Probing Quantum Reality - Weak Values and Double-Slit Trajectories

Jan Andreas Dziewior

München 2025

Probing Quantum Reality - Weak Values and Double-Slit Trajectories

Jan Andreas Dziewior

Dissertation
an der Fakultät für Physik
der Ludwig–Maximilians–Universität
München

vorgelegt von
Jan Andreas Dziewior
aus Hindenburg/Zabrze, Polen

München, den 09.01.2025

Erstgutachter: Prof. Dr. Harald Weinfurter
Zweitgutachter: Prof. Dr. Stephan Hartmann
Tag der mündlichen Prüfung: 20.03.2025

Amor fati: das sei von nun an meine Liebe! Ich will keinen Krieg gegen das Hässliche führen. Ich will nicht anklagen, ich will nicht einmal die Ankläger anklagen. Wegsehen sei meine einzige Verneinung! Und, Alles in Allem und Großen: ich will irgendwann einmal nur noch ein Ja-sagender sein!

Wir müssen zeitweilig von uns ausruhen, dadurch, dass wir auf uns hin und hinab sehen und, aus einer künstlerischen Ferne her, über uns lachen oder über uns weinen; wir müssen den Helden und ebenso den Narren entdecken, der in unsrer Leidenschaft der Erkenntniss steckt, wir müssen unsrer Thorheit ab und zu froh werden, um unsrer Weisheit froh bleiben zu können!

F. Nietzsche,
Die Fröhliche Wissenschaft, 1882

We do not know where we are "stupid" until we "stick our neck out", and so the whole idea is to put our neck out.

R. Feynman,
The Feynman Lectures on Physics III

All are architects of Fate,
Working in these walls of Time;
Some with massive deeds and great,
Some with ornaments of rhyme.

Nothing useless is, or low;
Each thing in its place is best;
And what seems but idle show
Strengthens and supports the rest.

For the structure that we raise,
Time is with materials filled;
Our to-days and yesterdays
Are the blocks with which we build.

Truly shape and fashion these;
Leave no yawning gaps between;
Think not, because no man sees,
Such things will remain unseen.

In the elder days of Art,
Builders wrought with greatest care
Each minute and unseen part;
For the Gods see everywhere.

Let us do our work as well,
Both the unseen and the seen;
Make the house, where Gods may dwell,
Beautiful, entire, and clean.

Else our lives are incomplete,
Standing in these walls of Time,
Broken stairways, where the feet
Stumble as they seek to climb.

Build to-day, then, strong and sure,
With a firm and ample base;
And ascending and secure
Shall to-morrow find its place.

Thus alone can we attain
To those turrets, where the eye
Sees the world as one vast plain,
And one boundless reach of sky.

H. W. Longfellow, The Builders, 1850

Zusammenfassung

Seit ihrer ersten Formulierung vor über hundert Jahren, ist Quantentheorie, wenn auch instrumental in der Entwicklung eines großen Teils moderner Technologie, begleitet von lebhaften Debatten und Kontroversen. Obgleich diese Arbeit nicht danach strebt Lösungen für solche Fragen vorzulegen, so ist ihr Hauptziel die Aufhellung einiger interpretatorischer Probleme, vor allem in Bezug auf das Verständnis von Interaktionen zwischen Quantensystemen und von Quantenmessungen. Dies wird vor allem mit eine Reihe von experimentellen Studien erreicht, welche sich mit grundlegenden Szenarien der Quantenmechanik befassen.

Um den Informationsfluss zwischen einem Quantensystem und dessen Umwelt zu untersuchen, wird ein offenes Quantensystem in einem integrierten optischen Wellenleiterarray simuliert, indem verschiedene Freiheitsgrade des Lichts mit System und Umwelt identifiziert werden. Dies ermöglicht die Beobachtung eines nicht-Markovschen Prozesses und eine Analyse des Informationsflusses aus dem System. Eine theoretische Studie stellt die Notwendigkeit heraus, die grundlegende Einstellung bezüglich statistischer Zertifizierung klarzustellen, wann immer Verschränkung mit beschränkten Ressourcen nachgewiesen wird. Sie demonstriert, wie in manchen Fällen frequentistische und bayessche Maße zu unterschiedlichen optimalen Strategien führen können. Die Messung einer nichtlokalen Observable, welche relativistischen Einschränkungen unterliegt, wird durch die Verwendung eines Messsystems in einem verschränkten Zustand experimentel realisiert. Dies lässt es zu, das Versagen der Produktregel für Systeme, die *postselected* sind, experimentell zu beobachten.

Ein zentrales Thema ist das Konzept des schwachen Wertes (*weak value*) eines Operators, der als effektive Beschreibung der Interaktion von Systemen angesehen werden kann, die *preselected* und *postselected* sind. Mit der Frage inwiefern schwache Werte Eigenschaften von einzelnen Quantensystemen und nicht bloß von Ensembles darstellen, befasst sich ein Experiment, welches eine grundsätzliche Ähnlichkeit zwischen Eigenwerten und schwachen Werten in Bezug auf die effektive Beschreibung von Interaktionen aufzeigt. Eine zweite experimentelle Untersuchung setzt eine Messung eines ungewöhnlich großen schwachen Wertes für nur ein einzelnes System mit erfolgreicher postselection um. Die Verwendung von schwachen Werten als Quantifikatoren effektiver Präsenz von Teilchen wird durch ein drittes Experiment motiviert, welches die Universalitäts Eigenschaft von schwachen Werten demonstriert, d.h. die Tatsache, dass ein bestimmter schwacher Wert der Projektion auf einen Ort zu der gleichen Modifikation der Effekte aller Interaktionen an diesem Ort führt.

Abschließend wird eine Analyse der nichtlokalen Eigenschaften der Bohmschen Mechanik durchgeführt. Es wird gezeigt, wie diese in grundlegenden Szenarien, wie z.B. dem EPR Szenario oder *delayed-choice* Experimenten, angewendet werden kann. Darüber hinaus, wird die Entwicklung eines Experiments dargestellt, welches darauf abzielt sogenannte "surrealistischen" Trajektorien zu verwirklichen, bei welchen die Bohmsche Zuschreibung von Trajektorien den Ergebnissen von welcher-Weg Beobachtungen widerspricht. Die experimentelle Umsetzung basiert auf einem Paar verschränkter Photonen, von denen eines das Interferenzfeld eines Doppelspaltes durchquert, während das andere die Rolle des dazugehörigen welcher-Weg Messapparats übernimmt. Durch die Verwirklichung einer echten *delayed-choice* Konfiguration in Verbindung mit der Möglichkeit die Zeitordnung der Operationen auf den beiden Photonen zu variieren, wird es möglich sein, verschiedene kausale Szenarien zu realisieren und die Nichtlokalität der Bohmschen Mechanik aufzuzeigen.

Abstract

Since its first formulation over a hundred years ago, quantum theory, while instrumental in the development of most contemporary technology, is accompanied by lively debates and controversies about its proper interpretation. While this study does not aim to provide solutions of such questions, its main goal is the clarification of several interpretational issues in particular with respect to the understanding of interactions between quantum systems and of quantum measurements. This is achieved chiefly through a series of experimental demonstrations addressing seminal scenarios of quantum mechanics.

To study information flow between a quantum system and its environment, integrated optical waveguide arrays are employed for the simulation of an open quantum system, where different degrees of freedom of light are identified with system and environment. This allows to observe non-Markovian evolution and analyze the information flow from the system. A theoretical study points out the necessity to clarify the foundational attitude towards statistical certification when entanglement detection is performed with limited resources. It demonstrates how, in some cases, Frequentist and Bayesian figures of merit imply different optimal strategies. The measurement of a nonlocal observable, which is subject to relativistic constraints, is realized experimentally by employing an entangled pointer state. This enables the observation of the failure of the product rule for pre- and postselected systems.

A major topic is the concept of a weak value of an operator, which can be regarded as an effective description of interactions with pre- and postselected systems. The question in what sense weak values represent properties of single quantum systems and not merely of ensembles is addressed in an experiment which shows a fundamental similarity between weak values and eigenvalues with respect to the effective description of interactions. A second experimental study implements a measurement of an anomalously large weak value on just a single successfully postselected system. The usage of weak values as quantifiers of effective particle presence is motivated by a third experiment which demonstrates the universality property of weak values, i.e., the fact that a particular weak value of local projection leads to the same modification of the effects of all interactions at that location.

Finally an analysis of the nonlocal properties of Bohmian mechanics is performed. It is shown how it can be applied to foundational scenarios, such as the EPR scenario or delayed-choice experiments. Furthermore, the development of an experiment is presented, which aims to realize so-called “surrealistic” trajectories, for which the Bohmian assignment of trajectories does not agree with the outcome of a which-path measurement. The experimental implementation is based on a pair of entangled photons, one of which traverses a double-slit interference field, while the other functions as the corresponding which-path measurement device. Through the realization of a true delayed-choice setup in conjunction with the possibility to vary the time-ordering of the operations performed on the two photons, it will become possible to realize various causal scenarios and to illustrate the nonlocality of Bohmian mechanics.

Contents

Zusammenfassung **vii**

Abstract **ix**

Contents **xi**

List of Abbreviations **xvii**

Introduction **1**

1 Quantum Mechanics **7**
1.1 Physical Reality 7
1.1.1 Beables and Elements of Reality 7
1.1.2 Realism and Operationalism 8
1.2 States of Physical Systems 9
1.2.1 Classical States 9
1.2.2 Quantum States 10
1.2.3 Probabilistic Connection to Phenomena 12
1.2.4 Interpretation of the Quantum State 13
1.3 Mixed States 15
1.3.1 Density Operators and Partial Description 15
1.3.2 Coherence and Decoherence 16
1.3.3 Proper and Improper Mixtures 17
1.4 Evolution 17
1.4.1 Schrödinger Equation 17
1.4.2 Relativistic Quantum Mechanics 18
1.4.3 Evolution of the Density Operator 19
1.4.4 Heisenberg Picture 20
1.5 Interaction 21
1.5.1 Interaction Picture 21
1.5.2 Weak Interactions and Weak Traces 22
1.6 Quantum Information and Communication 23
1.6.1 Information Theory 23

1.6.2 Accessibility and Distinguishability . . . 25
1.6.3 Channel Coding Theorems . . . 27
1.6.4 Qubits and Correlations . . . 28
1.7 Applications of Quantum Information . . . 30
1.7.1 Quantum Estimation Theory . . . 30
1.7.2 Quantum Cryptography . . . 31
1.7.3 Quantum Computation . . . 32
1.7.4 Quantum Simulation . . . 32
1.8 Open Quantum Systems . . . 33
1.8.1 Effective Evolution of Subsystems . . . 33
1.8.2 Markovian Master Equations . . . 33
1.8.3 Markovianity and Dynamical Maps . . . 35
1.8.4 Information Flow . . . 35

2 Quantum Measurement 37
2.1 Basic Concepts . . . 37
2.1.1 Measurement Postulates . . . 37
2.1.2 Incompatibility and Complementarity . . . 38
2.1.3 Uncertainty Relations and Mutually Unbiased Bases . . . 40
2.2 Formal Description of Quantum Measurement . . . 41
2.2.1 Indirect Measurement . . . 41
2.2.2 Generalized Observables . . . 42
2.2.3 Information-Disturbance Trade-Off . . . 44
2.2.4 Weak Measurements . . . 46
2.3 Measurements and Continuous Observables . . . 48
2.3.1 Canonically Conjugate Observables . . . 48
2.3.2 Wigner Representation . . . 50
2.3.3 Optimal Pointer States . . . 50
2.4 Properties of Quantum Measurements . . . 51
2.4.1 Informational Completeness and Quantum Tomography . . . 51
2.4.2 Quantum Non-Demolition Measurements . . . 52
2.4.3 Quantum Zeno Effect and Protective Measurements . . . 53
2.5 The Measurement Problem . . . 55
2.5.1 Decoherence . . . 55
2.5.2 Semantic Incompleteness . . . 55
2.5.3 Three Problems . . . 56
2.5.4 Collapse Theories . . . 57
2.5.5 Many Worlds Interpretation . . . 57
2.6 Measurements on Pre- and Postselected Systems . . . 58
2.6.1 Time-Symmetry in the Measurement Process . . . 58
2.6.2 Three Boxes, Pigeon Holes, and Cheshire Cats . . . 62
2.6.3 Practical Examples of Postselection . . . 63

3 Quantum Mechanics and Relativity **65**
3.1 Locality . . . 65
3.1.1 Minkowski Spacetime . . . 65
3.1.2 Formal Locality . . . 67
3.1.3 Locality of Interactions . . . 68
3.1.4 Local Causality . . . 69
3.1.5 Particles, Fields and Waves . . . 69
3.2 Bell's Theorem . . . 70
3.2.1 The EPR Argument . . . 70
3.2.2 No-Go Theorems for Hidden-Variables . . . 72
3.2.3 Empirical Test of Completeness . . . 72
3.2.4 The Theorem and its Consequences . . . 74
3.2.5 Analyses, Extensions and Generalizations . . . 77
3.2.6 Experimental Tests and Loopholes . . . 78
3.3 Entanglement . . . 79
3.3.1 Bipartite Entanglement . . . 79
3.3.2 Multipartite Entanglement . . . 81
3.3.3 Applications of Entanglement . . . 83
3.3.4 Entanglement Detection . . . 84
3.3.5 [**P11**] Valid and efficient entanglement verification with finite copies of a quantum state . . . 87
3.4 Spacetime Structure of Measurements . . . 97
3.4.1 Wheeler's Delayed Choice . . . 97
3.4.2 Generalized Delayed Choice . . . 99
3.4.3 Measurement of Nonlocal Observables . . . 101
3.4.4 [**P4**] Measurements of Nonlocal Variables and Demonstration of the Failure of the Product Rule for a Pre- and Postselected Pair of Photons 104

4 Light as a Quantum Object **111**
4.1 Classical Spectra and Fluctuations . . . 111
4.1.1 Electromagnetic Waves . . . 111
4.1.2 Spatio-Temporal Localization of Light Fields . . . 113
4.1.3 Spectral Properties of Light . . . 113
4.2 Classical Light Beams . . . 115
4.2.1 Paraxial Wave-Packets . . . 115
4.2.2 The Gaussian Beam . . . 116
4.2.3 Polarization of Paraxial Light . . . 118
4.2.4 Optical Energy Flow . . . 119
4.3 Quantization of the Electromagnetic Field . . . 121
4.3.1 Quantum Field Theory . . . 121
4.3.2 From the Classical to the Quantum Field . . . 124
4.3.3 Field Excitations . . . 125
4.3.4 Quantum Wave-Packets . . . 126

4.3.5 Time Evolution of the Field . . . 127
4.4 Field States and Quantum Fluctuations . . . 129
4.4.1 Quadrature Operators . . . 129
4.4.2 Field Fluctuations . . . 130
4.4.3 Classical and Non-Classical States . . . 132
4.5 Detection of Light . . . 135
4.5.1 Direct and Indirect Detection . . . 135
4.5.2 Photocount Statistics . . . 136
4.6 Coherence and Correlation Functions . . . 138
4.6.1 Interference and Coherence . . . 138
4.6.2 First-Order Correlation Function . . . 139
4.6.3 Higher-Order Correlation Functions . . . 140
4.6.4 Photon Bunching . . . 142
4.7 The Photon Wavefunction . . . 143
4.7.1 Wave-Mechanics of Light . . . 143
4.7.2 Operational Approach . . . 144
4.7.3 The Maxwell Wavefunction . . . 146
4.7.4 Interpretation of the Photon Wavefunction . . . 148

5 Quantum Optics Applied 151
5.1 The Quantum Toolbox of Paraxial Light . . . 151
5.1.1 Paraxial Hilbert Space . . . 151
5.1.2 The Free Evolution . . . 153
5.1.3 Interaction Picture and Transverse Fourier Transform . . . 155
5.1.4 Basic Linear Interactions . . . 155
5.1.5 Propagation through Media . . . 156
5.1.6 Beam-Splitters . . . 158
5.1.7 Mirrors and Lenses . . . 159
5.1.8 Birefringence . . . 161
5.2 Nonlinear Optical Processes . . . 163
5.2.1 Light in Nonlinear Media . . . 163
5.2.2 Parametric Amplification . . . 164
5.2.3 Spontaneous Parametric Down-Conversion . . . 165
5.2.4 The Laser . . . 168
5.3 The Double-Slit . . . 169
5.3.1 Optical Description . . . 169
5.3.2 Double-Slit Coherence . . . 170
5.3.3 Complementarity and Disturbance . . . 171
5.4 The Interferometer . . . 174
5.4.1 Basic Principles of Interferometry . . . 174
5.4.2 Second-Order Correlation Measurements . . . 176
5.4.3 Homodyne Detection and Optical Metrology . . . 178
5.4.4 Interferometric Complementarity . . . 180

5.5 Optical Waveguides . . . 181
5.5.1 Fiber Optics . . . 181
5.5.2 Integrated Waveguide Arrays . . . 182
5.5.3 Simulation of Open Quantum Systems . . . 183
5.5.4 [**P8**] Tracing Information Flow from Open Quantum Systems . . . 184

6 Weak Values 191
6.1 The Physical Meaning of Weak Values . . . 191
6.1.1 Definitions of Weak Values . . . 191
6.1.2 Reduced Expressions . . . 193
6.1.3 Weak Value Measurements . . . 194
6.1.4 Metrology and Tomography . . . 196
6.1.5 Deterministic Weak Values . . . 198
6.1.6 Robust Weak Values . . . 199
6.1.7 [**P1**] Weak value beyond conditional expectation value of the pointer readings . . . 202
6.1.8 [**P6**] Anomalous weak values via a single photon detection . . . 215
6.2 Weak Traces and Presence of Quantum Particles . . . 221
6.2.1 Particle Presence in Quantum Mechanics . . . 221
6.2.2 Weak Trace Approach . . . 221
6.2.3 Presence and the Weak Value of Local Projection . . . 223
6.2.4 Weak Three Box Scenario . . . 225
6.2.5 Criticism of the WTA . . . 226
6.2.6 [**P3**] Universality of local weak interactions and its application for interferometric alignment . . . 229

7 Nonlocal Effects in Bohmian Mechanics 239
7.1 Bohmian Mechanics . . . 239
7.1.1 Basic Principles . . . 239
7.1.2 Guiding Wave . . . 241
7.1.3 Variants of Bohmian Mechanics . . . 242
7.2 Measurement in Bohmian Mechanics . . . 243
7.2.1 Measurement Process . . . 243
7.2.2 Contextuality in Bohmian Measurement . . . 245
7.2.3 Delayed Choice Experiments . . . 247
7.3 The Nonlocality of Bohmian Mechanics . . . 249
7.3.1 Bohmian Explanation in the Bell-Scenario . . . 249
7.3.2 The Scenario of “Surrealistic” Trajectories . . . 251
7.3.3 Interpretation of the ESSW Scenario . . . 253
7.4 Weak Values and Photon Trajectories . . . 254
7.4.1 Relativistic Bohmian Mechanics . . . 254
7.4.2 Operational Definition Based on Weak Values . . . 255
7.4.3 Photon Trajectories . . . 257

7.5 Nonlocal Effects in the Photonic Double-Slit 258
7.5.1 Transverse Velocity Field of Gaussian Beam 258
7.5.2 Double-Slit Trajectories 260
7.5.3 ESSW-Trajectories 262
7.5.4 Bohmian Steering 264
7.6 Experimental Velocity Measurement 269
7.6.1 Weak Measurement of Bohmian Velocity 269
7.6.2 Coupling via Birefringent Crystal 270
7.6.3 Measurement Back-Action 273
7.7 Experimental Delayed Choice Investigation 274
7.7.1 Experimental Setup 274
7.7.2 Generation of the Double-Slit 277
7.7.3 Polarization Measurement 279
7.7.4 Interpretation of Experimental Results 281

Conclusion **285**

List of Publications **289**

Bibliography **293**

Acknowledgements **333**

List of Abbreviations

AAV	Aharonov, Albert, and Vaidman
ABL	Aharonov, Bergmann, and Lebowitz
APD	avalanche photo-diode
BAE	back-action evading
BM	Bohmian mechanics
BLP	Breuer, Laine, and Pirlo
BS	beam-splitter
CCO	canonically conjugate observables
CCP	common-cause principle
CCR	canonical commutation relation
CHV	contextual hidden variable(s)
CPTP	completely positive and trace preserving
CW	continuous wave
DST	direct state tomography
EBC	existence of Bell-correlations
EPR	Einstein, Podolsky and Rosen
FAPP	for all practical purposes
FC	free choice
GMBC	genuine multipartite Bell-correlations
GME	genuine mutlipartite entanglement
GRW	Ghirardi, Rimini, and Weber
HBT	Hanbury-Brown and Twiss
HWP	half-wave plate
IDT	information-disturbance trade-off
IID	independent and identically distributed
LC	local causality
LHS	left-hand side
LOCC	local operations and classical communication
MUB	mutually unbiased bases
MUS	minimal uncertainty states
MWI	many worlds interpretation
NCHV	non-contextual hidden variable(s)
PBS	polarizing beam-splitter
PHE	paraxial Helmholtz equation
POVM	positive operator valued measure
PPS	pre- and postselected systems
PPT	positive under partial transpose
PWF	photon wavefunction
QET	quantum estimation theory
QFT	quantum field theory
QIT	quantum information theory
QKD	quantum key distribution
QND	quantum non-demolition
QST	quantum state tomography
QWP	quarter-wave plate
RC	relativistic causality
RF	reference frame
RHS	right-hand side
RMSD	root mean square deviation
RS	Riemann and Silberstein
sLOCC	stochastic LOCC
SNL	shot noise limit
SNR	signal-to-noise ratio
SQL	standard quantum limit
SQM	standard quantum mechanics
SR	special relativity
TSVF	two-state-vector formalism
WTA	weak trace approach
WVA	weak value amplification

Introduction

Foreword

Science is the pursuit of truth.

Born out from the flames of the enlightenment, it is guided by the conviction that this truth can be attained, at least in a transient and tentative way, by the application of the human faculty of reason in combination with the experimental method. Its biggest enemy are not falsehood and error, which can be encountered in even the most honest pursuit of truth, but a betrayal of this core tenet. What really disintegrates science is the half-truth, the obscuration, the wanton desinformation, or to use Frankfurt's terminus technicus, simply the production of *bullshit*:

> It is just this lack of connection to a concern with truth – this indifference to how things really are – that I regard as of the essence of bullshit. [...] The bullshitter ignores these demands altogether. He does not reject the authority of the truth, as the liar does, and oppose himself to it. He pays no attention to it at all. By virtue of this, bullshit is a greater enemy of the truth than lies are. [922]

In this work the attempt was made to follow the holy tradition of the enlightenment and elucidate a minuscule fraction of the grand scientific pursuit in which the author had the utmost honor and pleasure to participate for a few years of his life, and to do it without producing bullshit. The goal was to present an as consistent and complete as possible account of the scientific work performed in the course of this doctoral thesis while connecting it thoroughly to the context of the corresponding fields. This naturally took time, time which could have maybe been spent on more fruitful endeavors, and of course, as with all lofty human goals, it was doomed to fail from the start. However, according to the benevolent council of Nietzsche, as printed on the preceding pages, certain failure should not discourage us in any way from trying, and in this spirit the author, following also the advice of Feynman, "sticks out his head" to present these pages to the reader in the hope that they might prove useful in one or the other way.

The Quantum Revolution

The subject is *quantum mechanics*, which does not just represent a particular physical theory but arguably *the* modern approach to physics permeating essentially every field of

contemporary natural science. Since its inception, over a century ago based on the pioneering work of Planck, Einstein, Bohr, Schrödinger, Heisenberg, Born, and others, it has revolutionized the manner in which humans think about the world. The first phase in the evolution of quantum physics was focused on the development of a quantum model for the atom and culminated in an intensive period of seminal work in the 1920s, which essentially established the non-relativistic form of the theory as it is known today. Its revolutionary character is exemplified by the fact that the fields of mechanics, electrodynamics and thermodynamics, as known at the end of the 19th century, are today commonly called "classical" physics in contrast to the new quantum physics [59, 520]. However, the term "classical" is also used to denote contemporary research fields which do not employ the formal apparatus of quantum mechanics or relativity, such as classical information theory.

After the initial period a second phase saw the unification of quantum theory with the theory of special relativity in the form of quantum field theory, which had found its formal completion by the end of the 1940s. In the second half of the century quantum field theory was applied beyond the domain of electromagnetic phenomena culminating in the formulation of the standard model of modern physics in the 1970s. During this time, based on Glauber's seminal insights, also *quantum optics* was born, i.e., the application of quantum field theory to the field of optics, which up to that point was mostly treated classically. Finally the fourth phase, which began in the 1990s and arguably lasts until today, is characterized by a combination of quantum physics and information theory. It has led to a new generation of quantum technology and is sometimes called the "second quantum revolution".

Apart from developments in physics and consequent influences on other sciences, since its beginning quantum mechanics has been closely connected with modern philosophy of science. The novel structure of quantum mechanics harmonized extremely well with the emerging school of logical positivism, which in a nutshell aimed to reduce all scientific propositions to statements about empirical observations. Hence, from an intricate fabric of respective influences between physics and philosophy emerged the hegemony of a non-realist view of quantum physics, which arguably remains the most held position until today [924, 918]. Note that non-realism by no means implies a renunciation of the scientific ideal of the search of truth as introduced in the beginning. Quite the contrary, it might be that any notion of a real world or an actual state of affairs are fundamentally unattainable, and the aim to provide a coherent and consistent account of observations is the closest science can come to a notion of truth. Some regard this insight on the limits of human knowledge itself as perhaps the most important and bitter truth learned from quantum mechanics. This conclusion, however, is by no means uncontested, and others are strongly convinced that there is no reason whatsoever to abandon the search for a rational description of an observer-independent physical world.

Such philosophical considerations never hindered the more practical application of quantum theory to various physical phenomena at hand. Today quantum physics is considered as the best confirmed theory in the history of physics and a large portion of contemporary technology is directly based on its utilization. Beyond this scientific mainstream, however, foundational questions linger on and remain in the focus of a small portion of

the efforts of physicists, including most parts of the present work, which searches for an understanding of the implications of quantum mechanics at the boundary of physics and philosophy of science. This does not mean that such efforts cannot also bear more practical fruit and in fact some arguably initially strictly foundational lines of investigation, such as, most famously, Bell's theorem, have lead to essential practical methods at the core of contemporary quantum technology.

Principal Questions

This work is mainly dedicated to two foundational approaches, namely weak values originating from an alternative time-symmetric formalism for quantum mechanics, and Bohmian mechanics, a realist interpretation, which provides ontological and causal explanations for quantum phenomena in opposition to the non-realist mainstream position. The Bohmian interpretation of quantum mechanics was developed by Bohm in the beginning of the 1950s and represented to some extent a rediscovery of previous ideas of de Broglie. It represented a new revolutionary approach to quantum mechanics, which was, however, for the largest part either ignored or not taken seriously. Weak values are a newer concept proposed at the end of the 1980s by Aharanov, Albert and Vaidman, shortly before the emergence of quantum information science. They are sometimes regarded as providing the possibility to extend the description of quantum systems beyond the commonly accepted domain, in particular ascribing properties to quantum systems independently of performed observations. In effect, the interpretation of weak values has also led to several controversies. The present thesis also contributes more technical results to the fields of open quantum systems as well as quantum measurement and information theory, which, however, are also intricately connected to the core problems of quantum mechanics and the foundations of physics. This connection can be formulated in terms of two main guiding questions also encapsulated in the title of this work:

> **Question 1:** To what extent and in what sense is it possible to provide accounts of quantum mechanics which allow a realist view of the physical world?
>
> **Question 2:** What can experimental investigations, in particular optical experiments, contribute to answering the first question?

The first question is addressed chiefly by a juxtaposition of three significantly different approaches to quantum mechanics, i.e., the standard textbook theory which rejects any ontological commitments, the Bohmian theory with an explicit realist interpretation and the time-symmetric two-state-vector approach, which, while not sharing the Bohmian concept of an observation-independent world, still adds features beyond the standard interpretation. However, while addressing these foundational issues, this work is first and foremost an experimental study. This means that the treatment of such questions is always closely linked to experimental investigations, in particular in the field of optics. In a series of optical experiments physical scenarios are realized which illustrate in a particularly glaring

manner the consequences and limits of the various foundational approaches. The analysis of these experiments then provides a path to answering the second question.

The Structure of this Work

The range of topics treated in this work makes it necessary to present a broad foundation, which allows to discuss the various facets of the experimental studies subject to this work in the proper context. Apart from Bohmian mechanics and the theory of weak values, four basic areas from the vast domain of quantum theory are of particular relevance, namely quantum information, open systems as well as quantum measurement from the theoretical and quantum optics from the experimental side. The final essential ingredient is the analysis of the connection of quantum theory with the tenets of special relativity as profoundly expressed in Bell's theorem, which represents the touchstone of any interpretation of quantum mechanics.

One particular challenge of this work is the development of a unified formalism to treat these distinct fields, which in the common practice of research sometimes have little overlap. Naturally, the manner in which quantum theory is formulated and employed varies immensely between application oriented efforts of experimentalists, the abstract language of quantum information theorists, and the ontological descriptions of Bohmian realists. Furthermore, non-relativistic and relativistic quantum theory are commonly treated in complete separation up to the point that they appear as two distinct theories. As this work is concerned with several of such fields, the attempt is made to provide a clear common formal and descriptive language to highlight the significant connections and common elements of the various areas of research.

The first two chapters cover the basic theoretical elements of quantum theory, with the second chapter focusing solely on the complex of quantum measurement. These chapters have a two-fold role. On the one hand they introduce the basic formalism, which forms the basis of all other considerations, but on the other hand they also present the minimal operational understanding of quantum theory, which represents its most common interpretation and which in the course of this work is compared with the two other approaches in focus. Chapter three discusses the consequences of a quantum description of physical systems in space-time under relativistic constraints, introducing Bell's theorem and the notion of quantum entanglement. In the context of the latter also the question is discussed how probabilistic conclusions about physical systems, in particular about the presence of entanglement, can be justified in the presence of significant statistical noise. Albeit primarily a technical result, also the statistical analysis of entanglement certification elucidates fundamental questions about the justification of probabilistic scientific conclusions. Additionally also an experimental scheme for the quantum nondemolition measurement of nonlocal observables is presented, which allows to experimentally observe the failure of the product rule for pre- and postselected systems.

In chapters 4 and 5 the way is paved to make the phenomenon of light available as an object of quantum theory to be employed as a tool in experiments probing the foundations

of quantum mechanics. In particular, through the discussion of the basic aspects of quantum field theory, the possibility of wave-mechanical description of photons is sketched, which forms the foundation for the description of all experiments treated in this work. Furthermore, only equipped with this notion of a photon wavefunction is it possible to apply optical experiments to the study of Bohmian mechanics. In particular in chapter 5 the basic optical setups of the double-slit and the interferometer are introduced. Finally, also a study is presented in which integrated optical devices are employed to probe the properties of information transfer in open quantum systems.

The last two chapters 6 and 7 are dedicated to detailed expositions of the concept of weak values and Bohmain mechanics, respectively. Two experiments provide illustrations of how weak values can be attributed to single pre- and postselected quantum systems. In the first it is shown that, at least from the perspective of the time-symmetric two-state-vector-formalism, systems described by a special type of so-called deterministic weak values affect other systems as if they were in eigenstates of the respective interaction operators, i.e., arguably in a classical manner. The second experiment demonstrates the possibility to observe an anomalous weak value on a single quantum system. A different question is addressed by a third experiment which illuminates the role of weak values in the context of the weak trace approach to past presence of quantum particles. The presence of the particle, as quantified by the weak value of local projection, is experimentally shown to universally modify all effective local interactions of the particle. In the last chapter the Bohmian perspective on quantum mechanics is introduced including in particular a discussion of contextuality in quantum measurement and the appearance of nonlocal influences. This realist theory is then applied to an experimental scenario in which, at least according to Bohmian mechanics, a photon traversing a double-slit field is nonlocally influenced by operations performed on a space-like separated second photon due to entanglement. The Bohmian description of this scenario is contrasted with standard quantum mechanics to accentuate the different features of the two approaches.

Technical Remarks

There exists only a finite set of commonly used Latin and Greek symbols and in order to avoid too unusual notations, it turned out to be beneficial to employ a small set of the more rarely occurring symbols in more than one manner. However, in each chapter the usage is unique. Whenever a symbol from a previous chapter is redeployed with a different meaning, the context directly clarifies the present definition.

Throughout this work operators are written in bold font, as, e.g., $\mathbf{a}$, the only exceptions being the symbol ρ denoting density operators and the symbol $\mathbb{1}$ for identity operators. Markers on top of symbols include the vector arrow $\vec{a}$ for two or three-dimensional spatial vectors, circumflexes $\hat{a}$ for unit or otherwise normalized vectors, and inverted circumflexes $\check{a}$ for spinors, i.e., vectorial quantities with entries not corresponding to spatial directions. The tilde symbol $\widetilde{a}$ is used both for Fourier transformed quantities as well as for states after postselection. Finally, estimators are written in fraktur font $\mathfrak{a}$.

To conserve precious space and to increase readability, for common expressions, names, as well as groups of authors acronyms are employed, which are also specified in a dedicated table. For the same reason whenever possible inline formulas are used, with an appropriately condensed notation. Inline fractions are written with the slash symbol as a/b, and the shorthand ∂_x is used for derivative $\partial/\partial x$. Also for denominators brackets are consequently neglected such that $1/ab$ is equivalent to $1/(ab)$, i.e., everything after an inline slash is considered part of the denominator. Furthermore, functional arguments are by default not written in inline expressions and only sometimes added for emphasis. For example while a function is defined as $\psi(x,t)$, it is typically referred to as ψ. On the rare occasions that functional arguments are also suppressed in centered formulas, this is always indicated explicitly in the text. Finally, throughout the text the abbreviations "RHS" and "LHS" are employed to denote the right-hand-side and left-hand-side of equations, respectively.

Due to its comparatively large extent, the bibliography has been divided into ten thematic categories. As with any taxonomy, the moment it is established a range of fringe cases appear, the attribution of which is ambiguous. Nevertheless, also these works have been sorted into respective categories to the best of the author's understanding, based on their main or most relevant topic. Notably works on physics from the first half of the 20th century and earlier have been assigned their own historical category. Finally, it should be pointed out with the strongest emphasis that this work has not been tainted in any manner by contact with natural language processors, i.e., "machines-that-think", the application of which has become so popular in our time.

Chapter 1

Quantum Mechanics

The aim of this chapter is to introduce the basic elements of quantum theory with the exception of quantum measurement which is relegated to a more specialized second chapter. The present chapter begins by discussing the concept of physical reality and pointing out its complicated relationship to quantum mechanics. It proceeds to introduce the basic concepts of the quantum formalism including the Hilbert space description with pure and mixed quantum states along with their evolution and the interaction between quantum systems. In this context also the distinction between the dispositional and descriptive functions of the theory is introduced leading over to a discussion of possible interpretations of the quantum state. Finally the treatment of quantum mechanics in terms of an information theory is sketched along with a summary of its major practical applications. The chapter then closes with an overview over the effective treatment of quantum systems as open systems. The components introduced in this chapter form the essential foundation for all other topics considered in this work.

1.1 Physical Reality

1.1.1 Beables and Elements of Reality

In classical physics, before the emergence of quantum mechanics, the connection between the mathematical content of physical theories and some notion of a *reality* was at least presumably clear [818, 521]. In this vein, famously, Einstein, Podolsky and Rosen (EPR) begin their seminal paper about quantum theory with the statement:

> ANY serious consideration of a physical theory must take into account the distinction between the objective reality, which is independent of any theory, and the physical concepts with which the theory operates. These concepts are intended to correspond with the objective reality, and by means of these concepts we picture this reality to ourselves. [18]

This paragraph captures exactly that element of classical physics which becomes highly contested in quantum physics. Physical theories are mathematical and consequently those

"physical concepts" are mathematical objects. However, classical theories crucially include, often only implicitly, a "correspondence" between at least some of those mathematical objects to a "picture" of an "objective reality". This connection is addressed by EPR with their influential definition.

Similarly, Bell establishes the concept of *beables* (in contrast to quantum mechanical observables) as those theoretical objects which "correspond to something real" [372, 370]. He gives the paradigmatic example of classical electrodynamics, where usually the potentials are considered to be only auxiliary mathematical constructs in contrast to the electric and magnetic fields which correspond to real things and asserts that

> ... if you are unable to give some special status to things like electric and magnetic fields (in classical electromagnetism), as compared with the vector and scalar potentials, and British sovereignty, then we cannot begin a serious discussion. [370]

In practice the classical intuition of correspondence to an underlying reality is mostly established by a body of experimental results, in which the theory is able to connect a large set of observable phenomena with a comparatively small set of theoretical objects and laws. This motivates to regard these objects as representing reality, even more so when, as Hacking argues, the net of their causal connections becomes so well understood that these objects become experimental tools themselves [923].

1.1.2 Realism and Operationalism

For the purpose of this work the term *realism* is broadly understood as denoting the aggregate of positions which in one way or another share the above-mentioned intuition of correspondence to an underlying reality. Arguably this view is omnipresent in classical physics but it is not the only manner how even classical theories can be viewed. An opposite position is the *operational* approach, as coined by Bridgman [2], where all physical statements are understood as statements about actions or operations [946]. In this context Hughes [925] has introduced the useful notions of the *descriptive* and *dispositional* functions of a scientific theory. While the descriptive character encapsulates the function of the theory as a representation of reality, the dispositional function pertains to its capacity to provide predictions for the behavior of empirical phenomena under certain circumstances. In effect, operationalism can be said to disregard the descriptive function of theories and attribute meaning to them exclusively from a dispositional perspective, in particular with respect to experimental interventions, i.e. operations. The distinction between the descriptive and dispositional functions of quantum mechanics represents a useful classification which is applied repeatedly throughout the following chapters.

In quantum mechanics operationalism is commonly connected with the so-called *Copenhagen interpretation*, a name coined by Heisenberg [924] and related to the fruitful collaboration of Heisenberg with Bohr in Copenhagen from 1926 to the 1927 Solvay conference [918, 992]. However, this term is notoriously ambiguous and also includes the ideas of several other founding fathers of quantum mechanics such as Pauli, Born, and also von Neumann [918, 931, 992, 944, 947]. In any case it introduces a decidedly operational and

non-realist element via the reinterpretation of the notion of *measurement*. Whereas in classical physics measurement was seen merely as a means to reveal existing properties of the real physical system, in the Copenhagen interpretation the measurement and the so-called *measurement apparatus*, i.e., the physical device interacting with the system in question, obtain fundamental meaning in themselves [966, 861, 521, 944]. The outcome of a measurement is an empirical phenomenon which is detached from an underlying reality and comes into existence due the interaction of a quantum system with a specific apparatus, see also the discussion of "complementarity" in Sec. 2.1.2. Typical slogans in this context are "unperformed experiments have no results" [1008] or "unasked questions have no answers", see, e.g., [91]. In operationalism an experiment is no longer a tool employed in the general endeavor "to understand the world" but in some sense becomes the object of science itself [966]. This point of view prompted a famous response by Einstein as recounted by Pais:

> We often discussed his notions on objective reality. I recall that during one walk Einstein suddenly stopped, turned to me and asked whether I really believed that the moon exists only when I look at it. The rest of this walk was devoted to a discussion of what a physicist should mean by the term "to exist". [1005]

Note that this opposition between realism and operationalism, *instrumentalism*, or, *idealism* in the context of quantum theory is part of a fundamental debate about the nature of science and human knowledge in general, which is and presumably also will still be going on as long as there is science. It is grazed in this work only to the extent as it forms a context to analyze some interpretations of quantum theory. See e.g. [920, 945, 998] as a starting point to get an overview over the enormous scale of this debate, which reaches far into antiquity, see, e.g., [933, 934, 914, 915, 913, 921, 930, 926, 928] for prominent examples.

1.2 States of Physical Systems

1.2.1 Classical States

In general physical theories are applied via *models* which simplify the complex content of the theory and make it applicable to the phenomena at hand [974, 923, 521]. A classical model contains *systems* with certain *degrees of freedom* described by sets of real valued *parameters*, where to each degree of freedom a single parameter is attributed. The set of real numbers parameterizing a certain system is its *state* which is commonly represented via a point in corresponding potentially high dimensional *phase-space* [925, 60, 225]. Of course such models involve idealizations and approximations such that there never exists a perfect correspondence between the mathematical model with its parameters and the quantified empirical phenomena.

Classical states have both descriptive as well as dispositional meaning. As illustrated by Bell's example of electromagnetic fields and potentials, usually in a classical model it

is clear that some parameters have the status of beables. The mass or the position of an extended body are thought of as corresponding to real *properties* of the world, which are fully described by the real values of the corresponding parameters. At the same time they have a clear dispositive function as they predict the outcomes of operations to measure mass or position. In the classical state the descriptive and dispositional aspects coexist unproblematically and are intuitively connected [225]. In fact, it is exactly this connection which is formulated in the definition of beables according to EPR:

> If, without in any way disturbing a system, we can predict with certainty (i.e., with probability equal to unity) the value of a physical quantity, then there exists an element of physical reality corresponding to this physical quantity. [18]

On the one hand the state is dispositional as it allows to predict the outcome of measurement and on the other hand EPR take all such certain predictions to indicate a descriptive quality of that phase space coordinate. The latter becomes even more explicit in Redhead's variation of the EPR definition:

> If we can predict with certainty, or at any rate with probability one the result of measuring a physical quantity at time t, then, at time t, there exists an element of reality corresponding to this physical quantity and having value equal to the predicted measurement result. [935]

In this formulation it is clarified that "predicting a value" means "predicting the outcome of a measurement" and furthermore a "value", i.e., a real number, is directly attributed to the corresponding element of reality.

1.2.2 Quantum States

The quantum notion of a physical state differs greatly from the classical approach. The state of a system, i.e., a *quantum state* is given as a unit vector $|\psi\rangle$ in a complex Hilbert space $\mathcal{H}$. Any single degree of freedom is thus no longer parametrized by a single number but by a higher dimensional vector, see, e.g., [54, 114, 925, 57, 95, 50] for details about the mathematical structure of discrete and continuous Hilbert spaces, states, and operators as well as the usual Dirac notation employed here.

Especially due to the strong influence of Bohr in early treatments of quantum mechanics, special emphasis was put on a transition from a classical description to a quantum description called the *correspondence principle* [521, 65, 76]. Based on an essential formal similarity between certain classical formalisms and quantum mechanics, a quantum description of a classical system is constructed by following the so-called procedure of *quantization*. In this process particular degrees of freedom of the system such as position and momentum become represented by a continuous Hilbert space with a corresponding state vector. In contemporary quantum physics the correspondence principle plays no longer a significant role and quantum systems without any classical analogues are considered [521, 65] the simplest example of which are fundamentally discrete degrees of freedom such particle spin, as first detected in the seminal *Stern-Gerlach experiment* [20], see also [85].

Due to the formal similarity of quantum mechanics to classical wave theory the expansion $\psi(x) = \langle x|\psi\rangle$ of the state vector $|\psi\rangle$ in a basis $|x\rangle$ of $\mathcal{H}$ and in fact sometimes even the state vector itself are commonly referred to as the *wavefunction* [220, 57, 73].

The linearity of the quantum formalism implies consequences for the description of a set of systems with exactly the same Hilbert space structure. In particular, a range of elementary types of systems is considered which are called elementary *particles*, where here the notion of "particle" is related to classical intuitions of the individuality and countability of physical systems [952]. However, in quantum mechanics elementary particles of the same type cannot be ascribed any individuality beyond differences in their states and are in this sense fundamentally *identical* [69, 79]. Thus, if their states are brought into at least partial overlap as a consequence of the joint evolution, quantum particles can *interfere*, where the term "interference" originates from optics as introduced in Secs. 5.3 and 5.4 and signifies the additive behavior of complex amplitudes due to the linearity of quantum mechanics [843]. Note that of course interference can also occur between different components of the state of a single particle and in fact multi-particle interference can always be regarded as the interference between components of a single system consisting of multiple particles.

The interference behavior for multiple particles is codified in the so-called *symmetry postulate* which states that joint states of identical particles must be invariant under the pairwise exchange of particles, i.e., they must be symmetric or anti-symmetric [69, 79]. In effect, all quantum particles and in extension also all composite quantum systems such as atoms are classified into two groups, namely *bosons* described by symmetric wavefunctions and *fermions* described by anti-symmetric ones. As long as the particles remain fully *distinguishable*, i.e., their states remain orthogonal at least with respect to a single degree of freedom, as discussed in Sec. 1.6.2, they can never interfere with each other. In such cases the symmetry postulate just obtains the "humble role" to rule out any statement about which particle is in which state and thus the symmetrization of the joint state can be forgone without any consequences for the empirical predictions [79]. In the context of statistical physics which involves a counting of possible configurations of particle states, the indinstiguishability of quantum particles leads to the famous *Bose-Einstein* distribution for bosons and along with the *Pauli exclusion principle* [34] to the *Fermi-Dirac distribution* for fermions, see also [62, 78, 77, 948]. This contrasts with classical Maxwell-Boltzmann statistics which is based on the individuality of particles.

Finally, an important technical issue, which concerns differences between discrete and continuous Hilbert spaces, should be noted at least briefly. Finite dimensional discrete Hilbert spaces allow for a much simpler mathematical treatment and as such are the primary object of quantum information theory as introduced in Sec. 1.6.1. A thorough mathematical treatment of continuous Hilbert spaces is much more complicated and poses a range of formal problems. In quantum mechanics, however, due to the requirement of normalizability of states, only *separable* Hilbert spaces are of relevance, i.e., Hilbert spaces with only a countably infinity of states [512, 95, 225]. While it is still possible to expand states from such Hilbert spaces in continuous bases, such as the eigenbasis of the position operator $\mathbf{x}$, it should be noted that these basis states themselves are only limits of physical states and not elements of the Hilbert space [83, 225].

1.2.3 Probabilistic Connection to Phenomena

Since a quantum state vector does not provide a single value to connect to empirical observations of real valued quantities such as spacetime coordinates, temperature, frequency, field strength, etc., additional formal structure is required. This dispositive function of the quantum state is established via so-called *observables*, a notion based on the term "beobachtbare Größe", i.e., "observable quantity", introduced by Heisenberg [22]. This notion reflects a fundamentally operational ansatz according to which meaningful physical properties have to be necessarily connected to certain measurement procedures [231]. In quantum mechanics an observable quantity is represented by a Hermitian operator $\mathbf{X}$ acting on the system's Hilbert space $\mathcal{H}$. As such $\mathbf{X}$ has a real-valued spectrum $\{x\}$ and it is the values in this spectrum which correspond to the possible values of the observable quantity, i.e., outcomes of measurements [231, 60]. In the jargon of quantum mechanics often both the operator as well as the observable quantity itself are denoted as "observable". Thus a common formulation is that "an observable $\mathbf{X}$ is measured", which is shorthand for "a measurement procedure is performed to determine the value of an observable quantity which is formally represented by the operator $\mathbf{X}$". Following this convention, also in this work the mathematical operators themselves are denoted as "observables" and the term "observable quantity" is used to explicitly denote associated measurement operations.

Since the state $|\psi\rangle$ in general is a superposition of eigenstates $|x\rangle$ of a given observable $\mathbf{X}$, no definite value is specified when the state of the system is given. Instead, the so-called *Born rule* as originally introduced by Born [7], provides the "statistical algorithm of quantum mechanics" [925] which gives a statistical prediction to observe certain values based on the given state of the system [931, 60, 75, 1010]. While for continuous observables $\mathbf{X}$ a probability density $p(x)$ over outcomes x is given, for discrete observables $\mathbf{A}$ with a spectrum $\{a_j\}$ discrete probabilities $p(j)$ to observe the outcomes a_j are provided. These probabilities are given by the squared modulus of the amplitude of the corresponding eigenvector $|x\rangle$ and $|a_j\rangle$ as

$$p(x) = |\langle x|\psi\rangle|^2 \tag{1.1}$$

$$p(j) = |\langle a_j|\psi\rangle|^2. \tag{1.2}$$

Accordingly, in the case of an observable with a subset of degenerate eigenvalues $a_j = a$ the probability to observe the value a is given by the sum of squared amplitudes of the respective eigenvectors or equivalently via the projection $\mathbf{\Pi}_a$ on the subspace spanned by them with

$$p(a) = \langle\psi|\mathbf{\Pi}_a|\psi\rangle. \tag{1.3}$$

This allows to define the *expectation value* $\langle\mathbf{A}\rangle$ in analogy to classical random variables as

$$\langle\mathbf{A}\rangle := \sum_j p(j)a_j = \langle\psi|\mathbf{A}|\psi\rangle. \tag{1.4}$$

The corresponding statistical variance $\mathrm{Var}(\mathbf{A})$ is given as

$$\mathrm{Var}(\mathbf{A}) := \sum_j p(j)\,(a_j - \langle \mathbf{A} \rangle)^2 = \langle \mathbf{A}^2 \rangle - \langle \mathbf{A} \rangle^2, \tag{1.5}$$

leading to the *standard deviation* $\Delta\mathbf{A} = \sqrt{\mathrm{Var}(\mathbf{A})}$. The concept of observables can be generalized further as discussed in Sec. 2.2.2.

1.2.4 Interpretation of the Quantum State

Although through the Born rule the dispositional function of the quantum state is clarified and for the most part uncontroversial, the question remains whether also a descriptive function with a potential correspondence to an underlying reality can be considered. Contrary to classical states there is no immediate intuition how to relate the state vector to a picture of a reality, especially given how experimental results are related probabilistically to projections on eigenstates of observables, a property sometimes called *non-objectivity* of observable quantities [222]. This becomes even more striking when considering the fundamental descriptive incompatibility of the Schrödinger and Heisenberg pictures of quantum states and their evolution, both of which, however, provide exactly the same empirical predictions as will be discussed in Section 1.4.4. In particular, while in the Schrödinger picture the quantum state evolves in time, it is time-invariant in the Heisenberg picture, where the observables evolve instead.

In any case any descriptive interpretation of the quantum states requires to add something more to the theory beyond the elements presented above, which already by themselves enable it to function so successfully as an operational theory. This is sometimes seen as a reason to stick to an operational interpretation and abandon any attempts to recover realism [856, 986], an attitude pointedly summarized with the slogan "shut up and calculate" by Mermin [1000, 1002]. This minimal pragmatic view is called "standard quantum mechanics" (SQM) in this work. The question of a correct interpretation of quantum mechanics, and in particular the descriptive status of the quantum state remains open until today, see e.g., [927, 222, 944, 994, 972, 976] for systematic overviews. Given the lack of generally accepted criteria to decide between those interpretations, it is not surprising that no consensus about the interpretation of quantum mechanics exists, neither in the physics nor in the philosophy communities, as indicated by several non-representative surveys [1013, 1015, 1004, 1014].

In general there are various options to group the different interpretations, but specifically with respect to the interpretation of the quantum state it is possible to identify three fundamental options, see Secs. 2.5 and 3.2.4 for different classifications of interpretations based on the solution of the measurement problem and Bell's theorem, respectively. Realist views can be divided into *psi-ontic* and *psi-epistemic* approaches [990, 1009]. Whereas in a psi-ontic interpretation the $|\psi\rangle$ itself is a beable or "ontic-state" [332], in a psi-epistemic view it encapsulates potentially only partial knowledge about other beables, which themselves are not part of the standard quantum theoretical description. Such parameters, not

present in SQM but considered crucial for the description of the real state of affairs, are commonly referred to as *hidden-variables* [963, 927, 861, 944, 68, 225]. In general both psi-ontic and psi-epistemic interpretations admit extensions via hidden-variables, but there are fundamental constraints on the structure of such approaches given by a set of seminal no-go theorems, as discussed in Sec. 3.2. The third major option is to view the quantum state as *not* connected to an underlying reality at all, but to consider it as description of a subjective state of knowledge or belief about empirical facts, more along the lines of an operational interpretation of quantum theory. While realistic interpretations are introduced in Sec. 2.5, examples of the third option are given by a minimal pragmatic view which strictly reduces the theory to its dispositive function as sketched above or most prominently by *Quantum Bayesianism* also called *QBism* [984, 985, 1001], in which the quantum state is explicitly viewed as the description of the subjective beliefs of agents.

A consequent operational position with a radical opposition to realistic interpretations of the quantum state is pointedly expressed by Peres:

> Many physicists, perhaps a majority, have an intuitive, realistic worldview and consider a quantum state as a physical entity. Its value may not be known, but in principle the quantum state of a physical system would be well defined. However, there is no experimental evidence whatsoever to support this naive belief. On the contrary, if this view is taken seriously, it may lead to bizarre consequences, called "quantum paradoxes." [sic] These so-called paradoxes originate solely from an incorrect interpretation of quantum theory, which is thoroughly pragmatic and, when correctly used, never yields two contradictory answers to a well-posed question. It is only the misuse of quantum concepts, guided by a pseudorealistic philosophy, that leads to paradoxical results. [422]

The same psychological habit of scientists is also pointed out by Norsen, albeit from a decidedly realist perspective:

> The reason for this schizophrenia, I suspect, is that orthodox quantum physicists are, after all, physicists. They cannot just "shut up and calculate" – not completely. They need some sort of visualizable picture of what, physically, the mathematical formalism describes, or they simply cannot keep track of what in the world they are talking about. [...] So they retain the classical picture while simultaneously, out of the other sides of their mouths, rejecting it. [883]

Remarkably these two authors, who hold diametrically opposite views with respect to the correct interpretation of quantum mechanics, share the basic conviction that a clear formulation of the interpretational stance is of crucial importance. The experimental scenarios considered in this work can aid in this goal by illustrating and clarifying crucial consequences of various interpretations.

1.3 Mixed States

1.3.1 Density Operators and Partial Description

Apart from state vectors quantum states can also be expressed as density operators ρ which formally correspond to maps on the respective Hilbert space $\mathcal{H}$. Valid density operators are Hermitian positive semi-definite operators with a unity trace [117, 95, 81, 61]. There exists a one-to-one correspondence between these two formulations. Any state vector $|\psi\rangle$ can be converted to a density operator via an outer product denoted as $\rho = |\psi\rangle\langle\psi|$. If a state can be described by such a rank-1 operator it is denoted as *pure*. If this is not the case the state is called *mixed*, a terminology introduced by Weyl with the originaly German terms *reiner Fall* and *Gemenge* [44]. Conversely, any density operator ρ, which always can be extended in its eigenbasis $\{|\phi_j\rangle\}$ as

$$\rho = \sum_j p(j)|\phi_j\rangle\langle\phi_j|, \tag{1.6}$$

where $p(j) \geq 0$ and $\sum_j p(j) = 1$, can be mapped to a state vector $|\Psi\rangle$ in a potentially higher dimensional Hilbert space $\mathcal{H}' = \mathcal{H} \otimes \mathcal{H}_{\text{aux}}$, via a *purification* [117, 95, 225]

$$|\Psi\rangle = \sum_j \sqrt{p(j)}\,|\phi_j\rangle \otimes |\xi_j\rangle \tag{1.7}$$

where $\{|\xi_j\rangle\}$ is a basis of $\mathcal{H}_{\text{aux}}$. Note that the auxiliary Hilbert space has to be sufficiently large with $\dim \mathcal{H}_{\text{aux}} \geq \text{rank}(\rho)$. The density operator ρ is then recovered via a partial trace $\rho = \text{tr}_{\text{aux}}(|\Psi\rangle\langle\Psi|)$. The amount of mixedness is quantified by the *purity* $\text{tr}(\rho^2)$ [95, 225]. It attains the maximal value of 1 for a pure state and the minimal value of $1/d$ for the so-called *maximally mixed state* $\mathbb{1}/d$ in a Hilbert space with dimension d. Throughout this work a shorthand notation for partial traces is employed whenever the traced out system is projected onto a pure state. For example in the case above, with an arbitrary state $|\xi\rangle$ of the auxiliary system, it holds that $\langle\xi|\Psi\rangle := \text{tr}_{\text{aux}}(\mathbb{1} \otimes |\xi\rangle\langle\xi|\,|\Psi\rangle\langle\Psi|)$. Finally, also the concept of orthogonality can be extended to potentially mixed states, by calling states "orthogonal" whenever they have disjoint *supports*, where the support of an operator is the defined as the subspace spanned by the subset of its eigenstates with nonzero eigenvalues [117].

From a dispositional point of view there is no difference between the state vector and the density operator formalism. The latter can be seen as providing effective predictions of measurement outcomes for observables $\mathbf{A}$ which act only on a subspace $\mathcal{H} \subseteq \mathcal{H}'$. Based on purification, the Born rule for density operators can be equivalently expressed via the Born rule for state vectors (1.3), when an observable $\mathbf{B}$ acting on $\mathcal{H}'$ is considered with $\mathbf{B} = \mathbf{A} \otimes \mathbb{1}$. The equivalence of predictive rules for density operators and state vectors can then be written as

$$p_j = \text{tr}(\rho|a_j\rangle\langle a_j|) = \langle\Psi|\mathbf{\Pi}_j|\Psi\rangle \tag{1.8}$$

where $\mathbf{\Pi}_j$ is a projector onto the subspace of $\mathcal{H}'$ spanned by $\{|\Phi_k^j\rangle\}$, which in turn is the subset of eigenvectors of $\mathbf{B}$ corresponding to its potentially degenerate eigenvalue b_j with

$|\Phi_k^j\rangle = |a_j\rangle \otimes |\xi_k\rangle$ and some basis $\{|\xi_j\rangle\}$ of $\mathcal{H}_{\text{aux}}$. The probability to observe outcome a_k given ρ can thus always be related to observing outcome b_k given $|\Psi\rangle$. In consequence, the expectation value of an observable $\mathbf{A}$ for a mixed state ρ in general can be expressed as $\langle \mathbf{A} \rangle = \text{tr}(\rho \mathbf{A})$ and similarly the variance as $\text{Var}(\mathbf{A}) = \text{tr}\big(\rho(\mathbf{A} - \langle \mathbf{A} \rangle)^2\big)$.

1.3.2 Coherence and Decoherence

A crucial difference between pure and mixed states can be illustrated by expanding the expectation values $\langle \mathbf{A} \rangle$ for a pure state $|\psi\rangle$ and a mixed state ρ in terms of a basis $\{\phi_k\}$ which is not the eigenbasis of $\mathbf{A}$ as

$$\langle \psi | \mathbf{A} | \psi \rangle = \sum_{j,k} a_j |c_k|^2 |\langle \phi_k | a_j \rangle|^2 + \sum_{j,k \neq l} a_j c_k c_l^* \langle a_j | \phi_l \rangle \langle \phi_k | a_j \rangle, \tag{1.9}$$

$$\text{tr}(\rho \mathbf{A}) = \sum_{j,k} a_j \rho_{kk} |\langle \phi_k | a_j \rangle|^2 + \sum_{j,k \neq l} a_j \rho_{kl} \langle a_j | \phi_l \rangle \langle \phi_k | a_j \rangle, \tag{1.10}$$

where c_k are the coefficients of $|\psi\rangle$ and ρ_{kl} the matrix elements of ρ with $\rho_{kl}^* = \rho_{lk}$ due to hermiticity. The first sum in both expressions, corresponding to the diagonal elements of ρ, represents a weighting of the eigenvalues with real-valued non-negative weights $|c_k|^2$ and ρ_{kk}, respectively. The value of the second sum, corresponding to off-diagonal elements of ρ is, however, crucially dependent on the complex phases and signs of the coefficients c_k and ρ_{kl}. As already mentioned this addition of products of complex amplitudes and not only real-valued probabilities is the signature of interference.

Since the density operator has significantly more parameters than the state vector, i.e., for states in a d-dimensional Hilbert space, the state vector has $2(d-1)$ free parameters and the density operator $d^2 - 1$, it is possible that the first sums are equal with $\rho_{kk} = |c_k|^2$, while the interference is suppressed for a mixed state with the extreme case of $\rho_{kl} = 0 \; \forall k, l$. In contrast, for a pure state it always holds that $|\rho_{kl}| = \sqrt{\rho_{kk}\rho_{ll}} \; \forall k, l$. This phenomenon of disappearance of interference is called *decoherence*, again generalizing the vocabulary of classical optics to quantum systems [529, 1011, 95, 70, 128, 327]. Decoherence is a gradual property which can be quantified by considering how much the modulus of the off-diagonal elements is decreased and several measures of decoherence have been proposed [128, 204]. Note that, in contrast to other properties, such as purity, coherence and decoherence are fundamentally basis-dependent properties.

Decoherence is sometimes also brought into relation with random phase fluctuations in an ensemble of systems [589, 529, 528, 225, 327]. If for example an expectation value of the form (1.9) is considered for an ensemble of systems in pure states, where between measurements on successive systems there is a uniformly distributed random rotation of phases between the coefficients c_k, the interference terms are canceled on average. This principle represents an important ingredient in the semi-classical modeling of certain states of light via mixed states as introduced in Sec. 4.3.5. Apart from that decoherence also plays an important role in the analysis of the quantum mechanical measurement problem as discussed in Sec. 2.5.1.

1.3.3 Proper and Improper Mixtures

In contrast to the statistical dispositional nature, the descriptive role of density operators is a more contested issue. As shown in Sec. 1.3.1 an expression in terms of a state vector is always possible for any state expressed even by a mixed density operator via purification. Thus, density operators can be viewed as describing subsystems, i.e., parts of larger systems which themselves are described by pure states. If the state vector is taken to have a descriptive function, or even an ontological interpretation, then the corresponding density operators of the subsystems gain their descriptive meaning exactly via their relation to the state vector. They constitute reduced partial descriptions of a subset of features of a greater system.

Following d'Espagnat [919, 920], such *improper* mixtures can be distinguished from *proper* ones, see also [953]. Proper mixtures are understood as describing ensembles of physical systems in explicitly different states $|\psi_j\rangle$, where the probabilities p_j are given by the corresponding relative frequencies. In this view the operator ρ can encapsulate subjective probabilities, expressing the ignorance about which type of system is currently at hand, in which case, after a measurement of a sub-ensemble the operator describing the remaining part of the ensemble might become updated. Alternatively, a proper mixture would also be realized if ρ would characterize a system about to be generated by a probabilistic source with propensities $p(j)$ to produce the state $|\psi_j\rangle$.

The existence of proper mixtures and even the distinction itself is subject of debate, see e.g., [957, 978, 993, 979, 996, 975]. In general, assuming that a universal wavefunction exhaustively describes the state of the physical universe, indeed there cannot be any proper mixtures and any statistical uncertainty of that type will always be the result of considering certain subsystems. On the other hand, if some phenomena are irreducibly described as classical or a least beyond the domain of quantum mechanics, then the ontological distinction between proper and improper mixtures seems clear and meaningful.

1.4 Evolution

1.4.1 Schrödinger Equation

The time evolution of classical systems in its totality is given by the collective changes of the system parameters, i.e., its phase-space trajectory. Dynamical laws are usually formulated as differential equations which express the change of one parameter as a function of the current value of all other parameters [932]. In contrast, in quantum theory evolution is expressed in terms of changes of the state vector or the density operator in the so-called *Schrödinger picture*, or alterntively in terms of changes of observables in the *Heisenberg picture*.

In the Schrödinger picture the most general transformation of a state vector $|\psi\rangle$ can be expressed via the action of a unitary operator $\mathbf{U}$ on the state [56]. The unitarity assures that the unit length of the vector is conserved and the probabilistic Born rule can be applied consistently. As in classical physics the evolution law is given in terms of a

differential equation, specifically the first-order *Schrödinger equation* [57, 50, 117, 86, 63, 56]

$$i\hbar\frac{\mathrm{d}}{\mathrm{d}t}\left|\psi\right\rangle = \mathbf{H}\left|\psi\right\rangle, \tag{1.11}$$

where $\mathbf{H}$ is the Hermitian *Hamilton* operator or *Hamiltionian*, an operator associated with the total energy of the system. This choice of dimension allows to recover the structure of the Hamilton formulation of classical mechanics, where the Hamiltonian corresponds to the energy of the system as a function of generalized positions and momenta. The Hamilton operator $\mathbf{H}$ of quantum mechanics can often be obtained through the correspondence principle by applying appropriate quantization rules to the classical Hamilton function, see e.g., [50].

For time-independent Hamiltonians, i.e., *conservative systems*, the Schrödinger equation is solved by the unitary evolution $\mathbf{U} = e^{-i/\hbar\mathbf{H}t}$ and for time-dependent Hamiltonians which commute with themselves at different times the unitary becomes [50, 82, 57]

$$\mathbf{U} = e^{-\frac{i}{\hbar}\int_{t_0}^{t}\mathbf{H}\mathrm{d}t} \tag{1.12}$$

For a general Hamiltonian the unitary is given via a *Dyson series*, see [57, 50]. In any case the unitarity of $\mathbf{U}$ is assured due to hermiticity of $\mathbf{H}$.

An essential feature of quantum evolution is its continuity which can be expressed when considering spatial wavefunctions and densities. According to the Born rule for a single particle with a spatial wavefunction $\psi(\vec{x},t) := \langle\vec{x}|\psi\rangle$ the spatial probability density p can be defined as $p(\vec{x},t) := \varrho^2(\vec{x},t)$, where ϱ is the modulus of the wavefunction according to its polar decomposition as $\psi = \varrho e^{i\varphi}$. As first suggested by Madelung [31], this allows to formulate a quantum *continuity equation* or *quantum flux equation* of the form [54, 50, 910, 819]

$$\frac{\partial}{\partial t}p(\vec{x},t) + \vec{\nabla}\vec{j}(\vec{x},t) = 0, \tag{1.13}$$

where $\vec{j}$ is the *probability current* defined as

$$\vec{j}(\vec{x},t) := \frac{1}{m}\mathrm{Re}\big[\psi^*(\vec{x},t)(-i\hbar\vec{\nabla})\psi(\vec{x},t)\big] = \frac{1}{m}\mathrm{Re}\big[\langle\psi|\vec{x}\rangle\langle\vec{x}|\vec{\mathbf{p}}|\psi\rangle\big] \tag{1.14}$$

for massive non-relativistic particles, with momentum operator $\vec{\mathbf{p}}$. The continuity equation forms the basis of pilot-wave interpretations, such as Bohmian Mechanics introduced in Sec. 7.1 and can also be generalized to relativistic massless particles, e.g., photons as discussed in Sec. 4.7.

1.4.2 Relativistic Quantum Mechanics

Sometimes the term "Schrödinger equation" is employed in a narrower sense to denote the original formulation as introduced by Schrödinger [40] for massive particle with a fixed mass

m and a kinetic energy operator $\vec{\nabla}^2/2m$ in the coordinate representation, see e.g. [520, 64, 819]. As this equation is manifestly non-relativistic the question arises whether quantum mechanics is a fundamentally non-relativistic theory [72, 952]. Indeed, while Schrödinger himself was unsuccessful in formulating a relativistic equation [72], there exist relativistic wave-equations for quantum particles which exactly correspond to the form of (1.11), such as the *Dirac equation* introduced by Dirac [14] in order to improve the quantum description of the hydrogen atom. It can be expressed as [58, 635, 71]

$$i\hbar\frac{\partial}{\partial t}\check{\Psi}(\upsilon) = \left(c^2 m\boldsymbol{\beta} + c(\vec{\boldsymbol{\alpha}}\cdot\vec{\mathbf{p}})\right)\check{\Psi}(\upsilon) \tag{1.15}$$

and describes the spatial and spin degrees of freedom of an electron in terms of the four component *spinor* $\check{\Psi}(\upsilon)$, which depends on the four component spacetime coordinate vector υ as introduced in Sec. 3.1. Furthermore, m is the electron rest mass, $\vec{\boldsymbol{\alpha}}$ a three component vector of operators $(\boldsymbol{\alpha}_x, \boldsymbol{\alpha}_y, \boldsymbol{\alpha}_z)$, and the dimensionless operators $\boldsymbol{\alpha}_j$ and $\boldsymbol{\beta}$ themselves are expressed as 4 by 4 matrices. Note that in contemporary formulations of the Dirac equation the operators and derivatives are conveniently expressed in terms of the four so-called *gamma matrices* γ_j, see e.g., [520, 71]. The four spinorial components of $\check{\Psi}$ correspond to two spin-eigenstates for particle and anti-particle solutions of the Dirac equation, respectively, such that the Dirac equation actually corresponds to a system of four coupled equations. Alternatively, it can be seen as the Schrödinger equation with a Hamiltonian $\mathbf{H}$ which has the matrix representation $\mathbf{H} = c^2 m\boldsymbol{\beta} + c(\vec{\boldsymbol{\alpha}}\cdot\vec{\mathbf{p}})$. In fact, at the time the equation was proposed by Dirac the meaning of the two negative-energy solutions to the equation was unclear and only later, after the experimental discovery of the positron by Anderson [5], were they identified with the anti-particle solution of the electron [520, 72, 71]. In consequence, in this work the Schrödinger equation is understood in the sense of Eq. (1.11) as the most general form of quantum mechanical wave-equations which can also be compatible with special relativity. The description of quantum systems in such terms is sometimes called *quantum wave mechanics* [64] to distinguish it from the other main formal approach to quantum mechanics, namely quantum field theory as introduced in Sec. 4.3.1.

1.4.3 Evolution of the Density Operator

Quantum mechanical evolution can also be expressed in terms of the density operator. In analogy to the Schrödinger equation differential equations can be formulated called *quantum master equations*, which generalize the classical formalism of master equations [50, 49, 98]. The simplest master equation for a unitary evolution governed by a Hamiltonian is the *von Neumann equation* $i\hbar\frac{\mathrm{d}}{\mathrm{d}t}\rho = [\mathbf{H}, \rho]$. As in many scenarios a treatment of the evolution of the full system is practically impossible, it is common to just consider the effective reduced evolution of a particular subsystem, i.e., an open system. This leads to more general forms of master equations as presented in Sec. 1.8.2. In general a state ρ is time-invariant if and only if it commutes with the Hamiltonian, in which case it is also called *stationary* [589, 57, 50]. Note, however, that each eigenstate of the Hamiltonian,

which is also stationary, experiences an oscillation of its global phase with a frequency $\omega = E/\hbar$, where E is the corresponding energy eigenvalue. This oscillation, however, is not present in the density operator formulation which is per definition independent of relative phases between its eigenstates.

Alternatively to a continuous formulation in terms of differential equations, the evolution of quantum systems is also often described via discrete transformations, so-called *dynamical maps* $\Lambda_{t_1}^{t_2}$, with $\Lambda_{t_1}^{t_2}[\rho(t_1)] = \rho(t_2)$ [49, 117, 56]. Such maps which act on operators are sometimes called *superoperators* [225] and written here with arguments in square brackets. Note that in general applying a certain map $\Lambda_{t_1}^{t_2}$ to an arbitrary quantum state or even to $\rho(t_3)$ at a different time t_3 will not yield a valid quantum state. In contrast, *completely positive* and *trace preserving* (CPTP) maps represent valid transformations for arbitrary quantum states and are thus also called *universal dynamical maps* [56]. Just as the unitarity in the case of state vectors the complete positivity and trace preservation assure that the resulting state is again a proper positive semidefinite density operator with unit trace allowing for a consistent application of the Born rule. The attribute "complete" indicates that if ρ is the state of a subsystem of a larger system, the state of the total system also remains positive semi-definite after the transformation.

A CPTP map $\mathcal{C}$ can always be written in the *operator-sum* representation [182, 174, 194, 195, 117, 56, 225] as

$$\mathcal{C}[\rho] = \sum_j \mathbf{K}_j \rho \mathbf{K}_j^\dagger, \tag{1.16}$$

where the *evolution operators* $\mathbf{K}_j$ satisfy the normalization condition $\sum_j \mathbf{K}_j^\dagger \mathbf{K}_j = \mathbb{1}$. Potentially trace reducing CP maps $\mathcal{T}$ also called *operations* can be expressed accordingly if the normalization condition is not enforced [95, 225]. This representation is also sometimes denoted as the *Kraus representation* after Kraus [115] with *Kraus operators* $\mathbf{K}$, see e.g., [212, 194, 195].

As shown by Lindblad [185], based on *Sinespring's dilation theorem* [203], it is possible to express an arbitrary master equation or CPTP map acting on a density operator as the action of a unitary operator on a pure state in a higher dimensional space in analogy to the purification of mixed states [174, 194, 195, 117, 95, 225]. Considering again the auxiliary Hilbert space $\mathcal{H}_{\text{aux}}$ and the purification $|\Psi\rangle$ with $\rho = \text{tr}_{\text{aux}}(|\Psi\rangle\langle\Psi|)$ as well as a suitable unitary $\mathbf{U}$ acting on $\mathcal{H} \otimes \mathcal{H}_{\text{aux}}$, any CPTP map $\mathcal{C}$ can be represented as

$$\mathcal{C}[\rho] = \text{tr}_{\text{aux}}\left(\mathbf{U}|\Psi\rangle\langle\Psi|\mathbf{U}^\dagger\right). \tag{1.17}$$

For trace reducing CP maps $\mathcal{T}$, a similar representation is also always possible, in which case, however, an additional projection onto a subspace of $\mathcal{H}_{\text{aux}}$ is required [312, 225].

1.4.4 Heisenberg Picture

As mentioned above the Heisenberg picture provides an alternative formulation of evolution in quantum mechanics, where the state vectors or density operators are fixed in time and

instead the observables are taken to evolve. The evolution of an observable is governed by the so-called *Heisenberg equation of motion*. For conservative systems and not explicitly time-dependent observables $\mathbf{X}$ this equation simplifies to $i\hbar\frac{\mathrm{d}}{\mathrm{d}t}\mathbf{X} = [\mathbf{X}, \mathbf{H}]$ [50, 57, 86], which, up to a sign flip, is similar to the von Neumann equation for the density operator, defined above in Sec. 1.4.3.

For a given Hamiltonian the Heisenberg picture leads to exactly the same unitary evolution operators as the Schrödinger picture. In consequence it provides the same predictions since the probability calculated via the Born rule stays the same no matter if the $\mathbf{U}$ is applied to the state or to the respective eigenspace of the observable. However, while both pictures are dispositionally equivalent they seem to imply vastly different and fundamentally incompatible descriptions of quantum systems. In one of them the quantum state expresses the time-evolving properties of the system, in the other it is at most a static description of some time-invariant properties. Most approaches to debates about interpretations of quantum mechanics consider the quantum state as the fundamental object as well as the prime candidate for a quantum ontology and are formulated exclusively in the Schrödinger picture. In particular, this holds for the two frameworks which are treated in this work, i.e., the Two State Vector Formalism and Bohmian Mechanics. Also Quantum Information Theory as introduced in Sec. 1.6 is typically formulated in terms of quantum states and their transformations. While, in contrast, the Heisenberg picture is chiefly employed in quantum field theory, there are also recent proposals to gain foundational insights from its application, see e.g. [682, 688, 689].

1.5 Interaction

1.5.1 Interaction Picture

When considering systems which can be conceptually separated into two or more subsystems a general total unitary evolution induces an *interaction* between those. For two systems $\mathcal{H}_1$ and $\mathcal{H}_2$ an interaction occurs whenever the unitary evolution operator acting on the joint space $\mathcal{H}_1 \otimes \mathcal{H}_2$ cannot be written in a product form as $U = U_1 \otimes U_2$, with subsystem unitaries U_1 and U_2 acting only on the respective subsystems [56].

Any two-system Hamiltonian can be decomposed as

$$\mathbf{H} = \mathbf{H}_F + \mathbf{H}_I \quad \text{with } \mathbf{H}_F = \mathbf{H}_1 \otimes \mathbb{1} + \mathbb{1} \otimes \mathbf{H}_2 \tag{1.18}$$

where $\mathbf{H}_1$ and $\mathbf{H}_2$ act on $\mathcal{H}_1$ and $\mathcal{H}_2$ respectively and are the so-called *free Hamiltonians* describing the individual evolution of the subsystems, while $\mathbf{H}_I$ is the *interaction Hamiltonian* encapsulating the interaction between them. Additionally, if $\mathbf{H}_F$ is time-independent the whole time-dependence is contained in the interaction Hamiltonian $\mathbf{H}_I$. The advantage of decomposition (1.18) is then that the total evolution $\mathbf{U}$ can be decomposed as $\mathbf{U} = \mathbf{U}_F\mathbf{U}_\mathrm{I}$, where simply $\mathbf{U}_F = e^{-i/\hbar\mathbf{H}_F t}$ and $\mathbf{U}_\mathrm{I}$ in general depends both on $\mathbf{H}_F$ and $\mathbf{H}_I$. If now all observables are transformed with $\mathbf{U}_F$ according to the Heisenberg picture, the total evolution of the states can be described according to the Schrödinger picture with

the Hamiltonian $\widetilde{\mathbf{H}}_I = \mathbf{U}_F^\dagger \mathbf{H}_I \mathbf{U}_F$, which is similar to $\mathbf{H}_I$ up to a unitary rotation. This so-called *interaction picture* [57, 49, 56] is employed for example in perturbative approaches where the solution of $\mathbf{H}_F$ is known and a small perturbation $\mathbf{H}_I$ is added. A further simplification occurs when $\mathbf{H}_F$ and $\mathbf{H}_I$ commute, in which case $\widetilde{\mathbf{H}}_I = \mathbf{H}_I$, i.e., the evolution of the states becomes completely independent of $\mathbf{H}_F$. If the interest of the description is focused on the interaction, it thus becomes possible to ignore the free evolution altogether and just consider suitably rotated observables [98]. In general the decomposition (1.18) is not unique and there is some freedom as to which parts of $\mathbf{H}$ are included in $\mathbf{H}_F$.

A typical scenario when considering interactions is that of two quantum systems which are in a product state $\rho = \rho_1 \otimes \rho_2$ prior to the interaction. The product state indicates that the systems are describable independently and the probability distributions or densities over the values of all possibles single system observables are uncorrelated, see also Sec.1.6.4. Due to the Hamiltonian $\mathbf{H}$ the joint state ρ is changed, which for each of the subsystems corresponds to a CPTP map Λ_j given by $\Lambda_j[\rho_j] = \mathrm{tr}_{\bar{j}}(\mathbf{U}_I \rho \mathbf{U}_I^\dagger)$, where $\bar{j}$ indicates the other index from the set $\{1, 2\}$, respectively. Λ_j is universal, i.e., a CPTP map for an arbitrary state ρ, if and only if the corresponding $\mathbf{U}$ is acting on a product state [95, 56]. This implies that even if the systems start in a product state, subsequent steps of the subsystem evolution will in general not correspond to CPTP maps.

1.5.2 Weak Interactions and Weak Traces

A special case of such state transformations due to interactions are so-called *weak interactions* or *weak coupling* [675, 680, 681, 225, 711, 741]. In this context typically the simplest finite-time interaction Hamiltonian is considered which has the form

$$\mathbf{H}_\mathrm{I} = g(t)\mathbf{A} \otimes \mathbf{X}, \tag{1.19}$$

where the Hermitian operators $\mathbf{A}$ and $\mathbf{X}$ act on the respective parts of the joint Hilbert space and the *coupling strength* $g(t)$ is a real valued parameter with proper dimension. The resulting unitary has the form

$$\mathbf{U} = e^{-i\varepsilon \mathbf{A}\otimes\mathbf{X}/\hbar}, \quad \text{with } \varepsilon := \int_\tau g(t)\mathrm{d}t, \tag{1.20}$$

where the *interaction strength* ε depends both on the duration of the interaction τ as well as the coupling strength g. Such an interaction is called *weak* if ε is sufficiently small such that higher order terms in ε can be neglected and the evolution can be approximated perturbatively for example to first order as $\mathbf{U} \approx 1 - i\varepsilon \mathbf{A} \otimes \mathbf{X}/\hbar$ [225, 276, 711, 741]. While such perturbative treatments of weak interactions are widely employed in the literature, in general the validity of this approximation is a non-trivial question. Thus in this work, instead of assuming a small interaction strength, the formal definition of weakness is always given by the limit $\varepsilon \to 0$, which allows to consider only the first non-vanishing order of ε. Of course this limit is a mathematical abstraction and is never realized exactly in any physical interaction. However, for a certain range of finite but sufficiently small values of ε called

the *weak regime* [711, 741, 712] typical physical scenarios are approximated extremely well. See e.g. [675, 714, 680, 673, 759, 695] for discussions of possible quantitative definitions of the weak regime and the validity of the perturbative approach in general. For general interaction Hamiltonians, which can be represented as

$$\mathbf{H}_I = \sum_j g_j(t)\mathbf{A}_j \otimes \mathbf{X}_j, \tag{1.21}$$

weakness can be defined similarly by requiring that all resulting interaction strength parameters ε_j given as in Eq. (1.20) in terms of integrated coupling strengths g_j are sufficiently small. This is the case for example in the limit $\tau \to 0$.

A consequence of weak coupling is that systems initially in a product state remain in a product state even after the interaction [225, 711, 98]. This approximation of the effect of weak interactions is a common ingredient in microscopic derivations of Markovian evolution in open system dynamics as discussed in Sec. 1.8.2. Furthermore, if one of the systems is initially in a pure state, e.g., $\rho = \rho_1 \otimes |\psi\rangle\langle\psi|$, the transformation induced by a first-order weak interaction can in general be approximated as a transformation to the pure state $|\psi'\rangle$ with

$$|\psi'\rangle \approx e^{i\langle\mathbf{Y}\rangle}\left(|\psi\rangle + \Delta\mathbf{Y}\,|\psi^\perp\rangle\right), \tag{1.22}$$

where $|\psi_\perp\rangle$ is a state orthogonal to $|\psi\rangle$, $\mathbf{Y} := \sum_j \varepsilon_j \operatorname{tr}(\rho_1\mathbf{A}_j)\mathbf{X}_j/\hbar$, and the expectation value and standard deviation of $\mathbf{Y}$ are evaluated with respect to $|\psi\rangle$. The orthogonal component has the form $|\psi_\perp\rangle = \exp(i\varphi)\big(\langle\mathbf{Y}\rangle - \mathbf{Y}\big)/\Delta\mathbf{Y}\,|\psi\rangle$ with a suitable phase φ. In the simple case of a product interaction (1.19) the amplitude of the orthogonal component simplifies to $\Delta\mathbf{Y} = \varepsilon\operatorname{tr}(\rho_1\mathbf{A})\Delta\mathbf{X}/\hbar$. Since the weak interaction transforms the initial pure system state into a different pure state it can also be represented as the effective unitary evolution

$$\mathbf{U}_{\text{eff}} \approx e^{i\langle\mathbf{Y}\rangle}\Big(\mathbb{1} - \Delta\mathbf{Y}|\psi\rangle\langle\psi_\perp| + \Delta\mathbf{Y}|\psi_\perp\rangle\langle\psi|\Big), \tag{1.23}$$

where higher orders of $\mathbf{Y}$ can be neglected in the weak regime. The appearance of an orthogonal component $|\psi^\perp\rangle$ with a small amplitude is called a *weak trace* [792, 804],**[P3]** and represents a central element of the weak trace approach to particle presence as discussed in Sec. 6.2. This formal description is easily generalized to a mixed state of the second system, in which case different weak traces appear for every component of the mixture.

1.6 Quantum Information and Communication

1.6.1 Information Theory

Information is an extremely broad concept with varying meanings and applications and is becoming more and more central in many disciplines, see e.g., [120]. In contrast, *information theory* is often taken to refer to a narrower scope of investigation started by the highly

influential mathematical formalization by Shannon [200, 118]. It considers information encoded in *messages* which are strings of symbols drawn from sets of admissible values, so-called *alphabets* [529, 174, 139]. The bit, a two-valued logical state, is introduced as the fundamental unit of information allowing to compare the information content of messages formulated in various alphabets.

A common way to model sources of messages are random variables X with values x, which correspond to the symbols of the alphabet and are distributed according to a probability distribution p. This allows to define the *Shannon entropy* H as $H(X) = -\sum_x p(x) \log p(x)$, where here and in the rest of this work "log" represents the logarithm with base 2 [117, 139]. The Shannon entropy captures the basic intuition that information is fundamentally related to the amount of possible configurations of symbols and acquisition of information to the reduction of this amount, e.g., via a better estimation of the value of parameters such as X [113, 529, 139]. Classical information theory then applies and refines statistical tools to tackle questions such as possible compression of information or correction of errors introduced by noisy transmission channels [117]. Note that the type of information considered here, i.e., information that can be encoded in abstract form, is sometimes referred to as *speakable* information and distinguished from *unspeakable* information which cannot [126]. An example of the latter are reference frames which define particular directions in space.

The field of *quantum information theory* (QIT) as pioneered in a seminal work by Schumacher [198] is nicely framed by Nielsen and Chuang as an approach to "treat quantum states *as if they were information*, and ask information-theoretic questions about those quantum states" [117]. QIT thus represents a tool to quantify the usefulness of quantum mechanical systems and their states for information theoretic tasks and is independent of any interpretation of quantum theory. It should be distinguished from certain interpretations which postulate that information is in itself a novel physical entity and quantum mechanics is the science of its properties with the quantum state being understood as a representation of subjective knowledge, see e.g., [970, 971, 969]. Nevertheless such interpretations can of course employ the techniques provided by QIT.

The basic mathematical tool of QIT is the quantum equivalent of the Shannon entropy, namely the *von Neumann entropy* S, which is defined as a function of the density operator ρ with [117, 194, 139]

$$S(\rho) = -\mathrm{tr}\left(\rho \log \rho\right). \tag{1.24}$$

The von Neumann entropy is equivalent to the Shannon entropy of the probability coefficients of any decomposition of ρ in an eigenbasis, i.e., the entropy of the set of eigenvalues of ρ. Thus, any pure state has zero entropy and the entropy reaches its maximum value of $\log d$ for the maximally mixed state $\mathbb{1}/d$.

Typically, QIT distinguishes two types of information. On the one hand it still considers classical information which is encoded in classical systems and behaves according to the rules of classical information theory. Additionally, however, quantum systems encode *quantum information*, which has a different character and crucially cannot be converted

without losses into classical information due to the probabilistic nature of quantum measurements [174]. In analogy to the classical bit, a quantum system with a two dimensional Hilbert space is taken to be the basic unit of quantum information and is denoted a *quantum bit* or *qubit*, as first introduced by Schumacher [198]. Accordingly, also with respect to *communication*, i.e., the transmission of information, classical channels which transmit classical information are distinguished from *quantum channels* which allow to transfer an arbitrary and unknown quantum state [162, 484]. Note that this can either happen directly via the physical propagation of a quantum system encoding the information, or also via other schemes such as quantum teleportation, as introduced in Sec. 3.3.3 Formally, deterministic quantum channels correspond to CPTP maps $\mathcal{C}$ and probabilistic channels to trace reducing CP maps $\mathcal{T}$ [95]. The conversion from classical to quantum information is given by parameter-dependent state preparation and the other direction via measurements which probabilistically extract the values of a classical parameter from a quantum state [174]. As a consequence in the context of QIT at least some mixed states are expressed in the form of proper mixtures, in particular in all cases where classical randomness affects the generation or transformation of quantum states. However, this does not necessarily imply any particular stance about the fundamental nature of mixed states. After all, the inclusion of classical randomness in QIT can be interpreted as a mere formal convenience, which refrains from explicitly expressing the origin of an only apparent randomness from a partial description of a unitarily evolving composite system, as discussed in Sec. 1.3.3.

1.6.2 Accessibility and Distinguishability

One classical approach to quantify information is to consider how well different symbols can be distinguished if only one of them is observed. The better the symbols can be distinguished the more *accessible* the information encoded in them. In this case the probability distribution over symbols $p(x)$ corresponds to the a priori knowledge about the symbol at hand, also called the *prior*. Typically, the information available about a random variable X is expressed in terms of its correlations with another random variable Y as encoded in the joint probability distribution $p(x, y)$ [162]. For example the values of Y can be thought of as being generated from X via a noisy classical channel [139]. A very useful quantity to capture the amount of information shared between the two variables is the *conditional entropy* $H(X|Y)$ defined as [117, 139]

$$H(X|Y) := -\sum_{x,y} p(x, y) \log \frac{p(x, y)}{p(y)}. \tag{1.25}$$

It captures the average uncertainty of X when conditioned on values of Y [139]. Consequently the difference between the unconditional and conditional entropy quantifies the information gain for the variable X from knowing Y. This difference is the so-called *mutual information* given by [117, 139]

$$I(X : Y) := H(X) - H(X|Y). \tag{1.26}$$

The maximal mutual information is $H(X)$, which corresponds to $H(X|Y) = 0$, i.e., full information in Y about X. In the classical case this maximum can always be attained by an optimal information extraction strategy or a lossless channel [117].

In the case of quantum information with quantum systems as carriers of information the information is encoded via an alphabet of different quantum states ρ_x distributed according to $p(x)$ which gives rise to the effective state $\rho = \sum_x p(x)\rho_x$ [117, 225]. The outcomes of any possible observations on ρ again can be expressed via a random variable Y. Then it is possible to provide an encoding-dependent limit on the maximally accessible information via the famous *Holevo bound* [169]

$$I(X:Y) \leq S(\rho) - \sum_x p(x)S(\rho_x), \tag{1.27}$$

see also [117, 194, 139]. Crucially, for certain some sub-optimal encoding strategies the Holevo bound can drop below $H(X)$, indicating that there exists no extraction strategy which can recover the full information about X. The bound is tight if and only if all ρ_x commute [194] in which case the bound exactly specifies the maximally attainable mutual information. The encoding is optimal if and only if the ρ_x are mutually orthogonal, which allows for extraction of the full information with an optimal strategy [117]. The fact that in some cases quantum information is at least partially inaccessible in the sense above is also related to the *no-cloning theorem* [151, 216, 125], which states that there cannot be a single process which reliably can copy different non-orthogonal quantum states [117, 196, 139, 84]. Another consequence of the Holevo bound is also that although the pure state of a qubit is described by a continuous parameter and thus in principle can store an infinite amount of information, still n qubits allow to transfer only n classical bits of information [117, 139, 111].

A special instance of the distinguishability problem is the two state discrimination problem, where based on a single optimal observation the decision has to be made whether state ρ_1 or ρ_2 is at hand. In this case it is useful to consider the weighted difference between the two states given by *Helstrom matrix* $\mathbf{\Delta}$ with $\mathbf{\Delta} = q\rho_1 - (1-q)\rho_2$, where q quantifies the prior. The average probability of an erroneous conclusion p_{err} for an optimal discrimination is then shown to be $p_{\text{err}} = (1 - ||\mathbf{\Delta}||)/2$, [95, 104], where $||\cdot||$ denotes the trace norm of an operator with $||\mathbf{A}|| = \text{tr}\big(|\mathbf{A}|\big)$ and the modulus of an operator is given as $|\mathbf{A}| = \sqrt{\mathbf{A}^\dagger\mathbf{A}}$. For an unbiased scenario with $q = 1/2$ the error probability can be expressed via the *trace distance* $\mathcal{D}_T(\rho_1, \rho_2) = \text{tr}(|\rho_1 - \rho_2|)/2$, which is a common distance measure for quantum states [117, 157, 111]. It reaches its maximal value of 1 if and only if the states are orthogonal.

The second important type of distance measures between quantum states is based on the *fidelity* F defined as [117]

$$F(\rho_1, \rho_2) := \text{tr}\left(\sqrt{\sqrt{\rho_1}\rho_2\sqrt{\rho_1}}\right), \tag{1.28}$$

which for two pure states $|\psi\rangle$ and $|\phi\rangle$ reduces to the simple scalar product $F(|\psi\rangle, |\phi\rangle) = |\langle\psi|\phi\rangle|$. Note that often also an alternative definition is used, where the fidelity is defined

as the square of the above quantity, see, e.g., [157, 139, 111]. According to *Uhlmann's theorem*, the fidelity of two mixed states is equivalent to the maximal fidelity achievable for any possible pair of purifications of the two [117, 139]. Crucially, the maximum is achieved when ρ_1 and ρ_2 are purified via correlation with the *same* subspaces of an extended Hilbert space. The fidelity implies the distance measures $\mathcal{D}_F = 1 - F$ and $\mathcal{D}'_F = \sqrt{1 - F^2}$, which are related to the trace distance via $\mathcal{D}_F \leq \mathcal{D}_T \leq \mathcal{D}'_F$ [117]. All three measures become equivalent for pure states. Finally, the so-called *Bures angle* $\mathcal{D}_B$ defined as $\mathcal{D}_B = \arccos F$ is also a useful distance measure [157].

1.6.3 Channel Coding Theorems

Another basic result of information theory are the so-called *coding theorems*. For example *Shannon's noiseless channel coding theorem* [200] addresses the scenario where messages constructed out of n symbols are encoded in $m = nR$ bits, where R is called the *compression rate* [117, 139]. A compression is called *reliable* if after its reversal the information can be fully recovered. The considered scenario is a source that chooses each subsequent symbol independently from the previous (and future) ones and according to the same distribution $p(x)$. As already pointed out by Shannon [200], such an *independent* and *identically distributed* (IID) source represents a reasonably good approximation for many realistic scenarios of information transmission [117]. The theorem states that for an IID source it is always possible to find a reliable compression with a rate $R > H(X)$ and impossible with $R < H(X)$ [117, 139].

The quantum analog is *Schumacher's quantum noiseless channel coding theorem* [173, 198], see also [117, 139]. As discussed in the preceding section, a source producing messages encoded in quantum information carriers can be associated with a certain quantum state ρ. Additionally, here it is assumed that the symbols are given by pure states $|\psi_x\rangle$, which are not necessarily pairwise orthogonal, such that $\rho = \sum_j p(x)|\psi_x\rangle\langle\psi_x|$. The compression maps a sequence $\bigotimes_n \rho$ from its space $\mathcal{H}^n$ to nR qubits in a *compressed space*. Subsequently, the compressed state is decompressed into an output state $\rho' \in \mathcal{H}^n$. The process is reliable if after decompression the potentially mixed states ρ'_x representing the recovered symbols in the output state, with $\rho' = \sum_x p(x)\rho'_x$, are equal to $|\psi_x\rangle\langle\psi_x|$. In general, however, they are not and the reliability is quantified via the fidelity $F(|\psi_x\rangle, \rho'_x)$ between corresponding symbols, averaged over all of them. In analogy to Shannon's coding theorem, the quantum version now states that whenever $R > S(\rho)$ a reliable compression strategy, i.e., a strategy with $F = 1$ can be found and for $R < S(\rho)$ no such strategy exists [173, 117, 139]. Both the classical as well as the quantum noiseless encoding theorems can be seen as providing operational interpretations for the Shannon and von Neumann entropies, respectively. Furthermore, both theorems are valid only for sufficiently large numbers of symbols when their relative frequencies converge to the probability $p(x)$.

Of course both in the classical as well as in the quantum case the channel coding theorems can be extended to channels with noise. In particular, the field of *quantum error correction* deals with approaches to encode and decode information in quantum systems in a noise resistant way, such that errors such as bit-flips or losses affect the transmitted

information as little as possible. See, e.g., [153, 117, 178, 111, 164, 225, 150] for overviews.

1.6.4 Qubits and Correlations

As qubits represent the basic units of quantum information the description of the properties of interacting systems of several qubits is central to QIT. While the qubit is similar to the classical bit in the sense that it is a two-dimensional system, it can be in any superposition of the two states leading to potential interference effects when undergoing evolution [529]. Commonly, the notation of the so-called *computational basis* $\{|0\rangle, |1\rangle\}$ is used for the standard basis of qubits. In this work also the notation

$$\begin{aligned} |+\rangle &= \frac{1}{\sqrt{2}}(|0\rangle + |1\rangle), \qquad & |\circlearrowleft\rangle &= \frac{1}{\sqrt{2}}(|0\rangle + i\,|1\rangle), \\ |-\rangle &= \frac{1}{\sqrt{2}}(|0\rangle - |1\rangle), \qquad & |\circlearrowright\rangle &= \frac{1}{\sqrt{2}}(|0\rangle - i\,|1\rangle), \end{aligned} \tag{1.29}$$

is used for superpositions of computational basis states. In practice, qubits and their states are realized by a plethora of different physical systems, examples of which are given in the next section. Since qubits are two-dimensional systems, typically only dichotomic measurements are considered, although also measurements with more outcomes can be performed by adding additional randomness via generalized measurements as introduced in Sec. 2.2.2. The prototypical dichotomic qubit measurement is of course given by the Stern-Gerlach experiment.

Arbitrary single qubit states ρ are commonly expressed by expansion in the orthonormal matrix-basis

$$\boldsymbol{\sigma}_0 = \begin{pmatrix} 1 & 0 \\ 0 & 1 \end{pmatrix}, \quad \boldsymbol{\sigma}_x = \begin{pmatrix} 0 & 1 \\ 1 & 0 \end{pmatrix}, \quad \boldsymbol{\sigma}_y = \begin{pmatrix} 0 & -i \\ i & 0 \end{pmatrix}, \quad \boldsymbol{\sigma}_z = \begin{pmatrix} 1 & 0 \\ 0 & -1 \end{pmatrix}, \tag{1.30}$$

which is typically formulated relative to the computational basis with the so-called *Pauli matrices* $\boldsymbol{\sigma}_x$, $\boldsymbol{\sigma}_y$, and $\boldsymbol{\sigma}_z$ [174, 117, 95, 225, 111]. The state of the qubit is then determined by three parameters $T_x, T_y, T_z \in [-1, 1]$ as $\rho = \frac{1}{2}\sum_k T_k \boldsymbol{\sigma}_k$, where the summation goes over the indices $\{0, x, y, z\}$ and $T_0 = 1$ due to the normalization constraint. The parameters can be obtained from the density operator via $T_k = \mathrm{tr}(\boldsymbol{\sigma}_k \rho)$, i.e., they correspond to expectation values $\langle \boldsymbol{\sigma}_k \rangle$ of the Pauli operators. By defining the vector of operators $\vec{\boldsymbol{\sigma}} := (\boldsymbol{\sigma}_x, \boldsymbol{\sigma}_y, \boldsymbol{\sigma}_z)$ the state becomes $\rho = \mathbb{1}/2 + \vec{b} \cdot \vec{\boldsymbol{\sigma}}$, where $\vec{b} := (T_x, T_y, T_z)$ is called the *Bloch vector* of ρ. The state of a single qubit can thus be conveniently visualized in the *Bloch ball*, a generalization of the *Poincaré sphere* describing the state of polarization of classical light, see e.g. [532, 111, 490] for illustrations. Pure states correspond to Bloch vectors of unity length and lie on the spherical shell of the Bloch ball. For qubits the trace distance is equivalent to half the euclidean distance between the Bloch vectors and for pure states the Bures angle corresponds to half of the geometrical angle between those [117, 111].

The decomposition of the density operator into a matrix basis can be generalized to discrete systems of arbitrary dimension by using *Gell-Mann* matrices λ_j [176] or other

matrix bases [132, 123], which all obey a similar algebra as the Pauli matrices. Such higher dimensional systems of dimension d are denoted as *qudits*, where sometimes also special names such as "qutrit" for a three dimensional system are used, see e.g. [117].

For composite systems of n qubits, the description in terms of the Pauli basis can be extended via the *correlation tensor* T, the entries $T_{k_1,k_2,\ldots,k_n}$ of which encode the state via the relation [504, 489, 206]

$$\rho = \frac{1}{2^n} \sum_{k_1,k_2,\ldots,k_n} T_{k_1,k_2,\ldots,k_n} \boldsymbol{\sigma}_{k_1} \otimes \boldsymbol{\sigma}_{k_2} \otimes \ldots \otimes \boldsymbol{\sigma}_{k_n}, \tag{1.31}$$

where each index k_j can take the same four values as for the single qubit. Accordingly the entries of the correlation tensor are given by $T_{k_1,k_2,\ldots,k_n} = \mathrm{tr}\big(\rho\, \boldsymbol{\sigma}_{k_1} \otimes \boldsymbol{\sigma}_{k_2} \otimes \ldots \otimes \boldsymbol{\sigma}_{k_n}\big)$. Correlation tensor elements with indices $k_j \in \{x, y, z\}$ for all j are referred to as *full correlations* and the remaining elements correspond to *marginal correlations*.

The product operators in expression (1.31) can be written as a product of commuting operators, e.g., $\boldsymbol{\sigma}_{k_1} \otimes \boldsymbol{\sigma}_{k_2} = \boldsymbol{\sigma}_{k_1} \otimes \mathbb{1} \cdot \mathbb{1} \otimes \boldsymbol{\sigma}_{k_2}$ in the case of a two-qubit state. This means that these operators can be simultaneously diagonalized and thus the values of the correlation tensor can be expressed as classical expectation values of products of random variables $\langle X_1 X_2 \ldots X_n \rangle$, where X_k represents the measurement outcomes for the k-th qubit, explaining the name of T. The extrema ± 1 of the correlation tensor elements are called *maximal correlation* and *maximal anti-correlation*, respectively. Note that the above usage of the term "correlation" is slightly different from the typical statistical notion, which identifies a lack of correlation with statistical independence by considering products of random variables which are centered and normalized, i.e., shifted and rescaled such that $\langle X \rangle = 0$ and $\Delta X = 1$, see, e.g., [119]. For such variables a non-vanishing correlation is equivalent to the impossibility to express the state as a product [174]. In contrast, according to the terminology employed here, even product states can exhibit non-vanishing correlations with respect to some observables.

While the correlations themselves are defined classically, multi-qubit states and quantum states in general can possess non-classical correlations in the sense that the amount of correlations is larger than possible for any classical states, as discussed in Sec. 3.3.1. In contrast, also for arbitrary non-commuting observables $\mathbf{A}$ and $\mathbf{B}$, it is possible to generalize the classical concept of correlations via the expectation value of their product $\langle \mathbf{AB} \rangle$, which has no classical analogue. This different notion of "correlation" is relevant for example in the case of field correlations in quantum optics as introduced in Sec. 4.6. Quantum correlations can also be expressed in a symmetrized manner with the centered *quantum covariance* C_{AB} defined in terms of the anti-commutator as [487, 130, 741, 567]

$$C_{AB} := \frac{1}{2} \langle \{ \mathbf{A} - \langle \mathbf{A} \rangle, \mathbf{B} - \langle \mathbf{B} \rangle \} \rangle = \frac{1}{2} \langle \{ \mathbf{A}, \mathbf{B} \} \rangle - \langle \mathbf{A} \rangle \langle \mathbf{B} \rangle. \tag{1.32}$$

1.7 Applications of Quantum Information

1.7.1 Quantum Estimation Theory

While the basic results of QIT presented in the previous section are based on the limit of messages with infinitely many symbols, in practice, quantum resources are limited and it is of great interest to understand the effects of a finite number of information carriers on which observations can be carried out. This problem is addressed by *Quantum Estimation Theory* (QET) which describes and analyzes approaches to gain information about the parameters describing the state of a quantum mechanical systems under investigation [113, 188]. In the most general sense this also includes the fields of quantum tomography and entanglement detection, as introduced in Secs. 2.4.1 and 3.3.4, respectively.

In general in estimation theory an *estimator* corresponds to a number $\mathfrak{A}$ which represents a guess about the unknown value of a physical parameter A. An estimator is called *unbiased* if its value converges to A for a repetition of the estimation process, i.e., if its expectation value $\mathbb{E}[\mathfrak{A}]$ is A. Otherwise $b(\mathfrak{A}) := \mathbb{E}[\mathfrak{A}] - A$ quantifies the *bias* of the estimator [113, 225]. For example, if the estimation task is to determine the expectation value of an observable $\mathbf{A}$ by repeatedly measuring it on n copies of a quantum state ρ and averaging the results, the probabilistic nature of observations on quantum systems, as introduced in Sec. 1.2.3, will lead to fluctuations of the measured value $\mathfrak{A}$ around $\langle \mathbf{A} \rangle$, with $\mathbb{E}[\mathfrak{A}] = \langle \mathbf{A} \rangle$. In particular, it can be shown that the statistical uncertainty $\Delta\mathfrak{A}$ of the estimation scales as $\Delta\mathfrak{A} = \Delta\mathbf{A}/\sqrt{n}$ [211]. This scaling of uncertainty is the hallmark of the repetition of an independent statistical process. It also appears for the *Poisson distribution* $p(m) = e^{-\mu}\mu^m/m!$, which describes the probability to observe m instances of an event in a certain time-interval, where $\mu = \mathbb{E}[m]$ is the average amount of occurrences for that interval, see, e.g., [529]. It crucially relies on the IID assumption that in each infinitesimal time-step there is a constant probability for the event to occur, which is completely independent from the number of past occurrences. For Poisson distributed events the variance is equal to the mean, i.e., $(\Delta m)^2 = \mu$. Thus, when considering n time-intervals the expected amount scales as $n\mu$, while the uncertainty scales as $\sqrt{n}\mu$. In effect, the uncertainty for an optimal estimator $\mathfrak{m}$ of the average amount μ scales as $\Delta\mathfrak{m} = \mu/\sqrt{n}$. Due to the probabilistic nature of quantum measurement, such independent statistical fluctuations are omnipresent in quantum mechanics, and the typical uncertainty with a scaling of $1/\sqrt{n}$ is known as *shot noise*. The quantity $\Xi := |\mathbb{E}[\mathfrak{A}]|/\Delta\mathfrak{A}$ can be used to quantify the quality of an estimation $\mathfrak{A}$ and here is called *signal-to-noise ratio* (SNR). In the case of shot noise it scales as $\Xi \propto \sqrt{n}$. Note, that commonly "signal-to-noise-ratio" is also defined as Ξ^2, see, e.g., [188].

A central application of QET is so-called *Quantum Metrology* in which the special properties of quantum systems are employed to achieve increased precision in the estimation of physical parameters [160, 159, 205, 192]. The primary metrological scenario is the estimation of a single parameter ε of a system of interest via an interaction with a set of n auxiliary systems, which are considered as mere tools to gain information about ε. While in this work such an auxiliary system is called *pointer*, commonly also the terms *probe* or

meter are used [225]. The interaction is given by the unitary operator $\mathbf{U} = e^{-\frac{i}{\hbar}\varepsilon\mathbf{H}}$, where $\mathbf{H} = \sum_{k=1}^{n} \mathbf{H}_\mathrm{s}$ and $\mathbf{H}_s$ describes the interaction of the system in question with a single pointer system. In general it can be shown that the uncertainty of any unbiased estimation $\mathfrak{e}$ of a parameter ε obeys the famous *Cramer-Rao bound* [113, 134, 135, 255, 225, 159, 190]

$$\Delta\mathfrak{e} \geq \frac{1}{\sqrt{mF_Q}}, \tag{1.33}$$

where m is the number of independent repetitions of the estimation and F_Q is the so-called *Fisher information*, which is defined based on the conditional probability distribution $p(\mathfrak{e}|\varepsilon)$. It quantifies how well different values of ε can be distinguished with a single estimation process. In the quantum case the Fisher information depends on the Hamiltonian $\mathbf{H}_s$, the measurement performed on the pointers as well as on the joint state ρ of the n pointer systems and of the system of interest. Since for special correlated n-pointer states the Fisher information can approach a scaling with n^2, quantum metrology allows for parameter estimation with a noise scaling of up to $1/n$, which is fundamentally better than the best scaling achievable with classical systems, i.e., $1/\sqrt{n}$ [184, 161, 225, 159, 205, 190]. In the context of quantum metrology the bound of $1/\sqrt{n}$ on the scaling is often called *shot-noise limit* (SNL) or *standard quantum limit* (SQL) and the improved bound of $1/n$ is usually referred to as the *Heisenberg limit*, alluding to the quantum mechanical uncertainty relations, as introduced in Sec. 2.1.3.

1.7.2 Quantum Cryptography

The unique properties of quantum systems also allow for so-called *quantum key distribution* (QKD) which is a method to securely send encryption keys in the adversarial scenario of *cryptography*, where a party A aims to send a message to another party B, while an adversary E attempts to access the message, see e.g., [152, 163, 191, 218]. In QKD the impossibility to distinguish non-orthogonal quantum states with a single measurement is employed to detect any attempt of an adversary to intercept the secret key. For example, in the famous *BB84* protocol as proposed by Bennett and Brassard [129] building on earlier work by Wiesner [214], A encodes the bits of a binary key in one of two randomly chosen bases states of a qubit without broadcasting the basis choice. Only after B has received and measured the quantum information carriers also choosing randomly between the bases, do the two parties share and compare their basis choices. At this point it is too late for the adversary E to utilize this information and any attempt to intercept and measure the state of the carriers will have become evident by a partial mismatch of the measurement outcomes for a subset of encoded bits in all cases where A and B had chosen the same basis by chance. Notable practical realizations of QKD include key distributions over large distances in fibers [210], via satellite communication [143] as well as using easily portable, even handheld devices [208].

1.7.3 Quantum Computation

QIT is less concerned with particular experimental phenomena and more with general properties common to all quantum systems. This culminates in the field of *Quantum Computation* in which, based on an idea by Feynman [154] and pioneering work by Deutsch [148], computational circuits comprised of quantum systems are pursued in analogy to classical computation [149, 124, 529, 147, 117, 174, 116, 121]. A quantum circuit consists of gates, i.e., unitary evolutions applied to single or several qubits. A set of gates is *universal* if it allows to approximate any unitary operation to arbitrary accuracy. Since in practice all devices are imperfect and subject to noise, a crucial ingredient of quantum computation is quantum error correction.

Quantum algorithms such as *Shor's factorization algorithm* [201] and *Grover's search algorithm* [166] have been proven to provide exponential and quadratic speedups over classical algorithms, respectively, and thus in the future quantum computers are expected to allow to tackle practical computational problems which are not solvable with classical computational resources [186, 117, 174, 121]. There exists a wide range of different experimental implementations of qubits and corresponding gates [112, 183], such as superconducting qubits [122], trapped ions [167, 189], neutral atoms [215], or photonic systems [629, 219, 187].

1.7.4 Quantum Simulation

A computationally hard problem is the simulation of quantum systems for which the amount of parameters increases exponentially with the number of systems [117]. In consequence, *quantum simulation*, as famously introduced by Feynman [154] as the first application of Quantum Computation, has emerged as a major field of research [156] in which the dynamical behavior of a system of interest is studied by considering a different, more controllable, more stable, or more easily observable system.

In general there are two approaches of quantum simulation. In *digital quantum simulation* a universal quantum computer is employed to study the evolution of a system of interest. The evolution of the latter is discretized and approximately mapped onto a suitable quantum circuit. This can be done efficiently for a broad range of practically encountered Hamiltonians. Alternatively, in *analog quantum simulation* a system is designed which has a similar Hilbert space structure and Hamiltonian as the system of interest. One advantage of analog simulation is that even in the presence of errors, which render the quantitative details of the simulation unreliable, often qualitative behavior such as phase transitions can be faithfully recovered and studied. A prime example is the simulation of various interacting many-body systems with ultracold quantum gases [165, 197].

1.8 Open Quantum Systems

1.8.1 Effective Evolution of Subsystems

As in classical physics quantum mechanical models are also based on considering certain subsystems of interest. In many cases such systems interact only very weakly with other systems, such that their evolution can be approximated very well by a unitary evolution, as discussed in Sec. 1.5.2. In such cases the system is called a *closed system*. However, a significant portion of experimentally encountered quantum systems of interest cannot be described well in this manner and the interaction with other systems has to be taken into account. Since in many such cases the total composite system possesses a very large number of degrees of freedom, it is often impossible to provide a full quantum description of the evolution, even if the Hamiltonian is known. The common solution is then to provide a reduced description focusing on the effective evolution of the system of interest, called an *open system*, modified by the interaction with the other systems, called the *environment*. While in principle any bipartite system can be regarded as an open system coupling to an environment, commonly very large environments are considered, i.e., systems which can be approximately described as having infinite degrees of freedom. Such environments are denoted as *reservoirs* or, if they are additionally in a thermal equilibrium, as *baths* [49].

As described in Sec. 1.4.3, the effective evolution of a subsystem can be given in terms of a quantum master equation or a dynamical map. Another common approach is to employ a *stochastic Schrödinger equation*, where the evolution is formulated based on a stochastic evolution of the system wavefunction, from which the reduced density matrix can be recovered via averaging of the various stochastic trajectories, see [109, 49, 225] for a detailed description. For certain typical scenarios there exist well-known quantum master equations such as the *quantum optical* master equation [529], describing the interaction between matter and electromagnetic radiation or the *Caldeira-Legett model* [92] which assumes an environment of harmonic oscillators especially suitable for applications in solid state physics.

Notably, also a conceptually different approach to quantum theory has been proposed, called the *open systems view* [977], in which the description in terms of open systems is not merely a practical necessity due to high system complexity, but the evolution of mixed quantum states according to master equations is explicitly regarded as the most fundamental form of quantum evolution. Additionally, the open systems view allows for more general forms of master equations and maps such that resulting evolution may be unphysical from the perspective of SQM. This work, however, follows the standard approach in which the evolution of any open system is always equivalent to a partial description of the unitary evolution of a larger composite system.

1.8.2 Markovian Master Equations

A crucial aspect of open system evolution is the flow of information between open system and environment. It is encapsulated in the concept of *Markovianity*. Classically, Marko-

vianity is defined for stochastic processes described by a vector of random variables $\vec{X}_t$ at different timesteps $t \in \{0, 1, 2, \ldots\}$ [98, 104, 90, 109]. The process is Markovian if and only if

$$p(\vec{X}_{j+1}|\vec{X}_j, \vec{X}_{j-1}, \ldots, \vec{X}_0) = p(\vec{X}_{j+1}|\vec{X}_j), \tag{1.34}$$

for every j. The corresponding interpretation is that such a process is *memoryless*, i.e., given the present state $\vec{x}_j$, the past states $\{\vec{x}_0, \vec{x}_1, \ldots, \vec{x}_{j-1}\}$ can provide no additional information for the prediction of the future states $\vec{x}_{j+1}$.

A straightforward translation of this concept to quantum mechanics would be to consider probability distributions over outcomes of observables. However, since in general quantum observables do not commute, such a definition of quantum Markovianity would be highly dependent on the choice of observable [104, 98]. In consequence, there exists a plethora of incompatible definitions of Markovian quantum processes the most important of which will be briefly sketched in the following.

A common approach to define Markovianity is to require that the master equation governing the evolution can be written in a particular form. One option to arrive at this equation is a so-called *microscopic derivation* in which certain simplifying assumptions are applied to a general total evolution of system and Hamiltonian, which are motivated by properties of classical Markovian systems [225, 98, 49, 100, 109, 104]. Commonly, there are three main assumptions employed in microscopic derivations of open system dynamics, the weak coupling approximation, as sketched in Sec. 1.5.2 which leads to a product state of system and environment, sometimes also referred to as *factorization approximation* or *Born approximation* [98], the *Markov approximation*, which assumes that the time scale of the system evolution is large compared to the lifetime of system-environment correlations and the *rotating-wave* or *secular* approximation which averages over rapidly oscillating terms in the evolution.

The microscopic approach with the three above-mentioned approximations leads to a comparatively restrictive definition of Markovian open system evolution. It is given by the *Lindblad master equation*, also called the *Gorini-Kossakowski-Sudarshan-Lindblad equation* (GKSL equation), of the general form [49, 100, 109, 98]

$$\frac{\mathrm{d}}{\mathrm{d}t}\rho = -\frac{i}{\hbar}[\widetilde{\mathbf{H}}, \rho] + \sum_{j=1}^{d^2-1} \gamma_j \Big(\mathbf{L}_j \rho \mathbf{L}_j^\dagger - \frac{1}{2}\{\mathbf{L}_j^\dagger \mathbf{L}_j, \rho\} \Big). \tag{1.35}$$

The term $[\widetilde{\mathbf{H}}, \rho]$ represents the unitary part of the evolution with the effective Hamiltonian $\widetilde{\mathbf{H}}$. The remaining $d^2 - 1$ terms, where d is the dimension of the system Hilbert space, correspond to a set of potential non-unitary components in the system evolution, the so-called *decay modes* of the system with *relaxation rates* $\gamma_j > 0$. The operators $\mathbf{L}_j$ are known as *Lindblad operators* and can always be chosen to be traceless and orthonormal [49, 98]. This definition of Markovianity is comparatively strict in the sense that it implies Markovian behavior also according to all other definitions presented here.

A possible generalization of GKSL equation is the time-dependent Lindblad equation which allows time-dependence of the parameters $\gamma_j(t)$, $\widetilde{\mathbf{H}}(t)$ and $\mathbf{L}_j(t)$ in Eq. 1.35 [109, 49,

98, 104]. It represents the most general form of a *time-local* master equation, in the sense that the change of ρ only depends on the current state and the equation does not involve an integration over the past [88]. As such it also considered as a potential definition of Markovian evolution at least for all times for which $\gamma_j(t) \geq 0$ for all decay modes j [98, 104].

1.8.3 Markovianity and Dynamical Maps

Apart from master equations another type of definitions of Markovianity is based on the properties of the dynamical maps describing the system evolution. Historically, one of the first definitions requires that the dynamical maps correspond to a dynamical semigroup [98, 109, 49], which is defined by the decomposition property

$$\Lambda_{t_1+t_2} = \Lambda_{t_2} \circ \Lambda_{t_1} \tag{1.36}$$

for a one parameter family of dynamical maps and $t_1, t_2 \geq t_0$. As the maps have just a single time parameter they are implicitly defined with respect to a common start time t_0. The semigroup property corresponds to a *time-homogeneous* evolution, i.e., the form of the evolution depends only on its duration and not on its starting time. Any evolution described by a Lindblad equation has the semigroup property and in fact, another motivation for the Lindblad form is that it is the most general form of master equation that can generate a dynamical semigroup [49]. Conversely, any continuous semigroup map Λ_t can be repesented by a GKSL equation [98]. Evolutions described by time-dependent Lindblad equations directly violate the time-homogeneity of semigroups and thus represent a less restrictive notion of Markovianity.

A generalization of the semigroup property is *divisability* which represents a very common and comparatively broad definition of Markovianity including all of the previous ones. It considers a two parameter family of maps $\Lambda_{t_1}^{t_2}$ with $t_2 \geq t_1 \geq t_0$. The family is *CP-divisible* if the maps are CPTP for all times and any map $\Lambda_{t_1}^{t_2}$ can be decomposed as

$$\Lambda_{t_1}^{t_2} = \Lambda_{t}^{t_2} \circ \Lambda_{t_1}^{t}, \tag{1.37}$$

for any time t, with $t_2 \geq t \geq t_1$ [502, 98, 90, 104]. The formulation in terms of a two-parameter family removes the requirement of time-homogeneity and consequently for continuous time-evolutions the requirement of CP divisibility is equivalent to requiring a time-dependent Lindblad form [98]. An ever broader notion of Markovianity is given by *P-divisibility* which is similar to CP-divisibility with the difference that it does not require complete positivity [90].

1.8.4 Information Flow

Finally, a third type of definition considers a notion of information flow and requires that no information flows back into the open quantum system during the evolution. In these approaches information is defined as the ability to distinguish initially different states of

the system after they have undergone the same evolution. As long as this amount is monotonously decreasing with time, the evolution is identified as Markovian and any time intervals with increasing information correspond to non-Markovianity. Two ways to define this distinguishability have been proposed. The first approach, denoted the *BLP-criterion* after its authors [89, 97], is based on quantifying the distance between quantum states with the trace distance $\mathcal{D}$, which corresponds to the unbiased discrimination problem as in Sec. 1.6.2. For any Markovian process it holds that

$$\mathcal{D}\big(\Lambda_{t_1}^{t_2}(\rho_1), \Lambda_{t_1}^{t_2}(\rho_2)\big) \leq \mathcal{D}\big(\rho_1, \rho_2\big) \tag{1.38}$$

for all times $t_1 < t_2$ and any pair of system states ρ_1, ρ_2.

Alternatively, a more general definition can be considered which requires a non-increasing distinguishabilty for any kind of biased prior. Then the process is defined as Markovian if and only if $\Lambda_{t_1}^{t_2}(\mathbf{\Delta}) \leq \mathbf{\Delta}$ for all times $t_1 < t_2$, all pairs of system states ρ_1, ρ_2 and any distribution of the prior $q \in [0, 1]$, where $\mathbf{\Delta}$ is the Helstrom matrix, as defined in Sec. 1.6.2 [93, 90, 104]. This is equivalent to requiring that the average probability of error for the discrimination cannot decrease with time. There are examples of maps which increase the distinguishability only for a biased prior, such as the uniform translation of states [99, 90]. Thus, the BLP criterion provides a broader notion of Markovianity than the generalized distinguishability criterion and in fact, it constitutes the broadest definition of Markovianity compared to all the other common definitions presented here. A process regarded as Markovian according to any other definition will also be BLP-Markovian. Conversely, the BLP-criterion yields the strictest witness for non-Markovianity and a detection of its violation implies non-Markovianty in all the other senses.

Chapter 2

Quantum Measurement

The special and contested role of measurement in quantum mechanics represents one of the pivotal points of the theory and distinguishes it decisively from classical theories. In consequence, it also represents the focus of the various interpretations. In this chapter an overview is given over the spectrum of possible treatments of quantum measurement. It begins with a brief summary of the basic measurement postulates as found in typical textbooks and introduces the basic concepts of complementarity and incompatibility. Subsequently, the formal apparatus of indirect measurement, generalized observables and quantum instruments is introduced, which forms the basis of a brief discussion of important properties of quantum measurement. Additionally, a section is dedicated to the critical implications of the standard account of quantum measurement, i.e., the measurement problem, as well as to its possible solutions. A special emphasis is put on canonical observables, weak measurements and measurements on pre- and postselected systems, which are of particular relevance for the subsequent chapters.

2.1 Basic Concepts

2.1.1 Measurement Postulates

As introduced in Sec. 1.2.3 the dispositive function of QM is based on observables, which encapsulate sets of possible outcomes of empirical observations. Crucially, the process of measurement, i.e., the connection of the quantum mechanical description of physical systems to these observations is not part of the dynamical formulation. Instead measurements are identified as a special class of physical processes in which the usual evolution governed by the Schrödinger equation is disrupted [232, 1010]. The characteristics of quantum measurements are commonly expressed in terms of two basic *postulates*, validated by the immense empirical success of QM, see e.g., [57, 50, 117].

The first postulate asserts that even if the measured system is in a superposition of eigenstates of an observable, always a single definite outcome is observed upon interaction with a suitable measuring system, i.e., the measurement apparatus, as already introduced

in Sec. 1.1.2. According to the postulate, whenever a quantum system is measured, the superposition of different states, i.e., a certain coexistence of distinct physical states, is not transferred to the apparatus. Instead the latter evolves probabilistically into a single definite state, corresponding to one particular eigenvalues of a measured observable, i.e., the outcome of the measurement. Given a certain quantum state of the system, the probability distribution over the possible outcomes is given by the Born rule as formulated in Eqs. (1.1) and (1.2). Thus, there is an "intrinsic randomness" in the standard description of quantum measurement, such that in general a particular measurement outcome cannot be predicted even with full knowledge of the quantum state [95].

The second measurement postulate, known as the *projection postulate* [225, 232], relates to the state of the system after the measurement. When a particular observable is measured and a definite outcome is observed, the state of the measured system itself evolves discontinuously into the corresponding eigenstate of the observable or alternatively is projected into the respective eigenspace in the case of degenerate eigenvalues. This is a fundamentally non-unitary process, known as *collapse* in which a part of the state vector disappears and a renormalization becomes necessary to arrive at a post-measurement description in terms of a valid quantum state [220, 117, 225, 232, 79, 1010]. While the usual quantum mechanical evolution is unitary and thus reversible, the collapse is fundamentally not. A common formulation is that the system is *found* in a certain state where "found" is used in contrast to "is" [819], and understood exclusively on an operational level as the empirical fact of a certain observation which does not indicate the revealing of an hitherto unknown element of reality. The attribution of a modified post-measurement state is also essential for the correct prediction of the future evolution of the system.

2.1.2 Incompatibility and Complementarity

If a measurement of an observable is repeated on the same quantum system, the same outcome will be observed with certainty, which is a property known as *repeatability* [222, 95, 225, 232, 314]. In such cases, at least in terms of the EPR criterion of reality [18] as introduced in Sec. 1.1.1, the system can be regarded as having the corresponding eigenvalue as an element of reality [803]. The collapse into an eigenstate of an observable is thus also called *objectification* of that property [222, 235]. However, for any observable there exists an infinite amount of observables which do not commute with it and thus cannot be simultaneously diagonalized. Accordingly such observables are called *incompatible* [54, 925, 258, 289]. In consequence, whenever a system is in an eigenstate of one observable, it will necessarily be in a superposition of eigenstates of an incompatible observable. Furthermore, if an incompatible observable is measured, the projection postulate leads to a modification of the state of the system such that it is no longer in an eigenstate of the first observable.

In principle the inability to assign definite values to all observables might be simply a consequence of the particular statistical prescriptions of QM, i.e., the Born rule. However, this is ruled out by the *Kochen-Specker theorem* [96] and other no-go theorems as introduced in Sec. 3.2.2, which assert the impossibility to recover the statistical predictions of QM by any simultaneous assignment of definite probabilities, i.e., $p \in \{0, 1\}$ to outcomes of

all observables [222, 925, 95, 101]. Expressed in language of EPR, this means that it is impossible to *complete* quantum mechanics in a manner that will lead to the same empirical predictions. A single quantum measurement can thus ever only yield partial information about values of observable quantities. Furthermore, in general any such measurement will necessarily disturb the state of the system, known as *quantum back-action* [161, 225]. In effect, the determination of an unknown quantum state of a particular system, i.e., quantum state tomography, as introduced in Sec. 2.4.1, has to involve measurements of several observables on ensembles of identically prepared systems.

Given the significant discrepancy between the classical understanding of measurement as revealing preexisting real properties of systems and the incompatibility of quantum observables, Bohr in his seminal Como lecture in 1927, as reprinted in [1], proposed the notion of *complementarity* as an entirely new perspective on physics [927, 236, 259]. It consists of two elements. The first is a fundamental conceptual separation between quantum and classical systems, which are described differently and are governed by different dynamical laws, a proposition known as the *Heisenberg cut* [222, 220, 521, 931, 225]. The measurement process then always corresponds to an interaction between a classical and a quantum system, which leads to a probabilistic collapse and thus a definite measurement outcome as required by the first of the measurement postulates. Note that in Bohr's view, this interaction cannot be described in physical terms since two fundamentally irreconcilable types of systems are involved. As written by Bohr in his response to EPR:

> This necessity of discriminating in each experimental arrangement between those parts of the physical system considered which are to be treated as measuring instruments and those which constitute the objects under investigation may indeed be said to form a *principal distinction between classical and quantum-mechanical description of physical phenomena.* [6]

Notably, Bohr adds in the next sentence that the exact placement of this cut is "largely a matter of convenience" [6], leaving its definition manifestly vague, as famously put by Bell:

> What exactly qualifies some physical systems to play the role of a 'measurer'? Was the wavefunction of the world waiting to jump for thousands of millions of years until a single-celled living creature appeared? Or did it have to wait a little longer, for some better qualified system ... with a Ph.D.? [966]

The second element of complementarity is an irreducible connection of observables and particular measurement procedures, where procedures corresponding to incompatible observables are mutually exclusive and cannot be performed jointly [54, 521, 931]. Measurements can thus lead to the objectification of one property but not the other. In this sense the properties are said be "complementary". Again in the words of Bohr:

> In fact, it is only the mutual exclusion of any two experimental procedures, permitting the unambiguous definition of complementary physical quantities, which provides room for new physical law, the coexistence of which might at first sight appear irreconcilable with the basic principles of science. It is just this entirely new situation as

> regards to the description of physical phenomena, that the notion of *complementarity* aims at characterizing. [6]

As already pointed out in Sec. 1.1.2, since properties of systems cannot be defined independently of measurement procedures, Bohr's view corresponds to a decidedly operational approach to physics. The goal is not to "disclose the essence of the phenomena" but only to understand "relations between the manifold aspects of our experience" [1]. The fact that measurement becomes a fundamental concept in the formulation of physics, with the corresponding impossibility to provide a physical description of measurement itself, is known as the *measurement problem* discussed in Sec. 2.5 along with possible solutions.

2.1.3 Uncertainty Relations and Mutually Unbiased Bases

The incompatibility of observables implies an irreducible indeterminacy both in the description of quantum systems, i.e., with respect to values of observable quantities, as well as in the prediction of results of future measurements, even if maximal attainable knowledge about the system is at hand [521]. The emerging tradeoff in the definiteness of a quantum state with respect to two observables has been first formulated by Heisenberg [21] for position and momentum and later extended to arbitrary observables [24, 44, 39], see also [927, 285, 228, 341] for overviews. It constitutes the famous *uncertainty relation* of quantum mechanics as given by

$$\Delta\mathbf{A}\Delta\mathbf{B} \geq \frac{1}{2}|\langle[\mathbf{A},\mathbf{B}]\rangle|, \tag{2.1}$$

which was tightened by Schrödinger into the improved form [42]

$$\Delta\mathbf{A}\Delta\mathbf{B} \geq \sqrt{\left(\frac{1}{2}|\langle[\mathbf{A},\mathbf{B}]\rangle|\right)^2 + (C_{AB})^2}, \tag{2.2}$$

written here in terms of the covariance as defined in Eq. (1.32). Uncertainty relations such as those above, i.e., written in terms of products or sums of statistical uncertainties have also been generalized to three or more observables, see e.g., [38, 301, 300, 275, 267].

A different approach to quantify the incompatibility of observables is given by *entropic uncertainty relations* with a seminal relation proposed by Maassen and Uffink for finite dimensional Hilbert spaces [307]. For two observables $\mathbf{A}$ and $\mathbf{B}$ as well as a state ρ, probability distributions $p(j)$ and $q(j)$ over the respective outcomes are given by $p(j) = |\langle a_j|\psi\rangle|^2$ and $q(j) = |\langle b_j|\psi\rangle|^2$. This allows to write the uncertainty in terms of a sum of Shannon entropies as

$$H(p) + H(q) \geq -2\log\Gamma, \tag{2.3}$$

where $\Gamma := \max_{jk}|\langle a_j|b_k\rangle|$ is the maximal overlap between the respective eigenstates. In contrast to the usual uncertainty relations, entropic relations have the advantage that the RHS is state independent. See e.g., [269] for a review about generalizations and applications

of entropic uncertainty relations. In particular, such relations form the basis of important security proofs for quantum cryptography protocols, see e.g., [287, 180, 155].

At least in the finite dimensional case the lower bound of relation (2.3) allows to define the concept of *maximally incompatible* observables, i.e., observables for which Γ is minimized. This is the case whenever a pair of observables acting on a Hilbert space of dimension d has sets of eigenstates which form a *mutually unbiased basis* (MUB), i.e., $|\langle a_j|b_k\rangle|^2 = 1/d$, for all j, k [250, 281]. In general the question about the maximal size of a set of MUB in a given Hilbert space still represents an open problem in quantum mechanics and solutions exists only in special cases with a general upper bound given by $d + 1$ [250, 281, 171]. Also the extension of the concept of MUB to infinite dimensional Hilbert spaces is non-trivial, where a possible definition can be given via the requirement of a constant overlap as in the finite dimensional case [339]. Note, however, that in the infite dimensional case there is no unambiguous value for that overlap and different pairs of observables with MUBs defined on the same Hilbert space can possess constant overlaps with different values. For example, the position and momentum bases can be regarded as MUB since the overlap is $|\langle x|p\rangle|^2 = 1/2\pi\hbar$. Notably, these operators also yield the state independent bound of $\hbar/2$ for the usual uncertainty relation (2.1).

2.2 Formal Description of Quantum Measurement

2.2.1 Indirect Measurement

Quantum mechanical measurement can be described in terms of an *indirect* measurement, first introduced by von Neumann in his seminal book [4], where the Heisenberg cut is placed in such a manner that part of the measurement apparatus is still modeled as a quantum mechanical system [222, 225]. As already introduced in Sec. 1.7.1 in the context of quantum estimation theory, such auxiliary measurement systems are called "pointers". In principle the measurement of the pointer is itself again a quantum measurement, which can be expressed as an indirect measurement by another pointer leading to the so-called *von Neumann chain* of correlated quantum systems, which would also include the experimenter itself if no cut were made at some point [4, 225].

In the simplest model of indirect measurement system and pointer are assumed to be initially in a pure product state $|\Psi\rangle = |\psi\rangle \otimes |\chi\rangle$ and subsequently become correlated after an interaction with a product Hamiltonian of the form (1.19). The joint state $|\Psi\rangle \in \mathcal{H} = \mathcal{H}_S \otimes \mathcal{H}_P$ of both systems after the interaction can be expressed as

$$|\Psi\rangle = \sum_j c_j \, |a_j\rangle \otimes |\chi_j\rangle \,, \tag{2.4}$$

where the $c_k = \langle a_k|\psi\rangle \in \mathbb{C}$ are the expansion coefficients of $|\psi\rangle$ in the countable eigenbasis of $\mathbf{A}$ and the different pointer states are given as $|\chi_j\rangle = \mathbf{U}_j \, |\chi\rangle$, where $\mathbf{U}_j = \exp(-i/\hbar \, \varepsilon a_j \mathbf{B})$ are effective unitary operators acting on the pointer system.

Due to the correlation between the states of the two systems the task of distinguishing the states $|a_j\rangle$ is now replaced by the task of distinguishing different states of the pointer by measuring in the basis of a suitable pointer observable $\mathbf{C}$ [225]. In information theoretic terms this interaction represents a strategy to extract information about the system, where the possible outcomes of $\mathbf{A}$ as expressed by the random variable X are encoded in the random variable Y corresponding to measurement outcomes on the pointer. As discussed in Sec. 1.6.2, the information about state with respect to $\mathbf{A}$ is most accessible if it is encoded in orthogonal states of the pointer. Accordingly, the indirect measurement of $\mathbf{A}$ is called an *ideal* or *von Neumann* measurement if the states $|\chi_j\rangle$ are pairwise orthogonal [225]. In this case, an optimal extraction strategy is given for example by an observable $\mathbf{C}$ for which all $|\chi_j\rangle$ are eigenvectors. A measurement of $\mathbb{1} \otimes \mathbf{C}$ on the joint state $|\Psi\rangle$ will then yield results according to the probability distribution $|c_j|^2$ correlated with the respective eigenstates $|a_j\rangle$.

The reduced *post-measurement state* of the system ρ'_S in a potentially non-ideal measurement becomes

$$\rho'_S = \sum_{j,k} c_j c_k^* \mu_{kj} |a_j\rangle\langle a_k|, \tag{2.5}$$

where the parameters $\mu_{jk} \in \mathbb{C}$ indicate the scalar product between the corresponding pointer states with $\mu_{jk} = \langle\chi_j|\chi_k\rangle$. If the collapse is taken to occur then dependent on the measurement performed on the pointer only parts of ρ'_S will be preserved, e.g., only the eigenstate $|a_j\rangle$ in the case of an ideal measurement, in which the pointer is found in $|\chi_j\rangle$. This is known as a *selective* measurement for which the density operator ρ'_S still expresses the average state in terms of a proper mixture, which crucially is independent of the action performed on the pointer [49, 225, 128, 279]. In fact, such selective measurements are the basis for the preparation of quantum systems in specific states [50]. In the other case when no cut is applied and thus no collapse occurs, the system is described by state ρ'_S in terms of an improper mixture This is called accordingly a *non-selective* measurement. In any case, in the absence of conditioning on the outcomes, the post-measurement state ρ'_S will correctly predict the probabilities for outcomes of future measurements on the system. Eq. (2.5) also shows the decohering effect of quantum measurement, i.e., the smaller the pairwise overlap $|\mu_{jk}|$, the more do the off-diagonal elements of ρ'_S vanish. Thus, the more the information about the state with respect to $\mathbf{A}$ becomes accessible to observations on the pointer, the more does ρ'_S decohere in the basis of $\mathbf{A}$, culminating in full decoherence in the case of an ideal measurement [49].

2.2.2 Generalized Observables

By allowing arbitrary interactions, pointer observables $\mathbf{C}$, and initial states of the pointer system, also more general measurements can be implemented in terms of the system-pointer model. As shown in the previous chapter, the interaction of the system in an arbitrary state ρ with an initially uncorrelated pointer in general will lead to a system evolution given by a quantum channel $\mathcal{C}[\rho]$, i.e., a CPTP map which can be written in operator-sum form (1.16).

In general each outcome corresponds to a certain trace reducing operation $\mathcal{T}_j$ represented in operator-sum form by a subset of the Kraus operators with $\mathcal{T}_j[\rho] = \sum_k \mathbf{K}_k^{(j)} \rho (\mathbf{K}_k^{(j)})^\dagger$, where $\sum_{jk} \mathbf{K}_k^{(j)} (\mathbf{K}_k^{(j)})^\dagger = \mathbb{1}$. The operations describe the evolution into the *conditional states* ρ_j, obtained when outcome j is selected, with [529, 225]

$$\rho_j := \frac{\mathcal{T}_j[\rho]}{\mathrm{tr}\big(\mathcal{T}_j[\rho]\big)} = \frac{\sum_k \mathbf{K}_k^{(j)} \rho (\mathbf{K}_k^{(j)})^\dagger}{\mathrm{tr}\big(\rho \sum_k (\mathbf{K}_k^{(j)})^\dagger \mathbf{K}_k^{(j)}\big)}, \tag{2.6}$$

where the probability $p(j)$ of outcome j corresponds to the trace of the conditional state before normalization as $p(j) = \mathrm{tr}\big(\mathcal{T}_j[\rho]\big)$. For example, an indirect measurement yielding the post-measurement state (2.5) can be expressed by operations $\mathcal{T}_j = \mathbf{K}_j \rho \mathbf{K}_j^\dagger$ with Kraus operators $\mathbf{K}_j = \sum_k \sqrt{\mu_{kj}}\, \mathbf{\Pi}_k$.

The Hermitian *operators* $\mathbf{M}_j := \sum_k (\mathbf{K}_k^{(j)})^\dagger \mathbf{K}_k^{(j)}$ as introduced by Ludwig [306] are called *measurement operators* [276] or *effects* [227]. They fulfill the relation $\sum_j \mathbf{M}_j = \mathbb{1}$ and thus form a so-called *positive operator valued measure* (POVM) [221, 117, 174, 95, 225, 230]. POVMs, also called *generalized observables* [174, 231], allow to specify the probability distribution over outcomes of a measurement operation without the need to specify in detail the interaction between system and pointer. Based on Gleason's theorem [94], they can be shown to represent the most general manner to construct a probability measure on quantum states [222, 95]. A POVM $\mathcal{M}$ and the corresponding quantum channel $\mathcal{C}$ can be unified in the concept of a *quantum instrument* $\mathcal{I} = (\mathcal{M}, \mathcal{C})$, as coined by Davies [273], which constitutes the most general representation of any measurement of a quantum system [316, 95, 230, 292]. Since, as discussed in Sec. 1.4.3, any CPTP map can be represented via a unitary evolution of an extended system, also any quantum instrument can be represented in terms of suitable unitary coupling between the system and a pointer along with the measurement of a pointer observable. In this sense the description of quantum measurement in terms of regular observables and unitary evolution might also be regarded as "most general", where quantum instruments just represent a convenient reduced description when only the system is of interest.

As clearly the same POVM can correspond to infinitely many different channels [117, 95, 225, 292], it is possible that a different amount of back-action on the system is induced by measurements which extract the same amount of information. This allows to classify measurements described by the same POVM in terms of induced disturbance and define *optimal measurements* as those which minimize this disturbance [222]. Whenever the operation $\mathcal{T}_j$ corresponding to a particular outcome j is comprised of multiple Kraus operators, unnecessary statistical noise is introduced [286, 312, 225]. Accordingly, *efficient* measurements consist exclusively of operations of the form $\mathcal{T}_j[\rho] = \mathbf{K}_j \rho \mathbf{K}_j^\dagger$ which can be expressed in terms of a single Kraus operator, leading to the POVM elements $\mathbf{M}_j = \mathbf{K}_j^\dagger \mathbf{K}_j$. In general for efficient measurements Kraus operators are related to measurement operators via a unitary operator $\mathbf{U}_j$ as $\mathbf{K}_j = \mathbf{U}_j \sqrt{\mathbf{M_j}}$ [220]. An example of such unitary transformations is given by the post-measurement state (2.5) as considered in the discussion of indirect measurement above, where the necessary decoherence due to extraction of information is

accompanied by a superfluous unitary rotation of the state, when the relative phases of the coefficients μ_{jk} are not equal for all j, k. This rotation represents an additional disturbance which does not affect the POVM. Thus, *minimally disturbing* measurements, i.e., measurement which lead to least average disturbance for arbitrary initial system states, can be defined by the requirement $\mathbf{K}_j = \sqrt{\mathbf{M}_j}$ [249, 225]. The latter type of instruments is sometimes called *Lüders instrument* [95, 292] after [29]. Note that Kraus operators can be freely mulitplied by an arbitrary global phase $e^{i\varphi}$, which has no physical relevance as it always cancels out.

Minimally disturbing measurements for which $\mathbf{M}_j = \mathbf{K}_j = \mathbf{\Pi}_j$ are called *projective measurements* and correspond to the usual quantum measurement based on Hermitian observables as introduced in the first chapter [117, 225]. If, furthermore, those observables are non-degenerate the ideal measurements, as described in the preceding Section 2.2.1, are obtained. Generalized measurements are repeatable, i.e., they lead to the same outcome upon a second application, if and only if they are projective [95, 225, 232, 314].

It is also possible to extend the notion of compatibility, as introduced in the previous section, to POVMs by distinguishing commutativity from *non-disturbance* and *joint-measurability* [292]. Two POVMs $\mathcal{M} = \{\mathbf{M}_j\}$ and $\mathcal{N} = \{\mathbf{N}_j\}$ are jointly measurable if there exists a third POVM $\mathcal{G} = \{\mathbf{G}_{jk}\}$ such that $\mathcal{M}$ and $\mathcal{N}$ can be recovered as marginals of $\mathcal{G}$, i.e., $\mathbf{M}_j = \sum_k \mathbf{G}_{jk}$ and $\mathbf{N}_j = \sum_k \mathbf{G}_{kj}$. Furthermore, $\mathcal{M}$ is non-disturbing with respect to $\mathcal{N}$ if there exist an instrument for the measurement of $\mathcal{M}$ which, for any arbitrary state, does not change the outcome statistics for a subsequent measurement of $\mathcal{N}$. Note that non-disturbance is asymmetric, i.e., even if $\mathcal{M}$ does not disturb $\mathcal{N}$, the opposite is not necessarily true. Finally also commutativity can be extended to POVMs via the definition $\forall j, k\ [\mathbf{M}_j, \mathbf{N}_k] = 0$. It can be shown that for an arbitrary pair $\mathcal{M}$ and $\mathcal{N}$ it holds that [292]

$$\text{commutativity} \quad \Rightarrow \quad \text{non-disturbance} \quad \Rightarrow \quad \text{joint-measurability}, \tag{2.7}$$

while the converse implications in general do *not* hold. In the case of projective POVMs, i.e., regular quantum observables, however, all these notions become equivalent as encompassed in the simple notion of compatibility introduced above.

While the concept of quantum instruments abstracts from observables with real-valued spectra, in principle arbitrary labels can be attached to the results [225]. In particular, so-called *contextual values* have been proposed [276, 277] to connect the formalism of generalized measurement to expectation values of observables. For an observable $\mathbf{A}$ and a POVM $\mathcal{M} = \{\mathbf{M}_j\}$ of size n the set of contextual values $\{\alpha_j\}$ is defined via the relation $\mathbf{A} = \sum_j \alpha_j \mathbf{M}_j$. Then, for any state ρ the expectation value of the generalized measurement $\langle \mathcal{M} \rangle := \sum_j \alpha_j \mathrm{tr}(\rho \mathbf{M}_j)$ will be equal to the expectation value of $\mathbf{A}$ as obtained by a projective measurement. Whenever $\dim \mathbf{A} \leq n$ such a set can always be found and, in the case of equality, it is uniquely determined [276].

2.2.3 Information-Disturbance Trade-Off

The properties of quantum measurement, in particular the existence of complementary observables, as introduced above, imply a principle of unavoidable disturbance of physical sys-

tems as a necessary consequence of measurement, captured by the slogan "no information without disturbance" [340, 259]. However, as sketched in the following, the exact quantification of an *information-disturbance trade-off* (IDT) is a non-trivial and contested issue. A hint of an IDT relation can already be gained from the simplest form of the preparation uncertainty relation (2.1) for the case of observables with a state-independent commutator such as position and momentum. In this case, after a projective measurement which extracts information about $\mathbf{A}$, the uncertainty $\Delta\mathbf{A}$ in the conditional post-measurement state is expected to be reduced compared to the initial state. This, according to the inequality, necessarily leads to an increase of the uncertainty of a complementary observable $\Delta\mathbf{B}$ in future measurements. The IDT is closely related to the no-cloning theorem introduced in Sec. 1.6.2, which in its quantitative formulation [140, 196, 575, 168] asserts that any such copying will necessarily disturb the state of the source system the more, the better the state is transferred onto the target system. In effect, also the measurements which can be performed on the two clones are not free from fundamental limitations of an IDT [257, 271, 256].

A fundamental intuition of measurement induced disturbance was first stated by Heisenberg when introducing the uncertainty relation [21] and later discussed in more detail based on the famous example of the *Heisenberg microscope* [3]. However, this treatment never went beyond the famous heuristic statement

$$p\,x \sim \hbar, \tag{2.8}$$

where x and p were loosely understood as quantifying error or disturbance for the position and momentum observations respectively [927, 226, 228, 341]. A first quantitative treatment was proposed only much later by Arthurs and Kelly [246] and the general question of a quantitative description of IDT relations in quantum mechanical measurements is still a lively topic of research, see [260, 261, 279, 324, 289] for overviews of the historical developments and [305, 274, 333, 336, 338] for examples of recent approaches.

A particularly influential contribution was given by Ozawa [319], with an alleged "universally valid reformulation" of the Heisenberg relation, further developed and improved in [290, 318, 317, 254, 342]. It is "universal" in the sense that it considers a general quantum instrument which measures observable $\mathbf{A}$ and quantifies the error as the root mean square deviation (RMSD) of the pointer readings corresponding to outcomes of $\mathbf{A}$. The disturbance is accordingly defined as the RMSD of subsequent measurements of observable $\mathbf{B}$. Ozawas relation was sometimes described as an "improvement" upon Heisenberg measurement-disturbance relation and its experimental confirmations [284, 326, 247, 299, 335] even prominently claimed to demonstrate "violations" of Heisenberg's relation. However, as pointed out by various authors [270, 262, 340], the presumable refutation of Heisenberg's uncertainty principle is based on a conceptual conflation of Heisenberg's heuristic arguments and the standard uncertainty relation (2.1) in terms of standard deviations, leading to a longer controversy, see e.g., [303, 263, 315, 244, 341]. Notably, an alternative formulation of a IDT relation has been introduced [264], where error and disturbance is suitably defined based on the distances between probability distributions of outcomes,

such that the product form of standard relation is exactly reproduced, even including the commutator on the RHS.

In summary, irrespective of historical considerations, three types of uncertainty relations should be carefully distinguished [261, 228, 263, 279]. The first type corresponds to *preparation uncertainties*, such as the relations (2.1) and (2.2), as well as their entropic counterparts such as (2.3), which quantify a trade-off in the uncertainties of a state with respect to two observables. Crucially preparation uncertainties are in general only relevant for cases in which only one of the two observables is factually measured on a single copy of the system. The other two types concern trade-offs when information about two observables is extracted from the *same* copy of the system either *simultaneously* or *sequentially*, corresponding to the concepts of joint-measurability and respective disturbance of POVMs, as defined above. Disturbance relations can also be distinguished based on the question whether they are state dependent or independent and whether they are concerned with results of observations on single copies of systems or on average results over the whole ensemble, see e.g., [340, 263, 279].

In recent years a plethora of further approaches to quantify the trade-off between information gain and state disturbance has emerged and a comprehensive overview of all types of different proposals lies far beyond the scope of this work. However, one particular hybrid approach, as proposed by Hashagen and Wolf [291], applicable to arbitrary quantum instruments, should be mentioned. It quantifies gained information via the distance of the probability distribution of the instrument outcomes to an ideal measurement and the error via the trace distance of the average post-measurement state to the initial state. In the experimental study **[P2]** this tradeoff relation is confirmed for a qubit system and pointer as well as shown to outperform an approach based on optimal cloning, where the information is extracted from an approximately cloned state.

2.2.4 Weak Measurements

In face of the unavoidable disturbance of quantum system due to any extraction of information so-called *weak measurements* represent the extreme case where the disturbance is made arbitrarily small at the cost of almost no information gain from a measurement on a single system. However, when sufficiently many identical copies of the state in question are available, weak measurements in principle allow to obtain arbitrarily precise information about an observable while inducing vanishingly small disturbance for each system [674, 675, 681, 727, 786, 751, 741, 677]. Weak measurements can be defined with a perturbative ansatz based on a continuous interaction strength parameter, as introduced in Sec. 1.5.2. While some authors consider higher orders of perturbation, this work follows the paradigm of a limit $\varepsilon \to 0$ [675, 681, 677], where only the first order, or alternatively the first non-vanishing order is considered. In the following an approximation sign will denote steps in which higher orders in ε are neglected.

As shown in Sec. 1.5.2, any weak interaction between the system and a pointer will leave a weak trace. In the case of a product Hamiltonian (1.19), the modified pointer state

can be written as

$$|\chi'\rangle \approx e^{-i\varepsilon\langle\mathbf{A}\rangle\mathbf{B}/\hbar}\,|\chi\rangle \tag{2.9}$$

Any change in the expectation value of the measured observable, is thus reflected linearly in a change of the effective unitary evolution parameter $\varepsilon\langle\mathbf{A}\rangle$. In effect, if some observable $\mathbf{C}$ is measured on the pointer system, the change of its expectation value due to the measurement can be expressed as

$$\delta\mathbf{C} := \langle\chi'|\mathbf{C}|\chi'\rangle - \langle\chi|\mathbf{C}|\chi\rangle \approx -\frac{i}{\hbar}\varepsilon\langle\mathbf{A}\rangle\langle[\mathbf{C},\mathbf{B}]\rangle. \tag{2.10}$$

Thus, as long as the expectation value of the commutator between $\mathbf{C}$ and the generator of the measurement interaction $\mathbf{B}$ does not vanish, the *shift* $\delta\mathbf{C}$ of the expectation value of $\mathbf{C}$ depends linearly on the expectation value of $\mathbf{A}$. Note that of course $\langle[\mathbf{C},\mathbf{B}]\rangle$ is strictly imaginary, such that the expression above is well defined.

The uncertainty $\Delta\mathbf{C}$ in the final pointer state is given as

$$\Delta\mathbf{C} \approx \Delta_0\mathbf{C} - \frac{i}{2\hbar}\varepsilon\langle\mathbf{A}\rangle\big(\langle[\mathbf{B},\mathbf{C}^2]\rangle - 2\langle\mathbf{C}\rangle\langle[\mathbf{C},\mathbf{B}]\rangle\big), \tag{2.11}$$

where $\Delta_0\mathbf{C} = \langle\chi|\mathbf{C}|\chi\rangle$ denotes the uncertainty in the initial pointer state. In effect, due to the relation

$$\langle\mathbf{A}\rangle \approx \delta\mathbf{C}\frac{i\hbar}{\varepsilon\langle[\mathbf{C},\mathbf{B}]\rangle}, \tag{2.12}$$

an unbiased estimator $\mathfrak{A}$ for the expectation value of $\mathbf{A}$ can be constructed based on averaging the outcomes of the measurement on $\mathbf{C}$ for a number n of weak measurements [675, 49, 681]. The SNR Ξ of the estimation then becomes

$$\Xi = \frac{|\mathbb{E}[\mathfrak{A}]|}{\Delta\mathfrak{A}} \approx \sqrt{n}\,\frac{|\varepsilon\langle\mathbf{A}\rangle|}{\Delta\mathbf{C}}\,\frac{|\langle[\mathbf{C},\mathbf{B}]\rangle|}{\hbar}. \tag{2.13}$$

Thus, no matter how weak the measurement, i.e., how small the disturbance of each individual system, the SNR can be made arbitrarily large by repeating the procedure on a large enough ensemble. For example, in the case of a qubit pointer with $|\chi\rangle = |0\rangle$, a generator $\mathbf{B} = \hbar\boldsymbol{\sigma}_y$, i.e., a rotation around the y-axis of the Bloch ball, and a pointer measurement of $\mathbf{C} = \boldsymbol{\sigma}_x$ the above expressions simplify to $\delta\mathbf{C} = \langle\mathbf{C}\rangle \approx \varepsilon\langle\mathbf{A}\rangle$, $\Delta\mathbf{C} \approx \Delta_0\mathbf{C}$, and $\Xi \approx \sqrt{n}\varepsilon\langle\mathbf{A}\rangle/\Delta\mathbf{C}$. Note that the scheme of weak measurements allows to determine the expectation value of an observable for an arbitrarily dimensional system with arbitrary precision even with a qubit pointer. In contrast, an ideal indirect measurement, as discussed in Sec. 2.2.1, requires a pointer which is at least of equal size as the system space.

The disturbance in weak measurements can be analyzed by deriving the corresponding quantum instrument. For a pointer readout of observable $\mathbf{C} = \sum_j c_j\boldsymbol{\Pi}_j$, the Kraus and

measurement operators $\mathbf{K}_j$ and $\mathbf{M}_j$ corresponding to an outcome j can be expressed as

$$\mathbf{K}_j \approx \sqrt{\langle\chi|\,\mathbf{\Pi}_j\,|\chi\rangle}\left(\mathbb{1} + \varepsilon\frac{\mathrm{Im}\big[\,\langle\chi|\,\mathbf{\Pi}_j\mathbf{B}\,|\chi\rangle\,\big] - i\mathrm{Re}\big[\,\langle\chi|\,\mathbf{\Pi}_j\mathbf{B}\,|\chi\rangle\,\big]}{\langle\chi|\,\mathbf{\Pi}_j\,|\chi\rangle}\mathbf{A}\right) \tag{2.14}$$

$$\mathbf{M}_j \approx \langle\chi|\,\mathbf{\Pi}_j\,|\chi\rangle\left(\mathbb{1} + 2\varepsilon\frac{\mathrm{Im}\big[\,\langle\chi|\,\mathbf{\Pi}_j\mathbf{B}\,|\chi\rangle\,\big]}{\langle\chi|\,\mathbf{\Pi}_j\,|\chi\rangle}\mathbf{A}\right). \tag{2.15}$$

Since a minimally disturbing measurement is given exactly if $\mathbf{K}_j = \sqrt{\mathbf{M}_j}$, for weak measurements minimal disturbance is achieved exactly if $\mathrm{Re}\big[\,\langle\chi|\,\mathbf{\Pi}_j\mathbf{B}\,|\chi\rangle\,\big] = \langle\{\mathbf{\Pi}_j, \mathbf{B}\}\rangle/2$ vanishes for any subspace j of $\mathbf{C}$. This also implies that $\langle\{\mathbf{B}, \mathbf{C}\}\rangle = 0$. The example of weak measurement with a qubit pointer introduced above, is also optimal in this sense.

2.3 Measurements and Continuous Observables

2.3.1 Canonically Conjugate Observables

Observables with continuous spectra, called *continuous observables* or *continuous variables* are present in many quantum scenarios and also represent useful tools in applications of QIT, see e.g., [136] for a review. Of particular importance are pairs of complementary continuous observables $\mathbf{X}$ and $\mathbf{Y}$, fulfilling the commutation relation $[\mathbf{X}, \mathbf{Y}] = iq\mathbb{1}$, with some dimensional scaling factor q. If the factor is $q = \hbar$ the commutation relation is typically called *canonical commutation relation* (CCR) [57, 50], where in this work this notion is used more broadly for arbitrary scaling factors q. Thus, while position $\mathbf{x}$ and momentum $\mathbf{p}$ are the paradigmatic example of the CCR, such relations also appear for pairs of observables acting on various infinite dimensional degrees of freedom, such as the quadratures of the electromagnetic field introduced in Sec. 4.4.1.

The CCR implies many important relationships between the observables such as the equivalence of commutation and derivative $[\mathbf{X}, f(\mathbf{Y})] = iq\,\partial_{\mathbf{Y}}\,f(\mathbf{Y})$ or the state independent uncertainty relation $\Delta\mathbf{X}\Delta\mathbf{Y} \geq q/2$. Note, however, that the CCR alone does not imply the relation $\langle x|\mathbf{Y}|\psi\rangle = -iq\partial_x\langle x|\psi\rangle$, where $|x\rangle$ is an eigenstate of $\mathbf{X}$, known from position and momentum. However, according to the *Stone - von Neumann theorem* [108, 174], there always exists a unitary transformation of $\mathbf{X}$ and $\mathbf{Y}$, which also recovers this relation. In the following, pairs of observables satisfying both the CCR and the latter relation will be called *canonically conjugate observables* (CCO). For CCO the overlap of the respective eigenstates $|x\rangle$ and $|y\rangle$ is determined up to an arbitrary factor $\gamma \in \mathbb{C}$ as $\langle x|y\rangle = \gamma e^{ixy/q}$, i.e., they possess MUB. In consequence the wavefunctions in x and y-representations form a Fourier pair, where throughout this work a symmetric form of the Fourier transform is achieved by choosing $\gamma = 1/\sqrt{2\pi q}$, leading also to the overlaps $\langle x|x'\rangle = \delta(x - x')/\sqrt{2\pi q}$ and vice versa for $\mathbf{Y}$. Furthermore, CCO are mutual generators of translations with e.g., $\langle x|\,e^{-i\varepsilon\mathbf{Y}/q}\,|\psi\rangle = \psi(x - \varepsilon)$. In general the unitary operator $\mathbf{U}_W$ defined as [340, 339, 111, 263]

$$\mathbf{U}_W(\varepsilon_x, \varepsilon_y) := e^{-i(\varepsilon_x\mathbf{Y} - \varepsilon_y\mathbf{X})/q} = e^{-i\varepsilon_x\mathbf{Y}/q}e^{i\varepsilon_y\mathbf{X}/q}e^{i\varepsilon_x\varepsilon_y/2q}, \tag{2.16}$$

sometimes called *Weyl operator*, describes a general translation also called *shift* of a state by ε_x and ε_y in the spaces of $\mathbf{X}$ and $\mathbf{Y}$, respectively.

For CCO the preparation uncertainty relation is minimized for so-called *minimal uncertainty states* (MUS), which can be expressed with a Gaussian wavefunction of the form [174, 225]

$$\psi(x) = \left(\frac{1}{2\pi\sigma^2}\right)^{\frac{1}{4}} e^{-\frac{(x-x_0)^2}{4\sigma^2}+iy_0(x-x_0/2)} \tag{2.17}$$

determined by three parameters $x_0 = \langle\mathbf{A}\rangle$, $y_0 = \langle\mathbf{B}\rangle$, and $\sigma = \Delta\mathbf{X}$. Accordingly, as required by Eq. (2.2) also the covariance C_{XY} vanishes for MUS. Since the Fourier transform of a Gaussian is also a Gaussian, in y-representation MUB states also have the same form with uncertainty $\Delta\mathbf{Y} = q/2\Delta\mathbf{X}$. The Fourier transform relation between CCO also implies a simple relation to observables $\mathbf{Z}$ which correspond to weighted sums of $\mathbf{X}$ and $\mathbf{Y}$ defined as

$$\mathbf{Z} := \varepsilon_x\mathbf{Y} - \varepsilon_y\mathbf{X}. \tag{2.18}$$

Eigenstates $|z\rangle$ of $\mathbf{Z}$ are then related to eigenstates of e.g., $\mathbf{X}$ as

$$\langle x|z\rangle = \frac{1}{\sqrt{2\pi q|\varepsilon_x|}} e^{i\left(xz+\varepsilon_y\frac{x^2}{2}\right)/q\varepsilon_x}. \tag{2.19}$$

The respective wavefunctions $\psi(x)$ and $\psi(z)$ are thus related via a *fractional Fourier transform* [103, 339]. A similar relation of course also holds for eigenstates of $\mathbf{Y}$. In effect, for MUS also the fractionally transformed states are Gaussians.

Indirect quantum measurements are often described in terms of CCO such as in the original example of von Neumann [4] where the initial state of the pointer $|\chi\rangle$ is given by a narrow function in the eigenspace of $\mathbf{Y}$ [675, 529, 49, 259]. In consequence, the evolutions $\mathbf{U}_j = \exp(-i\varepsilon a_j\mathbf{Y}/q)$ correspond to translations of the pointer distribution by distances proportional to the eigenvalues a_k of the measured observable $\mathbf{A}$, such that the probability distribution of the pointer readout $p(x)$ becomes

$$p(x) = \sum_j p(j)|\chi(x-\varepsilon a_j)|^2, \tag{2.20}$$

with the initial pointer state $\langle x|\chi\rangle = \chi(x)$, leading to the expectation value

$$\langle\mathbf{X}\rangle = x_0 + \varepsilon\sum_j p_j a_j = x_0 + \varepsilon\langle\mathbf{A}\rangle. \tag{2.21}$$

Thus, in the case of CCO the linear dependence of the pointer expectation value $\langle\mathbf{X}\rangle$ on $\langle\mathbf{A}\rangle$, which is the hallmark of weak measurements (2.10), holds for arbitrary interaction strengths ε. In the following such measurements are called *canonical measurements*. For a canonical measurement a sufficient condition for ideality is that the width $\Delta\mathbf{X}$ of χ is

small enough compared to the minimal difference between the eigenvalues, i.e., $\Delta\mathbf{X} \ll \varepsilon \min_{j,k} |a_j - a_k|$. A common figure of speech is that an ideal canonical measurement "*resolves* the eigenvalues of $\mathbf{A}$", see e.g., [529]. Degenerate eigenvalues of course cannot be resolved in general. Conversely, at least for non-pathological pointer states such as MUS, a weak measurement is realized if $\Delta\mathbf{X} \gg \varepsilon \max_{j,k} |a_j - a_k|$, since in this case the higher orders of ε in expression (2.9) can be neglected [681].

2.3.2 Wigner Representation

Although in general no joint probability distribution can be formulated for the values of the incompatible CCO, a range of representations in terms of quasi-probability distributions has been proposed, most famously the *Wigner distribution* also called *Wigner function* or *Wigner representation*, as introduced by Wigner [45]. It allows to formulate the quantum equivalent of a *phase-space representation* over the continuous outcome spaces $\Omega_X := \{x\}$ and $\Omega_Y := \{y\}$ of the CCO $\mathbf{X}$ and $\mathbf{Y}$ for any state ρ [529, 531, 136, 225]. The Wigner distribution W is a real valued function, which for a single degree of freedom can be defined as

$$W(x,y) = \frac{1}{\pi q} \int_{\Omega_Z} e^{2iyz/q} \langle x - z| \rho |x + z\rangle \, \mathrm{d}z, \tag{2.22}$$

where the space Ω_Z is equal to Ω_X, i.e., it is equivalent to $\mathbb{R}$ up to dimensional scaling factor. As originally introduced by Wigner this distribution can also be generalized to express the joint-state of any number n of continuous degrees of freedom [136, 225].

The Wigner distribution resembles a classical joint probability in many aspects [136, 225]. For example, it is normalized when integrated over Ω_X and Ω_Y and its marginals exactly correspond to the probability distributions for measurements of $\mathbf{X}$ and $\mathbf{Y}$. Furthermore, also the generalized overlap $\mathrm{tr}(\rho_1\rho_2)$ of two states ρ_1 and ρ_2 corresponds to the double integral over the product of their respective Wigner functions [225]. However, in general the Wigner function has also negative values, which is why a negative Wigner distribution is sometimes regarded as a criterion of "quantumness" or "non-classicality", as sketched in Sec. 4.4.3 in the context of quantum states of the electromagnetic field. In fact among pure states only Gaussian states, as introduced above correspond to a positive-definite Wigner function [225].

2.3.3 Optimal Pointer States

By considering measurement uncertainty and minimal state disturbance, it is possible to specify conditions on optimal pointer states for canonical measurements. If for example an arbitrary sum observable $\mathbf{Z}$, as defined in Eq. (2.18), is measured on an arbitrary pointer state $|\chi\rangle$, the resulting expectation value corresponds to a weighted sum of the expectation values of $\mathbf{X}$ and $\mathbf{Y}$ with

$$\langle \mathbf{Z} \rangle = \varepsilon_x \langle \mathbf{Y} \rangle - \varepsilon_y \langle \mathbf{X} \rangle. \tag{2.23}$$

The variance of the outcomes $\left(\Delta\mathbf{Z}\right)^2$, however, in general has the form

$$\left(\Delta\mathbf{Z}\right)^2 = \varepsilon_y^2 \left(\Delta\mathbf{X}\right)^2 + \varepsilon_x^2 \left(\Delta\mathbf{Y}\right)^2 + \varepsilon_x \varepsilon_y C_{XY}. \tag{2.24}$$

Thus, dependent on the signs of C_{XY}, ε_x, and ε_y the uncertainty can be reduced or increased. In particular, if the interaction parameters ε_x and ε_y are known, it is thus possible to choose a specific pointer state, such that the final uncertainty $\Delta\mathbf{Z}$ is minimized. Conversely, when choosing a MUS, for which always $C_{XY} = 0$, the resulting variance of $\mathbf{Z}$ has the simple form of a weighted sum of the variances of $\mathbf{X}$ and $\mathbf{Y}$.

A different sense in which a pointer states can be optimal is related to requiring minimal disturbance of the post-measurement state of the system, i.e., an optimal measurement. Assuming a canonical measurement of observable $\mathbf{A}$ with interaction strength ϵ, the generator $\mathbf{Y}$, an initially pure pointer state $|\chi\rangle$, and a pointer readout of $\mathbf{X}$ the Kraus and measurement operators $\mathbf{K}_x$ and $\mathbf{M}_x$ corresponding to outcomes x become [49]

$$\mathbf{K}_x = \sum_j \chi(x - \varepsilon a_j)|a_j\rangle\langle a_j|, \qquad \mathbf{M}_x = \sum_j |\chi(x - \varepsilon a_j)|^2 |a_j\rangle\langle a_j|. \tag{2.25}$$

Note that this description is only the limit of realistic measurements, since eigenstates of continuous observables are unphysical and always some coarse grained projective measurement of $\mathbf{X}$ is performed on the pointer instead. As introduced in Sec. 2.2.2, the requirement for minimal disturbance is $\mathbf{K}_x = \sqrt{\mathbf{M}_x}$, where a global phase on the Kraus operators can be neglected. For a canonical measurements this condition is satisfied independently of ε if and only if the phase of the wavefunction χ is constant, i.e., $\mathrm{Im}\left[\partial_x \chi\right] = 0$. For the CCO this also implies the condition $\langle\{\mathbf{X}, \mathbf{Y}\}\rangle = 0$. Thus, just as in the case of weak measurements, minimal disturbance implies a vanishing anti-commutator between the generator of pointer shift $\mathbf{Y}$ and the measured pointer observable $\mathbf{X}$.

2.4 Properties of Quantum Measurements

2.4.1 Informational Completeness and Quantum Tomography

A special type of measurements are procedures which try to determine the state of an ensemble of identically prepared quantum systems, called *quantum state tomography* (QST) or *quantum state estimation* [296, 223, 238]. QST is based on sets of *informationally complete* observables, which uniquely determine any quantum state through the corresponding set of expectation values [322, 95, 238]. For example, for a qubit the set of Pauli observables is informationally complete. An important tool of QST are so-called *symmetric informationally complete* POVMs (SIC-POVMs), see e.g., [325, 243, 288, 331]. A set of POVMs is symmetric if for any two POVMs $\mathcal{M}$ and $\mathcal{N}$ from the set it holds that all measurement operators $\mathbf{M}_j \in \mathcal{M}$ and $\mathbf{N}_k \in \mathcal{N}$ have equal overlaps $\mathrm{tr}(\mathbf{M}_j \mathbf{N}_k)$. SIC-POVMs correspond to *minimal* sets of informationally complete generalized observables which are

equally distributed with respect to the state space. Apart from states, also unknown quantum channels can be determined by preparing suitable sets of input states and performing QST on the output states, a procedure known as *quantum process tomography* [268, 311].

In experimental applications of QST due to finite statistics the measured expectation values will have a certain statistical error allowing only an approximate reconstruction of the state. In fact, these errors in the determination of state parameters might even lead to unphysical states, i.e., non-positive density operators. This makes it necessary to apply special reconstruction techniques, most prominently the *maximum-likelihood* method, which searches for the physical state yielding the measured values with highest probability [294, 296, 223]. However, these reconstruction methods are necessarily biased, causing systematic errors in the state estimation, see, e.g., [251, 199, 490] for analyses. Finally, since the experimental effort of QST scales exponentially with system size, especially for large quantum systems, the question of a most resource efficient QST is of crucial technical importance and various efficient approaches have been developed [296, 145, 308, 313, 328, 179, 490].

For continuous degrees of freedom a pair of CCO observables is not informationally complete even for pure states [702, 889, 95, 238]. Furthermore, since in practice the resolution of continuous observables is always necessarily coarse grained and for infinite dimensional discrete observables only a finite amount of projections into subspaces can be realized, any state reconstruction will be only approximate, independently of statistical errors. Typically this coarse graining is chosen fine enough such as to resolve the releveant features of the probability distributions with good approximation. Coarse grained informational completeness can be achieved for example by measuring the probability density of one non-degenerate continuous observable, together with the probability current [866, 889]. In fact, this method is applied in this work to measure a spatial wavefunction in one dimension in the context of the reconstruction of Bohmian trajectories, as described in Sec. 7.6. Another common scheme applied to the continuous degrees of freedom of the electromagnetic field is to measure suitable marginals of the Wigner distributions via optical interferometric homodyne detection as sketched in Sec. 5.4.3, which allows to reconstruct the full Wigner distribution and thus the state itself [223, 238].

2.4.2 Quantum Non-Demolition Measurements

In practice measurement operations are often described as projective measurements for simplification while the actual measurement interaction induces much more back-action than just a decoherence into the corresponding subspaces of the measured observable. A prime example are typical position measurements involving screens on which quantum particle impinge. In good approximation a flat screen allows to perform a coarse grained projective measurement of two position observables $\mathbf{x}$ and $\mathbf{y}$ corresponding to orthogonal spatial directions, where often square or rectangular subspaces are considered, i.e., so-called *pixels* on the screen. While the corresponding measurement operators $\mathbf{M}_{jk}$ are projectors defined by two intervals Ω_x^j and Ω_x^k in the outcomes spaces of $\mathbf{x}$ and $\mathbf{y}$, with $\mathbf{\Pi}_{jk} = \int_{\Omega_x^j \Omega_y^k} |x\rangle\langle x| \otimes |y\rangle\langle y| \, \mathrm{d}x\mathrm{d}y$, the corresponding channel is much different from the

corresponding projecting channel. Instead for massive particles such as electrons a complicated interaction with the material of the screen is involved which transforms the state of the particles much more significantly than just a projection into the subspace of the pixel and, in the case of photons, the particles are typically absorbed, i.e., destroyed and transformed into some excitation of the matter constituting the screen which necessitates a field theoretical description of the measurement interaction as sketched in Sec. 4.5. Another example are filters of spatial wavefunctions or polarization which can be described by a dichotomic observable. While for one of the outcomes, i.e, the "passing" through the filter, the system is in fact projected into the corresponding subspace, for the other outcome a much more significant disturbance or destruction takes place, the particular form of which depends on the filtering mechanism.

The examples presented above represent extreme cases of a disturbance of a quantum state due to measurement, which changes the statistical outcomes for a second application of the same measurement. In contrast, *back-action evading* (BAE) measurements are defined by the requirement $\forall j \, \mathrm{tr}(\rho \mathbf{M}_j) = \mathrm{tr}(\mathcal{C}[\rho] \, \mathbf{M}_j)$, i.e., that the probabilities for all outcomes are the same if the measurement is applied again to the non-selective post-measurement state $\mathcal{C}[\rho]$ [220, 49, 225]. A sufficient condition for BAE measurement of an observable $\mathbf{A}$ is that all Kraus operators commute with it, i.e., $\forall j \; [\mathbf{K}_j, \mathbf{A}] = 0$. A measurement is always BAE if it can be described in terms of a system-pointer model with an interaction Hamiltonian which commutes with the measured observable such as the prototypical product Hamiltonian considered in previous sections.

An even stricter notion of measurements which cause minimal disturbance is given by so-called *quantum non-demolition* (QND) measurements [253, 220, 252, 161, 225]. A QND measurement of an observable $\mathbf{A}$ is defined by the condition

$$\langle \chi | [\mathbf{A}, \mathbf{U}] | \chi \rangle = 0, \tag{2.26}$$

where $\mathbf{U}$ encompasses the total joint evolution of system and pointer and $|\chi\rangle$ the initial pure pointer state. It is a also implied by the stronger condition $[\mathbf{A}, \mathbf{U}] = 0$. While any QND measurement is BAE the converse is not true. For example a crucial ingredient of QND measurements is that any eigenstate of the observable is necessarily unperturbed, which is not necessarily the case for a non-efficient BAE measurements.

The practical implementation of QND measurements for various quantum systems, represents a significant technological challenge and is experimentally impossible for many observables [253, 252, 161]. A notable example is a measurement of the position of a photon [628], which does not destroy the particle and crucially also does not perturb its polarization degree of freedom. Furthermore, as discussed in Sec. 3.4.3, there exist fundamental limitations on the possibility of QND measurements of some observables due to relativistic constraints.

2.4.3 Quantum Zeno Effect and Protective Measurements

A famous consequence of the properties of quantum measurement is the so-called *quantum Zeno effect* [321, 298, 234, 642], a term coined by Misra and Sudarshan [310]. It describes

the possibility to slow down the evolution of a quantum system through repeated measurements. For a unitary evolution of the system according to a Hamiltonian $\mathbf{H}$, the probability $p(t)$ to find the system in its initial state $|\psi\rangle$ can be approximated to first non-vanishing order in the evolution time τ as [234]

$$p(\tau) = 1 - \left(\frac{\Delta \mathbf{H}}{\hbar}\right)^2 \tau^2 + \mathcal{O}(\tau^4). \tag{2.27}$$

If during time τ a number n of projective measurements including the projector $|\psi\rangle\langle\psi|$ are performed, then the probability to find the state in $|\psi\rangle$ in all of those measurements $p_n(\tau)$ is given by the product of the probabilities for each measurements as

$$p_n(\tau) \approx \left(1 - \left(\frac{\Delta \mathbf{H}}{\hbar}\right)^2 \left(\frac{\tau}{n}\right)^2\right)^n \approx 1 - \left(\frac{\Delta \mathbf{H}}{\hbar}\right)^2 \frac{\tau^2}{n} > p(\tau) \tag{2.28}$$

Thus, for short enough times τ, the state of the system can be forced to stay arbitrarily close to $|\psi\rangle$ if a sufficiently large amount of measurements is performed. Furthermore, for some types of Hamiltonians, there exists a regime of repetition times τ/n for which an increase of n actually leads to an accelerated decay known as the *anti-Zeno effect* [302, 298, 266]. Both effects have been observed experimentally, see e.g., [295, 265].

A concept closely connected to the Zeno effect are *protective measurements* as introduced by Aharonov and Vaidman [242], which correspond to measurements of a non-trivial expectation value of an observable $\mathbf{A}$ on a single copy of the state [241, 272, 337, 237]. In this scheme a weak measurement interaction with a small but effectively constant coupling strength g persists over some finite time interval τ, during which a system is projected back n times into its initial state $|\psi\rangle$. There can be scenarios in which such a projective operation can be implemented without knowing the state $|\psi\rangle$ such as switching on some unknown Hamiltonian which keeps the system in an unknown ground state [241, 272, 237]. If the free evolution of the pointer can be neglected, for example in the case that it commutes with the generator $\mathbf{B}$, the joint state $|\Psi\rangle$ of system and pointer after the n-th projection can be written as

$$|\Psi\rangle \approx \left(\mathbf{\Pi}_\psi \otimes \mathbb{1}\ (\mathbb{1} - \frac{i}{\hbar}\frac{g\tau}{n}\mathbf{A} \otimes \mathbf{B})\right)^n |\psi\rangle \otimes |\chi\rangle\,, \tag{2.29}$$

where $\mathbf{\Pi}_\psi = |\psi\rangle\langle\psi|$. Assuming a canonical measurement with the generator $\mathbf{B} = \mathbf{Y}$ and a measurement of the pointer observable $\mathbf{X}$ the shift of the expectation value becomes

$$\delta\mathbf{X} \approx n\varepsilon\langle\mathbf{A}\rangle. \tag{2.30}$$

Since canonical measurements do not increase the uncertainty $\Delta\mathbf{X}$, the effective change in the pointer expectation value can be made larger than the uncertainty for sufficiently high n. This allows to infer the expectation value $\langle\mathbf{A}\rangle$ from the protective measurement of a *single system* in an unknown states. Note that the protective scenario is formally equivalent to the weak coupling of the same pointer to n systems with interaction strength $\varepsilon = g\tau/n$.

2.5 The Measurement Problem

2.5.1 Decoherence

The formal apparatus of generalized quantum observables, as introduced in Sec. 2.2.2, allows to express the dispositive rules of quantum mechanics for any physical measurement scenario. Through the concept of quantum instruments it also predicts the statistics of outcomes of subsequent measurements, both on average as well as conditioned on the outcomes of previous measurements. Furthermore, based on the equivalence of generalized measurements and unitary system-pointer interaction, the dynamical laws of quantum mechanics allow to construct in principle an arbitrary deep description of the von Neumann chain, at least as far as the complexity of the involved systems and interactions permits. As more and more complex systems in the chain are reached, the field of *Decoherence* aims to provide an effective description of the emerging dynamical behavior through the formalism of open systems [346, 297, 224, 70, 327]. Note that the capital "D" is used to emphasize that while Decoherence is of course related to the generic phenomenon of decoherence due to interactions between quantum systems as introduced in the previous chapter, Decoherence as a research field, also called *decoherence program* [224, 1012], is engaged with the *specific* typical decoherence phenomena leading to *particular* effective evolutions of quantum systems.

An important result of Decoherence is the stability of macroscopic systems, i.e., it provides a physical explanation why macroscopic systems typically do not form coherent superpositions and thus do not interfere. Since the definite states of macroscopic systems are an empirical fact, they can be taken to represent a natural point where the Heisenberg cut is to be placed. Additionally, the Decoherence provides a natural criterion for the preferred basis in which the whole von Neumann chain collapses, i.e., the basis which contains definite macroscopic systems. This selection of a preferred basis is sometimes called *environment-induced superselection* or *einselection* [347, 49, 224]. In this sense decoherence is sometimes said to provide a "dynamical description of the quantum-to-classical transition" [320, 347, 224, 327].

2.5.2 Semantic Incompleteness

While for a range of typical systems Decoherence allows to trace the von Neumann chain from microscopic quantum systems to stable macroscopic objects, it does not solve the measurement problem [956, 964, 327, 942], i.e., the fundamental problem that QM cannot provide a physical explanation for the basic postulates of quantum measurement, as introduced in Sec. 2.1.2. It fully rests on deterministic unitary evolution and without additional theoretical structure still a Heisenberg cut has to be placed on some level of the description leading to a probabilistic ad hoc objectification. As expressed by Laundau and Lifshitz

> Thus quantum mechanics occupies a very unusual place among physical theories: it contains classical mechanics as a limiting case, yet at the same time it requires this limiting case for its own formulation. [53]

The metatheoretical requirement that the "measurement processes are governed by the same physical laws that they should test" can be called *semantic completeness* and is satisfied by many physical theories, for example the theory of relativity [931].

Of course from a strictly operational point of view, the semantic incompleteness of quantum mechanics does not pose a serious problem. As mentioned already in Sec. 1.2.4, according to some interpretations, chiefly QBism, even the quantum state itself does not represent a description of physical objects but only of subjective dispositive beliefs. Accordingly, neither the probabilistic nature of results nor the collapse are problematic, where the latter can be simply seen as an update of the subjective belief [422, 984, 1001, 1003]. Such operational approaches are entirely sufficient for the successful dispositive application of QM, i.e., they are sufficient *for all practical purposes* (FAPP) [966]. However, when physics is seen as an effort to, in the words of Bohr, actually "disclose the essence of the phenomena", be it only in an approximate and transient manner, a lingering on the level of an irreducibly dispositional character without any hope or ambition for descriptive content is entirely unsatisfactory. As put succinctly by Bell:

> Here are some words which, however legitimate and necessary in application, have no place in a *formulation* with any pretension to physical precision: *system*, *apparatus*, *environment*, *macroscopic*, *reversible*, *irreversible*, *observable*, *information*, *measurement*. [966]

2.5.3 Three Problems

Any descriptive interpretation of QM which solves the measurement problem, i.e., provides a physical explanation of the measurement process has to account for three critical aspects, as first formulated in terms of "three measurement problems" in an influential analysis by Maudlin [999], see also [222, 925, 995, 1011, 989]. The *problem of outcomes* concerns the uniqueness of the final measurement outcome, i.e., the question why only a single outcome is obtained in measurements performed on quantum systems in superposition states. This is also known as the *objectification problem* [222]. The second issue is the *problem of statistics* which corresponds to the question why the observed unique outcome happens to follow a probability distribution given by the Born rule. Finally, the *problem of effect* addresses the question why a collapsed state is the correct description of the future evolution of the system and what physical process leads to this collapse.

Given the contentious nature of quantum measurements, a myriad of possible solutions for the measurement problem have been proposed, each of which aims to provide answers to each of the three questions raised above. In fact, apart from clarifying the ontological content of QM, a solution of the measurement problem is the main motivation behind the various interpretations of quantum mechanics. Commonly three main realistic approaches are identified, namely *hidden-variable theories*, *collapse theories* and the *many worlds interpretation* (MWI), each providing a vastly different description of the physical world [944]. While the most prominent hidden-variable theory, Bohmian mechanics, is presented in more detail in chapter 7, in the following a brief overview over collapse theories and the MWI is given.

2.5.4 Collapse Theories

The fundamental concept of collapse theories, as first proposed by Ghirardi, Rimini, and Weber (GRW) [988] and in some sense already by Wigner [1022], is that the collapse of the wavefunction is a physical process, which immediately solves the problem of outcomes [944, 949, 950]. The particular variants of collapse theories then differ as to the exact physical mechanism of collapse, the ontological status of the wavefunction itself and its connection to experience. In Wigners interpretation a collapse occurs if a conscious observer becomes part of the von Neumann chain, as illustrated in the famous example of *Wigner's friend*. According to Wigner, since any conscious being has the experience of definite outcomes, the physical mechanism of collapse is to be found in the unique "physico-chemical structure" underlying consciousness, which can "modify the usual laws of physics" [1022].

Commonly "collapse theories" are understood in a more narrow sense as GRW-type theories in which the collapse mechanism is a universal element in the evolution of any quantum state, expressed explicitly in terms of an additional stochastic nonlinear term in the evolution equation [965, 1017, 1019, 950], as first proposed by Pearle [1007, 1006]. Unitary evolution thus becomes a limiting case and for sufficiently extended or massive systems the additional terms become relevant and lead to the nonunitary collapse. This modification of the evolution provides an explicit explanation for the problems of statistics and effect. Two prominent candidates for ontologies is either the psi-ontic so-called *mass-density ontology* [987, 965] where the wavefunction itself corresponds to a smeared out beable and the psi-epistemic *flash ontology* [967, 960, 1017], where the beables are point-like centers of the collapse events.

Due to the modified dynamics, collapse theories actually make predictions which differ from SQM and are thus testable. In particular, dependent on the parameters of the theory, superposition states of sufficiently massive or extended systems are impossible above a certain time-scale due to a very high probability of collapse. In consequence a range of experiments which produce superpositions of comparatively large systems can be regarded as tests of collapse theories, see [965, 950] for overviews. If for a certain scale of systems interference effects would disappear, and it could be verified that this is not due to environment-induced decoherence, this would constitute evidence for a physical collapse. See also [973] for a review of non-interferometric tests of collapse theories.

2.5.5 Many Worlds Interpretation

The MWI, based on the *relative state* interpretation proposed by Everett [983] and later pioneered by DeWitt [982], follows a decidedly different approach than collapse theories. While there are several variants, the essential core of the MWI is the exclusion of any collapse, either physical or add hoc due to a Heisenberg cut [1023, 980, 959, 1016, 943, 1010, 941, 1018, 954]. In the most common approach the ontology is exhausted by a single universal pure state, commonly called the *universal wavefunction*, which follows a strictly deterministic unitary evolution. In effect, observers themselves and in fact also the entire macroscopic world are part of a never collapsing von Neumann chain. The concept

of Decoherence then explains the emergence of a preferred decomposition of this global wavefunctions in terms of components which include well defined macroscopic objects [1024, 327, 942]. These components are commonly called *branches* or *worlds* [1010, 1019, 1018], or alternative even "universes" themselves in which case their totality is referred to as "the multiverse" [981, 941, 438]. A quantum process, which, similar to a measurement, involves the coupling of a quantum system with a system which is typically perceived in a definite state, i.e., a macroscopic object, then is said to *split* the world into several new ones, which crucially does not imply any deviation from unitary dynamics.

The MWI solves the problem of outcomes and effects by denying both the existence of objective outcomes and collapse. The experience of definite outcomes is typically explained by definite mental states of a conscious observer in each branch [982, 954]. This is taken to an extreme in the so-called *bare interpretation*, a gedankenexperiment by Albert [912], in which the post-interaction state $|\Psi\rangle$ of system and observer after a dichotomic measurement is assumed to be

$$|\Psi\rangle = \frac{1}{\sqrt{2}}\big(\,|\psi_A\rangle\,|o_A\rangle\,|u\rangle + |\psi_B\rangle\,|o_B\rangle\,|u\rangle\,\big) = \frac{1}{\sqrt{2}}\big(\,|\psi_A\rangle\,|o_A\rangle + |\psi_B\rangle\,|o_B\rangle\,\big)\,|u\rangle\,, \tag{2.31}$$

where the $\{|\psi_A\rangle\,, |\psi_B\rangle\}$ are two possible states of the system, $\{|o_A\rangle\,, |o_B\rangle\}$ represent the states of all the degrees of freedom of the observer which depend on the perceived outcome, and $|u\rangle$ represents the mental state of the observer corresponding to the conviction of having observed a unique outcome. Since the state $|u\rangle$ is the same in both branches, and thus factorizes, the observer will be in the definite state of being convinced of the uniqueness of outcomes, which factually is not the case.

Addressing the problem of statistics represents a notorious difficulty for the MWI, since it is non-trivial to explain the experience of quantum mechanical probability according to the Born rule, when, e.g., for a measurement with a discrete outcome space all options are always actualized [943, 1010, 958, 941, 1019, 1018]. The unitary evolution by itself only provides different amplitudes for each branch and no mechanism beyond that which could explain the empirically observed probabilities of particular outcomes, i.e., why observers "find themselves" in particular branches with the correct relative frequencies. The plethora of variants of the MWI which have been formulated propose a range of solutions for the problem of statistics, a survey of which would go far beyond the scope of this work, see e.g., [940, 445, 954] for overviews instead.

2.6 Measurements on Pre- and Postselected Systems

2.6.1 Time-Symmetry in the Measurement Process

The dynamical laws of QM, as expressed by unitary evolution, are fundamentally time-symmetric. In contrast, measurement collapse due to a selective measurement introduces an element of irreversibility and thus time-asymmetry into the description. However, as proposed early by Watanabe [809] as well as by Aharonov, Bergmann, and Lebowitz

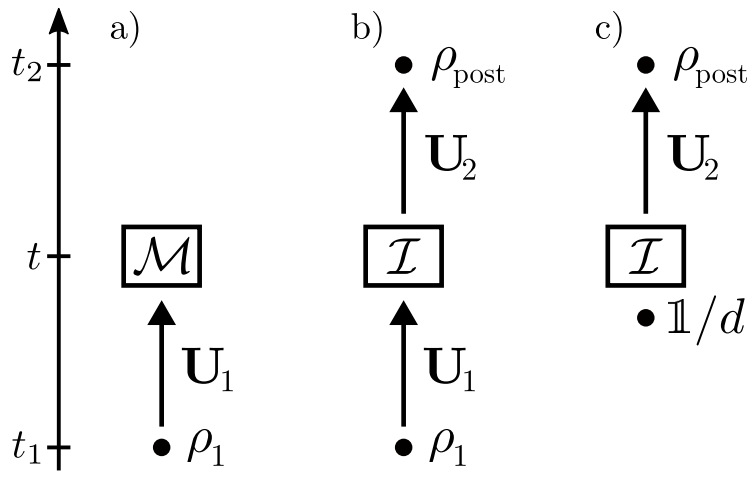

Figure 2.1: **Symmetry between Predicition and Retrodiction** The figure depicts three different measurement scenarios, a strictly predictive (a), a time-symmetric (b), and a strictly retrodictive (c). In scenario a) the system is preselected in the state ρ_1 at t_1 and evolves according to the unitary $\mathbf{U}_1$ until a measurement of the POVM $\mathcal{M}$ at time t. In b) the system additionally experiences an evolution according to $\mathbf{U}_2$ after the measurement and the outcomes of the measurement are conditioned on the postselection in state ρ_{post} at time t_2. Note that in contrast to a), also the quantum channel of the instrument $\mathcal{I}$ has to be taken into account. In case c) the system is preselected at an arbitrary time prior to the measurement in the least biased predictive state $\mathbb{1}/d$, is measured at time t and postselected at t_2 after evolution $\mathbf{U}_2$. If suitable states ρ_{post} are chosen, any distribution of outcomes obtainable in scenario a) can be reproduced in scenario c).

(ABL) [676], the standard statistical apparatus of QM can be seen simply as the *prediction* of outcomes of future measurements based on the outcomes of past ones and the same formalism can be employed to also express *retrodiction*. By including both prediction as well as retrodiction, the probabilities of outcomes of measurement on quantum systems can be expressed in a time-symmetric manner, which treats past and future boundary conditions on equal footing, see, e.g., [680, 673, 694, 762, 761, 796, 681, 278, 721, 777] for such time-symmetric approaches and [693] for a recent overview.

The formal equivalence of prediction and retrodiction can be shown by considering an arbitrary POVM $\mathcal{M} = \{\mathbf{M}_j\}$, measured at time t on system, prepared in some quantum state ρ_1 at time $t_1 < t$ and subject to the unitary evolution $\mathbf{U}_1$ between t_1 and t, as illustrated in Fig. 2.1a. The probability distribution of outcomes p_j is then given by the usual predictive relation $p_j = \mathrm{tr}\big(\mathbf{M}_j \rho_t\big)$, where $\rho_t = \mathbf{U}_1 \rho \mathbf{U}_1^\dagger$. Retrodiction can now be included by considering a conditioning on a future measurement, as shown in Fig. 2.1b. Since in this symmetrical scenario, the evolution after the measurement becomes equaly important, the description in terms of the POVM has to be extended to include the whole instrument $\mathcal{I}$ for which the post-measurement state is $\rho' = \sum_j \mathbf{K}_j \rho_t \mathbf{K}_j^\dagger$, where each outcome j is correlated with a conditional state $\rho'_j = \mathbf{K}_j \rho_t \mathbf{K}_j^\dagger / p_j$ and at this point of the derivation an efficient instrument is assumed. The system then evolves according to some unitary evolution $\mathbf{U}_2$

until a time t_2, at which it is in the state $\rho_2' = \sum_j p_j \mathbf{U}_2 \rho_j' \mathbf{U}_2^\dagger$. The crucial final step is a *postselection*, parametrized via a postselection state ρ_{post}, which is realized with a certain measurement at time t_2 together with a conditioning on only a subset of its outcomes.

In the case of a pure postselection state $|\phi\rangle$, the definition of the postselection is clear and simply corresponds to a conditioning on successful projection of ρ_2 onto $|\phi\rangle\langle\phi|$. However, in the general case of a mixed postselection ρ_{post} the interpretation of the postselection depends on the interpretation of the density operator, just as does the preparation. On a strictly operational level, the mixed postselection represents a randomized procedure in which the system is randomly postselected on one of the pure eigenstates $|\phi_j\rangle$ of $\rho_{\text{post}} = \sum_j q_j |\phi_j\rangle\langle\phi_j|$, chosen according to the probability distribution q_j. The average probability of successful postselection $p(\text{success})$ is then

$$p(\text{success}) = \sum_{jn} p_j q_n \langle\phi_n| \mathbf{U}_2 \rho_j' \mathbf{U}_2^\dagger |\phi_n\rangle = \text{tr}\big(\rho_2' \, \rho_{\text{post}}\big) \tag{2.32}$$

and the conditional postselection probability $p(\text{success}|j)$, given a certain outcome j accordingly is $p(\text{success}|j) = \text{tr}\big(\mathbf{U}_2 \rho_j' \mathbf{U}_2^\dagger \rho_{\text{post}}\big)$. Note, however, that crucially the randomness present in the postselection has to be independent from the randomness of measurement and preparation, i.e., they have to be purified with separate auxiliary degrees of freedom. This requirement of independent purification is exactly what makes it non-trivial to express a mixed postselection in terms of improper mixtures, i.e., irreducibly quantum randomness. A possible scheme is derived in Section V. of **[P1]**, as reprinted in Sec. 6.1.7.

By conditioning on successful postselection the probability distribution of outcomes j becomes modified as

$$p(j|\text{success}) = \frac{p(\text{success} \wedge j)}{p(\text{success})} = \frac{\text{tr}\big(\mathbf{U}_2 \mathbf{K}_j \mathbf{U}_1 \rho_1 \mathbf{U}_1^\dagger \mathbf{K}_j^\dagger \mathbf{U}_2^\dagger \rho_{\text{post}}\big)}{\sum_n \text{tr}\big(\mathbf{U}_2 \mathbf{K}_n \mathbf{U}_1 \rho_1 \mathbf{U}_1^\dagger \mathbf{K}_n^\dagger \mathbf{U}_2^\dagger \rho_{\text{post}}\big)}. \tag{2.33}$$

Thus, clearly the probability distribution p_j, observed for an arbitrary minimally disturbing POVM when preparing the system in state ρ_1 can be reproduced by a time reversal as shown in Fig. 2.1c, which involves a preparation of the system in the maximally mixed state $\mathbb{1}$ and a postselection on the state $\rho_{\text{post}} = \mathbf{U}_2 \mathbf{U}_1 \rho_1 \mathbf{U}_1^\dagger \mathbf{U}_2^\dagger$ at time t_2. In this case the state at time t resulting from the evolution of ρ_{post} back in time is equivalent to the state measured in the standard scenario, i.e., $\mathbf{U}_2^\dagger \rho_{\text{post}} \mathbf{U}_2 = \rho_t$. Note that if the instrument is not minimally disturbing, i.e., the Kraus operators are given as $\mathbf{K}_j = \mathbf{U}_j \sqrt{\mathbf{M}_j}$ with non-trivial and potentially varying unitaries, the situation is more complicated and a reproduction of the predictive statistics requires to perform different postselections dependent on the result j with $\rho_{\text{post}}^{(j)} = \mathbf{U}_j \mathbf{U}_2 \mathbf{U}_1 \rho_1 \mathbf{U}_1^\dagger \mathbf{U}_2^\dagger \mathbf{U}_j^\dagger$.

This possibility to reproduce outcome statistics via postselection represents a very general result which holds for arbitrary initial states ρ_1 and efficient instruments as long as the evolution of the system is unitary, i.e., reversible. However, since, as discussed in Sec. 1.4.3, any quantum channel can be dilated to a unitary evolution, such a time-reversal is in fact possible at least in principle for *any* scenario of a quantum measurement. The qualification "in principle" is necessary since there are of course FAPP irreversible processes such as

environment-induced decoherence. An inefficient instrument also corresponds to such a irreversible process since decoherence is introduced without the corresponding extraction of information, i.e., two different Kraus operators $\mathbf{K}_j$ are associated with the same outcome, making it impossible to apply the correct unitary $\mathbf{U}_j$ to the postselection states. Note, however, that this restriction only applies when the goal is to reproduce the outcome statistics via postselection using the *same* instrument as in the preselected case. Of course, if it is possible to choose the instrument, any behavior of a quantum system can be reproduced by an exclusively postselected system.

A special type of postselected scenario occurs if the postselection ρ_{post} commutes with the effective Kraus operators $\mathbf{K}'_j := \mathbf{U}_2\mathbf{K}_j$ or $\mathbf{K}''_j := \mathbf{U}_2\mathbf{K}_j\mathbf{U}_1$ for all outcomes j. In such cases the outcome statistics (2.33) would be unchanged if the postselection were performed directly before the action of the instrument $\mathcal{I}$ or even before the action of $\mathbf{U}_1$, respectively. While thus still the particular outcomes are generated only via conditioning on future results, there is a sense in which such a postselection can be effectively seen as a delayed preparation. Furthermore, when considering an instrument which is defined by the model of indirect measurement, as presented in Sec. 2.2.1, the various outcomes are correlated with different pointer states $|\chi_j\rangle$. Then, notably, if the postselection is commuting with the operation in the sense above, the reading of the pointer is determined by an incoherent mixture of the components $|\chi_j\rangle$ and, conversely, when the commutation is not given, the change in the distribution of outcomes corresponds to quantum interference between different pointer states.

The symmetry of expression (2.33) motivates to treat the preparation on equal terms as the postselection, which is why in the context of time-symmetrical QM it is called *preselection* ρ_{pre} accordingly, see, e.g., [676, 680, 762]. Thus, the final probability distribution of outcomes has to be regarded as a doubly conditioned distribution $p(j|\rho_{\text{pre}}, \rho_{\text{post}})$, conditioned both on a successful preselection and on a postselection. Just as the absence of a postselection can be modeled via $\rho_{\text{post}} = \mathbb{1}$, so can the absence of a preselection be expressed via a preparation in maximally mixed state, i.e., a "least biased predictive state" [278]. In consequence, any quantum system can be described as a *pre- and postselected system* (PPS). As it is always possible to express mixed pre- or postselection, as well as any non-unitary evolution via a purification, the time-symmetric description is more conveniently formulated in terms of pure states, taking into account all relevant degrees of freedom of all involved systems. This leads to the two-state-vector formalism, as introduced in Sec. 6.1.1. The latter also includes the concept of a "generalized state" which simply corresponds to a two-state description applied to subsystems. In conclusion, the dispositive indetermination of measurement outcomes in quantum mechanics opens the possibility to update the empirical description of a system conditioned on future information [680, 673, 681]. As put by Aharonov and Vaidman:

> In quantum mechanics, in contrast to classical mechanics, even if we have complete information about the past of a certain system, future measurements add information about the system at present. The maximum possible information about the quantum system based on the results of experiments performed both in the past and in the future is described by the generalized state [...]. It is a complete description of a

quantum system in the same sense that the quantum state in the standard approach is a complete description of a quantum system based on the results of experiments performed only in the past. [673]

2.6.2 Three Boxes, Pigeon Holes, and Cheshire Cats

The time-symmetric both predictive as well as retrodictive formula (2.33) can be rephrased by assuming pure pre- and postselection $|\psi\rangle$ and $|\phi\rangle$, both specified at time t such that no additional evolution has to be considered. If additionally only a projective measurement with projectors $\mathbf{\Pi}_j$ is considered, it simplifies to the famous *ABL-rule* [676] given as

$$p(j|\psi,\phi) = \frac{|\langle\phi|\mathbf{\Pi}_j|\psi\rangle|^2}{\sum_n |\langle\phi|\mathbf{\Pi}_n|\psi\rangle|^2}, \tag{2.34}$$

which described the conditional probability of observing outcome j [673]. This statistical prescription has been applied to simple prototypical pre- and postselected scenarios, which are described in figurative language allowing to contrast them easily with classical intuitions.

In the so-called *three-box-paradox*, as introduced by Aharonov and Vaidman [673], a system with a three-dimensional degree of freedom is considered, which is identified with a particle that can be found in a set of "boxes" $\{|A\rangle, |B\rangle, |C\rangle\}$. When the system is pre- and postselected in suitable states $|\psi\rangle$ and $|\phi\rangle$, which correspond to superpositions of boxes, a scenario can be constructed in which $p(A|\psi,\phi) = p(B|\psi,\phi) = 1$. Thus, the seemingly paradoxical result is obtained that the PPS particle will be found with certainty in box A as well as in box B. Note that this does not mean that (2.34) does not correspond to a proper probability distribution. Instead each test of the particle's presence in box j is given by a distinct sets of projectors $\{\mathbf{\Pi}_j, \mathbf{\Pi}_\perp\}$, with $\mathbf{\Pi}_j = |j\rangle\langle j|$ and $\mathbf{\Pi}_{j,\perp} = \mathbb{1} - \mathbf{\Pi}_j$. In effect, here and in the following the term "paradox" should not be understood as a failure of the theory e.g., through empirical results not reconcilable with it, but instead as a phenomenon violating classical physical intuitions or an apparent logical contradiction illustrating the need for a conceptual clarification [670, 768].

A related scenario is the so-called *pigeonhole paradox* [684, 686, 704] in which a set of three quantum systems is considered, each of which has the two dimensional degree of freedom, i.e., it can be in one of two boxes A or B. For suitably chosen pre- and postselection states the probability of succesfully measuring the system in a subspace corresponding to the projector $\mathbf{\Pi}_{\text{same}} := \mathbf{\Pi}^{jk}_{AA} + \mathbf{\Pi}^{jk}_{BB}$ is zero. Here the projector $\mathbf{\Pi}^{jk}_{nn} = \mathbf{\Pi}^{j}_{n} \otimes \mathbf{\Pi}^{k}_{n}$ is understood as the test whether particles j and k are both in box n and thus the projector $\mathbf{\Pi}_{\text{same}}$ corresponds to the test if both are in the same box. The result appears paradoxical since while there are three particles and only two boxes, no combination of two particles is ever found in the same box.

Finally, another famous paradox of that type is the so-called quantum *Cheshire cat* [684, 685, 708] consisting of a system which can be in one of two boxes but also possesses a second qubit degree of freedom. When such a system is pre- or postelected in a non-product state

between the spatial and the additional degree of freedom, a scenario can be constructed where the measurement of location with the projectors $\mathbf{\Pi}_A$ and $\mathbf{\Pi}_B$ finds the system with certainty in box A, while a local measurement of the other property, i.e., the projection onto $\mathbf{\Pi}_B \otimes \mathbf{\Pi}_j$, where $\mathbf{\Pi}_j$ is a particular state of the additional degree of freedom, also has non-vanishing probability. Speaking figuratively in reference to Carroll's famous tale, the "grin" of the Cheshire cat can be found were the cat itself cannot.

The interpretation of pre- and postselected scenarios such as these, has led to a prolonged controversy, see e.g., [701, 775, 736, 735, 800, 738, 745, 768, 681, 767, 807, 693]. All of the above paradoxes rest on an intuition similar to the EPR criterion of reality, as introduced in Sec. 1.1.1, where, based on the certainty or impossibility of measurement outcomes certain definite properties are associated with pre- and postselected ensembles. For example, since for no system in the pre- and postselected ensemble the Cheshire cat can be found in a certain box, it is concluded that this property corresponds to an element of reality for any member of the ensemble. If then a measurement of another property located in this box succeeds, the paradox is established. The common solution of all such paradoxes seems to be that even if the ascription of real properties in cases of probabilities 0 and 1 is valid, the pre- and postselection cannot be regarded as selecting a unique subensemble of quantum systems if arbitrary operations can be performed in between [701]. There is no reason to exclude that dependent on which measurements are factually performed, i.e., checking for example the presence in box A via $\{\mathbf{\Pi}_A, \mathbf{\Pi}_{A,\perp}\}$ or in box B via $\{\mathbf{\Pi}_B, \mathbf{\Pi}_{B,\perp}\}$, different subsensembles of systems are selected by the postselection. This means that there is no justification for the counter-factual attribution of properties, such as for example of "being in B" to particles in ensemble found with certainty in A [775, 735]. However, also an alternative solution has been proposed based on the concept of closest counterfactual worlds [802, 681]. The situation is different if the systems are described in terms of weak values, as described in Sec. 6.2.4, which are defined in the limit of vanishing disturbance.

Another aspect of the paradoxes emerging from the application of the ABL-rule (2.34) is a dependence on the *measurement context* [745, 767, 807]. Formally it is constituted by the dependence of denominator on the full set of projectors and not just on the outcome in question. Thus, even for the same projector $\mathbf{\Pi}_j$, the outcome probability depends in general on what other projectors or measurement operators are chosen. For example, in the three-box-paradox it is essential that exactly $\mathbf{\Pi}_j$ and $\mathbf{\Pi}_{j,\perp}$ are measured and in general the probability for outcome j is different if instead a triple of outcomes with projectors $\{\mathbf{\Pi}_A, \mathbf{\Pi}_B, \mathbf{\Pi}_C\}$ is employed. A similar effect is the failure of the *product rule* for PPS, i.e., the fact that even if the values of two *compatible* observables $\mathbf{A}$ and $\mathbf{B}$ are found with certainty to be a and b, the value of the product observable $\mathbf{AB}$ is not necessarily ab [442, 681, 671, 684]. This context dependence in pre- and postselected scenarios is a special case of the general contextuality of quantum observables as described in Sec. 3.2.2.

2.6.3 Practical Examples of Postselection

PPS are omnipresent in the experimental practice of quantum mechanics [765]. Apart from state preparation, experiments typically involve a plenitude of filtering procedures

preceding or coinciding with the final detection of the system in question. However, while formally the time-symmetric formalism allows to treat such pre- and postelection on equal grounds, fundamental practical differences remain. In particular, when a preparation yields an undesired outcome it is often possible to obtain the desired preselection state via application of a suitable unitary transformation [681, 671] or, if the latter is not possible at least the experiment can be aborted to conserve resources [765]. Both of these solutions are not available in the case of a failed postselection. However, while a preselection measurement has to be sufficiently non-demolition such as to achieve a certain conditional post-measurement state, this is not required of the postselection. In effect, there are many scenarios in which a postselection allows to realize a particular phenomenon with signficantly less experimental effort than just by tailoring a special preselected state.

One of the most basic physical examples of postselection is the dependence of the form of an interference pattern generated by polychromatic light on the frequency response functions of optical detectors [514, 517]. It is also present in everyday technological application such as optical telecom networks [700]. Furthermore, also many technological applications of QIT employ quantum states in particular of light which are only achieved via postselection. This includes postselection based quantum computing [177, 181], some schemes of optical quantum metrology [184, 765] as well as other heralded procedures such as teleportation or the generation of single photons and entanglement [455, 565, 667, 624]. Note, however, that while these applications of postselection are typically widely accepted as valid tools, attested by technological success, in particular in the case of teleportation the use of postselection has been also criticized at least at an early stage of the field [698]. A possible rebuttal to this particular criticism is the observation that for the teleportation experiments in question the postselection commutes with the relevant measurements, such that conceptually it can be regarded as a delayed preparation, as discussed in Sec. 2.6.1.

The scenario of quantum metrology represents a particularly important application of postelection [769, 159, 691, 692]. Given a system of interest, which interacts in a certain manner with pointer systems, in general the metrological resources can be quantified in three ways, i.e., the number of prepared pointers, the number of pointers interacting with the system of interest, or the number of detected pointer systems. Accordingly, sub-shot-noise sensitivity is called *super-sensitivity* if it is reached when counting interactions and *super-resolution* when only achieved through postselection. While some authors regard the number of interaction as the most fundamental metrological parameter of interest [159], there are also applications where both the preparation of probes as well as the interaction are much less resource intensive than the detection of the probes. A practical example of this scenario is detector saturation, where the detector has an upper limit on the rate of pointer systems it can detect, which is significantly lower than the rate with which the pointer systems can be prepared and made to interact. Additionally, usually the states necessary for super-sensitive metrology are highly sensitive to noise and, in contrast, postselection experimentally very simple [159]. In effect, in many cases postselection of pointers can yield a significant metrological advantage as exemplified in the procedure of weak value amplification, sketched in Sec. 6.1.4.

Chapter 3

Quantum Mechanics and Relativity

In this chapter the implications of relativistic constraints on the laws of quantum mechanics are investigated. Even without an explicitly covariant formulation, the clear formalism of quantum channels, operations and instruments allows to describe the profound implications of quantum theory on the spatio-temporal nature of physical systems. The chapter begins by introducing the notion of locality in the context of special relativity, which allows to present Bell's theorem about the consequences of the empirical behavior of quantum systems for any possible descriptive physical theory. Furthermore, based on the notion of Bell-correlations the concept of entanglement is introduced, alongside its most important properties and applications. The chapter closes with a discussion of the effects of quantum measurements and interactions on delocalized systems.

3.1 Locality

3.1.1 Minkowski Spacetime

The main insights of special relativity (SR) [17] is a maximal limit on the velocity of transmission of information, i.e., the velocity of light c and the *principle of relativity* which asserts that there is no single privileged reference frame [349, 422]. Together they imply significant consequences for a logically consistent description of physical systems in space and time. In particular, the comparison of times at different spatial locations is not well-defined and time has to be treated on equal footing as the three spatial dimensions, leading to a four dimensional coordinate system called *spacetime* in which coordinate points are given as *four-vectors* $v = (t, x, y, z)$ [349, 521, 422]. Due to the relativistic constraint of a maximal velocity spatial and temporal intervals are in general not invariant when transforming between descriptions in different reference frames, leading to the characteristic *length contractions* and *time dilations* of SR. Similarly, electromagnetic fields typically expressed in SR via a four-dimensional field-strength tensor, transform characteristically under changes of reference frame [523, 349]. In contrast, the *spacetime distance* between any two spacetime points as defined via the *Minkowski metric* is invariant for all *inertial*,

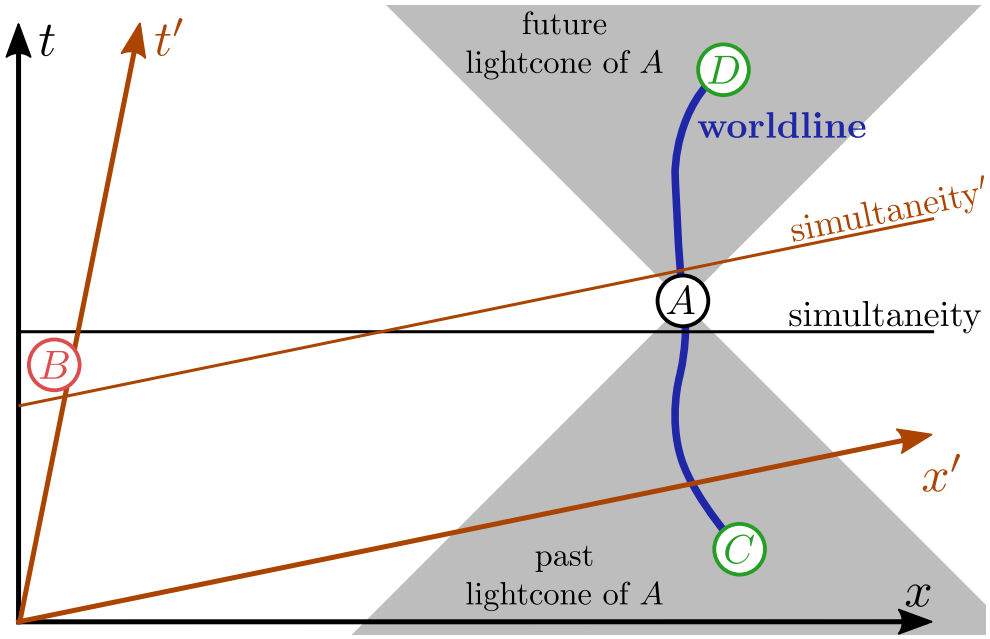

Figure 3.1: **Example Minkowski Diagram** The coordinate system (x', t') is boosted with respect to (x, t), where the tilt of the coordinate axes indicates the different definitions of same time and same location in the two reference frames and straight lines parallel to the spatial axes correspond to hyperplanes of simultaneity. The gray shaded areas represent the lightcone of event A. While C and D are time-like separated from A and thus it is possible to connect all three with a wordline, this is not possible for the space-like separated B. Instead, it is illustrated that dependent on the choice of coordinate system, B can occur before or after A and thus no definite time-ordering between the two events exists.

i.e., non-accelerated reference frames. Spacetime equipped with the Minkowski metric is called *Minkowski space* $\mathbb{M}$.

The full class of transformations under which the set of inertial frames is closed are called *Poincaré transformations* which include spacetime translations as well as *Lorentz transformations*, i.e., coordinate rotations and discontinuous changes in the velocity of the coordinate system, also called *boosts* [521, 580]. To additionally account for the effects of acceleration of the reference frame, which is equivalent to the effect of gravity, the theory of *general relativity* is necessary. However, the incorporation of general relativity into quantum theory still represents an open problem, see e.g., [955], and, for the range of phenomena treated in this work, a description in terms of SR is an excellent approximation.

The spacetime relations between physical objects are conveniently visualized via two-dimensional so called *Minkowski diagrams* in which only the dimension of time and a single spatial direction is depicted [349], as shown in Fig. 3.1. This allows to easily compare the description from the point of view of different reference frames for many practical scenarios which can be expressed in terms of a single significant spatial direction. In a Minkowski diagram, straight lines parallel to the spatial axis of a particular reference

frame represent hyperplanes of simultaneity, which differ for reference frames moving with different velocities. A *trajectory* $\vec{x}(t)$, i.e., a function which assigns a definite value for each of the three spatial coordinates at each point in time is represented in spacetime via a so called *world-line* [521, 349]. A pair of spacetime points defining a spacetime interval is called *time-like* if $c|t_2 - t_1| > |\vec{x}_2 - \vec{x}_1|$. Time-like separated points have a well-defined temporal ordering in any inertial reference frame and can be connected via a straight world-line with a velocity smaller than c, i.e., it is possible to send a signal from one of them to the other. The opposite case is denoted as *space-like* and equality in the expression above corresponds to *light-like* behavior. These relations are summarized in the concept of a *lightcone*, which for any spacetime point defines the region of points which are time-like related. Additionally, for many practical scenarios it is very useful to define *parties* or *sites*, which are given as confined spacetime regions, representing for example a certain laboratory in which an operation is performed for a certain amount of time. Usually several such parties are considered which are separated by spacetime distances much larger than their particular spacetime extensions, such that they can be essentially treated as single spacetime points with well-defined lightcones.

3.1.2 Formal Locality

The spacetime description of physical systems is fundamentally connected with the notion of *locality*, which can have different meanings, broadly divided into a formal and a physical meaning. Physical locality is typically connected to causal relationships between physical phenomena, as discussed in the next subsection. In consequence, the negation of locality called *nonlocality* also has different meanings dependent on which particular type of locality is absent.

The formal meaning of "locality" concerns the mathematical form of functions. A function is *local* if it has only on a single spacetime coordinate as its argument, i.e., when it is a map $\mathbb{M} \to \mathbb{S}$ from Minkowski space $\mathbb{M}$ to some output space $\mathbb{S}$. A basic example of a local function is the quantum wavefunction $\psi(\vec{x}, t)$ introduced in Sec. 1.2.2. The terms *time-local* and *space-local* are used to denote locality of a function solely with respect to time or space coordinates, respectively, i.e., a function can be time-local but not space-local and vice versa. A local function in the sense above is both time- and space-local.

Additionally, two local spacetime functions $f(\upsilon)$ and $g(\upsilon)$ are said to be *nonlocally connected* if the mapping between them has the form [562, 647]

$$f(\upsilon) = \int_{\mathbb{M}} g(\upsilon')K(\upsilon, \upsilon')\mathrm{d}\upsilon', \tag{3.1}$$

with a kernel function K which is not a delta function in the four spacetime coordinates, i.e., the value of f at point υ depends on the value of g at several points.

Finally, a local function is called *localized* in space at a particular point in time if at that time it has a spatial support which is confined on a certain reference length scale. The extreme of a localized function is the spatial delta function $\delta(\vec{x} - \vec{x}_0)$, which is fully localized at position $\vec{x}_0$. The opposite case is called *delocalized* in space accordingly and of

course in general a function can be localized in some spatial directions and delocalized in others. Also commonly, locality is not taken to require that the magnitude of the function vanishes completely outside the region of localization but it is sufficient that its values are below a certain threshold value or decay sufficiently fast, such as for example the tails of a Gaussian distribution. In the same manner it of course possible to define a function localized in time.

3.1.3 Locality of Interactions

The principle according to which physical influences always propagate through space with a finite speed, in contrast for example to Newtonian gravity, was present in human thought about nature since antiquity [918], and was coined *locality* or *Nahwirkungsprinzip* by Faraday around 1830 [521, 356]. The terms "influence" or "effect" here indicate a *causal* analysis of physical processes in which a certain physical event can be identified as a *cause* of another. In the physical description there are essentially two ways in which such a causal connection between two spacetime events can be established. The first option is the propagation of a localized physical system from one event to the other, such as for example in the case of a particle which is emitted at one location and absorbed at the other. Alternatively, also without propagating systems, a chain of interactions between physical systems located in between the two events can transfer the effect, as for example in the case of a wave propagating through a medium. Arguably this understanding of causal relationships is close to a *mechanist* understanding of causality [918], as developed by Salmon [939, 938]. The limited propagation speed of such physical effects leads to the principle of *locality of interactions*, which posits that during some finite time interval any physical interaction can affect only a finite spatial region around a point of interaction. Conversely, these interactions can be suppressed if the propagation of effects is blocked. As expressed pointedly by Wilczek:

> The concept of 'locality' [1], in the crude form that one can predict the behavior of nearby objects without reference to distant ones, is basic to scientific practice. Practical experimenters —- if not astrologers —- confidently expect, on the basis of much successful experience, that after reasonable (generally quite modest) precautions to isolate their experiments from the environment they will obtain reproducible results. [552]

Due to the the upper bound on the propagation velocity, a system of interest can even be regarded as perfectly isolated from systems which are sufficiently far away. It has been shown that, given the principle of relativity, locality of interactions necessarily implies a spatial continuum of degrees of freedom and accordingly all interactions in contemporary quantum field theory, as discussed in Sec. 4.3.1, are local and all effects are mediated via continuous field perturbations which propagate inside the light cone [512, 422, 552].

The principle that the causes of each physical phenomenon can only lie in its past, given by the past lightcone, is known as *relativistic causality* (RC), where here for simplicity, in

[1] The single quotes indicate a highlighting in the text.

contrast to [450, 453], it is taken to include the condition that any cause must always precede its effects and thus cannot lie in the *future* lightcone. An interaction which is nonlocal in this sense, i.e., is based on the propagation of a physical effect with a velocity larger than c, is commonly called "action-at-a-distance" or "Fernwirkung" as coined by Einstein, see e.g. [917]. The special role of the spatial degree of freedom in the context of interaction is also connected to the enduring question whether all physical measurements are ultimately reducible to position measurements [896, 918], as also discussed in Sec. 7.2.1.

3.1.4 Local Causality

In contrast to the mechanist notion of cause of effect, as described above, which is concerned with interactions, there exists also a statistical notion [951], as pioneered by Reichenbach [936]. It is typically defined based on statistical correlations between physical events, which can be for example settings of laboratory devices or outcomes of measurements. The sequence of events of a certain type can be described by a random variable with a corresponding probability distribution. Although for space-like separated events there is no unique definition of simultaneity, local sequences of events can be grouped into a joint distribution by, for example, considering their local time-ordering, which in turn allows to analyze their correlations. According to the *common cause principle* (CCP), formulated by Reichenbach, any statistical correlation between two events which does not disappear when their joint distribution is conditioned on the distribution of some other events indicates a causal connection between the two [936, 918, 377, 360, 951]. If in turn the correlation disappears, the conditioning is said to *explain* the correlation, and the condition event is referred to as a *decorrelating explanation*.

The statistical definition of causal influence has the great advantage that it is formulated in terms of empirically accessible observations and does not require a recourse to potentially unobservable microscopic events involved in mechanistic causal explanations, as discussed in the preceding subsection. It was Bell [368, 371] who first connected the physical notion of the locality of interactions with a statistical notion of causality. By considering events A and B at space-like separated sites, RC can be expressed based on the CCP via the statistical condition

$$\forall A, B, C \quad p(A|B, C) = p(A|C), \tag{3.2}$$

and vice versa for B, where C represents the totality of all events in the past of A. This statistical condition has been labeled *local causality* (LC) by Bell [371, 417, 450, 453].

3.1.5 Particles, Fields and Waves

The spacetime description of physical systems also allows to distinguish physical phenomena into *particles* and *fields* or *waves* [239, 997]. This stands in contrast to notion of "particles" introduced in Sec. 1.2.2, which pertains to identical elementary quantum systems. Although the distinction between particles and waves is not entirely clear cut [397,

952], particles are commonly associated with well-localized systems, sometimes up to the point of being identified with single point in space in which case they are called *point-like*. As such, particles typically possess at least to some degree of approximation a definite trajectory. In contrast, fields are continuous and delocalized objects characterized by a time-dependent potentially vector valued function $\vec{f}(\vec{x}, t)$ defined on spacetime. If a field represents an oscillating solution of a wave-equation, it is commonly called a "wave", such as the wavefunction of QM. Quantum fields, as introduced in Sec. 4.3, accordingly correspond to operator-valued functions on spacetime.

The *wave-particle duality* [240, 239] expresses the fact that quantum systems when described in terms of spatial wavefunctions possess both the characteristics of particles and waves. While their evolution and interaction is expressed in terms of delocalized waves governed by Schrödinger-type wave-equations, upon a spatial measurement the wave typically collapses to a much smaller volume in which the measurement takes place and the whole discrete package of the systems energy is found at that confined spacetime location. This duality of properties is not a problem from the point of view of a strictly operational dispositive understanding of QM, where the wavefunction is simply a tool to predict the outcomes of observations on the system. If, however, the wave is considered a beable, i.e., it is assigned a descriptive character, as for example a delocalized mass density in certain variants of collapse theories, the transition from wave to particle behavior represents a serious difficulty which essentially corresponds to the measurement problem in the spatio-temporal domain. In fact, as argued by several authors, for any psi-ontic theory the collapse of the wavefunction is itself an action-at-a-distance, in which an extended object, i.e., the wave, seizes to exist at remote locations due to some local measurement interaction [936, 939].

3.2 Bell's Theorem

3.2.1 The EPR Argument

One of the first and arguably most influential analyses of the problem with RC in quantum mechanics is the argument presented by EPR [18]. The gedankenexperiment introduces a pair of quantum particles at two space-like separated locations sharing a joint quantum state in which both their positions as well as their momenta are perfectly anti-correlated. As discussed in Secs. 2.1.2 and 2.1.3, due to the incompatibility of position and momentum measurements, it is impossible to formulate a quantum description of the system which predicts the values of both observable quantities for each particle with arbitrary precision, i.e., a precision below the limit implied by the uncertainty relation (2.1). Furthermore, RC implies the impossibility for a measurement at one site to have any effect on the other particle, in particular it cannot affect its real physical state if such is assumed to exist. The argument proceeds with the claim that by choosing to perform one of two complementary measurements, i.e., a position or a momentum measurement, on one of the particles, it is possible to predict the values of the respective observable quantity for the

other particle with certainty. Then, at least according to the EPR definition of beables, as discussed in Sec. 1.2.1, the values of these quantities must be causally connected to an underlying real physical state, which crucially must *simultaneously* determine the values of *both* complementary observable quantities [351]. This determination, however, is absent and even fundamentally impossible in SQM.

In summary there seem to exist two alternatives. Either the measurement at one site affects the physical state of the particle at the other, leading to a violation of RC, or the quantum mechanical underdetermination of measurement outcomes, as given by the uncertainty relations, is not the most exhaustive local description of physical systems, i.e., quantum mechanics is "incomplete" [927, 411]. Since EPR categorically reject a violation of RC, they opt for the latter. The conclusion seems to imply that there exists an alternative description of the systems, i.e., a hidden-variable theory as introduced in Sec. 1.2.4, which provides a local model predicting the results of both position as well as momentum measurements for each of the particles. In the ensuing decades of debates about the EPR argument this particular type of local hidden-variable theory postulated by EPR has been shown to be impossible in two distinct manners. First, as discussed in the next subsection, a series of no-go theorems has been formulated on strictly mathematical grounds, which assert that in general independently of relativistic considerations, it is impossible to formulate a hidden-variable theory which predicts the values of all complementary observables with certainty and is still dispositively consistent with quantum mechanics. Notably, these theorems do not rule out the general possibility of local hidden-variable theories of a more general nature. However, second, Bell's theorem, as discussed in detail in the remainder of this section, indicates the impossibility of the completion of quantum mechanics in a different sense by showing that the acceptance of a local hidden-variable theory of any kind would necessarily imply certain highly unusual properties of the physical universe, i.e., parallel worlds or superdeterminism.

Notably, several years after the original formulation of the EPR argument, Bohm introduced an even more simple and concise formulation of the EPR scenario [48, 373], around which, until today, most discussions about the seemingly nonlocal effects of quantum mechanics revolve. In Bohm's example the continuous spatial degrees of freedom from the EPR example are replaced by two correlated qubits, which were originally introduced as the spin degrees of freedom of spin-$\frac{1}{2}$ particles. The measured bivariate observables are the spin orientations in x, y and z-direction, as well as intermediate directions, which is the reason why typically a measurement setting is identified with the "orientation" or "direction of a measurement". The EPR argument is reproduced by assuming a singlet state of the two systems, where a perfect anti-correlation of results is observed when both particles are measured with respect to any product observable $\vec{b}\vec{\boldsymbol{\sigma}} \otimes \vec{b}\vec{\boldsymbol{\sigma}}$ with same projections at both sites. This provides a way to measure "an arbitrary component of the spin of [a] particle [...] without in any way disturbing that particle" [48] in analogy to the argumentation of EPR.

3.2.2 No-Go Theorems for Hidden-Variables

As already mentioned in Secs. 1.2.4 and 2.1.2, there exist a range of so called *no-go theorems*, first formulated by von Neumann [4], Gleason [94], Bell [87], as well as Kochen and Specker [96], which put significant restrictions on the possibility to explain results of quantum measurement in terms of hidden-variable models in a way compatible with the statistical predictions of quantum mechanics, see also [935, 102, 925, 413, 861, 66, 67, 80, 101]. This impossibility is encapsulated by a distinction between *contextual* (CHV) and *non-contextual* hidden-variable theories (NCHV), first introduced by Bell [87], who originally did not yet use these exact terms. In NCHV theories a set of system parameters is assumed such that the measurement of *any* quantum mechanical observable on the system is fully determined by those parameters, independently of the *context*, i.e., independently of other observables which are measured or properties of the measurement device. They correspond to a "map from observables to random variables which is such that the joint statistics of any family of commuting observables are preserved" [819]. Thus NCHV do not just concern the general possibility to explain measurement outcomes with physical models based on additional parameters not present in the quantum description, but crucially impose additional constraints on those parameters. In fact, the early no-go theorem by von Neumann [4], which considers only NCHV, has been very influential in fostering a prevailing but wrong conviction in the quantum physical community about a fundamental impossibility of hidden-variable extensions of quantum mechanics [918, 872, 920, 68, 105], leading, e.g., Bell to state that he "saw the impossible done" in Bohm's interpretation of quantum mechanics, as presented in Chapter 7 [829]. Early criticism of von Neumanns proof by Hermann [23] went unnoticed and only with Bell's distinction between CHV and NCHV, as motivated by Bohm's proposal [838], the possibility of hidden-variables was rehabilitated.

All no-go theorems for hidden-variables concern exclusively NCHV and are based on showing that it is impossible to simultaneously assign definite values to a set of observables defined on an at least three-dimensional Hilbert space. The non-contextuality is introduced by requiring that results of measurements of algebraic combinations of operators, e.g., sums or products, correspond to the same algebraic combination of the assigned values, see, e.g., [935, 91, 80, 67] for overviews. The impossibility of NCHV extensions has also been confirmed experimentally by the recording of corresponding measurement results for a suitable set of observables [110, 415, 107, 172, 629].

3.2.3 Empirical Test of Completeness

In a seminal insight by Bell, the question of the general possibility to complete quantum mechanics in a local manner was made empirically accessible by relating it to the statistical expression of relativistic causality, i.e., LC [368, 371]. Bell proposed an empirical test in which a particular set of results of measurements on a pair of quantum systems is observed, which fundamentally escapes a local causal explanation under a small set of very basic additional assumptions. This result is known as *Bell's theorem* [348, 355]. Note

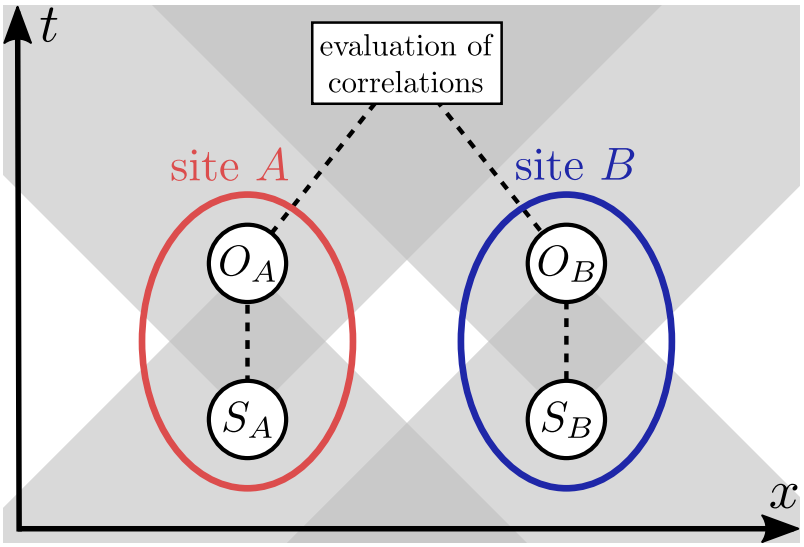

Figure 3.2: **Bell-Scenario** The settings S_j and observations O_j at sites A and B are sufficiently far away compared to their separation in time, such that the choice of each setting is space-like separated from the conclusion of the measurement process at the other site. Correlations between the outcomes can be evaluated at a spacetime point in the common future.

that, while the historical genesis of Bell's theorem is non-trivial and in particular the two formulations of 1964 [368] and 1976 [371] contain different but essentially equivalent arguments, the discussion presented here aims, following Wiseman's insightful account [450, 452], to describe the essential structure of Bell's theorem in a manner that clearly indicates the possible conclusions common to both formulations.

If indeed a more complete causal description of the EPR scenario exists, which can be reconciled with RC, LC indicates that in principle it should be possible to find a decorrelating explanation for all correlations between the two parties if all physical properties in the past are considered. This is of course unfeasible since it is practically impossible to be aware of all physical properties in the past of such complicated physical systems as measurement devices in laboratories. Furthermore, there might exist inaccessible hidden-variables which are unknown either merely for practical reasons or even due to some fundamental constraints. The ingenious solution proposed by Bell was to consider experimental interventions at the two sites, which can be considered as independent from all parameters in the past, as illustrated in Fig. 3.2. Taking into account interventions and hidden-variables, the condition of local causality (3.2) can be rewritten as [450, 453]

$$\forall\, O_A, O_B, S_A, S_B, C, \lambda \quad p(O_A|S_A, O_B, S_B, C, \lambda) = p(O_A|S_A, C, \lambda), \tag{3.3}$$

and vice versa for O_B where the events at each site j are divided into *observations* O_j and *settings* S_j, and the events in the past into accessible parameters C and hidden-variables λ. The settings S_j represent the experimental interventions which are assumed to be not causally linked to the past physical parameters of the systems, known as the assumption

of *free choice* (FC). Together with the CCP, FC implies that the settings S_A and S_B are statistically uncorrelated with C and λ.

A final assumption which is not stated explicitly in the original treatment by Bell is the actual existence of correlations such as those introduced in the EPR scenario, which here are called *Bell-correlations*. EPR take it for granted that upon measurement at each site a collapse occurs and a single definite record of an outcome is generated. After the records from both sites are brought together in the common future, correlations between outcomes can be evaluated. However, this is by no means the only logical possibility as for example, if the measurement apparatus and the local observers are also regarded as quantum systems, it could be that several incompatible records of the outcome persist in superposition at each site and a correlation of the various outcomes happens only in the common future. This is the case for example in the MWI, in which no correlation between the outcomes for the two space-like separated systems exists at any time before they are brought together. Here, this assumption is called *existence of Bell-correlations* (EBC). It has also been called "macroreality" [450, 453] or a "one-world" assumption [445].

Following Bell's original formulation, dichotomic measurements in two bases at each site are considered where the two outcomes for each basis are labeled identically. Then, if EBC is assumed to hold, a joint distribution of relative frequencies of outcomes $P(O_A, O_B|S_A, S_B, C)$ conditioned on the settings and empirically accessible parameters is given as

$$P(O_A^{(j)}, O_B^{(k)}|S_A^{(m)}, S_B^{(n)}, C) \approx \mathrm{tr}\left(\rho_C \cdot \mathbf{\Pi}_m^j \otimes \mathbf{\Pi}_n^k\right), \tag{3.4}$$

where $\mathbf{\Pi}_m^j$ is the projection onto the j-th eigenstate of the observable m at one of the sites with $j, k, m, n \in \{1, 2\}$ and the past known parameters are subsumed in the effective quantum state ρ_C. The expression above represents the dispositive quantum mechanical model for the prediction of the empirical results at the two sites, which becomes arbitrarily precise with an increasing number of measurements. Following [450, 453], the symbol "P" is used here in contrast to "p" for the probability distributions to indicate that P is an empirically obtained distribution.

3.2.4 The Theorem and its Consequences

The basic assumptions of Bell's theorem can be summarized as follows:

RC (Relativistic Causality)	Causes of an effect only lie in its past lightcone.
CCP (Common Cause Principle)	Correlated events are either causally connected or possess a decorrelating common causal explanation.
FC (Free Choice)	Experimental settings are causally independent from the relevant past parameters of the experimental scenario.
EBC (Existence of Bell-Correlations)	There exists a correlated distribution of definite outcomes at two space-like separated sites while the records are still separated.

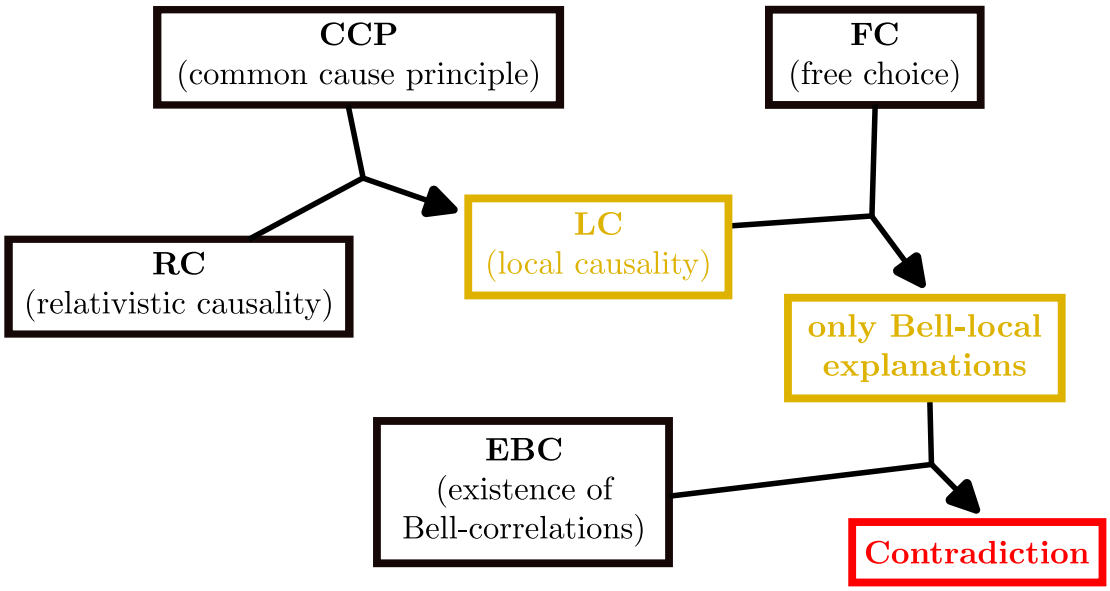

Figure 3.3: **Structure of Bell's Theorem** The black boxes indicate the four basic assumptions and the golden boxes derived propositions. The joined arrows indicate that the conjunction of two properties logically implies a third. RC and CCP together imply LC, which in turn together with FC implies the necessity to apply Bell-local models for an explanation of observed correlations. Assuming EBC, there exist correlations which cannot be explained by a Bell-local model and thus a contradiction emerges.

As illustrated in Fig. 3.3, RC and CCP together imply LC. From LC and FC it follows that any decorrelating explanation of that distribution has the form [450, 453]

$$P(O_A, O_B|S_A, S_B, C) = \sum_\lambda p(O_A|S_A, C, \lambda)p(O_B|S_B, C, \lambda)p(\lambda|C), \tag{3.5}$$

where the correlations in the joint distribution can be generated by appropriate dependence on the *local rules* $p(O_j|S_j, C, \lambda)$ on the hidden-variables. Such an explanation is called a *Bell-local* model [450, 453]. The point is now that there exist quantum states which lead to distributions P which cannot be reproduced by a Bell-local model. The most prominent manner to prove this is the so called *CHSH inequality* derived by Clauser, Horne, Shimony, and Holt [381] which is typically written in the form [1025, 355]

$$S_{\text{CHSH}} := \left|\mathbb{E}\left[S_A^{(1)}, S_B^{(1)}\right] - \mathbb{E}\left[S_A^{(1)}, S_B^{(2)}\right]\right| + \left|\mathbb{E}\left[S_A^{(2)}, S_B^{(1)}\right] + \mathbb{E}\left[S_A^{(2)}, S_B^{(2)}\right]\right| \leq 2, \tag{3.6}$$

where S_{CHSH} is known as the *S-value* and $\mathbb{E}\left[S_A^{(j)}, S_B^{(k)}\right]$ denotes the expectation value deduced from $P(O_A, O_B|S_A^{(j)}, S_B^{(k)}, C)$ for a measurement with setting j at site A and setting k at site B. Note that the operators are normalized such that the two results are ± 1. The bound of 2 can be violated if and only if the model is *not* Bell-local [388]. The maximal S-value achievable according to the laws of quantum mechanics, as given by the relation

(3.4), is $2\sqrt{2}$ [379, 404], which is sometimes called *Cirel'son bound* after Cirel'son [484, 629].

The impossibility to explain all empirically obtained distributions by Bell-local models leads to the prodigious conclusion that at least one of the four basic assumption has to be false. In fact, the negation of each of the four assumptions can be associated with a family of interpretations of quantum mechanics. The impossibility of FC is the hallmark of so-called *superdeterminism* [370, 991, 961] which broadly states that measurement settings are necessarily correlated with the hidden-variables in such a way that exactly reproduces the correlations. Usually they are regarded as introducing a huge explanatory cost since a hidden mechanism needs to be postulated which determines the outcome of any process to choose measurement settings no matter how complicated it is, see e.g. [962]. The negation of EBC is the defining property of MWIs, as introduced in Sec. 2.5, which negate collapse and posit that for any measurement all outcomes are realized and exist in parallel [438, 444, 445]. Another proposal, which also can be understood as a negation of EBC, is the postulate that the correlations are established via Einstein-Rosen bridges [19], which effectively suspend the space-like separation between the two sites [820, 409, 434, 403].

Commonly, FC and EBC are taken for granted and Bell's theorem is said to "rule out local realism", see e.g. [384, 432, 433, 437, 642], where the term was first used by Clauser and Shimony [380] as well as by Mermin [412]. Here "local" clearly is related to RC and its negation leads to theories which explicitly contain action-at-a-distance, such as Bohmian Mechanics introduced in Chapter 7 or GRW-type collapse theories. Notably, Bell himself also strongly advocated to take such options seriously, see, e.g., [87, 829, 968, 967]. A particularly extreme violation of RC is given by retro-causal approaches which admit a causal influence on the past [419, 429, 383]. In contrast, the other option to resolve the contradiction via a "negation of realism" is notoriously ill-defined in the literature on Bell's theorem, see, e.g., [410, 833, 416, 411, 450, 355] for criticisms. However, the causal analysis [450, 454, 453] presented here allows to provide a clear definition for this proposition as the negation of the general validity of the CCP. This means that if the other three assumption are kept, essentially no explanation in the conventional sense can be given for the observed correlations. This statement is far off from claiming a general impossibility of a realistic understanding of physics and also seems to be the way in which Bell understood a rejection of "realism" as he writes "... we have lost the idea that correlations can be explained, or at least this idea awaits reformulation" [370]. For example, as suggested in [377, 453], the notion of common causation and decorrelating explanation might be separated in the CCP to arrive at an entirely novel concept of common cause. In this case the question appears whether a theory not providing causal explanations is at all a proper *physical* theory and in what sense the other three assumptions can be said to be conserved. From a decidedly operationalist point of view, see, e.g. [447], a strictly dispositive prediction rule of the form (3.4), i.e., SQM, as defined in Sec. 1.2.4, is entirely sufficient as long as crucially it is consequently not attributed *any* descriptive meaning. However, the value of preserving RC or FC may be seen as questionable if the descriptive function of the theory is fundamentally lost, as put pointedly by Maudlin:

> But even supposing that somehow abandoning realism in quantum theory could preserve locality, we would have to wonder about the point of making such a bargain. Physicists have been tremendously resistant to any claims of non-locality, mostly on the assumption (which is not a theorem) that non-locality is inconsistent with Relativity. The calculus seems to be that one ought to be willing to pay any price - even the renunciation of pretensions to accurately describe the world - in order to preserve the theory of Relativity. But the only possible view that would make sense of this obsessive attachment to Relativity is a thoroughly realistic one! These physicists seem to be so certain that Relativity is the last word in space-time structure that they are willing even to forego any coherent account of the entities that inhabit space-time. [410]

In conclusion, any attempt to seek a more complete local theory, as motivated by the EPR argument, is shown to be destined to fail in the sense that even if quantum mechanics is not complete and an alternative theory is formulated, this theory will not be able to account for the phenomena in a manner consistent with local causality, unless of course it is superdeterministic or a version of the MWI.

Finally it should be also noted that a theory which violates RC does not necessarily lead to faster-than-light signaling, i.e., the condition of *signal-locality* given by [450, 453]

$$P(O_B|S_A, S_B, C) = P(O_B|S_B, C), \tag{3.7}$$

can still hold even if LC is violated. A violation of the above condition has not been observed and is implied neither by the standard formalism of quantum mechanics [352] nor by any of the major interpretations proposing solutions to the contradiction of Bell's theorem. However, since any theory that violates RC or FC has in principle the capability to violate signal-locality, this violation must be suppressed by additional parameters of the theory, which is known as *fine-tuning* [454].

3.2.5 Analyses, Extensions and Generalizations

Following the seminal impact of Bell's theorem, the original simple scenario, as proposed by Bohm and analyzed by Bell, with two parties and two dichotomic observables for each has been exhaustively analyzed and generalized to more complex scenarios, see, e.g., [421, 395, 402, 449, 382, 456, 484, 365, 376, 424, 375]. For example, Fine [388] has demonstrated that the existence of a Bell-local model is equivalent to the existence of a joint distribution $p(O_A, O'_A, O_B, O'_B)$ where O_j and O'_j are the outcomes given the two possible settings at site j. A notable result has also been given by Popescu and Rohrlich who showed that it is possible to achieve the maximal S-value of 4 in the CHSH inequality with a model not violating signal-locality [427]. A postulated device which can achieve such a degree of correlation is accordingly called a *Popescu-Rohrlich-Box* [642]. Finally, Mermin [414] as well as Greenberger *et al.* [391] have proposed a tripartite version of Bell's Theorem which only involves deterministic outcomes. If the parties share a so called *Greenberger-Horne-Zeilinger* (GHZ) state $|\text{GHZ}\rangle = \big(|000\rangle + |111\rangle\big)/\sqrt{2}$ [458, 353, 484, 480], the impossibility

of a generalized three-partite Bell-local explanation can even be proven for measurements with deterministic outcomes.

The properties of quantum correlations as illuminated by violations of Bell-type inequalities have also given rise to a resource theory of so called *Bell-nonlocality* [376, 375]. It classifies types of correlations $P(O_A, O_B|S_A, S_B)$, where the condition on C is usually not written explicitly, based on the amount of necessary resources to generate them, such as Bell-local models, quantum mechanical states or arbitrary non-signaling models. Unfortunately in this context the qualifier "Bell" is often neglected and the term "nonlocality" is used instead, see e.g. [529, 376, 405, 375, 439, 350, 406]. Of course, given the implications of Bell's theorem as presented above, this represents a catastrophic misnomer [392, 438, 457] since it is not related to locality in a general sense, as most appropriately captured by RC, but to the very special notion of Bell-locality which includes RC, CCP, and FC. To make matters worse, proponents of "nonlocality" as a resource by no means explicitly subscribe to a negation of LC through a negation of RC and thus this usage of the term blurs the clear structure of Bell's theorem. A different term, as for example "EPR-correlations" [448] or "Bell-correlations", as used throughout this work, seems more appropriate and independent of interpretation.

3.2.6 Experimental Tests and Loopholes

The experimental realization of Bohm's basic scenario is called a *Bell test* and typically consists of preparing an ensemble of bipartite quantum systems in the identical state ρ_C, distributing them among two remote laboratories, implementing an independent mechanism to choose the settings and record a sequence of results, leading to the empirical distribution $P(O_A, O_B|S_A, S_B, C)$. While pioneering experiment of this type have been performed by the groups of Clauser and Aspect [389, 364, 363, 362], they did not implement the conditions of Bell's scenario sufficiently well [354, 357, 629, 642]. In general despite its conceptional simplicity, an experimental realization of Bell's theorem is nontrivial due to practical limitations which introduce so-called *loopholes* for test.

The most obvious loophole called *locality loophole*, as discussed already by Bell [368], is related to the space-like separation of the measurement on each copy of the bipartite state [642]. In particular, the time from the process of choosing the setting to the finalization of the recording of the outcome has to be sufficiently small compared to the spatial separation of the laboratories. The first full closing of the locality loophole was achieved by Weihs *et al.* [446]. The second major loophole is related to a possible failure of the FC assumption and is called the *freedom of choice* loophole [642] or also misleadingly "free-will loophole" [350]. In general a correlation of the settings with the relevant past can never be fully excluded since, as mentioned above, it is at least practically impossible to know all physical parameters of the system. However, typically these correlations are made more and more unlikely by implementing complex randomized mechanisms to choose settings, in particular so called *quantum random number generators* which use the randomness of quantum measurements to choose settings [642]. The last loophole is commonly called the *detection loophole* [350] or *fair-sampling loophole* [642] and has a similar conspirato-

rial nature as the freedom of choice loophole, but in contrast to the latter can be closed. In essence, if a certain fraction of prepared systems is not detected, then there exists a Bell-local explanation for Bell-correlations if the local rules suitably prohibit any outcome of the measurement for a certain choice of local setting, e.g., via a loss of the local particle [418, 387, 374]. The detection loophole can be closed with sufficiently high experimental detection efficiencies, such as first achieved by Rowe *et al.* [432].

Only comparatively recently all three major loopholes have been closed simultaneously in four technologically challenging experiments [394, 390, 433, 431], all of which recorded a violation of the CHSH inequality, albeit with vastly varying significance. In all experiments the locality loophole was closed by a combination of sufficient space-like separation and fast experimental apparati, which were efficient enough to close the detection loophole. The freedom of choice loophole was also closed for all experiments by using fast random number generators along with fast mechanisms implementing the switching of the settings. Other experiments have aimed to further reduce the possible impact of FC violating correlations by basing the choices of settings either on human induced randomness [437] or extraterrestrial signals from astronomical objects positioned at close to opposite directions relative to earth, pushing the timescale on which the correlations have to persist back into the past to an order of 10^{10} years [430].

3.3 Entanglement

3.3.1 Bipartite Entanglement

Independently of how Bell's theorem is resolved, it allows to identify a certain special type of quantum states, namely those which can generate the Bell-correlations. It can be shown that such correlations cannot be established via a convex sum of product states as is the case for all classical correlations [448, 529, 174]. This motivates the definition of entangled states as states ρ which *cannot* be decomposed into a convex sum of product states as [174, 95, 484]

$$\rho \neq \sum_j p(j)\rho_j^A \otimes \rho_j^B, \tag{3.8}$$

where $p(j) > 0$ with $\sum_j p(j) = 1$ and the superscripts indicate the party. In the opposite case when the state *can* be written in the form above, it is called *separable*. While this formal definition is based on an analysis by Werner [448], the term "entanglement" is much older and a translation of the German term "Verschränkung", first introduced by Schrödinger to characterize quantum correlated systems as in the EPR scenario [41]. Note that, while entanglement is necessary to generate Bell-correlations, it is not sufficient, i.e., there are bipartite entangled states which cannot lead to correlations violating any Bell-inequality [448, 174]. While certainly connected, entanglement and the violation of Bell inequalities are thus distinct concepts. The basic definition of entanglement (3.8) is given for systems which are decomposed into two parties and this type of entanglement

is accordingly called *bipartite* entanglement. In the following the essential properties of bipartite entanglement are presented and in the next subsection also entanglement between more than two parties is discussed.

In the context of QIT, entanglement can be treated operationally as providing a resource for quantum information processing [484, 476]. In order to relate it to quantum operations, also quantum channels can be characterized based on their factorization properties in analogy to quantum states [174, 95, 484]. For a bipartite system a channel is called *local* if it consists of separate channels for each of the two systems, written as $\mathcal{C}_{\text{loc}} = \mathcal{C}_A \otimes \mathcal{C}_B$. An important subset of local channels are so called *local unitary channels* which apply a local unitary transformation to each of the parties. Bipartite states which are invariant under LU transformations are called *Werner* states [95]. Accordingly, a *separable* channel $\mathcal{C}_{\text{sep}}$ corresponds to a convex sum of local channels $\mathcal{C}_{\text{sep}} = \sum_j p(j)\mathcal{C}_A \otimes \mathcal{C}_B$ with $\sum_j p(j) = 1$. An important subset of separable channels are so called *local operations and classical communication* (LOCC) which can be modeled as a sequence of local operations at the two sites conditioned on preceding, intermediate, or subsequent exchange of classical information [174, 95, 484]. Note that there exist separable channels which are not LOCC. The concept of the *LOCC orbit* of a state ρ, i.e., the set of states into which ρ can be transformed via LOCC, defines a partial ordering in state space. It can be shown that for a given system all bipartite separable states are *LOCC equivalent*, i.e., they each lie pairwise in each other LOCC orbits. Entangled states lie outside this equivalence class and thus crucially cannot be generated from separable states via LOCC. If a greatest element exists in terms of the partial ordering via LOCC, i.e., a class of states with a LOCC orbit that spans the entire Hilbert space, these necessarily pure states are called *maximally entangled* states [95]. Since in general a classification of states in terms of LOCC orbits would require a continuum of parameters, the extended set of *stochastic* LOCC (sLOCC) was introduced in [475] to allow a more coarse grained classification [484]. In this context "stochastic" means that the CP maps are not TP, i.e., probabilistic, and a postselection has to be performed.

The quantification of entanglement via so called *entanglement measures*, i.e., maps from state space to non-negative real numbers, is an important problem both of foundational interest as of high practical relevance for the applications of entangled states as sketched below [174, 501, 484]. For pure bipartite states the situation is simple and entanglement can be quantified for example via the so called *entropy of entanglement*, which is the von Neumann entropy of the reduced states of the subsystems [460]. In the case of discrete local Hilbert spaces of same dimension d, for a maximally entangled state, the reduced states are the maximally mixed states $\mathbb{1}/d$ and the entropy of entanglement reaches the maximal value of $\log d$. It can be shown that for pure bipartite states all entanglement measures are equivalent to the entropy of entanglement [484].

In contrast to classical systems, for which it holds that $H(X,Y) \geq H(X)$, in QM the von Neumann entropy of the joint system can be smaller than the entropy of a subsystem, with an extreme case given by pure maximally entangled states. This property seems to be connected with Schrödingers intuition expressed as:

> Bestmögliche Kenntnis eines Ganzen schließt *nicht* bestmögliche Kenntnis seiner Teile ein — und darauf beruht doch der ganze Spuk. [41]

More precisely, there is a sense in which the joint description of quantum systems contains more information than just such classical correlations between the systems. In effect, for entangled states the quantum conditional entropy $S(\rho_{AB}|j) := S(\rho_{AB}) - S(\rho_j)$ with $j \in [A, B]$ can be negative [141, 142, 484]. While the conditional Shannon entropy can be interpreted as a measure of how much information one party needs to send to the other to recover the full joint probability distribution, a negative quantum entropy indicates that they share an even more powerful resource. For example, if the parties share states characterized by a negative conditional entropy they are always able to generate maximally entangled states just via LOCC [170]. Accordingly, the absolute value of the negative part of the conditional quantum entropy is called *coherent information* [170, 484].

Another property of entanglement of great practical relevance is the possibility to generate a small set copies of a highly entangled state from a larger set of copies of a less entangled one [463, 470]. This procedure is called *entanglement distillation* or *entanglement purification* [466, 174, 95, 459, 484]. Entanglement distillation requires some presence of entanglement in original state and furthermore, there exist types of entangled states which do not permit distillation called *bound entangled*. The concept of distillation originates from a proof given by Popescu [426] that some entangled states which possess Bell-local explanations can be transformed via sLOCC operations into states which violate a Bell-inequality [484].

Finally, it should be mentioned that an alternative definition of quantum correlations is provided by the so called *quantum discord* as introduced by Olliver and Żurek [496]. The authors point out an ambiguity in the definition of quantum conditional entropy and provide an alternative definition based on a specific basis in which the system conditioned upon is measured. The discord δ is then given by the difference $\delta = S'(\rho_{AB}|B_C) - S(\rho_{AB}|B)$ where the subscript C indicates a particular choice of basis for the conditioning. For an optimal choice of basis C the discord is minimized but if it does not vanish, the correlations are defined to not be classical, which in this case means that the information cannot be extracted without disturbing the total state of the system. This is not the case even for some separable states, which thus are regarded as quantum correlated in the sense of discord [496, 505].

3.3.2 Multipartite Entanglement

While the characterization and quantization of entanglement in bipartite systems already poses significant problems, the situation becomes even more complicated if entanglement involving a larger number of parties, called *multipartite* entanglement, is considered [484]. Nevertheless, some properties of bipartite entanglement can be generalized to multipartite systems such as bound entanglement, equivalence classes based on sLOCC or entanglement measures, see [459, 484]. A few important properties of multipartite entanglement will be sketched below and more details can be found, e.g., in the comprehensive reviews [484,

480].

Multipartite entanglement goes beyond the binary distinction between separable and entangled states and there are several options to define *entanglement structure*. If the total joint state can be written as a convex sum where each element is a product of the states of all parties, the state is called *fully separable* [484]. Conversely, a not fully separable state contains some form of entanglement. Furthermore, an entangled state is called *k-separable* if it can be written as a convex sum of states each being a product state with at least k-factors [474, 473]. Any k-separable state is thus also $(k-1)$-separable. Following a different concept, a state is called *k-producible* if it can be written as convex sum with factors that include at most k-parties [481, 479, 480]. A k but not $(k-1)$-producible pure state is said to be k-party entangled. Note that, crucially k-separability is concerned with the amount of partitions while k-producibility with the amount of entangled parties per partition. The extreme case of both concepts, i.e., 1-separability and n-producibility coincide and give rise to the notion *genuine multipartite entanglement* (GME) [481, 484, 480], i.e., a GME state is not even biseparable as well as n-producible but not $(n-1)$-producible.

A similar notion exists also for multipartite Bell-correlations, which here are called *genuine multipartite Bell-correlations* (GMBC). Note that common term is "genuine multipartite nonlocality" [361, 375], which is of course encumbered with the same terminological difficulties as "nonlocality". Generalizing the concept of a Bell-local model (3.5) to three parties, a first definition of GMBC was proposed by Svetlichny as correlations which *cannot* be decomposed in the form [435]

$$p(O_A, O_B, O_C|S_A, S_B, S_C) = \sum_{(j_1,j_2,j_3)} \sum_{\lambda} q_\lambda p(O_{j_1}, O_{j_2}|S_{j_1}, S_{j_2}, \lambda) p(O_{j_3}|S_{j_3}, \lambda), \tag{3.9}$$

where $q_\lambda \geq 0$ and the first sum goes over the three possible bipartitions with $j_k \in \{A, B, C\}$. As pointed out by other authors [361, 366], this definition is too strict since the elements of the decomposition can contain signaling correlations, even if the full three-partite joint distribution does not. Thus, a modified weaker definition of GMBC was proposed, where it is additionally required that the three non-factorized rules in Eq. 3.9 are non-signalling. In effect, some correlations which can be decomposed according to Svetlichny's definition and thus are not regarded as GMBC, are GMBC according to the modified definition since a decomposition into non-signaling terms is not possible. These conditions have been also generalized to an arbitrary number n of parties and it has been shown that for $n \geq 3$ Sveltichny's condition is strictly stronger than the modified condition while both are strictly stronger than the requirement of full factorization [366].

Even more so than for bipartite states, the quantification of multipartite entanglement presents a difficult problem for which no unique solution has been found [484]. A range of measures has been proposed which are typically required to satisfy a series of postulates, the most important of which is *monotonicity under LOCC*, i.e., the entanglement should be quantified such that LOCC operations cannot lead to an increase of entanglement. Other postulates include the requirement that entanglement is minimal for separable states and stays invariant under local unitary channels as well as several other conditions, see [174, 501, 484] for overviews.

A central problem in the context of multipartite entanglement is also the question of how entanglement and correlations are distributed among the various parties. For example, an essential property of multipartite entangled systems is a trade-off in the amount of correlations between the parties known as *monogamy of entanglement* [469, 497]. In general, if the reduced state of two parties contains a certain amount of entanglement, this imposes a limit on the maximal amount of entanglement between each of them and a third party [484]. A series of notable results also analyzes the necessity of certain correlations for the constitution of entanglement and in particular identifies GME states without any full correlations [487, 504, 507, 488]. Finally, an entropic quantity has been proposed to characterize multipartite correlations based on conditional mutual information called *k-partite dependence* **[P7]**. It quantifies the minimal informational advantage that a subset of k parties gains from cooperation.

3.3.3 Applications of Entanglement

One of the most famous applications of entanglement is so-called *quantum teleportation*, as first proposed by Bennett *et al.* [131], in which a single copy of an unknown quantum state is transferred reliably from site A to site B by exchanging only classical information, see also [1025, 133, 95, 484, 629]. While initially only proposed for discrete systems, it has also been generalized to continuous degrees of freedom by Vaidman [443]. The necessary prerequisite for teleportation is that A and B share a maximally entangled state, encoded in some local degrees of freedom at the two sites. Then in the basic protocol, e.g., party A can transfer an unknown state $|\psi\rangle$ encoded in another local degree of freedom to party B by first performing a joint projective measurement on its part of the entangled system and the local unknown state $|\psi\rangle$, which crucially involves projections into entangled subspaces, and subsequently transmitting the outcome to party B via a classical channel. Dependent on the outcome, B can then implement a suitable local unitary operation to recover the state $|\psi\rangle$ with certainty. Since the time-ordering in teleportation scenarios can be varied, e.g., when the entanglement between the two sites is established only after the measurement on site A, teleportation can also be realized in a delayed choice scenario as presented in Sec. 3.4.2. Quantum teleportation has been first experimentally realized by Bouwmeester *et al.* [565].

The principle behind teleportation is also the basis for *entanglement swapping*, where entanglement between parties A and B as well as between B and C is transformed into entanglement between A and C in a similar scheme [455, 464, 484, 629]. Combining entanglement swapping with distillation forms the basis of so called *quantum repeaters* [467, 629], which are devices allowing to efficiently establish entanglement between remote locations using e.g., photonic qubits, as introduced in Sec. 5.1.1, even in the presence of noise, loss, and errors. Together with the development of other technologies such as *quantum memory* [202, 629], i.e., systems which can store a certain quantum state for a comparatively long time, the technological aim is the creation of *quantum networks*, which are expected to lead to everyday applications of quantum communication, see e.g. [186, 175, 629, 213, 144].

A possible application of such quantum networks would be the facilitation of *entanglement based quantum cryptography* as proposed by Ekert [386]. In contrast to one-directional approaches, as sketched in Sec. 1.7.2, where one party sends quantum information, i.e., quantum systems to another, in this alternative scheme a source sends parts of an entangled state to the two parties. Since the capabilities of an eavesdropper to replicate the intercepted state of one party can only be based on the accessible local information, the probability to a violate Bell-inequality between the two parties is reduced the more information is gained by the eavesdropper, see also [486, 509]. Notably, the security of this approach is not only assured given the laws of quantum mechanics, but in fact for any theory respecting the no-signaling constraint [484]. Notable realizations of entanglement based cryptography are for example [207, 217, 127].

Finally, the generation of entanglement is also the foundation of so called *one-way quantum computing* as developed in [193, 138]. In this approach entanglement is already provided in the initial joint state of the qubits, typically a so called *cluster state* [137], and no implementation of further logical gates via qubit interactions is necessary [629]. Various computing circuits are implemented by appropriate successive single qubit measurements. Entanglement based photonic circuits are sometimes regarded as one of the main promising platforms for the development of quantum computation, see e.g., [209, 181, 158].

3.3.4 Entanglement Detection

For applications as those described above, the quantification and certification of entanglement are of crucial practical interest. Commonly two problems are distinguished, namely first, the purely mathematical problem to determine if a state is entangled or GME entangled if the full multipartite state ρ is known and second, the experimental problem to determine whether a multipartite physical system in an unknown state is entangled or not [95, 480, 477]. It has been shown that for general states even the first problem is highly non-trivial and scales unfavorably, i.e., exponentially, with system size [480, 478].

A possible criterion for entanglement can be formulated based on positive but not CP maps, as introduced in Sec. 1.4.3. When a positive map is applied to only one part of a composite state, in general the resulting total state will no longer be positive. However, for separable states positivity is sufficient for a positive output. This leads to a powerful criterion for entanglement called the *positive under partial transpose* (PPT) criterion. It considers a transposition acting on only one part of the state, which corresponds to a positive but non CP map [500, 483]. While a negative partial transpose represents a sufficient condition for entanglement, it is not a necessary one and there is a subset of entangled states that are PPT [482, 472]. Notably, all of such states can be proven to be bound entangled, i.e., to not admit a distillation. It remains an open question whether in general all bound entangled state are PPT states or whether there exist bound entangled states with a negative partial transpose [95, 459, 484, 171]. The PPT-criterion also motivates a bipartite entanglement measure called *negativity*, which is sensitive to how much the eigenvalues drop below zero for partially transposed states [508].

In the practical scenario of entanglement detection, the goal is often to determine

whether a state is entangled or not, without the experimental effort to perform a full QST. In such cases so-called *entanglement witnesses* are used which are functions of only a subset of experimental data necessary for QST and certify entanglement for a certain range of values [494, 468, 480, 477]. Typically, linear witnesses are employed, which correspond to linear observables $\mathbf{W}$ constructed such that $W := \mathrm{tr}(\rho\mathbf{W}) < 0$ only if the state is entangled [95, 484]. It can be shown that no linear witness is sensitive to all entangled states but that for any entangled state there exists a linear witness which detects it. Thus, especially if some prior knowledge is available, it is possible to perform entanglement detection by employing only a comparatively small set of measurement settings which is sufficient to calculate the value W of a suitably chosen witness operator. An example of a nonlinear witness for a multi-qubit state is the *full sector length* $S_F := \sum_j T_j^2$, where $\{T_j\}$ is the entire set of full correlations, as defined in Sec. 1.6.4. It can be shown that, for a system consisting of n qudits, $S_F > (d-1)^n$ is a sufficient criterion for entanglement, which even becomes necessary for pure states [206]. As S_F corresponds to a sum of non-negative elements it has the advantage that, in contrast to linear witnesses, only a subset of T_j have to be measured until the bound 1 is violated, which can further reduce experimental effort in certain practical scenarios of entanglement detection [491].

Since only entangled states can produce Bell-correlations, Bell-inequalities can also serve as entanglement witnesses. For example if the CHSH inequality is rewritten such that Bell-local states yield only positive values, it represents a linear entanglement witness [95, 484]. A crucial advantage of loophole-free Bell-tests lies in the possibility to certify entanglement even if some experimental features of the involved practical devices are unknown. This feature, commonly called *device independence* [461, 462, 498, 465], is of course also a crucial element of entanglement based quantum cryptography [218]. A different type of device independence is present in so called *random measurement* scenarios in which the transmissions channels or choices of settings are subjected to random local unitary rotations rendering usual approaches of entanglement detection useless. However, dependent on the particular scenario, it is still possible to gain information about local unitary invariant properties of the multipartite system, such as entanglement [282], **[P10]**. For example, in **[P5]** a scheme to detect even GME by only measuring local unitary random correlations was proposed and demonstrated experimentally for a four-qubit state.

Since the generation of entangled states for large multi-partite quantum systems as utilized in contemporary quantum technological applications is a resource-intensive task, it is of great practical interest to characterize these states using as few copies of the state as possible [492, 493, 489, 471, 495, 499, 477, 503, 510]. However, functions of the correlation tensor, such as W and S, allow definite conclusions about the entanglement of the state only in the limit of infinite statistics in which the correlation tensor elements can be determined without statistical noise. If the amount of copies per correlation tensor element is reduced, the conclusion about the character of the state becomes fundamentally probabilistic. How such probabilistic conclusions are to be drawn is not uniquely defined and depends on fundamental attitudes towards statistical inference, most prominently represented by the Frequentist and Bayesian approaches, see e.g., [929, 916, 937]. In **[P11]**, as reprinted in the next section, based on the framing of entanglement detection in form

of a statistical hypothesis test, a general analysis of possible probabilistic conclusions is developed, which can be applied to any entanglement witnesses based on correlation tensor elements. Notably, it shows that in the limit of very few copies of the entangled state, Frequentist and Bayesians figures of merit can lead to different prescriptions for an optimal usage of the available resources.

npj | quantum information www.nature.com/npjqi

ARTICLE OPEN

Check for updates

Valid and efficient entanglement verification with finite copies of a quantum state

Paweł Cieśliński[1]✉, Jan Dziewior[2,3,4], Lukas Knips[2,3,4], Waldemar Kłobus[1], Jasmin Meinecke[2,3,4], Tomasz Paterek[1,5], Harald Weinfurter[1,2,3,4] and Wiesław Laskowski[1,6]✉

Detecting entanglement in multipartite quantum states is an inherently probabilistic process, typically with a few measured samples. The level of confidence in entanglement detection quantifies the scheme's validity via the probability that the signal comes from a separable state, offering a meaningful figure of merit for big datasets. Yet, with limited samples, avoiding experimental data misinterpretations requires considering not only the probabilities concerning separable states but also the probability that the signal came from an entangled state, i.e. the detection scheme's efficiency. We demonstrate this explicitly and apply a general method to optimize both the validity and the efficiency in small data sets providing examples using at most 20 state copies. The method is based on an analytical model of finite statistics effects on correlation functions which takes into account both a Frequentist as well as a Bayesian approach and is applicable to arbitrary entanglement witnesses.

npj Quantum Information (2024)10:14 ; https://doi.org/10.1038/s41534-024-00810-3

INTRODUCTION

Quantum entanglement has long been recognized as an important prerequisite of modern quantum technologies. Its detection is accordingly a well-studied topic with a plethora of different methods available. The field has evolved towards strategies directly applicable to experimental data which inevitably is limited to a finite number of detection events. If this number is large, various forms of entanglement witnesses[1–3] provide reliable entanglement verification[4]. Interestingly, also the analysis of smaller data sets allows to detect entanglement[5], most recently with quantum state verification methods[6–8] and tailored game-like protocols in which particles are measured one by one[9–12]. These methods are of high practical relevance in all cases where only a limited amount or only partial data is accessible, e.g. when an inefficient source has to be characterized quickly or one is interested in entanglement detection in large-scale quantum systems.

The finiteness of data sets used to derive a conclusion about whether the state is entangled or not inevitably leads to a probabilistic nature of this conclusion. Common certification schemes aim to ensure a small error if the outcome of the method speaks in favour of entanglement, i.e. a small error of a false positive. Yet, in the case of low statistics, this might come at the price of a large probability of rejecting an actually entangled state, i.e. a false negative. This tradeoff is illustrated in Fig. 1, which shows that for smaller statistics one is required to go to more and more strict criteria to reliably distinguish between results compatible with entangled states and results compatible with separable states. In consequence, due to the increased strictness, it becomes also more and more improbable that an entangled state will pass the test. It thus becomes crucial to properly apply the apparatus of statistical hypothesis testing[13–15] to the scenario of entanglement certification in order to avoid significant misinterpretations of conclusions based on small sample sizes and to properly optimize the usage of these scarce resources.

Here, we analyse the consequences of limited datasets for the application of entanglement witnesses based on correlation functions. As mentioned above, there are competing interests in choosing a certification strategy. The first is achieving a certain level of validity, i.e. trust in a positive result of the entanglement certification. The second interest is to ensure that the test can correctly assess as many input states as possible, which we call its efficiency. In general, different certification strategies will exhibit different efficiencies even if they achieve the same validity and vice versa. Thus, both quantifiers should be taken into account when choosing an optimal test strategy. We develop an algorithm for the optimization of experimental entanglement tests which simultaneously ensures high validity with optimal efficiency while being independent of the system's size.

Although the general framework of statistical analysis which is employed here is well-known to statisticians, it has not yet been comprehensively applied in the field of entanglement certification, where it becomes especially relevant in the context of limited datasets. The present work contributes to closing this interdisciplinary gap. The results are illustrated with various examples where different entanglement witnesses are applied to general classes of quantum states. While our examples all consider systems of qubits (the most commonly encountered systems in quantum information), our general analysis is by no means limited to two-dimensional systems and can be applied to any witness which is a function of generalized correlation tensor elements.

RESULTS

Entanglement certification as hypothesis testing

There are two main approaches to statistical hypothesis testing, the Frequentist and the Bayesian one (see e.g. ref. [13] for a

[1]Institute of Theoretical Physics and Astrophysics, Faculty of Mathematics, Physics, and Informatics, University of Gdańsk, 80-308 Gdańsk, Poland. [2]Max Planck Institute for Quantum Optics, 85748 Garching, Germany. [3]Faculty of Physics, Ludwig Maximilian University, 80799 Munich, Germany. [4]Munich Center for Quantum Science and Technology, 80799 Munich, Germany. [5]School of Mathematics and Physics, Xiamen University Malaysia, 43900 Sepang, Malaysia. [6]International Centre for Theory of Quantum Technologies, University of Gdańsk, 80-308 Gdańsk, Poland. ✉email: pawel.cieslinski@phdstud.ug.edu.pl; wieslaw.laskowski@ug.edu.pl

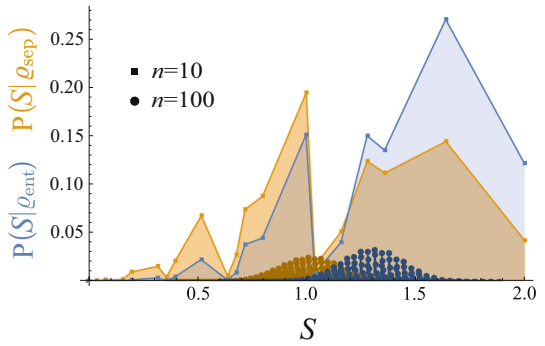

Fig. 1 Illustration of finite statistics effects on entanglement verification. The plot shows the probability distributions to obtain a specific value of a certain nonlinear entanglement witness S discussed in the "Methods" subsection "Certifying entanglement". The witness uses only two correlation measurements, each estimated either with $n = 10$ (squares) or $n = 100$ (circles) copies of the states. The probability distribution given an entangled state is marked in blue. The probability in orange is computed for a separable state that saturates the value of the witness in the case of infinite data sets, i.e. a separable state that tends to yield large values of S. For larger statistics (see circles), the two distributions have small overlap making it easy to verify that an entangled state was prepared. For smaller statistics (see squares) the overlap is very significant and care has to be taken even if big values of the witness are observed. More detailed discussion on this issue is provided in the "Results" subsection "Limited significance of entanglement certification". Here we develop universal tools, applicable to any entanglement witness, that extend it to the domain of finite statistics and can be employed to efficiently use every single copy of a state. For examples see the subsection "Optimizing entanglement certification strategies" in the "Results" section.

Frequentist and refs. [14,15] for a Bayesian perspective). These approaches employ different quantifiers to capture different figures of merit. In general, both are useful to statistically evaluate an entanglement certification scheme, but dependent on the context, such as e.g. the availability of prior information or the practical goal of certification, one of these frameworks might be more suited than the other. In the following, we will first express entanglement detection as a hypothesis test and subsequently show how it is statistically analysed from the Frequentist or Bayesian viewpoints.

Entanglement certification can be reduced to a so-called simple hypothesis test, where the parameter space contains just two elements corresponding to the two disjoint hypotheses 'the state is separable' and 'the state is entangled'. We denote the two parameters as 'sep' and 'ent', respectively. The outcome space $\mathcal{O}$ is given by the set of all possible outcomes generated by a particular entanglement detection function under consideration. Depending on the chosen approach to statistical inference, the theory of hypothesis testing now allows to construct the optimal test to choose between the two hypotheses for any given outcome $Q \in \mathcal{O}$.

In non-randomized tests the outcome space is divided into two disjoint sets $\mathcal{O}_{\mathrm{acc}}$ (acceptance set) and $\mathcal{O}_{\mathrm{rej}} = \mathcal{O} \setminus \mathcal{O}_{\mathrm{acc}}$ (rejection set) such that entanglement is certified whenever $Q \in \mathcal{O}_{\mathrm{acc}}$. Note, that sometimes it can be optimal to perform a (partially) randomized test, where there exists a subset of outcomes for which the decision between the hypotheses is made randomly. For simplicity, we present our analysis in terms of non-randomized tests and note that randomized test can be treated equivalently. Furthermore, the usefulness of a randomized test is illustrated in the generalized scenario part of the Optimizing Entanglement Certification Strategies section.

In typical entanglement certification schemes the outcomes Q approximate theoretical quantities Q^{∞} which are functions of the states that would be observed when the number of measurements tends to infinity. From this point on we use the superscript ∞ to indicate such ideal values. The inference of entanglement is usually justified by the fact that values in the acceptance set $\mathcal{O}_{\mathrm{acc}}$ cannot be attained by any separable state, i.e.

$$\mathrm{P}(Q^{\infty} \in \mathcal{O}_{\mathrm{acc}}|\mathrm{sep}) = 0. \tag{1}$$

If the experiment is performed with sufficient statistical data the experimental result Q approximates the theoretical Q^{∞} very well and thus a result in $\mathcal{O}_{\mathrm{acc}}$ entanglement can be certified essentially with certainty. Crucially, however, if the amount of empirical data is sufficiently small, the statistical fluctuations of the outcomes lead to a manifestly statistical nature of the conclusion and a proper analysis of the validity of the statistical inference becomes necessary.

Frequentist approach

In the Frequentist approach, the validity of the test is given by the level of confidence $q_{\mathrm{F}} = 1-\alpha$, that one or the other hypothesis is correct, with α being the level of significance. In our simple certification scenario, the significance α is the upper bound on the probability q_{F} with which the experiment will wrongly certify entanglement if the state is separable. As this is a statement about the average performance of the test, it does not allow any probabilistic assertions about the correctness of a particular single run of the procedure. For example, if we perform certification of entanglement with the values typically used for hypothesis testing, i.e. $q_{\mathrm{F}} = 95\%(\alpha = 5\%)$, but are given separable states only, we would certify the state to be entangled on average in roughly 5% of the runs.

In a certification scenario, the level of significance only depends on the likelihood of type I errors (false positives). Thus, to achieve a certain validity q_{F}, the acceptance set has to be chosen such that the likelihood of yielding a value in the acceptance set given a separable state is at most $1-q_{\mathrm{F}}$, i.e.,

$$\sum_{Q \in \mathcal{O}_{\mathrm{rej}}} \mathrm{P}(Q|\mathrm{sep}) \geq q_{\mathrm{F}}. \tag{2}$$

The likelihood function for the opposite hypothesis P(Q|ent) is irrelevant as far as the level of significance is concerned.

Although the distinction between types of errors in Frequentist inference is well known, particularly in the field of entanglement certification with small data sets, often the focus lies exclusively on the level of significance[5,9–11,16,17]. We want to argue, that in most practical applications, one is not only interested in a valid method but also in its ability to positively certify at least some entangled states. This tradeoff becomes particularly crucial in the case of very low statistics. Thus, hypothesis tests should also be optimized based on a second quantifier, the power of the test, which characterizes exactly this ability to provide a positive certification corresponding to minimizing e_2, the error of type II (probability of false negatives). The power r is given by

$$r = 1 - e_2 = \sum_{Q \in \mathcal{O}_{\mathrm{acc}}} \mathrm{P}(Q|\mathrm{ent}). \tag{3}$$

The concept of statistical power is essential for finding optimal tests and properly assessing the usefulness of statistical conclusions. See Fig. 2 for an illustration. Thus, in our terminology, the maximization of power corresponds to a maximization of the efficiency of the test.

Bayesian approach

In a Bayesian approach to certification, probabilities for both hypotheses can be calculated given a certain outcome, Q, i.e. P(ent|Q) and P(sep|Q) = 1−P(ent|Q). Validity in this context is

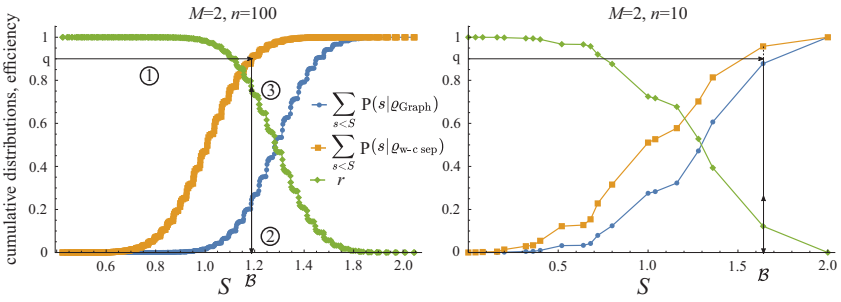

Fig. 2 Validity and power in the Frequentist approach applied to the nonlinear witness *S*. Given a required minimal, e.g., $q_F = 0.9$, an appropriate outcome space over the values of S (for definition see "Entanglement certification" in the Methods section) is chosen by specifying a bound $\mathcal{B}$ such that the separable correlations have at least q_F mass of its probability distribution below $\mathcal{B}$, i.e., the cumulative probability distribution of the worst case separable correlations (orange data) reaches q_F (arrows marked with encircled 1 and 2). For this bound, one then evaluates the cumulative probability of the entangled state (blue data). The power, r, is defined as one minus this probability and is plotted in green. The power at the determined bound is marked by an arrow with encircled 3. The higher the power, the better the entanglement detection works, i.e., the higher the probability to actually detect the entangled state as such (see Fig. 1). Reducing the statistics from $n = 100$ (left panel) to $n = 10$ (right panel) lowers the power of the detection from about 75% to about only 12% if the same validity $q_F = 0.9$ (level of significance 10%) is required.

readily identified with the Bayesian level of acceptance q_B, which is the minimal value of the posterior probability for which the hypothesis ent is accepted. Entanglement is thus certified whenever $P(\text{ent}|Q) \geq q_B$. This means that the acceptance set $\mathcal{O}_{\text{acc}}$ has to be chosen such that

$$P(\text{ent}|Q) \geq q_B, \quad \text{for all} \quad Q \in \mathcal{O}_{\text{acc}}, \tag{4}$$

i.e., whenever a value of $Q \in \mathcal{O}_{\text{acc}}$ is observed, the certification of entanglement is credible at least with degree q_B. Note, that as given by Bayes theorem, the posterior $P(\text{ent}|Q)$ is a function of both $P(Q|\text{sep})$ and $P(Q|\text{ent})$, as well as of the quotient of priors $P(\text{ent})/P(\text{sep})$.

To arrive at a formulation of Bayesian hypothesis testing in terms of validity and efficiency, one has to consider the connection between the level of acceptance and so-called loss functions. For a given outcome Q and weights β and $(1-\beta)$ for false positive and false negative respectively, the (posterior) loss function L_Q is given by

$$L_Q = \begin{cases} \beta\ P(\text{sep}|Q) & \text{if } Q \in \mathcal{O}_{\text{acc}} \\ (1-\beta)\ P(\text{ent}|Q) & \text{if } Q \in \mathcal{O}_{\text{rej}}, \end{cases} \tag{5}$$

i.e. the respective probability of error multiplied by the corresponding weight. It can be shown that for each Q this loss is optimized if the rejection and acceptance sets are chosen simply based on an acceptance level of $q_B = \beta$[14]. Thus for optimal tests, we can simply identify the acceptance level q_B with the (relative) weight β given to the error of false positive.

A priori, i.e., without the knowledge of the outcome Q, an expected loss L can be defined as

$$\begin{aligned} L = \sum_Q L_Q P(Q) &= q_B P(Q \in \mathcal{O}_{\text{acc}}|\text{sep}) P(\text{sep}) \\ &+ (1-q_B) P(Q \in \mathcal{O}_{\text{rej}}|\text{ent}) P(\text{ent}), \end{aligned} \tag{6}$$

which corresponds to a weighted sum of the probabilities for the errors of both types. This is also equivalent to the average loss if the procedure is applied multiple times. In analogy to the power for Frequentist tests, the average loss L allows to compare different Bayesian test strategies with equal acceptance levels. From a Bayesian perspective maximal efficiency of a test thus corresponds to minimal loss L.

Finally, let us also briefly mention why the relevant priors are not discussed in the usual detection of quantum entanglement, via witnesses, in the limit of many measurement results[4]. In such a case, when the number of state copies is large: $n \gg 1$, it is possible to choose acceptance sets $\mathcal{O}_{\text{acc}}$ for which it is practically impossible for a separable state to exceed the bound of the witness, i.e., $P(Q \in \mathcal{O}_{\text{acc}}|\text{sep}) \approx 0$, as discussed above. Therefore, Bayes rule simplifies and the posterior becomes $P(\text{ent}|Q) \approx 1$ independently of the priors. In consequence, for any outcome in the acceptance set entanglement is certified with validities $q_F \approx q_B \approx 1$ both from the Frequentist and the Bayesian perspective and the distinction between the two approaches becomes superfluous.

Effects of finite statistics

The standard experimental scheme for entanglement certification in qubit systems is based on the measurement of correlation functions or simply correlations $T_{\mu_1 \ldots \mu_N}$ defined by

$$T_{\mu_1 \ldots \mu_N} = \langle R_{\mu_1} \ldots R_{\mu_N} \rangle = \text{Tr}(\rho\, \sigma_{\mu_1} \otimes \cdots \otimes \sigma_{\mu_N}), \tag{7}$$

where σ_{μ_k} is the μ_kth local Pauli matrix of the kth party with $\mu_k \in \{0, x, y, z\}$ and σ_0 being the identity. The correlation is thus the average of the product of local measurement outcomes $R_{\mu_k} = \pm 1$ when suitable local Pauli measurements are executed. Note that definition (7) does not only include the full correlations, for which all parties perform measurements but also marginal correlations, i.e. values of T to which only a subset of parties contributes, which formally correspond to setting the remaining indices $\mu_k = 0$. To simplify the notation in the following we write the correlations as T_j, where the index $j \in [1, 4^N]$ indicates the set of chosen measurement settings over all parties.

Consider a broad class of procedures for entanglement certification, in which a quantity Q^∞, e.g., an entanglement witness, is calculated as a function of the correlations T_j. Note that by choosing Q^∞ tailored to witness various types of entanglement, e.g. genuine multipartite entanglement, one can employ the further discussed method for testing the statements about, e.g., genuine multipartite entanglement or biseparability. For the usual application of the conditions imposed by Q^∞, the actual correlation functions are estimated with a finite number of experimental trials. We denote the actually measured correlations resulting from finite statistics by τ_j.

Thus, instead of the ideal quantum mechanically predicted value Q^∞ based on T_j obtained in the limit of infinite statistics, experimentally we have only access to the modified value Q, calculated from τ_j. We therefore begin with modelling τ_j.

Let $\{n_j\}$ denote the number of state copies measured for each setting j, which can vary from setting to setting. For the jth

measurement setting, we have

$$\tau_j = \frac{n_j^+ - n_j^-}{n_j} \tag{8}$$

where $n_j^\pm$ are the numbers of trials in which the product of local results equals $R_{\mu_1}\cdots R_{\mu_N} = \pm 1$, with $n_j^+ + n_j^- = n_j$.

For large n_j we obtain $\tau_j \approx T_j$, but for small n_j the measured τ_j take potentially different values which are furthermore restricted to the discrete set $\tau_j \in \{-1, -1+\frac{2}{n_j}, \ldots, 1-\frac{2}{n_j}, 1\}$. Given an N-qubit state, expressed by its correlations T_j, it is possible to explicitly calculate the ideal probability distribution $\mathrm{P}(\tau_j)$ over these discrete values by employing the binomial distribution as demonstrated in Methods (Witnesses in finite statistics). The mean and variance of this distribution are given as

$$\langle \tau_j \rangle = T_j, \qquad \mathrm{Var}(\tau_j) = \sigma_j^2/n_j, \tag{9}$$

where σ_j^2 is a function of the ideal quantum prediction equal to $\sigma_j^2 = 1 - T_j^2$, see also[18]. Note that the variance depends on the correlation value itself, e.g. a perfect correlation has no variance. This already hints that the method is most useful for states with high values of T_j^2.

Considering a particular entanglement certification procedure with the outcome $Q = f(\tau_{j_1}, \ldots, \tau_{j_M})$ (M being the number of correlation measurements), it becomes possible to calculate explicitly the probability distribution over the outcomes

$$\mathrm{P}(Q) = \sum_{\substack{\tau_{j_1},\ldots,\tau_{j_M} \\ f(\tau_{j_1},\ldots,\tau_{j_M})=Q}} \prod_{k=1}^{M} \mathrm{P}(\tau_{j_k}). \tag{10}$$

In the "Methods", subsection "Witnesses in finite statistics" section, we illustrate this procedure for both linear[1–3] and non-linear entanglement witnesses[17,19–24]. The linear witness $\mathrm{W} = \sum_j a_j \sigma_j$, with expectation value $\mathrm{Tr}(\mathrm{W}\rho) = \sum_j a_j T_j$ denoted as E_W^∞, extension to finite statistics has the following properties:

$$\langle E_\mathrm{W} \rangle = E_\mathrm{W}^\infty, \quad \text{and} \quad \mathrm{Var}(E_\mathrm{W}) = \sum_j a_j^2 \mathrm{Var}(\tau_j). \tag{11}$$

For nonlinear witnesses, further work is required as one needs to calculate the effect of finite statistics on nonlinear functions of τ_j. We describe a general procedure in the "Methods" section and here briefly illustrate the case when the witness depends on the square of correlations. Its mean and variance read

$$\langle \tau_j^2 \rangle = T_j^2 + \mathrm{Var}(\tau_j), \qquad \mathrm{Var}(\tau_j^2) = \frac{2(n_j-1)(1-T_j^2)[(2n_j-3)T_j^2+1]}{n_j^3}. \tag{12}$$

Note that the mean value of the square has a consistent shift by exactly the variance of the estimation from the finite data. This is a consequence of taking the square—the negative values in the distribution are transformed into positive values leading to a systematic deviation. This fact is important in the experimental analysis of finite data sets and has already been addressed in ref. [25]. As a final illustration assume the quadratic witness $S^\infty = \sum_j^M T_j^2$ that sums up M squared correlations (see the subsection "Certyfing entanglement" in the "Methods" section), each measured with the same number of copies n, i.e. $n_j = n$. We obtain

$$\langle S \rangle = \frac{(n-1)S_M^\infty + M}{n}, \quad \text{with} \quad \mathrm{Var}(S) = \sum_{i=1}^{M} \mathrm{Var}(\tau_i^2), \tag{13}$$

where now apart from the statistical uncertainty also a shift of the mean value is present.

Limited significance of entanglement certification

The modelling of probability distributions for the outcomes of single correlation measurements now allows us to calculate explicitly the probability distribution over outcomes of the entanglement witnesses Q. This calculation is always based on particular state spaces corresponding to the hypotheses ent and sep. Initially, for simplicity, we consider a simple scenario, where the test is supposed to distinguish between having a particular entangled state of the form

$$\rho = \frac{3}{4}|\mathrm{GHZ}\rangle\langle\mathrm{GHZ}| + \frac{1}{4}\,\mathbb{1}/2^N, \tag{14}$$

or an arbitrary separable state. Here, $|\mathrm{GHZ}\rangle$ is an N-qubit GHZ state, for any N, and $\mathbb{1}/2^N$ corresponds to the so-called white noise with no correlations at all. Note that in realistic scenarios the expected distribution of input states might be more complicated as we also demonstrate below. The probability distributions corresponding to the sep hypothesis are modelled based on a worst-case estimation of correlations compatible with separability as discussed in detail in the "Methods" section (see the subsections "Estimating probability distributions" and "Correlations compatible with separability").

Now consider the linear witness $\mathrm{W} = \sigma_y \otimes \sigma_y \otimes \sigma_x \otimes \cdots \otimes \sigma_x - \sigma_x \otimes \cdots \otimes \sigma_x + 1$ with only $n = 10$ clicks per single correlation measurement, i.e., 20 state copies in total. Due to this very small number of data points, separable states can now give rise to outcomes in the acceptance set, i.e., $\mathrm{P}(E_\mathrm{W} < 0|\mathrm{sep}) > 0$, where we follow the convention that separable states admit $E_\mathrm{W}^\infty \geq 0$ in the case of infinite statistics. In fact, in this example, the probability that the witness is negative on a suitable separable state is as large as 41.5%. The straightforward solution seems to be to make the boundary more strict, i.e. require sufficiently negative values to certify entanglement. However, even with the strictest nontrivial bound of $-4/5$ we find that the violation by a separable state is still equal to 2.5%, i.e. $\mathrm{P}(E_\mathrm{W} \leq -4/5|\mathrm{sep}) = 2.5\%$. At the same time, the state ρ gives rise to values $E_\mathrm{W} < -4/5$ with probability of 26.7%. While it is clearly more probable for the entangled state to violate the bound than for any separable state, still, given the finite values of both probabilities, the question remains what the appropriate probabilistic conclusion about the quality of such certification should be.

The nonlinear criterion $S = \langle \sigma_y \otimes \sigma_y \otimes \sigma_x \otimes \cdots \otimes \sigma_x \rangle^2 + \langle \sigma_x \otimes \cdots \otimes \sigma_x \rangle^2$ has been illustrated in Fig. 1. Again we consider the sum of only two squared correlations, each estimated in 10 experimental trials. Our analytical tools return the plotted $\mathrm{P}(S|\mathrm{ent})$ based on the above-mentioned entangled state ρ. Figure 1 clearly illustrates that finite statistics leads to the violation of the bound of 1 by a separable state. Again the immediate solution seems to be making the bound more strict. We find that $\mathrm{P}(S = 2|\mathrm{sep}) = 4.2\%$, but at the same time $\mathrm{P}(S = 2|\rho) = 6.9\%$. With this bound, the procedure would wrongly certify entanglement (false positive) in at most only 4.2% of the cases, but at the same time, it would fail to correctly certify it (false negative) in roughly 93% of the cases where the state was entangled. Furthermore, for any single experiment yielding value $S = 2$, we are clearly not justified to conclude that the state is entangled, as a separable state might have given rise to the same value of S with a comparable probability.

This type of explicit calculation can be applied to any witness based on correlation values to evaluate whether it can be applied efficiently in the case of finite statistics. In particular, it becomes necessary to put $\mathrm{P}(Q \in \mathcal{O}_\mathrm{acc}|\mathrm{sep})$ in relation to the probability $\mathrm{P}(Q \in \mathcal{O}_\mathrm{acc}|\mathrm{ent})$ via a proper statistical analysis, either Frequentist or Bayesian.

Resource optimization

Based on the possibility of quantitatively evaluating any entanglement certification procedure in terms of validity and efficiency, we now tackle the question of how to best use a small number η of available copies of a multi-qubit quantum state. The experimental choice to be made is about the amount of settings M

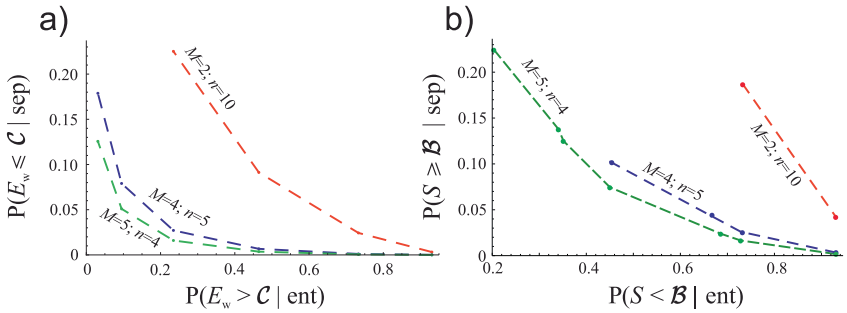

Fig. 3 Optimal use of 20 copies. Plot for ρ in Eq. (15) with $p = 3/4$, e.g. a GHZ state mixed with white noise. Panel (**a**) is for the linear witness, panel (**b**) for the quadratic witness. The discreteness of the outcome space for just 20 copies is clearly visible in the plot. To maximize validity and efficiency both probabilities need to be simultaneously minimized. This is best realized by dividing the 20 copies into 5 correlation measurements, each correlation estimated in 4 experimental runs.

and the distribution of the copies among those $\{n_j\}$, where $\Sigma_j n_j = \eta$. Furthermore, a suitable outcome space $\mathcal{O}_{\text{acc}}$ has to be chosen. By explicitly calculating the distributions P(Q|sep) and P(Q|ent), and assuming a certain prior the validity and efficiency of the procedure can be characterized, no matter if a Frequentist or Bayesian approach is chosen. In practice, a reasonable scenario could be to require a certain minimal validity and then choose a combination of experimental parameters with a suitable acceptance space, such as to maximize efficiency. This yields the following optimization problem:

> Given a certain minimal validity q_{min} and a total number η of state copies, what set of M observables, each estimated on $\{n_j\}$ copies of the state, and what acceptance set $\mathcal{O}_{\text{acc}}$ are to be chosen such that an observation of $Q \in \mathcal{O}_{\text{acc}}$ certifies entanglement with a validity $q \geq q_{\text{min}}$, while keeping the efficiency as high as possible.

Note that when Q is a function of marginal correlations corresponding to commuting operators it can be possible to measure them simultaneously from a single global measurement setting. This is the approach chosen in ref. [9], where a single state copy is used to obtain values for several marginal correlations providing the outcome for a linear witness. Thus, in general, given a function Q also of marginal correlations it is of high interest to group these into as few measurement settings as possible. Since our example witnesses S and W are solely based on full correlations this particular layer of optimization is not relevant for them.

Optimizing entanglement certification strategies

Scenario: First of all, let us emphasise that the proper statistical analysis is especially crucial in the case of a very limited data set composed of at most a few tens of data points. In the examples below we assume that no more than 20 copies of multi-particle state from a possibly entangled source have been successfully measured. The small amount of data makes it practically impossible to distinguish entangled states which are close to separable ones. Thus, the best candidates are states which are strongly non-classically correlated. Generalizing Eq. (14), here, we therefore consider mixed states of the form

$$\rho = p|\psi\rangle\langle\psi| + (1-p)\rho_{\text{n}}, \tag{15}$$

where a dominant admixture comes from a pure state $|\psi\rangle$, assumed to admit perfect correlations, and the remaining part, ρ_{N}, describes experimental noise. Since our theoretical analysis just depends on the number of correlations (measurement settings) it is thus independent of the number of involved particles. See ref. [26] for fidelity estimation with the same feature. Accordingly, we will not specify the state $|\psi\rangle$ exactly as the only parameters that enter the witnesses are correlations. We would like to emphasise this point, the methods work for any GHZ states, graph states, cluster states, absolutely maximally entangled states etc. Although in practice the perfect correlations of $|\psi\rangle$ will be reduced by various types of noise, which we consider via the addition of ρ_n, we show in the "Methods" subsection "Effects of different types of noise" that the probability to observe a certain measurement outcome depends almost entirely on the parameter p, and not a type of noise as long as it is uniform and unbiased. Clearly, it is possible to introduce a specific noise that results in different success probability characteristics. In such a case one can still apply our methods, but here we focus on random noises as they are the usual models of experimental imperfections. Thus, we restrict our examples to the case of white noise, i.e. $\rho_{\text{n}} = \mathbb{1}/2^N$. In effect, the model (15) encompasses a plethora of experimental situations that are of interest in quantum information.

Consider a certification scenario where we expect that the tested state is either from the family (15) or a separable state modelled according to the worst-case correlations compatible with separability (see Estimating Probability Distributions and Correlations Compatible with Separability in the Methods), with P(sep) = P(ent) = 1/2. We assume 20 available state copies and require a target validity of $q_{\text{F}} = q_{\text{B}} = 97.5\%$. This will help us to compare and highlight the differences in reasoning that occur from Frequentist and Bayesian perspectives on statistical inference. According to our optimization scheme, we want to determine the set of measurements, i.e., their amount M and in general also the measurement directions, together with an optimal distribution of clicks per setting $\{n_j\}$. For simplicity here, we restrict the presentation to cases where we assume that all n_j's are the same and equal to n, and hence we constrain the product $Mn = 20$. Let us first set $p = 3/4$ and specify the Bayesian loss function as Eq. (31).

Linear witness. To illustrate how to optimally distribute the 20 copies for the linear witness W, as an example we choose a procedure where the acceptance set is chosen via an upper bound $\mathcal{C}$. We extend the linear witness to M different settings as $E_{\text{W}}^{\infty} = T_1 - T_2 - \cdots - T_M + 1$. It turns out that the worst case separable state, i.e. the state which maximizes the probabilities in the acceptance set, for a sufficiently low bound $\mathcal{C}$ has the correlations $T_1 = -1/M$ and $T_i = 1/M$ for $i = 2, \ldots, M$. In Fig. 3a we plot P($E_{\text{W}} \leq \mathcal{C}$|sep) and P($E_{\text{W}} > \mathcal{C}$|ent), which are directly related to validity and efficiency. As the simultaneous optimization of the two quantifiers is based on keeping both probabilities as small as possible, clearly the optimal procedure is realized for $M = 5$ and $n = 4$.

From the Frequentist perspective to achieve the minimally required validity of 97.5%, a bound of $\mathcal{C}_F = -2.5$ has to be chosen, which leads to an efficiency of $r \approx 76.5\%$. The highest validity achievable with 20 state copies is 99.996% with a bound of $\mathcal{C}_F = -4$. However, it comes at the cost of efficiency of just $r \approx 6.9\%$.

The Bayesian framework requires $\mathrm{P}(\mathrm{ent}|E_W) \geq 97.5\%$ for all values in the acceptance set. This is satisfied if the bound $\mathcal{C}_B$ is chosen as -3. The associated efficiency, in this case, is given by the loss function of $L \approx 0.007$.

From the above results, one can see a clear difference in the choice of the acceptance sets for each reasoning. Namely, the Frequentist bound is less strict than the Bayesian counterpart, implying instances in which experimenters would disagree on the conclusions about the entanglement certification. For comparison, from the Frequentist perspective, the adjusted bound of $\mathcal{C}_B = -3$ that is optimal for the Bayesian approach results in the level of confidence given by 99.64% and the corresponding power of $r \approx 53.5\%$. As expected, for the lower bound confidence is increased and power reduced, however, we emphasise that in general the Bayesian approach does not always yield stricter acceptance sets.

Quadratic witness. Just as for the case of the linear witness, we introduce a bound $\mathcal{B}$ to define the acceptance set also in the example of the quadratic witness. Figure 3b presents the two relevant quantities $\mathrm{P}(S \geq \mathcal{B}|\mathrm{sep})$ and $\mathrm{P}(S<\mathcal{B}|\mathrm{ent})$. Again, the best use of copies is given by $n = 4$ and $M = 5$.

Based on the minimally required validity of 97.5%, we calculate the bound $\mathcal{B}$ for the Frequentist approach to be $\mathcal{B}_F = 4$ and in the Bayesian approach we get $\mathcal{B}_B = 5$. This leads to an efficiency of $r \approx 31.4\%$ and $L \approx 0.013$ respectively. Recall that the chosen priors for the Bayesian inference are $\mathrm{P}(\mathrm{ent}) = \mathrm{P}(\mathrm{sep}) = 0.5$. In general, the examined state is entangled iff $p > 1/(2^{N-1}+1)$[27]. Thus, given our state model, a more realistic scenario would take into account the cardinality of the separable states within the family (15) in the prior probabilities. For example, with a uniform distribution over p and $N = 4$, the natural prior is $\mathrm{P}(\mathrm{ent}) = 8/9$ and $\mathrm{P}(\mathrm{sep}) = 1/9$. This leads to the change of the acceptance set with $\mathcal{B}_B = 4$ and efficiency $L \approx 0.018$. With increasing N the efficiency in the Bayesian approach is changing. As the last example, for $N = 5$ the prior is $\mathrm{P}(\mathrm{ent}) = 16/17$ and $\mathrm{P}(\mathrm{sep}) = 1/17$, the Bayesian bound is given by $\mathcal{B}_B = 3.5$ and the corresponding efficiency reads $L \approx 0.015$.

Again, for equal priors Frequentist reasoning yields a greater acceptance set. However, here one can explicitly see that for more physically motivated priors this is no longer true and $\mathcal{C}_B$ can be smaller than $\mathcal{C}_F$. For all of the discussed cases, confidence and power are $(\mathcal{B} = 5, q_F = 99.8\%, r = 6.9\%)$, $(\mathcal{B} = 4, q_F = 97.6\%, r = 31.4\%)$ and $(\mathcal{B} = 3.5, q_F = 92.5\%, r = 54.9\%)$ respectively. Note that the last level of confidence does not meet the required validity condition.

Generalized scenario: Finally, in a more general example, we relax the condition of an equal amount of copies per setting and apply our optimization algorithm to determine the optimal amount of settings and distribution of state copies over these settings, such as to achieve optimal efficiency for certification with the quadratic witness S. It turns out that different certification strategies are found to be optimal, depending on whether a Frequentist or Bayesian approach is chosen. We calculate the distribution $\mathrm{P}(\rho_j|\mathrm{ent})$ based on the model of a family of noisy three-qubit GHZ states (14), with a mean $\bar{p} = 0.8$ and a standard deviation $\Delta p = 0.1$, such that for the entangled states

$$\mathrm{P}(p) = \begin{cases} \mathcal{N} \mathrm{e}^{-\frac{(p-\bar{p})^2}{2(\Delta p)^2}} & p \in [p_{\min}, 1] \\ 0 & \text{else}, \end{cases} \tag{16}$$

with proper normalization $\mathcal{N}$ and the lower bound $p_{\min} = 1/5$ given by the requirement that the states have to be entangled, see the quadratic witness example in the previous subsection. We set the maximal number of settings to $M = 3$, allow at most 13 state copies and require a minimal validity of 70%. Furthermore, we again choose not to model the separable state space and instead estimate $\mathrm{P}(S|\mathrm{sep})$ via the worst-case optimization used above. In this example for the prior, we assume that it is twice as likely to encounter an entangled state from our family than any separable state.

If the optimization is based on a Frequentist understanding of validity, i.e., achieving at least 70% confidence, it is optimal to use 12 of the 13 possible measurement runs and distribute them equally among the three settings as $n_1 = 4$, $n_2 = 4$ and $n_3 = 4$ (denoted as [444] for brevity). Figure 4a illustrates the resulting probability distribution $\mathrm{P}(S|\mathrm{ent})$ and the worst case distribution $\mathrm{P}(S|\mathrm{sep})$ obtained via the discussed optimization, where the best acceptance set turns out to be $\mathcal{O}_{\mathrm{acc}} = \{0, 1, 2.25, 3\}$. The probability $\mathrm{P}(S \in \mathcal{O}_{\mathrm{acc}}|\mathrm{sep})$ is only 29.8% and thus the confidence remains above 70% while at the same time the power $r = \mathrm{P}(S \in \mathcal{O}_{\mathrm{acc}}|\mathrm{ent})$ is maximized to 66.4%. Estimating also the Bayesian loss for this acceptance interval yields a value of 0.137. For comparison, Fig. 4b illustrates the estimated posterior distribution. From the Bayesian perspective, the acceptance set has to be chosen as $\{2.25, 3\}$ which leads to a minimal level of acceptance of 76.8% and a loss of 0.149. The corresponding power would be 65.6%.

This example illustrates two seemingly peculiar consequences of the need to use a worst-case estimation. The first concerns the benefit of using a randomized test. To maximize the power of the test, the outcomes 0 and 1 are included in the acceptance set. As seen in Fig. 4 these are not valuable points since they have a significantly higher likelihood given a separable state than an entangled state. In principle, it would be much more beneficial to add a point with a better likelihood ratio, but as the optimization shows in this case the confidence would drop below 70%. This problem is resolved by the Neymark–Pearson lemma[13], which proves that the optimal strategy consists of simply choosing the points with the best likelihood ratios (after corresponding optimization) and make a probabilistic conclusion whenever results with the lowest ratio are obtained. In this manner, the confidence level of 70% could be reached exactly while maximizing the power of the test even further. Second, the loss of the interval $\{0, 1, 2.25, 3\}$ is estimated to be smaller than the loss of the interval $\{2.25, 3.0\}$, while still the latter is chosen as the Bayesian optimum. This discrepancy is a consequence of the fact that different worst-case estimates are chosen to find the acceptance sets and to calculate the loss, as explained further in the "Methods" subsection "Estimating the probability distributions". These loss values are only used to compare the Bayesian performance given different distributions of measurement settings.

Figure 4d shows the posterior distribution for the optimal case according to the Bayesian approach, i.e. achieving at least 70% level of acceptance with as little expected loss as possible. It turns out that in this case, it is better to use only 11 of the 13 possible measurements and distribute them as [533] among the three settings. The requirement of $q_B \geq 70\%$ leads to the choice of acceptance set $\mathcal{O}_{\mathrm{acc}} = \{2.36, 3\}$ leading to a loss of 0.146, which is smaller than the value of 0.149 obtained with the distribution [444]. The corresponding power would be 50.4%. Conversely, as illustrated in Fig. 4c, with [444] only a power of 53.5% with a level of confidence of 71.1% (and a loss of 0.1603) can be reached from the point of view of the Frequentist approach making that choice suboptimal as compared with the best choice presented above. Note, that also here a randomized test would yield better results.

It might seem strange that in both cases a smaller than maximal number of copies is deemed optimal, but this is mainly a consequence of the strong discreteness of the outcome space. Indeed the maximal number of 13 measurements might provide

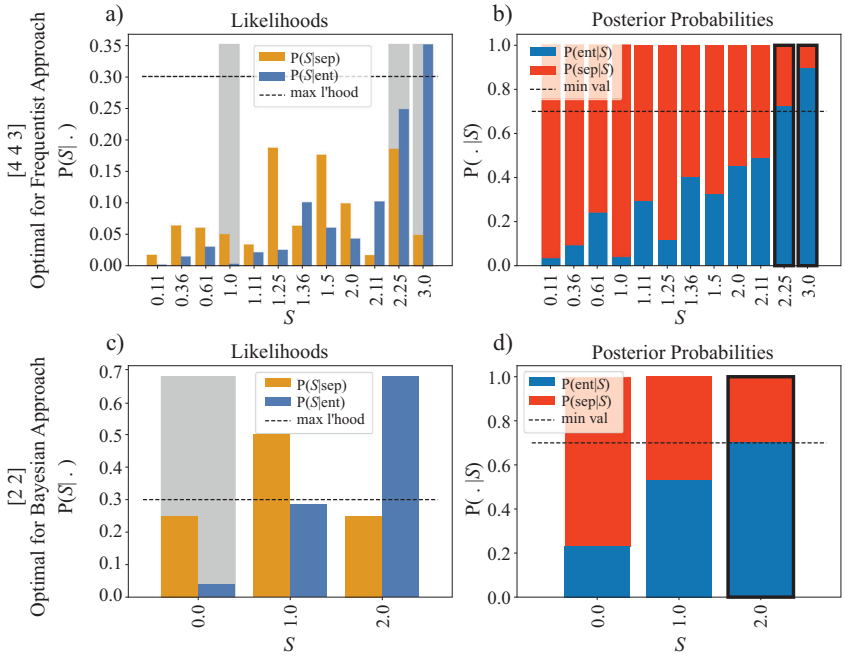

Fig. 4 Optimal choices of distributions of states for Bayesian and Frequentist figures of merit. Panel **a** shows the estimated distributions P(S|ent) (blue bars) and P(S|sep) (orange bars) for the choice [444] which is optimal from the Frequentist point of view. Note that the shown P(S|sep) is actually the worst-case estimate $G_{acc}(Q)$, optimized for one particular acceptance set. The acceptance set $\mathcal{O}_{acc} = \{0, 1, 2.25, 3\}$ (marked by the grey background) is chosen by maximizing $P(S \in O_{acc}|ent)$, i.e., includes as much as possible of blue bar length while not allowing $P(S \in O_{acc}|sep)$ (estimated by $G_{acc}(S \in O_{acc}|sep)$) to exceed $1-70\% = 30\%$ (dashed black line), i.e., not getting too much orange bar length into the acceptance set. A power of 66.4% is reached. Panel **b** shows the posterior probability P(ent|S) for that choice of experiment. The acceptance set (marked by the black boxes) is given by all values of S for which $P(ent|S) = 1-P(sep|S) \geq 70\%$ (dashed horizontal line) leading to $\mathcal{O}_{acc} = \{2.25, 3\}$. Note, that the posterior is based on the point-wise worst-case optimization G_S which is different from the one employed in panel a), see Estimating Probability Distributions in the Methods. Panels **c** and **d** show the respective distributions for the choice [533] optimal from the Bayesian point of view. With the acceptance set $\mathcal{O}_{acc} = \{2.36, 3\}$ for the Bayesian analysis, it leads to a smaller estimated loss. On the other hand, the optimal Frequentist power of 53.5% with the interval {0.58, 2.36, 3} is significantly lower than for the first testing strategy. Note, for example in panel (**c**) it might appear that choosing, say the point 1.22 instead of 0.58 might be more beneficial for the Frequentist. However, it needs to be taken into account that the shown distribution is obtained from a worst-case optimization for $\mathcal{O}_{acc} = \{0.58, 2.36, 3\}$ and that with appropriate parameters $G_{acc}(S \in \{1.22, 2.36, 3\}|sep) \geq 30\%$ can be achieved.

maximal information about the state. However, the ability to harness this information within the given bounds on the levels of confidence and acceptance is restricted by the need to choose the acceptance and rejection sets from a small number of outcomes. It can thus happen that for a smaller number of measurements, the probabilities distribute more favourably such that the relevant quantifiers can reach better values.

Finally, it is important to keep in mind that although we subsume the level of confidence and level of acceptance by the term validity, they quantify different figures of merit which correspond to different practical interests. While the Frequentist is only interested in the average correctness of the conclusion of the certification method, the Bayesian wants to quantify the correctness of the conclusion on a case-by-case basis (and becomes dependent on the prior). Note, for example, that with the distribution [444] although it is much more probable for a separable state to yield a value 1 than for an entangled state (see Fig. 4a, given that result, the Frequentist would still certify entanglement as this decision increases the overall power without violating the significance level. On the other hand, if, as done here, a worst-case optimization of correlations compatible with separability is used, the Frequentist approach requires prior assumptions only to estimate the power (by modelling the space of entangled states) and can provide an assertion of the confidence which is completely independent of all priors.

DISCUSSION

In entanglement certification, it is usually of interest to achieve a sufficiently high validity, i.e. be sufficiently convinced that the certification does not falsely conclude entanglement. Here we showed explicitly that for small data sets it is necessary to consider not only P(Q|sep), i.e. the probability of a separable state to yield particular values of the witness Q, but also P(Q|ent) of entangled states. Such proper design of an experiment is necessary if we are to make robust conclusions in the presence of finite statistics and allows us to define and evaluate the validity and efficiency of the method. Only with these two quantifiers, it becomes possible to optimize the usage of the available experimental resources.

We have introduced a universal procedure that allows the extension of any entanglement witness to the domain of finite statistics. It is based on an analytical calculation of probability distributions over possible outcomes when estimating correlation functions experimentally with finite resources. Based on these probability distributions we recalled the measures of validity and efficiency, applicable to any entanglement detection scheme, from the points of view of both Frequentist and Bayesian interpretation. Illustrative examples were provided based on linear as well as nonlinear witnesses and broad families of states.

The methods introduced here are directly applicable to raw data and should be especially helpful for a resource-efficient estimation of the performance of a known apparatus subject to

variations of external parameters or in multipartite experiments with rare detection events, e.g., multi-photon setups based on coincidence clicks. For example, our scheme could be employed to quickly certify the quality of a large quantum processor before a time-consuming computation task.

METHODS

Certifying entanglement

Linear witnesses W admit the following expansion in terms of the Pauli basis

$$\mathrm{W} = \sum_j a_j \sigma_j. \tag{17}$$

The expectation value $E_\mathrm{W} \equiv \langle \mathrm{W} \rangle$ given a particular state ρ, is then a linear function of the correlations T_j given by

$$E_\mathrm{W} = \mathrm{Tr}(\mathrm{W}\rho) = \sum_j a_j T_j. \tag{18}$$

Measuring each correlation and computing the expectation value of the witness function provides information about the separability of the state. Constructions of such functions are tailored to a specific entangled state for which $E_\mathrm{W} < 0$, whereas the expectation value on separable states is never negative. For example, a linear witness detecting entanglement of a three-qubit GHZ state could be chosen as

$$\mathrm{W} = \sigma_y \otimes \sigma_y \otimes \sigma_x - \sigma_x \otimes \sigma_x \otimes \sigma_x + 1, \tag{19}$$

where the constant ensures that the witness is non-negative on separable states and negative on the GHZ state $(|000\rangle + |111\rangle)/\sqrt{2}$, written in the standard σ_z basis.

Entanglement in state ρ can also be revealed via nonlinear witnesses. As an example we consider the scheme introduced in ref. [19]. Consider the so-called correlation length S defined by

$$S \equiv \sum_{j=1}^{3^N} T_j^2, \tag{20}$$

which is the sum of all *full* correlations squared. Accordingly, the sum goes only up to 3^N (the marginal correlations are not included). It has been proven[17,20–24] that a value of $S > 1$ certifies entanglement. Since S sums up only non-negative terms, entanglement is verified as soon as a subset of M correlations violates the bound, i.e., $S_M > 1$. We omit the subscript whenever the number of measured settings is clear.

Witnesses in finite statistics

Since the product of qubit measurement results is either equal to $+1$ or -1, the probability that in n trials we obtain n_+ products equal to $+1$ is given by the binomial distribution:

$$\mathrm{p}_i(n_+) = \binom{n}{n_+} \left(\frac{1+T_i}{2}\right)^{n_+} \left(\frac{1-T_i}{2}\right)^{n_-}, \tag{21}$$

where $(1 \pm T_i)/2$ is the probability to obtain the product equal to ± 1 in a single trial, estimated from the ideal quantum mechanical prediction. All random variables are assumed to be independent and identically distributed. Using Eq. (8) the correlation τ_i is also binomially distributed as

$$\mathrm{P}(\tau_i) = \mathrm{p}_i\left(\frac{n}{2}(1+T_i)\right). \tag{22}$$

Note that due to the finiteness of n also τ_i can take on a finite set of values $\{-1, -1+\frac{2}{n}, \ldots, 1-\frac{2}{n}, 1\}$.

In the case of nonlinear witnesses, these correlations have to be further processed. We illustrate this process using the quadratic witness S since it can be easily generalized to any power. In order to write the probability distribution of different values of S we first note that

$$\mathrm{P}(\tau_i^2) = \mathrm{P}(\tau_i) + \mathrm{P}(-\tau_i) \quad \text{for} \quad \tau_i \neq 0, \tag{23}$$

because both values $\pm\tau_i$ give the same square. In the special case of $\tau_i = 0$, the probability $\mathrm{P}(\tau_i^2)$ is just given by $\mathrm{P}(\tau_i = 0)$. Since S is defined as the sum of squares, a particular value of S can be realized in many ways, e.g. the value $S = 1$ can be achieved if any one $\tau_i^2 = 1$ and all the other squared correlations are zero, or when all $\tau_i^2 = 1/M$, etc. The same reasoning applies to the linear case. Assuming that all the squared correlations τ_i^2 are independently distributed, the values of S satisfy:

$$\mathrm{P}(S) = \sum_{\tau_1^2 + \cdots + \tau_M^2 = S} \mathrm{P}(\tau_1^2) \cdots \mathrm{P}(\tau_M^2). \tag{24}$$

These distributions were used in the "Results" section to derive mean values and variances of the introduced quantities.

Estimating the probability distributions

For a simple hypothesis test, determining validity and efficiency requires the calculation of the two likelihoods $\mathrm{P}(Q|\mathrm{sep})$ and $\mathrm{P}(Q|\mathrm{ent})$. In practice, however, the parameter space is more complicated and one has to consider the full subspaces $\mathcal{H}_\mathrm{sep}$ and $\mathcal{H}_\mathrm{ent}$ of separable and entangled states. These spaces would be modelled via distributions $\mathrm{P}(\rho_j|\mathrm{sep})$ and $\mathrm{P}(\rho_j|\mathrm{ent})$ of separable and entangled states ρ_j and each of those states would give rise to certain likelihood of outcomes $\mathrm{P}(Q|\rho_j)$. Although one option would be to expand the discussion towards so-called composite hypothesis tests, the simple scenario can be recovered by reducing these state spaces to single parameters ('sep' and 'ent'). This is done by considering the average distributions of outcomes given a separable or entangled state with

$$\mathrm{P}(Q|\mathrm{sep}) = \sum_j \mathrm{P}(Q|\rho_j)\mathrm{P}(\rho_j|\mathrm{sep}), \tag{25}$$

$$\mathrm{P}(Q|\mathrm{ent}) = \sum_j \mathrm{P}(Q|\rho_j)\mathrm{P}(\rho_j|\mathrm{ent}). \tag{26}$$

Unfortunately, evaluating such expressions is notoriously daunting[28].

In some cases, it is possible to avoid the modelling of the state space and instead consider a worst-case distribution of values Q. For $\mathrm{P}(Q|\mathrm{sep})$ this distribution can either be calculated point-wise for each Q, denoted as G_Q, or for the whole acceptance interval $\mathcal{O}_\mathrm{acc}$, denoted as G_acc. These distributions have to satisfy

$$\forall_{\rho \in \mathcal{H}_\mathrm{sep}} \, \forall_{Q \in \mathcal{O}_\mathrm{acc}} \quad \mathrm{G}_Q(Q) \geq \mathrm{P}(Q|\rho) \quad \text{and} \tag{27}$$

$$\forall_{\rho \in \mathcal{H}_\mathrm{sep}} \quad \mathrm{G}_\mathrm{acc}(Q \in \mathcal{O}_\mathrm{acc}) \geq \mathrm{P}(Q \in \mathcal{O}_\mathrm{acc}|\rho), \tag{28}$$

where G_Q is stronger in the sense that it satisfies the condition for G_acc as well, i.e. $\mathrm{G}_\mathrm{acc}(Q \in \mathcal{O}_\mathrm{acc}) \leq \sum_{Q \in \mathcal{O}_\mathrm{acc}} \mathrm{G}_Q(Q)$. The strategy to find the upper bounds is based on finding a set of M correlations T_j corresponding to $\tilde{\rho}$ such that $\mathrm{P}(Q|\tilde{\rho})$ satisfies the criterion in question. Note that $\tilde{\rho}$ might not even be a proper density matrix which is why we refer to such correlations as compatible with separability. Furthermore, in the case of G_Q the value at each Q can correspond to a different $\tilde{\rho}$.

G_acc can be used straightforwardly to choose Frequentist acceptance sets by modifying condition (2) to

$$\sum_{Q \in \mathcal{O}_\mathrm{acc}} \mathrm{P}(Q|\mathrm{sep}) \leq \sum_{Q \in \mathcal{O}_\mathrm{acc}} \mathrm{G}_\mathrm{acc}(Q|\mathrm{sep}) \leq 1 - q_\mathrm{F}. \tag{29}$$

If the criterion is satisfied for G_acc it will also be satisfied for the actual distribution $\mathrm{P}(Q|\mathrm{sep})$. Thus, the estimation can only lead to a stricter choice of the acceptance set and ensures that the minimal level of significance is attained.

In the Bayesian case for each outcome Q the minimal validity q_B is assured as in Eq. (4), by providing a lower bound on $\mathrm{P}(\mathrm{ent}|Q)$

using G_Q as

$$\mathrm{P}(\mathrm{ent}|Q)=\frac{\mathrm{P}(Q|\mathrm{ent})\mathrm{P}(\mathrm{ent})}{\mathrm{P}(Q|\mathrm{sep})\mathrm{P}(\mathrm{sep})+\mathrm{P}(Q|\mathrm{ent})\mathrm{P}(\mathrm{ent})}\geq\frac{\mathrm{P}(Q|\mathrm{ent})\mathrm{P}(\mathrm{ent})}{G_Q(Q)\mathrm{P}(\mathrm{sep})+\mathrm{P}(Q|\mathrm{ent})\mathrm{P}(\mathrm{ent})}\geq q_B. \tag{30}$$

To estimate the expected loss, however, it is sufficient to employ the weaker worst-case estimate G_{acc} since the scenario is considered a priori, i.e. before a particular outcome Q is known. It is thus sufficient to only maximize the probability in the whole interval $\mathcal{O}_{acc}$, independently of how $G_{acc}(Q)$ is related to P(Q|sep) point-wise. The loss (6) is thus estimated as

$$\begin{aligned}L &= q_B\mathrm{P}(Q\in\mathcal{O}_{acc}|\mathrm{sep})\mathrm{P}(\mathrm{sep})+(1-q_B)\mathrm{P}(Q\in\mathcal{O}_{rej}|\mathrm{ent})\mathrm{P}(\mathrm{ent})\\ &\leq q_B G_{acc}(Q\in\mathcal{O}_{acc})\mathrm{P}(\mathrm{sep})+(1-q_B)\mathrm{P}(Q\in\mathcal{O}_{rej}|\mathrm{ent})\mathrm{P}(\mathrm{ent}).\end{aligned} \tag{31}$$

Since different worst-case estimates are employed, i.e. G_Q to find the acceptance interval and G_{acc} to estimate the loss, it is no longer the case that the optimal choice of acceptance intervals minimizes the loss. However, the worst-case estimate of the loss with G_{acc} is still useful to compare scenarios with different numbers of copies and distributions of copies over settings, for each of which G_Q has been used as a rule to find the acceptance sets.

In analogy to P(Q|sep) in principle, both the Frequentist and the Bayesian approach could proceed given a lower bound on P(Q|ent). However, this is completely unfeasible for several reasons. For example, for the non-linear witness S: (i) entangled states can easily yield very small values of S due to statistical fluctuations, (ii) some entangled states have small (or even vanishing) S^∞[29–32], (iii) there are bad choices of measurement settings, e.g. ones that give S^∞ close to 1. Thus, P(S|ent) is obtained by modelling a certain state distribution $\mathrm{P}(\rho_j|\mathrm{ent})$, which fits the currently employed apparatus for state generation, as illustrated in Results (Optimizing Entanglement Certification Strategies). Similar problems appear for linear witnesses. Note, that the probability distributions $\mathrm{P}(\rho_j|\mathrm{sep})$ and $\mathrm{P}(\rho_j|\mathrm{ent})$ do not describe a statistical uncertainty of the form encountered in mixed states. Instead, they capture prior expectations as to what separable or entangled states are to be submitted to the certification procedure. In other words, due to nonlinearity of the function $\mathrm{P}(Q|\rho_j)$ it does not hold that $\mathrm{P}(Q|\mathrm{sep})=\mathrm{P}(Q|\overline{\rho}_{\mathrm{sep}})$ with a mean separable state $\overline{\rho}_{\mathrm{sep}}=\sum_j\rho_j\mathrm{P}(\rho_j|\mathrm{sep})$ and similarly for P(Q|ent).

Correlations compatible with separability

We have written an optimization algorithm in order to find the set of correlation functions that maximize the probabilities in the acceptance sets while being compatible with separability, i.e. the correlations do not violate the witness in the limit of infinite sample size. It verifies that for equal distribution of copies over the settings, i.e. each $n_i=n$ for each $i=1,\ldots,M$, and sufficiently high bound on the linear witness $\mathcal{C}$ ($\mathcal{B}$ for the non-linear witness) all of the correlations can be taken as $T_i=1/M$ ($T_i^2=1/M$). The algorithm can be also applied to a model probability distribution over Q for separable states and arbitrary distributions of copies as well as more complicated disjoint acceptance sets (see the "Results" subsection "Optimizing entanglement certification strategies").

The basic algorithm works as follows. We compute P(Q) and the cumulative probability function. They are parameterized with to-be-determined correlations $\{T_1,T_2,\ldots,T_M\}$ as well as the bound defining the acceptance set. The heart of the computation is the numerical maximization of $\sum_{Q\in\mathcal{O}_{acc}}\mathrm{P}(Q)(\mathrm{P}(Q)\forall_{Q\in\mathcal{O}_{acc}})$, for the fixed value of bound, with respect to $\{T_1,T_2,\ldots,T_M\}$. We constrain the set of possible correlations to those that yield $W^\infty\geq 0$ for the linear and $S^\infty\leq 1$ for the non-linear witness, with each $T_i\in[-1,1]$. Two widely available out-of-the-box methods were used for finding the maximum: simulated annealing and Nelder-Mead algorithm[33,34]. Both gave similar results with the Nelder–Mead method being more precise in the considered problem. The output of the algorithm is a list of $\{T_1,T_2,\ldots,T_M\}$ that maximizes $\sum_{Q\in\mathcal{O}_{acc}}\mathrm{P}(Q)(\mathrm{P}(Q)\forall_{Q\in\mathcal{O}_{acc}})$ for the given bound, or any other acceptance set, under the stated constraints.

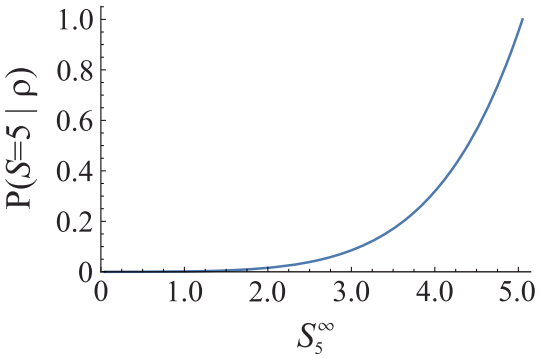

Fig. 5 The efficiency of entanglement detection for different noises ρ_n and their admixtures p in Eq. (15). The plot shows the probability of measuring $S=5$ given ρ (vertical axis) as a function of S_5^∞ (horizontal axis). The plotted curve assumes white noise and is given analytically as $[(1+6p^2+p^4)/8]^5$. The data for the other types of noise, i.e., pure and mixed noises according to Eqs. (33) and (34), overlap with the presented one. Thus, different types of unbiased noises are not relevant to the considered criteria.

Effects of different types of noise

We analyse here the effects due to different forms of noise in Eq. (15) on the efficiency of the entanglement certification. In particular, we consider the following unbiased noises

$$\rho_{\mathrm{wn}}=\mathbb{1}/2^N,\quad \text{white noise} \tag{32}$$

$$\rho_{\mathrm{rp}}=|\psi_{\mathrm{r}}\rangle\langle\psi_{\mathrm{r}}|,\quad \text{Haar random pure state noise} \tag{33}$$

$$\rho_{\mathrm{wn}}=\rho_{\mathrm{r}},\quad \text{random mixed states}, \tag{34}$$

where Haar randomness refers to the sampling of states according to the rotationally invariant measure. Data for the random states was computed numerically by scanning p in the range [0.5, 1] with steps of 0.01, sampling 1000 random four-qubit states for each p, choosing the five biggest correlations, computing S_5^∞ and finally the probability of $S=5$ in finite statistics. In this way, practically all the values of S_5^∞ were scanned. These calculations have shown that the probability of success does not depend on the kind of noise and it is described solely by the value of p. The probability of success $\mathrm{P}(S=5|\rho)$ for a continuous choice of p is presented in Fig. 5.

DATA AVAILABILITY

The data supporting figures are available at https://doi.org/10.48550/arXiv.2208.01983.

Received: 20 July 2023; Accepted: 11 January 2024;
Published online: 24 January 2024

REFERENCES

1. Horodecki, M., Horodecki, P. & Horodecki, R. Separability of mixed states: necessary and sufficient conditions. *Phys. Lett. A* **223**, 1 (1996).

2. Horodecki, R., Horodecki, P., Horodecki, M. & Horodecki, K. Quantum entanglement. *Rev. Mod. Phys.* **81**, 865 (2009).
3. Gühne, O. & Tóth, G. Entanglement detection. *Phys. Rep.* **474**, 1–75 (2009).
4. Arrazola, J. M. et al. Reliable entanglement verification. *Phys. Rev. A* **87**, 062331 (2013).
5. Blume-Kohout, R., Yin, J. O. S. & van Enk, S. J. Entanglement verification with finite data. *Phys. Rev. Lett.* **105**, 170501 (2010).
6. Zhu, H. & Hayashi, M. Efficient verification of pure quantum states in the adversarial scenario. *Phys. Rev. Lett.* **123**, 260504 (2019).
7. Wang, K. & Hayashi, M. Optimal verification of two-qubit pure states. *Phys. Rev. A* **100**, 032315 (2019).
8. Zhang, W.-H. et al. Experimental optimal verification of entangled states using local measurements. *Phys. Rev. Lett.* **125**, 030506 (2020).
9. Dimić, A. & Dakić, B. Single-copy entanglement detection. *npj Quantum Inf.* **4**, 11 (2018).
10. Saggio, V. et al. Experimental few-copy multipartite entanglement detection. *Nat. Phys.* **15**, 935 (2019).
11. Morris, J., Saggio, V., Gočanin, A. & Dakić, B. Quantum verification and estimation with few copies. *Adv. Quant. Tech.* **5**, 2100118 (2022).
12. Saggio, V. & Walther, P. Few-copy entanglement detection in the presence of noise. *Ann. Phys.* **534**, 2100597 (2022).
13. Lehmann, E. L. & Romano, J. P. *Testing Statistical Hypotheses* (Springer, Cham, 2005).
14. Robert, C. P. *The Bayesian Choice* (Springer, New York, NY, 2013).
15. Berger, J. O. *Statistical Decision Theory and Bayesian Analysis* (Springer, New York, NY, 2010).
16. Jungnitsch, B. et al. Increasing the statistical significance of entanglement detection in experiments. *Phys. Rev. Lett.* **104**, 210401 (2010).
17. Tran, M. C., Dakić, B., Arnault, F., Laskowski, W. & Paterek, T. Quantum entanglement from random measurements. *Phys. Rev. A* **92**, 050301R (2015).
18. Knips, L. et al. How long does it take to obtain a physical density matrix? arXiv:1512.06866 (2015).
19. Badziag, P., Brukner, C., Laskowski, W., Paterek, T. & Żukowski, M. Experimentally friendly geometrical criteria for entanglement. *Phys. Rev. Lett.* **100**, 140403 (2008).
20. Hassan, A. S. M. & Joag, P. S. Separability criterion for multipartite quantum states based on the Bloch representation of density matrices. *Quantum Inf. Comp.* **8**, 773 (2008).
21. Hassan, A. S. M. & Joag, P. S. Experimentally accessible geometric measure for entanglement in *n*-qubit pure states. *Phys. Rev. A* **77**, 062334 (2008).
22. Hassan, A. S. M. & Joag, P. S. Geometric measure for entanglement in *n*-qudit pure states. *Phys. Rev. A* **80**, 042302 (2009).
23. Tran, M. C., Dakić, B., Laskowski, W. & Paterek, T. Correlations between outcomes of random measurements. *Phys. Rev. A* **94**, 042302 (2016).
24. Knips, L., Schwemmer, C., Klein, N., Wieśniak, M. & Weinfurter, H. Multipartite entanglement detection with minimal effort. *Phy. Rev. Lett.* **117**, 210504 (2016).
25. Knips, L. et al. Multipartite entanglement analysis from random correlations. *npj Quantum Inf.* **6**, 51 (2020).
26. Flammia, S. T. & Liu, Y.-K. Direct fidelity estimation from few Pauli measurements. *Phys. Rev. Lett.* **106**, 230501 (2011).
27. Pittenger, A. O. & Rubin, M. H. Geometry of entanglement witnesses and local detection of entanglement. *Phys. Rev. A* **67**, 012327 (2003).
28. Li, W., Han, R., Shang, J., Ng, H. K. & Englert, B.-G. Sequentially constrained Monte Carlo sampler for quantum states. Preprint at https://arxiv.org/abs/2109.14215 (2021).
29. Kaszlikowski, D., De, A. S., Sen, U., Vedral, V. & Winter, A. Quantum correlations without classical correlations. *Phys. Rev. Lett.* **101**, 070502 (2008).
30. Laskowski, W., Markiewicz, M., Paterek, T. & Wieśniak, M. Incompatible local hidden-variable models of quantum correlations. *Phys. Rev. A* **86**, 032105 (2012).
31. Schwemmer, C. et al. Genuine multipartite entanglement without multipartite correlations. *Phys. Rev. Lett.* **114**, 180501 (2015).
32. Tran, M. C. et al. Genuine n-partite entanglement without n-partite correlation functions. *Phys. Rev. A* **95**, 062331 (2017).
33. Inc., W. R. *Mathematica, Version 13.1* (W.R. Inc., Champaign, IL, 2022).
34. Virtanen, P. et al. SciPy 1.0: fundamental algorithms for scientific computing in Python. *Nat. Methods* **17**, 261–272 (2020).

ACKNOWLEDGEMENTS

We thank Borivoje Dakić for useful discussions. This research was supported by the DFG (Germany) and NCN (Poland) within the joint funding initiative 'Beethoven2' (2016/23/G/ST2/04273, 381445721), by the DFG under Germany's Excellence Strategy EXC-2111-390814868 and by the BMBF project QuKuK (16KIS1621). P.C. is supported by the National Science Centre (NCN, Poland) within the Preludium Bis project (Grant No. 2021/43/O/ST2/02679). W.L. acknowledges partial support from the Foundation for Polish Science (IRAP project ICTQT, Contract No. 2018/MAB/5, co-financed by EU via the Smart Growth Operational Programme). T.P. is supported by the Polish National Agency for Academic Exchange NAWA Project No. PPN/PPO/2018/1/00007/U/00001. J.D. acknowledges support from the Ph.D. programme IMPRS-QST.

AUTHOR CONTRIBUTIONS

P.C., W.L. and L.K. started the project. P.C. and L.K. formulated the finite statistics model for entanglement witnesses. J.D. analysed and performed a careful statistical analysis, further developed by J.D., P.C., L.K. and W.K. P.C., J.D., L.K. and J.M. prepared detailed examples and perfected the resource optimization strategy. W.L., T.P. and H.W. supervised the project. All authors contributed to analysing the results, as well as writing the manuscript.

COMPETING INTERESTS

The authors declare no competing interests.

ADDITIONAL INFORMATION

Correspondence and requests for materials should be addressed to Paweł Cieśliński or Wiesław Laskowski.

Reprints and permission information is available at http://www.nature.com/reprints

Publisher's note Springer Nature remains neutral with regard to jurisdictional claims in published maps and institutional affiliations.

Open Access This article is licensed under a Creative Commons Attribution 4.0 International License, which permits use, sharing, adaptation, distribution and reproduction in any medium or format, as long as you give appropriate credit to the original author(s) and the source, provide a link to the Creative Commons license, and indicate if changes were made. The images or other third party material in this article are included in the article's Creative Commons license, unless indicated otherwise in a credit line to the material. If material is not included in the article's Creative Commons license and your intended use is not permitted by statutory regulation or exceeds the permitted use, you will need to obtain permission directly from the copyright holder. To view a copy of this license, visit http://creativecommons.org/licenses/by/4.0/.

© The Author(s) 2024

3.4 Spacetime Structure of Measurements

3.4.1 Wheeler's Delayed Choice

Delayed choice scenarios, as pioneered by Wheeler in terms of seminal gedankenexperiments [1021, 1020], allow to exclude certain physical mechanisms of complementarity by analyzing the spacetime structure of quantum measurements [997, 378]. They are based on establishing a simple scenario which allows to clearly distinguish two complementary types of phenomena as depicted in Fig. 3.4. In this experimental configuration, most commonly realized in form an interferometer as introduced in Sec. 5.4, in a first step the spatial wavefunction of the system is separated into two disjoint but comparatively well-localized parts ψ_α and ψ_β, which propagate towards two detectors. The propagation and the detectors are arranged such that each component can reach only one of the detectors, which is denoted as "case P" for "particle". These detectors can be modeled as sufficiently extended such that they implement a coarse grained projective position measurement which differentiates just between the two subspaces corresponding to the two components of the wavefunction. In the second step, depending on an experimental setting S, which crucially is either chosen in space-like separation from the first step or even in its future, a unitary operation $\mathbf{U}$ can be implemented which transforms the state of the system such that instead superpositions $\psi_\pm := \big(\psi_\alpha \pm \exp(i\varphi)\psi_\beta\big)/\sqrt{2}$, where φ is some relative phase, propagate towards the detectors. This case is depicted in right panel of Fig. 3.4 and denoted as "case W" for "wave". The fact that, assuming RC, the choice of the setting can have no causal influence on the behavior of the system at the first step $\mathbf{U}_{\text{sep}}$ constitutes the "delayed choice" character of the scenario. Note that, while in Wheeler's original interferometric gedankenexperiment the paths of the wavefunction components cross, this has no relevance for the scenario and case P in Fig. 3.4 is fully equivalent to Wheeler's case without the beam splitter. However, as discussed in Sec. 7.2.3, these two scenarios differ significantly from the perspective of the Bohmian interpretation.

For equal amplitudes of ψ_α and ψ_β, in case P, the rules of quantum mechanics predict an irreducibly random single detection event at one of the detectors, with equal probabilities of detection. Wheeler then effectively considers a model realist interpretation R, which takes a particular detection event as evidence that a particle "has traveled only *one* route", corresponding either to the trajectory of component ψ_α or ψ_β [1020]. In case W, i.e., if the unitary transformation is performed, the detection probabilities depend on the relative phase φ between the two components and for a suitable phase relation fully destructive interference towards one of the detectors can be realized such that the other projection succeeds with certainty. Accordingly, in this case the model interpretation R is taken to conclude that the particle "has arrived by both routes" since their relative phase is of relevance [1020]. The fact that these two modes of propagation correspond to the intuitions of wave-particle duality, as discussed in Sec. 3.1.5, are the reason why they are sometimes also denoted as "particle behavior" and "wave behavior", respectively [397, 436, 997]. The conclusions according to interpretation R would then be that in dependence of the chosen measurement the past of the system is definite and either corresponds to a particle, i.e.,

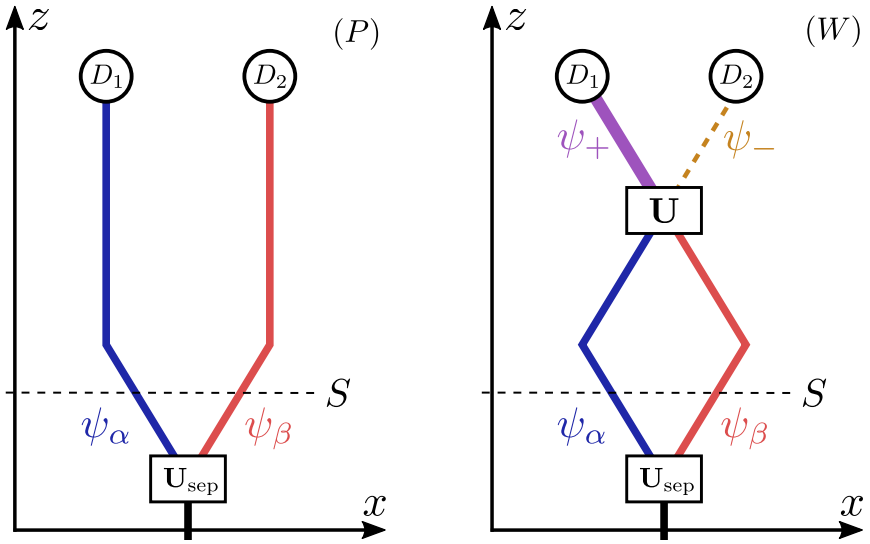

Figure 3.4: **Wheeler-Type Delayed Choice Scenario** The panels show two possible spatial propagations of the wavefunction of a quantum system, dependent on the choice of setting S. In both cases the spatial wavefunction of the system is initially separated via $\mathbf{U}_{\text{sep}}$ into two components propagating along two distinct paths in positive z-direction. The time where the setting is chosen in relation to the propagation is depicted as a horizontal dashed line. While in case (P) each of the components ψ_α and ψ_β reaches a separate detector, in case (W), due the additional unitary operation $\mathbf{U}$, instead the superpositions $\psi_\pm$ propagate towards the respective detectors. The thick and dashed line used for ψ_+ and ψ_-, respectively, indicate a case where the relative phase between the two paths is chosen such that ψ_- is vanishingly small and thus only detector D_1 registers detection events.

propagation along a single trajectory, or a delocalized wave. Thus, in the delayed choice scenario, the choice of the setting S in the future appears to have "an unavoidable effect on what we have a right to say about the already past history" of the particle [1020].

Bar retrocausality, the effective dependence of the past on the future setting represents a refutation of the particular realistic interpretation R [1021, 1020, 397, 997]. As an alternative Wheeler and others propose an interpretation of Bohr's principle of complementarity, with a special emphasis on the fact that the properties of a quantum system are fundamentally undefined until irreversible macroscopic records are created by some classical measurement apparatus. In the words of Wheeler, where in his example the particle is a photon:

> It is wrong to speak of the "route" of the photon [...] It is wrong to attribute a tangibility to the photon in all its travel from the point of entry to its last instant of flight. A phenomenon is not yet a phenomenon until it has been brought to a close by an irreversible act of amplification [...] we find that nature at the quantum level is not a machine that goes its inexorable way. Instead what answer we get depends on the question we put, the experiment we arrange, the registering device we choose. We are inescapably involved in bringing about that which appears to be

> happening. [1020]

Nevertheless, at least in some formulations, Wheeler seems to admit certain statements about the unmeasured past of the particle based on theoretical considerations. For example he writes:

> ... the lesson presents itself rather as this, that the past has no existence except as it is recorded in the present. It has no sense to speak of what the quantum of electromagnetic energy was doing except as it is observed or *calculable*[2] from what is observed. [1021]

While thus in Wheeler's view there appears to be a sense in which the past can be described based on present observations, such inferences do not have the same character as empirical observation and are fundamentally theory dependent. As emphasized by Wheeler:

> What we call reality consists [...] of a few iron posts of observation between which we fill in by an elaborate papier-mache [sic] construction of imagination and theory. [1020]

3.4.2 Generalized Delayed Choice

The concept of delayed choice has been generalized and implemented experimentally in various quantum systems, e.g., [393, 398, 401, 436, 407, 396], see also [997] for a comprehensive overview. The formal essence of a generalized delayed choice scenario is given by the fact that a system-pointer interaction does not determine the form of the corresponding quantum instrument, which instead crucially depends on the observable measured on the pointer. Thus, as illustrated in Fig 3.5a, after the measurement-interaction has taken place, it is possible to induce a space-like separation between system and pointer and only then choose which pointer observable $\mathbf{C}$ to measure at the site of the pointer. While the non-selective post-measurement state of the system depends only on the system-pointer interaction $\mathbf{U}$, the initial system state ρ, and the initial pointer state $|\chi\rangle$, the conditional system states ρ_j also depend on the choice of $\mathbf{C}$, as described in Sec. 2.2.2. The resulting instrument is given by the Kraus operators $\mathbf{K}_j = \langle c_j| \mathbf{U} |\chi\rangle$, where $|c_j\rangle$ are eigenstates of $\mathbf{C}$ corresponding to outcome j. Thus, when conditioning on the outcomes j in a common future of system and pointer, any operations or measurements performed on the system, even while in spatial separation from the pointer, can still effectively be described in terms of these conditional states. This of course also holds true if the pointer observable is chosen and measured not only in space-like separation of the operations performed on the system but in their future, as depicted in Fig. 3.5b, and the time-ordering in fact has no effect on the conditioned outcomes [422, 997].

The effect on the conditional system states can be illustrated with the simple example of the measurement of a qubit system with a qubit pointer, where $\mathbf{U} = \exp(-i\pi \boldsymbol{\sigma}_x \otimes \boldsymbol{\sigma}_x/4)$ and $|\chi\rangle = |0\rangle$. Then for the choice of pointer observables $\mathbf{C} = \boldsymbol{\sigma}_y, \boldsymbol{\sigma}_x$ the system is

[2] emphasis added

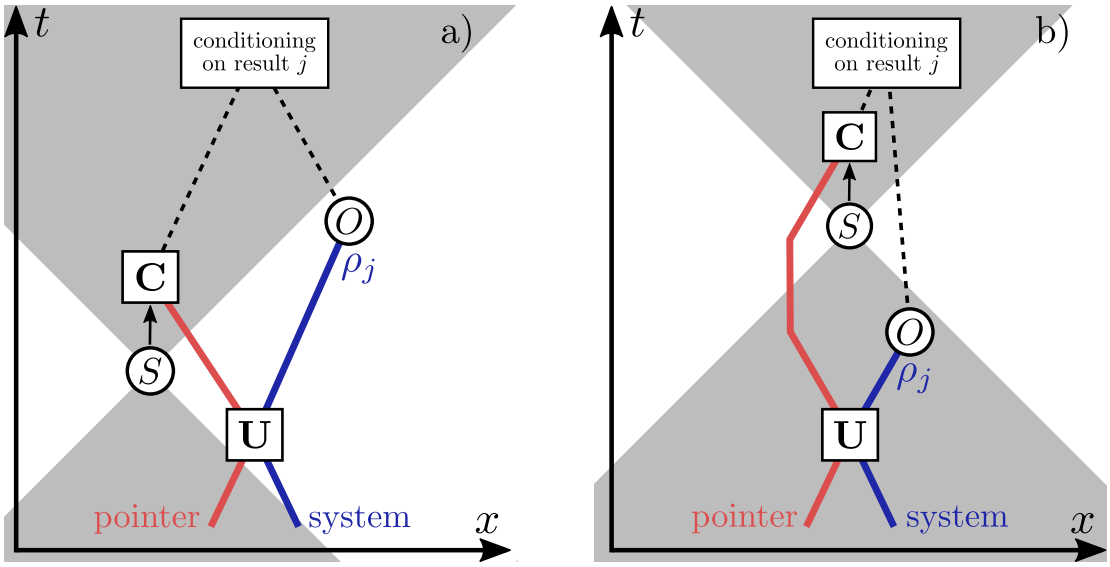

Figure 3.5: **Generalized Delayed Choice Scenarios** In the first scenario a), after a general local interaction **U**, system and pointer become space-like separated. This interaction can for example consist in the generation of pair of entangled qubits which are then distributed to two sites. After a choice of setting S, the corresponding pointer observable C is measured and, in a common future, the results of operations O on the system are conditioned on the outcomes of the pointer measurement. For outcome j the behavior of the system is exactly such as if it had been in the respective conditional state ρ_j. The same behavior is observed in scenario b), when choice S is already in the causal future of the operation.

effectively projected onto the eigenbases of $\boldsymbol{\sigma}_x$ and $\boldsymbol{\sigma}_y$, respectively. Furthermore, if the observable $\boldsymbol{\sigma}_z$ is measured on the pointer, the POVM elements become proportional to the identity although the channel is not the identity channel. However, when additionally only conditioning on the pointer outcome 0, the corresponding operation becomes the identity and the interaction is effectively reversed, an effect commonly denoted as *quantum erasure* [330, 329, 304, 293, 639, 233, 997, 642]. For more complex systems the effective conditional states of the system can differ significantly, e.g., correspond to separable or entangled states, as in the delayed choice entanglement swapping scenario [420, 399, 408, 997]. The general phenomenon that conditioning on outcomes at one site influences the effective conditional state at a space-like separated site beyond only classical correlations is also known as *quantum steering* [451, 400, 423, 440].

A common interpretation of delayed choice experiments follows Wheeler to opt for a radically operational approach. For example Ma *et al.* write:

> It is a general feature of delayed-choice experiments that quantum effects can mimic an influence of future actions on past events. However, there never emerges any paradox if the quantum state is viewed only as a "catalog of our knowledge" [...] without any underlying hidden-variable description. Then the state is a probability list for all possible measurement outcomes and not a real physical object. The relative

> temporal order of measurement events is not relevant, and no physical interactions or signals, let alone into the past, are necessary to explain the experimental results. [...] In light of quantum erasure and entanglement swapping, one might like to even say that some registered phenomena do not have a meaning unless they are put in relationship with other registered phenomena... [997]

In consequence, statements of the form "one can decide *a posteriori* whether two systems were entangled or separable" [997] can be made, which far from implying retrocausality simply consequently follow the operationalist paradigm and identify "were" with "have been found". While such a view represents a consistent interpretation, also alternative explanations of delayed choice experiments are provided by any interpretation which reproduces the standard dispositive structure of QM. In particular, in contrast to the artificial interpretation R as introduced above, all three major realist approaches, i.e., MWI, collapse theories, and pilot-wave hidden-variable theories are specifically designed to provide explanations for *all* quantum mechanical predictions. Thus, all of them provide consistent realist accounts of what the state of system and pointer *was* for any conceivable delayed choice scenario.

In essence, delayed choice experiments represent special cases of measurement scenarios with postselection and, as demonstrated in Sec. 2.6.1, the effective behavior of any quantum system can be changed significantly by conditioning on suitable postselection, going so far that, at least in principle, the characteristics of *any* solely preselected system can be reproduced by postselection only. Notably, any delayed choice scenario with space-like separation as in Fig. 3.5a, which establishes Bell-correlations between the outcomes of the pointer measurement and the measurements on the system, is effectively a Bell test and its interpretation will thus require the violation of at least one of the four basic assumptions of Bell's theorem. If such correlations are not present, the particular scenario is explainable by local-causal models, as is the case for example for Wheelers initial gedankenexperiment described in the preceding section [378, 425]. While, in conclusion, delayed choice experiments cannot be expected to refute any consistent interpretation of QM, they nevertheless constitute highly illustrative test-beds which can highlight the principles and mechanisms underlying the various theories as well as their more or less desirable properties. This is exactly the spirit of the delayed choice experiment presented in Chapter 7.

3.4.3 Measurement of Nonlocal Observables

Another context in which the spacetime relations between measurements are of crucial importance are QND measurements of so called *nonlocal observables* [359, 367, 441]. A nonlocal observable is defined as an observable which acts on space-like separated degrees of freedom, such as the product observables $\mathbf{C} = \mathbf{A} \otimes \mathbf{B}$ measured in the context of a violation the CHSH inequality (3.6). While the expectation values of such observables are routinely measured in quantum experiments, their QND measurement is highly non-trivial.

For example in the case of a two-qubit measurement with Pauli observables, the product observables $\mathbf{C}$ can all be written in the form $\mathbf{C} = \vec{b}_A\vec{\boldsymbol{\sigma}} \otimes \vec{b}_B\vec{\boldsymbol{\sigma}} = \mathbf{\Pi}_p - \mathbf{\Pi}_m$, where the

projectors $\mathbf{\Pi}_p$, $\mathbf{\Pi}_m$ are associated with the eigenvalues $+1$ and -1, respectively, and each corresponds to a two-dimensional subspace spanned by a pair of maximally entangled states. In consequence those entangled states are eigenstates of $\mathbf{C}$. However, in typical measurements of such observables, e.g., during QST, as introduced in Sec. 2.4.1, local measurements in the eigenbases of $\vec{b}_j\vec{\boldsymbol{\sigma}}$ are performed, such that the instrument is given by the inefficient operations

$$\mathcal{T}_p[\rho] = \mathbf{\Pi}_{pp}\rho\mathbf{\Pi}_{pp} + \mathbf{\Pi}_{mm}\rho\mathbf{\Pi}_{mm} \quad \text{and} \quad \mathcal{T}_m[\rho] = \mathbf{\Pi}_{pm}\rho\mathbf{\Pi}_{pm} + \mathbf{\Pi}_{mp}\rho\mathbf{\Pi}_{mp}, \tag{3.10}$$

where $\mathbf{\Pi}_{jk} = \mathbf{\Pi}_j^{\text{sgl}} \otimes \mathbf{\Pi}_k^{\text{sgl}}$ and $\mathbf{\Pi}_{p/m}^{\text{sgl}}$ corresponds to the eigenstates of $\vec{b}_j\vec{\boldsymbol{\sigma}}$ with eigenvalues ± 1. While this measurement is still BAE, it clearly is not QND, where in particular any post-measurement state is separable, both in the selective as well as in the non-selective case. Note that in practice this conceptual inefficiency is often of no consequence, as even stronger back-action is induced by the interaction with the measurement device such as total destruction of the system in case of photonic detection, see Sec. 4.5. However, after such a measurement, entanglement between A and B cannot be recovered even effectively via postselection, i.e., LOCC.

Measurements of nonlocal observables represent a special case of nonlocal quantum channels $\mathcal{C}[\rho]$, which act on systems in the state ρ shared by several space-like separated parties [367, 422]. Since there is no unique notion of simultaneity between events at the various sites, such channels have to be defined on some hyperplane of simultaneity also called *spacetime foliation* [410]. Channels which do not allow for signaling between the two sites are called *causal operations*. An example of causal operations are the delayed choice steering scenarios discussed above, such as teleportation or quantum erasure, where the influence between the two sites is only effective, i.e., it only appears when conditioning on outcomes in the common future and not instantaneously relative to some spacetime foliation. Crucially, however, it is possible to formulate CPTP maps acting on multipartite systems which are *not* causal operations if the parts are in space-like separation. In effect, through the no-signaling condition, SR imposes significant constraints on the possibility to implement such channels and thus also on the measureability of nonlocal observables, as discussed below [358, 359, 428, 521, 441]. Furthermore, even stricter constraints are imposed by the requirement of *localizable channels*, i.e., channels which include only local unitary interactions between the local part of the system and local part of the pointer. As a consequence, due to the locality of physical interactions not all causal operations are physically realizable [367].

As shown by Aharonov *et al.* [359] for a subset of nonlocal product observables $\mathbf{C} = \mathbf{A} \otimes \mathbf{B}$, QND measurements correspond to causal operations and thus adhere to the no-signaling constraint. However, in general the locality of interactions inhibits the realization of a nonlocal measurement of observable $\mathbf{C}$ via a simple product Hamiltonian of the form $\mathbf{H} = g\mathbf{C} \otimes \mathbf{D}$, where $\mathbf{D}$ is some generator acting on the various parts of a delocalized pointer degree of freedom. In effect, the sufficient condition for QND $[\mathbf{C}, \mathbf{U}] = 0$, with $\mathbf{U} = \exp(-i\hbar\mathbf{H}/t)$, as introduced in Sec. 2.4.2, cannot be trivially satisfied. However, by choosing an appropriate initial pointer state $|\chi\rangle$, a QND measurement of $\mathbf{C}$ can be

achieved even with a local interaction involving product Hamiltonians at the two sites, which is of the form $\mathbf{H} = g\mathbf{A} \otimes \mathbf{D}_A + \mathbf{B} \otimes \mathbf{D}_B$. A practical scheme of this type, based on using entangled pointer states, has been proposed by Vaidman and experimentally realized in [**P4**], as reproduced in the next section. After the two parts of the entangled pointer have interacted with the respective parts of the system at the two sites, local measurements are performed on the pointer, such that when conditioning on those results in the common future, effectively a QND instrument for $\mathbf{C}$ is realized. Due to the QND nature of this measurement, it is possible to perform a measurement of $\mathbf{C}$ on a PPS, where the outcome probabilities are given by the ABL-rule, as introduced in Sec. 2.6.2. In particular, by choosing suitable pre- and postselection, the violation of the product-rule was demonstrated by comparing the results of the QND measurement of $\mathbf{C}$ to separate measurements of $\mathbf{A}$ and $\mathbf{B}$.

3.4.4 [P4]

PHYSICAL REVIEW LETTERS **122,** 100405 (2019)

Measurements of Nonlocal Variables and Demonstration of the Failure of the Product Rule for a Pre- and Postselected Pair of Photons

Xiao-Ye Xu,[1,2] Wei-Wei Pan,[1,2] Qin-Qin Wang,[1,2] Jan Dziewior,[3,4] Lukas Knips,[3,4] Yaron Kedem,[5] Kai Sun,[1,2] Jin-Shi Xu,[1,2] Yong-Jian Han,[1,2] Chuan-Feng Li,[1,2,*] Guang-Can Guo,[1,2] and Lev Vaidman[6,†]

[1]*CAS Key Laboratory of Quantum Information, University of Science and Technology of China, Hefei 230026, People's Republic of China*

[2]*Synergetic Innovation Center of Quantum Information and Quantum Physics, University of Science and Technology of China, Hefei 230026, People's Republic of China*

[3]*Max-Planck-Institut für Quantenoptik, Hans-Kopfermann-Straße 1, 85748 Garching, Germany*

[4]*Department für Physik, Ludwig-Maximilians-Universität, 80797 München, Germany*

[5]*Department of Physics, Stockholm University, AlbaNova University Center, 106 91 Stockholm, Sweden*

[6]*Raymond and Beverly Sackler School of Physics and Astronomy, Tel-Aviv University, Tel-Aviv 69978, Israel*

(Received 14 May 2018; revised manuscript received 26 January 2019; published 15 March 2019)

We report the first implementation of the von Neumann instantaneous measurements of nonlocal variables, which becomes possible due to technological achievements in creating hyperentangled photons. Tests of reliability and of the nondemolition property of the measurements have been performed with high precision, showing the suitability of the scheme as a basic ingredient of numerous quantum information protocols. The method allows us to demonstrate for the first time with strong measurements a special feature of pre- and postselected quantum systems: the failure of the product rule. It has been verified experimentally that for a particular pre- and postselected pair of particles, a single measurement on particle A yields with certainty $\sigma_x^A = -1$, a single measurement on particle B yields with certainty $\sigma_y^B = -1$, and a single nonlocal measurement on particles A and B yields with certainty $\sigma_x^A \sigma_y^B = -1$.

DOI: 10.1103/PhysRevLett.122.100405

All known interactions in nature are local. It was thus believed (e.g., Ref. [1]) that measurements of nonlocal variables (variables that are related to more than one region of space) are impossible. However, Aharonov and his coauthors [2,3] showed theoretically that some nonlocal variables can be measured. For two separate locations, the sum of local variables, $A + B$, and the modular sum $(A + B)$ mod c are always measurable. On the other hand, they also showed that some other nonlocal variables cannot be measured as this would lead to superluminal signaling. Note that if we do not require the measurement to be nondemolition, then theoretically all nonlocal variables are measurable [4], but the procedure places high demands on entanglement resources [5–7].

Aharonov's main motivation was to shed light on relativistic quantum field theory [2,8–11], but the main impact of the analysis of measurements of nonlocal variables was in the field of quantum information [12–20]. In particular, it allowed an efficient method for teleportation [21] and was the basis for cryptographic protocols [22–25].

In this work, we demonstrate the measurement of nonlocal variables in its original sense, the one that is closest to the standard von Neumann definition of measurement in quantum mechanics [26]. Note that there exists an alternative scheme [27] alongside a particular proposal for its implementation [28,29], which, however, has the drawback of being a probabilistic measurement; i.e., even with ideal devices it might not provide an outcome.

After performing and testing our measurement procedure, we apply it to show the peculiar phenomenon of the failure of the product rule for two separate (and thus commuting) local variables, which can take place only for pre- and postselected quantum systems [30–32]. There have been several demonstrations of the failure of the product rule for weak values—the outcomes of weak measurements [33–35] in the context of the Hardy paradox [30]. These, however, are very different results, obtained from many measurements on an ensemble of particles. In our scenario, we are able to violate the product rule using strong nondemolition measurements, providing direct information about single pairs of particles. We show below that the same cannot be done in the setting of the Hardy paradox.

Let us start by spelling out the properties of a von Neumann measurement. It has to be reliable, nondemolition, and instantaneous.

Reliability: If the initial state is an eigenstate of the measured nonlocal variable, the corresponding eigenvalue is found with certainty.

 © 2019 American Physical Society

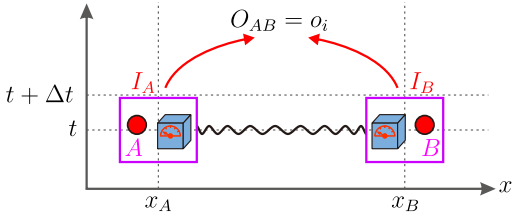

FIG. 1. Measurement scheme of a nonlocal variable. Entangled parts of the measuring device in locations A and B couple simultaneously to the respective parts of the system for a short time. The locally obtained records I_A and I_B provide, when brought together, the eigenvalue o_i of the nonlocal variable O_{AB} of the system.

Nondemolition property: If the initial state is an eigenstate of the measured nonlocal variable, the state is not changed. This ensures repeatability, namely, that identical consecutive measurements all agree with the reading of the first measurement.

Instantaneousness: The standard definition in nonrelativistic quantum mechanics is that the measurement process has a negligible duration. According to the principles of relativistic quantum mechanics, there is no physical mechanism that allows a local observer simultaneous coupling to spatially separated parts of a physical system. Thus, a measurement of a nonlocal observable must consist of two separate local couplings at distinct spatial locations followed by the creation of macroscopic records. In addition to the requirement of negligible duration of these local couplings, together with the respective creation of local records, we require that the processes at the two locations are spacelike separated. The measurement coupling and creation of macroscopic records, which specify the result of the measurement, happen instantaneously and simultaneously in some Lorentz frame, e.g., that of the observer.

To satisfy the above requirements, our scheme for the measurement of nonlocal variables has two stages (see Fig. 1). In the first stage, spatially separated measuring devices ("pointers") interact locally with the respective components of the system. In the second stage, immediately after, macroscopic records are created via local measurements of the measuring device. To gain nonlocal information from these local measurements, the crucial element in our scheme is the preparation of the measuring device in a nonlocal entangled state.

We perform a measurement of the product of polarization operators of two photons separated in space. The measuring device is given by the path degree of freedom (d.o.f.) of the photons themselves, which is measured interferometrically (see Fig. 2). In this setting, the local macroscopic records correspond to ports of the interferometer in which the detectors eventually click. The meaning of "nondemolition" is that the polarization state of the pair of photons in the corresponding pair of ports is still the initial (possibly entangled) polarization state as long as it starts in an eigenstate of the nonlocal variable. While in our experiment there is no spacelike separation of the local

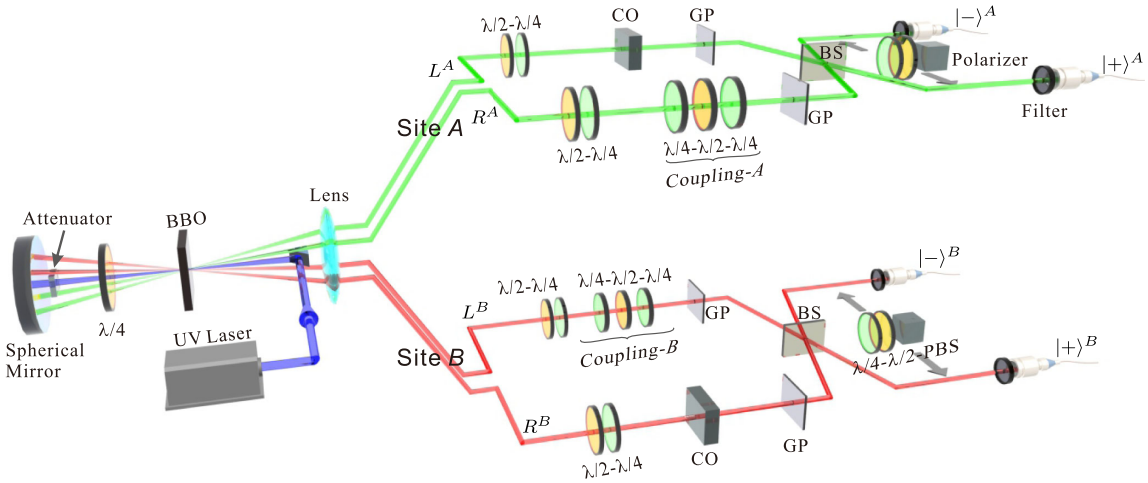

FIG. 2. Experimental setup. The two-photon, path-polarization, hyperentangled state is generated from the SPDC using $\beta - BaB_2O_4$ (BBO) crystal in a round-tripping confocal structure [36,37]. Photon A will be in the upper layer (green lines), while the lower layer is site B (red lines). The attenuator and sets of $\lambda/2$-$\lambda/4$ wave plates prepare the polarization state. The local coupling between the system (polarization d.o.f.) and the measuring device (path d.o.f., L and R) is realized by sets of wave plates ($\lambda/4$-$\lambda/2$-$\lambda/4$) in a particular arm of the interferometer. For the nonlocal measurement, two such local couplings are applied. In the other arms, compensation crystals (CO) ensure identical optical path length. The relative phases are tuned using thin glass plates (GP) before bringing the arms to interference using a polarization insensitive beam splitter (BS). For testing the nondemolition property, polarization filters composed of a set of $\lambda/4$-$\lambda/2$ plates and a polarization beam splitter (PBS) are placed in front of the detectors.

measurement processes, each one consisting of a coupling in one arm of the interferometer and the detector click, which provides the macroscopic record, our scheme in no way relies on the proximity of the two parties and thus allows for a modification with a spacelike separation of the local measurements.

The Hilbert spaces of photon polarization states and of the states of a spin $-\frac{1}{2}$ particle are isomorphic, which allows us to use a more familiar language of spin operators. Expressed with spin operators, our measurement corresponds to the measurement of $\sigma_z^A\sigma_z^B$ on two remote particles. There is no general method for the measurement of the product of variables belonging to remote locations; however, $\sigma_z^A\sigma_z^B = (\sigma_z^A + \sigma_z^B) \bmod 4{-}1$, so the measurement of this product is equivalent to the measurement of a modular sum, which is proven to be possible [3]. For the polarization d.o.f., we use the correspondence

$$\sigma_z|\uparrow_z\rangle = |\uparrow_z\rangle \leftrightarrow |H\rangle, \qquad |\downarrow_z\rangle \leftrightarrow |V\rangle, \tag{1}$$

with $|H\rangle$ and $|V\rangle$ identifying horizontal and vertical polarization, respectively. Similarly, for the measuring device, which we mark with "$\sim$" in the spin notation,

$$\tilde{\sigma}_z|\tilde{\uparrow}_z\rangle = |\tilde{\uparrow}_z\rangle \leftrightarrow |L\rangle, \qquad |\tilde{\downarrow}_z\rangle \leftrightarrow |R\rangle, \tag{2}$$

where $|L\rangle$ and $|R\rangle$ denote the two arms the photons can take at both locations.

The measurement scheme requires us to correctly match the preparation of the initial pointer state, the interaction Hamiltonian, and the pointer measurement. We prepare the measuring device in the entangled state,

$$|\Psi^+\rangle^{AB} \equiv \frac{1}{\sqrt{2}}(|\tilde{\uparrow}_z\rangle^A|\tilde{\downarrow}_z\rangle^B + |\tilde{\downarrow}_z\rangle^A|\tilde{\uparrow}_z\rangle^B), \tag{3}$$

and perform local pointer measurements in the plane perpendicular to $\tilde{\sigma}_z$. The interaction Hamiltonian is

$$H = g(t)[(\mathbb{1}^A - \sigma_z^A)(\mathbb{1}^A - \tilde{\sigma}_z^A) + (\mathbb{1}^B - \sigma_z^B)(\mathbb{1}^B + \tilde{\sigma}_z^B)], \tag{4}$$

where $\int g(t)dt = \pi/4$.

Given a polarization state that is an eigenstate of $\sigma_z^A\sigma_z^B$ with eigenvalue $+1$, the interaction Hamiltonian (4) does not change the state $|\Psi^+\rangle^{AB}$ of the measuring device. On the other hand, for an eigenstate with eigenvalue -1, the state of the measuring device is changed to

$$|\Psi^-\rangle^{AB} \equiv \frac{1}{\sqrt{2}}(|\tilde{\uparrow}_z\rangle^A|\tilde{\downarrow}_z\rangle^B - |\tilde{\downarrow}_z\rangle^A|\tilde{\uparrow}_z\rangle^B). \tag{5}$$

The states $|\Psi^+\rangle^{AB}$ and $|\Psi^-\rangle^{AB}$ can be distinguished reliably using our simultaneous local measurements in A and in B, after the records have been combined. In both cases, after the interaction, the system and the pointer are not entangled with each other and the system state is not changed. This makes the measurement nondemolition. Note that the product of spin operators in other directions can also be measured in this way, when the Hamiltonian is adapted accordingly. In addition, a strictly local spin measurement can be achieved using this scheme when only one of the two local coupling terms is present in the interaction Hamiltonian.

In our experiment (as shown in Fig. 2), a vertically polarized ultraviolet ($\lambda = 406.7$ nm) laser beam is focused and reflected to pump a 0.5-mm-thick BBO crystal (type-1 cut at 29.11°). Because of the degenerate spontaneous parametric down-conversion (SPDC), horizontally polarized photon pairs are emitted in a cone with apex angle 3° (postselected by spectral filters centered at $\lambda = 813.4$ nm with bandwidth $\Delta\lambda = 3$ nm). After passing a wave plate, acting as $\lambda/4$ for 813.4 nm light, with optical axis oriented at 45°, both the pump laser and the emitted photons are reflected by a spherical mirror with a 150-mm radius. While the polarization of previously produced photon pairs is converted to vertical, a second pass through the BBO of the pump can produce another pair of horizontally polarized photons.

The two processes overlap both spatially and temporally due to the confocal structure and the long coherence time. A positive lens ($f = 150$ mm) transforms the conical parametric emission into a cylindrical one, preparing a so-called entanglement ring [37]. By selecting four points in the ring, we obtain the two-photon four-qubit hyperentangled state, maximally entangled both in the polarization and spatial d.o.f., while separable between the two. The spatial state reads $|\Psi^+\rangle^{AB} = (1/\sqrt{2})(|L\rangle^A|R\rangle^B + |R\rangle^A|L\rangle^B)$. An attenuator near the spherical mirror together with the wave-plate sets in the four arms of the interferometer allow us to prepare arbitrary polarization states.

The two parts of the interaction Hamiltonian of Eq. (4) at the two sites A and B are each implemented by sets of wave plates, introducing a conditional phase shift of π for horizontally polarized photons in the right arm at site A and in the left arm at site B. Using glass plates, we tune the interferometer such that without interaction we get complete correlation between clicks of the detectors in sites A and B. Then, observing the clicks corresponds to a "spin" measurement in some unknown direction in the $x-y$ plane, which, however, is the same for the two particles. In the notation of the photon states, these are the measurements in the basis $|\pm\rangle \equiv (1/\sqrt{2})(|L\rangle \pm e^{i\varphi}|R\rangle)$ with unknown phase φ, which is equal at both sites. In this notation, the states of the measuring device (3) and (5) are

$$|\Psi^+\rangle^{AB} = \frac{e^{-2i\varphi}}{\sqrt{2}}(|++\rangle^{AB} - |--\rangle^{AB}), \tag{6a}$$

$$|\Psi^-\rangle^{AB} = \frac{e^{-2i\varphi}}{\sqrt{2}}(|+-\rangle^{AB} - |-+\rangle^{AB}), \tag{6b}$$

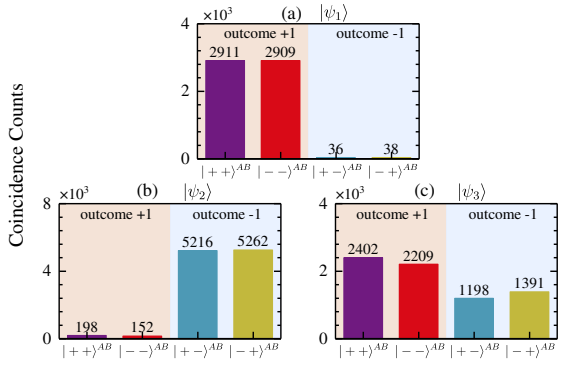

FIG. 3. Reliability test. Coincidence counts on various pairs of detectors for the three polarization states of Eq. (7). The states $|\psi_1\rangle$ and $|\psi_2\rangle$ are eigenstates of the nonlocal variable $\sigma_z^A\sigma_z^B$. The percentage of outcomes for state $|\psi_3\rangle$ corresponds well to the initial superposition.

where we used the shortcut notation $|++\rangle^{AB} \equiv |+\rangle^A|+\rangle^B$, etc. Thus, the correlations and the anticorrelations of the outcomes for the measurements of $|+\rangle$ and $|-\rangle$ in the path d.o.f. allow us to distinguish between the eigenstates $+1$ and -1 of the product operator of the system.

We test the reliability and the nondemolition property of our measurement procedure for three different states,

$$|\psi_1\rangle = |\uparrow_z\rangle^A|\uparrow_z\rangle^B, \tag{7a}$$

$$|\psi_2\rangle = \frac{1}{\sqrt{2}}(|\uparrow_z\rangle^A|\downarrow_z\rangle^B + i|\downarrow_z\rangle^A|\uparrow_z\rangle^B), \tag{7b}$$

$$|\psi_3\rangle = \sqrt{0.5}|\uparrow_z\rangle^A|\uparrow_z\rangle^B + \sqrt{0.1}|\uparrow_z\rangle^A|\downarrow_z\rangle^B - i\sqrt{0.2}|\downarrow_z\rangle^A|\uparrow_z\rangle^B + \sqrt{0.2}|\downarrow_z\rangle^A|\downarrow_z\rangle^B. \tag{7c}$$

The results of the reliability test are presented in Fig. 3. For $|\psi_1\rangle$ and $|\psi_2\rangle$, only 1.3% and 3.2% of the events are erroneous, respectively. State $|\psi_3\rangle$, which is not an eigenstate of the nonlocal operator, leads to 64% events corresponding to outcome $+1$ and 36% to outcome -1, roughly agreeing with the theoretical predictions of 70% and 30%, respectively.

To confirm that the measurement is nondemolition, we perform state verification measurements by adding polarization analyzers directly in front of the detectors. We test the polarization in one of the pairs of output ports, between which coincidences are expected, and repeat the test for the same measurement time with differently set filters. For the state $|\psi_1\rangle$, the results are very robust, as shown in Fig. 4(a), as only 0.2% changed their polarization. This measurement verifies that the output state is indeed $|\uparrow_z^A\rangle|\uparrow_z^B\rangle$. The entangled state $|\psi_2\rangle$ requires two tests. The first measurement in the basis σ_z^A, σ_z^B shows that the state corresponding to the -1 outcome ($|+-\rangle^{AB}$) of $|\psi_2\rangle$ is in a superposition

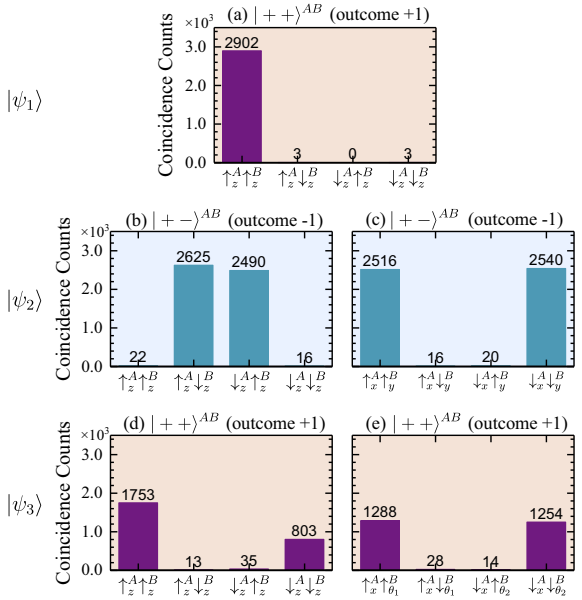

FIG. 4. Test of nondemolition property. (a) $|\psi_1\rangle$ is measured on the detectors $|++\rangle^{AB}$ in the σ_z^A, σ_z^B basis using polarization filters to verify that the state is unaltered during the coupling. (b,c) For $|\psi_2\rangle$, the measurements were done on detectors $|+-\rangle^{AB}$ in bases σ_z^A, σ_z^B and σ_x^A, σ_y^B. (d) State $|\psi_3\rangle$ was measured first in the σ_z^A, σ_z^B basis. To fix the phase relation between $|\uparrow_z^A\rangle|\uparrow_z^B\rangle$ and $|\downarrow_z^A\rangle|\downarrow_z^B\rangle$, a second measurement (e) was conducted with projections also containing rotated states with $|\uparrow_{\theta_1}\rangle = (\sqrt{0.5}|\uparrow_z\rangle + \sqrt{0.2}|\downarrow_z\rangle)/\sqrt{0.7}$ and $|\uparrow_{\theta_2}\rangle = (\sqrt{0.5}|\uparrow_z\rangle - \sqrt{0.2}|\downarrow_z\rangle)/\sqrt{0.7}$. The results prove that we performed nondemolition measurements of nonlocal variables.

(or mixture) of $|\uparrow_z^A\rangle|\downarrow_z^B\rangle$ and $|\downarrow_z^A\rangle|\uparrow_z^B\rangle$ according to Fig. 4(b). The second measurement in basis σ_x^A, σ_y^B (with $\sigma_x \equiv |\downarrow_z\rangle\langle\uparrow_z| + |\uparrow_z\rangle\langle\downarrow_z|$ and $\sigma_y \equiv i|\downarrow_z\rangle\langle\uparrow_z| - i|\uparrow_z\rangle\langle\downarrow_z|$) [see Fig. 4(c)] fixes the phase relation between those contributions. In both bases, we get only 0.7% errors. For state $|\psi_3\rangle$, we test the projection onto the subspace corresponding to outcome $+1$ in the ports $|++\rangle^{AB}$. Again, we observe a good correspondence with theoretical predictions [see Figs. 4(d) and 4(e)].

In the second part of the experiment, we use our technique of measurement of nonlocal variables to demonstrate the failure of a product rule for pre- and post-selected quantum systems.

Before presenting our measurement, we show that the failure of the product rule appearing in the Hardy paradox [30] (which was demonstrated using weak measurements [33–35]) cannot be observed using von Neumann measurement. Such a measurement would allow superluminal communication between Alice at site A and Bob at remote site B. In this case, Alice would be able to change the probability distribution at Bob's site instantaneously.

Assume that a nondemolition measurement of $\mathbf{P}_1^A\mathbf{P}_1^B$ is performed at time t with $\mathbf{P}_1^A \equiv |1\rangle\langle 1|^A$ and $\mathbf{P}_1^B \equiv |1\rangle\langle 1|^B$. Just before t, Bob prepares the state $(1/\sqrt{2})(|0\rangle^B + |1\rangle^B)$ and performs a projection measurement of this state immediately after time t. If, also just before t, Alice prepares state $|0\rangle^A$, then at time t the state in the two sites is an eigenstate of $\mathbf{P}_1^A\mathbf{P}_1^B$ with eigenvalue 0, so the nonlocal measurement will not change the state and Bob will find $(1/\sqrt{2})(|0\rangle^B + |1\rangle^B)$ with probability 1. If, instead, Alice, just before t, prepares state $|1\rangle^A$, the nonlocal measurement will either lead to state $|1\rangle^A|0\rangle^B$ for the outcome $\mathbf{P}_1^A\mathbf{P}_1^B = 0$ or to state $|1\rangle^A|1\rangle^B$ for the outcome $\mathbf{P}_1^A\mathbf{P}_1^B = 1$. In both cases, the probability for Bob to find the state $(1/\sqrt{2})(|0\rangle^B + |1\rangle^B)$ is $\frac{1}{2}$, and Alice would have changed the probability distribution of Bob's outcomes instantaneously by her state preparation.

For our demonstration of the failure of the product rule, we measure the product $\sigma_x^A\sigma_y^B$, instead of measuring a product of projection operators, which *is* measurable in the von Neumann sense. In our example, we have a pair of particles for which we know with certainty that a single local measurement of σ_x^A or of σ_y^B results in the outcome -1. If, however, we measure the product $\sigma_x^A\sigma_y^B$, it will also provide the outcome -1 with certainty, instead of the naively expected product outcome $+1$.

To this end, we preselect the singlet state $(1/\sqrt{2})(|\uparrow_z\rangle^A|\downarrow_z\rangle^B - |\downarrow_z\rangle^A|\uparrow_z\rangle^B)$ and postselect the product state $|\uparrow_y\rangle^A|\uparrow_x\rangle^B$ [31]. Indeed, the initial state is anticorrelated for all directions, so $\sigma_x^A = -1$ follows immediately from postselection of $|\uparrow_x\rangle^B$ and $\sigma_y^B = -1$ follows immediately from postselection of $|\uparrow_y\rangle^A$. We can see that $\sigma_x^A\sigma_y^B = -1$ with certainty by noticing that the outcome $+1$ can never occur. If prior to the postselection the nonlocal measurement yields $\sigma_x^A\sigma_y^B = +1$, the initial state is projected on the space spanned by states $|\uparrow_x\rangle^A|\uparrow_y\rangle^B$ and $|\downarrow_x\rangle^A|\downarrow_y\rangle^B$. Then, in the basis of σ_y^A and σ_x^B, the projected state is $-(1+i)/2(|\uparrow_y\rangle^A|\downarrow_x\rangle^B + |\downarrow_y\rangle^A|\uparrow_x\rangle^B)$. Since it is orthogonal to the postselected state $|\uparrow_y\rangle^A|\uparrow_x\rangle^B$, the postselection will never be successful, and thus the outcome of the measurement will always be $\sigma_x^A\sigma_y^B = -1$.

To implement this measurement of $\sigma_x^A\sigma_y^B$, we only need a simple modification of our measurement scheme. The interaction Hamiltonian is changed to

$$H = g(t)[(\mathbb{1}^A - \sigma_x^A)(\mathbb{1}^A - \tilde{\sigma}_z^A) + (\mathbb{1}^B - \sigma_y^B)(\mathbb{1}^B + \tilde{\sigma}_z^B)], \qquad (8)$$

which is achieved experimentally in a straightforward way by modifying the settings of the wave plates at the two sites accordingly. The measurement procedure is then completely analogous to the measurement of $\sigma_z^A\sigma_z^B$. For the local measurements of σ_x^A and σ_y^B, the coupling at the respective opposite site is switched off by setting the optical axis of the wave plates at zero, such that the interaction Hamiltonians become $H = g(t)(\mathbb{1}^A - \sigma_x^A)(\mathbb{1}^A - \tilde{\sigma}_z^A)$ and $H = g(t)(\mathbb{1}^A - \tilde{\sigma}_z^A)(\mathbb{1}^B + \tilde{\sigma}_z^B)$.

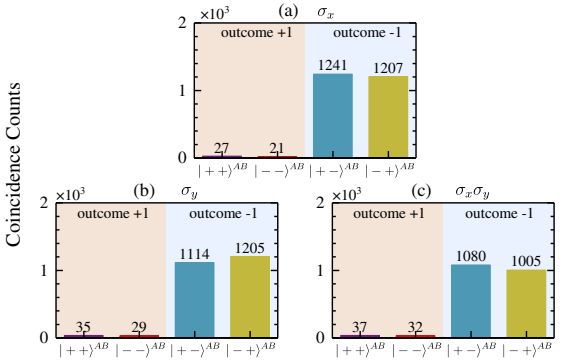

FIG. 5. Experimental results for demonstrating the failure of the product rule. Coincidence counts in pairs of detectors for measurement of local and nonlocal variables: (a) σ_x^A, (b) σ_y^B, (c) $\sigma_x^A\sigma_y^B$. In all three cases, the system is preselected in a singlet state and postselected in the product state $|\uparrow_y^A\downarrow_x^B\rangle$.

The results are presented in Fig. 5. As in the nonlocal measurement of $\sigma_z^A\sigma_z^B$ explained above, the correlations and the anticorrelations of the outcomes for the measurements of $|+\rangle$ and $|-\rangle$ in the path d.o.f. allow us to distinguish between the eigenstates $+1$ and -1 of the product operator of the system. Figure 5(a) shows $\sigma_x^A\sigma_y^B = -1$ with very high precision. For the local measurement at site A (B), we use the same procedure without the interaction at site B (A) such that, again, the observed anticorrelations, Figs. 5(b) and 5(c), clearly demonstrate $\sigma_x^A = -1$ and $\sigma_y^B = -1$.

We have performed the first experimental implementation of von Neumann measurements of nonlocal variables. We also demonstrated a peculiar property of pre- and postselected composite systems: the failure of the product rule for commuting observables. The experiment sheds light on the fundamental question of the physical meaning of nonlocal variables. The high fidelity of the experimental results demonstrates that the method is potentially useful for quantum information applications.

This work was supported by National Key Research and Development Program of China (No. 2017YFA0304100 and No. 2016YFA0302700), the National Natural Science Foundation of China (No. 11474267, No. 61327901, No. 11774335, No. 61322506, and No. 11821404), Key Research Program of Frontier Sciences, CAS (No. QYZDY-SSW-SLH003), Anhui Initiative in Quantum Information Technologies (No. AHY020100 and No. AHY060300), the Fundamental Research Funds for the Central Universities (No. WK2470000026), the National Postdoctoral Program for Innovative Talents (No. BX201600146), China Postdoctoral Science

Foundation (No. 2017M612073), the Israel Science Foundation Grant No. 1311/14, and the German-Israeli Foundation for Scientific Research and Development Grant No. I-1275-303.14. J. D. and L. K. gratefully acknowledge support by the international Max-Planck-Research School for Quantum Science and Technology (IMPRS-QST) and the International Ph.D. Program ExQM from the Elite Network of Bavaria, respectively.

*cfli@ustc.edu.cn
†vaidman@post.tau.ac.il

[1] L. D. Landau and R. Peierls, Extension of the uncertainty principle to relativistic quantum theory, Z. Phys. **69**, 56 (1931).
[2] Y. Aharonov and D. Z. Albert, States and observables in relativistic quantum field theories, Phys. Rev. D **21**, 3316 (1980).
[3] Y. Aharonov, D. Z. Albert, and L. Vaidman, Measurement process in relativistic quantum theory, Phys. Rev. D **34**, 1805 (1986).
[4] L. Vaidman, Instantaneous Measurement of Nonlocal Variables, Phys. Rev. Lett. **90**, 010402 (2003).
[5] S. Bandyopadhyay, G. Brassard, S. Kimmel, and William K. Wootters, Entanglement cost of nonlocal measurements, Phys. Rev. A **80**, 012313 (2009).
[6] S. R. Clark, A. J. Connor, D. Jaksch, and S. Popescu, Entanglement consumption of instantaneous nonlocal quantum measurements, New J. Phys. **12**, 083034 (2010).
[7] B. Groisman and S. Strelchuk, Optimal amount of entanglement to distinguish quantum states instantaneously, Phys. Rev. A **92**, 052337 (2015).
[8] Y. Aharonov and D. Z. Albert, Is the usual notion of time evolution adequate for quantum-mechanical systems? I, Phys. Rev. D **29**, 223 (1984).
[9] Y. Aharonov and D. Z. Albert, Is the usual notion of time evolution adequate for quantum-mechanical systems? II. Relativistic considerations, Phys. Rev. D **29**, 228 (1984).
[10] D. Beckman, D. Gottesman, A. Kitaev, and J. Preskill, Measurability of Wilson loop operators, Phys. Rev. D **65**, 065022 (2002).
[11] G. Ghirardi, Local measurements of nonlocal observables and the relativistic reduction process, Found. Phys. **30**, 1337 (2000).
[12] S. Popescu and L. Vaidman, Causality constraints on nonlocal quantum measurements, Phys. Rev. A **49**, 4331 (1994).
[13] D. Beckman, D. Gottesman, M. A. Nielsen, and J. Preskill, Causal and localizable quantum operations, Phys. Rev. A **64**, 052309 (2001).
[14] L. Vaidman, L. Goldenberg, and S. Wiesner, Error prevention scheme with four particles, Phys. Rev. A **54**, R1745 (1996).
[15] C. H. Bennett, D. P. DiVincenzo, C. A. Fuchs, T. Mor, E. Rains, P. W. Shor, J. A. Smolin, and W. K. Wootters, Quantum nonlocality without entanglement, Phys. Rev. A **59**, 1070 (1999).
[16] Y. Kedem and L. Vaidman, Modular Values and Weak Values of Quantum Observables, Phys. Rev. Lett. **105**, 230401 (2010).
[17] B. Groisman and B. Reznik, Measurements of semilocal and nonmaximally entangled states, Phys. Rev. A **66**, 022110 (2002).
[18] L. Yu, R. B. Griffiths, and S. M. Cohen, Fast protocols for local implementation of bipartite nonlocal unitaries, Phys. Rev. A **85**, 012304 (2012).
[19] G.-P. Guo, C.-F. Li, and G.-C. Guo, Quantum nondemolition measurement of nonlocal variables and its application in quantum authentication, Phys. Lett. A **286**, 401 (2001).
[20] W. Dür and J. I. Cirac, Nonlocal operations: Purification, storage, compression, tomography, and probabilistic implementation, Phys. Rev. A **64**, 012317 (2001).
[21] L. Vaidman, Teleportation of quantum states, Phys. Rev. A **49**, 1473 (1994).
[22] O. Cohen, Quantum cryptography using nonlocal measurements, Helv. Phys. Acta **70**, 710 (1997).
[23] H. Buhrman, N. Chandran, S. Fehr, R. Gelles, V. Goyal, R. Ostrovsky, and C. Schaffner, Position-based quantum cryptography: Impossibility and constructions, SIAM J. Comput. **43**, 150 (2014).
[24] S. Beigi and R. König, Simplified instantaneous non-local quantum computation with applications to position-based cryptography, New J. Phys. **13**, 093036 (2011).
[25] H.-K. Lau and H.-K. Lo, Insecurity of position-based quantum-cryptography protocols against entanglement attacks, Phys. Rev. A **83**, 012322 (2011).
[26] J. von Neumann, *Mathematische Grundiagen der Quantenmechanik* (Springer-Verlag, Berlin, 1932); *Mathematical Foundations of Quantum Mechanics* (English translation) (Princeton University, Princeton, NJ, 1955).
[27] A. Brodutch and E. Cohen, Nonlocal Measurements via Quantum Erasure, Phys. Rev. Lett. **116**, 070404 (2016).
[28] Z.-Q. Wu, H. Cao, H.-L. Zhang, S.-J. Ma, and J.-H. Huang, Experimental proposal for performing nonlocal measurement of a product observable, Opt. Express **24**, 27331 (2016).
[29] K. Edamatsu, Quantum measurement and uncertainty relations in photon polarization, Phys. Scr. **91**, 073001 (2016).
[30] L. Hardy, Quantum Mechanics, Local Realistic Theories, and Lorentz-Invariant Realistic Theories, Phys. Rev. Lett. **68**, 2981 (1992).
[31] L. Vaidman, Lorentz-Invariant "Elements of Reality" and the Joint Measurability of Commuting Observables, Phys. Rev. Lett. **70**, 3369 (1993).
[32] Y. Aharonov, A. Botero, S. Popescu, B. Reznik, and J. Tollaksen, Revisiting Hardy's paradox: Counterfactual statements, real measurements, entanglement and weak values, Phys. Lett. A **301**, 130 (2002).
[33] W. Irvine, J. Hodelin, C. Simon, and D. Bouwmeester, Realization of Hardys Thought Experiment with Photons, Phys. Rev. Lett. **95**, 030401 (2005).
[34] J. S. Lundeen and A. M. Steinberg, Experimental Joint Weak Measurement on a Photon Pair as a Probe of Hardy's Paradox, Phys. Rev. Lett. **102**, 020404 (2009).

[35] K. Yokota, T. Yamamoto, M. Koashi, and N. Imoto, Direct observation of Hardy's paradox by joint weak measurement with an entangled photon pair, New J. Phys. **11**, 033011 (2009).

[36] P. G. Kwiat, Hyper-entangled states, J. Mod. Opt. **44**, 2173 (1997).

[37] M. A. Ciampini, A. Orieux, S. Paesani, F. Sciarrino, G. Corrielli, A. Crespi, R. Ramponi, R. Osellame, and P. Mataloni, Path-polarization hyperentangled and cluster states of photons on a chip, Light Sci. Appl. **5**, e16064 (2016).

Chapter 4

Light as a Quantum Object

The goal of this chapter is to present the theoretical basis for an expression of the phenomenon of light in the formalism of QM. While the previous sections focused on the properties of quantum mechanics in general, this chapter lays the essential foundation to connect this formalism to empirical phenomena. As such it is crucial both for the description of the optical experiments treated in this work as well as for the understanding of the application of the Bohmian theory, as presented in Chapter 7, to photons. The chapter begins with a brief sketch of the formalism of classical optics including the theory of paraxial fields typically encountered in the laboratory. Subsequently the basic elements of quantum field theory are introduced which allows to formulate the essential aspects of free space quantum optics. The final result of this chapter is the introduction of the photon wavefunction, which allows to treat quantum optical systems, including single photons, in the formalism of wave-mechanics.

4.1 Classical Spectra and Fluctuations

4.1.1 Electromagnetic Waves

The laws of classical electrodynamics are expressed in the set of four Maxwell equations, which govern the spacetime relationships between the electric and magnetic vector fields $\vec{E}$ and $\vec{B}$ as well as the current density $\vec{j}$ and the charge density ϱ, all of which are functions of position $\vec{x}$ and time t, see e.g. [526, 514, 517, 523]. For the purpose of this work it is mostly sufficient to consider the *free space* field or *free field*, i.e., assume vanishing charge and current densities. Interaction with matter are only relevant in the context of nonlinear optics and waveguide structures, as discussed in Secs. 5.2 and 5.5, respectively. Both the electric as well as the magnetic field are conveniently expressed via the electromagnetic vector potential $\vec{A}$, with $\vec{E} = -\partial_t \vec{A}$ and $\vec{B} = \vec{\nabla} \times \vec{A}$. Here and below the *Coulomb Gauge* $\vec{\nabla}\vec{A} = 0$ is used, which does not affect the $\vec{E}$ and $\vec{B}$ fields but assures that plane waves in $\vec{A}$ are transverse. The Maxwell equation implies a wave-equation, which for the free field

has the simple form [526, 517]

$$\vec{\nabla}^2 \vec{A}(\vec{x},t) = \frac{1}{c^2}\frac{\partial^2}{\partial t^2}\vec{A}(\vec{x},t). \tag{4.1}$$

A complete set of solutions to the wave-equation is given by harmonic plane waves $\vec{s}\,e^{i(\vec{k}\vec{x}-\omega_k t)}$, where the *wavevector* or *k-vector* corresponds to the direction of propagation, ω_k is the frequency of the harmonic oscillation, and $\vec{s}$ denotes a certain direction of polarization. In optics such single frequency oscillations are called *monochromatic*. In free space, the *wavenumber* $k = |\vec{k}|$ is related to the frequency via $\omega_k = ck$ and the *wavelength* $\lambda = c\tau_\omega$ is the propagation distance equivalent to one period of oscillation $\tau_\omega = 2\pi/\omega_k$. A single full harmonic oscillation is called a *cycle*. It is possible to express any general free field $\vec{A}(\vec{x},t)$ as a linear decomposition into plane wave modes as [662]

$$\vec{A}^{(+)}(\vec{x},t) = \sum_p \hat{s}_p \int_{\mathbb{R}^3} c_{\vec{k},s}\, e^{i(\vec{k}\vec{x}-\omega_k t)}\, \frac{\mathrm{d}^3 k}{\sqrt{2\pi}^3}, \tag{4.2}$$

where $c_{\vec{k},s} \in \mathbb{C}$ are the amplitudes of the respective plane wave components and the summation is performed over two orthonormal polarization vectors $\hat{s}_1$ and $\hat{s}_2$. Here the complex notation for the field amplitude $\vec{A}^{(+)}$ is chosen, which is called *complex analytic signal*, where the physical field is given as [618, 514, 525]

$$\vec{A}(\vec{x},t) = 2\mathrm{Re}\big[\vec{A}^{(+)}(\vec{x},t)\big] = \vec{A}^{(+)}(\vec{x},t) + \vec{A}^{(-)}(\vec{x},t) \tag{4.3}$$

with $\vec{A}^{(-)} = \big(\vec{A}^{(+)}\big)^*$. Typically, strictly for convenience of calculations, the imaginary part is chosen such that $A^{(+)}$ has only positive frequency components, i.e., time-dependence exclusively of the form $e^{-i\omega_k t}$. Note that time-evolution of the field due to interactions with matter in general can be expressed in terms of time-dependent amplitudes $c_{\vec{k},s}(t)$. In the case of the free field, however, constant amplitudes are sufficient and the full extent of the time-evolution is given by the periodic harmonic oscillation of each component. Such a time-evolution, which is independent from the distance to the origin of time, is commonly denoted as *stationary* [514]. The plane-wave components are also called *modes* since they represent eigenstates of the free field evolution.

A harmonic oscillation of the general form $e^{i(\nu(\vec{x})-\omega t)}$ is fully determined by the *phase* $\nu(\vec{x}) - \omega t$ with *temporal phase* ωt and a *spatial phase* $\nu(\vec{x})$. In the case of plane waves the spatial phase is given by $\nu(\vec{x}) = \vec{k}\vec{x}$ and indicates a propagation in a single direction. Spherical waves with $\nu(\vec{x}) = k|\vec{x}|$ and standing waves with $\nu(\vec{x}) = 0$ are other paradigmatic examples of spatial phases [514, 511]. The two-dimensional spatial hypersurfaces on which $\nu(\vec{x})$ is constant are called *phase-fronts* and in the case of plane waves correspond to parallel planes perpendicular to $\vec{k}$. The *phase-velocity* v_{ph} is the velocity with which the phase fronts of monochromatic fields propagate in space and is given as $v_{\mathrm{ph}} = \omega/|\vec{\nabla}\nu(\vec{x})|$, which is simply $\omega/k = c$ in the case of plane wave modes [517, 514]. This motivates the definition of the so-called *local k-vector* $\vec{k}_{\mathrm{loc}} := \vec{\nabla}\nu(\vec{x})$ as the normal of the phase-front [560]. Finally,

while in general the polarization can vary over the field, in the following paragraphs of this section, exclusively for the benefit of a simpler notation, a single polarization is assumed and the vectorial character of the field is neglected accordingly.

4.1.2 Spatio-Temporal Localization of Light Fields

The plane wave modes of the field decomposition (4.2) are infinitely extended in time and space, in contrast to typically empirically encountered light which exhibits some localization in spacetime. Such localized fields must thus always be given by superpositions of plane-wave modes and are called *multi-mode* light accordingly. In this context "localization" by no means implies that the field completely vanishes at some spacetime point, but rather that outside of a finite region around a point $(\vec{x}_0, t_0)$ the field amplitude decays with some characteristic function, i.e., $|\vec{A}(\vec{x}, t)| \to 0$ for $|\vec{x} - \vec{x}_0| \to \pm\infty$ or $|t - t_0| \to \pm\infty$. Since any superposition of harmonic modes with equal frequency results again in the same effective frequency of oscillation, temporal localization is necessarily connected to a non-sharp spectral distribution, i.e., a superposition of various spectral modes also called *polychromatic* light. By integrating the k-space on spherical shells with constant $|\vec{k}|$, the general stationary field from Eq. (4.2) can be expressed as [618, 514]

$$A^{(+)}(\vec{x}, t) = \int_0^\infty \widetilde{A}^{(+)}(\vec{x}, \omega)\, e^{-i\omega t}\, \mathrm{d}\omega, \tag{4.4}$$

where $\widetilde{A}^{(+)}(\vec{x}, \omega) \in \mathbb{C}$ is called *spectral amplitude* of the field. Eq. (4.4) indicates that the temporal and spectral amplitudes of the field form a Fourier pair for any location $\vec{x}$ [517]. Based on the spectral amplitude it is possible to define a local *spectral density* G, also called *power spectrum* as [618, 517]

$$G(\vec{x}, \omega) = \frac{|\widetilde{A}^{(+)}(\vec{x}, \omega)|^2}{\int_0^\infty |\widetilde{A}^{(+)}(\vec{x}, \omega)|^2\, \mathrm{d}\omega}, \tag{4.5}$$

which characterizes the field in terms of the presence of various frequency components. Furthermore, for typical paraxial beams, as described below, the spectral amplitude factorizes as $\widetilde{A}^{(+)}(\vec{x}, \omega) \approx \widetilde{A}^{(+)}(\omega) e^{i\omega\tilde{\nu}(\vec{x})}$ and a position-independent spectral density $G(\omega)$ can be defined for the whole beam. Apart from an effective temporal offset of $\tilde{\nu}(\vec{x})$, the time evolution for any location $\vec{x}$ of the field is then uniquely defined by G. In general a classical uncertainty relation between the temporal width Δt of $|A^{(+)}(\vec{x}, t)|^2$ and the spectral width $\Delta\omega$ of $G(\vec{x}, \omega)$ can be formulated which has the form $\Delta t \Delta\omega \geq 1/2$.

4.1.3 Spectral Properties of Light

For fields with sufficiently narrow spectra, the time evolution can be expressed via a decomposition into the product of a fast harmonic, i.e., stationary *carrier* oscillation with the mean frequency $\bar{\omega}$ from the spectrum and a much slower varying *envelope* function [514,

525]. In this case the whole field can be called *quasi-stationary* or a *wave-group*. Light fields with approximately bell-shaped temporal envelope functions, such as, e.g., Gaussians, are commonly called *pulses*. The carrier-envelope decomposition seizes to be useful if the spectral bandwidth reaches one octave, i.e., $\Delta\omega \approx \bar{\omega}$, in which case the pulse can be as short as $\Delta t \approx \tau_\omega/4\pi$. In the optical range this corresponds to a spectral width in the order of few hundred terahertz or nanometers, respectively, as is the case with so-called *ultra-short* pulses of light [606]. The optical fields which are subject to this work never have spectra broader than a few nanometers and are thus all extremely well approximated by a carrier envelope decomposition.

In analogy to phase-fronts it is possible to define hypersurfaces of maximal amplitude at a given time t, which for a general wave-group not necessarily coincide with a phase-front [514]. If they do, the beam is called *homogeneous*, if they do not, accordingly *inhomogeneous*. The velocity of these surfaces is called *group-velocity* v_{gr} and given as [514]

$$v_{\mathrm{gr}} = \frac{1}{|\vec{\nabla}(\frac{\partial\nu(\vec{x})}{\partial\omega})_{\bar{\omega}}|}, \tag{4.6}$$

where the derivative is evaluated at the mean frequency.

In media the frequency dependence of $\nu(\vec{x})$ is related to a frequency dependence of the *refractive index* $n(\omega)$. For example in the case of plane waves the general non-free wave-equation fixes the relation $k = n(\omega)\omega/c$. If n is not constant the wave-group is said to experience *dispersion* and the derivative $\partial\nu(\vec{x})/\partial\omega$ is called a *dispersion relation*, which connects spatial and temporal properties, typically associated with momentum and energy, respectively. In the case of *normal dispersion*, i.e., $\partial n(\omega)/\partial\omega > 0$ around $\bar{\omega}$ the group velocity is slower than the phase velocity and in the opposite case of *anomalous dispersion* the group velocity is accordingly faster [517, 514]. In non-dispersive media the phase and group velocities are equal and given by c/n. A difference of phase and group velocities in general leads to a temporal broadening of the light, which, although negligible in most cases of sufficiently spectrally narrow beams, begins to play an essential role for example in optical data transfer with short pulses [636, 537]. The electromagnetic fields subject to this work mostly propagate in air, which at standard conditions has a refractive index of $n \approx 1$ and is extremely well approximated as a non-dispersive medium [517, 514]. In effect, the fields outside of optical components can be essentially regarded as free fields.

Light emitted by optical sources typically exhibits random fluctuations, which cannot be easily expressed by an explicit time dependent field $A^{(+)}(\vec{x}, t)$ but can be modeled as fluctuations of the coefficients $c_{\vec{k},s}$ in Eq. (4.2). If the fluctuations happen on sufficiently short time-scales and are sufficiently uniformly distributed, i.e., *ergodic*, the time average over them can be modeled as an effectively broadened spectral density [618, 517, 514, 525, 524], see also Sec. 4.3.5. The spectral changes due to rapid random temporal fluctuations are called *spectral broadening* accordingly. A typical example of such ergodic fluctuations are so-called *phase fluctuations*, modeled as shifts of the carrier phase by a uniformly distributed random phase offsets, which additionally can be randomly distributed in time [517, 514]. Note that, in this case, the spectrum does not reflect a particular spectral wavefunction $A^{(+)}(\vec{x}, \omega)$ which can be Fourier transformed into a particular time-evolution of the

field $A^{(+)}(\vec{x},t)$ but instead corresponds to an ensemble of possible time-evolutions each characterized by a specific random composition of fluctuations leading to the same spectral density. As discussed below in Sec. 4.6.2, the spectral density uniquely characterizes the first-order coherence properties of classical light.

An example of a particularly practically useful spectral distribution is a so-called *optical frequency comb*, see e.g. [586, 668]. Frequency combs as first developed by Hall and Hänsch [595, 594] are classical light fields, which in the time-domain correspond to a sequence of pulses with a stable phase relation, i.e., a single common carrier oscillation. In the frequency-domain this translates to a spectrum given by several narrow peaks, called *comb lines* with a width corresponding to the pulse repetition frequency as well as an envelope function determined by the shape and width of the temporal pulse shape. Crucially, the distances between the comb lines in frequency space can be determined with high precision from a time-domain measurement of the comparatively slow repetition frequency. Furthermore, also their joint offset, which depends on the ratio of pulse repetition rate and carrier frequency, can be measured precisely through various techniques, such as a superposition with a frequency doubled signal [586]. The application of such combs is primarily based on the measurement of *beat notes*, i.e., comparatively slow field oscillations with difference frequencies, appearing whenever two close spectral components are superposed. While, as discussed in Sec. 4.5.1, optical oscillations themselves are of course too fast to be resolved, the beat notes can be measured with high precision if the two frequencies are sufficiently close. In effect, a frequency comb provides a broad set of well-known reference frequencies which are so narrowly spaced that, when superposed with an arbitrary unknown oscillating signal, at least one sufficiently slow beat note appears. Together with an additional conventional frequency measurement which identifies the closest comb lines, it thus becomes possible to determine the frequency of any unknown signal with unprecedented precision. Frequency combs represent an indispensable tool in many contemporary optical applications which require precise knowledge of frequencies, such as atomic spectroscopy or optical clocks [586, 668].

4.2 Classical Light Beams

4.2.1 Paraxial Wave-Packets

Due to the propagating nature of light in free space, free light fields are often spatially localized in only two spatial directions, with the third direction corresponding to the mean direction of propagation. The spatial shape along the propagation direction, usually coinciding with the coordinate z-direction, is then closely connected with temporal localization Δt. The z-direction is called *longitudinal* and the x- and y-directions *transverse*. Stationary or at least quasi-stationary light fields with transverse localization are commonly called *beams* [636]. If instead also the longitudinal and thus temporal localization is sufficiently narrow, i.e., close in length-scale to the transverse localization, the light field is called *wave-packet* [512, 524, 662, 600, 74].

Just as temporal and thus longitudinal localization requires a superposition of spectral modes, leading to a certain spectral density $G(\omega)$, so does transverse localization require a superposition of plane-wave modes with different k-vectors, leading to a certain distribution $p(\vec{k})$ of directions in the plane wave decomposition of the beam. For the beam to remain transversely localized over a certain propagation length, the distribution of allowed transverse momenta must be sufficiently narrow around the origin of k-space. This leads to the definition of a special class of fields, called *paraxial* beams, which can be broadly characterized by the conditions [893]

$$k_x, k_y \ll k_z \Longleftrightarrow k \approx k_z, \tag{4.7}$$

where formally different orders of paraxial approximation can be considered. Paraxial fields can be well approximated by the decomposition as $A^{(+)}(\vec{x},t) = A_s^{(+)}(\vec{x},t)e^{i(kz-\omega t)}$, where it is implied that all short-scale spatial dependence is contained in e^{ikz} and $A_s(\vec{x},t)$ varies much less on comparable length scales, i.e., its decomposition into plane wave modes has only very little contribution of modes with large $k_x, k_y \approx k$ [581]. Combining the paraxial approximation with wave equation (4.1) leads to the *paraxial Helmholtz equation* (PHE) for a harmonic mode $\vec{A}(\vec{x},t) = \vec{A}_s(\vec{x})e^{-i\omega t}$ given as [662, 530, 893]

$$i\frac{\partial \vec{A}_s(\vec{x})}{\partial z} = -\frac{1}{2k}\vec{\nabla}_\perp^2 \vec{A}_s(\vec{x}), \tag{4.8}$$

where $\vec{\nabla}_\perp$ is the exclusive nabla operator for the transverse directions x and y. The PHE has the character of a wave equation between the longitudinal coordinate z and the two transverse coordinates. In effect, the evolution of the transverse field can be expressed in dependence of the longitudinal position of the beam, where the role of the z-coordinate is equivalent to the usual role of time, as e.g., in the Schrödinger equation [893]. Any field propagating in free space, and thus also any beam evolving according to the PHE will experience *diffraction*, i.e., a spatial broadening, which in the case of a longitudinally extended beam happens in the transverse direction [636]. Thus typical beams are characterized by a distinguished longitudinal position z_0 of minimal transverse width, called the *focus*, and have diverging widths with increasing distance $|d|$ from the focus, where $d = z - z_0$. The minimal width is commonly called the *waist* of the beam. At longitudinal distances sufficiently far from the focus paraxial beams can be approximated very well by a set of rays with a suitable distribution of directions, leading to a linearly increasing width characterized by an angle of *divergence*.

4.2.2 The Gaussian Beam

Commonly, two classes of monochromatic, i.e., stationary solutions of the PHE are considered the *Gauss-Hermite* and *Gauss-Laguerre* beams [605, 513, 525, 527, 511, 662, 530]. Both correspond to possible transverse electromagnetic modes (TEM) of optical resonators, where Gauss-Laguerre beams are additionally eigenstates of the so-called *orbital angular momentum* of light, see, e.g., [554, 559, 583]. Beams which can be described by one of these

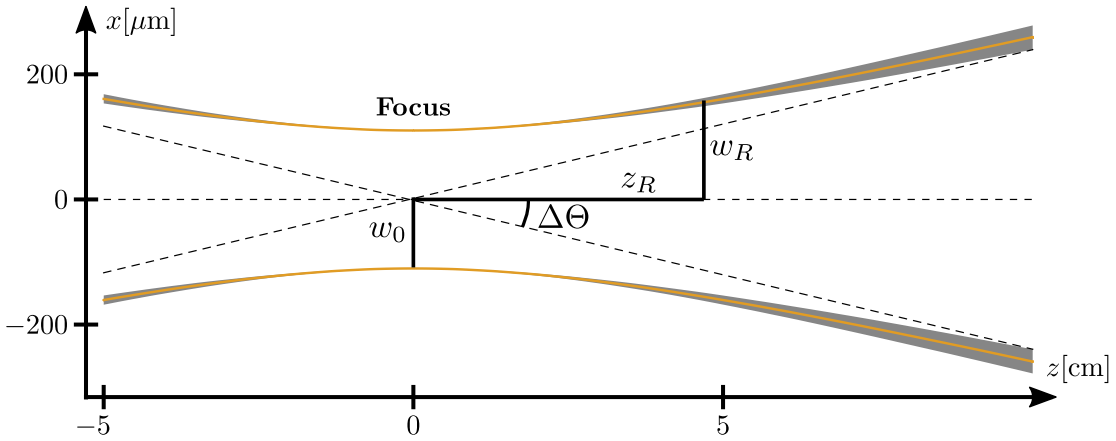

Figure 4.1: **Properties of the Gaussian Beam** The figure depicts the basic beam parameters z_R, $\Delta\Theta$, w_0, as well as the beam width $w_R = \sqrt{2}w_0$ at a distance of z_R from the waist position. The drawn edges of the beam (yellow lines) correspond to the respective widths $w(z)$, which for large distances from the focus asymptotically approach the limit of ray-optics (indicated as tilted dashed lines). Furthermore, the effect of finite spectral width is illustrated, where the shaded areas represent the range of widths for a spectrum with wavelengths in the range $[\lambda - \Delta\lambda, \lambda + \Delta\lambda]$ ($\lambda = 810$nm, $\Delta\lambda = 70$nm). For typical spectral widths of a few nanometers, the effect would not be visible in the figure.

mode are commonly called *transverse single mode* in contrast to *longitudinal single mode* beams, which are monochromatic. The fundamental mode of both classes is the *Gaussian beam*, defined as [518, 513, 511, 662, 530, 515]

$$A^{(+)}(\vec{x}) = A_0 \frac{w_0}{w(z)} \exp\left(-\frac{x^2+y^2}{w^2(z)}\right) \exp\left(i\left(kz + k\frac{x^2+y^2}{2R(z)} - \phi_G(z)\right)\right) \tag{4.9}$$

and depicted in Fig. 4.1, where A_0 is factor with a suitable dimension. The Gaussian beam is characterized by the single parameter z_R called the *Rayleigh range* or *Rayleigh length*, which determines both the waist $w_0 = \sqrt{z_R\lambda/\pi}$ as well as the divergence angle $\Delta\Theta = \sqrt{\lambda/\pi z_R}$. The z-dependent width $w(z)$ and *radius of curvature* $R(z)$ can also be parametrized by z_R and are given by

$$w(z) = w_0\sqrt{1+\left(\frac{z}{z_R}\right)^2}, \quad R(z) = z\left(1+\left(\frac{z_R}{z}\right)^2\right), \tag{4.10}$$

respectively. The so-called *Guoy phase* $\phi_G(z) = \arctan(z/z_R)$ represents a phase change of π between $z = \pm\infty$, which is very slow varying compared to kz. At longitudinal distances around the focus, which are significantly smaller than the Rayleigh range, the beam is approximately non-diverging and denoted as *collimated*. Note that in Eq. (4.9) the polarization has been not written and the general polarization properties of paraxial beams will be discussed in the next section.

For a monochromatic Gaussian beam the time dependence is given by an additional factor $e^{-i\omega t}$ and in the case of a quasi-monochromatic beam a slowly varying temporal envelope factor $f(t-cz)$ can be added. Note that the latter corresponds to the special case of a beam with a *resting focus*, i.e., a time-invariant transverse shape of the beam [662]. Strictly speaking even a quasi-stationary beam has a finite spectral width and thus will exhibit a correspondingly modified spatial mode, as also illustrated in Fig. 4.1. However, for sufficiently narrow spectra this effect is negligible and the beam is very well approximated by the spatial mode corresponding to the central frequency.

The Gaussian beam corresponds to a minimally diffracting beam, which means that for any given waist it has the minimally possible divergence angle. Accordingly, a typical quantifier of beam quality is the so-called M^2 *parameter* which corresponds to the increase of divergence compared to a Gaussian beam with the same waist w_0, i.e., $M^2 := \Delta\Theta/\Delta\Theta_G$, where $\Delta\Theta_G = \lambda/\pi w_0$ [613]. Finally also the calculation of the propagation of a Gaussian beam through an optical system is significantly simplified since the *ABCD-matrix* formalism of ray optics can be applied, see, e.g., [518, 517, 530], if the z-dependent state of the beam is expressed as a single complex parameter q_z, where

$$\frac{1}{q_z} = \frac{1}{R(z)} + \frac{i\lambda}{\pi w^2(z)} \tag{4.11}$$

and the transformations are given as

$$q' = \frac{Aq+B}{Cq+D}. \tag{4.12}$$

4.2.3 Polarization of Paraxial Light

Due to the transversality constraint the range of possible polarizations of the paraxial beam is reduced. In effect, at least in the first-order paraxial approximation employed here, it is possible to express the polarization at each position in the form [558]

$$\vec{A}^{(+)}(\vec{x},t) = \begin{pmatrix} A_H^{(+)}(\vec{x},t) \\ A_V^{(+)}(\vec{x},t) \\ \frac{i}{k}\left(\frac{\partial}{\partial x}A_H^{(+)}(\vec{x},t) + \frac{\partial}{\partial y}A_V^{(+)}(\vec{x},t)\right) \end{pmatrix} e^{i(kz-\omega t)}, \tag{4.13}$$

where $A_H^{(+)}$ and $A_V^{(+)}$ are two slowly varying amplitude functions corresponding to orthogonal polarizations, each of which can for example be given by the slowly varying part of a Gaussian beam. Note that due to the beam divergence there is a non-vanishing polarization component in longitudinal direction. However, orthogonality of the two polarization components is ensured since in paraxial approximation terms of order $(\partial_r A_j^{(+)}/k)^2$ with $r \in \{x,y\}$ are neglected. Throughout this work the y-direction is defined as the vertical direction of the spatial reference frame and thus the symbols H and V are chosen to denote horizontal and vertical polarization of the electric field.

A very useful representation of the polarization of paraxial beams is given by the *Stokes formalism*, which allows to express the polarization at any spacetime coordinate in terms of three real valued dimensionless parameters called the Stokes parameters $\mathcal{Z}_j$ [532, 514, 296, 530]. Here they are defined in terms of the electric field as

$$\begin{aligned}\mathcal{Z}_1(\vec{x},t) &= \frac{1}{N}\left(\left|E_H^{(+)}(\vec{x},t)\right|^2 - \left|E_V^{(+)}(\vec{x},t)\right|^2\right)\\ \mathcal{Z}_2(\vec{x},t) &= \frac{1}{N}\,2\mathrm{Re}\big[E_H^{(+)}(\vec{x},t)\,E_V^{(-)}(\vec{x},t)\big]\\ \mathcal{Z}_3(\vec{x},t) &= \frac{1}{N}\,2\mathrm{Im}\big[E_H^{(+)}(\vec{x},t)\,E_V^{(-)}(\vec{x},t)\big],\end{aligned} \tag{4.14}$$

with normalization $N = \left|E_H^{(+)}\right|^2 + \left|E_V^{(+)}\right|^2$. While $\mathcal{Z}_1$ and $\mathcal{Z}_2$ quantify degrees of the two orthogonal *linear* polarizations, $\mathcal{Z}_3$ corresponds to the degree of *circular* polarization. Instead of the Stokes parameters the polarization can also be expressed equivalently in terms of the two complex parameters

$$\alpha_H(\vec{x},t) := \frac{E_H^{(+)}(\vec{x},t)}{\sqrt{N}}, \qquad \alpha_V(\vec{x},t) := \frac{E_V^{(+)}(\vec{x},t)}{\sqrt{N}}, \tag{4.15}$$

which represent the entries of the so-called *Jones vector* [532, 517, 530].

For a *homogeneously polarized* paraxial field, the polarization is fully described either by three real or two complex parameters, which are all independent of the spacetime coordinate $(\vec{x},t)$. However, crucially this does not imply that the directions of the fields $\vec{E}$ and $\vec{B}$ are fixed as well. Instead small variations of polarization direction are present as given by expression (4.13).

4.2.4 Optical Energy Flow

The behavior of electromagnetic energy in a light beam is captured by *Poynting's theorem*, which states that the flow of electromagnetic energy in vacuum obeys a continuity equation of the form [514, 523]

$$\frac{\partial}{\partial t}u(\vec{x},t) + \vec{\nabla}\vec{S}(\vec{x},t) = 0 \tag{4.16}$$

where the electromagnetic energy density u and the *Poynting vector* $\vec{S}$ are given by

$$u(\vec{x},t) = \frac{1}{2}\left(\epsilon_0|\vec{E}(\vec{x},t)|^2 + \frac{1}{\mu_0}|\vec{B}(\vec{x},t)|^2\right) \tag{4.17}$$

$$\vec{S}(\vec{x},t) := \frac{1}{\mu_0}\vec{E}(\vec{x},t)\times\vec{B}(\vec{x},t), \tag{4.18}$$

respectively, where E and B refer to the real valued fields and the constants ϵ_0 and μ_0 are the *vacuum permittivity* and *vacuum permeability*, respectively. The time-averaged

Poynting vector is called the *Poynting current*, and the classical intensity I_{class} is the absolute value of the Poynting current with $I_{\text{class}} = |\langle \vec{S}(\vec{x},t)\rangle_t|$, where the subscript t indicates a time averaging [537]. The intensity characterizes the surface density of average energy flow for a propagating field.

For quasi-stationary fields it is possible to define a time-dependent intensity as the average Poynting current over one oscillation cycle with [514, 558, 560, 537]

$$I_{\text{class}}(\vec{x},t) \approx \frac{1}{\tau}\left|\int_t^{t+\tau} \mathrm{d}t'\, \vec{S}(\vec{x},t')\right| \approx \left|\vec{S}_{\text{avg}}(\vec{x},t)\right|, \tag{4.19}$$

with the time-averaged Poynting vector $\vec{S}_{\text{avg}}$ defined as

$$\vec{S}_{\text{avg}}(\vec{x},t) := \frac{2}{\mu_0}\mathrm{Re}\big[\vec{E}_s^{(+)}(\vec{x},t) \times \vec{B}_s^{(-)}(\vec{x},t)\big], \tag{4.20}$$

where the amplitudes $\vec{E}_s^{(+)}$ and $\vec{B}_s^{(-)}$ contain only the slow time variation of the field and are approximately constant during the period τ_ω of carrier frequency ω. For an ideal harmonic, i.e., stationary field all above approximations become equalities and the intensity time-independent. During a stationary oscillation in free space, $\vec{S}$ is oriented along a single axis, such that the intensity provides the cumulative energy flow density in the direction of that axis. In the following the approximate character of the time-averaged Poynting current will be neglected in the case of quasi-monochromatic light for convenience of presentation.

The time-averaged Poynting current of a quasi-monochromatic field can be decomposed into two parts, called *orbital current* $\vec{S}_O$ and *spin current* $\vec{S}_S$, with $\vec{S}_{\text{avg}} = \vec{S}_O + \vec{S}_S$ [558, 560, 559]. In general this definition is ambiguous since different decompositions are implied when considering electric and magnetic fields, where a possibility of a unique definition is given by averaging the two expressions [560]. However, for paraxial beams this ambiguity disappears and the orbital current can be written for example in terms of electrical field as [558, 560, 559, 564]

$$\vec{S}_O(\vec{x},t) = c\frac{2\varepsilon_0}{k}\mathrm{Im}\big[\vec{E}_s^{(-)}(\vec{x},t)(\vec{\nabla})\vec{E}_s^{(+)}(\vec{x},t)\big], \tag{4.21}$$

where the notation with "$(\vec{\nabla})$" implies that the scalar product is taken between the field vectors, i.e., $\big(\vec{a}(\vec{\nabla})\vec{b}\big)_j := \sum_k a_k \partial_j b_k$. In contrast, the spin current in the paraxial case is given as [558, 560, 559]

$$\vec{S}_S(\vec{x},t) = c\frac{\varepsilon_0}{k}\vec{\nabla} \times \mathrm{Im}\big[\vec{E}_s^{(-)}(\vec{x},t) \times \vec{E}_s^{(+)}(\vec{x},t)\big]. \tag{4.22}$$

It is divergence free per definition, i.e., $\vec{\nabla}\vec{S}_S = 0$ such that it does not contribute to the net energy flow $\vec{\nabla}\vec{S}$. In general the fact that additional curl terms can be added to the Poynting vector without affecting the optical continuity equation (4.16) represents an ambiguity in its definition [514, 523, 560, 559].

The orbital part is independent of the type of polarization and corresponds to the local k-vector averaged over all polarization components with [558, 560, 834]

$$\vec{S}_O(\vec{x},t) = c\,u(\vec{x},t) \sum_{j\in\{H,V\}} |\alpha_j(\vec{x},t)|^2\ \hat{k}^{(j)}_{\text{loc}}(\vec{x},t), \tag{4.23}$$

with Jones vector coefficients α_j and the unit local k-vector $\hat{k}^{(j)}_{\text{loc}} = \vec{\nabla}\nu_j/k$ defined based on the polar decomposition $E^{(+)}_j = |E^{(+)}_j|e^{i\nu_j}$. The expression for the spin current can also be simplified to

$$\vec{S}_S(\vec{x}) = \frac{c}{2}\,u(\vec{x},t)\ \hat{s}_z \times \big(\mathcal{Z}_3(\vec{x},t)\hat{\sigma}_{\text{osm}}(\vec{x},t) + \mathcal{Z}_2(\vec{x},t)\hat{\delta}_{\text{loc}}(\vec{x},t)\big) \tag{4.24}$$

where $\hat{s}_z$ is the unit vector in z-direction, $\hat{\delta}_{\text{loc}} := \big(\vec{k}^{(H)}_{\text{loc}} - \vec{k}^{(V)}_{\text{loc}}\big)/k$ is the normalized difference between the local k-vectors, and $\hat{\sigma}_{\text{osm}} := \big(\vec{k}^{(H)}_{\text{osm}} + \vec{k}^{(V)}_{\text{osm}}\big)/k$ is the normalized sum of the so-called *osmotic* k-vectors defined as

$$\vec{k}_{\text{osm}}(\vec{x},t) = \text{Re}\big[\frac{\vec{\nabla}\psi(\vec{x},t)}{\psi(\vec{x},t)}\big] = \frac{\vec{\nabla}\varrho(\vec{x},t)}{\varrho(\vec{x},t)}, \tag{4.25}$$

for a general complex scalar field $\psi = \varrho e^{i\varphi}$. This definition is motivated by the concept of *osmotic velocity* [882, 835, 879, 873] as sometimes employed in Bohmian mechanics, see also Sec. 7.6.1. The spin part (4.24) clearly contributes only a transverse energy flow, which depends both on the local polarization as well as on its change. It vanishes for a strictly linearly polarized beam since in this case $\mathcal{Z}_3 = \hat{\delta}_{\text{loc}} = 0$.

For a homogeneous polarization of the paraxial field the components of the two currents simplify to

$$\vec{S}_O = c\,u(\vec{x},t)\,\hat{k}_{\text{loc}}(\vec{x},t), \tag{4.26}$$

$$\vec{S}_S = c\,u(\vec{x},t)\,\mathcal{Z}_3\big(\hat{s}_z \times \hat{k}_{\text{osm}}(\vec{x},t)\big) \tag{4.27}$$

where $\hat{k}_{\text{osm}} := \vec{k}_{\text{osm}}/k$. In conclusion, the net energy flow of a homogeneously polarized paraxial field, as expressed by $\vec{S}_O$, corresponds to a flow with velocity c in the direction of the local k-vector. Additionally $\vec{S}_S$ represents a divergence free, polarization-dependent, and purely transverse contribution to the flow, which vanishes for linear polarization and is maximal for circular polarization.

4.3 Quantization of the Electromagnetic Field

4.3.1 Quantum Field Theory

The quantization of electromagnetic radiation lies at the historical origin of quantum theory. By proposing a quantization of the emitted energy of black body radiation, Planck

was able to provide a theoretical explanation [36, 37, 35] of Wien's law and the Stefan-Boltzmann law, describing the influence of temperature on spectrum and amount of radiated energy, respectively [526, 517, 600, 540]. The model assumes that the matter in the walls of the black body consists of oscillators which admit only a set of discrete frequencies ν and connects these frequencies to discrete Energies E via the relation $E = h\nu$, where h is *Planck's constant*, already introduced in Sec. 1.4.1 as a fundamental constant in the dynamics of quantum processes, e.g. in the Schrödinger equation (1.11). A statistical analysis of the possible distributions of the discrete portions of energy among the oscillators then allows to deduce the temperature dependencies. Another crucial historical step was provided by Einstein's explanation of the photoeffect [16], postulating that not only the mechanism of radiation emission is quantized but the radiation field itself [641, 526, 551]. Conceptions of light momentum such as exhibited in Compton scattering [12] strengthened the notion of light particles [526, 239], which were eventually denoted as "photons" by Lewis [28]. It should be noted that just like Planck's law, also the photoeffect possesses an explanation which does not require a quantization of the field if the absorption process is quantized analogously to the emission process [524]. This type of explanations in which the electromagnetic field is considered in a classical, non-quantized manner and the matter with which it interacts as a quantum system, is commonly denoted as *semi-classical*. In fact, a large range of quantum optical phenomena can be treated semi-classically [531, 529], leading to a prolonged controversy in the 1960s and 70s with respect to the question whether the phenomenon of the Lamb shift [25], usually regarded as an effect of field quantization, possesses a semi-classical explanation, see [627] for a recounting.

The first comprehensive systematic formulation of the quantization of the electromagnetic field was given by Dirac [13]. Based on this seminal work, over the following two decades a novel theoretical approach to quantum theory called *quantum field theory* (QFT) was developed culminating in the introduction of a unified formalism by Dyson [15], see [534] for a detailed historical overview. In modern terms the electromagnetic radiation and its interaction with matter is described by *quantum electrodynamics* (QED), which is one of the most prominent instances of a QFT. In fact, a large portion of modern physics, can be seen as "special applications of quantum electrodynamics to selected physical systems" [512]. QED forms an essential part of the *standard model* of physics, which represents a unified theory for three of the four fundamental forces in the framework of QFT, i.e., the strong, the weak and the electromagnetic force, excluding gravitation [548, 550].

Typically QFT is confronted with significant mathematical difficulties such that very few realistic problems possess exact solutions. Instead the vast majority of work in QFT is based on perturbative approaches, where the problem is expanded in orders of weak interaction strength [526, 952]. In this context *Feynman diagrams* [543] have emerged as a very useful tool. One of the main problems of QFT is the appearance of infinities, i.e., non-converging integrals. It is solved with the approach of *renormalization* in which the infinities are "subtracted out", which means that free unobservable parameters of the theory are given finite or even infinite values which cancel out the infinities [538]. Since it is non-trivial that by changing a finite amount of parameters, a potentially infinite amount of divergencies can be eliminated, a special class of *renormalizable* QFTs can be identified.

In light of such formal problems, QFT is sometimes regarded less as a closed fundamental theory but rather as an open research program which provides "an approximate scheme to carry out calculations based on perturbation theory" [512]. *Effective field theories* with a limited range of applicability are formulated, which are valid for example only at certain energy scales where the divergencies do not occur [534, 552, 952]. Nevertheless QFT demonstrates enormous explanatory power through very good agreement with empirical results.

The fundamental element of QFT are *quantum fields*, i.e., operator-valued functions defined on the whole spacetime continuum. As already sketched in Sec. 3.1, quantum fields, although they are global objects, allow to express all interactions in a form compatible with the principles of SR by letting all influences between various parts of the physical system propagate with finite speed over the field [521, 552]. In effect, QFT admits a covariant formulation reconciling quantum theory with SR, which is difficult to achieve in the wave-mechanical formalism [534, 535]. With respect to quantum mechanical particles, which are identified as excitations of the field, QFT allows to describe creation and annihilation processes where the particle number is not conserved, identifies fundamental forces with the exchange of particles, and includes the existence of anti-particles [552, 534, 526, 952]. It is also especially suited to describe systems with a large number of particles, for example in the context of condensed matter theory. It is an open question whether fields or particles are more fundamental and which should be regarded as the fundamental beables of QFT and Quantum Theory in general [952]. In particular some authors point out that the predictions of QFT are grounded to a large extent in a "particle representation"[851], such as, e.g., the scattering experiments at CERN or other colliders [592].

A quantum field description can be established from a scalar field, such as the classic electromagnetic field or a quantum mechanical spacetime wave function, by using the correspondence principle. In the process of field quantization the spacetime coordinates are treated as continuous indices to define a set of a continuous infinity of quantum systems, one for each spacetime point [55, 526, 521, 666, 552]. Formally this means that the scalar functions are replaced by operators, which are regarded as dynamical variables according to a Heisenberg picture [637]. The state vectors acting on the field then just encode the state of the respective field modes in an abstract way, for example as occupation numbers in the case of a quantization in terms of harmonic oscillators, and in particular have no spatial character which could be expressed via a position operator. Instead all dynamics and spatial dependence is based on the field operators themselves, which obey an infinite amount of pairwise commutation relations between the field at different spacetime points [552, 952]. Usually the quantization process is simplified by initially considering only a finite volume allowing for only a countable infinity of *field modes*, i.e., possible states of the classical field given by the size and form of the volume toghether with appropriate boundary conditions, and then considering the limit where the size of this volume goes to infinity [526, 529, 531, 524]. Since field quantization is sometimes applied to a quantum wavefunction, it is sometimes also referred to as "second quantization" [542], although this term is not universally accepted, for example by authors who regard a formalism based on wavefunctions as more fundamental, see, e.g., [666].

4.3.2 From the Classical to the Quantum Field

Typically field quantization is based on considering an arbitrary electromagnetic field in a finite volume, which can be expressed as [529, 525]

$$\vec{A}^{(+)}(\vec{x},t) = \sum_j c_j \vec{b}_j(\vec{x}) e^{-i\omega_j t}, \tag{4.28}$$

where the summation is performed over a complete set of countably infinite orthonormal harmonic modes with spatial amplitudes $\vec{b}_j$. They conform to the Maxwell equations in the sense that the terms $\vec{b}_j e^{-i\omega_j t}$ represent harmonic solutions of frequency ω_j to the wave equation under appropriate boundary conditions given by the volume under consideration, sometimes called the "quantization cavity" [524]. The proper dimension is contained in the complex amplitudes c_j which specify the particular field. While in the classical theory the imaginary part of the complex analytic signal can be in principle chosen arbitrarily, in the context of field quantization, as discussed below, it is crucial that the components $\vec{A}^{(+)}$ and $\vec{A}^{(-)}$ correspond exclusively to positive and negative frequency components.

Although the field expansion of the form (4.28) is well suited to treat a large range of optical phenomena, it is not relativistically covariant, which, as written above, in general is one of the main advantages of quantum field theory [55, 526]. The technical reason for this is that it relies on the Hamiltonian formulation of electrodynamics which treats time and space on a different footing. To arrive at a covariant expression of a quantum field, a path integral formulation based on the Lagrangian can be used where the field is expressed via the relativistic field strength tensor unifying the treatment of both electric and magnetic fields as well as of space and time coordinates [526, 521, 638]. As for the subjects treated in this work and in fact a large portion of quantum optics in general a discussion in a single reference frame is absolutely sufficient, a covariant formulation is not necessary and will not be pursued further.

The classical field is described by the set of continuous amplitudes $\{c_j\}$. Quantization is achieved by effectively discretizing the range of values these amplitudes can take, very similar to the original idea proposed by Planck. In the case of an expansion into harmonic modes as in (4.28), this discretization is done by applying the formal apparatus of the quantum mechanical harmonic oscillator, see, e.g., [55, 526, 529, 525, 531, 524]. While the basic harmonic oscillator describes an oscillation in space due a harmonic potential, the same formalism is now applied to the harmonic oscillation in the space of the electromagnetic field. In effect, for each mode j the amplitude c_j is thus replaced by the annihilation and creation operators $\mathbf{a}_j$ and $\mathbf{a}_j^\dagger$ as

$$c_j \to \sqrt{\frac{\hbar}{2\omega_j \epsilon_0}}\, \mathbf{a}_j, \qquad c_j^* \to \sqrt{\frac{\hbar}{2\omega_j \epsilon_0}}\, \mathbf{a}_j^\dagger, \tag{4.29}$$

leading to a quantum field of the form

$$\vec{\mathbf{A}}^{(+)}(\vec{x},t) = \sum_j \sqrt{\frac{\hbar}{2\omega_j \epsilon_0}}\, \mathbf{a}_j\, \vec{b}_j(\vec{x}) e^{-i\omega_j t}, \tag{4.30}$$

with $\vec{\mathbf{A}}^{(-)} = \left(\vec{\mathbf{A}}^{(+)}\right)^\dagger$ and $\vec{\mathbf{A}} = \vec{\mathbf{A}}^{(+)} + \vec{\mathbf{A}}^{(-)}$. The factor $\sqrt{\hbar/2\omega_j\epsilon_0}$ is chosen such that each excitation of the harmonic mode j corresponds to the energy quantum $\hbar\omega_j$. The *field operators* $\mathbf{a}_j$ and $\mathbf{a}_j^\dagger$ obey the usual commutation relations, $[\mathbf{a}_j, \mathbf{a}_{j'}] = [\mathbf{a}_j^\dagger, \mathbf{a}_{j'}^\dagger] = 0$ and $[\mathbf{a}_j, \mathbf{a}_{j'}^\dagger] = \delta_{jj'}$.

4.3.3 Field Excitations

The field operators are always understood as acting on a quantum state vector $|\psi_j\rangle$ in a continuous separable Hilbert space $\mathcal{H}_E$, which according to the correspondence principle constitutes the quantum mechanical representation of the classical electromagnetic field. A countably infinite basis of $\mathcal{H}_E$ is given by the *number states* or *Fock states* $|n_j\rangle$, which are eigenstates of the *number operator* $\mathbf{n}_j = \mathbf{a}_j^\dagger\mathbf{a}_j$, with the eigenvalues $n_j \in \mathbb{N}$, indicating the occupation number of mode j. The total state of the field is specified by the joint state $|\Psi\rangle$ of all modes called the *multimode field state*, which in Fock representation can be written as [531, 524]

$$|\Psi\rangle = \sum_{n_1,n_2,n_3,\ldots} c_{n_1,n_2,n_3,\ldots} |n_1, n_2, n_3, \ldots\rangle \in \mathcal{H}_F \otimes \mathcal{H}_F \otimes \mathcal{H}_F \otimes \ldots \tag{4.31}$$

Of course in general the field can also be an arbitrary mixed state ρ. The quantum mechanical equivalent to a zero field is the *vacuum state* $|0\rangle := |0, 0, 0, \ldots\rangle$ with zero occupation for all modes.

The quantized description of the electromagnetic fields leads to the minimal definition of a *photon* as an elementary excitation of a mode of the field with discrete energy $\hbar\omega_j$ [512, 525]. In particular in this case the photon is monochromatic, i.e., has a single well-defined frequency ω_j, and is associated with an extended but time-independent spatial function $\vec{u}_j$. While in the quantum case the description in terms of positive and negative frequency parts $\vec{\mathbf{A}}^{(+)}$ and $\vec{\mathbf{A}}^{(-)}$ still contains redundancy, it is fundamentally connected to the occurrence of both annihilation and creation of field excitations [589].

The quantization of energy in the field can be seen by considering the total field Hamiltonian $\mathbf{H}$ given by [526, 529, 525]

$$\mathbf{H} = \sum_j \hbar\omega_j \left(\mathbf{n}_j + \frac{1}{2}\right), \tag{4.32}$$

which is the Hamiltonian for a system of infinitely many independent quantum harmonic oscillators. Notably, the expectation value of the total field energy is divergent even for the vacuum state yielding the so-called *zero-point* energy $\sum_j \hbar\omega_j/2$, which is a basic example of the above-mentioned divergences typically encountered in QFT [511]. The absolute amount of zero-point energy has no known empirical consequences, but its relative changes are the basis of several physical phenomena [526, 529, 525, 524, 547] such as the Casimir effect [11, 545]. In the latter a change of field geometry, which affects only the mode structure of the field and thus the zero-point energy leads to a very small but measurable [650, 609]

attractive or repulsive force between two conductors, even in the absence of any field excitations.

Finally a general free field can be described by letting the quantization volume go to infinity and Fourier expand the field, e.g., in a basis of plane wave modes as [525, 662, 647]

$$\vec{\mathbf{A}}^{(+)}(\vec{x},t) = \sum_p \hat{s}_p \int_{\mathbb{R}^3} \sqrt{\frac{\hbar}{2\omega_k \epsilon_0}}\, \mathbf{a}_{\vec{k},p}\, e^{i(\vec{k}\vec{x}-\omega_k t)}\, \frac{\mathrm{d}^3 k}{\sqrt{2\pi}^3}, \tag{4.33}$$

in analogy to the corresponding mode decomposition of the classical field (4.2). Here, each mode corresponds to a well-defined photon momentum of $\vec{p} = \hbar\vec{k}$. In the continuous case, the $\mathbf{a}_{\vec{k},s}$ represent an annihilation operator density and fulfill the commutation relation $[\mathbf{a}_{\vec{k},p}, \mathbf{a}^\dagger_{\vec{k}',p'}] = \sqrt{2\pi}^3 \delta^{(3)}(\vec{k}-\vec{k}')\delta_{s,s'}$. Accordingly the joint Hilbert space of the field, becomes a continuum of continuous mode spaces. Note that expression (4.2) fully describes the classical field in the sense that it provides both the *structure* of the field via the form of the field modes and the *content* of the field via the corresponding amplitudes $c_{\vec{k},s}$. In contrast, the operator $\mathbf{A}^{(+)}$ can be seen as providing only the mode structure, while the content of the field is given by the respective field state $|\Psi\rangle$. Following the general idea of QFT as described above, Eq. 4.33 corresponds to a replacement of the classical field by a continuum of quantum harmonic oscillators, where each mode, i.e., each point in Fourier space corresponds to an independent oscillator [589]. The corresponding Hamiltonian becomes [647]

$$\mathbf{H} = \sum_p \int_{\mathbb{R}^3} \hbar\omega_k\, \mathbf{a}^\dagger_{\vec{k},p} \mathbf{a}_{\vec{k},p}\, \frac{\mathrm{d}^3 k}{\sqrt{2\pi}^3}, \tag{4.34}$$

where, following common practice, the zero-point energy has been neglected.

4.3.4 Quantum Wave-Packets

The quantization of the field in terms of plane wave modes (4.33) is not well suited to express the state of typical light beams, which would correspond to complicated superpositions of excitations. Instead the usual strategy is to rewrite the field in terms of different mode compositions and introduce appropriately transformed field operators, leading to simple field states. By introducing an amplitude function $\xi(\vec{k})$, which for example can be proportional to the spatial Fourier transform of some classical beam mode $A^{(+)}(\vec{x},t)$, such as, e.g., a Gaussian beam, it is possible to define *photon-wavepacket creation operator* as [581, 524, 662, 647]

$$\mathbf{a}^\dagger_{\xi,p} = \int_{\mathbb{R}^3} \mathbf{a}^\dagger_{\vec{k},p} \xi(\vec{k}) \frac{\mathrm{d}^3 k}{\sqrt{2\pi}^3} \tag{4.35}$$

with a certain polarization p. Analogously a corresponding annihilation operator $\mathbf{a}_\xi$ can be defined with complex conjugate $\tilde{\xi}^*(\vec{k})$. By requiring that the amplitude function ξ is

normalized according to the standard scalar product

$$(\xi|\xi') := \int_{\mathbb{R}^3} \xi^*(\vec{k})\xi'(\vec{k})\frac{\mathrm{d}^3k}{\sqrt{2\pi}^3}, \tag{4.36}$$

the operators $\mathbf{a}_{\xi,p}$ and $\mathbf{a}^\dagger_{\xi,p}$ again fulfill the commutation relation $\left[\mathbf{a}_{\xi,p}, \mathbf{a}^\dagger_{\xi,p}\right] = 1$ and thus lead to the same number state algebra as in the case of discrete single mode states (4.30). The operator $\mathbf{a}^\dagger_\xi$ corresponds to a single-photon excitation in a superposition of plane wave modes, potentially with different frequencies ω. As such it no longer has the simple meaning of an excitation with well-defined energy and momentum as in the case of plane wave excitations, but extends the notion of a single photon to potentially unsharp energies and momenta. In general these wavepackets modes do not need to be pairwise orthogonal such that the field operators for two wavepackets with different amplitude functions ξ and ξ' fulfill the commutation relation [581, 662]

$$\left[\mathbf{a}_{\xi,p}, \mathbf{a}^\dagger_{\xi',p'}\right] = \delta_{p,p'} \int_{\mathbb{R}^3} \xi^*(\vec{k})\xi'(\vec{k})\frac{\mathrm{d}^3k}{\sqrt{2\pi}^3}. \tag{4.37}$$

Even if $\xi(\vec{k})$ is the Fourier transform of some stationary classical spatial field amplitude $A^{(+)}(\vec{x},t)$ at some time t, in general the spatial form of the wavepacket field is not the same, i.e., in general $\mathbf{A}^{(+)}(\vec{x},t) \neq A^{(+)}(\vec{x},t)\mathbf{a}_\xi$. The reason for this is the factor of $1/\sqrt{\omega_k}$ in the integral (4.33) which effectively represents a weight in the Fourier transform to position space. It is a consequence of the fact that each spectral mode corresponds to a different single-photon energy and thus its contribution to the resulting field is modified accordingly. For sufficiently monochromatic wavepackets, however, ω_k can be approximated via a mean frequency $\bar{\omega}$ and, e.g., a Gaussian spatial beam shape $A^{(+)}(\vec{x},t)$ obtained from $\xi(\vec{k})$ [524, 662]. Another consequence of the weighting factor is that the field amplitudes $A^{(+)}_1(\vec{x},t)$ and $A^{(+)}_2(\vec{x},t)$ resulting from orthogonal k-space amplitudes $\xi_1(\vec{k})$ and $\xi_2(\vec{k})$ with $(\xi_1|\xi_2) = 0$ are not necessarily orthogonal themselves [647], which has to be accounted for when formulating a wave-mechanical description of photons, as discussed in Sec. 4.7.

4.3.5 Time Evolution of the Field

The free field, as introduced above in (4.30) or (4.33), is stationary in the sense that it contains time-evolution only as the harmonic oscillation of each mode. As discussed above, for harmonic oscillations the only relevant temporal parameter is the *phase* which determines the relative time inside a cycle. Nevertheless, collective excitations are possible, which while still stationary in the strict sense, have a more complicated time-dependence such as for example the propagating wave-packet excitations, discussed above. To incorporate non-stationary time-evolution of the field it is necessary to consider QED interactions with matter, i.e., other quantum systems, see, e.g., [524]. This leads to a field with additional time evolution which can either be included in the Heisenberg picture by adding time dependence to the creation and annihilation operators, or expressed in terms of an interaction

picture with time-varying amplitudes or matrix elements of the field states, which is the formalism chosen here, using the time-dependent density operators $\rho(t)$.

In general in optical processes a vast range of timescales are involved, spanning at least 15 orders of magnitude, from the oscillations of the electromagnetic field in the optical spectrum, which has a period of femtoseconds to temporal drifts of optical components in the lab in the order of seconds [618, 517]. Thus, when describing the time-evolution of fields it is crucial to take the respective timescale into account. A crucial reference is given by a certain time-scale of measurement typically characterized by a duration τ_I over which the fields are necessarily integrated. This can for example correspond to the integration time of an optical detector as discussed in the next section. While in general the field will vary over the integration time as well as between subsequent measurements, a stationary description is possible for time-variations which can be modeled as classical random fluctuations [514, 517], as already sketched in Sec. 4.1.3 in the context of spectral broadening.

In principle two types of classical field fluctuations can be distinguished based on whether the characteristic timescale of the fluctuations is slower or faster than τ_I. Fast fluctuations, i.e., happening on a short timescale, often stem from randomness in the source generating the light, and typical sources, such as thermal sources or lasers, have their own characteristic types of fluctuations [589, 618, 612, 517, 514, 524]. A typical example are phase fluctuations, which for propagating single mode fields are commonly modeled as a sequence of harmonic *wavetrains* containing a certain number of cycles interrupted by a discontinuous change of the phase, see, e.g., [517] for an illustration. A simple example of decidedly slow fluctuations, i.e., happening on a comparatively long timescale, would be typical modifications of the optical setup introduced or noticed by the experimenter as for example random rotations of polarization, see, e.g., **[P5]**.

In the case of fast fluctuations the field exhibits a large number of states during the integration time of τ_I. A convenient approach in optics it then to translate this time averaging into an ensemble average over these various fields [589, 618, 524]. If the fluctuations are produced by an ergodic random process during each period of integration, they are effectively sampled from the same distribution independently of the starting point of the integration. For such ergodic fluctations and sufficiently large integration times the ensemble average then becomes stationary. This allows to express the coherence properties of light, which are strongly influenced by time-dependent fluctuations via stationary ensemble averages. In the quantum formalism this corresponds to employing a time-independent mixed state ρ, where the mixture is understood as proper. The long term evolution of the field can still vary leading to a time-dependent $\rho(t)$, which however, can be regarded as constant on the timescale τ_I. This description transfers very well to a full quantum description of the fluctuations via a quantum interaction of the field with another quantum systems. In this latter case the evolution is deterministic and the mixture is improper, resulting from a description of the field as an open system, see e.g. [578] and also Secs. 1.3.3 and 1.8.

If on the other hand fluctuations are present which are significantly slower than the integration time τ_I, then effectively each particular measurement j encounters a different stationary field ρ_j, at least with respect to the long term fluctuations [529]. However, since

each particular field measurement is a quantum measurement, subject to a fundamental quantum uncertainty as discussed in the next section, in general the field measurement will have to be repeated several times. Thus, effectively, apart from the averaging, due to time integration and the quantum average over superpositions of pure field states, a third average over the slow fluctuations is performed. If that fluctuation is sufficiently ergodic, again it is equivalent to an ensemble with a time-independent probability distribution $p(j)$ and can be expressed via a time-independent density operator $\rho = \sum_j p(j)\rho_j$, potentially extending the ensemble already given by short term fluctuations. In summary, any fluctation due to an ergodic interaction that happens on a timescale sufficiently shorter or sufficiently longer than the characteristic integration time of the measurement τ_I can be modeled as an ensemble average over an effectively free field [604].

4.4 Field States and Quantum Fluctuations

4.4.1 Quadrature Operators

Apart from uncertainty due to classical fluctuations which can be expressed as ensemble averages, the quantum field also exhibits irreducible uncertainty due to its quantum nature, which is absent in the classical description. Thus, even for pure states of the field, no definite values can be associated with the continuous observables of electric and magnetic fields $\vec{\mathbf{E}}^+$ and $\vec{\mathbf{B}}^+$ and they are usually only characterized by expectation values and standard deviations. In general it is of course also formally possible to provide the full probability density of field values for each spacetime point. Note that this is not a probability density over space or time but over the space of field values E or B at a particular spacetime point. While the following discussion only treats the electric field, a similar treatment is of course also possible for the magnetic field. Furthermore, the focus lies on a single mode field, which is entirely sufficient to give an overview over characteristic states of the field and their properties.

The electric and magnetic quantum fields $\vec{\mathbf{E}}^+$ and $\vec{\mathbf{B}}^+$ can be obtained from the vector potential field $\vec{\mathbf{A}}^{(+)}$ via the same relations as in the classical case. In the case of a decomposition into harmonic modes (4.33) an especially useful representation of the electric quantum field is given in terms of dimensionless, hermitian and crucially time-independent so-called *quadrature operators* $\mathbf{X}_1$ and $\mathbf{X}_2$, which in analogy to the usual classical field quadratures are defined as proportional to real and imaginary parts of the field operators, with [529, 524, 637]

$$\mathbf{X}_1 = \frac{\mathbf{a} + \mathbf{a}^\dagger}{\sqrt{2}}, \qquad \mathbf{X}_2 = \frac{\mathbf{a} - \mathbf{a}^\dagger}{\sqrt{2}i}. \tag{4.38}$$

The field operator $\mathbf{E} = \mathbf{E}^{(+)} + \mathbf{E}^{(-)}$ of a particular single harmonic mode j or $\vec{k}$ can then be expressed as

$$\mathbf{E}(\vec{x}, t) = \sqrt{\frac{\hbar\omega}{\epsilon_0}}\, |b(\vec{x})| \left(\mathbf{X}_1 \sin\Theta(\vec{x}, t) - \mathbf{X}_2 \cos\Theta(\vec{x}, t) \right), \tag{4.39}$$

with the effective phase $\Theta(\vec{x},t) = \omega t - \nu(\vec{x})$, where the spatial shape of the mode is decomposed into polar form as $b(\vec{x}) = |b(\vec{x})|e^{i\nu(\vec{x})}$. Here and below, the j or k-vector indices as well as the polarization, i.e., the vectorial character of the field, are not written explicitly in the case of a single mode field. Given that the harmonic oscillation of the field mode is formally completely equivalent to the standard quantum harmonic oscillator of mass m, the quadrature operators can be associated with oscillator position and momentum via the relations $\mathbf{x} = \sqrt{\hbar/m\omega}\,\mathbf{X}_1$ and $\mathbf{p} = \sqrt{m\hbar\omega}\,\mathbf{X}_2$ [529, 525, 637]. Note that here the notions "position" and "momentum" do not refer to location and direction in actual space but are instead abstract concepts capturing the excitation of a single mode of the electric quantum field. This identification allows to apply the formalism already established for the canonical observables $\mathbf{x}$ and $\mathbf{p}$, see Sec. 2.3.1, to the quadratures, which obey the commutation relation $[\mathbf{X}_1, \mathbf{X}_2] = i$.

The expression of the field in terms of quadrature operators allows to write the time-dependent field eigenstates $|E\rangle$ defined through the usual relation $\mathbf{E}\,|E\rangle = E\,|E\rangle$ in terms of the quadrature eigenstates $|x_1\rangle$ and $|x_2\rangle$ with eigenvalues $x_1, x_2 \in \mathbb{R}$. Using Eq. (2.19) the time-dependent field eigenstate $|E(t)\rangle$ can be expressed, e.g., as a function of x_1 with

$$|E(t)\rangle = \frac{1}{\sqrt{2\pi|a|}} \int_{\mathbb{R}} \mathrm{d}x_1 e^{-\frac{i}{a}(Ex_1 - b\frac{x_1^2}{2})}\,|x_1\rangle\,, \tag{4.40}$$

where the phase dependence is contained in the parameters $a = \sin\Theta$ and $b = \cos\Theta$. For spacetime points at which $a = 0$ or $b = 0$, the above formula is not necessary as the field operator is trivially equal to the two quadrature operators. The quadrature eigenstates can also be expressed in the number state basis as [529, 525, 637]

$$|x_1\rangle = \sum_{n=0}^{\infty} e^{-\frac{x_1^2}{2}} \frac{H_n(x_1)}{\pi^{\frac{1}{4}}(2^n n!)^{\frac{1}{2}}}\,|n\rangle\,, \quad |x_2\rangle = \sum_{n=0}^{\infty} e^{-\frac{x_2^2}{2} - in\pi/2} \frac{H_n(x_2)}{\pi^{\frac{1}{4}}(2^n n!)^{\frac{1}{2}}}\,|n\rangle\,, \tag{4.41}$$

where H_j are the *Hermite polynomials* of order j.

4.4.2 Field Fluctuations

Just as position and momentum eigenstates, also the quadrature and field eigenstates are not normalizable and thus unphysical. This means that the field can never be in an eigenstate and always has an unavoidable non-vanishing uncertainty, commonly denoted as *quantum fluctuations* [612, 338]. This uncertainty is lower bounded via the uncertainty relation $\Delta\mathbf{X}_1\Delta\mathbf{X}_2 \geq 1/2$ [524, 637]. In general the field expectation value $\langle\mathbf{E}\rangle$, sometimes called the *coherent signal* [589, 524], has a phase-dependent standard deviation $\Delta\mathbf{E}$. Even the vacuum field with a mean field of $\langle\mathbf{E}\rangle = 0$ has non-vanishing so-called *vacuum fluctuations* $\Delta\mathbf{E}(\vec{x}) = |b(\vec{x})|\sqrt{\hbar\omega/2\epsilon_0}$, which, however, have no phase dependence [55, 531], as illustrated in Fig. 4.2a. Quantum field fluctuations provide the explanation for many critical quantum-optical phenomena such as spontaneous emission, i.e., the decay of an excited atomic state from a meta-stable equilibrium, or the Lamb shift already mentioned above,

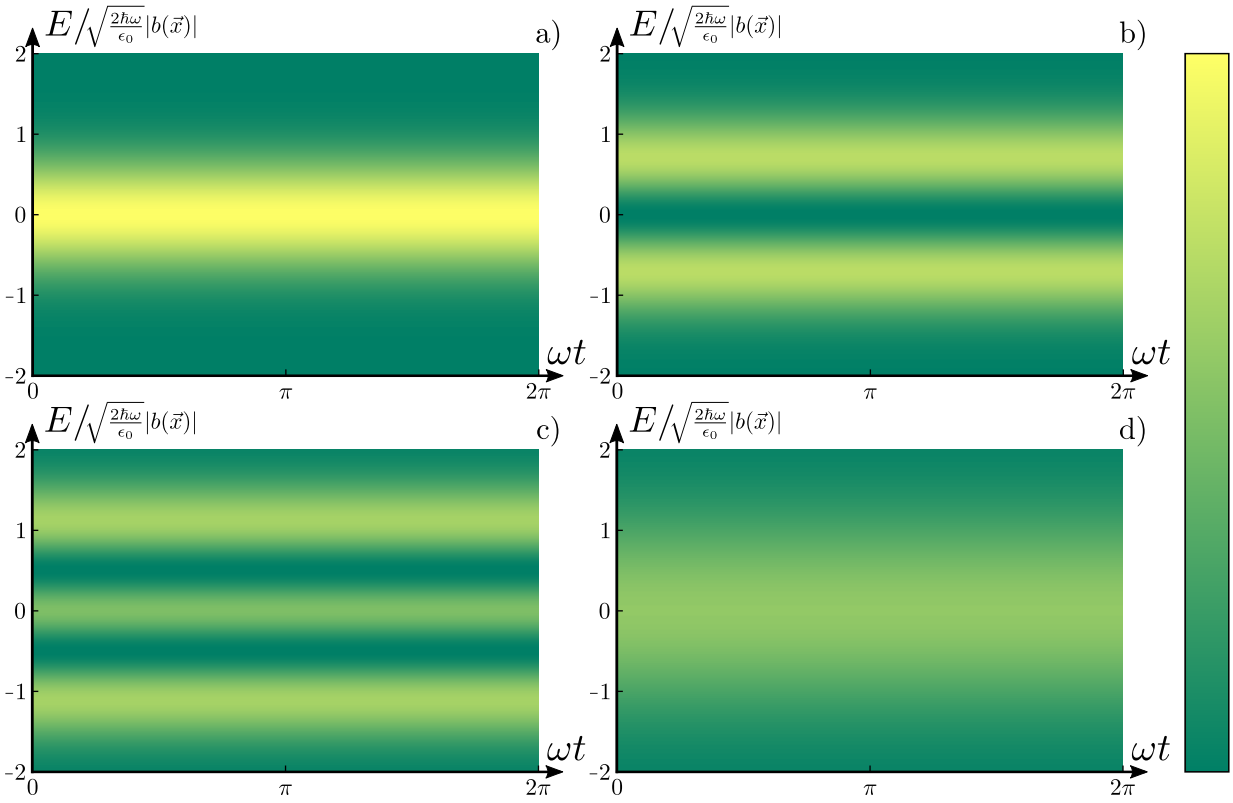

Figure 4.2: **Probability Density for Various Field States - Part 1** The probability density $p(E,t) = \langle E(t)|\rho|E(t)\rangle$ is displayed over one cycle of the mode oscillation. The corresponding linear color scale is referenced by the vertical bar on the right. Panel a) shows the distribution for the vacuum state, which corresponds to a coherent state and thus exhibits a Gaussian distribution at each point in time. In the case of the number states $|1\rangle$ and $|2\rangle$, shown in panels b) and c), respectively, the distribution can be seen as the result of the interference between a continuum of oscillations uniformly distributed in phase, which leads to the plotted lobe structures. For the thermal state with $\bar{n} = 1$, depicted in panel d), the interference patterns of each number state are superposed incoherently, resulting again in a Gaussian field distribution.

the observation of which was an important milestone in the development of QFT [531, 524].

In the case of photon number states $|n\rangle$, which correspond to a definite finite amount of energy in the field, the coherent signal is still vanishing, with a field uncertainty that scales as $\Delta\mathbf{E}(\vec{x}) = |b(\vec{x})|\sqrt{2\hbar\omega/\epsilon_0}\,\sqrt{n+1/2}$ [524, 338]. The vanishing of the field expectation value at each point in space and time can be related to a maximal fluctuation of the phase of the field. An oscillation with maximal phase uncertainty is completely smeared out over time and thus no longer an oscillation [524]. Quantifying phase uncertainty in the field is not trivial due to formal difficulties encountered when trying to define a Hermitian phase operator $\boldsymbol{\varphi}$ [529, 525, 524]. One possible definition was suggested by Susskind and Glogower [652] who considered the polar decompositon of the field operator as $\mathbf{a} = \sqrt{\mathbf{n}}e^{i\boldsymbol{\varphi}}$.

It leads to phase distribution $p(\varphi) = 1/2\pi|\langle e^{i\varphi}|\psi\rangle|^2$ for an arbitrary pure mode state $|\psi\rangle$, where $|e^{i\varphi}\rangle$ are eigenstates of the operator $e^{i\boldsymbol{\varphi}}$ and the factor $1/2\pi$ is needed since the eigenstates are not orthogonal [529]. Although no rigorous uncertainty relations exist, nevertheless a certain tradeoff between number uncertainty $\boldsymbol{\Delta n}$ and phase uncertainty has been identified [612, 529, 524]. In particular an unsharp number of photons is required for any field with a well-defined oscillation phase. The field distributions for number states with $n = 1$ as well as $n = 2$ photons are shown in Figs. 4.2b and c, respectively.

4.4.3 Classical and Non-Classical States

It was first argued by Glauber [590, 588, 589] that *coherent states* represent a single mode quantum field which is closest to a classical oscillation with a well defined phase, see e.g. [657, 529, 525, 531, 524, 546, 637] for more recent treatments. Coherent states of the form $|\alpha\rangle = e^{-|\alpha|^2/2}\sum_{n=0}^{\infty}\alpha^n/\sqrt{n!}\,|n\rangle$, characterized by single complex parameter α, are eigenstates of the annihilation operator and have been originally introduced by Schrödinger [40] as harmonic oscillator states with expectation values that behave in a classical manner. Note that the vacuum state also falls under this definition. An equivalent definition is based on the action of the unitary *displacement operator* $\mathbf{D}(\alpha) = \exp(\alpha\mathbf{a}^\dagger - \alpha^*\mathbf{a})$, with $|\alpha\rangle = \mathbf{D}(\alpha)\,|0\rangle$, where $\mathbf{D}^\dagger\mathbf{a}\mathbf{D} = \mathbf{a} + \alpha$. For coherent states the photon number is Poisson distributed with $\bar{n} = \langle\mathbf{n}\rangle = (\Delta n)^2 = |\alpha|^2$. Furthermore, the quadrature expectation values are given respectively as $\langle\mathbf{X}_1\rangle = \sqrt{2}|\alpha|\cos\theta$ and $\langle\mathbf{X}_2\rangle = \sqrt{2}|\alpha|\sin\theta$, where $\alpha = |\alpha|e^{i\theta}$. In consequence the coherent signal $\langle\mathbf{E}\rangle$ at any position $\vec{x}$ exactly corresponds to a harmonic oscillation with complex amplitude $|b(\vec{x})|\sqrt{\hbar/2\omega\epsilon_0}\,\alpha$. In the eigenspaces of both quadratures coherent states are Gaussians, i.e., MUS and minimize the quadrature uncertainty relation with equal uncertainties $\Delta\mathbf{X}_1 = \Delta\mathbf{X}_2 = 1/\sqrt{2}$. In this special case a simple relation holds between the field uncertainty and the two quadrature uncertainties with

$$\Delta\mathbf{E}(\vec{x},t) = \sqrt{\frac{\hbar\omega}{\epsilon_0}}\,|b(\vec{x})|\left((\Delta\mathbf{X}_1)^2\sin^2\Theta(\vec{x},t) + (\Delta\mathbf{X}_2)^2\cos^2\Theta(\vec{x},t)\right)^{\frac{1}{2}}. \tag{4.42}$$

Coherent states thus still exhibit irreducible quantum fluctuations, which, however, as illustrated in Fig. 4.3a, are independent of space and time since both quadrature uncertainties are equal. Since the fluctuations are also independent of the parameter α, in the classical limit $|\alpha| \to \infty$ they vanish compared to the strength of the coherent signal and the classical oscillation is recovered. This coincides with a scaling of the phase uncertainty with $1/\sqrt{\langle\mathbf{n}\rangle}$ [529, 524].

Whenever one of the quadrature uncertainties is smaller than $1/\sqrt{2}$, i.e., smaller than the vacuum fluctuations, the state is called *squeezed*. In that case the uncertainty relation dictates that the uncertainty of the other quadrature is larger which leads to a phase dependent change of the field fluctuations over the oscillation cycle [612], as shown in Fig. 4.3b. While sometimes additionally it is required that squeezed states also minimize the quadrature uncertainty, see, e.g., [657, 529, 511, 225], other authors, such as, e.g., [525, 531, 524, 549, 637] distinguish such *ideal* squeezed states from general squeezed states only

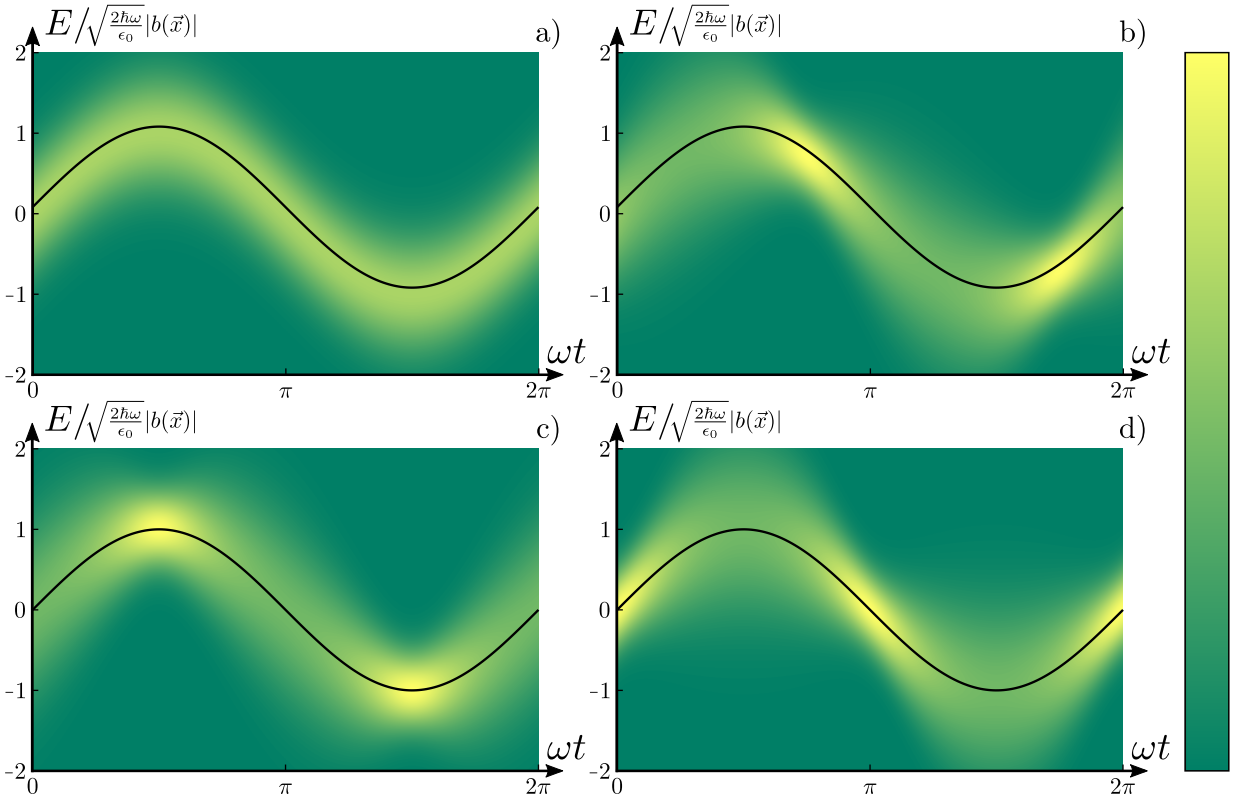

Figure 4.3: **Probability Density for Various Field States - Part 2** All four states have $|\alpha| = 1$ and the squeezed states a squeezing factor of $|\xi| = 0.4$. While for the coherent state (a) the field fluctuations are invariant over the whole cycle, they change for an arbitrary squeezed state (b). Panels c) and d) show the special cases of perfect amplitude and phase squeezing, respectively.

characterized just by a one sufficiently small quadrature uncertainty. Formally, minimal uncertainty squeezed states $|\alpha_\xi\rangle$, also called *coherent squeezed states* are given by $|\alpha_\xi\rangle = \mathbf{D}(\alpha)\mathbf{S}(\xi)\,|0\rangle$, where $\mathbf{S}(\xi) = \exp\left((\xi^*\mathbf{a}^2 - \xi\mathbf{a}^{\dagger 2})/2\right)$ is the unitary *squeezing operator* with the complex squeezing parameter $\xi = |\xi|e^{i\vartheta}$. The form of the squeezing operator also motivates the interpretation of squeezed states as "two-photon coherent states" which is how they were originally introduced by Yuen [665]. Although the squeezing always increases the mean photon number as $\langle\mathbf{n}\rangle = |\alpha|^2 + \sinh^2|\xi|$, it does not change the coherent signal which is the same as for the respective coherent state $|\alpha\rangle$. The phase ϑ of the squeezing parameter determines characteristic in-phase quadrature operators $\mathbf{X}_1'$ and $\mathbf{X}_2'$, which in general are phase shifted with respect to $\mathbf{X}_1$ and $\mathbf{X}_2$, and given by the relation $\mathbf{X}_1' + i\mathbf{X}_2' = (\mathbf{X}_1 + i\mathbf{X}_2)e^{-i\vartheta/2}$. The uncertainties of these quadratures are changed by the squeezing to $\Delta\mathbf{X}_1' = e^{-|\xi|}/\sqrt{2}$ and $\Delta\mathbf{X}_2' = e^{|\xi|}/\sqrt{2}$, where $|\xi|$ is called the *squeezing factor*. In terms of in-phase quadrature operators the field uncertainty can again be expressed in the simple form of Eq. (4.42). This points at two special cases of squeezing, namely when the squeezing is perfectly in or out of phase with the field oscillation determined by

the phase θ. If the coherent and squeezing phases are aligned as $\theta = \vartheta/2$, the maximal value of the field oscillation coincides with minimal field uncertainty, see Fig. 4.3c. Such a state is accordingly called *amplitude squeezed*, exhibits a reduced number uncertainty and a correspondingly increased phase uncertainty due to the fact that the fluctuations on the flanks of the oscillation are necessarily increased. In some sense number states can be seen as limiting case of amplitude squeezing, which, however, is discontinuous since for number states the quadrature uncertainty relation is no longer minimized. The opposite case with maximal fluctuation on the peaks and minimal fluctuation on the flanks as shown in Fig. 4.3d is called *phase squeezed* and exhibits an increased photon number uncertainty along with a better defined phase. Phase squeezed states are especially useful in interferometric sensing, as discussed in Sec. 5.4.3. The deviations from a Poissionian distribution due to the increased or reduced photon number uncertainties are commonly called *super* and *sub-poissonian statistics*, respectively. In general light with sub-Poissonian statistics is sometimes also called *photon-number squeezed* [524].

Practically encountered fields will generally be at most only approximately described by the special pure states described above and usually given by a superposition of those or even a general density operator ρ indicating some average over pure field states. A common but again somewhat idealized example of such a statistical state of a single mode is the *chaotic* or *thermal state* ρ_{th} given by $\rho_{\text{th}} = \sum_n p_{\text{th}}(n)|n\rangle\langle n|$, where $p_{\text{th}}(n) \propto \exp(-n\frac{\hbar\omega}{k_B T})$ with *Boltzmann constant* k_B and equilibrium temperature T, is the thermal distribution characteristical for the energy distribution of many processes in thermal equilibrium, also appearing in Planck's law [618, 529, 525, 524, 338]. In the limit $T \to 0$ the thermal state approaches the vacuum. The vacuum is thus the unifying limit of number states, coherent states as well as thermal states, with $n = 0$, $\alpha = 0$ and $T = 0$, respectively. In the quantum field description of thermal states the resulting photon number variance is super-Poissonian with $(\Delta\mathbf{n})^2 = \langle\mathbf{n}^2\rangle + \langle\mathbf{n}\rangle$, which is increased by $\langle\mathbf{n}\rangle$ compared to the classical description of a thermal state. Due to this correspondence, following a terminology introduced by Einstein, sometimes the first term is called the "wave contribution" and the second the "particle contribution", where the latter becomes negligible in the limit of high mean photon numbers, i.e., high temperatures [524, 338]. Just as number states, thermal states fields do not possess a coherent signal and have a field uncertainty similar to number states with $\Delta\mathbf{E}(\vec{x}) = |b(\vec{x})|\sqrt{2\hbar\omega/\epsilon_0}\,\sqrt{\bar{n} - 1/2}$. However, the corresponding field distribution is Gaussian, as shown in Fig. 4.2d for $\bar{n} = 1$.

Finally, it should be mentioned that there exist a range of typical phase-space representations for the field state of a single mode of light, which are based on the correspondence between the quadrature operators and position and momentum. Apart from the Wigner distribution already mentioned in Sec. 2.3.2, another example is *P-representation* developed by Glauber and Sudarshan [590, 651], where the field state is expanded in terms of coherent states $|\alpha\rangle$ and the parametrization $\alpha = x_1 + ix_2$, with coordinates x_1 and x_2 is employed [529, 531, 637, 338]. Along with the representations also several criteria have been proposed which quanitify the non-classicality of a state, i.e., the degree to which its properties deviate from those of classical states. For example, negative values both of the P-distribution as well as the Wigner distribution, as obtained, e.g., for number states,

cannot be explained by classical states of the light field. Another criterion is the so-called *Mandel parameter* $Q_M = (\Delta\mathbf{n})^2/\langle\mathbf{n}\rangle - 1$ [617], which quantifies how much the photon number variance differs from the Poissonian case. While classical states also can lead to super-Poissonian distributions with $Q_M > 0$, only quantum light can yield a sub-Poissonian distribution with $Q_M < 0$ [524, 637, 338].

4.5 Detection of Light

4.5.1 Direct and Indirect Detection

In classical optics, observations are typically formulated as the measurement of *intensity*, as defined in Sec. 4.2.4, which characterizes the surface density of energy flow for a propagating field. An appropriately oriented detector will detect the light power $\int_A I_{\text{class}} \mathrm{d}^2 r$ in each surface element A, which for example can correspond to the pixel of a camera or the aperture of a photo-detector. The quantum description of light detection is based on the absorption of photons from the field due to an interaction with the material of the detector, called *direct detection* of the field. While usually the field excitation is lost in the process of direct detection, a notable exception are quantum optical QND measurements, which allow to measure the photon number without changing it. Possible realizations of QND measurements are for example the nonlinear *optical Kerr-effect* in which the phase of a probe beam is shifted dependent on the number of photons [531], see also Sec. 5.2.1, or interactions of photons with atoms in a cavity [593, 628].

In practice the temporal properties of optical detectors can be characterized by two durations, i.e., the integration time τ_I, and a *dead-time* τ_D. As defined in Sec. 4.3.5, the integration time indicates the time over which a particular field is interacting with the detector. This interaction can be essentially continuous and limited merely by technical properties of the detector or it can consist of discrete absorption events fundamentally limited by the characteristic timescale of the light-matter interaction underlying the detection process. The dead-time characterizes a potentially slightly varying time-interval in between integration events, during which the detector cannot record, i.e., which limits how closely subsequent measurements can follow each other. Of course there exist types of detectors, such as photo-diodes, which have no dead-time, i.e., $\tau_D = 0$. Furthermore, it is sometimes the case that optical detectors are time-triggered on the source successfully preparing a certain state, such as in the case of heralded single-photon sources, as sketched in Sec. 5.2.3.

The integration times of typical optical detectors are significantly larger than the carrier oscillation of the detected light field and thus no subcycle resolution is possible. For example, while typical contemporary electronic detectors can reach integration times of as low as a few picoseconds, this still involves an integration over thousands of optical cycles. So-called *avalanche photodiodes* (APDs) with single-photon sensitivity can have significantly lower integration times determined by the timescale of the interaction of the field and the semiconductor material, see, e.g., [573, 513, 511], but instead typically have

dead-times in the order of tens of nanoseconds.

In order to achieve subcycle resolution of the light-field, alternative methods are used, which can be broadly characterized as *indirect detection*. Special techniques based on the control of electrical processes via microwaves allow to reach picosecond resolution using for example so-called *streak cameras*, see e.g. [606], which map the time-evolution to a spatial distribution. By instead applying optical pulses to control the detection, it becomes possible to increase the resolution even further, leading to a method called *electro-optic sampling* [599] in which the rotation of the polarization of an ultra-short optical probe pulse, due to a nonlinear interaction with the optical field in question, can be used to scan the latter with subcycle resolution. Although in the end still photons are absorbed, the detection can be understood as "indirect", insofar as it involves the correlation of the temporal evolution of the field with another resolvable degree of freedom such as the spatial modes or the polarization of a probe pulse.

Instead of this technologically very challenging search for higher time-resolution, typically in quantum optics interferometric methods such as homodyne and heterodyne detection are employed to investigate periodic and thus phase-dependent subcycle properties, such as squeezing. In these schemes two quickly oscillating signals are superposed, such that a measurement of the resulting comparatively slowly varying intensity contains information about the relative short time-scale behavior of the two fields [657, 529, 531, 569, 524, 338]. See Sec. 5.4.3 for more details. While ultimately also such indirect interferometric measurements involve a direct detection of a superposition of fields, they extract very different information about the particular component fields compared to a direct detection of any single one of them.

4.5.2 Photocount Statistics

In general, following an ansatz proposed by Glauber [590, 589], the photon absorption process of detectors sensitive to the electrical field can be modeled via the transition amplitude $\langle f|\mathbf{E}^{(+)}|\psi\rangle$ from an arbitrary initial multi-mode field state $|\psi\rangle$ to some final field state $|f\rangle$, where the positive frequency field component corresponds to a single annihilation event [529, 525, 531, 637]. The spatial and temporal dependence of the different field modes, quantifies how much each contributes to the probability of annihilation, i.e., detection at a particular spacetime point $(\vec{x}, t)$. Here, again for convenience of notation a single polarization is considered and the direction of the field is not written explicitly. Note that in general, dependent on the properties of the detector, photons in different polarization or spectral modes will be absorbed with different probabilities, which would require additional mode-dependent weights in the expression for the transition amplitude [604]. In the following detectors with no frequency or polarization dependence will be assumed, which is a good approximation given the type of detectors employed in this work and the comparatively narrow spectral width of the light.

The probability density for the annihilation of a single photon at a certain spacetime point is proportional to the *average field intensity* $I(\vec{x}, t) = \mathrm{tr}\big(\rho\mathbf{I}(\vec{x}, t)\big)$, which corresponds to the transition probability integrated over all possible final field states, where the *intensity*

operator is given by $\mathbf{I}(\vec{x},t) := \mathbf{E}^{(-)}(\vec{x},t)\mathbf{E}^{(+)}(\vec{x},t)$ and "average" here means an average over the full multi-mode field state ρ [604, 529, 531, 524]. The average field intensity I is sometimes also called the "average photon flux" of the field [616]. Note that here, following the common convention of notation, a dimensionality factor of $2c\varepsilon_0$ is neglected in the definition of intensity. An identical dependence on the intensity operator can be derived by considering the simple QED model of an interaction of single atom with a radiation field [524]. The same holds for a generalization to detectors consisting of many atoms and finally essentially for all typical macroscopic light detectors based on photoionization, including the human eye, see, e.g., [589, 601, 618, 529, 525, 531, 524].

As discussed above, optical detectors for technical reasons necessarily observe over a minimal finite integration time τ_I and integrate over several cycles. In each of this time-intervals a certain number m of photons will be absorbed, which will be subject to quantum fluctuations. Thus in general the expected *photocount* m will be a random number following a probability distribution $p(m)$. Based on the spacetime probability density for detection given by the quantum intensity I, it is possible to derive the statistical distribution of detector counts $p(m)$ in a time-interval τ_I for a certain detector surface as [601, 618, 578, 529]

$$p(m) = \mathrm{tr}\Big(\rho : \frac{\big(\kappa_D \bar{\mathbf{I}}(\vec{x},t)\big)^m}{m!} e^{-\nu_D \bar{\mathbf{I}}(\vec{x},t)} : \Big) \tag{4.43}$$

with the time-averaged intensity operator $\bar{\mathbf{I}}$ given by

$$\bar{\mathbf{I}}(\vec{x},t) := \frac{1}{\tau_I}\int_t^{t+\tau_I} \mathbf{E}^{(-)}(\vec{x},t')\mathbf{E}^{(+)}(\vec{x},t')\mathrm{d}t', \tag{4.44}$$

and κ_D being an effective, detector specific efficiency parameter with appropriate dimension. Here, the commonly used *normal ordering* notation $: \circ :$ has been employed, where the colons indicate that after the multiplication of all elements in the sums contained in the expression $\circ$, the operators are reordered such that creation operators are always to the left of the corresponding annihilation operators [589, 529, 525, 531, 637]. In the case of a single mode this expression simplifies significantly to [529, 524, 146]

$$P(m) = \mathrm{tr}\Big(\rho : \frac{(\mu_D \mathbf{n})^m}{m!}\, e^{-\mu_D \mathbf{n}} : \Big), \tag{4.45}$$

where the *quantum efficiency* $\mu_D \in [0,1]$ quantifies the sensitivity of the detector to this particular mode and corresponds to the probability that given a pure single-photon state, that photon will be detected during the integration time τ_I. Note that, while the form of Eq. 4.45 is similar to a Poisson distribution, it is written in terms of non-commuting operators and thus in general can lead to non-Poissonian statistics. In particular it takes into account back-action of the detection on the field where the absorption of a certain amount of excitations changes the amount of excitations left in the field [524]. This is illustrated most strikingly by the example of a perfect detector with $\mu_D = 1$ acting on number states $\rho = |n\rangle\langle n|$, in which case $p(m) = \delta_{mn}$.

While in classical detector models the shot noise originates from a discretization of the photoionization process, for quantum models the shot noise is already present in the field and the detector transfers it to the photocurrent [524]. Due to the inherently discrete nature of photon detection, a reduced quantum efficiency will in general lead to differences in statistics between the photocount and the photon number distribution. For some states such as coherent and thermal states, which are described by Poissonian and thermal distributions respectively, also the measured distributions will be Poissonian and respectively thermal with accordingly reduced mean count numbers of $\bar{m} = \mu\langle \mathbf{n} \rangle$ [529]. For other states, in particular states with sub-Poissonian statistics this simple relation no longer holds. For example, for number states $|n\rangle$ a reduced quantum efficiency leads to a photocount distribution which is no longer δ_{mn} and instead nonzero for all $m \leq n$ [529]. Thus, a sufficiently high quantum efficiency is necessary to observe non-classical photon statistics. Apart from the efficiency in practice optical detectors are typically also further characterized by their spectral range, background noise and by the minimal number of photons they are able to resolve [579]. For example the APDs employed in this work have no number resolution and give the same signal independently of the number of photons. Since, however, in the experiments the probability to encounter a light field with two or more photons during one period of integration is very small, the detection is effectively a single-photon detection. Alternatively, in so-called *multiplexed* photon detection, the light field is probabilistically distributed among several APDs or to the same APD at different times, allowing to detect multi-photon states [644, 338].

4.6 Coherence and Correlation Functions

4.6.1 Interference and Coherence

A typical scenario in optics is a superposition of two or more fields. For example for two fields with $\vec{\mathbf{E}} = \vec{\mathbf{E}}_1 + \vec{\mathbf{E}}_2$ the resulting field intensity operator depends on the component fields as

$$\mathbf{I}(\vec{x}, t) = \mathbf{I}_1(\vec{x}, t) + \mathbf{I}_2(\vec{x}, t) + \left(\vec{\mathbf{E}}_1^{(-)}(\vec{x}, t) \vec{\mathbf{E}}_2^{(+)}(\vec{x}, t) + \vec{\mathbf{E}}_2^{(-)}(\vec{x}, t) \vec{\mathbf{E}}_1^{(+)}(\vec{x}, t) \right). \tag{4.46}$$

Note that now full vectorial fields are considered and the definition of the intensity operator is generalized accordingly. Typically instead of using two distinct fields with different indices the resulting field is equivalently expressed as a superposition of two instances of a single global field $\vec{\mathbf{E}}$ evaluated at two different spacetime points $(\vec{x}_1, t_1)$ and $(\vec{x}_2, t_2)$, which have been brought into superposition at the point $(\vec{x}, t)$ via some particular field evolution. A typically example of this are the interference experiments described in Secs. 5.3 and 5.4. As discussed above, the mean photocount in direct detection of the field is proportional to the averaged intensity

$$I(\vec{x}, t) = I(\vec{x}_1, t_1) + I(\vec{x}_2, t_2) + 2\mathrm{Re}\big[\mathrm{tr}\big(\rho \vec{\mathbf{E}}^{(-)}(\vec{x}_1, t_1) \vec{\mathbf{E}}^{(+)}(\vec{x}_2, t_2)\big)\big]. \tag{4.47}$$

Here it is again assumed that on the timescale of integration the field can be regarded as stationary for times in suitably small time-regions around t_1 and t_2 and all random temporal field fluctuations can be expressed as ensemble averages. The last term of the above expression is an instance of a quantum mechanical interference term, as introduced in Sec. 1.3.2. The value $\left|\mathrm{tr}\left(\rho\vec{\mathbf{E}}_1^{(-)}\vec{\mathbf{E}}_2^{(+)}\right)\right|$ corresponds to the *optical coherence* between the two fields and quantifies the extent to which the resulting intensity can deviate from the simple sum of the two individual field intensities.

Historically, the terms "interference" and "coherence" originate from the descriptions of field superpositions in classical optics and have been subsequently generalized to quantum fields. An extremely useful classical tool to conveniently characterize the relevant coherence properties of quantum fields are optical *correlation functions*. The analysis of optical phenomena in terms of such functions has a long history in classical optics, see, e.g., [514], and their quantum generalization, as first introduced by Glauber [590], forms a cornerstone of the modern formalism of quantum optics [637, 579].

4.6.2 First-Order Correlation Function

The form of the interference term in the expression for the field intensity (4.47) motivates the definition of the normalized *first-order correlation function* $g^{(1)}$ as [589, 618, 517, 531, 514, 524, 637]

$$g^{(1)}(\vec{x}_1, t_1, \vec{x}_2, t_2) := \frac{\mathrm{tr}\left(\rho\vec{\mathbf{E}}^{(-)}(\vec{x}_1, t_1)\vec{\mathbf{E}}^{(+)}(\vec{x}_2, t_2)\right)}{\sqrt{I(\vec{x}_1, t_1)I(\vec{x}_2, t_2)}}, \tag{4.48}$$

also called the *mutual coherence function* between the fields at the two spacetime points [618, 517, 514]. The first-order correlation function corresponds to the non-centered quantum correlation between the two component fields, as introduced in Sec. 1.6.4. As such it is commonly regarded as providing a measure of the correlation of both statistical as well as quantum fluctuation of the two field components [601, 618, 514, 637]. Note, however, that since the optical correlation function is non-centered it is sensitive only to a special type of correlations and in general may vanish in cases where there are actually very high correlations between the two fields. Conversely, it also may be non-zero for fields which are completely uncorrelated with respect to centered correlations. In any case the correlation function captures the fact that coherence does not depend on the strength of individual fluctuations of the two fields but instead on a joint property expressed in the form of a product expectation value. The first-order correlation function $g^{(1)}$ is a complex number with an absolute value between 0 and 1, corresponding to *incoherence* and *full coherence*, respectively. Medium absolute values indicate *partial coherence* [589, 618, 517, 514, 524]. For $(\vec{x}_1, t_1) = (\vec{x}_2, t_2)$ it trivially holds that $g^{(1)} = 1$. Furthermore any pure single mode state has full coherence for any pair of spacetime points with $g^{(1)} = \exp\left(i(\Theta_1 - \Theta_2)\right)$ [524], with effective phase $\Theta_j = \omega t_j - \nu(\vec{x}_j)$ as defined in Sec. 4.4.1.

In the case $t_1 = t_2$, $g^{(1)}$ quantifies *spatial coherence* between two points $\vec{x}_1$ and $\vec{x}_2$, which for fields with a distinguished direction, such as propagating paraxial fields can be

be further divided into *longitudinal* and *transverse* coherence [517]. In the same manner a *region of coherence* can be defined, in which the coherence does not fall below a certain value, by considering a set of points $\vec{x}_2$ defined by some characteristic radius r with $|\vec{x}_1 - \vec{x}_2| < r$ [514]. *Temporal coherence* can be defined analogously in the case $\vec{x}_1 = \vec{x}_2$, where for general propagating fields this distinction is not unique since field components originating from different spatial points, can be superposed at the same location at another point in time [618, 524].

An important special case of temporal coherence is the *first-order auto-correlation function* $g^{(1)}(\vec{x}_1, t, \vec{x}_1, t+\tau)$ defined via a time difference τ, also called *self-coherence* [618, 514]. In the case of stationary fields it is independent from t and commonly written as $g^{(1)}(\tau)$. In fact the time-independence of the first-order auto-correlation function is a necessary condition for the stationarity of a field [589]. The first-order auto-correlation functions allows to define a *coherence time* τ_c, which characterizes the timescale at which the coherence of a field breaks down, i.e., $g^{(1)}(\tau) \approx 1$ for $\tau \ll \tau_c$ and $g^{(1)}(\tau) \approx 0$ for $\tau \gg \tau_c$ [517, 524]. For example in the case of a state ρ given by an ensemble of field states with random phase fluctuations happening on the timescale τ_c, for much smaller time durations the state can effectively be expressed as pure and has full coherence. On much longer timescales the fluctuations effectively lead to a mixture of fields with uniformly distributed differing phases leading to vanishing coherence. For quasi-stationary homogeneously polarized classical fields this relation is generalized by the *Wiener-Khintchine theorem* which states that the first-order auto-correlation function $g^{(1)}(\vec{x}, t, \vec{x}, t+\tau)$ forms a Fourier transform pair with the spectral density $G(\vec{x}, \omega)$, as introduced in Sec. 4.1.2 [618, 525, 524]. Thus spectral broadening in general leads to a reduction of coherence time. For paraxial fields the latter can also be related to a *coherence length* l_c via the propagation velocity c, with $l_c = c\tau_c$. Accordingly the coherence length defines a characteristic difference of spatial propagation distances at which the coherence breaks down. For approximately Gaussian spectral densities the coherence length can be written as $l_c = \lambda^2/\Delta\lambda$, where $\Delta\lambda$ is the spectral width expressed in terms of wavelength uncertainty [517].

4.6.3 Higher-Order Correlation Functions

The definition of coherence functions can be generalized with normalized *nth order correlation functions* $g^{(n)}$ defined as [589, 525, 637]

$$g^{(n)}(q_1, \ldots, q_n, q_{n+1}, \ldots, q_{2n}) = \frac{\mathrm{tr}\big(\rho \mathbf{E}^{(-)}(q_1) \cdots \mathbf{E}^{(-)}(q_n) \mathbf{E}^{(+)}(q_{n+1}) \cdots \mathbf{E}^{(-)}(q_{2n})\big)}{\prod_{j=1}^{2n} \sqrt{I(q_j)}}, \quad (4.49)$$

where here the shorthand notation $q_j := (\vec{x}_j, t_j)$ for spacetime coordinates is employed and only a single polarization mode is considered. The definition with an equal amount of creation and annihilation operators is not the most general, but accounts for all scenarios in which photon counting measurements, as described above, are performed. When additionally taking into account different polarizations of the field components, the correlation functions have to be replaced by appropriate *correlation tensors*, see, e.g., [618, 525].

Just as the first-order correlation function quantifies coherence in detection of the superposition of two fields at a single spacetime point, the higher order correlation functions can be used to quantify the joint absorption probability at several spacetime points, where at each point several fields can be superposed [589, 637]. In general for a state with a finite maximal number of excitations, such as the number states $|n\rangle$, all correlation functions $g^{(n')}$ with $n' > n$ vanish. Furthermore, due to the commutation relations of the creation and annihilation operators, the correlation functions are invariant under the permutations inside the two sets of spacetime coordinates for positive and negative frequency parts, respectively. Also, similar to $g^{(1)}$, again for stationary fields, all correlation functions are invariant under time-translations of all points by the same amount τ and thus effectively only depend on $(2n-1)$ time-differences [589]. Coherence can be attributed to a field as a whole if it is equally coherent for all possible choices of coordinates $\{q_1, \ldots, q_{2n}\}$. A field for which $|g^{(n)}| = 1$ for all $n \leq m$ is called *m-th order coherent*. As eigenstates of the annihilation operator, single mode coherent states are coherent to arbitrary order as well as for any choice of coordinates and thus are instances of *fully coherent fields* [589, 637].

Of particular importance is the second-order correlation function evaluated at two distinct spacetime points q_1 and q_2 as $g^{(2)}(q_1, q_2, q_1, q_2)$, which can be written in the form [637]

$$g^{(2)}(\vec{x}_1, t_1, \vec{x}_2, t_2) := \frac{\mathrm{tr}\big(\rho : \mathbf{I}(\vec{x}_1, t_1)\mathbf{I}(\vec{x}_2, t_2) : \big)}{I(\vec{x}_1, t_1)I(\vec{x}_2, t_2)}. \tag{4.50}$$

Historically this quantum version of second-order correlation function represented one of the first important results of quantum optics, as it provided a quantum mechanical description of intensity interferometry experiments [589, 651, 618, 529, 637], first performed by Hanbury-Brown and Twiss, and discussed in Sec. 5.4.2. It quantifies the probability densities of joint photon annihilation at the two spacetime points, commonly denoted as photon *coincidences* [524, 637]. In analogy to the first-order self-coherence, also a second-order *intensity auto-correlation function* can be defined for a single spatial location with $\vec{x} = \vec{x}_1 = \vec{x}_2$ and a stationary field as [529, 524, 637, 579]

$$g^{(2)}(\tau) := \frac{\mathrm{tr}\big(\rho : \mathbf{I}(\vec{x}, t)\mathbf{I}(\vec{x}, t+\tau) : \big)}{I^2(\vec{x}, t)}, \tag{4.51}$$

where t is arbitrary and $g^{(2)}(\tau) \in [0, \infty[$ due to the positivity of intensity. It corresponds to the joint probability density of successive photon detections at the location $\vec{x}$ with a time difference of τ [657, 669, 529, 531]. A value of $g^{(2)}(\tau) = 1$ indicates that the joint detection probability is equal to the product of the intensities, which corresponds to statistical independence between the two detection events, i.e., Poissonian statistics. A value $g^{(2)}(\tau) > 1$ indicates an increased probability density of joint detection at time-differences τ and conversely values $g^{(2)}(\tau) < 1$ a reduced one. Thus, although $g^{(2)}(\tau)$ only quantifies the probability density for pairs of counts, a $g^{(2)}(\tau) < 1$ for all τ in some interval $[0, \tau']$ implies sub-Poissonian statistics for photon counting over integration times smaller than τ' and conversely super-Poissonian statistics in the opposite case of $g^{(2)}(\tau) > 1$ [669]. For stationary single mode states $g^{(2)}$ is independent of τ, where for coherent

states the constant $g^{(2)}(\tau) = 1$ corresponds to a Poissonian number distribution for any time-interval. Accordingly for the super-Poissonian thermal states $g^{(2)}(0) = 2$ and for the sub-Poissonian number states $|n\rangle$ the relation $g^{(2)}(0) = 1 - 1/n$ holds [657, 531, 637, 524]. In the limit of $n \to \infty$ the detection statistics for number states thus approach the statistical independence exhibited by coherent states, which corresponds to the transition from a binomial to a Poissonian distribution.

4.6.4 Photon Bunching

Apart from integrated photon statistics, the variation of $g^{(2)}(\tau)$ with τ indicates how the detection events are distributed in time [669, 531, 511]. If $g^{(2)}(\tau)$ is monotonously rising in some time-interval $[0, \tau']$, i.e., $g^{(2)}(\tau_1) \leq g^{(2)}(\tau_2)$ for $0 \leq \tau_1 < \tau_2 \leq \tau'$ and $g^{(2)}(0) < g^{(2)}(\tau')$ this indicates that the detection events tend to be separated in time, which is commonly denoted as *photon anti-bunching*. Correspondingly in the opposite case of a falling $g^{(2)}(\tau)$ they tend to be grouped closer together, denoted as *photon bunching*. For fields characterized by a finite coherence time τ_c the expectation value of the product of the intensity operators factorizes for long time-differences $\tau \gg \tau_c$ leading to $g^{(2)}(t) \approx 1$ [529]. If such fields have sub-Poissonian statistics on short timescales, i.e., $g^{(2)}(0) < 1$ they will thus necessarily exhibit anti-bunching on some potentially larger timescale. An analog relation exists between super-Poissonian behavior and bunching. It should be noted, however, that in general the fluctuation of integrated counts and their distribution in time are independent properties and there exist both super-Poissonian states with anti-bunching, as well as sub-Poissonian states with bunching [616, 669, 529, 524].

Considering for example the extremely sub-Poissonian single-photon state $|1\rangle$ with $g^{(2)}(\tau) = g^{(2)}(0) = 0$ any detection at some time t means a vanishing probability of detection at any other point in time $t + \tau$. However, there is neither bunching nor anti-bunching of detection events for the trivial reason that only a single count can occur. In practice measurements of a vanishing $g^{(2)}(\tau)$ for $\tau \geq 0$ are the typical experimental signature of so-called *single-photon sources* [579]. Typically, however, these sources produce a sequence of multi-mode light pulses, as introduced in the next section, with a certain repetition rate f_P, each containing only a single excitation. The value of $g^{(2)}(\tau)$ at the timescale $1/f_P$ of pulse succession then of course is no longer vanishing and rises very rapidly from zero as $\tau \to 1/f_P$. In this sense a single-photon source produces anti-bunched light and in fact an ideal single-photon source can be seen as the limiting case of maximal anti-bunching [529]. In practical applications the rate of pulse succession is known and sufficiently small, such that on shorter experimentally accessible timescales effectively single-photon states are available.

In general any observations of light which involves a measurement of $g^{(1)}$ can be explained by the classical theory. Thus, to motivate the need for a quantum description, experimental scenarios are necessary which involve dependence on $g^{(2)}$ or higher order correlation functions [589, 529, 524, 642]. Indeed such experiments have represented important milestones in the development of quantum optics, where, apart from the already mentioned intensity interforemtry experiments, notable examples include the first obser-

vation of photon anti-bunching by Kimble *et al.* [603] or the detection of differences in photon number variance between chaotic and coherent light by Arecchi [556]. Furthermore, if some sort of quantum advantage is to be pursued, for example in metrologicial scenarios, as discussed in Sec. 5.4.3, it is of course to be found per definition only in effects involving higher order correlation functions. Note, however, that crucially it would represent a logical fallacy to conclude that the possibility of a classical explanation implies that measurements of $g^{(1)}$ do not correspond to quantum phenomena. Just because an alternative description exists, does not change the nature of a phenomenon, and any scenario of classical optics can of course be treated in the quantum formalism as well. In effect, experiments with so-called "classical" light, when cast in the proper quantum formalism, using, e.g., the wave-mechanical description derived below, can provide a useful illustration of general quantum properties of physical systems. In particular this also holds for the works **[P1,P3,P8]** as reproduced in Secs. 6.1.7, 6.2.6, and 5.5.4 of this work.

4.7 The Photon Wavefunction

4.7.1 Wave-Mechanics of Light

Before the advent of QFT, relativistic wave-mechanical descriptions of massive particles have been formulated [72, 71, 952], most notably the Dirac theory of the electron [14], as already mentioned in Sec. 1.4.2. Historically, many of those particles have been known before the invention of quantum mechanics and, motivated by de Broglies insight into the wave-nature of matter [9, 10], a quantum formalism has been developed to treat them [72]. Only in a second step, with QFT these wave-functions have been "upgraded" to field operators allowing to deal more conveniently with many particle states and scenarios where particle number is not conserved [561, 627, 952]. While in modern physics electrons are of course fully included in the field theoretical standard model, nevertheless a range of problems exist where the Dirac equation is still useful.

The historical development of the quantum theory of the light is characterized to some extent exactly in the opposite manner where a wave theory, i.e., electromagnetism came first, and a discovery of a particle nature of light came after, leading to the development of QFT as described above [562]. Thus, in contrast to matter waves, the treatment of the light field as waves is commonly regarded as classical [531], and contemporary textbooks usually do not include a wave-mechanical description of light particles, i.e., photons. Furthermore, the great explanatory success of QED also had the consequence that no immediate need for an alternative description of light was apparent [562]. However, the electromagnetic wave-theory, as expressed via a linear wave-equation, shares significant structural similarities with QM [523], which motivates the question whether a wave-mechanical description of photons in terms of a *photon wave-function* (PWF) might be possible [531, 877].

Indeed, while the PWF is usually not established formally, both in textbooks as well as in the daily jargon of physicists there is a range of formulations which refer to "states" of photons, especially in the context of quantum information applications, see, e.g., [583].

In the context of interferometry, commonly questions such as "which path did the photon take through the interferometer" or "what slit did the photon go through" are posed [647]. Expressions such as those go far beyond the minimal meaning of the notion of "photon" as a single delocalized excitation of a global electromagnetic field mode, but instead seem to treat it as a localized particle propagating through space. Another example of such a treatment is the very common introduction of quantum superpositions in the beginning of textbooks or lectures via the polarization *state* of *a* photon [561, 562, 600], see, e.g., [50]. While starting with such a clearly wave-mechanical treatment of light, these textbooks usually do not develop it further and reintroduce the photon at a later point as a field excitation in the framework of QFT. Also the common statement that "a photon only interferes with itself", which can be traced back to Dirac, implies some notion of a photon quantum state which is usually not specified [561]. This practice to treat photons like a "fuzzy globule of light that travels this way or that way through pieces of optical equipment" or the light beam as consisting "streams of globules, like bullets from a machine gun" has prompted some criticism [524], most notably from Lamb [608], who advocates strongly for the abandonment of such uses of the notion of "photon".

The formal and conceptual problems which have been connected with the PWF can be broadly grouped in three issues, the problem of photon localization on length scales smaller than the wavelength, the problem of negative photon energies, and the problem of proper relativistic transformation of the photon description. In fact several authors have claimed the fundamental impossibility to construct a PWF in the position representation. While the details of these objection are of great interest, a comprehensive discussion goes beyond the scope of this work. Seminal historical contributions to the debate have been given by Landau and Peierls [26], Pauli [33], Newton and Wigner [32], as well as by Bohm [48]. The reader is referred to various newer summaries of the debate for example in [512, 820, 525, 645, 531, 877, 627, 600, 640, 563, 602, 631, 952]. Nevertheless all three problems are illustrated in the derivation below, alongside possible solutions.

4.7.2 Operational Approach

Despite the various objections and no-go theorems, a consistent quantum mechanical description of the photon has been developed [561, 645, 627, 635]. To a certain extent it allows to place the common figures of speech about the traveling photon mentioned above on a firm foundation. The central idea is to overcome the localization problems by broadening the notion of a wavefunction. Following an operational ansatz the PWF is defined based on the probability to detect the photon at a certain location based on the quantum optical model of direct detection, as introduced in Sec. 4.5, see, e.g. [561, 645, 531, 877, 627, 647, 893]. Since the detection events of a photon can be identified with length scales which are several orders of magnitude below the wavelength, such as, e.g., in case of absorption by an atom, such events can be regarded as an effective photon localization. As described above, light detection is commonly based on the transition matrix of the positive frequency electrical field operator $\mathbf{E}^{(+)}$, which in the case of a single-photon excitation has only overlap with the vacuum as the final state [655] leading to the definition [627, 647,

626, 563]

$$\vec{\psi}(\vec{x},t) \propto \langle 0|\vec{\mathbf{E}}^{(+)}(\vec{x},t)|1\rangle, \tag{4.52}$$

of a PWF ψ, where $|1\rangle$ denotes the product state of single-photon excitations in all modes.

For a given single-photon wave-packet mode with a certain polarization, characterized by a momentum amplitude function ξ, as defined in Sec. 4.3.4, the above relation is satisfied with the so-called *energy-density photon wavefunction* (EPWF), which can be written as the weighted Fourier transform [562, 645, 647, 640, 563]

$$\vec{\psi}(\vec{x},t) = \int_{\mathbb{R}^3} \sqrt{\hbar\omega_k}\, \hat{s}_{\vec{k}}\, \xi(\vec{k}) e^{i(\vec{k}\vec{x}-\omega_k t)} \frac{\mathrm{d}^3k}{\sqrt{2\pi}^3}, \tag{4.53}$$

where $\hat{s}_{\vec{k}}$ denotes the corresponding polarization for each of the plane wave modes. The name "EPWF" is motivated precisely by the fact that the factor of $\sqrt{\hbar\omega_k}$ is the square root of mode energy and thus the expectation value of the expected total energy $\langle \mathbf{H}\rangle$ of the field is given as [562, 563]

$$\langle \mathbf{H}\rangle = \int_{\mathbb{R}^3} \hbar\omega_k\, |\xi(\vec{k})|^2 \frac{\mathrm{d}^3k}{\sqrt{2\pi}^3}. \tag{4.54}$$

In the following the qualification "energy" will be neglected and "PWF" identified with "EPWF".

As mentioned above in Sec. 4.3.4, for orthogonal k-space amplitude functions ξ_1 and ξ_2 the resulting real space wavefunction ψ_1 and ψ_2, obtained via the transform (4.53), are not necessarily orthogonal. This constitutes a serious problem since the orthogonality of states should not depend on the representation in a particular basis. The solution is to define a modified scalar product in position space, denoted as $\langle \psi_1||\psi_2\rangle$, which has the form [562, 647]

$$\langle \psi_1||\psi_2\rangle := \frac{4\pi}{\hbar c} \int_{\mathbb{R}^3} \frac{\mathrm{d}^3x}{\sqrt{2\pi}^3} \int_{\mathbb{R}^3} \frac{\mathrm{d}^3x'}{\sqrt{2\pi}^3} \frac{\vec{\psi}_1^*(\vec{x},t)\vec{\psi}_2(\vec{x}',t)}{|\vec{x}-\vec{x}'|^2}. \tag{4.55}$$

In contrast to the usual quantum mechanical scalar product, which due to the orthogonality of position eigenstates reduces to a single integral, the above expression is manifestly *nonlocal* in the sense that each spatial value of one function is multiplied by all other spatial values of the other function [647]. It also clearly indicates the impossibility to define orthogonal position eigenstates and thus a position operator $\vec{\mathbf{x}}$ for the photon, at least in general. Apart from the nonlocality of the expression, the scalar product has the advantage to be invariant under relativistic transformations which alleviates objections related to the transformation behavior of the PWF [562, 647]. Crucially, however, the energy expectation value has a local form in position space with [647, 563]

$$\langle \mathbf{H}\rangle = \langle \psi||\mathbf{H}||\psi\rangle = \int_{\mathbb{R}^3} \vec{\psi}^*(\vec{x},t)\vec{\psi}(\vec{x},t)\, \frac{\mathrm{d}^3x}{\sqrt{2\pi}^3}, \tag{4.56}$$

where again the special scalar product is indicated by the double-bars || and the local form can be recovered by considering the Fourier transformed expression. It is the locality of the energy expectation value in position space, which allows to interpret the squared modulus of ψ as proportional to the probability density of the photon $p(\vec{x},t)$ with the normalization $p(\vec{x},t) := |\vec{\psi}(\vec{x},t)|^2/\langle \mathbf{H} \rangle$. Note that, in contrast to the scalar product (4.55), the energy is not invariant under relativistic transformation, which is the expected behavior as for example in the case of *Doppler shifts* [523].

For the definition of the momentum representation of the wave-function, two options have been proposed. When the simple identification $\vec{\psi}(\vec{k}) := \hat{s}_{\vec{k}}\xi(\vec{k})$ is chosen as in [645, 635, 647], the momentum space wavefunction remains dimensionless, i.e., it can be interpreted as a probability amplitude, but the Fourier transform has the weighted form of eq. (4.53). The other option is to define $\vec{\psi}(\vec{k}) := \sqrt{\hbar\omega_k}\hat{s}_{\vec{k}}\xi(\vec{k})$ as in [561, 562, 563], which leads to a regular Fourier transform between position and momentum space wavefunctions, but also gives the absolute squared momentum wavefunction the dimension of energy density in k-space. Thus it also necessitates a modification of the scalar product in momentum space, which has to be [563]

$$\langle \psi_1 || \psi_2 \rangle := \int_{\mathbb{R}^3} \frac{1}{\hbar\omega_k} \vec{\psi}_1^*(\vec{k}) \vec{\psi}_2(\vec{k}) \frac{\mathrm{d}^3 k}{\sqrt{2\pi}^3}. \tag{4.57}$$

In contrast to the scalar product in position space, however, it still remains local in k-space. Since the difficulties with the definition of photon wavefunction result from the weighting factor in the Fourier transform (4.53), they disappear in the case of monochromatic field states, for which the notion of a PWF seems simple. However, crucially the finite energy of single photons fundamentally requires a description in terms of wave-packets localized in time, i.e., multiple modes [562, 600, 580].

4.7.3 The Maxwell Wavefunction

Instead of starting with the QFT notion of a photon and then deriving the PWF via the operational argument of an energy denstiy wavefunction as mentioned above, the same result can also be obtained without any recourse to field theory in a derivation analogous to the Dirac equation. Essentially it is based on identifying the Maxwell equations as a relativistic wave equation for a massless quantum particle of spin-1, a connection which initially has been made by Majorana and later fully developed by Białynicki-Birula [561, 562], see also [653]. The first step is to define the complex field [561, 562, 877, 653]

$$\vec{F}(\vec{x},t) = \frac{1}{\sqrt{2}} \left(\sqrt{\varepsilon_0}\vec{E}(\vec{x},t) + i\frac{\vec{B}(\vec{x},t)}{\sqrt{\mu_0}} \right), \tag{4.58}$$

also called the *Riemann-Silberstein vector* (RS). It can been interpreted as the complex amplitude of field energy density and is related to the energy density via $u = \vec{F}^*\vec{F}$. Employing the RS vector, it is possible to put the free space Maxwell equations, along with

the transversality condition $\vec{\nabla}\vec{F} = 0$, into the compact operator form [561, 562, 635, 647, 602]

$$i\hbar\frac{\partial}{\partial t}\vec{F} = c(\vec{\mathbf{s}}\cdot\vec{\mathbf{p}})\vec{F} \tag{4.59}$$

Where the momentum operator is defined as $\vec{\mathbf{p}} := -i\hbar\vec{\nabla}$ and the *spin-operator* $\vec{\mathbf{s}} = (\mathbf{s}_x, \mathbf{s}_y, \mathbf{s}_z)$ consists of the three spin matrices with matrix elements $(\mathbf{s}_j)_{kl} = -i\epsilon_{jkl}$, which are the generator of rotations for spin-1 particles around the three spatial axes x, y and z [561, 562, 647]. Note that, due to the transversality condition, the photon polarization has only two orthogonal components and thus effectively behaves like a spin-1/2 particle. The RS vector also corresponds to a possible complex analytical signal for the electric field with $\vec{E} = 2\mathrm{Re}\big[\vec{F}/\sqrt{2\epsilon_0}\big]$ and also provides a complex form for the magnetic field with $\vec{B} = 2\mathrm{Re}\big[-i\vec{F}\sqrt{\mu_0/2}\big]$. Note, however, that these complex analytical signals in general contain both positive as well as negative frequency parts. Since the equation above has the same form as a Schrödinger equation with Hamiltonian $\mathbf{H} = c\vec{\mathbf{s}}\cdot\vec{\mathbf{p}}$, this motivates the identification of the RS vector $\vec{F}$ with the spinor representation of the photon wavefunction $|\psi\rangle$ up to a normalization constant [561, 562, 563].

In terms of the Maxwell equations the spin-operator can be seen as the operator notation for the cross product with $(\vec{\mathbf{s}}\cdot\vec{v})\vec{w} = i\vec{v}\times\vec{w}$ for any pair of vectors $\vec{v}$ and $\vec{w}$. However, it also allows to connect the PWF to the relativistic formalism in which the product of momentum on the spin defines the *helicity* of a particle [561, 562, 563]. It turns out that right and left-circular polarization are eigenstates of helicity, i.e., of the Hamiltonian, with positive and negative frequencies respectively. Thus when decomposing $\vec{F}$ into negative and positive frequency parts as $\vec{F} = \vec{F}^{(+)} + \vec{F}^{(-)}$, where $\vec{F}^{(+)}$ is the projection of $\vec{F}$ onto right circular polarization and $\vec{F}^{(-)}$ the left-circular component correspondingly. This motivates the reformulation of the wave-equation in an extended Hilbert space by adding a two dimensional polarization space as [561, 562, 563]

$$i\hbar\frac{\partial}{\partial t}|\Psi\rangle = \boldsymbol{\sigma}_z \otimes \mathbf{H}\,|\Psi\rangle\,, \tag{4.60}$$

where the position representation of $|\Psi\rangle$ corresponds to the normalized six component spinor $\check{F} = (\vec{F}^{(+)}, \vec{F}^{(-)*})$. This equation effectively just contains two decoupled equations of the form (4.59), differing only by a sign such that each helicity represents a positive energy solution. This finally also solves the problem of the negative frequency components present in the field by identifying them with different photon helicities. Crucially, since $\vec{F}$ is a complex field, in general $\vec{F}^{(-)} \neq \big(\vec{F}^{(+)}\big)^*$, i.e., the photon can be in arbitrary superpositions of helicities. In analogy to the Dirac formalism, the spinor notation $\check{F}$ allows to conveniently express relativistic boosts under which the two helicity components obtain a relative phase [653, 563]. Note that the equations are only decoupled for the free field and interactions with matter induce also interactions between the two helicity components.

Similar to the probability density $p(\vec{x}, t)$, also the probability current $\vec{j}$ of the photon can be defined by identifying the normalized Poynting vector, expressed as $\vec{S} = c\check{F}^*(\boldsymbol{\sigma}_z \otimes \vec{\mathbf{s}})\check{F}$,

with the probability current [561, 531, 877]

$$\vec{j}(\vec{x},t) = \vec{S}(\vec{x},t)/\langle \mathbf{H} \rangle. \tag{4.61}$$

This allows to formulate an effective quantum continuity equation of the form (1.13) also for the photon [561, 877].

For a description in a single reference frame, the doubling of the spinor is not necessary and the summed RS vector $\vec{F}$ together with wave-equation (4.59) can be used. As this is exactly equivalent to the classical electromagnetic wave-equation, the solutions in momentum space are given by the wave-packet amplitude functions $\xi(\vec{k})$. The requirement of a local expression for the position space energy expectation value then again leads to the same scalar products and transformations as presented above. Finally, the PWF can also be quantized leading to the full QFT description of the electromagnetic field, reproducing a similar hierarchy of quantum theories for massive particles [647, 563].

When taking into account the full QED interactions of the quantum field with charged matter, the description via the PWF becomes much more involved as the interaction essentially corresponds to a multitude of photon annihilation and creation processes [561, 562, 563, 600]. However, at least in homogeneous media, i.e., media which classically can be described by a constant index of refraction, an effective wave-equation of the same form as (4.60) can be formulated by exchanging the vacuum constants ε_0 and μ_0 by the phenomenological parameters ε and μ. Crucially, this allows to describe the propagation of single photons with the apparatus of classical optics. It should be noted, however, that in this case no simple interpretation of $\check{F}$ as the wavefunction of a single photon is possible [600]. In inhomogenoues media the wave-equation becomes more complicated as the two helicities no longer evolve independently and in general their wave-equations are coupled [561, 562, 563].

Finally, the PWF also allows to express the quantum optical correlation functions. In the case of $g^{(1)}$ the situation is simple and by considering the operational definition (4.52) it is evident that $g^{(1)}(\vec{x}_1,t_1,\vec{x}_2,t_2) = \vec{\psi}^*(\vec{x}_1,t_1)\vec{\psi}(\vec{x}_2,t_2)$ [655, 579]. Accordingly quantum values of $g^{(2)}$ for two-photon states can be recovered by formulating properly symmetrized two-photon wavefunctions [647, 626] and the same approach can then be generalized to n-photon wavefunctions and n-th order correlation functions [653].

4.7.4 Interpretation of the Photon Wavefunction

In summary, it is possible to distinguish three types of interpretations for the photon, either as an elementary excitation of the quantum field, operationally as the click of a photodetector, or as a fundamental quantum particle described by a wave-function [647, 952]. Accordingly, the PWF formalism can either be interpreted as a stand-alone theory of quantum particles such as the Dirac equation or alternative as a convenient tool to effectively describe the states and dynamics of quantum fields when the system is restricted to a single-photon or few-photon subspace. In fact it is implicitly used in many quantum information applications based on single photons such as quantum cryptography, where it

often gives a clearer and simpler description of the scenario at hand than a description via QFT [653]. While the PWF allows to define a local photon density which transforms consistently under Lorentz boosts and gives meaning to the negative frequency components of the field as states of opposite helicity, of course it cannot account for field theoretical effects such as quantum fluctuations and photon creation and annihilation [635, 626, 653, 637]. Thus even expressing the state of, e.g., a single photon via a PWF, no naive connection to a classical electromagnetic field can be established and in particular the global phase of the oscillation is undefined. Note, however, that stochastic models of light have been proposed, which combine a description in terms of an electromagnetic wavefunction with statistical noise, see, e.g., [778].

Since the wave-mechanical description presented above holds both for wave-packets as well as for quasi-stationary beams, the PWF emerges as an immensely useful tool which allows to treat single-photon experiments on the same footing as experiments with coherent laser light [561]. Furthermore, the correspondence between the PWF and the Maxwell field, as established by the RS-vector, indicates that such a description is not only a convenient formalism which is artificially attached to classical phenomena, but in fact can be seen as a genuinely quantum theory also in the context of so-called "classical" light. In this sense it could be said that the PWF provides a description of optical experiments on a single-photon level and points to an inherently quantum nature of the wave-theory of light. A view of a similar type seems to have also been expressed by Glauber, who in his famous Les Houches lectures, in the context of classical statistical description of optical fields, writes:

> One of the properties of the "semi-classical" approaches that makes them elementary is that they deal with ordinary numbers and functions. They make no use of the apparatus of non-commuting operators which, it may appear, ought to be part of any formal quantum mechanical description of the field. Later in these lectures we shall show that for a certain class of fields there need be no error in a statistical description of the field which is based upon such ordinary functions as we find by solving the wave equation. It is possible to describe these fields fully by means which are rather similar to those used in the classical theory of noise. Where such a description is available it means that there need be nothing incorrect about the so-called "classical" or "semi-classical" approaches except their names, which then become totally misleading. [589]

Chapter 5

Quantum Optics Applied

While the previous chapter focused on the theoretical description of light as a quantum object, this chapter discusses the practical utilization of light in quantum experiments. It opens with the introduction of the quantum formalism of paraxial light based on the PWF, which can be applied to single-photon experiments as well as to laser light. This includes also the description of the basic building blocks of free-space linear optics such as beam-splitters and waveplates. Subsequently fundamental elements of nonlinear optics are sketched as a basis for the description of the light sources employed in the context of this work, i.e., lasers and entangled photon-pair sources. The chapter proceeds with the description of the optical double-slit and the interferometer, which represent the main paradigmatic experimental scenarios for quantum experiments. It closes with an overview over applications of optical waveguides, in particular for the simulation of open quantum systems.

5.1 The Quantum Toolbox of Paraxial Light

5.1.1 Paraxial Hilbert Space

A plethora of contemporary quantum experiments is based on paraxial light fields in free space, which can be described very conveniently by the PWF. In the paraxial case the description simplifies significantly since the weighting factor $\sqrt{\omega_k}$ in the Fourier transform between momentum and position wavefunctions (4.53) can be approximated as $\sqrt{k_z/c}$ [647]. This leads to a spinorial wavefunction $\check{\psi}$ of the form

$$\check{\psi}(\vec{x},t) = \frac{\check{F}(\vec{x},t)}{\sqrt{\langle \mathbf{H} \rangle}} \approx \begin{pmatrix} \hat{s}_R(\vec{x})\, \psi_R(\vec{x})\, \zeta_R(z-ct) \\ \hat{s}_L(\vec{x})\, \psi_L(\vec{x})\, \zeta_L(z-ct) \end{pmatrix} \tag{5.1}$$

where R and L indicate right and left circular polarization, and ψ_j as well as ζ_j represent the weakly and strongly spatially varying parts of the scalar spatial wavefunction for polarization j, respectively. Also here the transverse shape of the beam has been assumed to be time-independent, i.e., $\psi_j(\vec{x})$ is independent of t, which is the typical case of beams with

resting foci, as introduced in Sec. 4.2.2. Note that, although the polarization unit vectors $\hat{s}_R$ and $\hat{s}_L$ have spatial dependence, they are not free parameters and in the paraxial case the vectorial state of wavefunction is fully specified according to Eq. (4.13) by just the two scalar components $\psi_R(\vec{x})$ and $\psi_L(\vec{x})$.

Since for paraxial beams the transverse part of the integration (4.53) is independent of k_z, the slowly varying terms ψ_j in (5.1) are equivalent to solutions of the classical wave-equation such as the Gaussian Beam, and by itself obeys the PHE (4.8). Accordingly, the standard scalar product can be applied in the transverse directions allowing the definition of position eigenstates and thus the usual position operators $\mathbf{x}$ and $\mathbf{y}$. This means that there is a well-defined notion of transverse photon localization. The same does not hold for ζ_j, which in the case of a polychromatic photon wave-packet is different from the classical solutions and is connected to a nonlocal scalar product [647]. For the range of scenarios treated here, this is, however, not a problem since the spatial localization along the longitudinal direction is not of interest and only the total overlap of the longitudinal parts is relevant as a contribution to the first-order correlation function of the field.

Due to the fact that in first-order paraxial approximation the field vector for the two polarization eigenstates is fully specified by two scalar wavefunctions ψ_R and ψ_L, a common notation is to collapse the six-dimensional spinor $\check{\psi}$ into a two-dimensional complex Hilbert space corresponding to polarization. Thus the polarization of a paraxial beam effectively represents a qubit [511]. Furthermore, since, as discussed in Sec. 4.7.3, the description in a single reference frame does not require the Lorentz invariant helicity eigenstates, commonly the basis $\{|H\rangle, |V\rangle\}$ of horizontal and vertical polarization of the electric field is employed as the primary representation, and the Pauli operators are defined accordingly such that these states are eigenstates of the $\boldsymbol{\sigma}_z$ operator. The amplitudes of these polarization eigenstates then become exactly equivalent to the entries of the Jones vector as defined in Eq. (4.15). To derive the polarization dependent energy flow, as introduced in Sec. 4.2.4, for the PWF, the polarization at each location can be converted back into a three component vector by using expression (4.13). In the following the polarization indices of ψ_j and ζ_j will only be written explicitly if the polarization is not homogeneous.

Finally the additional degree of freedom of *path* can be added to the wavefunction. A path is a localized spacetime region which defines a local coordinate system in which the wavefunction is paraxial to the local z-axis. Optical processes in which the wavefunction changes its direction of propagation far outside the paraxial regime, such as, e.g., reflections, can thus still be described via paraxial wavefunctions, where differently rotated and mirrored coordinate systems are used for the regions through which the wavefunction passes before and after reflection, as illustrated in Fig. 5.1. In effect, the notion of a path allows to conveniently describe fields which consist of several wavefunctions which are locally paraxial but propagate in different directions [629].

In conclusion, the full state of paraxial wavefunctions can be expressed as an element of the joint Hilbert space $\mathcal{H}_{\text{light}}$ of five degrees of freedom of light given as

$$\mathcal{H}_{\text{light}} = \mathcal{H}_{\text{path}} \otimes \mathcal{H}_{\text{pol}} \otimes \mathcal{H}_x \otimes \mathcal{H}_y \otimes \mathcal{H}_L, \tag{5.2}$$

where $\mathcal{H}_{\text{path}}$ is the discrete space of paths, $\mathcal{H}_{\text{pol}}$ is the two-dimensional qubit space of

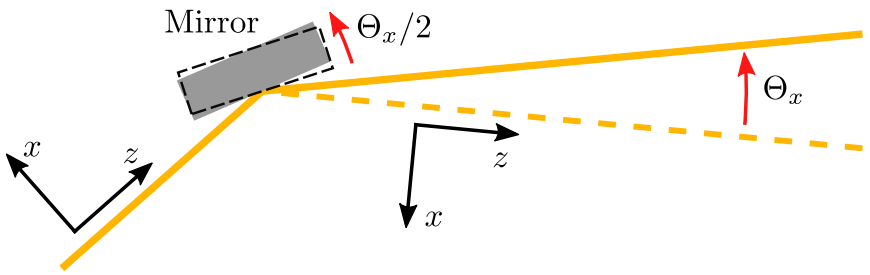

Figure 5.1: **The Concept of a Beam Path** The paraxial description of the light field is preserved by redefining the coordinate system upon deflection of the beam at the mirror. In contrast, for deflections about small angles or small changes of deflection direction, the coordinate system can be held fix and the paraxial description of the beams can be modified by incorporating a small additional transverse angle Θ_x. In the typical experiments described here, all strong reflections happen in the horizontal xz-plane, such that the vertical y-direction remains fixed.

polarization, $\mathcal{H}_x$ and $\mathcal{H}_y$ are the continuous spaces of transverse spatial directions x and y, and $\mathcal{H}_L$ the continuous longitudinal Hilbert space of the z-direction, which also effectively encodes all temporal and spectral properties of the photon [568]. The Hilbert space $\mathcal{H}$ can also be seen as definition of the photon as an elementary particle, corresponding to a set or *bundle* of properties [948], as defined in Sec. 1.2.2. For convenience, also the space $\mathcal{H}_{\text{light}}^{\text{sgl}}$ is defined, which corresponds to

$$\mathcal{H}_{\text{light}}^{\text{sgl}} = \mathcal{H}_{\text{pol}} \otimes \mathcal{H}_x \otimes \mathcal{H}_y \otimes \mathcal{H}_L, \tag{5.3}$$

i.e., $\mathcal{H}_{\text{light}}$ without the path degree of freedom. It can be employed whenever only a single path is of interest, such as, e.g., for the discussion of the double-slit in Sec. 5.3.

5.1.2 The Free Evolution

The free Hamiltonian for a system described by the paraxial PWF involves no coupling between the discrete and continuous degrees of freedom. While path and polarization remain invariant under the free evolution, the combination of transverse and longitudinal evolution corresponds to the diffraction of a propagating wave-packet. The propagation in z-direction with constant velocity c as expressed with the parameter $(z - ct)$ of ζ, entails that effectively the time coordinate t and longitudinal coordinate z can be treated equivalently. In particular time displacements have the same effect as differences in propagation length which is the basis of interferometry, as introduced below. Since typical interferometric experiments, such as those treated in this work, consist of several wavefunction components which travel along paths of similar length before being superposed, it is convenient to express the longitudinal parts in terms of the shifted coordinate $z' := z - ct$ which is moving with the common propagation velocity c of all components. Note that this is to be understood as a strictly non-relativistic convenient coordinate notation for the experimental rest frame and not as a Lorentz boost, i.e., not as a description from the point of view of a moving reference frame. It accounts for the fact that when considering

superpositions of quasi-stationary wavefunctions which have propagated along different paths, the effective quantity of interest is only a longitudinal offset due to a relative difference of propagation-length, which also includes a certain difference in carrier phase. In consequence, also the longitudinal component of the wavefunction is regarded as invariant under the free evolution and relative longitudinal displacements are expressed as the action of a unitary shift-operator as introduced below.

The equivalence between the longitudinal coordinate and time also allows to view the stationary dependence of the transverse shape on the longitudinal coordinate z as an evolution in time and express the slowly varying part of the wavefunction as $\psi(\vec{x}) \rightarrow \psi(x, y, t)$ which then can be written as a state vector $|\psi\rangle \in \mathcal{H}_T$ in the transverse Hilbert space $\mathcal{H}_T = \mathcal{H}_x \otimes \mathcal{H}_y$. If the coherence length of the wave-packet is sufficiently small compared to the longitudinal length-scale on which ψ changes significantly, the latter is effectively the same over the whole longitudinal extension of the wavepacket. In this case $\psi(x, y, t)$ exactly corresponds to the temporally varying transverse shape of the whole wave-packet as it propagates through space. The more the longtudinal wavefunction ζ approaches the monochromatic regime, however, the more the longitudinal shape becomes distributed over a region of significant transverse variation. Nevertheless, also in such cases a continuum of time-shifted functions $\psi(x, y, t - t_0)$ corresponds to the transverse evolution of fixed points $\zeta(t_0)$ of the longitudinal wavefunction. Thus, here, ψ is normalized with respect to the transverse direction and the remaining factors are absorbed in ζ such that the whole spacetime wavefunction can still be used to obtain the normalized first-order correlation function.

By replacing the z-coordinate in the PHE with time t via $z = ct$, it is possible to express the transverse time-evolution in terms of quantum mechanical wave-equation. In fact this equation is exactly equivalent to the Schrödinger equation of a free massive particle of effective mass $m_{\text{eff}} = \hbar\bar{k}_z/c$ [581, 308, 893] given by

$$i\hbar\frac{\partial}{\partial t}|\psi\rangle = \frac{\mathbf{p}_T^2}{2m_{\text{eff}}}|\psi\rangle =: \mathbf{H}_T|\psi\rangle\,, \tag{5.4}$$

where $\mathbf{p}_T = \mathbf{p}_x \otimes \mathbf{p}_y$ is the paraxial momentum operator and $\mathbf{H}_T$ the transverse Hamiltonian. In position representation $\mathbf{p}$ can be expressed as $\langle xy|\,\mathbf{p}\,|\psi(t)\rangle = -i\hbar\vec{\nabla}_\perp\psi(x, y, t)$, where $|xy\rangle := |x\rangle \otimes |y\rangle$ are eigenstates of the transverse position operator $\mathbf{r}_T = \mathbf{x} \otimes \mathbf{y}$. In the following a quasi-monochromatic paraxial beam with carrier frequency ω is assumed for which the effective mass can be simply approximated as $m_{\text{eff}} = \hbar k/c$. The Schrödinger equation above exactly reproduces the diffraction of the paraxial wavefunction including the evolution of the phase-front curvature, where the beam width w as defined for the Gaussian beam (4.9) can be related to the standard deviation of position with $w = 2\Delta\mathbf{x}$ and vice versa for the y-direction. Note that, for an increasingly broadened spectrum, the approximation of the transverse evolution via single effective mass proportional to $\bar{k}_z$ becomes less and less valid and the diffraction experienced by the different spectral components becomes more distinct. This leads to a modification of the transverse wave-function correlated with the different longitudinal spectral modes, as already discussed in Sec. 4.2.2 and illustrated in Fig. 4.1.

5.1.3 Interaction Picture and Transverse Fourier Transform

The free evolution of the transverse part can be seen as an effective Fourier transform of the position wavefunction, when expressing the evolution in the interaction picture. Since the momentum operator commutes with Hamiltonian it is time-invariant in the interaction picture and thus $\mathbf{p}(t) = \mathbf{p}_0 = \mathbf{p}$, where the subscript 0 indicates the operator at time $t_0 = 0$. Here, for illustration just the x-direction is considered and the corresponding subscript neglected. All results of course hold the same also for the y-direction. In contrast to the stationary momentum operator, the Heisenberg evolution of the position operator becomes [42]

$$\mathbf{x}(t) = e^{\frac{i}{\hbar}\mathbf{H}_T t}\mathbf{x}_0 e^{-\frac{i}{\hbar}\mathbf{H}_T t} = \mathbf{x}_0 + \frac{\mathbf{p}_0}{m_{\text{eff}}}t. \tag{5.5}$$

In consequence with increasing time t a position measurement shows less and less the expectation value of position at time t_0 and more and more the one of momentum. In fact, as discussed in Sec. 2.3.1, a position measurement at time t or equivalently at longitudinal position $z = ct$ shows a fractional Fourier transform of the initial wavefunction at t_0, approaching a full transform in the far field $t \to \infty$. In the following the operator $\mathbf{x}(t)$ will be written as $\mathbf{x}_z$ with eigenstates $|x_z\rangle$.

Assuming that for the initial wavefunction the quantum covariance C_{xp} vanishes, the time-dependent variance $\Delta\mathbf{x}_z$ can be expressed according to Eq. (2.24) as [42]

$$(\Delta\mathbf{x}_z)^2 = (\Delta\mathbf{x}_0)^2 + \left(\frac{z}{m_{\text{eff}}c}\right)^2 (\Delta\mathbf{p}_0)^2 . \tag{5.6}$$

This implies that at the critical longitudinal position $z_{\text{crit}} = k\hbar\Delta\mathbf{x}_0/\Delta\mathbf{p}_0$ position and momentum uncertainties contribute in an equal manner to the total uncertainty and in this sense z_{crit} can be seen as the point where the Fourier transform is half completed. In the case of beams with minimal uncertainty transverse profiles, i.e., $\Delta\mathbf{p}_0\Delta\mathbf{x}_0 = \hbar/2$, the critical position exactly coincides with the Rayleigh range z_R.

5.1.4 Basic Linear Interactions

Having established the space of degrees of freedom of paraxial light as well as its free evolution, a significant portion of experimental scenarios can now be described by a range of basic interactions which are additionally introduced. As all of these interactions involve the interaction of light with matter, a fundamental description in terms of a single photon is potentially rather complicated. However, it is possible to express them as effective interactions between the five degrees of freedom of the free PWF using the simple formalism of classical linear optics. In this context "linear" denotes independence of the interaction from the intensity or photon number. Nonlinear optical effects are discussed in the next section. Note that here the term "interaction" is applied not to the interaction of distinct quantum systems but for coupling between different degrees of freedom of the same particle, which satisfies the formal definition of interaction presented in Sec. 1.5. Following the

paradigm of analog quantum simulation, as introduced in Sec. 1.7.4, such interactions can be seen as simulating any quantum interaction of the same form.

The basic effective interactions relevant in this work are approximately local both in time and space compared to transverse and longitudinal time and length scales of the light and are thus always described by unitary operators of the form

$$\mathbf{U} = \mathbf{\Pi}_j \otimes \mathbf{U}_m + \mathbf{\Pi}_{j,\perp} \otimes \mathbb{1}, \tag{5.7}$$

where $\mathbf{\Pi}_j$ is a projection on path j, $\mathbf{\Pi}_{j,\perp} := \mathbb{1} - \mathbf{\Pi}_j$ denotes the projection on the remaining paths, and $\mathbf{U}_m$ is a time-independent unitary operator acting on the Hilbert space of the four remaining degrees of freedom. In the following various interactions will be discussed by presenting typical operators $\mathbf{U}_m$. The only exception from this form are local interactions between the paths themselves, which can occur if the paths cross in space. Since most interactions commute with the free evolution, usually only the particular durations, implicit in the form of $\mathbf{U}_m$, and the order of the interactions are of relevance. This of course does not hold for focusing or dispersing elements, such as lenses, or transverse deflections as described below.

Finally, it should be mentioned that there exist one basic component of free-space optical experiments, which does not correspond to a unitary interaction, namely a polarization dependent transmitter commonly called a *polarizer* [530, 537]. A polarizer placed in a certain path j acts on $\mathcal{H}_{\text{path}} \otimes \mathcal{H}_{\text{pol}}$ and effectively corresponds to the projector $\mathbf{\Pi}_{\text{pol}}$ with

$$\mathbf{\Pi}_{\text{pol}} := \mathbf{\Pi}_j \otimes |\phi\rangle\langle\phi| + \mathbf{\Pi}_{j,\perp} \otimes \mathbb{1}, \tag{5.8}$$

where $|\phi\rangle$ is some polarization state. Since potentially a part of the state is projected out, in general a renormalization is necessary after the application of a polarizer. The polarizers employed in this work are absorptive glass polarizers, i.e., they absorb one of the two components of polarization. See, e.g., [537] for details and other possible implementations of polarizers.

5.1.5 Propagation through Media

A basic effective interaction between path and the spatial degree of freedom is given by the propagation through a medium with plane parallel input and output facets as illustrated in Fig. 5.2. A typical experimental example is a glassplate placed in the path of the light. As introduced in Sec. 4.1.3, in the classical formalism of optics the interaction between a light field and a typical non-absorptive homogeneous medium can be described effectively by a refractive index $n > 1$. For a plane wave propagating over the length L in the medium, the effective evolution is the same as for a wave propagating in free space over the length nL. This is the basis for the definition of the *optical path-length* $l = nL$, where L is called the *geometrical path-length* [514, 530]. According to the same principle, a paraxial propagation in a medium over the geometrical distance L can be modeled as a time-retardation by $\delta t = (1 - n)L/c < 0$ relative to a wave-packet in free space, both for the longitudinal as well as for the transverse components. Accordingly two unitary

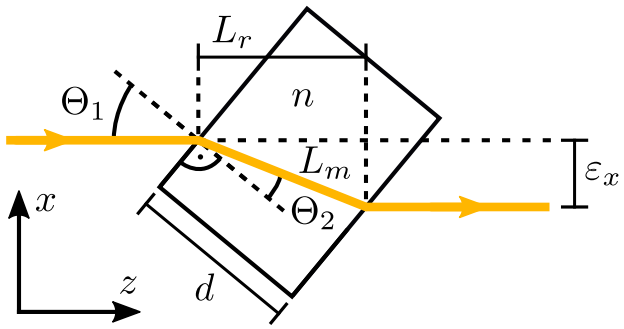

Figure 5.2: **Propagation through plane-parallel Medium** Upon entrance into the medium with $n > 1$ the propagating beam is refracted towards the surface normal, where the two angles Θ_1 and Θ_2 are related via Snell's law. Since the refraction is symmetric, after exiting at the parallel output facet of the medium, the same propagation direction is restored. Due to the different propagation direction in the medium, which can be far from paraxial, the beam effectively aquires a spatial offset of ε_x. To calculate the effective retardation, it is necessary to compare the geometrical path length L_m inside the medium multiplied with its refractive index n and the reference length L_r, i.e., the length the light would have traversed if the medium had not been there.

time-displacement operators $\mathbf{U}_z(n, L)$ and $\mathbf{U}_T(n, L)$ can be defined. While $\mathbf{U}_z$ acts on $\mathcal{H}_L$ with $\zeta(ct) \to \zeta(ct + c\delta t)$, $\mathbf{U}_T$ acts on $\mathcal{H}_T$ and can be expressed in terms of the transverse Hamiltonian as

$$\mathbf{U}_T(n, L) = e^{\frac{i}{\hbar c}\mathbf{H}_T(n-1)L}. \tag{5.9}$$

If the temporal width is much larger than δt, the absolute shift of the temporal envelope can be neglected. However, in any case the shift will lead to a phase-shift $\delta\varphi$ for the light in this path which is given by $\delta\varphi = \delta t\omega$, where ω is the carrier frequency of the longitudinal part of the PWF. Thus, for notational convenience, the phase-shift is often distinguished from the longitudinal time-delay by defining the operator $\mathbf{U}_z^{\varphi} = \exp(-i\delta\varphi)\mathbf{U}_z$ and writing the phase-shift explicitly. In the case of dispersive media with frequency dependent refractive index or absorptive media with complex n, more complicated deformations of the spatial wavefunctions and non-unitary effects have to be taken into account.

As also illustrated in Fig. 5.2 when the central propagation axis is not parallel to the normal of the incidence plane of the medium, the medium effectively introduces a transverse displacement of the beam due to refraction at the boundary between the medium and free space. By placing the transverse x-direction in the plane constituted by surface normal and propagation direction z, the total effect of a propagation through a medium can be expressed by the effective unitary operator $\mathbf{U}_{\text{med}}$ acting on $\mathcal{H}_x \otimes \mathcal{H}_{\text{L}}$ as

$$\mathbf{U}_{\text{med}} := e^{i\delta\varphi}e^{-i\epsilon_x\mathbf{k}_x}\,\mathbf{U}_T(n, L) \otimes \mathbf{U}_z^{\varphi}(n, L), \tag{5.10}$$

with effective displacement $\varepsilon_x = d\sin(\theta_1 - \theta_2)/\cos\theta_2$, where d is the thickness of the medium, θ_1 its tilt with respect to the beam, and θ_2 the refracted angle inside the medium,

as obtained by Snell's law $\sin\theta_1 = n\sin\theta_2$. To calculate the effective retardation The geometrical path length L_m inside the medium is given by $L_m = d/\cos\theta_2$ and the reference path L_r without the medium as $L_r = \sqrt{L_m^2 - \varepsilon_x^2}$. Since the path inside the medium is not parallel to the reference path, to conform with the definition of the retardation operator (5.9) the effective geometrical path-length

$$L = \frac{nL_m - L_r}{n-1} = d\frac{n - \cos(\theta_1 - \theta_2)}{(n-1)\cos\theta_2} \tag{5.11}$$

has to be used in $\mathbf{U}_{\text{med}}$, which for small angles simplifies to $L \approx d$. As $\mathbf{U}_{\text{med}}$ commutes with the free evolution, longitudinal displacements of the medium leave the final state invariant. If the transverse wavefunction is sufficiently broad, the transverse displacement can often be neglected while the small longitudinal path difference still is of comparable order as the carrier wavelength and thus leads to significant phase-shift. In effect, this makes slightly tilted glassplates a very useful tool to adjust the relative phase between different optical paths.

5.1.6 Beam-Splitters

The basic interaction which allows to split a single paraxial wavefunction into a superposition of wavefunctions propagating along distinct paths is called *beam-splitting* and is realized by optical devices called *beam-splitters* (BS). In the language of QFT a beam-splitter can be defined via a local operation which annihilates photons from two input paths A and B and creates superpositions of photons in two output paths C and D, also called input and output *ports*. The corresponding unitary operator $\mathbf{U}_{\text{BS}}$ is defined as [524, 610, 629]

$$\mathbf{U}_{\text{BS}} := \frac{e^{i\varphi}}{\sqrt{2}}\big(T\mathbf{a}_C^\dagger\mathbf{a}_A + e^{i\vartheta}R\mathbf{a}_C^\dagger\mathbf{a}_B + e^{i\vartheta}R\mathbf{a}_D^\dagger\mathbf{a}_A - e^{2i\vartheta}T\mathbf{a}_D^\dagger\mathbf{a}_B\big) \tag{5.12}$$

where the annihilation operator $\mathbf{a}_j$ denotes an integral over the annihilation operator density $\mathbf{a}_{k,p}$ of modes corresponding to path j, the amplitudes $T, R \geq 0$ with $T^2 + R^2 = 1$ parametrize the splitting ratio between the two ports, the phase ϑ represents a relative phase introduced between the two paths, and φ is an arbitrary additional global phase. As in practice a beam-splitter usually corresponds to optical transmission of one part of the wavefunction and reflection of the other, the amplitudes T and R are usually connected to optical *transmittivity* and *reflectivity*, respectively. It should be noted, as already mentioned above, that the beam-splitter operators presented in this subsection are of course defined without any additional projectors, i.e., *not* defined relative to expression (5.7), in contrast to the operators for all remaining components.

In the formalism of the PWF the unitary operator of the beam-splitter can instead be expressed as

$$\mathbf{U}_{\text{BS}}^{\text{PWF}} := \frac{e^{i\varphi}}{\sqrt{2}}\Big(T|C\rangle\langle A| + e^{i\vartheta}R|C\rangle\langle B| + e^{i\vartheta}R|D\rangle\langle A| - e^{2i\vartheta}T|D\rangle\langle B|\Big), \tag{5.13}$$

and thus acts exclusively on $\mathcal{H}_{\text{path}}$. Note that (5.13) is simply the matrix representation of (5.12) for a single-photon subspace, where the latter, has of course the advantage to allow a simple description also of multi-photon interference phenomena. In any case, the unitarity of a beam-splitter necessarily implies that it also functions as a mode merger, i.e., it overlaps the wavefunctions coming in from different input ports at both output ports. Since beam-splitters also involve a propagation of the beams through an extended medium with $n > 1$, in general they also introduce different time-shifts for the transmitted and reflected components. In the following such time-shifts are neglected, since configurations are assumed in which they cancel out when considering the total propagation of overlapping wavefunctions through all the beam-splitters employed in their splitting and merging.

A special type of beam-splitter is the *polarizing beam-splitter* (PBS), which can be described as an interaction between path and polarization. For each of the input ports, it transfers only one of the polarization components to each of the output ports, which in general leads to a change of the polarization state [629]. Since in usual experimental scenarios the beam propagation direction is horizontal with respect to the experimental reference frame, horizontal and vertical polarizations are eigenstates of a typical polarizing beam-splitter. Accordingly the unitary operator $\mathbf{U}_{\text{PBS}}$ acting on the Hilbert space $\mathcal{H}_{\text{path}} \otimes \mathcal{H}_{\text{pol}}$ can be expressed as

$$\begin{aligned}\mathbf{U}_{\text{PBS}}^{\text{PWF}} := e^{i\varphi}\Big(&T|CH\rangle\langle AH| + e^{i\vartheta}R|CV\rangle\langle BV| \\ &+e^{i\vartheta}R|DV\rangle\langle AV| - e^{2i\vartheta}T|DH\rangle\langle BH|\Big).\end{aligned} \tag{5.14}$$

5.1.7 Mirrors and Lenses

Another crucial optical element are planar mirrors which are optimized for polarization independent high reflectivity [513, 530]. The effect of such mirrors on the paraxial direction of propagation and the induced parity inversion is usually absorbed into the definition of paths, as illustrated above in Fig. 5.1. Nevertheless given a certain paraxial path, mirrors can be slightly tilted to introduce small angular deflections, i.e., an interaction between path and transverse degrees of freedom. Note that here the term "deflection" is used to indicate that in contrast to a reflection no parity inversion takes place. For a mirror, which is tilted in the xz-plane of input and output coordinate systems the corresponding unitary operator $\mathbf{U}_M$ is given by

$$\mathbf{U}_m = \mathbf{U}_M(t_1, t_2) := e^{i\epsilon_k \mathbf{x}}, \tag{5.15}$$

where ϵ_k is the angular displacement with the dimension of wavenumber, corresponding to the transverse angle $\theta_x \approx \varepsilon_k/k$, and the unitary operator describes the evolution for the time interval $[t_1, t_2]$, which is assumed to be much shorter than the timescale of the transverse free evolution. Note that in general a mirror might also introduce a deflection in y-direction, which can be expressed analogously.

If the remaining interactions commute with the free Hamiltonian, instead of specifying a certain time where the unitary operator acts, it is also possible to express the action

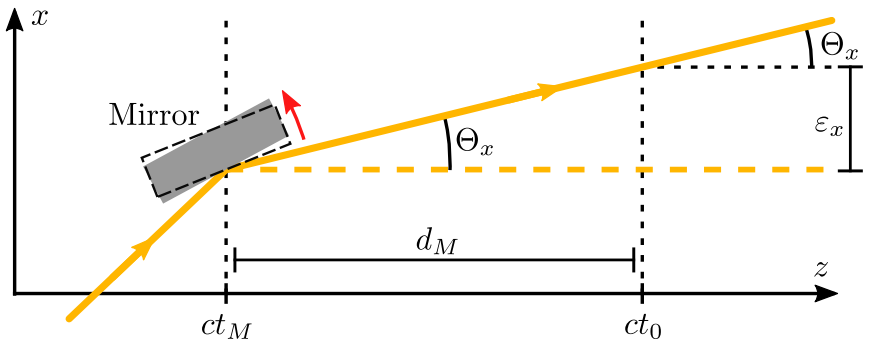

Figure 5.3: **Effective Displacement due to Mirror** A small tilt of a mirror at some longitudinal position ct_M is equivalent to the introduction of a beam tilt by an angle Θ_x, along with an additional displacement ε_x at a different longitudinal position ct_0, where the relative distance is d_M.

with respect to a reference time t_0 chosen, e.g., as the time when the evolution traverses the waist of a beam. As illustrated in Fig. 5.3, introducing an angular deflection at a longitudinal distance $L = c(t_0 - t_M)$ from ct_0, where ct_M is the longitudinal position of the mirror, is equivalent to introducing the same deflection at location ct_0, together with an additional displacement $\varepsilon_x \approx L\theta_x$. The effective time-independent unitary for the mirror at t_1 can then be expressed as

$$\mathbf{U}_M = e^{i(\varepsilon_k \mathbf{x} - \varepsilon_x \mathbf{k}_x)} = e^{i\varphi} e^{i\varepsilon_k \mathbf{x}} e^{-i\varepsilon_x \mathbf{k}_x} = e^{-i\varphi} e^{-i\varepsilon_x \mathbf{k}_x} e^{i\varepsilon_k \mathbf{x}} \tag{5.16}$$

where the distance of the mirror from ct_0 is encoded in the strength of the additional displacement ϵ_x. The action of the mirror effectively corresponds to a Weyl operator (2.16) and the joint application of deflection and displacement is equivalent to a subsequent application up to global phase. Finally, it should be noted that, for purely geometrical reasons, the parity transformation induced by a reflection introduces a phase of π between the linear polarization direction parallel to the mirror surface and the orthogonal direction. The same effect of course also occurs for reflections at beam-splitters. Since a path can involve several reflections, usually only the final polarization state is of relevance when considering superpositions of light from different paths and the effect can be completely neglected when each path involves the same parity of reflections.

A local interaction between path and transverse degrees of freedom which clearly does not commute with the free evolution is the action of a lens. The unitary transformation $\mathbf{U}_L$ induced in the paraxial approximation over a short time interval $[t_1, t_2]$ by a thin lens can be expressed as [519, 530]

$$\mathbf{U}_m = \mathbf{U}_L(t_1, t_2) := e^{-i\frac{k}{2f}(\mathbf{x}^2 + \mathbf{y}^2)}, \tag{5.17}$$

where f is the focal length of the lens. In the case of a Gaussian beam this transformation can be conveniently calculated with the method of Matrix optics, as described in Sec. 4.2.2. Lenses are particular useful to shape the transverse wavefunction according to the experimental requirements and can also be used for example to perform a full Fourier transform

of the transverse degrees of freedom, without the need to go to the far field of Fraunhofer diffraction [519, 530], as introduced below in Sec. 5.3.1. By using *cylindrical lenses* the same effects can be applied to only one of the two transverse directions of the beam.

5.1.8 Birefringence

While all interactions introduced so far involve only coupling between the path and one other degree of freedom, so-called *birefringent* optical elements allow polarization dependent effects on the spatial modes. A typical example extensively used in the experiments described in this work is a unixaial birefringent plane parallel crystal [516, 530, 537]. A uniaxial crystal is an homogenous approximately non-dispersive medium which is anisotropic, i.e., characterized by a single distinguished direction called *optical axis*. The crystal possesses two different refractive indices, which depend on the particular material, where the *extraordinary* index of refraction n_E is associated with the optical axis and the *ordinary* index n_O corresponding with the remaining transverse plane. When light propagates inside such an unixaial crystal, two special polarization directions can be distinguished, namely the *ordinary polarization* component which is perpendicular to the optical axis, and the *extraordinary component* which lies in the plane defined by propagation direction and optical axis. The two polarization components experience different indices of refraction, which is n_O for the ordinary component and an effective index n_{eff} with a value between n_O and n_E for the extraordinary components, where the exact value of n_{eff} depends on the relative orientation between the local k-vector of the extraordinary component and the optical axis. This does not only lead to different refraction angles for the two polarization components at the crystal boundary but additionally to the so-called *walk-off* of the extraordinary component. The walk-off is a result of the anisotropy of the medium, which leads to a Poynting current which is no longer parallel to the local k-vector, i.e., the mean propagation direction of the light is changed.

The combination of polarization dependent refraction and walk-off in general leads to different propagation directions through the crystal for the two polarizations, which in turn results in different transverse displacements, time-shifts and in general an inhomoegenous polarization state for the free light outside of the crystal, even in the case of an initially homogeneous polarization. The effective unitary operator $\mathbf{U}_{\text{BR}}$, again acting for a short time-interval on all parts of the Hilbert space of the PWF except the path can be written as

$$\begin{aligned}\mathbf{U}_m = \mathbf{U}_{\text{BR}} := e^{i\varphi_E}\mathbf{\Pi}_E \otimes e^{-i\epsilon_E \mathbf{k}_E}\,\mathbf{U}_T(n_{\text{eff}}, L_E) \otimes \mathbf{U}_z(n_{\text{eff}}, L_E) \\ + e^{i\varphi_O}\mathbf{\Pi}_O \otimes e^{-i\epsilon_O \mathbf{k}_O}\,\mathbf{U}_T(n_O, L_O) \otimes \mathbf{U}_z(n_O, L_O),\end{aligned} \tag{5.18}$$

where $\mathbf{\Pi}_j$ with $j \in [O, E]$ are projectors on the two polarization eigenstates and ϵ_j the effective displacements in the two transverse directions $\mathbf{k}_j$, which in the general case are not necessarily parallel. The longitudinal time-shift is divided into phase and envelope parts, as introduced in Eq. 5.10, where also the crystal tilt has to be taken into account when calculating the effective lenghts L_j. Notably, this evolution commutes with the free Hamiltonian. See also [715, 867, 909] for more detailed descriptions of the properties of

uniaxial birefringent crystals.

By using particular configurations of several birefringent crystals it is possible to avoid all effects on the spatial degrees of freedom and achieve a local change of polarization only. A typical tool of this type are *waveplates* [530, 537], which usually are designed in so-called *zero-order* configurations of two successive birefringent crystals with perpendicular orientations of optical axes. In this case each polarization component experiences both the evolution as the ordinary and as the extraordinary component, which leads to an effective cancellation of the relative longitudinal shifts and the same transverse displacement behavior as for an isotropic medium. By choosing slightly different thicknesses for the two crystals it is possible to introduce a well-controllable phase-shift between two linear polarization eigenstates $|\phi_1\rangle$ and $|\phi_2\rangle$, which are determined by the orientation of the optical axes of the crystals. Since the phase-shift is determined by the ratio of optical path length difference and wavelength, and, additionally, in general the refractive index is wavelength dependent, waveplates work as intended only for light with a sufficiently narrow spectrum around a central wavelength for which the waveplate is specifically designed. For a so-called *half-wave plate* (HWP) the relative shift is exactly π, i.e., half of a cycle, leading to the unitary evolution $\mathbf{U}_{\mathrm{HWP}}$ of the form

$$\mathbf{U}_m = \mathbf{U}_{\mathrm{HWP}} := e^{i\varphi} \left(|\phi_1\rangle\langle\phi_1| - |\phi_2\rangle\langle\phi_2| \right), \tag{5.19}$$

where in general additionally a global phase of φ is acquired. In effect, the HWP allows to transform between different linear polarizations. Note that the waveplates are typically assumed to be sufficiently thin, such that the global retardation can be neglected. A phase shift of $\pi/2$, accordingly leads to a *quarter wave-plate* (QWP) described by the unitary $\mathbf{U}_{\mathrm{QWP}}$ with

$$\mathbf{U}_m = \mathbf{U}_{\mathrm{QWP}} := e^{i\varphi} \left(|\phi_1\rangle\langle\phi_1| \pm i|\phi_2\rangle\langle\phi_2| \right) \tag{5.20}$$

$$= e^{i\varphi} \left(|R\rangle\langle\phi_1'| + |L\rangle\langle\phi_2'| \right), \tag{5.21}$$

where $|\phi_1'\rangle \propto |\phi_1\rangle \pm |\phi_2\rangle$ and $|\phi_2'\rangle \propto |\phi_1\rangle \mp |\phi_2\rangle$. The QWP thus allows to transform between the two circular polarizations and two linear polarization states determined by the waveplate's rotation. See, e.g., [490] for a more detailed discussion of the transformations induced by waveplates. In a similar manner, as described, e.g., in [715, 909] and employed in the experiment introduced in 7.7.2, a pair of thick birefringent crystals of approximately equal thickness can be used to generate zero-order beam separations in which the relative longitudinal and transverse effects on the two polarization eigenstates cancel out.

Of course there are also many more optical components, which also can be described in the formalism of the PWF, such as liquid crystal retarders or Dove prisms, but their description lies outside the scope of this work. The selection of evolutions and interactions of the five degrees of freedom, as described above, is entirely sufficient to describe all free space experiments which are subject of this thesis and in fact many experiments with paraxial photons.

5.2 Nonlinear Optical Processes

5.2.1 Light in Nonlinear Media

Apart from the linear optical processes described in the previous section, also nonlinear effects play a crucial role in optical experiments. Commonly, however, while the interactions themselves are mediated by nonlinear processes the effective output states depend linearly on the input states, such that the whole optical setup can be effectively described as a series of linear interactions, and accordingly is called a *linear optical network* [610, 629]. In the context of this work nonlinear effects are relevant only for the generation of particular states of light and all other nonlinear effects can be safely neglected.

A common way to describe nonlinear optical processes is to start with a classical description and then introduce field operators at a later point, whenever necessary to capture particular quantum effects. The basic formalism of classical nonlinear optics is based on the concept of the *polarization* $\vec{P}$ of a medium, which has the dimension of a dipole moment density and corresponds to an inhomogeneity in the charge distribution in the medium induced by an electromagnetic field. In the case of an instantaneous, i.e., frequency independent response of the medium, it can be expanded in orders of electric field strength $\vec{E}$ as [629, 515]

$$P_j(\vec{x},t) = \epsilon_0 \left(\sum_k \chi^{(1)}_{jk} E_k(\vec{x},t) + \sum_{kl} \chi^{(2)}_{jkl} E_k(\vec{x},t) E_l(\vec{x},t) + \mathcal{O}(E^3) \right), \tag{5.22}$$

where P_j and E_j represent the j-th components of polarization and electric field, respectively and the coefficients $\chi^{(j)}$ are called j-th order *susceptibilities* of the medium. While the first-order susceptibility represents a 3×3 matrix, the higher order susceptibilities are given as tensors of rank $j+1$. In typical media the higher order susceptibilities are much smaller than the components of $\chi^{(1)}$, such that only for high intensity light, provided for example by focused lasers, the effects of nonlinearities become significant. Note that the description in terms of susceptibility represents an effective phenomenological description in the sense that many different nonlinear physical mechanisms can lead to effectively the same relations between field and polarization $\vec{P}$ [515].

According to *Larmor's theorem* [27] any moving charges generate electromagnetic radiation and thus crucially new components of the electromagnetic field can appear as an effect of a time-varying polarization of the medium [511, 515]. A simplified expression of such a process, which fits to many practical scenarios, can be given by decomposing the field into a sum of monochromatic components and considering specific frequency components of the polarization. Then, for a general medium with a frequency dependent response, the polarization component of frequency ω can be written as a function of second-order susceptibility as [524, 515, 566]

$$P_j(\omega) = \sum_{jkl} \sum_{\substack{mn \\ \omega_n \pm \omega_m = \omega}} \chi^{(2)}_{jkl}(\omega, \omega_m, \omega_n) E_k(\omega_m) E_l(\omega_n), \tag{5.23}$$

where in contrast to Eq. (5.22) the susceptibility is now also frequency dependent. Note that, since second-order nonlinear effects can only generate sum and difference frequencies for pairs of frequency components of the field, the summation is restricted by the condition $\omega_n \pm \omega_m = \omega$. The above expression encapsulates many basic processes of nonlinear optics such as sum- and difference-frequency generation of fields with two different frequency components, or second-harmonic generation for single frequency fields. Similarly, for monochromatic fields, the third-order susceptibility can lead to third-harmonic generation or alternatively an oscillation of the polarization with the same frequency as the field. Crucially, the latter effect corresponds to an intensity dependent change of the index of refraction, known as the *optical Kerr-effect* [515]. It has many useful applications and can be used for example to perform QND measurements of photon number by inducing an effective interaction between a high intensity light field and single photons [525, 531, 723] or to implement intensity dependent self-focusing of light fields, known as *Kerr-lensing* [577, 601, 664].

In general in a particular medium the susceptibility has non-vanishing components only for certain frequencies and directional modes. Semi-classically, this frequency dependence can be seen as originating from the particular spatial distribution of the atomic dipoles oscillating in the material, such that the respective frequency is only radiated if the oscillations are in phase. Accordingly, the determination of possible emission frequencies and directions for a given input field is called *phase-matching* [516, 511, 629, 515, 566]. For example for sum-frequency generation with paraxial fields, the phase-matching condition can be expressed in terms of the mean k-vectors of the respective fields with the relation

$$\delta\vec{k} = \vec{k}_1 + \vec{k}_2 - \vec{k}_S = 0, \tag{5.24}$$

where $\vec{k}_S$ is the wave-vector of the sum-frequency. The quantity $\delta\vec{k}$ is called k-vector *mismatch* and for $\delta\vec{k} = 0$ so-called *perfect* phase-matching is achieved.

A typical method to tune the phase-matching is the use of birefringent crystals as nonlinear media, which provide different indexes of refraction for differently polarized field components. By tuning the orientation of the crystal, the effective refractive indices for the different polarizations can be adjusted which allows to achieve phase-matching for the desired frequencies and directions of radiation. For such second-order processes with three frequency components, different *types* of phase-matching are distinguished dependent on the relation of the polarization states of the lower frequency modes, where *type-I* corresponds to equal and *type-II* to orthogonal polarizations [629, 515]. Furthermore, dependent on the k-space composition of the modes, *collinear* and *non-collinear* processes are distinguished.

5.2.2 Parametric Amplification

In many cases the classical formalism of nonlinear optics as described above can be connected to the formalism of QFT. A simplified picture is given by so-called *photon energy-level diagrams* [524, 515] in which the conversion between different frequency modes is

considered on the level of single-photon excitations and absorptions in the corresponding modes. Such diagrams are especially suited for processes in which the net energy flow between medium and fields, both incoming and radiated, is zero, called *parametric processes*. An important example of such a parametric process is difference frequency generation in which a second-order nonlinear effect creates radiation with the frequency $\omega = \omega_2 - \omega_1$, for two input frequencies ω_1 and ω_2. When considering this process on a single-photon level, it becomes clear that for the removal of one excitation of high frequency ω_2 not only a photon of frequency ω is created, but also, due to energy conservation, an additional photon of input frequency ω_1. Thus a side effect of difference frequency generation is the amplification of the lower input frequency, a process known as *optical parametric amplification* [529, 531, 524, 511, 515, 566]. In this context the high frequency field with frequency ω_2 providing the energy is called the *pump*, the amplified frequency ω_1 the *signal*, and the byproduct difference frequency ω the *idler*.

In a simple semi-classical approach to the description of parametric amplification the pump field is treated classically and signal and idler as quantum fields. For the general case that signal and idler frequencies correspond to different modes, either due to different frequencies or different propagation directions, the resulting Hamiltonian can be shown to be [529, 525, 531]

$$\mathbf{H}_{\mathrm{PA}} = \hbar\omega_1 \mathbf{n}_A + \hbar\omega_2 \mathbf{n}_B + i\hbar\chi_\alpha^{(2)}\big(\mathbf{a}_A^\dagger \mathbf{a}_B^\dagger e^{-i\omega t} - \mathbf{a}_A \mathbf{a}_B e^{i\omega t}\big), \tag{5.25}$$

where here the subscripts $\{A, B\}$ denote signal and idler modes, respectively, and $\chi_\alpha^{(2)}$ is an effective coupling constant which depends on the scalar second-order susceptibility of the medium as well as on the amplitude α of the pump with pump frequency ω. The terms $\hbar\omega_j \mathbf{n}_j$ represent the free Hamiltonians of the two modes and the last term the interaction part. In the degenerate case with $\mathbf{a}_A = \mathbf{a}_B$, in which a factor of $1/2$ has to be added to the Hamiltonian to account for the degeneracy of the modes [529], the resulting unitary interaction operator exactly corresponds to the squeezing operator $\mathbf{S}(\xi)$, as introduced in Sec. 4.4.3, where the squeezing parameter is given as $\xi = \chi_\alpha^{(2)} t$. Assuming an initially coherent state of the signal mode, the Hamiltonian leads to amplitude squeezing by the factor $|\chi_\alpha^{(2)} t|$ and thus parametric amplification represents one of the methods to generate squeezed states of light [657, 612, 529, 531, 524, 511], first realized by the group of Kimble [661]. Since squeezing implies that different parts of the oscillation cycle are affected differently by the amplification, in this sense the latter can be said to be a "phase-sensitive" process. In the case of two different modes $\mathbf{a}_A$ and $\mathbf{a}_B$ the amplification induces correlations in the fluctuations of the two modes leading the a *two-mode squeezed state* [612, 529, 525, 524, 136, 338], which in general depends on the initial state of signal and idler modes and is given by the action of the two-mode squeezing operator $\mathbf{S}_2(\xi) = \exp(\xi^* \mathbf{a}_A \mathbf{a}_B - \xi \mathbf{a}_A^\dagger \mathbf{a}_B^\dagger)$.

5.2.3 Spontaneous Parametric Down-Conversion

In contrast to parametric amplification in which the decay of the pump photons into signal and idler is stimulated by the signal field, the same process can also occur spontaneously

due to quantum fluctuations. Since in this case the experimental goal is the generation of a two-mode squeezed state of light itself, the terms "signal" and "idler" are no longer fitting. However, they are still broadly used to denote the two components of the resulting signal. As in this scenario a small part of the high frequency excitations of a coherent pump beam is converted into two photonic excitations with lower energies, which sum up to the pump energy, this process is commonly called *spontaneous parametric down-conversion* (SPDC) or also *parametric fluorescence* [525, 524, 629, 515, 566, 338, 642]. Formally, this process can be expressed via the action of the Hamiltonian $\mathbf{H}_{\mathrm{PA}}$ for some finite time, where crucially the excited modes $\mathbf{a}_1$ and $\mathbf{a}_2$ correspond to propagating wave-packet modes [524]. In effect, the resulting state is given by an application of the two-mode squeezing operator $\mathbf{S}_2$ to the two signal modes, which are initially in the vacuum state, leading to the two-mode state $|\Psi\rangle = \mathbf{S}_2 |0\rangle$. The indefinite photon number of correlated photons in the signal fields is related to the fact that also an indefinite number of photons from the coherent pump state participates in the down-conversion process. The second-order correlation function (4.51) of $|\Psi\rangle$ between the two modes at zero time-difference is super-Poissonian, with $g^{(2)}(0) > 1$, and falls for increasing τ, i.e., the detection events for the two modes are bunched [529, 524]. This motivates the use of SPDC, together with suitable postelection, to create photon-pair states or, as described below, even multi-photon states with a definite number of photons.

In the number state representation the state $|\Psi\rangle$ can be written as [529, 642]

$$|\Psi\rangle = \sqrt{1 - \tanh^2 |\xi|} \sum_{n=0}^{\infty} \left(-\frac{\xi \tanh |\xi|}{|\xi|} \right)^n |nn\rangle \,, \tag{5.26}$$

where the amplitude for each component $|nn\rangle$ is of leading order ξ^n. By postselecting on the detection of a coincidence of n photons in each of the modes, i.e., conditioning of all prior measurements on that particular successful detection event, effectively an experiment with the state $|nn\rangle$ can be realized. As mentioned in Sec. 4.5.1, however, typically APDs without photon number resolution are employed for the detection of single photons such that the detection of coincidences allows only for postslection on the subspace $\mathbf{\Pi}_{\bar{0}} = \mathbb{1} - |0\rangle\langle 0|$. If the goal is the creation of a *pair state* $|11\rangle$, the typical approach is to choose not too high pump intensities such that all higher order terms in ξ can be neglected. For the effective generation of multi-photon states, multiplexed postselection is a common solution, see, e.g., [328] for an experimental realization. Finally, a partial postselection applied on the pair state is also the principle behind the generation of so-called *heralded* single photons, in which case, however, the single photons are produced at random times, where the durations of the time-intervals between successive production events follow a falling exponential distribution [511, 579].

While the Hamiltonian $\mathbf{H}_{\mathrm{PA}}$ corresponds to a single pump mode with frequency ω and just two signal modes, in general the phase-matching condition (5.24) is satisfied for a continuum of signal mode pairs. Additionally, in practice any pump has a finite spectral width and no phase-matching is perfectly selective, such that the range of excited signal modes is even larger. In effect, the resulting field state is significantly more complicated than just $|\Psi\rangle$ and corresponds to a superposition of several such states [525]. Furthermore,

the two detectors used for the detection of coincidences usually project only on a subset of the down-converted modes such that each detector also registers photon detections without a pair at the other detector. The conditioning on coincidences thus not only projects out the vacuum but also such uncorrelated detection events, called *singles*. In practice, single counts can also result from imperfect filtering of a pump mode which has a finite spatial overlap with the detectors. Note that the reduced single mode state of $|\Psi\rangle$ corresponds to a thermal state.

Although the state $|\Psi\rangle$ is entangled, the postselected pair state $|11\rangle$ represents a separable product state. To generate an entangled two-photon state, as used in a plethora of quantum experiments and routinely applied in quantum technology, it is necessary to coherently overlap two SPDC processes [642]. One type of approaches is based on bringing the pump field into equal superposition of two modes C and D in each of which a SPDC process with signal sub-modes A_j and B_j, with $j \in \{C, D\}$ is implemented. In effect, when considering postselection on the two-photon subspace, the SPDC results in the four-mode state $|\Psi_{\text{pair}}\rangle$ with

$$|\Psi_{\text{pair}}\rangle = \frac{1}{\sqrt{2}} \left(|\Psi_C\rangle + |\Psi_D\rangle \right) = \frac{1}{\sqrt{2}} \left(|1010\rangle + |0101\rangle \right), \tag{5.27}$$

where the notation $|n_{A_C} n_{A_D} n_{B_C} n_{B_D}\rangle$ has been used to denote the mode occupation. In an alternative scheme a similar state can also be produced with a single pump mode, which couples to a range of mode pairs, by postselection on a coherent superposition of two of the latter. Such an approach has been realized in the seminal design of a type-II polarization-entangled photon source by Kwiat *et al.* [607]. By combining superpositions of pump states with postselection on superpositions of modes, also more complicated entangled states can be generated, such as so-called *hyper-entangled* states [629], which involve independent entanglement of the photons across several degrees of freedom, as used in the experiment **[P4]**, presented in Sec. 3.4.4. The entangled two-photon source employed in the trajectory experiment, described in Ch. 7, follows the design developed in [584], which implements a doubling of the pump-mode and colinear type-I so-called *quasi-phasematching* in a periodically-poled birefringent crystal [629, 515]. See [909] for an excellent overview over the corresponding details, setup, and tuning of the source.

The state $|\Psi_{\text{pair}}\rangle$ is typically conveniently expressed in the wave-mechanical formalism using a two-photon wave function [627, 647, 626]. For example, if modes A_C and A_D are localized in the same region, they can be identified with the Hilbert space of a photon A and vice versa for a second photon B with modes B_C and B_D. Then the field states $|1010\rangle$ and $|0101\rangle$ from (5.27) correspond to the two-photon states $|C_A C_B\rangle$ and $|D_A D_B\rangle$, respectively. The state $|\Psi_{\text{pair}}\rangle \in \mathcal{H}_A \otimes \mathcal{H}_B$ can then be written as

$$|\Psi\rangle = \frac{1}{\sqrt{2}} \left(|C_A C_B\rangle + |D_A D_B\rangle \right), \tag{5.28}$$

which corresponds to an entangled bipartite state. Note that, while the state above happens to be symmetric, this is not the case in general for two-photon states and, as discussed in

Sec. 1.2.2, usually an additional symmetrization is required when two-particle interference is to be properly described.

5.2.4 The Laser

The principal light source which underlies the vast majority of contemporary experiments and applications of optics is the *laser*, as first successfully implemented by Maiman [615], where the acronym "LASER" stands for "light amplification by stimulated emission of radiation". The laser represents a prime example of a non-parametric nonlinear process in which energy is continuously transferred to the light field via an interaction with a nonlinear medium. The basic structure of a laser consists of this so-called *gain medium* enclosed by an optical cavity as well as a mechanism that supplies energy to the gain medium, commonly called *pumping* [517, 513, 525, 511, 530, 623]. The cavity typically consists of one essentially fully reflective and another highly reflective mirror surface, such that a high field intensity builds up inside the cavity of which only a small portion is transmitted as emerging laser light. If the field intensity of a particular cavity mode is sufficiently high, preferential emission from the medium into that mode is stimulated due to the nonlinear response of the medium. This enables lasers to generate high intensity light with a very narrow range of spectral and spatial modes.

In general two regimes of laser operation can be distinguished, characterized by a *threshold* corresponding to a certain pump power at which a transition between the two regimes occurs [517, 513, 524, 511]. For low pump powers below the laser threshold the stimulated emission is not the dominant effect and typically several cavity modes are excited simultaneously. Above the threshold, due to stimulation of emission, the whole pump power is transferred to only a small subset of modes suppressing emission into the others, commonly called *quenching*. Since the stimulation is phase-sensitive, the amplification results in approximately coherent states of the light. In the basic type of laser operation, called *continuous-wave* (CW) operation, this process is allowed to continue for a time which can be effectively regarded as infinite compared to the length of a cycle. Of course also CW laser light has only a finite coherence length, which, however, typically has a macroscopic length scale, such that the light is well-approximated by a single mode coherent state. See [529, 525, 524, 623] for comprehensive overviews both of the semi-classical as well as the quantum theory of the laser.

An alternative to CW operation are so-called *pulsed lasers*, which generate sequences of pulses, i.e., light fields localized in time, as discussed in Sec. 4.1.3. Such pulses can be generated for example by rapidly turning the pumping on an off in which case, however, there is no fixed relation between the carrier phases of successive pulses. Thus, if the goal is to generate pulsed fields corresponding to the frequency combs introduced in Sec. 4.1.3, an additional mechanism is required in order to achieve phase-coherent amplification of a continuum of spectral modes, called *mode-locking* [623]. This can be realized for example by adding a mechanism for saturable absorption into the cavity, e.g., via a combination of Kerr-lensing with the choice of a gain region which is smaller than the cavity modes, such that pulsed high intensity light obtains a better overlap with the gain region through

self-focusing [664]. CW modes, which have only small peak intensity and thus exhibit vanishing self-focusing, are thus effectively quenched, leading to emission into high peak intensity wave-packet modes.

There exists a wide range of technical realizations of the laser principle which can be broadly categorized with respect to the employed gain medium. Common types are gas lasers, dye laser, and solid state lasers. See [513, 530, 634] for overviews over the more practical aspects of laser physics. The experiments performed in the context of this work are based on solid state lasers, with additional external cavities in so-called *Littrow configuration* [585, 614, 596] allowing for a finer mode selection and thus narrower spectral widths.

5.3 The Double-Slit

5.3.1 Optical Description

The prototypical optical double-slit is a special case of a *Fresnel-Kirchhoff diffraction* scenario in which a propagating light field is spatially filtered via partial absorption at a two dimensional *aperture* described by a real transverse transmission function $\Omega(x, y)$ [514, 517, 530, 537]. Assuming a large distance between the aperture and the light source, the incoming field can be approximated as a plane wave and commonly the simple case of paraxial light propagation in z-direction is considered, i.e., perpendicular to the aperture. Then in the *Fraunhofer* limit of imaging at an infinitely distant plane parallel to the aperture the resulting spatial pattern simply corresponds to the Fourier transform of the transmission function Ω. This description of diffraction also holds approximately in regions which are sufficiently far from the aperture such that the phase-fronts of the light field are approximately plane. This region is called *far field*, accordingly. In contrast, the *near field* represents the region close to the aperture where the effects of phase-front curvature are significant and which can be well approximated with the more general *Fresnel* theory of diffraction [514, 517, 530, 821], which also holds in the far-field. Note that the separation into near and far field is not a clear distinction but rather a gradual statement about the quality of the respective approximations.

A double-slit corresponds to a transmission function Ω_{DS} which can be expressed as the sum of two identical transmission functions Ω displaced by a distance of b in x-direction. Usually a "slit" is understood as infinitely extended in the orthogonal y-direction such that the description reduces to a two-dimensional problem for which only the x and z-directions are of interest. However, the essential condition for a two-dimensional description is that Ω factorizes into x and y dependent parts Ω_x and Ω_y, which is why in the following "slit" is used more broadly to denote such factorizing transmission functions. In effect, a general transmission function for a double-slit can be written as $\Omega_{\mathrm{DS}}(x, y) := \big(\Omega_x(x - b/2) + \Omega(x + b/2)\big)\Omega_y(y)$. The transverse field amplitude $A_\perp^{(+)}$ in the Fraunhofer regime then

becomes [517, 537, 822]

$$\vec{A}_{\perp}^{(+)}(x,y) \approx \vec{A}_0 \cos\left(abx/2\right) \Upsilon_x(ax)\Upsilon_y(ay), \tag{5.29}$$

where $\vec{A}_0$ is an effective amplitude that depends on the initial field and the constant $a = k/z_D$ translates transverse momenta to far field positions with z_D being the longitudinal distance to the aperture. The intensity pattern thus corresponds to a sinusoidal oscillation with a spatial frequency $k_{\mathrm{DS}} = kb/2z_D$, which depends linearly on the separation between the two slits b, modulated by an envelope function which corresponds to the Fourier transform Υ_x of the horizontal slit function. The amplitude in vertical y-direction remains independent of x and simply corresponds to the Fourier transform Υ_y of the vertical slit function. The sinusoidal modulation of the transverse intensity along the axis of the slit is the hallmark of double-slit interference.

While the Fraunhofer limit gives a simple description for the interference pattern in the far-field, a general description in the near-field is more complicated. However, for paraxial light the formalism of the paraxial wavefunction $|\Psi\rangle \in \mathcal{H}_{\mathrm{light}}^{\mathrm{sgl}}$, as introduced in Sec. 5.1.1, can be applied, where here the path state is assumed to be identical and is thus neglected. An effective double-slit can be constructed by superposing two identical paraxial beams Ψ with

$$\Psi_{\mathrm{DS}}(\vec{x},t) = \frac{1}{2}\Big(\Psi(\vec{x} - b\hat{e}_x, t) + \Psi(\vec{x} + b\hat{e}_x, t)\Big). \tag{5.30}$$

The amplitude for any horizontal plane after the slit plane is then given by the fractional Fourier transform of the initial slit function Ψ_{DS}. For double-slits constructed from paraxial beams, the typical behavior described above, i.e., an illumination of the aperture with plane waves, is achieved when the effective position of the aperture is chosen to coincide with a longitudinal position at which the beam has plane phase-fronts, such as in the waist of a Gaussian beam.

5.3.2 Double-Slit Coherence

While, so far, an illumination of the double-slit with a plane wave has been assumed, the resulting pattern is modified if there is a more complicated relationship between the fields at the two slits. In the simplest case a relative phase is induced between the two otherwise identical components, which for example would be obtained if the slit is illuminated with spherical waves having a sufficiently small curvature compared to the size of the slits. In the far field, such a relative phase of φ between the two slits would simply lead to a phase shift of φ for the sinusoidal spatial interference pattern.

To account for general differences between the two fields corresponding to the two slits the apparatus of optical coherence, as introduced in Sec. 4.6.2, can be employed. In the simplest scenario [618, 529, 531, 637] the two slits are modeled as point-like pinholes such that the field at a plane after the double-slit can be modeled as a sum of spherical wave fields $\vec{\mathbf{E}}^{(+)}(\vec{r},t) = \vec{\mathbf{E}}^{(+)}(\vec{r}_\alpha,t_\alpha)/s_\alpha + \vec{\mathbf{E}}^{(+)}(\vec{r}_\beta,t_\beta)/s_\beta$, where $\vec{r}_j$ with $j = \alpha,\beta$ are the positions

of the two silts α and β, $s_j := |\vec{r} - \vec{r}_j|$ are respective distances to the location in question, and $t_j = t - s_j/c$ the effective propagation times. Assuming equal illumination for both pinholes, the variation of intensity at a sufficiently far location is then given by the first-order correlation function as $I(\vec{r}, t) \propto 1 + \mathrm{Re}\big[g^{(1)}(\vec{r}_\alpha, t_\alpha, \vec{r}_\beta, t_\beta)\big]$. Thus, while the phase of $g^{(1)}$ determines the spatial phase of the interference pattern, its modulus determines the amplitude. The latter is related to the *visibility* $\mathcal{V}$ defined as [618, 517, 531, 637]

$$\mathcal{V} := \frac{I_{\max} - I_{\min}}{I_{\max} + I_{\min}}. \tag{5.31}$$

In this simple scenario the visibility is approximately constant and equal to the modulus of the first-order correlation function with $\mathcal{V} = |g^{(1)}|$. As with any property dependent only on $g^{(1)}$, it is immediately clear that the same type of patterns are observed for any light field with equal first-order coherence, such as, e.g., coherent laser light and single photons [529].

For paraxial beams, the coherence effects can be taken into account by considering the overlaps of the polarization and longitudinal degrees of freedom. A typical example involves two homogeneously polarized transverse spatial states $|\psi_j\rangle \otimes |\phi_j\rangle \in \mathcal{H}_x \otimes \mathcal{H}_y$, which, as discussed above, factorize with respect to x and y-directions, such that the total state $|\Psi_j\rangle \in \mathcal{H}^{\mathrm{sgl}}_{\mathrm{light}}$ of slit j can be written as $|\Psi_j\rangle = |P_j\rangle\,|\psi_j\rangle\,|\phi_j\rangle\,|\zeta_j\rangle$, with some polarization state $|P_j\rangle$ and the longitudinal component $|\zeta_j\rangle$. The interference pattern then depends on the fractionally Fourier transformed amplitudes $\widetilde{\psi}_j(x_z) = \langle x_z|\psi\rangle$ and $\widetilde{\phi}_j(y_z) = \langle y_z|\phi\rangle$, where $|x_z\rangle$ is an eigenstates of the operator $\mathbf{x}_z$, as defined in Sec. 5.1.3, on the overlaps $\eta_{\mathrm{pol}} := |\langle P_\alpha|P_\beta\rangle|$ and $\eta_L := |\langle\zeta_\alpha|\zeta_\beta\rangle|$, as well as on the effective relative phase between the slits φ. For equal amplitudes of the two slits-components, the transverse intensity distribution can be written as

$$I(x_z, y_z) \propto \Big(|\widetilde{\psi}_\alpha(x_z)|^2 + |\widetilde{\psi}_\beta(x_z)|^2 + 2\eta_{\mathrm{pol}}\eta_L \mathrm{Re}\big[\widetilde{\psi}^*_\alpha(x_z)\widetilde{\psi}_\beta(x_z)e^{i\varphi}\big]\Big)|\widetilde{\phi}(y_z)|^2, \tag{5.32}$$

where crucially the y-dependence factorizes at all longitudinal positions z. In the far field for a sufficiently broad envelope function again a sinusoidal oscillation of the pattern emerges at least in a region sufficiently close to the center $x_z = 0$, with a visibility given by $\mathcal{V} \approx \eta_{\mathrm{pol}}\eta_L$, see Fig. 5.4. With a reduction of coherence between the two slits the interfrence term becomes suppressed and the intensity distribution starts to correspond more to an incoherent sum of the single slit intensities.

5.3.3 Complementarity and Disturbance

The double-slit represents a seminal physical scenario, which was persistently employed to illustrate crucial quantum optical effects in the history of physics, see, e.g., [541] for a historical overview. Early double-slit interference patterns as recorded by Young [46] were seen as a proof for the wave nature of light. In contrast, the experiments performed by Taylor a hundred years later in the context of nascent quantum theory [43], showed that these interference patterns persisted even if the intensity was lowered so significantly that

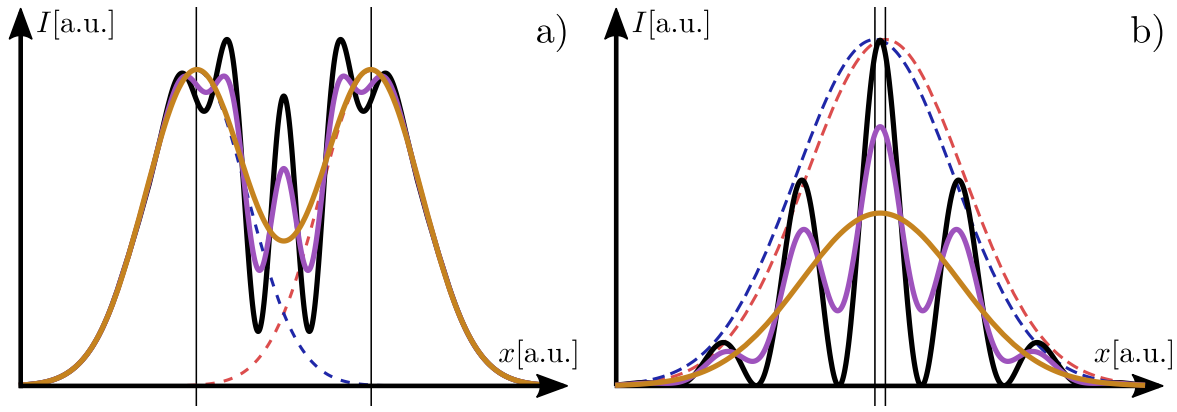

Figure 5.4: **Gaussian Double-Slit Interference Patterns** The two panels show double-slit interference patterns in horizontal direction x for Gaussian slits, calculated according to Eq. (5.32), at distances $z \approx 3.35 z_R$ (a) and $z \approx 90.2 z_R$ (b), with a separation of $b = 6w_0$. The dependence of the intensity distribution on the visibility is indicated by the solid colored lines, where black, purple, and brown correspond to visibility values of $\mathcal{V} = 1, 0.5, 0$, respectively. The dashed colored lines indicate the fractionally transformed envelope functions corresponding to the two slits, where in panel b), for better illustration, these envelopes are multiplied by a factor of 4. At the medium distance (in the order of z_R) in panel a) there is only small overlap of the envelope functions and only a small portion of the interference fringes appears. For the comparatively far distance (significantly larger than z_R) in panel b) the two beams have undergone a large amount of diffraction, such that the envelopes overlap almost perfectly, which approximates the Fraunhofer regime very well.

only few "indivisible units" of light energy, i.e., photons were present in the double-slit setup at any point in time, which seemed to imply a combination of wave and particle behavior for quantum systems. In the context of these results the double-slit scenario became one of the principal test beds to illuminate and test the predictions of quantum mechanics [33, 925, 51, 239, 822, 642]. Accordingly it and its extension to multi-slit interference have been realized with single photons [630, 557], as well as with other systems such as electrons [656], neutrons [323], neutral atoms [106], or even large molecules [245].

Double-slit experiments with single particles, most easily realized with light, are uniquely suited to demonstrate the complementarity of quantum mechanics. In this context the two relevant observables are the position observable in the near field $\vec{\mathbf{x}}_0 = \vec{\mathbf{x}}$ and the position observable in the far field $\vec{\mathbf{x}}_\infty \propto \vec{\mathbf{p}}$, which due to the free space propagation, effectively corresponds to the momentum of the near field wavefunction, see Eq. 5.5. Furthermore, in the near field typically a coarse grained position measurement is considered, which consists solely of two projectors onto the subspaces $\mathbf{\Pi}_\alpha$ and $\mathbf{\Pi}_\beta$ associated with each of the slits α and β, respectively. Accordingly, such a measurement is called a *which path* or *which way* measurement [531, 229], and sometimes formulations are used such as "it tells through which slit the particle went", see, e.g., [857, 1025], which seem to imply that this type of measurements provides some information about the past trajectory of the particle. As discussed in Sec. 3.4.2 in the context of delayed choice experiments, crucially the descriptive

and dispositive character of such statements has to be carefully distinguished.

In general the which-path measurement can be modeled as an interaction with a pointer which leads to a joint state $|\Theta\rangle$ of the form

$$|\Theta\rangle = \frac{1}{\sqrt{2}}\big(\,|\Psi_\alpha\rangle\,|\chi_\alpha\rangle + |\Psi_\beta\rangle\,|\chi_\beta\rangle\,\big), \tag{5.33}$$

where $|\Psi_j\rangle \in \mathcal{H}^{\mathrm{sgl}}_{\mathrm{light}}$ and $|\chi_j\rangle$ are the corresponding pointer states. As discussed in Sec. 2.2.1, the properties of the instrument then depend on the product of the pointer states $\langle\chi_\alpha|\chi_\beta\rangle$ as well as on the chosen pointer observable. From Eq. (5.32) it becomes clear that a non-selective measurement has exactly the same decohering effect as a reduced overlap of polarization and longitudinal degrees of freedom and for an ideal which-way measurement with $\langle\chi_\alpha|\chi_\beta\rangle = 0$ the double-slit visibility is entirely lost. Thus, from the perspective of SQM, an objectification of the path property leads to a change in the observable momentum distribution. Accordingly, a weakening of the which-path measurement leads to only a partial coherence loss. When considering conditional post-measurement states, various steering scenarios can be realized, as discussed in the context of delayed choice measurements in Sec. 3.4.2. For example by postselecting on equal superpositions of pointer states $|\chi\rangle = \big(\,|\chi_\alpha\rangle + \exp(i\varphi)\,|\chi_\beta\rangle\,\big)/\sqrt{2}$, a fully coherent double-slit pattern can be achieved, at least as much as the coherence between the two slit-components permits, with a phase fully controlable by the choice of postselection phase φ. In particular, the postselection with $\varphi = 0$ corresponds to a quantum erasure.

In the history of double-slit experiments this connection of the loss of interference visibility to the basic postulates of quantum measurements was not entirely clear and in the 1990s a lively debate ensued, regarding the question in which sense the loss of interference due to measurement back-action from which-path measurement can be modeled as a disturbance of photon momentum, see, e.g., [722, 233, 228, 229] for overviews. Such a picture goes back as far as to Bohr who writes about the double-slit:

> In fact, the renunciation in each experimental arrangement of the one or the other of two aspects of the description of physical phenomena [...] depends essentially on the impossibility, in the field of quantum theory, of accurately controlling the reaction of the object on the measuring instruments, i.e., the transfer of momentum in case of position measurements, and the displacement in case of momentum measurements. [6]

Bohr regards this description in terms of disturbance merely as useful picture and proceeds to repeat that fundamentally complementary quantities cannot be *defined* simultaneously, which makes it meaningless to consider their mutual disturbance. Note that the IDT relations discussed in Sec. 2.2.3 are of course well-defined independent of interpretation, as they do not consider the disturbance of system properties existing independently of measurement but disturbances of states or of outcome distributions.

Nevertheless, the concept of a physical mechanism for disturbance with simultaneously defined position and momentum has persisted in the history of quantum mechanics, most famously exemplified in Feynmans lectures, where a which-path measurement in a single

electron double-slit by scattering of light is described, with P_{12} being the distribution on the screen:

> Anyway, the light exerts a big influence on the electrons. By trying to "watch" the electrons we have changed their motions. That is, the jolt given to the electron when the photon is scattered by it is such as to change the electron's motion enough so that if it might have gone to where P_{12} was at a maximum it will instead land where P_{12} was a minimum; that is why we no longer see the wavy interference effects. [51]

This picture was shown to be highly misleading by Scully, Englert and Walther [329], who pointed to the possibility of a particular which-path measurement which does not disturb the wavefunctions ψ_α and ψ_β at all and thus crucially does not affect the distribution on the screen in any way when applied to a single slit. In a seminal experiment by Dürr *et al.* [280] a measurement of that type was realized, which, while not avoiding completely all disturbance of the component wavefunctions, could nevertheless reduce this disturbance to such an extent that the resulting disturbance of the probability distributions could *not* explain the disappearance of the interference pattern. From the corresponding debate [654, 334, 283, 344, 343, 1025, 722, 233, 228] the consensus emerged that while an IDT indeed fully accounts for the complementarity, this tradeoff has to be considered on the level of quantum states and distributions and not in a classical picture of random disturbance of well-defined momentum due to a position measurement. In conclusion, for a which-path measurement the laws of quantum mechanics do not impose any disturbance beyond the decoherence due to the distinguishability of the two paths and this decoherence can fully account for even total loss of interference visibility. Until today the double-slit remains a main reference to illustrate and discuss foundational questions of QM and it is particularly fruitful in the explanation of the physical mechanisms of Bohmian mechanics, see Sec. 7.5.

5.4 The Interferometer

5.4.1 Basic Principles of Interferometry

The oscillation of the electromagnetic radiation in the visible spectrum is removed from direct human experience, which can resolve events on the order of seconds or hundreds of milliseconds, by 14 or 15 orders of magnitude. Accordingly, as discussed in Sec. 4.5.1, temporal subcycle resolution of light is currently only achievable with extreme technological effort. In contrast, for propagating fields, the, in human standards, comparatively high velocity of light maps this oscillation over length scales of hundreds of nanometers, which are only 4 orders of magnitude below directly resolvable length scales of millimeters. The fundamental principle of interferometry is thus to translate temporal differences into spatial ones [618, 569]. The enormous difference in scales then explains why the interferometer represents such an immensely powerful tool in optics and why it has been possible to probe the properties of light via interferometric experiments since hundreds of years.

The core of any interferometer is the superposition of two or more field components, the relations between which can be investigated by controlling experimentally accessible spatial

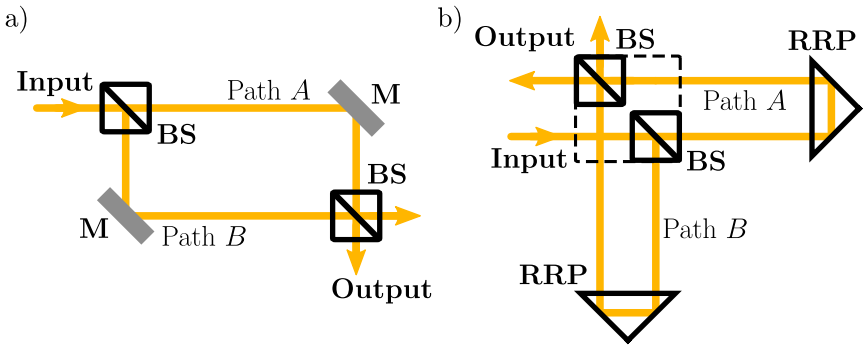

Figure 5.5: **Mach-Zehnder Interferometers** The two panels shown equivalent configurations of the MZI, where here in both cases the input beam-splitters separate paths A and B with an angle of 90 degrees. While in the standard version (a) two mirrors (M) redirect the beams towards the output beam-splitter, in the folded configuration (b), the mirrors are replaced by retro-reflecting prisms (RRP) instead. As indicated by the large dashed box, the folded configuration has the advantage of potentially allowing the use of only a single beam-splitter, reducing the amount of necessary optical components and thus increasing stability.

parameters. There is a plethora of possible realizations of optical interferometers, which can be coarsely divided into wave-front-separating and amplitude-separating configurations. Also the double-slit can be seen as interferometer, which depending on the realization is wave-front-separating as in the case of illumination of an aperture or amplitude-separating as in case of the splitting and subsequent overlap of two paraxial beams. See, e.g., [514, 517] for overviews over the extraordinarily rich field of interferometric methods in optics.

One of simplest interferometric setups based on amplitude separation of paraxial beams is the *Mach-Zehnder-Interferometer* (MZI) [531, 524, 511, 544, 629] as first proposed by Zehnder [47] and Mach [30], depicted in Fig. 5.5a. It establishes a two-dimensional path degree of freedom with path transformations induced by two beam-splitters, called the *input* and *output* beam-splitter, respectively, where additionally two mirrors redirect the beams towards the output beam-splitter. The region between the two beam-splitter is denoted as the *inner* part of the MZI and the paths outside of input and output beam-splitters, as input and output *ports*, respectively. In Fig. 5.5b also an alternative so-called *folded* configuration of the MZI is depicted, where the mirrors are replaced by retro-reflecting prisms, as used in two of the experiments described in Sec. 6. Note that, while in the examples of Fig. 5.5 the beam-splitters perform a right angle beam-separation, this is by no means required in a MZI.

For any superposition of paraxial beams, e.g., at one of the output ports of the MZI, the transverse intensity distribution depends on the first-order auto-correlation function $g^{(1)}(x, y, t, \tau)$ parametrized only by the two transverse coordinates, the absolute time t as well as the effective time difference $\tau = \delta l/c$ between two paths A and B [514, 517, 524]. The latter parameter encapsulates the interferometric translation from a well-controllable difference in optical path δl to effective time offset τ. A typical spatially-resolving measurement of the first auto-correlation function is given by imaging of the transverse mode

with a spatially-resolving detector, such as, e.g., a camera. Commonly also the total intensity at the output ports is considered, i.e., $g^{(1)}$ averaged over the whole transverse field. For quasi-monochromatic fields a variation of the optical path-length difference between the two arms, leads to a sinusoidal oscillation of the total intensity at the two output ports, which allows to define *interferometric-visibility* similarly to the spatial visibility for the double-slit (5.31). Due to the unitarity of all involved processes, which also implies conservation of energy, the dependence on the output intensity at the two output ports on the interferometric phase φ has an offset of π, i.e., the sum of the total intensities at the two ports is constant. In the extreme case of maximal intensity at one and minimal intensity at the other output port, the ports are commonly denoted as *bright* and *dark port*, respectively. Of course for smaller visibilities these terms loose their significance as the intensities at the two ports change less with variation of phase and remain more equal. By measuring the output intensity for different values of optical path difference, the MZI allows to reconstruct the whole first-order auto-correlation function and thus in effect also the spectral density of the light [514, 524].

In terms of the paraxial PWF, as defined in Sec. 5.1.1, the total state of the light inside an MZI-type interferometer $|\Psi\rangle \in \mathcal{H}_{\text{light}}^{\text{sgl}}$ can be written as

$$|\Psi\rangle = \alpha_A |\psi_A\rangle |P_A\rangle |\zeta_A\rangle |A\rangle + e^{i\varphi}\alpha_B |\psi_B\rangle |P_B\rangle |\zeta_B\rangle |B\rangle , \tag{5.34}$$

where $\alpha_j \in \mathbb{R}$ with $\alpha_A^2 + \alpha_B^2 = 1$ denote the moduli of the amplitudes of the light in the two paths and φ is again a phase-shift resulting from small-scale relative difference in optical path length which essentially leaves the slow variation of the longitudinal wavefunctions unaffected. The full state consists of the transverse spatial components $|\psi_j\rangle \in \mathcal{H}_x \otimes \mathcal{H}_y$, some polarization states $|P_j\rangle$, the longitudinal components $|\zeta_j\rangle$, and the two path states $|A\rangle$ and $|B\rangle$. Thus for an output port which corresponds, e.g., to transmission of path A and reflection of path B, the visibility simplifies to the product of overlaps of the beams in their three degrees of freedom with $\mathcal{V} = \alpha_A\alpha_B rt\eta_T\eta_{\text{pol}}\eta_L$, where additionally $\eta_T := |\langle\psi_A|\psi_B\rangle|$ denotes the overlap of the transverse modes. By extending the principle of the MZI to multiple paths, higher dimensional discrete degrees of freedom can be implemented, alongside suitably unitary transformations.

In interferometric experiments the notion of the PWF allows to consistently employ a description of photons as localized particles, which propagate through interferometers and "arrive at" or "pass through" the beam-splitters. Furthermore, since interferometers have total path lengths on the order of tens of centimeters and, for typical spectral widths of down-converted photons of a few nanometers, the coherence length is on the order of hundreds of microns, it is meaningful to state that at a certain point in time a photon "is inside" the interferometer, in the sense that it has a vanshingly small probability to be detected outside.

5.4.2 Second-Order Correlation Measurements

Interferometric experiments allow to illustrate and investigate second-order correlation properties of light fields, in particular non-classical behavior. An early success of the quan-

tum optical formalism of correlation functions was the explanation of so-called *intensity interferometry* experiments as first performed by Hanbury-Brown and Twiss (HBT) [570, 572, 571, 522]. The goal of the original HBT experiment was to measure the angular diameter of a distant star via a stellar interferometer, which consists of two spatially separated mirrors focusing the respective components of incident light on photodetectors. The relevant signal was the change of correlation between the two measured intensities upon a variation of mirror distance, i.e., the second-order correlation function g^2 (4.50), which, crucially, is independent of the relative phase between the lightfields at the two mirrors. This allowed to deduce the angular diameter of the star by considering the reduction of second-order coherence with increasing mirror distance [589, 517, 531]. Compared to hitherto applied techniques of stellar interferometry which aimed to measure the first-order correlation function via superposition of two light fields, the HBT method had the great advantage that no phase stability was necessary and in general all short-timescale fluctuations in the signal where averaged out due to the photoelectric intensity measurement. While the intensity correlations of the HBT experiment still possesses a classical explanation, nevertheless Glauber's field theoretical explanation, in terms of photon bunching detected by a measurement of the second-order correlation function, represented a seminal milestone in the development of quantum optics [529, 531, 629, 637, 642].

Cases of optical interference without any classical description are given by one and two-photon interference. In fact already the behavior of single photon arriving at one of the ports of beam-splitter is non-classical when a measurement of the second-order correlation function between the two output ports is considered. Since $g^{(2)} = 0$ for the single-photon state, trivially no coincidences between the photo-counts at the two output ports will be detected. Notably, the resulting singe-photon two-mode state $|\Psi\rangle = \big(\,|1_A 0_B\rangle + |0_A 1_B\rangle\,\big)/\sqrt{2}$ even represents at least formally an entangled state of the light field [524]. Due to finite detector integration time and crucially also to dead-time of typical detectors with single-photon resolution, $g^{(2)}(\tau)$ usually cannot be directly measured by a single detector placed at a particular location for arbitrary short time-differences τ. Thus a single beam-splitter in combination with two detectors at the output ports is the common practical method to measure the second-order correlation function and in particular to characterize the quality of single-photon sources [524, 579]. Dependent on the relative distance of the detectors from the beam-splitter, different time-delays τ can be tested.

When two single-photon fields arrive at the two input ports of a beam-splitter, a two-photon interference effect can be observed, as first measured by Hong, Ou, and Mandel (HOM) [597]. For perfect coherence between the two input fields, there is full destructive interference between the output components with a photon in each of the arms. In consequence photon-bunching occurs, i.e., the photons are detected always in the same output port, without any coincidences between the two ports. If the coherence is reduced, e.g., by introducing a time-delay for one of the arriving photons, coincidences appear. The typical experimental signature of two-photon interference is thus a *HOM-dip*, i.e., a reduction and subsequent increase in the coincidence rate as a coherence parameter is tuned to and away from values corresponding to full coherence [524, 544, 629, 338]. In the context of the undefined phase of single photons, the bunching can be seen as a "Solomonic solution" in

which in some sense the output ports are in a superposition of maximally constructive and destructive interference [610].

The result of the HOM experiment changes significantly if the two photons are in an entangled singlet state with respect to one of their internal degrees of freedom, such as, e.g., polarization, with

$$|\Psi_{\text{sgl}}\rangle = \frac{1}{\sqrt{2}}\big(\mathbf{a}^\dagger_{AH}\mathbf{a}^\dagger_{BV} - \mathbf{a}^\dagger_{AV}\mathbf{a}^\dagger_{BH}\big)\,|0\rangle\,, \tag{5.35}$$

which can be also expressed in terms of a symmetrized two-photon PWF of the form

$$|\Psi_{\text{sgl}}\rangle = \frac{1}{2}\big(\,|H\rangle\,|V\rangle - |V\rangle\,|H\rangle\,\big) \otimes \big(\,|A\rangle\,|B\rangle - |B\rangle\,|A\rangle\,\big), \tag{5.36}$$

neglecting the continuous spatial degree of freedom. Note that the state above corresponds to a product of an anti-symmetric polarization state with an anti-symmetric path state. In this case the opposite behavior occurs in the HOM-scenario and perfect coincidences are observed in terms of a "HOM-peak", which respresents the experimental signature of fermions. In this manner, fermionic states and behavior can be realized in certain degrees of freedom of bosonic particles [629, 621]. Furthermore, such state-dependent bunching behavior is also used to distinguish between different polarization entangled two-photon states in so-called *Bell-state analyzers* [659, 629].

5.4.3 Homodyne Detection and Optical Metrology

As mentioned in Sec. 4.5.1, typical photodetectors have insufficient time-resolution to resolve subcycle properties of quantum light, in particular the quadrature variances. Knowledge of the latter does not only allow to detect squeezing but also to distinguish, e.g., a thermal field with a Poissonian number distribution from a coherent state. A principal strategy to enable such measurements for light-fields with sufficiently narrow spectra is the interferometric overlap of the unknown field in question with another well-known and controllable light field in a coherent state, commonly called *local oscillator*. Two cases are distinguished, namely whether the local oscillator has the same or a different oscillation frequency from the unknown signal, called *homodyne* and *heterodyne detection*, respectively [657, 612, 529, 525, 531, 524, 146]. In both schemes, to recover information it is necessary that the phases of the signals are stable, i.e., in homodyne detection the relative phase between the signals has to be constant and in heterodyne schemes the phase drift between the fields has to correspond exactly to the difference frequency. In typical experiments this phase stability is achieved by using the same source for the local oscillator as well as for the generation of the quantum field of interest [136].

In the quantum optical homodyne detection scheme as first proposed by Yuen and Shapiro [643] the signal arriving at port B of the beam-splitter is significantly weaker than the local oscillator at input port A. In this case, assuming for simplicity perfect photodetectors, the mean photocounts $\langle \mathbf{m}_j \rangle$ and their variances $\mathrm{Var}(\mathbf{m}_j)$ at the two output

ports $j \in \{C, D\}$ are given as [612, 529, 531]

$$\begin{aligned} \langle \mathbf{m}_C \rangle &= T^2|\alpha|^2 + R^2\langle \mathbf{n} \rangle + 2TR|\alpha|\langle \mathbf{X}_2' \rangle, \quad \mathrm{Var}(\mathbf{m}_C) \approx T^4|\alpha|^2 + 4T^2R^2|\alpha|^2\mathrm{Var}(\mathbf{X}_2'), \\ \langle \mathbf{m}_D \rangle &= R^2|\alpha|^2 + T^2\langle \mathbf{n} \rangle - 2TR|\alpha|\langle \mathbf{X}_2' \rangle, \quad \mathrm{Var}(\mathbf{m}_D) \approx R^4|\alpha|^2 + 4T^2R^2|\alpha|^2\mathrm{Var}(\mathbf{X}_2'), \end{aligned} \tag{5.37}$$

where α is the coherent amplitude of the local oscillator and $\mathbf{X}_2'$ is the rotated quadrature component, as defined in Sec. 4.4.3, phase-shifted proportionally to the relative phase between signal and local oscillator. Note that, since the local oscillator is much stronger than the signal, only terms in second order of $|\alpha|$ are retained in the expressions for the variances and additionally the calculation also simplifies significantly since the two input fields are in a product state. In *ordinary* homodyne detection an asymmetric beam-splitter is employed with a measurement in only one output port [612, 531]. For example with $T \ll R$, in port C, the contribution of the local oscillator which is independent on the relative phase can be significantly reduced allowing to resolve the subcycle changes of quadrature fluctuations in the signal by scanning the relative phase between the input fields.

Alternatively, in *balanced* homodyne detection a symmetric beam-splitter with $R \approx T$ is chosen, and the photocurrents from both detectors subtracted. Note that, in this case, just as in the HBT scheme, correlations between intensity fluctuations persist in the photocurrents and thus, assuming again ideal photodetectors, the resulting fluctuation of the difference current is proportional to the standard deviation of the photocount difference operator $\mathbf{m}_{\mathrm{diff}} := \mathbf{n}_C - \mathbf{n}_D$ with [612, 529, 531, 524]

$$\langle \mathbf{m}_{\mathrm{diff}} \rangle \approx \Delta\mathbf{m}_{\mathrm{diff}} \approx 2|\alpha|\Delta\mathbf{X}_2'. \tag{5.38}$$

Thus in the balanced scheme the phase-dependent fluctuation of the photocurrent allows to determine the quadrature fluctuations without any contribution of noise from the local oscillator. Furthermore, since the scanning of the phase rotates $\mathbf{X}'$ to arbitrary linear combinations of the two quadratures, also a full QST of the signal field state can be performed [146], as first realized by Smithey *et al.* [649]. Heterodyne detection schemes employ similar strategies, such as, e.g., for the detection of non-degenerate two-mode squeezed states, where the frequency of the local oscillator is placed exactly in the middle of the two signal frequencies [612, 146].

Finally, as first proposed by Caves [574] in the context of interferometric detection of gravitational waves, the combination of squeezed states and balanced homodyne detection also allows to improve metrological sensitivity. The proposed scenario is the determination of relative path difference in an MZI with a coherent state of amplitude α in one input port and an arbitrary and comparatively weak field in the other. When choosing an interferometric phase, with approximately equal intensity at both output ports, the electric difference signal I_{diff} for a balanced detection is given as [338]

$$I_{\mathrm{diff}} \propto \langle \mathbf{m}_{\mathrm{diff}} \rangle = \delta\varphi \left(|\alpha|^2 - \langle \mathbf{n}_{\mathrm{dark}} \rangle \right) \tag{5.39}$$

where $\delta\varphi$ represents a small variation of the relative phase between the two arms and $\langle \mathbf{n}_{\mathrm{dark}} \rangle$ the expected photon number of the signal at the dark input port. It can be shown

that for an injection of squeezed vacuum at the dark input port the fluctuation of the difference operator can be expressed as [531, 338]

$$\mathrm{Var}(\mathbf{m}_{\mathrm{diff}}) = |\alpha|^2 e^{-2|\xi|} + \sinh^2|\xi| \tag{5.40}$$

Thus, if no input, i.e., the vacuum state, is injected at the dark port, the phase can be estimated with a SNR of $\Xi = |\delta\varphi\,\alpha| = |\delta\varphi|\sqrt{n}$, corresponding to the SNL. In contrast, when the appropriate quadrature of the vacuum is squeezed, the SNR can become $\Xi \approx |\delta\varphi|\sqrt{n}\exp(|\xi|)$, beating the SNL of classical interferometry. This increase of sensitivity can be interpreted as reduced phase-noise due to phase-squeezing in the added vacuum. The SNR can be improved even further by injecting two-mode entangled states into the MZI such as two-mode squeezed vacuum or so-called *noon states* $|\mathrm{NOON}\rangle = (|n,0\rangle + |0,n\rangle)/\sqrt{2}$ [184, 161, 159, 646, 338]. Notably, it has been shown that optimal metrological states for two-mode interferometric estimation strategies involve GME entanglement between all particles [485, 506]. Thus, while the SNL is fundamentally based on the statistical independence of detection events, quantum optical metrology in some sense harnesses "cooperative behavior among the photons" [161]. Quantum metrological advantage has been first demonstrated experimentally by the group of Kimble [663] and famously applied at the LIGO detector for gravitational waves [553].

5.4.4 Interferometric Complementarity

Just as in the case of double-slit, also in MZI-type interferometers which-path measurements can be performed. They can be modeled again as an interaction with an auxiliary quantum system or another degree of freedom acting as a pointer system, which leads to a similar joint state as in the case of the double-slit (5.33). In consequence, just as for the double-slit any extraction of which-path information necessarily leads to a loss of interferometric visibility. Note that a very simple experimental method to obtain such which-path information is the usage of the other degree of freedom of the paraxial beams as an effective pointer, i.e., for example perform a rotation of the polarization state of the field in one of the two arms. The more orthogonal the two polarizations become, the more visibility is lost and the more which-path information can be obtained from a polarization measurement at one of the output ports. Since the path degree of freedom in a MZI interferometer is essentially a qubit, in fact when identifying the internal path basis $\{|A\rangle, |B\rangle\}$ with the eigenbasis of the $\boldsymbol{\sigma}_z$ operator, the which-path measurement represents a measurement of $\boldsymbol{\sigma}_z$ on the path degree of freedom. Conversely, the measurement of output intensity represents a projection onto one of the eigenstates of $\boldsymbol{\sigma}_{\mathrm{out}} = \cos(\varphi)\boldsymbol{\sigma}_x + \sin(\varphi)\boldsymbol{\sigma}_y$, where φ is the effective phase-difference between the state components from the two arms after passing the output beam-splitter.

The simple qubit structure of the path degree of freedom allows to formulate a general quantitative IDT relation between which-path information and visibility for the MZI. As first proposed by Jaeger, Shimony, and Vaidman [598] and later independently by Englert [582], the gain in which-path information can be quantified by the distinguishability

of the corresponding pointer states, which is given by their trace distance $\mathcal{D}_T$ as defined in Sec. 1.6.2. The lack of disturbance is simply taken to correspond to the amount of visibility $\mathcal{V}$, leading to the trade-off relation [598, 582]

$$\mathcal{D}_T^2 + \mathcal{V}^2 \leq 1, \tag{5.41}$$

which is saturated exactly for efficient which path measurements, i.e., for pure initial pointer states.

5.5 Optical Waveguides

5.5.1 Fiber Optics

An important tool for the practical handling of electromagnetic radiation and propagating waves in general are so-called *waveguides*, which allow to control the propagation of the respective wave phenomenon. In the optical domain the foremost implementation of waveguides are *optical fibers*, which in their simplest form consist of an elongated cylindrical *core* with some index of refraction n_{core}, transversely surrounded by a *cladding*, i.e., another medium with a lower index of refraction $n_{\text{clad}} < n_{\text{core}}$ [533, 517, 523, 530, 537]. Due to the principle of *total internal reflection* any plane-wave components with transverse angles of incidence $\Theta > \Theta_C = \arcsin(n_{\text{clad}}/n_{\text{core}})$ are fully reflected at the boundary between the two media, where Θ_C is called the *critical angle*. Accordingly given an external medium with refractive index n from which light enters the fiber, the angle $\Theta_A = \arcsin\left(\sqrt{n_{\text{core}}^2 - n_{\text{clad}}^2}/n\right)$, defined with respect to the propagation axis, is called *acceptance angle*. Only plane-wave components with transverse angles below the acceptance angle can be guided by the fiber. For convenience the acceptance angle is commonly expressed in terms of the *numerical aperture* $\text{NA} = n \sin \Theta_A$.

Typically optical fibers are flexible and as long as not bent too much, allow close to lossless propagation of light along freely controllable directions over distances, at which free space light would undergo significant diffraction. In practice instead of the discontinuous change of refractive index as described above, called *step-index* profile, often optical fibers are also designed with a gradually changing refractive index of the core corresponding to a so-called *graded-index* profile, which, however, does not change the general guiding principle [533, 530].

For core sizes with comparable dimensions as the wavelength, the fiber can support only a finite number of transverse modes for any given frequency and if the frequency is too low, i.e., the wavelength too large, no guiding might be possible at all [533, 517, 523, 530, 537]. In the frequency range, for which only a single transverse mode is guided, the fiber is denoted as *single mode* and for larger frequencies as a *multi mode* fiber. For cylindrical single mode fibers with a step-profile the fundamental transverse modes can be approximated as Gaussian profiles with a width w given as [533]

$$w = \frac{2r_c}{\sqrt{2 \log V}}, \qquad \text{with } V := k r_c \sqrt{n_{\text{core}}^2 - n_{\text{clad}}^2}, \tag{5.42}$$

where r_c is the core radius and V the so-called *waveguide parameter*, which depends on the frequency through the wavenumber k.

Since the size of the mode exiting a typical single mode fiber is on the order of only a few wavelengths, the resulting beam has a large divergence. Thus, typically, convex lenses are placed in a small distance behind the end-facets of fibers to refocus the beam after it has sufficiently expanded propagating from fiber to lense. In a reverse configuration the same lenses can be used to focus a free-space beam into a fiber. Accordingly such lenses are called *fiber-collimators* and sometimes also *fiber-couplers*, where, alternatively, the latter term is also used to denote devices allowing the transfer of light from one fiber to another, such as the directional couplers introduced in the next subsection.

5.5.2 Integrated Waveguide Arrays

Another crucial application of waveguide structures are integrated optical systems, in which linear and nonlinear optical networks are implemented in a small and scalable manner by the creation of waveguide structures in various transparent materials, see [632, 587] for an overview. One possible platform for integration are laser-written waveguides in silica [619, 622], which are created by inducing local changes of the refractive index in the substrate through illumination with focused laser pulses. Such systems allow to encode qubits and higher dimensional degrees of freedom in a set of discrete paths, where unitary transformations are achieved by relative phase shifts, which are tunable by *thermo-optic effects* as well as so-called *directional couplers*, which effectively correspond to beam splitters [619, 537, 622, 587]. Also, polarization dependent components such as partially and fully polarizing beam splitters or waveplates can be realized. In contrast to equivalent systems in free-space, integrated circuits are significantly more stable, which makes them more suitable to implement complex structures, see, e.g., [633, 658] for examples.

Instead of modeling the whole electromagnetic field inside the waveguide structure a common approach to its formal description is the so-called *coupled mode theory*, in which the fields inside the individual waveguides are approximated as single modes and the transitions between those discrete states is described as quantum mechanical tunneling [533, 620, 576]. The strength of the coupling between the various modes depends on their distance and, e.g., directional couplers are realized by bringing waveguides closer together for a certain propagation length. An alternative configuration is given by a set of parallel waveguides which are spaced closer together such that they couple continuously. In a typical scenario with a planar waveguide geometry, the distances between the parallel waveguides are chosen such that there is only non-vanishing coupling between neighboring modes. In terms of coupled-mode theory this scenario exactly corresponds to a so-called *tight-binding model* as commonly employed for the description of processes in solid-state physics [555, 576]. The corresponding Hamiltonian $\mathbf{H}_{\mathrm{TB}}$ is diagonal with respect to two differently coupling polarization components $p \in \{H, V\}$ and can be written as [555, 591,

576]

$$\mathbf{H}_{\mathrm{TB}} = \hbar \sum_p \left(\sum_j \beta_j^p \mathbf{n} + \sum_{j \neq k} \kappa_{jk} (\mathbf{a}_j^p)^\dagger \mathbf{a}_k^p \right), \tag{5.43}$$

where β_j^p is the polarization dependent *propagation constant* for waveguide j and κ_{jk}^p the *coupling constant* between waveguides j and k, with $(\kappa_{jk}^p)^* = \kappa_{kj}^p$.

5.5.3 Simulation of Open Quantum Systems

In [**P8**], as reprinted in the next section, an integrated waveguide array is employed to perform a simulation of an open quantum system. While the experiment is performed with CW laser light, it can be related to a tight binding Hamiltonian using the formalism of the PWF, where the effective Hilbert space $\mathcal{H}$ is given as the product of polarization and path Hilbert spaces $\mathcal{H}_{\mathrm{pol}} \otimes \mathcal{H}_{\mathrm{path}}$. By identifying the polarization degree of freedom with a qubit system and the path degree of freedom with the environment, the polarization dependent coupling between the waveguides effectively corresponds to a system-environment interaction. While in this case the arguably extremely small discrete environment does not capture all properties of open system dynamics, it still represents a valid model system for certain effects which are common to all open quantum systems. In this context the small size of the system becomes a feature as it can be described both via unitary as well as via reduced dynamics and the full joint state of system and environment can be evaluated.

The BLP-criterion, as defined in Sec. 1.8.4, is applied and extended to investigate properties of information flow between system and environment. Apart from witnessing non-Markovian evolution, the main focus of the study lies on the question whether the information that is removed from the system actually is stored in the environment itself or rather in correlations between system and environment. It is found that for the basic tight-biding Hamiltonian (5.43) there is never information in the environment which is not also still in the system, and all information removed from the system is stored exclusively in the system-environment correlations. Finally, an alternative waveguide array structure is proposed which would lead to a full transfer of the initial system state into the environment, and consequently also to a full transfer of information.

Check for updates

RESEARCH ARTICLE

LASER & PHOTONICS REVIEWS

www.lpr-journal.org

Tracing Information Flow from Open Quantum Systems

Jan Dziewior, Leonardo Ruscio, Lukas Knips, Eric Meyer, Alexander Szameit, and Jasmin D. A. Meinecke*

Open quantum systems are highly relevant, both for practical applications as well as for fundamental questions about the nature of information and its transfer, encompassing for example decoherence and memory effects. Quantum mechanics introduces additional complexity to the transfer of information, e.g., storage of information in non-classical correlations. Yet, some of these aspects tend to be neglected by the usual framework of open system research. In this work, photons are used in a waveguide array to implement a quantum simulation of the coupling of a qubit with a low-dimensional discrete environment. Using the trace distance between quantum states as a measure of information, different types of information transfer are analyzed. Extending the usual perspective which is focused on the system alone, the presence of information is also investigated in the environment.

1. Introduction

In recent years, growing attention has been given to the investigation of open quantum systems,[1–6] which are ubiquitous in quantum science, where many experimental systems have significant interactions with their environment.[7–12] Although their description is significantly more involved compared to isolated systems,[13] it allows to capture omnipresent effects as decoherence and other instances of state deterioration as well as memory effects in a unified manner.

Especially for quantum information applications, a point of particular interest is the flow of information from and to the open system, usually captured by the concept of Markovianity. This concept is classically well-understood and identifies stochastic processes as *Markovian* if they are memory-less, such that the future of the process depends only on the present state, but not on its past.[14,15] Given the impossibility to measure a quantum process at intermediate time steps without disturbing the evolution, a straightforward generalization of this notion to the quantum realm is not possible and thus several nonequivalent definitions exist, based on, e.g., the semigroup property or divisibility, see Refs. [14, 16]. This work employs an experimentally friendly definition based on the variation of the distinguishability of system states, quantified by their trace distance, which was proposed by Breuer, Laine, and Piilo (BLP).[17–19] As the BLP notion of Markovianity is comparatively broad, conversely a violation of the BLP criterion also indicates non-Markovianity according to other criteria such as CP-divisibility or semigroup behavior.

In the field of open systems research, the focus naturally lies on the dynamics of the open system, which is analyzed in terms of a quantum master equation or effective dynamical maps.[15] Also the information flow and memory effects are usually expressed in terms of information present in, lost from or returned to the system. However, questions as for example where information lost from the system actually flows to, i.e., whether it actually is transferred from the system to the environment or becomes stored in correlations between the two, are usually not in focus.[16] A few works address this topic and at least consider system environment correlations in more detail,[20–25] or the storage of system information in the environment.[26]

In our approach we extend the scope of investigation by explicitly asking where the information lost from the system flows to, in particular, to what extent it reaches the environment, as this can have fundamental implications on memory effects and possibilities to retrieve information in application scenarios, e.g., when parts of a system and hence carriers of information are lost. This shift in perspective allows us to analyze a taxonomy of several classes of information transfer emerging naturally, some of which are illustrated in **Figure 1**.

J. Dziewior, L. Ruscio, L. Knips, J. D. A. Meinecke
Max-Planck-Institut für Quantenoptik
Hans-Kopfermann-Straße 1, 85748 Garching, Germany
E-mail: jan.dziewior@physik.lmu.de

J. Dziewior, L. Ruscio, L. Knips, J. D. A. Meinecke
Fakultät für Physik
Ludwig-Maximilians-Universität
Schellingstraße 4, 80799 München, Germany

J. Dziewior, L. Ruscio, L. Knips, J. D. A. Meinecke
Munich Center for Quantum Science and Technology (MCQST)
Schellingstraße 4, 80799 München, Germany

E. Meyer, A. Szameit
Institut für Physik
Universität Rostock
Albert-Einstein-Str. 23, 18059 Rostock, Germany

J. D. A. Meinecke
Institut für Festkörperphysik
Technische Universität Berlin
10623 Berlin, Germany

The ORCID identification number(s) for the author(s) of this article can be found under https://doi.org/10.1002/lpor.202400737

© 2025 The Author(s). Laser & Photonics Reviews published by Wiley-VCH GmbH. This is an open access article under the terms of the Creative Commons Attribution-NonCommercial-NoDerivs License, which permits use and distribution in any medium, provided the original work is properly cited, the use is non-commercial and no modifications or adaptations are made.

DOI: 10.1002/lpor.202400737

ADVANCED SCIENCE NEWS
www.advancedsciencenews.com

LASER & PHOTONICS REVIEWS
www.lpr-journal.org

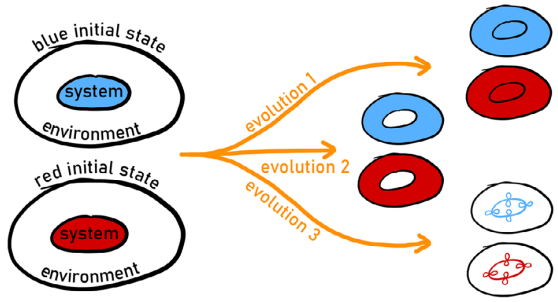

Figure 1. Concept of information and information flow between system and environment. Here, *information* is defined as the distinguishability between two initial states of a quantum system (depicted as colors blue and red). Initially, this information is in the system only. After an evolution of type 1, the information from the system is duplicated into the environment such that measurements on system or environment alone are sufficient to distinguish case blue from case red. In contrast, after evolution 2 the information flows fully into the environment and measurements on the system alone do not enable to distinguish between the two versions. Finally, evolution 3 depicts a completely different case, where the information becomes stored exclusively in the correlations between system and environment, such that only a joint measurement of both allows to recover the relevant information.

We investigate different types of information flow in an experimental quantum simulation using integrated photonic waveguide arrays.[27,28] The simulation is implemented by identifying the polarization as the quantum system and the path as the environment. This allows to effectively realize an open system through the interaction between these two degrees of freedom by harnessing polarization-dependent coupling. In the past, such simulations have been proposed for discrete quantum walks[29–31] and realized in free space optical systems or single optical fibers based on coupling polarization to either path[32,33] or frequency/time,[34–39] investigating common questions such as decoherence dynamics or the presence of non-Markovianity. In contrast, employing laser-written structures in silica opens the path to the scalability necessary to match the complexity of more realistic systems while preserving a high degree of control.

The regular structure of our integrated circuit allows to analytically calculate the full time evolution of system and environment states, thus expanding the usual perspective focused solely on the effective evolution of the open system. We clearly observe a non-Markovian evolution of the system qubit and investigate the flow of information to the environment. By extending the concept of the BLP criterion we distinguish different manners in which the information is encoded in our system. Furthermore, we propose a different type of array with a decisively different type of information flow, where all information is removed from the system and transferred to the environment.

2. Tracing Information

Following the BLP criterion, we here define information as the ability to distinguish between two quantum states. Any choice of two states ρ_1 and ρ_2 corresponds to a certain amount of distinguishing information encoded in the parameters characterizing the two states. This distinguishability is quantified via the trace distance D between the two states, defined as

$$D(\rho_1,\rho_2)=\frac{1}{2}\|\rho_1-\rho_2\|=\frac{1}{2}\mathrm{tr}\left(\sqrt{(\rho_1-\rho_2)^2}\right). \tag{1}$$

To trace the flow of information, we consider two initially perfectly distinguishable pure test states of the system, ρ_1 and ρ_2. For these two test states, a certain unitary interaction with the environment results in changed reduced states of system $\rho_i^S=\mathrm{tr}_E(\rho_i^{S\wedge E})$ and environment $\rho_i^E=\mathrm{tr}_S(\rho_i^{S\wedge E})$, where $\rho_i^{S\wedge E}$ is the joint state of system and environment after the evolution in the two cases with $i=1,2$. After the interaction, even via optimal measurements on the system it might become harder or even impossible to decide in which of the two test states the system initially has been. This corresponds to an information loss from the *system*, quantified by the trace distance $D_S=D(\rho_1^S,\rho_2^S)$. Conversely, after the interaction, it might become possible to infer the initial test state via optimal measurements on the *environment*, indicating information transfer to it, quantified via the trace distance $D_E=D(\rho_1^E,\rho_2^E)$.

To analyze how a particular interaction transfers information, we choose different pairs of test states. After the interaction the pairs might be distinguishable to varying degree by measurements on the system or the environment or even allow distinguishability only from joint measurements. This allows to characterize the interaction by its different transfer behavior of information in dependence of the choice of information encoding in test states. This analysis also includes the original application of the BLP criterion to witness non-Markovian information backflow, in the case where, D_S increases with time.

3. Experimental Section

3.1. Waveguide Arrays as Open Quantum Systems

In order to implement the quantum simulation of an open quantum system we use polarized photons propagating in an array of evanescently coupled waveguides. The polarization and the path degrees of freedom form a composite system equivalent to an open quantum system (polarization) coupled to an environment (path). A sketch of the experimental setup is shown in **Figure 2**a. The array, laser-written in fused silica (SiO_2),[40] is composed of five waveguides with a separation of 33μm lying in a plane parallel to the surface of the chip. The waveguides have an elliptical cross section introducing birefringence into the system as well as a polarization-dependent evanescent coupling between the waveguides.

We consider only single photon processes and thus the Hamiltonian H acting on the Hilbert space of system and environment $\mathcal{H}_S\otimes\mathcal{H}_E$ which best describes our scenario[27] can be written as

$$H=\sum_{\pi=\mathrm{H,V}}P_\pi\otimes\left(\sum_{m=1}^{M}\beta_m^\pi P_m+\sum_{j=m\pm1}\kappa_{j,m}^\pi|m\rangle\langle j|\right), \tag{2}$$

with $M=5$ and projectors P_π and P_m on polarization π and path m. β_m^π and κ_{jm}^π represent the propagation constant for waveguide

© 2025 The Author(s). Laser & Photonics Reviews published by Wiley-VCH GmbH

18638899, 0, Downloaded from https://onlinelibrary.wiley.com/doi/10.1002/lpor.202400737 by Jan Dziewior - MPI 356 Quantum Optics , Wiley Online Library on [16/02/2025]. See the Terms and Conditions (https://onlinelibrary.wiley.com/terms-and-conditions) on Wiley Online Library for rules of use; OA articles are governed by the applicable Creative Commons License

ADVANCED SCIENCE NEWS
www.advancedsciencenews.com

LASER & PHOTONICS REVIEWS
www.lpr-journal.org

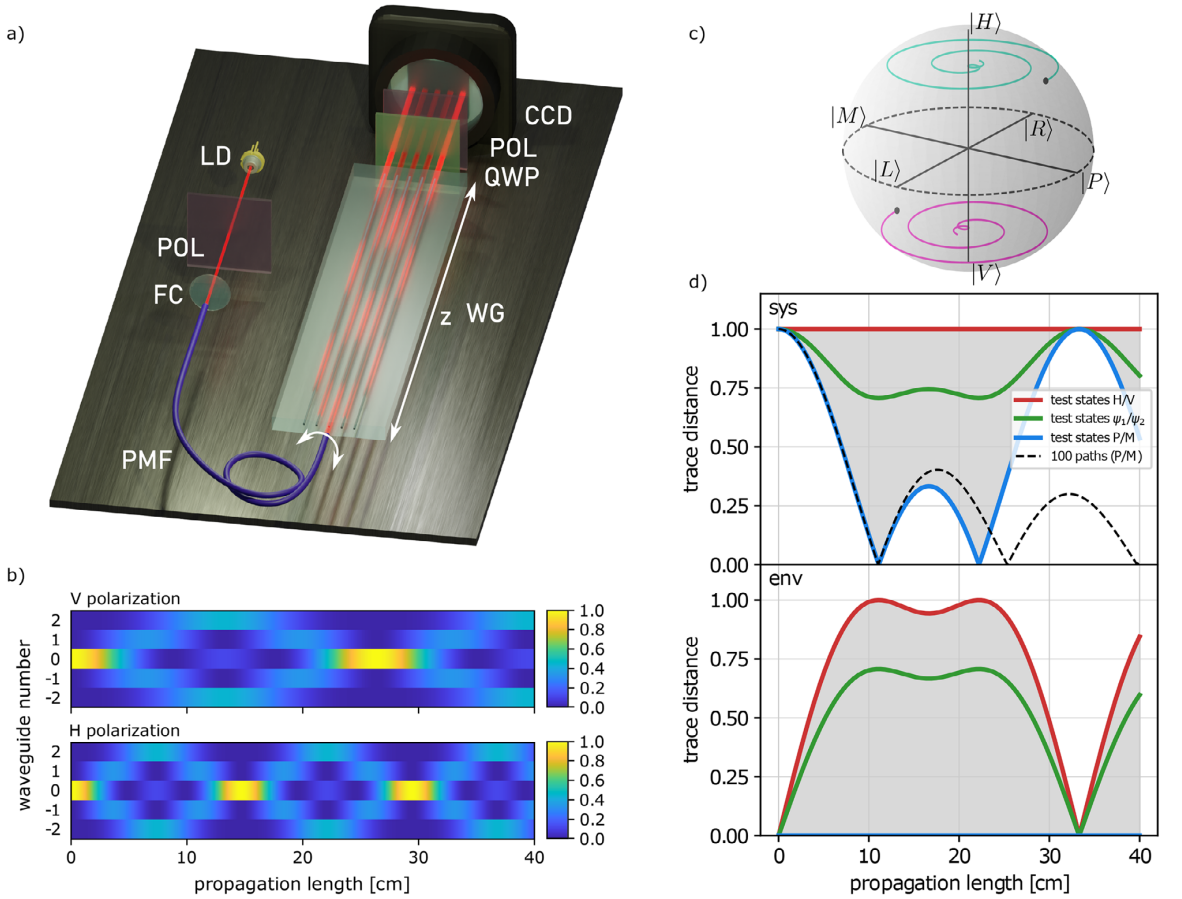

Figure 2. Experimental setup and simulations. a) Experimental setup consisting of a linearly polarized 780 nm laser (LD) coupled to the chip via a PM fiber. At the output of the waveguide chip (WG), polarization state tomography is performed using a $\lambda/4$ waveplate (QWP), a polarizer (POL) and a CCD camera. Waveguide chips with different lengths z were used to measure at various propagation lengths. b) Transverse probability distributions of photons in the waveguide array as function of the propagation length for the input states $|\mathrm{H}\rangle$ and $|\mathrm{V}\rangle$. c) Simulated evolution of the polarization states for $|\psi_1\rangle$ (upper turquoise curve) and $|\psi_2\rangle$ (lower purple curve) inside the Bloch sphere. d) Simulations of polarization and path trace distance behavior for different pairs of orthogonal test states $|\mathrm{H}\rangle$ and $|\mathrm{V}\rangle$ (red curves), $|\mathrm{P}\rangle$ and $|\mathrm{M}\rangle$ (blue curves) as well as $|\psi_1\rangle$ and $|\psi_2\rangle$ (green curves). Here and in the remaining plots, the gray area signifies the possible range of trace distances under variations of pairs of orthogonal test states. The dashed black line corresponds to a simulation of an equivalent system with 100 waveguides, where the finite size of the system does not yet come into effect.

m and the coupling constant from waveguides j to m for polarization π, respectively. While it is possible to further separate the Hamiltonian into free and interaction parts, in general this does not simplify the description since the interaction part remains of the same form as (2). However, it can be brought into a traceless form with $\sum_{m,\pi} \beta_m^\pi = 0$ where the free part just corresponds to an offset term, resulting in a global phase.

The Hamiltonian is a pure dephasing Hamiltonian,[15] since it is diagonal along a system basis, in our case the basis of horizontal (H) and vertical (V) polarization. In consequence, the resulting evolution

$$U(t) = e^{iHt} = |\mathrm{H}\rangle\langle\mathrm{H}| \otimes U^{\mathrm{H}}(t) + |\mathrm{V}\rangle\langle\mathrm{V}| \otimes U^{\mathrm{V}}(t) \tag{3}$$

is also diagonal with effective environment unitaries U^π given by

$$U^\pi(t) = \exp\left[it\left(\sum_{m=1}^{M} \beta_m^\pi P_m + \sum_{j=m\pm1} \kappa_{j,m}^\pi |m\rangle\langle j|\right)\right]. \tag{4}$$

Thus, for our system, H and V polarizations are eigenstates of the evolution U such that the total evolution can be separated into two polarization conserving parts corresponding to these states.

We numerically simulated the two intensity distributions of the two polarizations, as shown in Figure 2b, based on the simplest possible non-trivial model for our system where all propagation and coupling constants only depend on the polarization and are the same across the waveguides with $\beta_j^\pi = \beta^\pi$ and $\kappa_{j,j\pm1}^\pi = \kappa^\pi$

© 2025 The Author(s). Laser & Photonics Reviews published by Wiley-VCH GmbH

18638899, 0, Downloaded from https://onlinelibrary.wiley.com/doi/10.1002/lpor.202400737 by Jan Dziewior - MPI 356 Quantum Optics , Wiley Online Library on [16/02/2025]. See the Terms and Conditions (https://onlinelibrary.wiley.com/terms-and-conditions) on Wiley Online Library for rules of use; OA articles are governed by the applicable Creative Commons License

ADVANCED SCIENCE NEWS
www.advancedsciencenews.com

LASER & PHOTONICS REVIEWS
www.lpr-journal.org

for all j. For this and all following simulations as well as in the experimental realization we always start with an initial path state $\rho_I^E = |3\rangle\langle 3|$ given by coupling all light into the central waveguide. In this scenario the Hamiltonian can be significantly simplified by separating free and interaction parts, H_F and H_I, leading to

$$H_F = \beta\sigma_z \otimes \mathbb{1} + \kappa_0 \mathbb{1} \otimes C_E, \tag{5}$$

$$H_I = \kappa\sigma_z \otimes C_E \tag{6}$$

respectively. Here, σ_z is the third Pauli operator, C_E denotes the coupling operator for the waveguides with $C_E = \sum_{j=m\pm1} |m\rangle\langle j|$, $\beta^{H/V} = \beta_0 \pm \beta$ as well as $\kappa^{H/V} = \kappa_0 \pm \kappa$, with appropriate choices of β_0, β, κ_0, and κ. The global phase term $\beta_0 \mathbb{1} \otimes \mathbb{1}$ is again neglected.

3.2. Simulation of Information Flow

Employing the trace distance Equation (1) between pairs of states, it is instructive to first determine the full range of information flow between system and environment by analyzing paradigmatic cases. Given the structure of our system, it becomes clear that no information loss is to be expected for the eigenstates $|\mathrm{H}\rangle$ and $|\mathrm{V}\rangle$ as pair of test states ρ_1 and ρ_2. On the other hand, for a pair such as $|\mathrm{P}\rangle = (|\mathrm{H}\rangle + |\mathrm{V}\rangle)/\sqrt{2}$ and $|\mathrm{M}\rangle = (|\mathrm{H}\rangle - |\mathrm{V}\rangle)/\sqrt{2}$ the trace distance is expected to be most sensitive since equal weights are given to the two eigenstates of the evolution. Additionally, we consider an intermediate case with the pair $|\psi_1\rangle = (|\mathrm{H}\rangle + |\mathrm{P}\rangle)/\sqrt{2+\sqrt{2}}$ and $|\psi_2\rangle = (|\mathrm{V}\rangle - |\mathrm{M}\rangle)/\sqrt{2+\sqrt{2}}$.

We start with a numerical simulation of the expected information flow based on the simple model described above, shown in Figure 2d. Initially, we see maximum distinguishability in the system, which in the course of the evolutions drops indicating a loss of the information from the system. For the pair $|\mathrm{P}\rangle$ and $|\mathrm{M}\rangle$, the information is completely lost. Subsequently, however, the trace distance increases again, which witnesses non-Markovianity. The appearance of non-Markovianity is a consequence of the form of the Hamiltonian and does not hinge on the finite boundaries of our system. Indeed, with five waveguides we observe distinct state recurrence for H and V polarizations, i.e., the initial path states are restored for each of the polarizations after finite time (Figure 2b) and even the total state of system and environment will eventually evolve back into the initial state as happens in any finite dimensional system with time-indepentent unitary evolution. However, the appearance of non-Markovian behavior does not depend on this recurrence as illustrated by the dashed black line in Figure 2d corresponding to a simulation with 100 waveguides. For this system, non-Markovianity is observed, although the boundary is not reached in the timescale of the evolution.

The particular structure of the information loss is furthermore illustrated for the case of $|\psi_1\rangle$ and $|\psi_2\rangle$ via the evolution of the system states in the Bloch sphere in Figure 2c. It corresponds to a dephasing process in the $\{\mathrm{H}, \mathrm{V}\}$-basis together with a change of the relative phase between the H and V components. These two effects combine into the spiralling evolution of the states, where the Bloch vectors remain pointing in opposite directions.

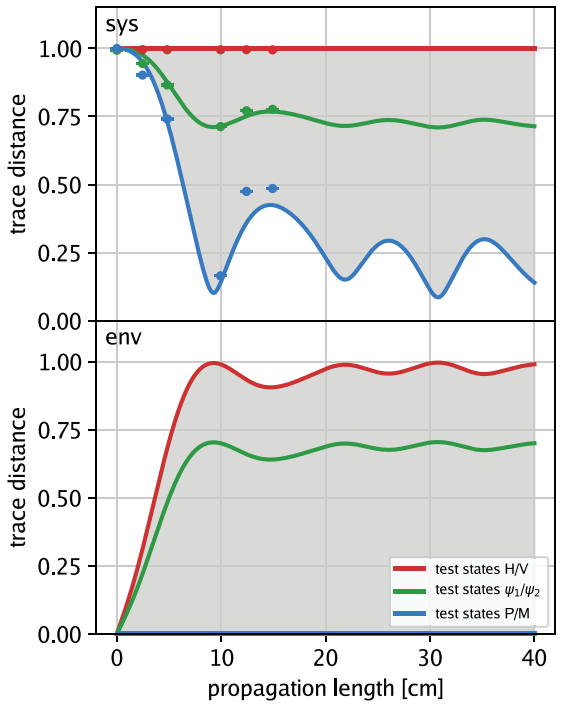

Figure 3. Experimental data and fit of theoretical model. The first datapoint of each curve at length zero stems from measurements in free space (without the array) and the remaining results are obtained using arrays of five different lengths. The statistical errorbars lie inside the dots. The solid lines represent simulations based on the theoretical model including varying propagation constants.

3.3. Measurement Results

We perform the experiment with the same pairs of states and observe the evolution of the information in the system. In order to achieve the time-resolved quantum state tomography of the polarization, we employ five chips of different lengths with arrays of waveguides written with the same writing parameters, thus leading to the same Hamiltonian. The results are presented as data points in **Figure 3**.

Just as in our simulation the system exhibits an almost maximal information loss followed by a significant gain for the pair $\{|\mathrm{P}\rangle, |\mathrm{M}\rangle\}$, no significant information loss for $\{|\mathrm{H}\rangle, |\mathrm{V}\rangle\}$, and an intermediate behavior for $\{|\psi_1\rangle, |\psi_2\rangle\}$. It is also clearly possible to certify non-Markovian behavior in the evolution. When considering only the relative behavior of the information between the three pairs, these results are explained very well by the simple theoretical model used for Figure 2d. However, the time evolution of the information flow is noticeably different, which stems from the fact that the actual physical array exhibits variations of the parameters which are not included in the model. A noticeable deviation from the simple model is expected to originate from small fluctuations of the laser system during the writing of the array, which result in different propagation constants for each waveguide. Modeling these variations by allowing different parameters β_k for the five waveguides already allows to fit an evolution which

© 2025 The Author(s). Laser & Photonics Reviews published by Wiley-VCH GmbH

18638899, 0, Downloaded from https://onlinelibrary.wiley.com/doi/10.1002/lpor.202400737 by Jan Dziewior - MPI 356 Quantum Optics , Wiley Online Library on [16/02/2025]. See the Terms and Conditions (https://onlinelibrary.wiley.com/terms-and-conditions) on Wiley Online Library for rules of use; OA articles are governed by the applicable Creative Commons License

ADVANCED SCIENCE NEWS
www.advancedsciencenews.com

LASER & PHOTONICS REVIEWS
www.lpr-journal.org

is much closer to the observed results, shown as solid lines in Figure 3.

4. Information Flow in the Experiment

To understand the different evolutions we observed in the experiment we provide a theoretical analysis of our system. The state ρ^S of the open system, i.e., the polarization qubit, is parameterized in terms of correlation tensor elements $\{T_x, T_y, T_z\}$ as

$$\rho^S = \frac{1}{2}\left(\mathbb{1} + T_x\sigma_x + T_y\sigma_y + T_z\sigma_z\right), \tag{7}$$

with the Pauli matrices $\{\sigma_x, \sigma_y, \sigma_z\}$. For the environment we allow an arbitrary initial state ρ^E, where a pure state corresponds to a coupling into a coherent superposition of waveguide modes and a mixed one for example to a certain amount of incoherence between those.

The Hamiltonian implies a system master equation which can be expressed in time-local Lindblad form as

$$\dot{\rho}^S(t) = -i\left[\tilde{H}(t), \rho^S(t)\right] + \gamma(t)\left(\sigma_z\rho^S(t)\sigma_z - \rho^S(t)\right) \tag{8}$$

where both the effective Hamiltonian $\tilde{H}(t) = \sigma_z\dot{\mu}(t)/2$ as well as the single decay mode with rate $\gamma(t)$ can be written in terms of the complex parameter $\chi(t) := \mathrm{tr}\left(U^V(t)\rho^E(U^H(t))^\dagger\right)$ with $|\chi(t)| \in [0,1]$. The rotation rate in the Hamiltonian corresponds to the change of the phase of $\chi(t)$ with $\mu(t) = \arg(\chi(t))$ and the decay rate by $\gamma(t) = -\dot{G}(t)/G(t)$, where $G(t) = |\chi(t)|$ is called the "decoherence function."[16]

For an initially pure system state $|\psi\rangle$, the master equation leads to the system state $\rho^S(t)$ at time t

$$\rho^S(t) = \frac{1}{2}\left(\mathbb{1} + G(t)\left(T'_x(t)\sigma_x + T'_y(t)\sigma_y\right) + T_z\sigma_z\right), \tag{9}$$

where the correlation tensor elements are transformed as $T'_x(t) = T_x\cos\mu(t) - T_y\sin\mu(t)$ and $T'_y(t) = T_y\cos\mu(t) + T_x\sin\mu(t)$, respectively.

Additionally, by considering for example the total unitary evolution (3), also the time evolution of the state of the environment $\rho^E(t)$ can be derived as

$$\rho^E(t) = \langle P_H\rangle\, U^H\rho^E(U^H)^\dagger + \langle P_V\rangle\, U^V\rho^E(U^V)^\dagger, \tag{10}$$

where the expectation values are taken over the initial system state ρ^S, with $\langle P_{H/V}\rangle = (1 \pm T_z)/2$ and the time dependence is contained in the unitaries with $U^\pi = U^\pi(t)$.

Using Equations (9) and (10) the amount of information in system and environment can be calculated in dependence on the choice of initial information encoding. For two initial test states ρ_1^S and ρ_2^S parametrized by $\{T_x^1, T_y^1, T_z^1\}$ and $\{T_x^2, T_y^2, T_z^2\}$ the trace distances D_S and D_E between the effective system states and between the environment states after the evolution, respectively, are given as

$$D_S(t) = \frac{1}{2}\sqrt{\delta T_z^2 + G(t)^2(\delta T_x^2 + \delta T_y^2)}, \tag{11}$$

$$D_E(t) = \frac{1}{2}\sqrt{\left(1 - G(t)^2\right)\delta T_z^2} \tag{12}$$

with $\delta T_k = T_k^1 - T_k^2$. These equations hold for any unitary with a diagonal form as U with arbitrary U^H and U^V. In particular, they do not depend on the size or structure of the environment and thus are valid also for much more complicated systems with continuous reservoirs or heat baths. Equation (11) corresponds to the known evolution of distinguishability in the case of a decoherence process, as for example described in Ref. [16]. In particular, whenever $G(t)$ increases, the process is certified to be non-Markovian according to the BLP criterion which in this case exactly corresponds to negative rate $\gamma(t)$ indicating a violation of CP-divisibility. By additionally considering Equation (12), it now becomes possible to trace the information flow between system and environment.

5. Types of Information Flow to Environment

5.1. Classical Information Flow

We can distinguish two completely different types of information flow for the information encoded either in T_z or alternatively in T_x and T_y. As seen from Equation (11), the information encoded in T_z never leaves the system and is at least partially duplicated in the environment whenever $G(t) < 1$. φ-dependent information on the other hand is never stored in the environment as becomes clear from the absence of the parameters T_x and T_y from Equation (12). Consequently, this information must become stored exclusively in the correlations between system and environment, whenever it is lost from the system. Additionally, a clear trade-off becomes apparent. The more information encoded in T_z is transferred to the environment, the more is necessarily lost from the complementary parameters T_x and T_y. Thus, system decoherence appears as a necessary and sufficient condition for information transfer to the environment, i.e., G also quantifies the amount of information in the environment. This is in accordance with well-known quantum complementarity relations and the no-cloning theorem,[41–47] which would be violated if significant information about one parameter could be extracted from the system while leaving the information stored in the other parameters intact. Concurringly, the information encoded in T_z remains in the system and can be even fully copied to the environment for $G(t) = 0$. Thus, albeit the system becomes entangled with the environment, the information transfer due to the decoherence process itself in this case is *classical* in the sense that in principle it could be transmitted by a classical channel after a quantum measurement.

5.2. Quantum Information Flow

The special form of information flow in our experimental system naturally implies the question whether simple time-independent Hamiltonians such as H are also suitable to implement more general types of evolutions. In particular, a genuinely *quantum* information flow occurs when a sufficiently large amount of information about several parameters is transferred into the environment such that this process could not be realized by a classical channel anymore.

© 2025 The Author(s). Laser & Photonics Reviews published by Wiley-VCH GmbH

18638899, 0, Downloaded from https://onlinelibrary.wiley.com/doi/10.1002/lpor.202400737 by Jan Dziewior - MPI 356 Quantum Optics , Wiley Online Library on [16/02/2025]. See the Terms and Conditions (https://onlinelibrary.wiley.com/terms-and-conditions) on Wiley Online Library for rules of use; OA articles are governed by the applicable Creative Commons License

ADVANCED SCIENCE NEWS
www.advancedsciencenews.com

LASER & PHOTONICS REVIEWS
www.lpr-journal.org

The extreme of such an information flow is a full transfer of the system's quantum state into a subspace of the environment, realized by a generalized swap operation U_S with

$$U_S = \sum_{j,k=1}^{2} |\phi_j\rangle\langle\phi_k| \otimes |\chi_k\rangle\langle\chi_j| + \mathbb{1} \otimes P_\perp, \tag{13}$$

where $\{|\phi_1\rangle, |\phi_2\rangle\}$ is a system basis, $\{|\chi_1\rangle, |\chi_2\rangle\}$ is a pair of orthogonal environment states and $P_\perp$ is the projector into the respective orthogonal subspace of the environment.

A possible practicable solution to experimentally achieve a genuine quantum information flow to the environment, is to additionally introduce a polarization rotation into the waveguides around an axis different than z. This can be achieved for example by introducing a rotation of the ellipticity into the waveguides.[48,49] The effective Hamiltonian in this case H' contains the Hamiltonian H and an additional polarization rotation with

$$H' = H + \sum_{m=1}^{M} (\alpha_m^x \sigma_x + \alpha_m^y \sigma_y) \otimes P_m, \tag{14}$$

where α_m^x and α_m^y represent the rotation rates around the x and y-axis of the Bloch sphere for waveguide m respectively. Note that H' cannot be written in diagonal form for the system and thus no longer corresponds to a pure dephasing process.

By choosing suitable parameters for propagation, coupling and rotation for H' we are able to numerically simulate an evolution where all information about all system parameters is simultaneously transferred to the environment, as shown in **Figure 4**. For each timestep we optimized over pairs of orthogonal test states from all possible directions of the Bloch sphere to determine the cases of maximal and minimal information transfer. In the simulated time interval the state, and thus all information is periodically swapped between system and environment, with approximately a full swap (up to local unitaries) realized at the propagation length $l = 9.6$ cm.

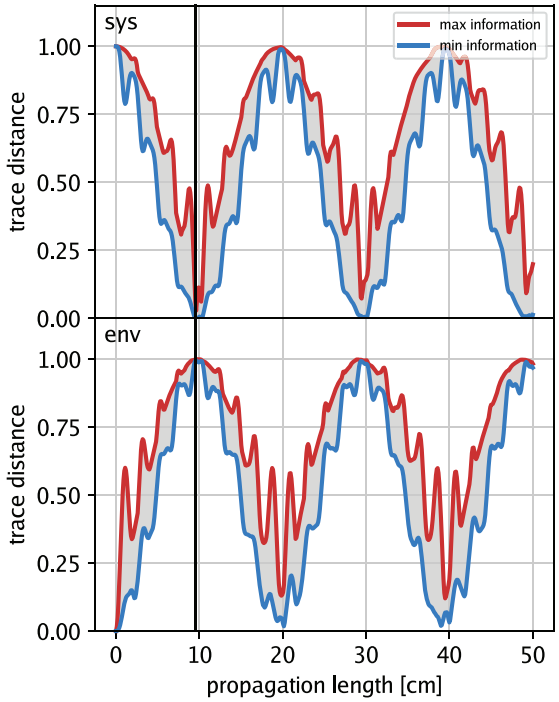

Figure 4. Evolution of information present in system and environment for specific parameters of H'. The two curves in each plot are obtained via optimization (independently for system and environment) over all possible Bloch sphere directions for pairs of orthogonal test states. The upper curve (red) always indicates the best case trace distance, where the lower curve (blue) corresponds to the worst case. At propagation length $l = 9.6$ cm (vertical marker) the unitary is (up to product unitaries) approximately equivalent to a generalized swap U_S, with a worst case trace distance in the environment of 0.995.

6. Discussion

In this work, we investigated the quantum simulation of open quantum systems in optical waveguide arrays both experimentally and theoretically, which leads to a new perspective on the information flow between open systems and their environments. By using multiple waveguide arrays with different lengths we obtained a stable window into the evolution of the system and were able to perform a time-resolving state tomography. This allowed to observe non-Markovian evolution of the open system and to identify different types of information flow.

Conceptually, we extended the BLP measure as a general quantifier for the presence of information. This enables to trace the information lost from our experimental system and identify our scenario as a special case of information transfer to the environment, which can be regarded as classical, in the sense that only information encoded in one type of parameter is copied to the environment. Through further theoretical analysis we derived a tradeoff relation for our scenario, requiring information encoded in a certain parameter to be lost from the system if information stored in another parameter is gained in the environment, which we confirmed via simulations. Conversely, we also demonstrated that the platform of optical waveguide arrays is suitable to implement a broad range of different scenarios by showing the simulation of a theoretical example with full quantum state transfer between system and environment.

Our results form the basis of a comprehensive analysis of information flow between open system and environment from a new perspective, which is sensitive to the presence of information in the environment. In particular, it allows to investigate to which extent statements about the information present in the environment can be based on observations on the system alone. Another possible extension of our research is the analysis of deeper quantum phenomena arising from the interference of several photons interacting with a common or with separate environments, in particular with respect to effects originating from entanglement.

Acknowledgements

The authors thank Harald Weinfurter for fruitful discussions and extensive support. The authors also thank Julian Roos for constructive exchange about open quantum systems. This work was supported

© 2025 The Author(s). Laser & Photonics Reviews published by Wiley-VCH GmbH

18638899, 0, Downloaded from https://onlinelibrary.wiley.com/doi/10.1002/lpor.202400737 by Jan Dziewior - MPI 356 Quantum Optics , Wiley Online Library on [16/02/2025]. See the Terms and Conditions (https://onlinelibrary.wiley.com/terms-and-conditions) on Wiley Online Library for rules of use; OA articles are governed by the applicable Creative Commons License

ADVANCED SCIENCE NEWS
www.advancedsciencenews.com

LASER & PHOTONICS REVIEWS
www.lpr-journal.org

by the DFG Beethoven 2 Project No. WE2541/7-1, Germany's Excellence Strategy EXC-2111-390814868 as well as by the BMBF (project QuKuK, grant no. 16KIS1621). A.S. acknowledges funding from the European Research Council (grant no. 899368 'EPIQUS'), the Deutsche Forschungsgemeinschaft (grants SZ 612/9-2, SZ 276/20-1, SZ 276/21-1, SZ 276/27-1, IRTG 2676/1-2023 "Imaging of Quantum Systems," project no. 437567992, and SFB 1477 "Light-Matter Interactions at Interfaces," project no. 441234705), and the Alfried Krupp von Bohlen and Halbach Foundation. J.D. acknowledges support by the international Max-Planck-Research school for Quantum Science and Technology (IMPRS-QST), and J.D.A.M. acknowledges support of the MCQST START fellowship.

Open access funding enabled and organized by Projekt DEAL.

Conflict of Interest

The authors declare no conflict of interest.

Data Availability Statement

The data that support the findings of this study are available from the corresponding author upon reasonable request.

Keywords

integrated optics, open quantum systems, quantum information

Received: May 21, 2024
Published online:

[1] J. T. Barreiro, M. Müller, P. Schindler, D. Nigg, T. Monz, M. Chwalla, M. Hennrich, C. F. Roos, P. Zoller, R. Blatt, *Nature* **2011**, *470*, 486.
[2] S. Maniscalco, J. Piilo, F. Intravaia, F. Petruccione, A. Messina, *Phys. Rev. A* **2004**, *69*, 052101.
[3] A. Chiuri, C. Greganti, L. Mazzola, M. Paternostro, P. Mataloni, *Sci. Rep.* **2012**, *2*, 968.
[4] S. Mostame, J. Huh, C. Kreisbeck, A. J. Kerman, T. Fujita, A. Eisfeld, A. Aspuru-Guzik, *Quantum Inf. Process.* **2017**, *16*, 1.
[5] I. de Vega, D. Alonso, *Rev. Mod. Phys.* **2017**, *89*, 015001.
[6] Á. Cuevas, A. Geraldi, C. Liorni, L. D. Bonavena, A. De Pasquale, F. Sciarrino, V. Giovannetti, P. Mataloni, *Sci. Rep.* **2019**, *9*, 3205.
[7] W. G. Unruh, *Phys. Rev. A* **1995**, *51*, 992.
[8] M. J. Biercuk, H. Uys, A. P. VanDevender, N. Shiga, W. M. Itano, J. J. Bollinger, *Nature* **2009**, *458*, 996.
[9] T. Monz, P. Schindler, J. T. Barreiro, M. Chwalla, D. Nigg, W. A. Coish, M. Harlander, W. Hänsel, M. Hennrich, R. Blatt, *Phys. Rev. Lett.* **2011**, *106*, 130506.
[10] J. Preskill, *Quant. Inf. Comput.* **2013**, *13*, 0181.
[11] E. Paladino, Y. M. Galperin, G. Falci, B. L. Altshuler, *Rev. Mod. Phys.* **2014**, *86*, 361.
[12] F. K. Malinowski, F. Martins, T. B. Smith, S. D. Bartlett, A. C. Doherty, P. D. Nissen, S. Fallahi, G. C. Gardner, M. J. Manfra, C. M. Marcus, F. Kuemmeth, *Phys. Rev. X* **2018**, *8*, 011045.
[13] M. A. Nielsen, I. L. Chuang, *Quantum Computation and Quantum Information: 10th Anniversary Edition*, 10th ed., Cambridge University Press, USA **2011**.
[14] L. Li, M. J. Hall, H. M. Wiseman, *Phys. Rep.* **2018**, *759*, 1.
[15] H.-P. Breuer, F. Petruccione, *The Theory of Open Quantum Systems*, Oxford University Press, Oxford **2007**.
[16] H.-P. Breuer, *J. Phys. B: At., Mol. Opt. Phys.* **2012**, *45*, 154001.
[17] H.-P. Breuer, E.-M. Laine, J. Piilo, *Phys. Rev. Lett.* **2009**, *103*, 210401.
[18] E.-M. Laine, J. Piilo, H.-P. Breuer, *Phys. Rev. A* **2010**, *81*, 062115.
[19] H.-P. Breuer, E.-M. Laine, J. Piilo, B. Vacchini, *Rev. Mod. Phys.* **2016**, *88*, 021002.
[20] J. Maziero, F. M. Zimmer, *Phys. Rev. A* **2012**, *86*, 042121.
[21] A. Pernice, J. Helm, W. T. Strunz, *J. Phys. B: At., Mol. Opt. Phys.* **2012**, *45*, 154005.
[22] J. H. Reina, C. E. Susa, F. F. Fanchini, *Sci. Rep.* **2014**, *4*, 7443.
[23] K. Roszak, L. Cywiński, *Phys. Rev. A* **2015**, *92*, 032310.
[24] H.-B. Chen, C. Gneiting, P.-Y. Lo, Y.-N. Chen, F. Nori, *Phys. Rev. Lett.* **2018**, *120*, 030403.
[25] M. Strzałka, D. Kwiatkowski, L. Cywiński, K. Roszak, *Phys. Rev. A* **2020**, *102*, 042602.
[26] M. Ziman, P. Štelmachovič, V. Bužek, M. Hillery, V. Scarani, N. Gisin, *Phys. Rev. A* **2002**, *65*, 042105.
[27] M. Gräfe, R. Heilmann, M. Lebugle, D. Guzman-Silva, A. Perez-Leija, A. Szameit, *J. Opt.* **2016**, *18*, 103002.
[28] T. Meany, M. Gräfe, R. Heilmann, A. Perez-Leija, S. Gross, M. J. Steel, M. J. Withford, A. Szameit, *Laser Photonics Rev.* **2015**, *9*, 363.
[29] F. Elster, S. Barkhofen, T. Nitsche, J. Novotný, A. Gábris, I. Jex, C. Silberhorn, *Sci. Rep.* **2015**, *5*, 13495.
[30] N. P. Kumar, S. Banerjee, R. Srikanth, V. Jagadish, F. Petruccione, *Open Syst. Inform. Dynam.* **2018**, *25*, 1850014.
[31] J. Naikoo, S. Banerjee, C. M. Chandrashekar, *Phys. Rev. A* **2020**, *102*, 062209.
[32] A. Salles, F. de Melo, M. P. Almeida, M. Hor-Meyll, S. P. Walborn, P. H. Souto Ribeiro, L. Davidovich, *Phys. Rev. A* **2008**, *78*, 022322.
[33] K. A. G. Fisher, R. Prevedel, R. Kaltenbaek, K. J. Resch, *New J. Phys.* **2012**, *14*, 033016.
[34] B.-H. Liu, L. Li, Y.-F. Huang, C.-F. Li, G.-C. Guo, E.-M. Laine, H.-P. Breuer, J. Piilo, *Nat. Phys.* **2011**, *7*, 931.
[35] J.-S. Tang, C.-F. Li, Y.-L. Li, X.-B. Zou, G.-C. Guo, H.-P. Breuer, E.-M. Laine, J. Piilo, *Europhys. Lett.* **2012**, *97*, 10002.
[36] D. Valente, M. F. Z. Arruda, T. Werlang, *Opt. Lett.* **2016**, *41*, 3126.
[37] Z.-D. Liu, H. Lyyra, Y.-N. Sun, B.-H. Liu, C.-F. Li, G.-C. Guo, S. Maniscalco, J. Piilo, *Nat. Commun.* **2018**, *9*, 3453.
[38] Z.-D. Liu, Y.-N. Sun, B.-H. Liu, C.-F. Li, G.-C. Guo, S. Hamedani Raja, H. Lyyra, J. Piilo, *Phys. Rev. A* **2020**, *102*, 062208.
[39] H. Lyyra, O. Siltanen, J. Piilo, S. Banerjee, T. Kuusela, *Phys. Rev. A* **2022**, *106*, 032603.
[40] A. Szameit, S. Nolte, *J. Phys. B: At., Mol. Opt. Phys.* **2010**, *43*, 163001.
[41] W. Heisenberg, *The Physical Principles of the Quantum Theory*, University of Chicago Press, Chicago **1930**.
[42] W. K. Wootters, W. H. Zurek, *Nature* **1982**, *299*, 802.
[43] G. Jaeger, A. Shimony, L. Vaidman, *Phys. Rev. A* **1995**, *51*, 54.
[44] B.-G. Englert, *Phys. Rev. Lett.* **1996**, *77*, 2154.
[45] M. Ozawa, *Phys. Rev. A* **2003**, *67*, 042105.
[46] P. Busch, P. Lahti, R. F. Werner, *Phys. Rev. Lett.* **2013**, *111*, 160405.
[47] L. Knips, J. Dziewior, A.-L. K. Hashagen, J. D. A. Meinecke, H. Weinfurter, M. M. Wolf, *arXiv* **2018**.
[48] R. Heilmann, M. Gräfe, S. Nolte, A. Szameit, *Sci. Rep.* **2014**, *4*, 4118.
[49] M. Ehrhardt, R. Keil, L. J. Maczewsky, C. Dittel, M. Heinrich, A. Szameit, *Sci. Adv.* **2021**, *7*, 9.

© 2025 The Author(s). Laser & Photonics Reviews published by Wiley-VCH GmbH

18638899, 0, Downloaded from https://onlinelibrary.wiley.com/doi/10.1002/lpor.202400737 by Jan Dziewior - MPI 356 Quantum Optics , Wiley Online Library on [16/02/2025]. See the Terms and Conditions (https://onlinelibrary.wiley.com/terms-and-conditions) on Wiley Online Library for rules of use; OA articles are governed by the applicable Creative Commons License

Chapter 6

Weak Values

Based on the results derived in previous chapters this chapter discusses weak values as the first of the two special topics of this work. In its first part the formal definitions, common interpretations and main applications of weak values are presented. This includes the concepts of deterministic and robust weak values, which both can be seen as motivating a view of weak values as properties of single pre- and postselected quantum systems. The second part of the chapter focuses on the weak trace approach to particle presence and its connection to weak values. After introducing the weak trace approach as a consistent and operationally motivated concept as well as highlighting its connection to the weak value of local projection, it is shown how the latter corresponds to a quantification of the universal modification of effective interactions of pre- and postselected systems. The chapter closes with a discussion of the seminal nested interferometer scenario and the general controversy surrounding the weak trace approach.

6.1 The Physical Meaning of Weak Values

6.1.1 Definitions of Weak Values

In 1988 Aharonov, Albert, and Vaidman (AAV) [675] introduced the *weak value* of a quantum mechanical observable as a novel concept in the formal description of quantum mechanical systems. It represents a generalization of the description of properties of quantum systems in terms of expectation values of observables and is based fundamentally on a time-symmetric formulation of quantum mechanics called the *two-state-vector formalism* (TSVF) [680, 673, 681, 671]. The TSVF describes PPS, as defined in Sec. 2.6, using pure states and defines for each point in time t a *two-state*

$$\langle \phi(t)| \, |\psi(t)\rangle \,, \tag{6.1}$$

which contains both a *forward-evolving* state $|\psi\rangle$ as well as a *backward-evolving* state $|\phi\rangle$, in contrast to the standard description which just involves a preparation corresponding to the preselection. While in the following the term “two-state” is used for brevity, commonly

the longer term "two-state-vector" is employed in the literature. Note that in general a two-state does not necessarily exist. A sufficient condition for its existence is given by the requirement that an ideal measurement, as defined in Sec. 2.2.1, is performed at a future point in time $t_2 > t$ on the system and all other degrees of freedom it has interacted with. Furthermore, some authors postulate, in analogy to the universal wavefunction of the MWI, a universal backwards evolving wavefunction [670, 678, 683], such that a two-state is defined for any quantum degree of freedom at any point in time.

Given a certain two-state $\langle\phi|\ |\psi\rangle$ of the system, the weak value $(\mathbf{A})_w$ of an observable $\mathbf{A}$ at time t is defined as [675, 680, 673, 681, 672, 677]

$$(\mathbf{A})_w := \frac{\langle\phi(t)|\mathbf{A}|\psi(t)\rangle}{\langle\phi(t)|\psi(t)\rangle}. \tag{6.2}$$

In general the weak value is a complex quantity. While the modulus of the numerator lies in the spectrum of $|\mathbf{A}|$, the denominator can take values with arbitrarily small modulus $|\langle\phi|\psi\rangle| \in [0, 1]$. This can lead to weak values with a magnitude far outside the spectrum of the observable. Weak values which are complex or outside of the spectrum are called *anomalous* weak values. For orthogonal pre- and postselection the weak value is not defined.

The definition of the weak value can be generalized to cases without complete postselection, called *partial postselection*, with the definition [810, 681, 813, 711]

$$(\mathbf{A})_w = \frac{\langle\psi(t)|\mathbf{\Pi}_\phi(t)\mathbf{A}|\psi(t)\rangle}{\langle\psi(t)|\mathbf{\Pi}_\phi(t)|\psi(t)\rangle}, \tag{6.3}$$

where $\mathbf{\Pi}_\phi$ is a projector acting on the Hilbert space of the forward evolving state $|\psi\rangle$. This definition is motivated in a two-fold manner. For one it reduces to the standard weak value (6.2) in the case that $\mathbf{\Pi}_\phi$ is a rank-1 projector and secondly it reproduces the dispositive meaning of the weak value also in the absence of full postselection as discussed in the next subsection. In fact without any postselection, i.e., $\mathbf{\Pi}_\phi = \mathbb{1}$ the weak value becomes equivalent to the expectation value of the observable given the forward evolving state only, i.e., $(\mathbf{A})_w = \langle\psi|\mathbf{A}|\psi\rangle$. In the absence of a universal backward evolving wavefunction, Eq. (6.3) has to be regarded as the most general definition of the weak value, which, with the help of suitable purification, allows to assign weak values to observables in *any* quantum mechanical scenario. An example of partial postselection is given by the operational definition of Bohmian velocity, as presented in Sec. 7.4.2. Furthermore, in **[P1]**, **[P6]**, and **[P3]**, as reprinted in Secs. 6.1.7, 6.1.8, and 6.2.6, respectively, reduced expressions for the weak value are employed, which, as discussed in the next subsection, represent effective formulations of scenarios with partial postselection.

The description of PPS is significantly simplified when the free evolution can be neglected in the time interval $[t_1, t_2]$ between pre- and postselection. In such cases the weak value is constant in the whole interval and can be calculated by simply replacing the time dependent pre- and postselection states by the respective states at times t_1 and t_2. Alternatively, there are also scenarios in which the operator $\mathbf{A}$ commutes with the free evolution

leading again to a constant weak value which can be calculated at an arbitrary point in time $t \in [t_1, t_2]$, in particular even at t_1 or t_2.

6.1.2 Reduced Expressions

In typical cases the observable $\mathbf{A}$ is acting not on the full purified Hilbert space $\mathcal{H}$, but only on one part of the system or only on one specific degree of freedom, i.e., $\mathbf{A} = \mathbf{A}_0 \otimes \mathbb{1}$ with $\mathbf{A}_0$ acting on a reduced space $\mathcal{H}_0$ and $\mathcal{H} = \mathcal{H}_0 \otimes \mathcal{H}_R$. Then, given a complete postselection, the definition of the weak value (6.2) can be reformulated in terms of the reduced states in $\mathcal{H}_0$. However, since the definition of the weak value involves scalar products between the full states $|\psi\rangle, |\phi\rangle \in \mathcal{H}$, it is imperative to take into account how the reduced states are purified. In general employing an arbitrary basis $\{|\xi_j\rangle\}$ of $\mathcal{H}_R$, the pre- and postselection states can be written as

$$|\psi\rangle = \sum_j c_j |\psi_j\rangle |\xi_j\rangle , \qquad |\phi\rangle = \sum_j d_j |\phi_j\rangle |\xi_j\rangle \tag{6.4}$$

where $c_j, d_j \in \mathbb{C}$ and the states $|\psi_j\rangle, |\phi_j\rangle \in \mathcal{H}_0$, with $c_j |\psi_j\rangle = \langle \xi_j | \psi \rangle$ and vice versa for $|\phi_j\rangle$, do not necessarily form two orthogonal sets. By tracing out $\mathcal{H}_R$ the *generalized two-state* [673, 681]

$$\sum_j a_j \langle \phi_j | \ |\psi_j\rangle \tag{6.5}$$

can be defined, with $a_j = c_j d_j^* \in \mathbb{C}$. The reduced expression for the weak value then becomes

$$(\mathbf{A})_w = (\mathbf{A}_0 \otimes \mathbb{1})_w = \frac{\sum_j a_j \langle \phi_j | \mathbf{A}_0 | \psi_j \rangle}{\sum_j a_j \langle \phi_j | \psi_j \rangle}. \tag{6.6}$$

Note that, while for any given two-state $\langle \phi | \ |\psi\rangle$, a generalized reduced two-state can be constructed, this construction is not unique and essentially depends on the arbitrary choice of a basis of $\mathcal{H}_R$.

With only partial postselection $\mathbf{\Pi}_\phi$ in general a reduced description cannot be formulated using a generalized two-state. However, in some cases the weak value can be expressed in terms of forward and backward evolving mixed states ρ_{pre} and ρ_{post} acting on $\mathcal{H}_0$, as introduced in Sec. 2.6.1. Assuming a sufficiently large remaining space $\mathcal{H}_R$, i.e., with $\dim \mathcal{H}_R \geq \big(\operatorname{rank} \operatorname{tr}_R(|\psi\rangle\langle\psi|) + \operatorname{rank} \mathbf{\Pi}_\phi\big)$, where tr_R represents the partial trace over $\mathcal{H}_R$, it is possible to separate the rest Hilbert space $\mathcal{H}_R$ into two parts $\mathcal{H}_R^{(1)}$ and $\mathcal{H}_R^{(2)}$ with $\mathcal{H}_R = \mathcal{H}_R^{(1)} \otimes \mathcal{H}_R^{(2)}$, where $\mathcal{H}_R^{(2)}$ represents the part which is uncorrelated with the preselection state of the degree of freedom described by $\mathcal{H}_0$. The forward evolving state can be written as

$$|\psi\rangle = \Big(\sum_j c_j |\psi_j\rangle |\xi_j'\rangle \Big) |\zeta\rangle , \tag{6.7}$$

with normalized coefficients $c_j \in \mathbb{C}$, some arbitrary basis $\{|\xi'_j\rangle\}$ of $\mathcal{H}_R^{(1)}$, and $|\zeta\rangle$ being the forward evolving state in $\mathcal{H}_R^{(2)}$. Note that, again, the states $|\psi_j\rangle \in \mathcal{H}_0$ do not necessarily form an orthogonal set. With respect to $\mathcal{H}_0$, the forward evolving state can then be represented by the density operator

$$\rho_{\text{pre}} = \sum_j |c_j|^2 |\psi_j\rangle\langle\psi_j|, \tag{6.8}$$

where it is crucial that the no postselection is performed on $\mathcal{H}_R^{(1)}$, i.e., $\langle\xi'_j|\mathbf{\Pi}_\phi|\xi'_k\rangle = \delta_{jk}$.

Together with the state $|\zeta\rangle$, the partial postselection $\mathbf{\Pi}_\phi$ then effectively constitutes a backward evolving density operator ρ_{post} with

$$\rho_{\text{post}} = \frac{\text{tr}_R\big(\mathbf{\Pi}_\phi|\zeta\rangle\langle\zeta|\big)}{\text{tr}\big(\mathbf{\Pi}_\phi|\zeta\rangle\langle\zeta|\big)}. \tag{6.9}$$

The weak value (6.3) then can be rewritten as the convenient expression [**P1**]

$$(\mathbf{A})_w = \frac{\text{tr}\big(\rho_{\text{post}}\mathbf{A}_0\rho_{\text{pre}}\big)}{\text{tr}\big(\rho_{\text{post}}\rho_{\text{pre}}\big)}. \tag{6.10}$$

For example for any given basis $\{|b_j\rangle\}$ of $\mathcal{H}_0$, arbitrary postselection states

$$\rho_{\text{post}} = \sum_j p_j |b_j\rangle\langle b_j| \tag{6.11}$$

can be constructed by choosing

$$\mathbf{\Pi}_\phi = \mathbb{1}_{R1} \otimes \sum_j |b_j\rangle\langle b_j| \otimes |\zeta_j\rangle\langle\zeta_j|, \tag{6.12}$$

$$|\zeta\rangle = \sum_j \sqrt{p_j}\,|\zeta_j\rangle \tag{6.13}$$

where $\mathbb{1}_{R1}$ is the identity of $\mathcal{H}_R^{(1)}$ and $\{|\zeta_j\rangle\}$ are elements of some basis of $\mathcal{H}_R^{(2)}$. Note that $\mathbf{\Pi}_\phi$ can be seen as the non-selective effect of a quantum instrument, which consists of projectors onto the joint states $|b_j\rangle\,|\zeta_j\rangle$. As discussed in Sec. 2.6.1, the practical meaning of a mixed postselection is the projection on a randomly chosen state $|b_j\rangle$. Thus, in the language of QIT, the preselection state $|\zeta\rangle$ can be seen simply as a source of randomness for the choice of this postselection. In [**P1**], as reprinted in the next section, also an alternative scheme for the construction of mixed postselection states is described.

6.1.3 Weak Value Measurements

While expectation values obtain their dispositive meaning as averages over outcomes for measurements of quantum mechanical observables, the situation is different for weak values.

In particular, since a weak value is defined at a particular point in time t with respect to a two-state, the future evolution of the system, at least until a complete postselection, is of equal importance as its past evolution [680, 879, 672, 731]. In effect, in general for a single system weak values cannot be connected to outcomes of strong measurements as those necessarily disturb the evolution of the system. However, when considering sufficiently weak measurements, as defined in Sec. 2.2.4, weak values can be measured to arbitrary precision on ensembles of equally pre- and postselected systems [879, 681].

For the typical measurement interaction $\mathbf{U}_I = \exp(-i\varepsilon \mathbf{A} \otimes \mathbf{B}/\hbar)$ of product form, as also employed in all three works reprinted in this chapter, and the initial pointer state $|\chi\rangle$, the pointer state $\widetilde{\rho}_\chi$ after interaction and conditioning on the postselection is given as

$$\widetilde{\rho}_\chi = N \operatorname{tr}_S\big(\mathbf{\Pi}_\phi \otimes \mathbb{1} \cdot \mathbf{U}_I |\psi\rangle\langle\psi| \otimes |\chi\rangle\langle\chi| \mathbf{U}_I^\dagger\big), \tag{6.14}$$

with proper normalization N and the partial trace over the system tr_S. In general this state can be approximated to first order in ε as the pure state $|\widetilde{\chi}\rangle$ with [675, 670, 814, 741]

$$|\widetilde{\chi}\rangle \approx e^{-i\varepsilon (\mathbf{A})_w \mathbf{B}/\hbar} |\chi\rangle\,. \tag{6.15}$$

Here $(\mathbf{A})_w$ corresponds to the general expression (6.3), which reduces to (6.2) in cases of complete postselection. Again in the absence of any postselection the final pointer state just depends on the expectation value of $\mathbf{A}$, as already shown in Eq. 2.9. The form of the effective pointer state (6.15) represents the dispositive definition of weak values and also justifies the expression for the weak value with partial postselection.

Since in weak measurements eigenvalues are not resolved, the particular complex values of $(\mathbf{A})_w$ can be determined for an ensemble of PPS by measuring the expectation values of suitable observables on the pointer $|\widetilde{\chi}\rangle$. For a general pointer observable $\mathbf{C}$ the shift $\delta\mathbf{C}$ of the expectation value is given as [760]

$$\delta\mathbf{C} \approx -i\frac{\varepsilon}{\hbar}\mathrm{Re}\big[(\mathbf{A})_w\big]\langle[\mathbf{C},\mathbf{B}]\rangle + \frac{\varepsilon}{\hbar}\mathrm{Im}\big[(\mathbf{A})_w\big]\langle\{\mathbf{C},\mathbf{B}\}\rangle. \tag{6.16}$$

While the real part of the weak value has a similar effect as the expectation value in regular weak measurements (2.10), an additional term depending on the imaginary part and the anti-commutator of $\mathbf{B}$ and $\mathbf{C}$ appears. The real part is commonly determined by considering non-commuting pointer observables $\mathbf{B}$ and $\mathbf{C}$ as well as a minimally disturbing measurement such that the anti-commutator and thus the dependence on the imaginary part disappears. In contrast, the imaginary part can be obtained by simply measuring the shift of the expectation value of $\mathbf{B}$, i.e., with $\mathbf{C} = \mathbf{B}$.

Typically weak measurements are often performed with continuous pointers and MUS, such that using, e.g., $\mathbf{B} = \mathbf{p}$ and $\mathbf{C} = \mathbf{x}$, the famous relations [733, 814, 813, 711, 741, 712]

$$\begin{aligned} \delta\mathbf{x} &= \varepsilon \mathrm{Re}\big[(\mathbf{A})_w\big] \\ \delta\mathbf{p} &= 2\frac{\varepsilon}{\hbar}\,(\Delta\mathbf{p})^2\,\mathrm{Im}\big[(\mathbf{A})_w\big], \end{aligned} \tag{6.17}$$

are obtained. As shown in **[P3]**, reproduced in Sec. 6.2.6, in the case of MUS the expressions above remain valid for arbitrary interaction strengths ε if the change of the weak value due

to the non-negligible measurement interaction and resulting entanglement between system and pointer is taken into account. Another example of a typical weak value measurement is given by a qubit pointer [814], where $\mathbf{B} = \boldsymbol{\sigma}_x$, $\mathbf{C} = \boldsymbol{\sigma}_y$, and $\boldsymbol{\sigma}_z|\chi\rangle = \pm|\chi\rangle$, or any permutation of the three Pauli operators. Then for the shifts $\delta\boldsymbol{\sigma}_y$ and $\delta\boldsymbol{\sigma}_x$ the respective expressions, as given above, are recovered in approximation for sufficiently small ε. The first weak value measurement was performed by Ritchie *et al.* [771], and since than weak values have been measured in various types of pre- and postselected quantum systems, such as, e.g., [781, 766, 783], having even been found to occur in standard technological applications [700]. As already mentioned above, all the works reprinted in this chapter also represent examples of such weak value measurements.

Note that some authors do not take formal expressions as (6.2) and (6.3) as the defining condition of the weak value and instead define it as the conditioned average outcome of weak measurements, see, e.g., [810, 813, 741]. From this point of view it is natural to regard the requirement of weak interaction strength for the measurement of weak values as an undesired restriction of the applicability of the theory and in effect sometimes modified expressions for weak values are proposed, which take into account higher orders of the expansion in orders of interaction strength ε [813, 741, 712, 743]. However, the latter approach represents a stark departure from the standard approach to weak values [680, 681, 677], as presented here, in which the weak value is defined independently of measurements and represents a property of PPS at a particular moment in time. As mentioned above, if a system becomes entangled with another due to a measurement which is not weak, the solution is thus not to redefine the weak value but rather to express it either in terms of the joint state of both systems or, in case of observables acting only a subsystem, via the proper reduced expression, as derived in Sec. 6.1.2. This weak value can then always be measured via weak interaction with a third system. Such reduced expressions are used for the description of the experimental weak value measurements **[P6]** and **[P3]**, see Secs. 6.1.8 and 6.2.6, respectively.

6.1.4 Metrology and Tomography

The fact that weak values can be anomalous and in particular lie arbitrarily far outside the eigenvalue spectrum of $\mathbf{A}$, in connection with the possibility to measure them in weak interactions, has motivated their application in quantum metrology in an approach known as *weak value amplification* (WVA) [712, 732, 740, 791, 757]. The typical scenario of interest is an interaction of the form $\mathbf{U}_I$ with an unknown parameter ε. By preparing two systems in suitable states and postselecting one of them in a state almost orthogonal to the preselection, the effective change of the state of the other system is given by Eq. (6.15), where the weak interactions strength ε is multiplied by a large factor. From the perspective of the standard formalism this can be seen as a particular instance of close to destructive interference between pointer components corresponding to various eigenvalues of the measured observable, which represent an instance of so-called *super-oscillations* [697, 696, 679, 834].

If the amplification factor is too large the approximation breaks down and with it also

the amplification effect. Thus, WVA is only useful in a weak regime with sufficiently small interaction strength ε. While, as already mentioned, the exact quantitative definition of the weak regime is non-trivial, a sufficient condition is given by [681, 813]

$$\frac{\varepsilon}{\hbar}|(\mathbf{A})_w| \ll \Delta\mathbf{x}, \tag{6.18}$$

in the case of canonical measurements. Thus, at least in general only pointer shifts much smaller than the pointer width $\Delta\mathbf{x}$ can be amplified efficiently. Note, however, that for particular observables $\mathbf{A}$ defined on sufficiently large PPS this condition is not necessary and anomalously large pointer shifts of the order $\Delta\mathbf{x}$ or greater can be generated, as discussed in Sec. 6.1.6.

Assuming a complete postselection, the probability of postselection p_{post} is given by $p_{\text{post}} = |\langle\psi|\phi\rangle|^2$. Thus for a number n_{pre} of prepared systems and pointers, only a fraction $n_{\text{post}} \approx p_{\text{post}} n_{\text{pre}}$ is expected to successfully pass the postselection and be detected. Furthermore, the modulus of the weak value is bounded also in dependence on the probability of postselection as

$$|(\mathbf{A})_w| \leq \frac{|a_{\max}|}{\sqrt{p_{\text{post}}}}, \tag{6.19}$$

where $a_{\max}$ is the eigenvalue of $\mathbf{A}$ with maximal modulus. Since again for a weak canonical measurement the uncertainty of the pointer is not increased, the SNR Ξ_{weak} of the estimation of ε on an ensemble of PPS using weak value amplification becomes

$$\Xi_{\text{weak}} = \frac{|\mathbb{E}[\mathfrak{e}]|}{\Delta\mathfrak{e}} \approx \sqrt{n_{\text{post}}}\frac{|\varepsilon \text{Re}\big[(\mathbf{A})_w\big]|}{\Delta x} \leq \sqrt{n_{\text{pre}}}\frac{|\varepsilon a_{\max}|}{\Delta x}, \tag{6.20}$$

where $\mathfrak{e}$ is the estimator of ε, as defined in Sec. 1.7.1. Thus, when counting prepared or interacting systems, clearly for canonical measurements WVA cannot provide any advantage compared to a technique with preselection only. In particular, by choosing $|\psi\rangle = |a_{\max}\rangle$, best metrological performance can be achieved. The above result has been generalized for arbitrary systems and interactions, showing that in general no advantage can be provided by WVA when counting prepared and interacting systems [159, 705, 720, 740, 791]. However, clearly when conditioning on successful postselection and considering the number of detected pointers n_{post} only, a significant metrological advantage is obtained [732, 794, 692], corresponding to super-resolution, as defined in Sec. 2.6.3.

Another crucial advantage of WVA occurs when the detection is not shot-noise limited, i.e., other sources of noise, commonly called *technical noise*, are dominant [718, 732, 791, 725, 779, 739, 757]. In such cases the SNR does not scale with $\sqrt{n}$ but with some other function $f(n)$ with $\partial_n f < 1/2\sqrt{n}$ in some range of n. Then WVA can provide a metrological advantage for any type of resource counting as long as

$$f(p_{\text{post}} n_{\text{pre}}) > \sqrt{p_{\text{post}}} f(n_{\text{pre}}). \tag{6.21}$$

An extreme case of such a scenario is detector saturation for which even $\partial_n f \leq 0$.

WVA has been successfully employed to measure various small effects, see, e.g., [729, 709, 716, 816, 806, 755, 747, 805, 815] for examples. By implementing WVA with, e.g., pulsed light it is possible to reuse the systems, which did not pass postselection [713, 752, 742], an approach known as *photon recycling*. Note, however, that this effectively just corresponds to a repetition of several WVA measurements, where the systems and pointers employed in subsequent repetitions happen to be those which have been rejected in previous ones. Since these rejected systems need to be prepared anew via suitable unitary operations, photon recycling does not affect the counting of prepared systems and can only conserve resources connected to the source of light.

Apart from metrology, the properties of weak values have also motivated a particular technique for the QST called *direct state tomography* (DST) [751, 750, 812, 712, 753, 642]. In this state estimation scenario the unknown quantity is the forward evolving state ρ and, with knowledge of the interaction, various weak values can be constructed by a suitable choice of postselection states. A measurement of these weak values then allows to reconstruct the full density operator ρ. DST is direct in the sense that state parameters, such as the entries of density operator corresponding to complementary observables, can be determined with a single measurement interaction [751, 750, 790]. The reader is also referred to the work [715] for a discussion of some of the details, merits and disadvantages of DST as well as to [774, 754, 756, 776, 790, 707, 737] for examples of experimental realizations. The interferometric alignment procedure developed in **[P3]**, see Sec. 6.2.6, where effectively the coupling strength parameters of a weak interaction are determined, combines the principle of repeated weak measurements under varying postselection states from DST with the increased precision gained from WVA.

6.1.5 Deterministic Weak Values

When considering the effects of weak interactions on pointer states for product interactions, i.e., Eqs. (2.9) and (6.15), no formal difference between the expressions for the pointer state $|\chi'\rangle$ and for the pointer state $|\widetilde{\chi}\rangle$, additionally conditioned on a postselection, becomes apparent. In the limit $\varepsilon \to 0$, both expressions resemble the pointer state $|\chi_j\rangle$ after interaction with a system preselected in the eigenstate $|a_j\rangle$ of $\mathbf{A}$, where

$$|\chi_j\rangle = e^{-i\varepsilon a_j \mathbf{B}/\hbar} |\chi\rangle \,. \tag{6.22}$$

Arguably this particular type of effect on a pointer has a special role in quantum measurements as it results from an interaction with a system in an eigenstate, which, at least according to the definition of EPR, as presented in Sec. 1.2.1, corresponds to an element of reality. In consequence Vaidman has proposed an extended definition of elements of reality:

> If we are certain that a procedure for measuring a certain variable will lead to a definite shift of the unchanged probability distribution of the pointer, then there is an element of reality: the variable equal to this shift. [803]

Note, however, that in this particular definition "reality" does not denote a correspondence with an ontological reality, as defined in Sec. 1.1.1, i.e., it is not about beables. Instead it establishes a different epistemic concept of "reality", which is defined based on FAPP observable phenomena. There are two ways in which a measurement procedure can diverge from Vaidman's condition, i.e., *not* reveal an element of reality, either by changing the pointer distribution or by introducing an indefinite change in the pointer state.

As discussed in [**P1**], reproduced below in Sec. 6.1.7, the disturbance of the pointer in the case of only partial postselection is in general indefinite since the pointer is in a mixed state. In contrast, after a complete postselection of the system, the pointer state, while disturbed, remains pure and in this sense represents a non-probabilistic state. Accordingly, weak values corresponding to complete pre- and postselection are called *deterministic* weak values in contrast to general *non-deterministic* weak values such as expectation values. Thus, while the form (6.22) with a_j replaced by $(\mathbf{A})_w$ is also only an approximation of the final pointer state $|\widetilde{\chi}\rangle$, the latter is already pure, in contrast to $|\chi'\rangle$, which, as discussed in Sec. 1.5.2, is only an approximation for a mixed state $\rho'_\chi \approx |\chi'\rangle\langle\chi'|$. In [**P1**] it is proven that in general deterministic weak values lead to pointer states which are not only pure but in a crucial manner closer to undisturbed shifted pointer states than ρ'_χ. In particular it is shown that in any case in which $(\mathbf{A})_w = \langle\mathbf{A}\rangle = a_j$, the Bures distance $\mathcal{D}_B(|\chi_j\rangle, |\widetilde{\chi}\rangle)$ scales as ε^2 while $\mathcal{D}_B(|\chi_j\rangle, \rho'_\chi)$ scales only with ε. In this sense, the effective interaction of a pointer with a system described by a deterministic weak value leads to a "definite shift" of the undisturbed pointer distribution and thus in the time-symmetric framework such weak values have the same empirical signature as eigenvalues.

Apart from the general proof, [**P1**] also contains an experimental demonstration of the different scaling of the pointer disturbances in the two scenarios. As in many optical weak value experiments, different degrees of freedom of a paraxial beam are used to represent system and pointer. In this case the polarization qubit corresponds to the system, and the transverse spatial wavefunction in horizontal direction to the pointer. The interaction between these two degrees of freedom is implemented in one path of a MZI, where the other path contains the undisturbed transverse wavefunction, i.e., the undisturbed pointer state. A measurement of the interferometric visibility then corresponds to a measurement of the two distances between the respective disturbed pointer states and the undisturbed one, confirming the different scalings with interaction strength ε. Note that throughout [**P1**] the term "robust" is used to denote deterministic weak values as defined here, which is better reserved for a different property, as discussed below.

6.1.6 Robust Weak Values

Typically weak values are measured via the estimation of weak pointer shifts based on repeated measurements on large ensembles of pointer systems. In general an anomalously large real weak value cannot be reliably observed in a canonical measurement on a single copy of the PPS. However, for special types of weak values, called *robust weak values*, it is in principle possible to measure an arbitrary large anomalous weak value on a single copy of the system [687, 680, 672].

A robust weak value can be obtained for a sum observable $\mathbf{A}$ defined on a sufficiently large system as

$$\mathbf{A} := \sum_{j=1}^{n} \mathbf{A}_j = \mathbf{A}_1 \otimes \mathbb{1} \otimes \mathbb{1} \otimes \ldots + \mathbb{1} \otimes \mathbf{A}_2 \otimes \mathbb{1} \otimes \ldots + \ldots, \tag{6.23}$$

where the Hilbert space of the system can be decomposed into n parts as $\mathcal{H} = \bigotimes_{j=1}^{n} \mathcal{H}_j$ and each operator $\mathbf{A}_j$ acts only on the subspace $\mathcal{H}_j$. Furthermore, a scenario is considered where pre- and postselection factorize over the various parts of the system, such that

$$|\psi\rangle = \bigotimes_j |\psi_j\rangle\,, \qquad |\phi\rangle = \bigotimes_j |\phi_j\rangle\,, \tag{6.24}$$

which results in the weak value

$$(\mathbf{A})_w = \sum_j (\mathbf{A}_j)_w = \sum_j \frac{\langle\phi_j|\mathbf{A}_j|\psi_j\rangle}{\langle\phi_j|\psi_j\rangle}. \tag{6.25}$$

For a canonical measurement, the pointer shift $\delta\mathbf{x}$ is given by the exact relation

$$\delta\mathbf{x} = \varepsilon \mathrm{Re}\big[(\mathbf{A})_w\big] = \varepsilon \sum_j \mathrm{Re}\big[(\mathbf{A}_j)_w\big]. \tag{6.26}$$

Assuming, e.g., n equal operators $\mathbf{A}_j = \mathbf{A}_0$ as well as the same pre- and postselection states for each part of the system, the shift becomes $\delta\mathbf{x} = n\varepsilon(\mathbf{A}_0)_w$. Crucially, for appropriate pre- and postselection states the final pointer uncertainty scales with lower order than n, such that for sufficiently high n even an anomalous weak value can be resolved [680].

In **[P6]**, as reproduced below in Sec. 6.1.8, a measurement of such a robust weak value is experimentally realized based on a single reading of the measurement device, i.e., without statistical averaging over measurements on an ensemble of systems. Instead of coupling to a large system, a canonical measurement of the same anomalous weak value is performed on a number $n = 7$ of identically pre- and postselected qubits all coupling to the same pointer. As shown in **[P6]**, this is exactly equivalent to the scenario of a robust weak value discussed above. In the experiment the robust weak value is resolved via a canonical measurement by achieving a pointer shift of $\delta\mathbf{x} \approx 4\Delta\mathbf{x}$ for an anomalous weak value with $|(\mathbf{A})_w| \approx 2.5|a_{\max}|$.

Since the initial introduction of weak values, their meaning has been the subject of significant debate, as summarized in [794]. A central issue is the question whether the outcomes of weak value measurements reveal quantum properties of single PPS [727, 677, 699, 772, 693] or are merely statistical effects emerging from the large uncertainty of weak measurements performed on an ensemble [744, 730], some authors even claiming that they can be modeled classically [719]. This controversy is of course also related to the general question about the nature of the wavefunction, as sketched in Sec. 1.2.4. As shown both by the concept of deterministic weak values, which indicate a fundamental difference between

certain weak values and statistical expectation values, and by the possibility to measure robust weak values, it is possible to consistently attribute weak values to single quantum systems [680, 794].

In consequence the weak value can be seen as a candidate for the definition of *inter-phenomena*, as coined by Reichenbach [936], which "assert something about what happens between the localized phenomena", i.e., between pre- and postselection. This is also how statements that the TSVF "provides maximal possible information about the quantum system" [673, 681] can be understood. Accordingly, in particular the real part of the weak value has been taken to represent the actual physical state of affairs, most famously in studies of tunneling times [785, 784] and of momentum transfer in the context of double-slit complementarity [810, 811, 722, 309], a view which has been called "realistic straight forward interpretation" [789]. The latter interpretation also fits naturally to a connection of weak values with the MWI in which case they correspond to the epistemic reality of each branch while the fundamental ontology is exhausted by the universal forward evolving wavefunction [803, 681, 801, 792, 1018, 798]. In contrast, some authors go even further to propose a nonlocal and retrocausal weak value based ontology denoted as "weak reality" in which novel types of particles are defined via a set of weak values [688, 808].

6.1.7 [P1]

PHYSICAL REVIEW A **96**, 032114 (2017)

Weak value beyond conditional expectation value of the pointer readings

Lev Vaidman,[1] Alon Ben-Israel,[1] Jan Dziewior,[2,3] Lukas Knips,[2,3] Mira Weißl,[2,3] Jasmin Meinecke,[2,3] Christian Schwemmer,[2,3] Ran Ber,[1] and Harald Weinfurter[2,3]

[1]*Raymond and Beverly Sackler School of Physics and Astronomy, Tel-Aviv University, Tel-Aviv 69978, Israel*

[2]*Max-Planck-Institut für Quantenoptik, Hans-Kopfermann-Straße 1, 85748 Garching, Germany*

[3]*Department für Physik, Ludwig-Maximilians-Universität, 80797 München, Germany*

(Received 10 November 2016; revised manuscript received 2 May 2017; published 19 September 2017)

It is argued that a weak value of an observable is a robust property of a single pre- and postselected quantum system rather than a statistical property. During an infinitesimal time a system with a given weak value affected other systems as if it had been in an eigenstate with eigenvalue equal to the weak value. This differs significantly from the action of a system preselected only and possessing a numerically equal expectation value. The weak value has a physical meaning beyond a conditional average of a pointer in the weak measurement procedure. The difference between the weak value and the expectation value has been demonstrated on the example of photon polarization. In addition, the weak values for systems pre- and postselected in mixed states are considered.

DOI: 10.1103/PhysRevA.96.032114

I. INTRODUCTION

Contrary to classical physics, in quantum mechanics physical observables or, in short, variables might not have definite values even if the full quantum description of the system is given. If the system is in a superposition or a mixture of eigenstates corresponding to different eigenvalues, then only an expectation value of a variable is defined. But since, in general, this value cannot be measured given a single system, the expectation value is commonly regarded as a statistical property of an ensemble of quantum systems. If, however, the system is in an eigenstate of the observable, a measurement on a single system is enough to observe the corresponding eigenvalue. This constitutes the definite nature of the eigenvalue in contrast to the statistical nature of the expectation value.

Again, contrary to classical physics, even if we have complete information about the preparation of a system, the outcomes of future measurements are in general not determined. The two-state vector formalism [1,2] uses such future results to describe systems in between two measurements. It employs two quantum states, the usual one defined by the preparation and the backward evolving state defined by the result of the postselection. For describing the coupling to variables of a pre- and postselected system the concept of a *weak value* has been introduced [3]. It was accepted with harsh criticism [4–6], but its significance was appreciated in a number of experiments performing weak measurements in a regime of anomalous weak values achieving unprecedented precision in measuring small parameters [7,8]. New proposals and experiments continue to appear [9–15]. Still, a controversy regarding the usefulness of anomalous weak values for parameter estimation and metrology compared to conventional methods based on strong measurements arose [16–29]. Moreover, even the quantum nature of weak values was questioned [30–37].

Weak values were introduced as outcomes of weak measurements [3], which have large uncertainty in the pointer position. Thus, in experiments, the weak value is obtained as a statistical average of the pointer readings. Even among proponents of this concept the weak value is frequently understood as a mere generalization of the expectation value for the case when the quantum system is postselected, i.e., a conditional expectation value [38,39].

In this paper we argue that although we obtain weak values from many measurement outcomes, they represent definite properties of single pre- and postselected quantum systems. Furthermore, we show a fundamental equality between weak values and eigenvalues, concerning the interaction of quantum systems.

This holds when the system is described by a pure two-state vector and also when it is described by a *generalized two-state vector* [40]. In addition, we generalize the definition of weak values for genuine mixed pre- and postselected states [41]. Then, but only then, the weak value has a statistical nature.

II. COMPARING WEAK VALUES AND EXPECTATION VALUES

The weak value of a variable A is defined for a single quantum system preselected in a state $|\psi\rangle$ and postselected in a state $|\varphi\rangle$ as

$$A_w \equiv \frac{\langle\varphi|A|\psi\rangle}{\langle\varphi|\psi\rangle}. \tag{1}$$

In our analysis we stay within the framework of the standard quantum theory describing the system and systems it interacts with using wave functions only. Our feature of interest is the interaction of a quantum system, which is operationally defined as the measurable change in the state of external systems after a certain interaction period. In particular we view the weak value (as well as the eigenvalue and the expectation value) as a description of this interaction. In case of the weak value, the measurable change of the external system is the result of an interaction followed by postselection. The interaction of a pre- and postselected system and thus the weak value are considered only after the postselection.

While the definition of the weak value is based on the pure two-state vector with states $|\psi\rangle$ and $|\varphi\rangle$ considered at a particular time t, its operational meaning as stated above relies on interactions with other systems which create entanglement. The way to deal with this problem is by a delicate play of

 ©2017 American Physical Society

limits. We should consider a short period of time around time t to evaluate the action of the system on other systems. The change in the other systems should be large enough to be seen, but the back action on the system should be small enough, such that the change in the two-state vector describing the system can be neglected. Since we allow an unlimited ensemble of experiments with identical pre- and postselection, the required limits are achievable.

We start our analysis with a von Neumann measurement Hamiltonian coupling a quantum system to a continuous pointer system defined by its position Q:

$$H_{\rm int} = gAP, \tag{2}$$

where P is a conjugate momentum to Q and g is a coupling constant. We assume that at time $t = 0$ the system was prepared in state $|\psi\rangle$ and, shortly after, at time $t = \epsilon$ was found in state $|\varphi\rangle$. For simplicity of calculations, we assume that the pointer at time $t = 0$ is in a Gaussian state:

$$\Phi_0 = \frac{1}{(2\pi)^{1/4}\sqrt{\Delta}} e^{-\frac{Q^2}{4\Delta^2}}. \tag{3}$$

For a comparison of different cases, we consider the pointer state after the interaction with the system and the postselection measurement at time $t = \epsilon$. Let us consider a particle with the integer spin observable

$$A \equiv S_z = \sum_j j|j\rangle\langle j|. \tag{4}$$

If, e.g., the spin state is the eigenstate $|1\rangle$, i.e., the variable has the eigenvalue $A = 1$, then at time $t = \epsilon$, independently of the result of the postselection measurement, the pointer state is shifted:

$$\Phi_{\rm e} = \frac{1}{(2\pi)^{1/4}\sqrt{\Delta}} e^{-\frac{(Q-g\epsilon)^2}{4\Delta^2}}, \tag{5}$$

where we have set $\hbar \equiv 1$ here and throughout the rest of the paper. If the system is not in an eigenstate of A, the pointer state might also be distorted.

To compare various cases we evaluate the effect of the interaction by calculating the distance between quantum states expressed by the Bures angle. The distance between the initial state of the measuring device (3) and the final state (5) is

$$D_A(\Phi_0, \Phi_{\rm e}) \equiv \arccos|\langle\Phi_0|\Phi_{\rm e}\rangle| = \frac{g\epsilon}{2\Delta} + O(\epsilon^3). \tag{6}$$

The amplitude of the additional orthogonal component is of the order of $\frac{g\epsilon}{2\Delta}$, but since our theoretical small parameter is $\epsilon \ll \frac{\Delta}{g}$, we take into account only the lowest order of ϵ.

Consider now a pre- and postselected system with $A_w = 1$, but in which both preselection and postselection do not include the eigenstate $|1\rangle$. A two-state vector which provides this weak value is

$$\langle\varphi|\,|\psi\rangle = \tfrac{1}{\sqrt{5}}(\langle -1| - 2\langle 0|)\ \ \tfrac{1}{\sqrt{2}}(|-1\rangle + |0\rangle). \tag{7}$$

After the postselection, the state of the pointer variable is

$$\Phi_{\rm w} = \mathcal{N}(\epsilon)\left(2e^{-\frac{Q^2}{4\Delta^2}} - e^{-\frac{(Q+g\epsilon)^2}{4\Delta^2}}\right) \approx \mathcal{N}'(\epsilon)e^{\frac{-Q^2g^2\epsilon^2}{4\Delta^4}}\Phi_{\rm e}. \tag{8}$$

Note that because $\Delta^2/g\epsilon \gg \Delta$, the distortion factor $e^{\frac{-Q^2g^2\epsilon^2}{4\Delta^4}}$ is almost constant relative to $\Phi_{\rm e}$. Therefore $\Phi_{\rm w}$ is effectively a Gaussian centered around $A_w = 1$ and is thus very close to $\Phi_{\rm e}$ as seen from the Bures angle

$$D_A(\Phi_{\rm e}, \Phi_{\rm w}) = \frac{g^2\epsilon^2}{2\sqrt{2}\Delta^2} + O(\epsilon^4). \tag{9}$$

The characteristic distance between states after the interaction for the time ϵ is approximately $\frac{g\epsilon}{2\Delta}$, so when the additional distance is proportional to ϵ^2, it can be neglected. Thus, in the limit of short interaction times, the pre- and postselected system with some weak value interacts with other systems in the same manner as a system preselected in an eigenstate with a numerically equal eigenvalue. Not only are the expectation values of the positions of the pointers essentially the same but the full quantum states of the pointers are almost identical.

The situation changes considerably when the system is only preselected in a state with the expectation value $\langle A\rangle = 1$, which, however, is not the eigenstate $|1\rangle$. To show this, assume that the particle is in the state

$$|\psi\rangle = \tfrac{1}{\sqrt{2}}(|0\rangle + |2\rangle). \tag{10}$$

At time $t = \epsilon$, now without postselection, the pointer system is not described by a pure state, but by a mixture. The density matrix describing this mixture is

$$\rho_{\rm ex} = \frac{1}{2\sqrt{2\pi}\,\Delta}\left(e^{-\frac{Q^2+Q'^2}{4\Delta^2}} + e^{-\frac{(Q-2g\epsilon)^2+(Q'-2g\epsilon)^2}{4\Delta^2}}\right). \tag{11}$$

The distance between $\rho_{\rm ex}$ and $\Phi_{\rm e}$, the state of the pointer after coupling to an eigenstate (5), is

$$D_A(\Phi_{\rm e}, \rho_{\rm ex}) \equiv \arccos(\sqrt{\langle\Phi_{\rm e}|\rho_{\rm ex}|\Phi_{\rm e}\rangle}) = \frac{g\epsilon}{2\Delta} + O(\epsilon^3). \tag{12}$$

This is a significantly larger distance than (9). In fact, the distance (12) is of the same order as (6) and cannot be neglected for small ϵ.

While the pointer states (8) and (11) correspond to similar probability distributions, they are fundamentally different. As in the case of an eigenstate (5), the final pointer state (8) corresponds to a shift of the original distribution given by a single number, the weak value. In this sense, we call eigenvalues and weak values "robust." The situation changes significantly when the system is prepared in a superposition of eigenstates. This results in a mixture of pointer distributions (11), which cannot be described by a single parameter anymore, but by several parameters, namely, all eigenvalues corresponding to the superposed eigenstates. Consequently, this pointer is in a statistical mixture of independent distributions in stark contrast to the other cases. In the above example, the statistical character of the expectation value is reflected in (11), which represents the mixture of two independent distributions centered around the eigenvalues 0 and 2.

Note that if we add postselection on the original state (10), such that $A_w = 1$, then the final state of the external system converges to that of the eigenvalue case with $A = 1$, again.

The system evolves as in the eigenvalue case also when the weak value is anomalously large and lies very far from the range of the actual eigenvalues. It might be equal to an eigenvalue which is not present in the pre- and postselected states, or it might be equal to a nonexisting "hypothetical"

eigenvalue of the system, as in the canonical example [3]. For example, a system described by the two-state vector

$$\langle\varphi|\,|\psi\rangle = \frac{1}{\sqrt{20\,201}}(100\langle -1| - 101\langle 0|)\;\frac{1}{\sqrt{2}}(|-1\rangle + |0\rangle) \tag{13}$$

has a weak value of 100. Then, the distance between the states of the external system at time $t = \epsilon$ in this case and in the case when the system has an eigenvalue $A = 100$,

$$D_A(\Phi_e, \Phi_w) = \frac{100\times 101 g^2\epsilon^2}{4\sqrt{2}\Delta^2} + O(\epsilon^4), \tag{14}$$

is larger than (9), but still scales favorably with ϵ^2. As will be shown in Sec. IV, the resulting scaling order is not restricted to these examples, but holds in general.

III. EXPERIMENTAL DEMONSTRATION

Our claim that the interaction with a pre- and postselected system described by some weak value is similar to the standard interaction with a system described by a numerically equal eigenvalue, but different from the interaction with a system described by a numerically equal expectation value, is tested experimentally. Our system is the polarization degree of freedom of the Gaussian light beam. The "other" or "pointer" system is the transverse position of the beam. The variable A of the system includes the polarization operator $\mathcal{P}$:

$$\mathcal{P}|H\rangle = |H\rangle, \quad \mathcal{P}|V\rangle = -|V\rangle. \tag{15}$$

The coupling to this variable is achieved by passing the beam through a birefringent crystal which shifts the beam according to its polarization. We consider situations in which the weak value and expectation value equal 0. The operator $\mathcal{P}$ has only eigenvalues ± 1, but effectively we can perform the experiment also for A with the eigenvalue 0 by removing the birefringent element from the beam or tilting it so that there is no shift.

We start by preparing light in the state

$$|\psi\rangle = \tfrac{1}{\sqrt{2}}(|H\rangle + |V\rangle) \equiv \tfrac{1}{\sqrt{2}}(|1\rangle + |-1\rangle). \tag{16}$$

Then, effectively, we have the three cases of interest: (i) without the crystal, the *eigenvalue* $A = 0$; (ii) with the crystal, preselection only of the state (16) with *expectation value* $\langle A\rangle = 0$; and (iii) pre- and postselection of the same state (16) with the *weak value* $A_w = 0$.

Coupling to a state with "eigenvalue" 0 causes no change of the state of the pointer system, meaning that the Gaussian beam is not shifted, and Φ_e has the form of (3).

Coupling to the state (16) with expectation value 0 leads to the mixed state of the pointer described by density matrix

$$\rho_{ex} = \frac{1}{2\sqrt{2\pi}\,\Delta}\left(e^{-\frac{(Q+g\epsilon)^2+(Q'+g\epsilon)^2}{4\Delta^2}} + e^{-\frac{(Q-g\epsilon)^2+(Q'-g\epsilon)^2}{4\Delta^2}}\right). \tag{17}$$

For postselected systems, the coupling to a state with weak value 0 leads to the pointer state

$$\Phi_w = \mathcal{N}\left(e^{-\frac{(Q-g\epsilon)^2}{4\Delta^2}} + e^{-\frac{(Q+g\epsilon)^2}{4\Delta^2}}\right). \tag{18}$$

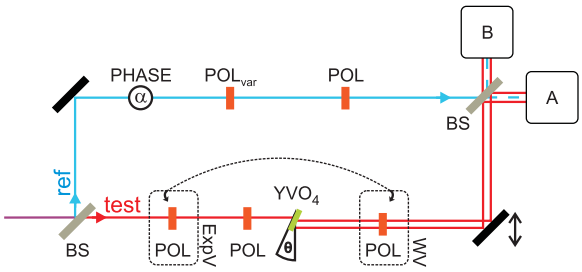

FIG. 1. Experimental setup for comparing pointer wave functions. By varying the phase α, we can change between constructive and destructive interference in order to measure the maximal visibility and thus to find the Bures angle. The first polarizer in the reference beam (ref) is used to vary the intensity of the reference beam. The postselection polarizer in the test beam (test) used when analyzing the weak value (WV) case is removed and put in front of the YVO_4 when observing the expectation value in the test arm (ExpV) to keep the number of optical components equal. Note that for practical reasons a folded Mach-Zehnder interferometer, i.e., a nondegenerate version of a Michelson interferometer, is used, where the phase can be scanned by means of a retroreflecting prism coupled to a piezo. The shift of the center of the test beam caused by the YVO_4 is compensated by a lateral displacement of the beam.

The distances between the states and the reference Φ_e given by (3) behave according to the results of the first example, (12) and (9), and are given by

$$D_A(\Phi_e, \rho_{ex}) \simeq \frac{g\epsilon}{2\Delta}, \tag{19}$$

$$D_A(\Phi_e, \Phi_w) \simeq \frac{g^2\epsilon^2}{4\sqrt{2}\Delta^2}. \tag{20}$$

The center of the beam is the same in all cases; the difference between the states is only due to different distortions of the initial Gaussian beam. Our method to measure this difference is to perform an interference experiment between the reference beam and the beam distorted by the measurement interaction for the two other cases. It is based on the following simple relation between maximal obtainable visibility of the interference between two beams and the Bures angle between their quantum states:

$$\arccos \mathcal{V}_{max} = D_A. \tag{21}$$

This formula holds when the visibility is maximal under variation of all parameters: alignment, relative intensity, and—in the case of interference between pure and mixed state—unitary transformation of auxiliary degrees of freedom, the polarization in our case. It follows from the well-known expression for the pure states, $\mathcal{V}_{max} = |\langle\Psi|\Phi\rangle|$, and from Uhlmann's theorem [42] about purification of mixed states.

In our experiment we use a balanced Mach-Zehnder interferometer where the incoming beam is preselected in the specified polarization (16) (see Fig. 1). In one arm of the interferometer, the spatial mode remains Gaussian ($\lambda = 780\,\text{nm}$, beam waist $w = 2\Delta = 813\,\mu\text{m}$) and can therefore be described by (3). The state in this arm, Φ_e, is used as reference. In the other arm we insert a yttrium orthovanadate (YVO_4) crystal (of thickness $d = 4.52\,\text{mm}$), which causes

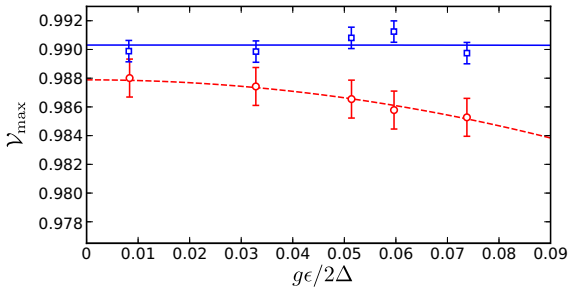

FIG. 2. Maximally achievable visibility for different couplings $g\epsilon$ in the interference experiment between the undisturbed beam and the test beam (weak value case, blue boxes with blue solid line; expectation value case, red circles with red dashed line) as a function of the coupling strength $g\epsilon/2\Delta$. The lines represent the theoretical curves with fitted offsets. Each setting was measured ten times to reduce the errors introduced by the optimization procedure.

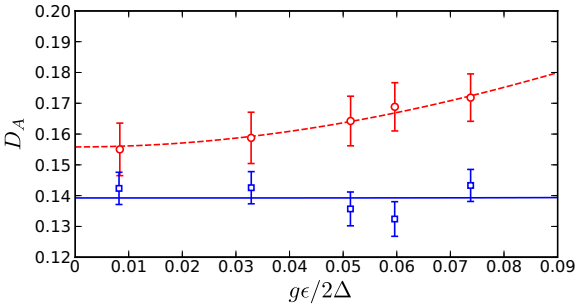

FIG. 3. Bures angles between the spatial state of the undisturbed beam (3) and the spatial states of the beam coupled to the weak value $A_w = 0$ (blue boxes with blue solid fitted line) and the expectation value $\langle A\rangle = 0$ (red circles with red dashed fitted line) as a function of the coupling strength $g\epsilon/2\Delta$. The fitting according to Eqs. (24) and (23) includes offset parameters ξ_1 and ξ_2 appearing due to imperfections of the optical setup.

a transversal shift according to the action of $\mathcal{P}$ from (15), thus coupling the (Gaussian) spatial mode of the beam to the different polarizations. For a tilting angle θ, the beam separation is

$$\delta x = d\left(\frac{\sin(\theta-\theta^{(o)})}{\cos(\theta^{(o)})} - \frac{\sin(\theta-\theta^{(e)})}{\cos(\theta^{(e)})}\right), \tag{22}$$

where $\theta^{(i)} = \arcsin\left(\frac{\sin(\theta)}{n^{(i)}}\right)$ is obtained via Snell's law for $i \in \{o,e\}$ with o (e) denoting the ordinary (extraordinary) beam. Varying the tilting angle θ mimics varying the interaction time ϵ according to $\delta x = 2g\epsilon$.

For the expectation value case the system is described by density matrix (17). For the weak value case (18) we add, behind the YVO_4 crystal, a polarization filter aligned in the original polarization state (16). In order to find the maximal visibility for different interaction strengths, the alignment of the interferometer was optimized and the relative intensities of the arms were varied by means of the first polarizer in the reference arm. There was no need to vary the reference polarization since in our setup the optimal polarization does not depend on the interaction strength.

Figure 2 presents our results for the observed visibility values for the two cases. The action of the crystal leads to the intended (spatial) pointer shifts, resulting in the Bures angles $\frac{g\epsilon}{2\Delta}$ and $\frac{g^2\epsilon^2}{4\sqrt{2}\Delta^2}$ for the expectation value case and the weak value case, respectively. The precision of the measurement is not sufficient to observe the tiny reduction of visibility in the weak value case when increasing $g\epsilon$ in the range available in the experiment given by the properties of the crystal. However, the decrease of visibility for the expectation value case can clearly be resolved.

With real optical components, the maximal visibility is limited, in our experiment to about 99.0% for $g\epsilon = 0$, mainly due to coupling to higher-order spatial modes. These imperfections can be modeled by a fixed pointer shift with amplitude ξ into a Hilbert-space direction orthogonal to the initial pointer state. Because of the high dimensionality of the Hilbert space of the pointer, it is unlikely that the imperfections are collinear to the intended shift and we assume them to be orthogonal.

Taking into account the influence of the imperfections, the dependences of the Bures angle given in (19) and (20) change to

$$D_A(\Phi_e,\rho_{ex}) = \sqrt{\xi_1^2 + \left(\frac{g\epsilon}{2\Delta}\right)^2}, \tag{23}$$

$$D_A(\Phi_e,\Phi_w) = \sqrt{\xi_2^2 + \left(\frac{g^2\epsilon^2}{4\sqrt{2}\Delta^2}\right)^2}, \tag{24}$$

respectively. Due to slight differences in the setup, the parameters ξ_1 and ξ_2, i.e., the offsets, are not exactly equal.

The Bures angles as functions of $g\epsilon$ for both cases are shown in Fig. 3 together with the corresponding least-squares fits according to (23) and (24) with ξ_1 and ξ_2 being the only fit parameters. We observe a good agreement with the theory [(23) and (24)] in both cases. While the Bures angle remains almost constant in the weak value case, it increases significantly for the expectation value case, which underpins our theoretical claim.

IV. GENERALIZATION OF THE RESULT TO ARBITRARY SYSTEMS

A system with a weak value behaves in general in the same manner as a system described by an eigenvalue, not just for coupling to a Gaussian state through the Hamiltonian (2). For the limit of an infinitesimally small time ϵ, the evolution of the system interacting with the pre- and postselected system according to the Hamiltonian (2) is

$$\Phi(Q) = \Phi_0(Q - g\epsilon A_w). \tag{25}$$

This holds not just for Gaussian distributions but for a wide class of wave functions with the Fourier transform reducing fast enough for large P. Yet, it is not directly applicable for coupling to a pointer with a discrete spectrum (see Appendix A for the case of a spin pointer). What is generally true is that for a pre- and postselected system the weak value (as an eigenvalue) should replace the corresponding operators in any interaction Hamiltonian, even when it is different from (2).

Note, however, that unlike eigenvalues, if in a nonlinear Hamiltonian there appears, say, A^3, it should not be replaced by $(A_w)^3$ but by the weak value of the respective operator, i.e., by the complex number $(A^3)_w$, which is in general different. In Appendix A we demonstrate the difference between coupling to systems described by weak values and systems described by expectation values for the case of a very different system than what was analyzed above, a spin-$\frac{1}{2}$ particle [43].

The different scaling behavior demonstrated in the previous examples can be derived for arbitrary states and interactions. Consider two systems, coupled by the Hamiltonian

$$H_{\rm int} = gAB, \tag{26}$$

where A is a variable of the system, B is a variable of the second system which we call the pointer system, and g is a coupling constant. The system is preselected in state $|\psi\rangle$ and postselected in state $|\phi\rangle$. The pointer system is prepared in state $|\Phi_0\rangle$. Its state after the postselection of the system is

$$|\Phi_{\rm w}\rangle = \mathcal{N}\langle\varphi|e^{-ig\epsilon AB}|\psi\rangle|\Phi_0\rangle. \tag{27}$$

If the system state $|\Psi\rangle$ is an eigenstate with eigenvalue $A = a$, numerically equal to the above weak value $A_w = a$, then the pointer ends up in the state

$$|\Phi_{\rm e}\rangle = e^{-ig\epsilon aB}|\Phi_0\rangle. \tag{28}$$

Estimating the distance between these two states by expanding the exponents (including those in normalization factor $\mathcal{N}$) in powers of ϵ gives the Bures angle

$$D_A(\Phi_{\rm e},\Phi_{\rm w}) = |(A^2)_w - a^2|\sqrt{\langle B^4\rangle - \langle B^2\rangle^2}\frac{g^2\epsilon^2}{2} + O(\epsilon^3), \tag{29}$$

where $\sqrt{\langle B^4\rangle - \langle B^2\rangle^2}$ is computed at the time of preselection, i.e., for $|\Phi_0\rangle$. Note that the first order of ϵ vanishes in all cases.

Now consider the first system to be preselected in the state $|\psi\rangle = \Sigma\alpha_k|a_k\rangle$ written in terms of eigenstates of A without postselection. The expectation value $\langle A\rangle$ is assumed to be numerically equal to a. We will compare the mixed state of the external system after the interaction

$$\rho_{\rm ex} = \Sigma|\alpha_k|^2 e^{-ig\epsilon a_k B}|\Phi_0\rangle\langle\Phi_0|e^{ig\epsilon a_k B} \tag{30}$$

to the state $|\Phi_{\rm e}\rangle$ corresponding to coupling to the eigenvalue a (actual or hypothetical). Straightforward calculation based on (12), in which we expand in powers of ϵ, yields the Bures angle

$$D_A(\Phi_{\rm e},\rho_{\rm ex}) = \Delta A\Delta B g\epsilon + O(\epsilon^2), \tag{31}$$

where the uncertainties ΔA and ΔB are again those of the initial state. In contrast to the weak value case the first order of ϵ does not drop out unless the system is preselected in an eigenstate of A or if the pointer system is prepared in an eigenstate of B.

We have shown that the distance in the weak value case generally scales with a higher order than in the expectation value case. Thus, in the weak interaction limit, the distance in the weak value case is infinitesimally small compared to the distance in the expectation value case. In this limit we may say that the coupling specified by the weak value is identical to the coupling specified by an eigenvalue. The coupling given by an expectation value is clearly different. The application of (29) and (31) to several specific cases is considered in Appendix B.

Care has to be taken for a complex weak value which cannot be an eigenvalue. In this case the statement that in the interaction Hamiltonian the operator corresponding to a variable of a pre- and postselected system should be replaced by the weak value remains correct. Consequently, the effective Hamiltonian of systems coupled to a pre- and postselected system is, in general, non-Hermitian [44]. In Appendix C we demonstrate the effect of a system with an imaginary weak value on other systems. The scaling of the distance when the pre- and postselected system characterized by a complex weak value is coupled to an arbitrary system is identical to that obtained for the real weak value case given by (29).

V. GENERALIZATION OF WEAK VALUES FOR MIXED PRE- AND POSTSELECTED STATES

A natural way to generalize the expression for weak values (1) to density matrices is

$$A_w \equiv \frac{{\rm tr}(\rho_{\rm post}A\rho_{\rm pre})}{{\rm tr}(\rho_{\rm post}\rho_{\rm pre})}. \tag{32}$$

For pure pre- and postselection states the density matrices describing the system are $\rho_{\rm pre} = |\psi\rangle\langle\psi|$, $\rho_{\rm post} = |\varphi\rangle\langle\varphi|$, and the validity of this ansatz is immediately seen. In the following, we will show that the expression (32) for a weak value at time t correctly shows the average effect of the system coupled to other systems at time t through variable A also for a case of a genuine *mixed two-state vector*:

$$(\rho_{\rm post},\rho_{\rm pre}). \tag{33}$$

We do not expect that in a genuinely mixed case the weak value will be robust as an eigenvalue. It can be shown that for external systems coupled to the system through variable A the deviation of the final states from the final states in the case of a numerically equal eigenvalue of A is of order ϵ. This is similar to the case of the expectation value.

In order to introduce the concept of a mixed two-state vector, we need to clarify how to pre- and postselect onto genuinely mixed states. The concept of a mixed forward evolving state is well understood. The mixed state $\rho_{\rm pre}$ is obtained by preparation of a state entangled with an ancilla (A_1). The state of the system remains mixed provided no measurement has been carried out on A_1 after the preparation. The future of the ancilla is unknown and this is what ensures that the state of the system is mixed.

In order to obtain a mixed backward evolving state we cannot just perform a postselection measurement of a state entangled with another ancilla (A_2). We need also to ensure that no measurement has been carried out on A_2 *before* the postselection measurement. But since A_2 was created in a possibly known state, we have to erase its past [45].

The scheme for the creation of a mixed two-state vector (33) at time t, $t_1 < t < t_2$, is described in Fig. 4. At time t_1 we prepare an entangled state with A_1 and ensure that no measurement is performed on it after creation of the entangled state. This provides a preselected mixed state. Shortly before time t_2 we prepare a maximally entangled state of A_2 and ancilla A_3. This erases the past of A_2 relative to time t_2

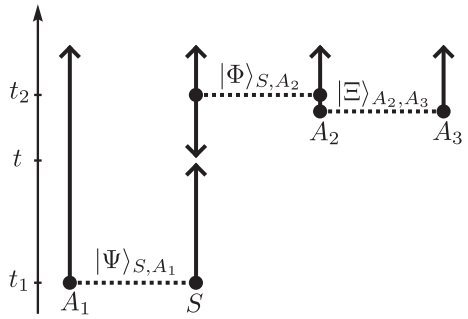

FIG. 4. Preparation of a mixed two-state vector $(\rho_{\rm post},\rho_{\rm pre})$. System S and ancilla A_1 are prepared at t_1 in an entangled state $|\Psi\rangle_{S,A_1}$ such that the reduced density matrix of S is $\rho_{\rm pre}$. The system is then found at t_2 in another entangled state $|\Phi\rangle_{S,A_2}$ with ancilla A_2 such that the reduced density matrix of S is $\rho_{\rm post}$. Just before t_2, ancilla A_2 was prepared in a maximally entangled state with yet another ancilla A_3. At intermediate times all ancilla systems are protected to avoid any interaction.

by connecting it to the future of A_3 which can be ensured to be unknown. (Another way to create a genuinely mixed backward evolving state might be realized by crossed in time nonlocal measurements, which were used in the first continuous variables teleportation scheme [46], removing the need for the third ancilla.)

The preselected mixed state, described by density matrix

$$\rho_{\rm pre}=\sum_k p_k|\psi_k\rangle\langle\psi_k|, \tag{34}$$

is created by preparing an entangled state with A_1:

$$|\Psi\rangle_{S,A_1}=\sum_k\sqrt{p_k}|\psi_k\rangle|k\rangle_1. \tag{35}$$

The postselected mixed state, described by density matrix

$$\rho_{\rm post}=\sum_i \tilde{p}_i|\phi_i\rangle\langle\phi_i|, \tag{36}$$

is created by first preparing a maximally entangled state between A_2 and A_3,

$$|\Xi\rangle_{A_2,A_3}=\frac{1}{\sqrt{N}}\sum_{i=1}^{N}|i\rangle_2|i\rangle_3, \tag{37}$$

and shortly afterwards, at time t_2, performing a postselection measurement of the entangled state

$$|\Phi\rangle_{S,A_2}=\sum_i\sqrt{\tilde{p}_i}|\phi_i\rangle|i\rangle_2. \tag{38}$$

Straightforward application of the formula (32) for a weak value of A for this mixed two-state vector yields

$$A_w=\frac{\sum_{i,k}\tilde{p}_i\,p_k\langle\psi_k|\phi_i\rangle\langle\phi_i|A|\psi_k\rangle}{\sum_{i,k}\tilde{p}_i\,p_k|\langle\phi_i|\psi_k\rangle|^2}. \tag{39}$$

In Appendix D we prove that this is the correct expression and by this show the validity of the expression for weak values (32) for a mixed two-state vector.

Systems described by mixed states, with various ways of obtaining information from future measurements, have been discussed before [38,41,47–49]. What allowed us to derive the symmetrical expression (32) is our special procedure for introducing the backward evolving mixed state.

The weak value (32) is not analogous to an eigenvalue in the sense described in the previous sections. What we have here is a statistical weak value, as explained in Appendix D. The pointer is in a mixed state similar to the expectation value case discussed before.

It is important to note that pre- and postselected systems described by a *generalized two state vector* [40]

$$\sum_{k=1}^{N}\alpha_k\langle\phi_k|\,|\psi_k\rangle \tag{40}$$

are not described by a genuine mixed two-state vector and the weak value for such a system is robust as for a system described by a pure two-state vector.

The generalized two-state vector arises when the system and ancillas are described together by a pure two-state vector. It is postulated that between the pre- and postselection the ancilla is isolated and there is coupling to the system only. A simple construction for the generalized two-state vector (40) is the following two-state vector describing the system and ancilla:

$$\frac{1}{\sqrt{N}}\sum_{k=1}^{N}\langle\phi_k|\langle k|\;\sum_{k=1}^{N}\alpha_k|\psi_k\rangle|k\rangle, \tag{41}$$

where $\{|k\rangle\}$ is an orthonormal basis of states of the ancilla. Naively one can apply (32) for the case of a generalized two-state vector, too. Indeed, (41) tells us that the system is prepared in a mixed state since it is entangled with an ancilla, and that it is also postselected in some other mixed state. But applying formula (32) in this case is a mistake. We cannot trace out the ancilla in preparation and in postselection separately, because it is the same ancilla. Indeed, from (41) we obtain

$$\rho_{\rm post}=\frac{1}{N}\sum_{k=1}^{N}|\phi_k\rangle\langle\phi_k|,\quad \rho_{\rm pre}=\sum_{k=1}^{N}|\alpha_k|^2|\psi_k\rangle|\langle\psi_k|. \tag{42}$$

Substituting in (32) yields

$$A_w=\frac{\sum_{i,k}|\alpha_k|^2\langle\psi_k|\phi_i\rangle\langle\phi_i|A|\psi_k\rangle}{\sum_{i,k}|\alpha_k|^2|\langle\phi_i|\psi_k\rangle|^2}, \tag{43}$$

which is obviously different from the correct expression defined in [40]:

$$A_w\equiv\frac{\sum\alpha_k\langle\phi_k|A|\psi_k\rangle}{\sum\alpha_k\langle\phi_k|\psi_k\rangle}. \tag{44}$$

This weak value for the generalized two-state vector (40) is equal to the standard weak value of the combined system with the two-state vector (41), $A_w=(A\otimes I)_w$, as defined in (1). For weak values defined for generalized two-state vectors, it should therefore also be true that for coupling to other systems during infinitesimal time the system behaves as a system in an eigenstate.

VI. WEAK VALUES AND WEAK MEASUREMENTS

In this section we want to connect our results with the general literature on weak values which considers it as an outcome of weak measurements, and define a procedure for specifying the weak value for situations when the postselection measurement does not specify the backward evolving state of involved systems completely. In such cases the system is described neither by a pure two-state vector nor by a generalized two-state vector, nor by a mixed two-state vector. Such a situation occurs when the system is coupled to an external system which is not postselected. Here, we will consider an example of a measurement procedure which would represent a weak measurement in the limit of weak coupling or a small period of time between pre- and postselection. We, however, take a finite time τ and a finite strength of the interaction g.

We consider a spin variable (4) pre- and postselected in the same states as in (13). But while (13) describes a two-state vector at a particular time, we take the forward evolving state from (13) as the preselected state at time $t = 0$ and the backward evolving state from (13) as the postselected state at some finite time τ. For simplicity, we consider a coupling of the system to a spin pointer, prepared in the initial state $|\Phi_0\rangle = |\uparrow_x\rangle$, with interaction Hamiltonian (A1) as described in Appendix A. Note that the final state of the spin pointer can only be read with a tomographic analysis involving a large ensemble.

If the interaction of this system with a spin pointer was very weak, we would expect the spin of the pointer to rotate by the angle $\theta = 100g\tau$ in proportion to the weak value $A_w = 100$ corresponding to the two-state vector (13). For an arbitrary strength of the interaction the state of the spin and the pointer spin at time τ immediately before the postselection is

$$\tfrac{1}{2}(|0\rangle|\uparrow\rangle + |0\rangle|\downarrow\rangle + e^{ig\tau}|-1\rangle|\uparrow\rangle + e^{-ig\tau}|-1\rangle|\downarrow\rangle). \quad (45)$$

The state of the pointer spin at time τ immediately after the postselection of the system is

$$|\Phi_\tau\rangle = \frac{(100e^{ig\tau} - 101)|\uparrow\rangle + (100e^{-ig\tau} - 101)|\downarrow\rangle}{\sqrt{40\,402 - 40\,400\cos(g\tau)}}. \quad (46)$$

This is a pure state of the spin rotated around the z axis. Only in the limit of a weak measurement, i.e., $g\tau \to 0$, the angle θ of this rotation corresponds to $A = 100$. The continuous line on the plot in Fig. 5 shows the dependence of the relative shift of the pointer variable $\frac{\theta}{g\tau}$ on the strength of the measurement interaction.

During the finite measurement interaction, the system couples to (and entangles with) a pointer, which is not postselected. Therefore, the system itself is not described by a pure two-state vector, and thus the basic definition (1) at an intermediate time t cannot be applied. The system is also not described by a mixed two-state vector if no special procedures as the one presented in the previous section are performed. In order to find the weak value, we here present two approaches—a more general one and a special but simpler procedure. Our general approach uses the same "trick" as in the proof of Appendix D. We rely on the fact that future operations cannot change any measurable property at present. Taking into account the assumption of a vanishingly weak coupling at time t to external systems, we can calculate the final state of the pointer. Then we introduce a verification measurement of this pointer state which we know will effectively succeed with certainty. Therefore, the weak value as a description of the shift of the pointer state, in case this measurement is successfully performed, has to be (in the limit of a small coupling to the external systems) equal to the weak value in our experiment without the verification measurement. With the measurement, the composite system, including the pointer, is described by a pure two-state vector which allows us to calculate the generalized two-state vector of the system. Finally, this gives the weak value at any intermediate time of any variable of the system.

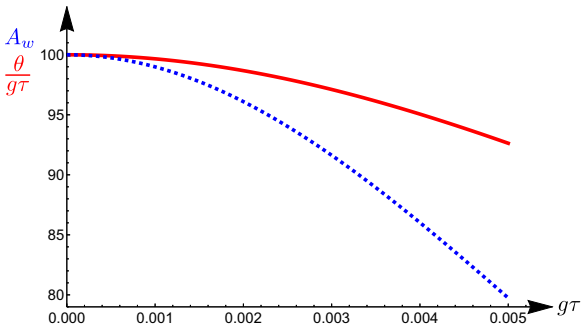

FIG. 5. The pointer reading and the weak value as a function of the strength of the measurement interaction. The pointer reading $\frac{\theta}{g\tau}$ (calibrated to correctly show eigenvalues of A) is given by the continuous red line. The weak value A_w is given by the blue dashed line.

The second method we present for calculating A_w can be applied here because the variable A commutes with the interaction Hamiltonian, and thus A_w at $t = \tau$, the time of the postselection, is A_w during the whole period. At time $t = \tau$, just before the postselection, the composite system is described by mixed two-state vector (it is mixed only in the forward evolving state), so we can directly apply (32). The entangled state of the system and the spin pointer just before time τ is (45), so the system is described by a forward evolving density matrix:

$$\rho_{\text{pre}} = \begin{pmatrix} 0 & 0 & 0 \\ 0 & \frac{1}{2} & \frac{1}{2}\cos(g\tau) \\ 0 & \frac{1}{2}\cos(g\tau) & \frac{1}{2} \end{pmatrix}. \quad (47)$$

The backward evolving state is given in (13). The formula (32) yields the weak value at $t = \tau$, and thus at all times:

$$A_w = \frac{201}{40\,402 - 40\,400\cos(g\tau)} - \frac{1}{2}. \quad (48)$$

The dependence of the weak value on the strength of the measurement interaction is shown by the dotted line in Fig. 5.

In the previous sections, we argued that the weak value of a physical variable at time t characterizes an effective coupling to this variable at this moment. At first glance, the

discrepancy between the final reading of the spin pointer used in our measurement procedure and the weak value (which remains constant during the interaction) seems contradictory to the previous sections, since we might expect that the pointer spin rotates as if the system has a (hypothetical) eigenvalue equal A_w. The reason for the discrepancy is the entanglement between the system and the pointer, so we have to consider the evolution of the whole composite system. The weak value (48) remains relevant for coupling of the system to external systems which are currently not entangled with our system.

VII. DISCUSSION

There is a fundamental difference between the outcomes of coupling to a variable of a quantum system depending on whether it is in a state corresponding to some eigenvalue of that variable or whether it is in a superposition of states with different eigenvalues, even when the expectation value is numerically equal to the aforementioned eigenvalue. The eigenvalue is an observable property of a single quantum system. A pointer coupled to that system changes its state in a well-defined manner that is manifested in the certainty of the result of a projection measurement on the final pointer state. Coupling to a system in a superposition with a certain expectation value results in a pointer state with a corresponding expectation value, yet there is no complete measurement of the pointer system which succeeds with certainty. The manifestation of the expectation value of a variable of the system is a statistical average of results of measurements performed on an ensemble.

The weak value, introduced as an outcome of a weak measurement, is traditionally considered to be a conditional expectation value and, as such, a property of a pre- and postselected ensemble. We have shown, however, that it has meaning for a single system. In the limit of coupling for a short time, the pointer state becomes identical to the pointer state coupled to the system in a state described by a numerically equal eigenvalue. It is measurably different from the case of coupling to a system in a superposition state with a numerically equal expectation value.

Our demonstration of the weak value as a property of a single pre- and postselected system shows that recent classical statistical analogies of weak values [30], which can be formulated only given an ensemble, are artificial.

Let us now discuss our result in light of different interpretations of quantum mechanics. The weak value has ontological meaning in only some of them; nevertheless, it is a useful tool regardless of interpretation. All interpretations agree about experimental results and are consistent with the "shut up and calculate" approach. In all interpretations, after the postselection measurement, predictions about the outcomes of possible measurements on systems coupled to our pre- and postselected system are the same.

Natural candidates for interpretations in which weak values might have ontological meaning are time-symmetric approaches. The strongest ontological meaning is in the interpretation due to Aharonov [50]. According to this interpretation, in addition to the usual forward evolving wave function, there is a real ontological wave function evolving backward in time. It corresponds to particular outcomes of all quantum experiments performed in the future, when it is assumed that every experiment has a single outcome. Both forward and backward evolving quantum states are ontological and thus weak values are ontological entities, too. This interpretation, however, is far from being widely accepted.

Consistent or decoherent histories interpretations [51,52] also have pre- and postselection on equal footing. Yet, it seems that these approaches are talking about reality in classical terms and the only values associated with physical variables are eigenvalues [53]. In another interpretation in which a backward evolving state is present, the transactional interpretation [54], ontological meaning is also attributed only to eigenvalues while the weak value is considered as a sort of amplitude [55].

A more popular interpretation (for which one of us is arguably the strongest proponent [56]) is the many-worlds interpretation (MWI) originated by Everett [57]. In MWI only the forward evolving wave function has ontological physical meaning, but in every world we have a particular outcome of the postselection measurement, so within each world the weak value has an ontological meaning as in the Aharonov interpretation [58].

Weak measurements are useful for analyzing the Bohmian interpretation [59]. For a particular postselection, weak values yield local currents which allow one to verify calculations of Bohmian trajectories [60,61]. Also, when the postselection measurement is completed, there is an effective collapse of the wave function of the pointer to that observed in our experiment. However, the weak values do not have ontological meaning in the Bohmian picture. The ontology includes only the forward evolving wave functions and Bohmian positions, the motions of which supervene solely on the forward evolving wave function. Weak values of local projections do not coincide with Bohmian trajectories [62].

Weak values also do not have an ontological meaning in collapse interpretations, since only the (forward evolving) wave function is ontological [63,64]. Similarly, they also have no ontological meaning in the Copenhagen interpretation and in its modern derivative, quantum Bayesianism [65], which distance themselves from reality. However, none of these interpretations would dispute our results about predictions regarding measurements of the pointer.

While we argue that the weak value is closer to an eigenvalue than to an expectation value, there is an important aspect in which the weak value differs both from the eigenvalue and expectation value cases. Eigenvalues and expectation values have a meaning for the coupling in the present, past, and future. The weak value has a meaning for the coupling only in the past, at times after the postselection. It is relevant only to the question of describing the interaction of a pre- and postselected system in the past.

The weak value requires the two-state vector formalism for its definition [1,66]. Standard formalism, without a backward evolving quantum state, lacks this concept. There, one has to involve entanglement of the system with the pointer. Postselection on the state of the system then collapses the pointer to a particular state. The weak value formalism allows us to simplify the standard description: for weak coupling

we can replace entanglement and collapse with an effective evolution determined by the weak value. In Aharonov's interpretation, one can say that this is what actually happens, while in the MWI one can say that this is what happens in each world. Nevertheless, in any interpretation one can use the weak value as a simple way to make predictions regarding changes of states of systems coupled to a pre- and postselected system.

VIII. CONCLUSIONS

We have analyzed the concept of the weak value. Although it can be viewed as a statistical entity, i.e., the average reading of a measuring device, it has the deeper meaning of a property associated with a single quantum system similar to an eigenvalue when the quantum state of the system is a corresponding eigenstate. We have shown theoretically and experimentally that the pre- and postselected system coupled to external systems through a particular variable affects these systems at any infinitesimal period of time as if it were in an eigenstate corresponding to an eigenvalue numerically equal to the weak value.

In the experiment we observe different effects on the pointer state for the cases of preselected photons (without postselection) with expectation value $\langle A\rangle = 0$ and pre- and postselected photons with $A_w = 0$. Our results demonstrate that the nature of the weak value is different from the nature of the expectation value. The measurements confirm that the weak value describes the interaction in the same way an eigenvalue does.

This opens rich possibilities to emulate otherwise unachievable eigenvalues by employing suitable pre- and postselected systems with the respective eigenvalues, as demonstrated in our experiment. For example, it allows us to mimic the behavior of complex eigenvalues as they occur in systems with $\mathcal{PT}$-symmetry breaking using ordinary quantum systems [67]. Furthermore, the lack of distortion of the wave function of the pointer, even in weak measurements with anomalously large weak values, represents the foundation of precision measurements employing the principle of weak amplification.

We have analyzed the concept of weak values for systems pre- and postselected in mixed states and derived a formula for weak values of variables of systems described by density matrices. Note, however, that due to the statistical nature of mixed states the coupling to systems described by a mixed two-state vector is in general not equivalent to the coupling to an eigenvalue and the nature of weak values in this case has a genuine statistical element.

ACKNOWLEDGMENTS

This paper has been supported in part by the Israel Science Foundation Grant No. 1311/14, the German-Israeli Foundation for Scientific Research and Development Grant No. I-1275-303.14, and by the German excellence initiative Nanosystems Initiative Munich. L.K. acknowledges support by the international Ph.D. program ExQM from the Elite Network of Bavaria, J.D. acknowledges support by the international Max-Planck-Research school for Quantum Science and Technology (IMPRS-QST), and J.M. acknowledges support by a fellowship from the German Academic Exchange Service.

APPENDIX A: ANALYSIS OF A MEASUREMENT WITH A SPIN POINTER

The interaction Hamiltonian with a spin system is given by

$$H_{\rm int} = gA\sigma_z. \tag{A1}$$

We repeat the analysis of the cases of various pre- and postselections of our system considered in Sec. II, but now coupled to the spin. We take the initial state of the spin to be

$$|\Phi_0\rangle = |\uparrow_x\rangle = \tfrac{1}{\sqrt{2}}(|\uparrow\rangle + |\downarrow\rangle), \tag{A2}$$

which has maximal sensitivity to the coupling (A1).

When the system has the eigenvalue $A = 1$, the coupling for time ϵ causes the rotation to the quantum state

$$|\Phi_{\rm e}\rangle = \tfrac{1}{\sqrt{2}}(e^{-ig\epsilon}|\uparrow\rangle + e^{ig\epsilon}|\downarrow\rangle), \tag{A3}$$

such that

$$D_A(\Phi_0,\Phi_{\rm e}) = g\epsilon. \tag{A4}$$

When the system is pre- and postselected and described by the two-state vector (7) corresponding to $A_w = 1$, the final state of the measuring device is

$$|\Phi_{\rm w}\rangle = \mathcal{N}[(2 - e^{ig\epsilon})|\uparrow\rangle + (2 - e^{-ig\epsilon})|\downarrow\rangle]. \tag{A5}$$

This state is very close to the state given by (A3) resulting in the Bures angle

$$D_A(\Phi_{\rm e},\Phi_{\rm w}) = (g\epsilon)^3 + O(\epsilon^5). \tag{A6}$$

For the case of a system preselected in the state given in (10) without postselection, the density matrix representing the measuring device after the interaction is

$$\rho_{\rm ex} = \begin{pmatrix} \frac{1}{2} & \frac{1}{4}(1+e^{-4ig\epsilon}) \\ \frac{1}{4}(1+e^{4ig\epsilon}) & \frac{1}{2} \end{pmatrix}. \tag{A7}$$

This mixed state is far from the final state in case of coupling to the eigenvalue described by (A3), which gives

$$D_A(\Phi_{\rm e},\rho_{\rm ex}) = g\epsilon + O(\epsilon^3). \tag{A8}$$

Postselection on the same state, which corresponds to the weak value $A_w = 1$, leads to a coupling which is again similar to the coupling to the eigenvalue $A = 1$. The distance between the states of the external system in these cases is proportional to ϵ^3. This is also true for the distance between the case $A_w = 100$

obtained when the system is described by (13) and the state of the system with eigenvalue $A = 100$. Thus, also in the case of coupling to a system very different from the Gaussian beam, described by a weak value and a numerically equal eigenvalue, the couplings are the same (in the limit of weak interaction), while the coupling to a system described by a numerically equal expectation value is different.

APPENDIX B: CONSISTENCY OF THE GENERAL RESULTS WITH EXAMPLES CONSIDERED IN THE PAPER

In Sec. IV we obtained general expressions for coupling to systems described by weak values (29) and expectation values (31), respectively. Here we show that these results are consistent with analyses of the examples in previous sections.

In Sec. II the spin $A = S_z$ was measured by a continuous pointer according to (2) with $B = P$. For the initial Gaussian pointer state we obtain

$$\langle P^2\rangle = \frac{1}{4\Delta^2}, \quad \langle P^4\rangle = \frac{3}{16\Delta^4}. \tag{B1}$$

For a spin described by the two-state vector (7) it holds that

$$(S_z)_w = a = 1, \quad \left(S_z^2\right)_w = -1. \tag{B2}$$

Plugging these into (29) yields (9).

When the spin is described by the two-state vector (13) we have

$$(S_z)_w = 100, \quad \left(S_z^2\right)_w = -100, \tag{B3}$$

which allows one to obtain (14).

The formula (29) works for coupling to the spin (A1) when $B = \sigma_z$ as well. For the initial pointer spin state (A2), we obtain

$$\left\langle\sigma_z^2\right\rangle = \left\langle\sigma_z^4\right\rangle = 1. \tag{B4}$$

Together with (B2) it shows that (29) is in agreement with (A6).

The general expressions are also confirmed by the examples in the expectation value case. For example, considering the continuous pointer with $B = P$, coupled to the spin $A = S_z$ in the initial state (10), yields the uncertainties

$$\Delta P = \frac{1}{2\Delta}, \quad \Delta S_z = 1. \tag{B5}$$

Plugging these into (31) results in an estimate of the distance consistent with (12).

APPENDIX C: WEAK VALUES WHICH ARE NOT REAL NUMBERS

For the coupling (2) to a continuous variable system, the pointer wave function is "shifted" as in (25) even if the weak value is complex. Note, however, that the presence of the imaginary part in A_w requires adding a normalization factor. To demonstrate this behavior we will consider coupling to the photon polarization (15) with weak value $A_w = i$ obtained for initial state (16) and the postselected state

$$\langle\phi| = \tfrac{1}{\sqrt{2}}(\langle 1| + i\langle -1|). \tag{C1}$$

The pointer state after the postselection is

$$\Phi_{\rm w} = \mathcal{N}\left(e^{-\frac{(Q-g\epsilon)^2}{4\Delta^2}} - ie^{-\frac{(Q+g\epsilon)^2}{4\Delta^2}}\right), \tag{C2}$$

while the state shifted by the imaginary "eigenvalue" i is

$$\Phi_{\rm e} = \mathcal{N}'e^{-\frac{(Q-ig\epsilon)^2}{4\Delta^2}}. \tag{C3}$$

Straightforward calculation shows that the distance between these states is small:

$$D_A(\Phi_{\rm w},\Phi_{\rm e}) = \frac{g^2\epsilon^2}{2\sqrt{2}\Delta^2} + O(\epsilon^4). \tag{C4}$$

If the coupling is to a spin variable (A1) instead of a continuous transverse degree of freedom, and we start again with the initial state of the measuring device $|\Phi_0\rangle = |\uparrow_x\rangle$, then the effective evolution of the spin is a rotation around the y axis instead of the z axis [68]. It is approximately the same as the evolution under an effective non-Hermitian Hamiltonian in which the polarization operator is replaced by i. The distance between the states in this case is

$$D_A(\Phi_{\rm w},\Phi_{\rm e}) = \frac{2g^3\epsilon^3}{3} + O(\epsilon^5). \tag{C5}$$

APPENDIX D: PROOF OF THE WEAK VALUE FORMULA FOR MIXED STATES

We want to prove the expression for the weak value (32) for a mixed two-state vector by deriving it from the basic definition (1). However, our procedure, Fig. 4, does not provide a pure backward evolving state even for the composite system which includes our system and the three ancilla systems. In order to resolve this issue we consider a verification measurement in the future, chosen such that it will have a definite result, thus providing the required backward evolving state.

The act of performing this verification measurement cannot change any measurable property at time t. Having a large enough pre- and postselected ensemble of systems (with their own ancilla systems) as described, the weak value of A at time t is a measurable property: the average shift of pointers weakly coupled at time t to the systems in the pre- and postselected ensemble. In the limit where the weak coupling does not change the evolution, we can calculate the quantum state of the composite system after the whole process. A verification measurement of this state at t_3 then will effectively succeed with certainty. It will provide the pure backward evolving state with the same weak value (in the limit) as without the verification measurement, which is the weak value we wish to know.

Let us proceed with the proof. At time t_1 we start with an entangled state of the system and ancilla A_1, $|\Psi\rangle_{S,A_1}$, see Fig. 6. Shortly before t_2 we prepare a maximally entangled state of ancillas A_2 and A_3, $|\Xi\rangle_{A_2,A_3}$. Thus, before the postselection measurement at time t_2, the total state of the system and the

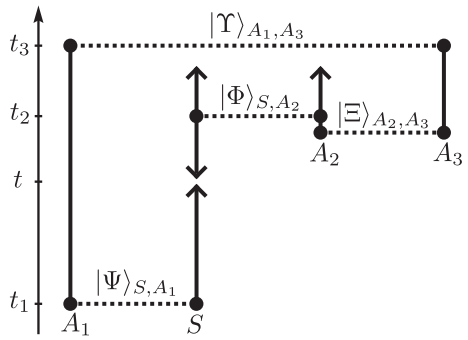

FIG. 6. In order to calculate the weak value, a (hypothetical) verification measurement is introduced at t_3 which provides a pure two-state vector for the system and ancilla A_1 and thus a generalized two-state vector for the system.

three ancilla systems is

$$\left(\sum_k \sqrt{p_k}|\psi_k\rangle|k\rangle_1\right)\left(\frac{1}{\sqrt{N}}\sum_{i=1}^{N}|i\rangle_2|i\rangle_3\right). \tag{D1}$$

The postselection measurement of the system and A_2 leaves ancilla systems A_1 and A_3 in the state

$$|\Upsilon\rangle_{A_1,A_3} = \mathcal{N}\sum_{i,k}\sqrt{\tilde{p}_i\, p_k}\langle\phi_i|\psi_k\rangle|k\rangle_1|i\rangle_3. \tag{D2}$$

We consider a verification measurement at t_3 of state $|\Upsilon\rangle_{A_1,A_3}$, which effectively succeeds with certainty. Thus, the state of the system and the three ancilla systems evolving backward in time from t_2 is

$$\left(\sum_j \sqrt{\tilde{p}_j}\langle\phi_j|\langle j|_2\right)\left(\mathcal{N}\sum_{i,k}\sqrt{\tilde{p}_i\, p_k}\langle\psi_k|\phi_i\rangle\langle k|_1\langle i|_3\right). \tag{D3}$$

After evolving backwards through the Bell-type measurement of A_2 and A_3, the backward evolving state toward time t is

$$\langle\Omega|_{S,A_1} = \mathcal{N}\sum_{i,k}\tilde{p}_i\sqrt{p_k}\langle\psi_k|\phi_i\rangle\langle\phi_i|\langle k|_1. \tag{D4}$$

We have obtained a pure two-state vector of the system and A_1 at time t with pre- and postselected states given by (35) and (D4). This allows us to apply (1) to find the weak value of A:

$$\begin{aligned} A_w = (A\otimes I_1)_w &= \frac{\langle\Omega|A\otimes I_1|\Psi\rangle}{\langle\Omega|\Psi\rangle} \\ &= \frac{\sum_{i,j,k}\tilde{p}_i\sqrt{p_j}\sqrt{p_k}\langle\psi_k|\phi_i\rangle\langle\phi_i|\langle k|_1 A\otimes I_1|\psi_j\rangle|j\rangle_1}{\sum_{i,j,k}\tilde{p}_i\sqrt{p_j}\sqrt{p_k}\langle\psi_k|\phi_i\rangle\langle\phi_i|\langle k|_1|\psi_j\rangle|j\rangle_1}. \end{aligned} \tag{D5}$$

This result reduces to the same expression as in (39), which provides the proof of our general formula (32).

In our proof we have assumed that the verification measurement at t_3 effectively succeeds with certainty, which holds in the limit of vanishing interaction at time t. This is enough for the proof since the weak value is defined at the limit, but the tiny probability for the failure of this measurement, which always exists, is crucial for the nature of the weak value of the genuinely mixed two-state vector.

The weak value (32) is not analogous to an eigenvalue in the sense described in the previous sections. Only the center of the affected pointer distribution shifts in the same manner as in the case of coupling to a system with a numerically equal eigenvalue. In fact, it is the same situation as for the system described by an expectation value, where after the coupling the pointer is in the mixed state (30). The mixture with a tiny probability of an orthogonal pointer state (in case of the failure of the verification measurement) is equivalent to the mixture of almost identical states with comparable probabilities obtained via weak coupling to a system in a superposition of eigenstates.

[1] Y. Aharonov, P. G. Bergmann, and J. L. Lebowitz, Time symmetry in the quantum process of measurement, Phys. Rev. **134**, B1410 (1964).

[2] Y. Aharonov and L. Vaidman, The two-state vector formalism: An updated review, Lect. Notes Phys. **734**, 399 (2007).

[3] Y. Aharonov, D. Z. Albert, and L. Vaidman, How the Result of a Measurement of a Component of the Spin of a Spin-$\frac{1}{2}$ Particle Can Turn Out to Be 100, Phys. Rev. Lett. **60**, 1351 (1988).

[4] A. J. Leggett, Comment on "How the Result of a Measurement of a Component of the Spin of a Spin-$\frac{1}{2}$ Particle can Turn out to be 100," Phys. Rev. Lett. **62**, 2325 (1989).

[5] A. Peres, Quantum Measurements with Postselection, Phys. Rev. Lett. **62**, 2326 (1989).

[6] Y. Aharonov and L. Vaidman, Aharonov and Vaidman Reply, Phys. Rev. Lett. **62**, 2327 (1989).

[7] O. Hosten and P. Kwiat, Observation of the spin Hall effect of light via weak measurements, Science **319**, 787 (2008).

[8] P. B. Dixon, D. J. Starling, A. N. Jordan, and J. C. Howell, Ultrasensitive Beam Deflection Measurement Via Interferometric Weak Value Amplification, Phys. Rev. Lett. **102**, 173601 (2009).

[9] G. Strübi and C. Bruder, Measuring Ultrasmall Time Delays of Light by Joint Weak Measurements, Phys. Rev. Lett. **110**, 083605 (2013).

[10] X.-Y. Xu, Y. Kedem, K. Sun, L. Vaidman, C.-F. Li, and G.-C. Guo, Phase Estimation with Weak Measurement Using a White Light Source, Phys. Rev. Lett. **111**, 033604 (2013).

[11] L. Zhou, Y. Turek, C. P. Sun, and F. Nori, Weak-value amplification of light deflection by a dark atomic ensemble, Phys. Rev. A **88**, 053815 (2013).

[12] G. Jayaswal, G. Mistura, and M. Merano, Observing angular deviations in light-beam reflection via weak measurements, Opt. Lett. **39**, 6257 (2014).

[13] O. S. Magaña Loaiza, M. Mirhosseini, B. Rodenburg, and R. W. Boyd, Amplification of Angular Rotations Using Weak Measurements, Phys. Rev. Lett. **112**, 200401 (2014).

[14] K. Lyons, J. Dressel, A. N. Jordan, J. C. Howell, and P. G. Kwiat, Power-Recycled Weak-Value-Based Metrology, Phys. Rev. Lett. **114**, 170801 (2015).
[15] M. Hallaji, A. Feizpour, G. Dmochowski, J. Sinclair, and A. M. Steinberg, Weak-value amplification of the nonlinear effect of a single photon, Nat. Phys. **13**, 540 (2017).
[16] C. Ferrie and J. Combes, Weak Value Amplification is Suboptimal for Estimation and Detection, Phys. Rev. Lett. **112**, 040406 (2014).
[17] G. C. Knee and E. M. Gauger, When Amplification with Weak Values Fails to Suppress Technical Noise, Phys. Rev. X **4**, 011032 (2014).
[18] A. N. Jordan, J. Martínez-Rincón, and J. C. Howell, Technical Advantages for Weak-Value Amplification: When Less is More, Phys. Rev. X **4**, 011031 (2014).
[19] D. Das and Arvind, Estimation of quantum states by weak and projective measurements, Phys. Rev. A **89**, 062121 (2014).
[20] J. Lee and I. Tsutsui, Merit of amplification by weak measurement in view of measurement uncertainty, Quantum Stud.: Math. Found. **1**, 65 (2014).
[21] S. Pang and T. A. Brun, Improving the Precision of Weak Measurements by Postselection Measurement, Phys. Rev. Lett. **115**, 120401 (2015).
[22] L. Zhang, A. Datta, and I. A. Walmsley, Precision Metrology Using Weak Measurements, Phys. Rev. Lett. **114**, 210801 (2015).
[23] A. Nishizawa, Weak-value amplification beyond the standard quantum limit in position measurements, Phys. Rev. A **92**, 032123 (2015).
[24] G. B. Alves, B. M. Escher, R. L. de Matos Filho, N. Zagury, and L. Davidovich, Weak-value amplification as an optimal metrological protocol, Phys. Rev. A **91**, 062107 (2015).
[25] S. Pang and T. A. Brun, Suppressing technical noise in weak measurements by entanglement, Phys. Rev. A **92**, 012120 (2015).
[26] Y. Susa and S. Tanaka, Statistical hypothesis testing by weak-value amplification: Proposal and evaluation, Phys. Rev. A **92**, 012112 (2015).
[27] G. I. Viza, J. Martínez-Rincón, G. B. Alves, A. N. Jordan, and J. C. Howell, Experimentally quantifying the advantages of weak-value-based metrology, Phys. Rev. A **92**, 032127 (2015).
[28] T. Denkmayr, H. Geppert, H. Lemmel, M. Waegell, J. Dressel, Y. Hasegawa, and S. Sponar, Experimental Demonstration of Direct Path State Characterization by Strongly Measuring Weak Values in a Matter-Wave Interferometer, Phys. Rev. Lett. **118**, 010402 (2017).
[29] J. Harris, R. W. Boyd, and J. S. Lundeen, Weak Value Amplification Can Outperform Conventional Measurement in the Presence of Detector Saturation, Phys. Rev. Lett. **118**, 070802 (2017).
[30] C. Ferrie and J. Combes, How the Result of a Single Coin Toss Can Turn Out to be 100 Heads, Phys. Rev. Lett. **113**, 120404 (2014).
[31] A. Brodutch, Comment on "How the Result of a Single Coin Toss can Turn out to be 100 heads," Phys. Rev. Lett. **114**, 118901 (2015).
[32] M. F. Pusey, Anomalous Weak Values are Proofs of Contextuality, Phys. Rev. Lett. **113**, 200401 (2014).
[33] J. Dressel, K. Y. Bliokh, and F. Nori, Classical Field Approach to Quantum Weak Measurements, Phys. Rev. Lett. **112**, 110407 (2014).
[34] A. Karanjai, E. G. Cavalcanti, S. D. Bartlett, and T. Rudolph, Weak values in a classical theory with an epistemic restriction, New J. Phys. **17**, 073015 (2015).
[35] J. Dressel, Weak values as interference phenomena, Phys. Rev. A **91**, 032116 (2015).
[36] D. Sokolovski, The meaning of "anomalous weak values" in quantum and classical theories, Phys. Lett. A **379**, 1097 (2015).
[37] A. C. Ipsen, Disturbance in weak measurements and the difference between quantum and classical weak values, Phys. Rev. A **91**, 062120 (2015).
[38] H. M. Wiseman, Weak values, quantum trajectories, and the cavity-QED experiment on wave-particle correlation, Phys. Rev. A **65**, 032111 (2002).
[39] J. Dressel, M. Malik, F. M. Miatto, A. N. Jordan, and R. W. Boyd, *Colloquium*: Understanding quantum weak values: Basics and applications, Rev. Mod. Phys. **86**, 307 (2014).
[40] Y. Aharonov and L. Vaidman, Complete description of a quantum system at a given time, J. Phys. A **24**, 2315 (1991).
[41] R. Silva, Y. Guryanova, N. Brunner, N. Linden, A. J. Short, and S. Popescu, Pre- and postselected quantum states: Density matrices, tomography, and Kraus operators, Phys. Rev. A **89**, 012121 (2014).
[42] A. Uhlmann, The "transition probability" in the state space of a $*$-algebra, Rep. Math. Phys. **9**, 273 (1976).
[43] S. Wu and K. Mølmer, Weak measurements with a qubit meter, Phys. Lett. A **374**, 34 (2009).
[44] Y. Aharonov, S. Massar, S. Popescu, J. Tollaksen, and L. Vaidman, Adiabatic Measurements on Metastable Systems, Phys. Rev. Lett. **77**, 983 (1996).
[45] L. Vaidman, Backward evolving quantum states, J. Phys. A **40**, 3275 (2007).
[46] L. Vaidman, Teleportation of quantum states, Phys. Rev. A **49**, 1473 (1994).
[47] Y. Aharonov, S. Popescu, J. Tollaksen, and L. Vaidman, Multiple-time states and multiple-time measurements in quantum mechanics, Phys. Rev. A **79**, 052110 (2009).
[48] G.-D. Lin, C. Monroe, and L.-M. Duan, Weak Values are Universal in Von Neumann Measurements, Phys. Rev. Lett. **106**, 230402 (2011).
[49] D. Tan, S. J. Weber, I. Siddiqi, K. Mølmer, and K. W. Murch, Prediction and Retrodiction for a Continuously Monitored Superconducting Qubit, Phys. Rev. Lett. **114**, 090403 (2015).
[50] Y. Aharonov, E. Cohen, E. Gruss, and T. Landsberger, Measurement and collapse within the two-state vector formalism, Quantum Stud.: Math. Found. **1**, 133 (2014).
[51] R. B. Griffiths, Consistent histories and the interpretation of quantum mechanics, J. Stat. Phys. **36**, 219 (1984).
[52] M. Gell-Mann and J. B. Hartle, Quantum mechanics in the light of quantum cosmology, in *Complexity, Entropy and the Physics of Information*, edited by W. H. Zurek (Addison-Wesley, Reading, MA, 1990), pp. 425–459.
[53] R. Griffiths, Particle path through a nested Mach-Zehnder interferometer, Phys. Rev. A **94**, 032115 (2016).
[54] J. G. Cramer, The transactional interpretation of quantum mechanics, Rev. Mod. Phys. **58**, 647 (1986).

[55] R. Kastner, The transactional interpretation, counterfactuals, and weak values in quantum theory, Stud. Hist. Phil. Mod. Phys. **39**, 806 (2008).

[56] L. Vaidman, Many-Worlds Interpretation of Quantum Mechanics, in *Stanford Encyclopedia of Philosophy*, edited by E. N. Zalta, http://plato.stanford.edu/entries/qm-manyworlds (2014).

[57] H. Everett, III, "Relative State" Formulation of quantum mechanics, Rev. Mod. Phys. **29**, 454 (1957).

[58] L. Vaidman, Time symmetry and the many-worlds interpretation, in *Many Worlds? Everett, Quantum Theory, and Reality*, edited by S. Saunders, J. Barrett, A. Kent, and D. Wallace (Oxford University Press, Oxford, UK, 2010), pp. 582–596.

[59] D. Bohm, A suggested interpretation of the quantum theory in terms of "hidden" variables. I, Phys. Rev. **85**, 166 (1952).

[60] H. M. Wiseman, Grounding Bohmian mechanics in weak values and bayesianism, New J. Phys. **9**, 165 (2007).

[61] D. H. Mahler, L. Rozema, K. Fisher, L. Vermeyden, K. J. Resch, H. M. Wiseman, and A. Steinberg, Experimental nonlocal and surreal Bohmian trajectories, Sci. Adv. **2**, e1501466 (2016).

[62] Y. Aharonov and L. Vaidman, About position measurements which do not show the Bohmian particle position, in *Bohmian Mechanics and Quantum Theory: An Appraisal*, edited by J. T. Cushing, A. Fine, and S. Goldstein (Kluwer Academic, Dordrecht, The Netherlands, 1996), pp. 141–154.

[63] P. Pearle, Reduction of the state vector by a nonlinear Schrödinger equation, Phys. Rev. D **13**, 857 (1976).

[64] G. C. Ghirardi, A. Rimini, and T. Weber, Unified dynamics for microscopic and macroscopic systems, Phys. Rev. D **34**, 470 (1986).

[65] C. M. Caves, C. A. Fuchs, and R. Schack, Quantum probabilities as Bayesian probabilities, Phys. Rev. A **65**, 022305 (2002).

[66] Y. Aharonov and L. Vaidman, Properties of a quantum system during the time interval between two measurements, Phys. Rev. A **41**, 11 (1990).

[67] P. A. Kalozoumis, C. V. Morfonios, F. K. Diakonos, and P. Schmelcher, $\mathcal{PT}$-symmetry breaking in waveguides with competing loss-gain pairs, Phys. Rev. A **93**, 063831 (2016).

[68] S. Sponar, T. Denkmayr, H. Geppert, H. Lemmel, A. Matzkin, J. Tollaksen, and Y. Hasegawa, Weak values obtained in matter-wave interferometry, Phys. Rev. A **92**, 062121 (2015).

6.1.8 [P6]

Rebufello et al. *Light: Science & Applications* (2021)10:106
https://doi.org/10.1038/s41377-021-00539-0

Official journal of the CIOMP 2047-7538
www.nature.com/lsa

LETTER Open Access

Anomalous weak values via a single photon detection

Enrico Rebufello[1], Fabrizio Piacentini[1], Alessio Avella[1], Muriel A. de Souza[2], Marco Gramegna[1], Jan Dziewior[3,4], Eliahu Cohen[5], Lev Vaidman[6], Ivo Pietro Degiovanni[1] and Marco Genovese[1]

Abstract

Is it possible that a measurement of a spin component of a spin-1/2 particle yields the value 100? In 1988 Aharonov, Albert and Vaidman argued that upon pre- and postselection of particular spin states, weakening the coupling of a standard measurement procedure ensures this paradoxical result[1]. This theoretical prediction, called *weak value*, was realised in numerous experiments[2–9], but its meaning remains very controversial[10–19], since its "anomalous" nature, i.e., the possibility to exceed the eigenvalue spectrum, as well as its "quantumness" are debated[20–22]. We address these questions by presenting the first experiment measuring anomalous weak values with just a single click, without the need for statistical averaging. The measurement uncertainty is significantly smaller than the gap between the measured weak value and the nearest eigenvalue. Beyond clarifying the meaning of weak values, demonstrating their non-statistical, single-particle nature, this result represents a breakthrough in understanding the foundations of quantum measurement, showing unprecedented measurement capability for further applications of weak values to quantum photonics.

Weak values (WVs), as introduced in ref. [1], represent one of the most interesting and intriguing quantum measurement paradigms. In that influential work, the outcome of the measurement of the spin component was 100, while in the chosen units its maximal eigenvalue was just 1. However, weakening the coupling in the measurement procedure made the uncertainty in an individual measurement much larger than 1 (and even than 100), thus this "anomalous" value was observed only after averaging over a very large number of readings of the pointer variable. While averaging is a standard practice in many measurement protocols, postselection is not, hence the legitimacy of the statistical analysis was questioned[20–22]. Understanding this matter is fundamental not only for clarifying the meaning of WVs, but also in view of significant applications in quantum metrology[3–5,23,24]. In this work, we present a *robust weak measurement*, an experiment in which a single reading of the measuring device, coupled to the system only once, provides a WV and, in particular, an anomalous one. Postselection still plays a crucial role, but the anomalous outcome no longer arises from a statistical analysis. We measured an observable with eigenvalues in the range $[-7, 7]$. The WV of the observable of the pre- and postselected system on which a single-click measurement was performed was 18.7, and our single click yielded 21.4 ± 4.5, see Fig. 1.

This is a surprising result, since the expectation value of the observable in the preselected state was only 2.2. It would not be surprising that postselection on the eigenstate corresponding to a maximal eigenvalue (i.e., 7) slightly increased the measured value, but only up to 7, not beyond (in fact, in our experiment the expectation value corresponding to the postselected state was also just 2.2).

The main theoretical basis for our experiment is the work in ref. [25], which preceded the introduction of WVs[1], extended here by constructing a new method allowing a feasible experimental implementation. The easiest way to explain this work is via weak measurements performed on a system consisting of n particles with a single measuring device, see Sec. VII of ref. [26]. Within the standard weak

Correspondence: Fabrizio Piacentini (f.piacentini@inrim.it)
[1]INRIM, Strada delle Cacce 91, I-10135 Torino, Italy
[2]National Institute of Metrology, Quality and Technology—INMETRO, Av. Nossa Senhora das Graças, 50, Duque de Caxias, RJ 25250-020, Brazil
Full list of author information is available at the end of the article

© The Author(s) 2021
Open Access This article is licensed under a Creative Commons Attribution 4.0 International License, which permits use, sharing, adaptation, distribution and reproduction in any medium or format, as long as you give appropriate credit to the original author(s) and the source, provide a link to the Creative Commons license, and indicate if changes were made. The images or other third party material in this article are included in the article's Creative Commons license, unless indicated otherwise in a credit line to the material. If material is not included in the article's Creative Commons license and your intended use is not permitted by statutory regulation or exceeds the permitted use, you will need to obtain permission directly from the copyright holder. To view a copy of this license, visit http://creativecommons.org/licenses/by/4.0/.

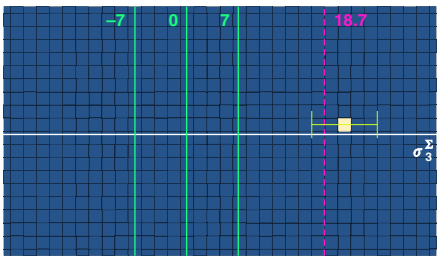

Fig. 1 Single detection event yielding an anomalous weak value of σ_3^Σ. The vertical solid lines show the borders and centre of the eigenvalue spectrum of our observable, while the dashed line indicates its weak value calculated according to the experimental parameters, i.e., $(\sigma_3^\Sigma)_w = 18.7$. The experimental point, shown in white, gives the value $(\sigma_3^\Sigma)_w^{1\text{ click}} = 21.4$. The uncertainty, represented by the horizontal green bars, is specified by calculating the width of the spatial wave function of the quantum particle before the detection, and confirmed by repeating the experiment many times

measurement procedure, in which each particle has its own measuring device, the uncertainty of measuring the sum of variables $A^\Sigma \equiv \sum_{k=1}^n A_k$, where A_k corresponds to particle k, scales like $\sqrt{n}$ because of the contributions of the n measuring devices. In our procedure for measuring A^Σ, we couple a single measuring device to all particles and thus, importantly, the final uncertainty is the one of the single measuring device involved, avoiding the $\sqrt{n}$ increase. This allows extracting an anomalous WV $(A^\Sigma)_w$ by coupling the measuring device only once to each part of the system, and observing only a single click of the measuring device.

In our experimental demonstration, the measured variable is the sum of polarisation variables of n photons:

$$\sigma_3^\Sigma \equiv \sum_{k=1}^{n} \sigma_3^{(k)} \tag{1}$$

where $\sigma_3 \equiv |H\rangle\langle H| - |V\rangle\langle V|$, and $H(V)$ is the horizontal (vertical) polarisation. All photons are preselected in the state

$$|\psi_\alpha\rangle = \cos\alpha|H\rangle + \sin\alpha|V\rangle \tag{2}$$

and postselected in the state

$$|\psi_\beta\rangle = \cos\beta|H\rangle + \sin\beta|V\rangle \tag{3}$$

When states (2) and (3) are almost orthogonal, we obtain an anomalously large weak value

$$(\sigma_3^\Sigma)_w = \frac{\langle\psi_\beta|\sigma_3^\Sigma|\psi_\alpha\rangle}{\langle\psi_\beta|\psi_\alpha\rangle} \tag{4}$$

All photons are coupled to the same measuring device, so the interaction Hamiltonian is

$$\mathcal{H} = g(t) \sum_{k=1}^{n} \sigma_3^{(k)} \otimes p_x \tag{5}$$

where a well localized $g(t)$ defines the time of the measurement, $\int g(t)\,dt = 1$, and p_x is the conjugate momentum of the pointer variable x with the initial quantum state modelled by the Gaussian

$$\chi(x) = \frac{1}{\sqrt{\Delta\sqrt{2\pi}}} e^{-x^2/4\Delta^2} \tag{6}$$

The strength of the measurement interaction in Eq. (5) is characterized by $\frac{1}{\Delta}$, which has to be chosen carefully: for a single-click measurement the uncertainty cannot be too large, but also the coupling cannot be too strong, as it changes the WV[19,27]. Moreover, although the system has a well-defined WV of the measured observable at every moment between pre- and postselection, the measuring device, in general, does not indicate this WV, because of entanglement between system and measuring device, see Fig. 5 in ref. [22]. Somewhat surprisingly, in the case of coupling to a Gaussian pointer, the expectation value of the pointer after the measurement exactly equals this WV. Since, in the present scenario, the WV is constant in time during the measurement interaction, we can extract it at the moment just before the postselection, by calculating the quantum state after the interaction and knowing the postselection state.

To make the explanation more transparent, let us first consider a case for $n = 1$. The state of the photon and the measuring device before the postselection is

$$\cos\alpha|H\rangle|\chi_+\rangle + \sin\alpha|V\rangle|\chi_-\rangle \tag{7}$$

where $|\chi_+\rangle$ and $|\chi_-\rangle$ denote Gaussians shifted by 1 and -1, respectively. Thus, the photon has a mixed polarisation state described by the density matrix ρ_α, that can be expressed in the $\{|H\rangle, |V\rangle\}$ basis as

$$\rho_\alpha = \begin{pmatrix} \cos^2\alpha & e^{-\frac{1}{2\Delta^2}}\sin\alpha\cos\alpha \\ e^{-\frac{1}{2\Delta^2}}\sin\alpha\cos\alpha & \sin^2\alpha \end{pmatrix} \tag{8}$$

Postselecting on $|\psi_\beta\rangle$, the WV is given by (see Eq. (32) in ref. [22])

$$(\sigma_3)_w = \frac{\mathrm{tr}(|\psi_\beta\rangle\langle\psi_\beta|\sigma_3\rho_\alpha)}{\mathrm{tr}(|\psi_\beta\rangle\langle\psi_\beta|\rho_\alpha)} = \frac{\mu^2 - \nu^2}{\mu^2 + \nu^2 + 2\mu\nu e^{-\frac{1}{2\Delta^2}}} \tag{9}$$

where $\mu = \cos\alpha\cos\beta$ and $\nu = \sin\alpha\sin\beta$.

It is straightforward to generalise the calculation for $n > 1$. We define the joint pre- and postselected states of the n photons as, respectively, $|\Psi_\alpha\rangle = \bigotimes_{k=1}^{n} |\psi_\alpha^{(k)}\rangle$ and $|\Psi_\beta\rangle = \bigotimes_{k=1}^{n} |\psi_\beta^{(k)}\rangle$. The WV is

$$\begin{aligned} \left(\sigma_3^\Sigma\right)_w &= \frac{\langle\Psi_\beta|\sigma_3^\Sigma \,\mathrm{tr}\left(U^\Sigma|\Psi_\alpha\rangle\langle\Psi_\alpha|\otimes|\chi\rangle\langle\chi|\left(U^\Sigma\right)^\dagger\right)|\Psi_\beta\rangle}{\langle\Psi_\beta|\mathrm{tr}\left(U^\Sigma|\Psi_\alpha\rangle\langle\Psi_\alpha|\otimes|\chi\rangle\langle\chi|\left(U^\Sigma\right)^\dagger\right)|\Psi_\beta\rangle} \\ &= \frac{\sum_{k,l=0}^{n}\binom{n}{k}\binom{n}{l}\mu^{k+l}\nu^{2n-k-l}(2k-n)\gamma_{kl}}{\sum_{k,l=0}^{n}\binom{n}{k}\binom{n}{l}\mu^{k+l}\nu^{2n-k-l}\gamma_{kl}} \end{aligned} \tag{10}$$

where $U^\Sigma = e^{-i\sum_{k=1}^{n}\sigma_3^{(k)}\otimes p_x}$, $\gamma_{kl} = e^{-\frac{(k-l)^2}{2\Delta^2}}$, and the trace is taken over the pointer system only. Our Gaussian pointer, after the measurement, shows $\langle x\rangle = \left(\sigma_3^\Sigma\right)_w$ with uncertainty $\Delta x = \sqrt{\langle x^2\rangle - \langle x\rangle^2}$, where

$$\langle x^2\rangle = \frac{\sum_{k,l=0}^{n}\binom{n}{k}\binom{n}{l}\mu^{k+l}\nu^{2n-k-l}\left((n-k-l)^2+\Delta^2\right)\gamma_{kl}}{\sum_{k,l=0}^{n}\binom{n}{k}\binom{n}{l}\mu^{k+l}\nu^{2n-k-l}\gamma_{kl}} \tag{11}$$

The experiment directly testing this prediction, see Fig. 2a, is very difficult.

The following observation leads to a more feasible test of our predictions. In the Hamiltonian in Eq. (5) the variables $\sigma_3^{(k)}$ are constants of motion, therefore it does not matter when the interaction with every photon takes place. In particular, we can perform the couplings one after another. In this case, however, we can use just one photon instead of n, pre- and postselecting it n times according to the states in Eqs. (2) and (3), see Fig. 2b. The observable, i.e., the sum of polarisation variables of n photons, is replaced by the sum of polarisation variables of the same photon at n different times, which is much easier to measure, since the spatial degree of freedom of this single photon can play the role of the measuring device.

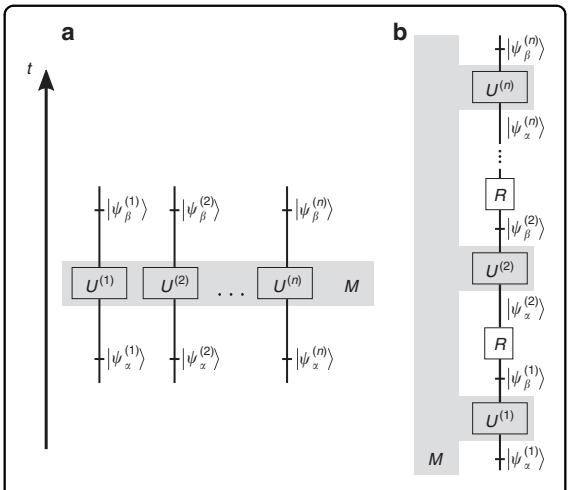

Fig. 2 Robust weak measurement: theoretical framework. a A measuring device M is coupled simultaneously to n particles of a pre- and postselected system. **b** The measuring device is coupled to the same particle at n times with particular pre- and postselection at each time. After each postselection onto $|\psi_\beta^{(k)}\rangle$, a unitary rotation R restores the preselection state $|\psi_\alpha\rangle$

We consider the case $n = 7$, which is large enough to see the predicted effect. In Fig. 3 we show the WV $\left(\sigma_3^\Sigma\right)_w$ and the pointer uncertainty Δx (Eqs. (10) and (11), respectively) for $\alpha = 0.62$ and $\Delta = 5.84$, as a function of β. By choosing $\beta = 2.53$, one obtains a theoretical final state of the pointer showing 18.7 ± 4.5, granting an optimal reading of the anomalous WV in terms of relative uncertainty. Note that the final width of the pointer is smaller than the initial width, due to a subtle narrowing effect[28].

The experimental setup is shown in Fig. 4. It is composed of a set of $n = 7$ blocks in which a birefringent crystal pair realises the weak interaction, preceded by a half-wave plate and followed by a polarising plate. While the polarising plate performs the postselection, the half-wave plate rotates the polarisation of the photon outgoing the previous block to set the preselection state. The EMCCD placed at the end of the $n = 7$ blocks detects the arrival position of the photon. A detailed description of the setup is provided in the Methods section.

The single-click experiment presented in Fig. 1 yielded 21.4, in agreement with the predicted value within the theoretical uncertainty.

We tested our theoretical analysis a posteriori by performing a multi-click experimental run with the same parameters α, β and Δ, to record the distribution shown in Fig. 5. The mean value of this multi-click distribution, 18.59, is very close to the theoretical WV $\left(\sigma_3^\Sigma\right)_w = 18.7$, given by Eq. (10). The statistical uncertainty is only 0.09, thus the remaining discrepancy is due to imprecision in the parameters α, β, Δ fixing the theoretical value. Some deviations are caused by imperfections in the optical elements, e.g., the birefringent crystals (details in the Supplementary Material). The width of the multi-click distribution in Fig. 5 turns out to be 4.5, in full agreement with the theoretical predictions.

As in all weak measurements in which the pointer variable of the polarisation measurement of a photon is its transverse degree of freedom, the probability distribution in Fig. 5 is identical to the intensity pattern of the electromagnetic wave on the screen which can be calculated using Maxwell equations (see refs. [4,29]). This is a sufficiently narrow distribution to allow a robust measurement of the WV via the detection of a single quantum particle. In the framework of classical physics, this bizarre result is hidden in the peculiar interference phenomena of

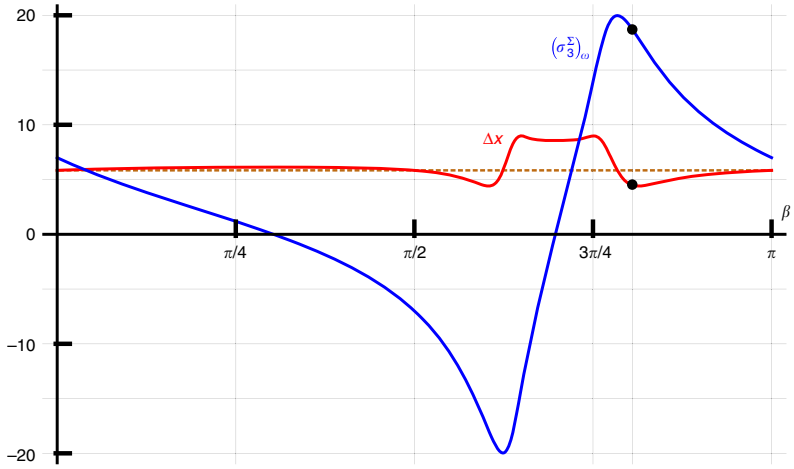

Fig. 3 Predicted weak value and pointer uncertainty. Predicted values for the WV $(\sigma_3^\Sigma)_w$ (solid blue line) and the final pointer uncertainty Δx (solid red line) for $n = 7$, $a = 0.62$ and $\Delta = 5.84$, as a function of β. The initial photon distribution width Δ is included as a dashed brown line. The two black dots on the curves denote the $(\sigma_3^\Sigma)_w = 18.7$ and $\Delta x = 4.5$ obtained for $\beta = 2.53$, the parameters chosen for our experimental demonstration

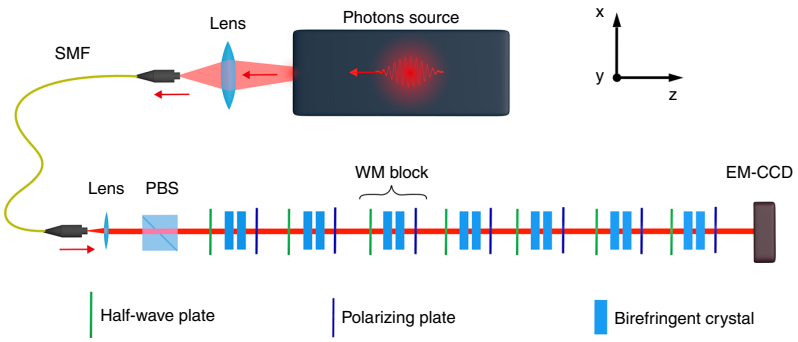

Fig. 4 Experimental setup. Our photon source exploits type-I spontaneous parametric down conversion. Generated signal photons at 702 nm are spectrally-filtered, injected in a single-mode fibre and then collimated in a Gaussian mode to be used in the experiment, while idler photons at 920 nm are detected by a Single-Photon Avalanche Detector in order to monitor the stability of the source. The robust weak measurement is obtained by means of the $n = 7$ identical blocks put after the initial PBS. A spatially-resolving detector (EM-CCD camera operating in the photon counting regime) is used to determine the final position of the detected photons

superoscillations[30,31]. Thus, the quantum formalism of robust weak values, apart from describing a genuinely quantum effect for the case of measurement with an external pointer, naturally incorporates this classical interference effect.

To increase confidence in our results, we repeated the experiment for a few sets of different parameters leading to less anomalous WVs (and even a non-anomalous one). All results are presented in Table 1 (see the Supplementary Material for additional information). The results are influenced by uncertainties originating from the calibration procedure. However, when the purpose is not to find a precise numerical value of the polarisation WV, but to test the single-click measurement method versus an ensemble measurement, the calibration uncertainty is irrelevant. The experimental data shown in Table 1 fit the theoretical predictions well, proving the possibility of measuring an anomalous WV with a single detection.

Theoretical calculations, see Fig. 3, show that the final uncertainty of the pointer is close to the initial beam width Δ. Thus, faced with a new task of estimating $(\sigma_3^\Sigma)_w$ in which somebody else fixes the pre- and postselected states of the system, a single click on our detector is capable of providing the WV with an uncertainty of the same order of magnitude as the width of the initial beam even for anomalous WVs.

In summary, our results offer a deeper understanding of the meaning of WVs, providing a significant contribution to the development of quantum measurement in the weak coupling regime. Estimating anomalous WVs with a single-click breaks the common belief that the WV is a statistical concept of conditional expectation value[13]. Our findings, going well beyond refs. [22,32], stress the non-statistical, single-particle nature of WVs, demonstrating how a single-click measurement can provide a WV estimate even for anomalous WVs. Furthermore, this experiment suggests a viable possibility for amplification methods effectively reducing the uncertainty contribution associated with the measurement of the pointer. This paves the way for future practical applications of the robust weak measurement paradigm.

Methods

In our experimental setup, shown in Fig. 4 (further details in the Supplementary Material), photons in a multi-thermal distribution with a mean photon number per pulse $\ll 1$ are produced by type-I spontaneous parametric down-conversion (SPDC). This guarantees a short coherence time (~150 fs), avoiding unwanted self-interference effects due to internal reflections. The SPDC occurs in a $10 \times 10 \times 5$ mm $LiIO_3$ crystal, pumped by the second harmonic generation (398 nm) of a 76 MHz mode-locked laser at 796 nm. The signal photons are spectrally filtered and coupled to a single-mode fibre. At the end of the fibre, the photons are collimated in a Gaussian mode and sent to the free-space path where the robust weak measurement experiment occurs. After passing through an initial polarising beam splitter (PBS), used to suppress any residual circular polarisation component, the signal photons go through $n = 7$ identical blocks, each implementing three steps: preselection, weak coupling and postselection. Each photon enters every block in a linear polarisation state, due to either the first PBS or the postselection of the previous block. Every block begins with a quartz half-wave plate, implementing a unitary rotation R aligning the photon polarisation axis to the direction corresponding to the initial (preselected) state $|\psi_\alpha\rangle$. Then, a birefringent unit composed of a pair of birefringent crystals is responsible for the weak interaction. The first calcite crystal, 2 mm long, has the extraordinary (e) optical axis lying in the $x-z$ plane, forming an angle of $\pi/4$ with respect to the z direction. This generates a spatial walk-off (of ~0.2 mm) along the x direction for the horizontally-polarised photons, reducing the overlap between the horizontal and vertical polarisation components. The second crystal of each unit is a 1.1 mm long calcite crystal with the optical e-axis lying along the y direction. It generates no spatial walk-off, and its role is to compensate the temporal walk-off induced by the first crystal. The last component of each block is a polarising plate, postselecting the photons in the state $|\psi_\beta\rangle$. After the $n = 7$ blocks, the photons are detected

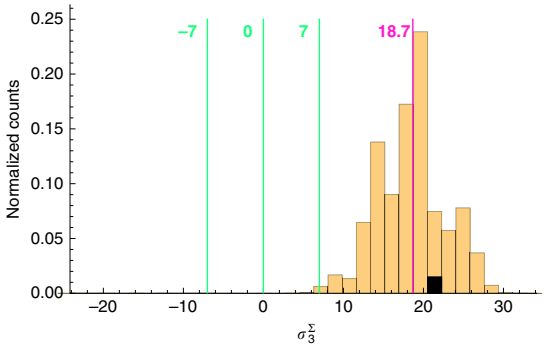

Fig. 5 Measurement of anomalous weak value. Normalized histogram of the photon counts along the x axis of the EM-CCD (see Methods) for repetitions of the single-click experiment (with unchanged parameters). The black square indicates the first click of the run, corresponding to the single-click experiment. The green lines indicate the borders and centre of the eigenvalue spectrum of our observable. The purple line shows the expected (theoretical) weak value $(\sigma_3^\Sigma)_w$

Table 1 Results for the various parameters of the measurement setup

#	1	2	3	4	5	6	7	8	9	10
	α	β	Δ	$(\sigma_3^\Sigma)_w$	$\Delta[(\sigma_3^\Sigma)_w]$	$(\sigma_3^\Sigma)_w^{\exp}$	$\Delta_{\text{stat}}[(\sigma_3^\Sigma)_w^{\exp}]$	$(\sigma_3^\Sigma)_w^{1\text{click}}$	$\Delta(\sigma_3^\Sigma)_w^{1\text{click}}$	Δx
(a)	0.62	2.53	5.84	18.7	0.9	18.59	0.09	21.4	4.5	4.5
(b)	0.62	2.53	3.18	9.8	0.8	10.51	0.02	10.9	3.8	5.0
(c)	0.52	2.62	2.96	11.4	0.5	11.07	0.08	14.1	3.4	2.8
(d)	0.52	0.88	3.09	1.3	0.4	0.97	0.05	−2.6	4.6	3.6

Columns 1-4 describe the preparation parameters and the corresponding weak value $(\sigma_3^\Sigma)_w$. Column 5 shows the systematic uncertainty in the experimental implementation of $(\sigma_3^\Sigma)_w$ due to the uncertainties in the preparation parameters α, β and Δ (which incorporate inhomogeneities in birefringent crystals and other experimental imperfections). Column 6 shows the experimental mean values obtained by repeating the single-photon experiments (EM-CCD dark counts subtracted). The statistical uncertainty in these experiments is shown in column 7. Column 8 presents the experimental weak values $(\sigma_3^\Sigma)_w^{1\text{click}}$ extracted from a single detection event. The uncertainty in column 9 represents the quantum uncertainty of the pointer variable experimentally obtained from repeated measurements with the same parameters as the single-click experiment (see histogram in Fig. 5). Column 10 contains the predicted final uncertainty of the pointer, Δx, calculated from the parameters α, β, and Δ

by a spatially resolving detector, i.e., an Electron Multiplying CCD (EM-CCD) device able to work in the linear analogue regime as well as in the photon counting regime (details in ref. [33]). To calibrate our system, we identify the extremal positions of the pointer on our EM-CCD, i.e. the position of the $|V\rangle$ polarisation state, corresponding to the eigenvalue $\sigma_3^\Sigma = -7$ and then the position of the state $|H\rangle$, corresponding to $\sigma_3^\Sigma = 7$. This allows us to define the zero point as the centre between the readings for $\sigma_3^\Sigma = \pm 7$, and also scale the pointer variable accordingly.

Acknowledgements
We acknowledge the European Union's Horizon 2020 and the EMPIR Participating States in the context of the projects 17FUN01 "BeCOMe" and 17FUN06 "SIQUST", the European Union's Horizon 2020 FET-OPEN project grant no. 828946 "PATHOS", the National Science Foundation—U.S.-Israel Binational Science Foundation Grant No. 735/18. EC was supported by Grant No. FQXi-RFP-CPW-2006 from the Foundational Questions Institute and Fetzer Franklin Fund, a donor advised fund of Silicon Valley Community Foundation, the Israel Innovation Authority under Projects No. 70002 and No. 73795, the Quantum Science and Technology Program of the Israeli Council of Higher Education, and the Pazy Foundation. JD acknowledges support from the PhD program IMPRS-QST.

Author details
[1]INRIM, Strada delle Cacce 91, I-10135 Torino, Italy. [2]National Institute of Metrology, Quality and Technology—INMETRO, Av. Nossa Senhora das Graças, 50, Duque de Caxias, RJ 25250-020, Brazil. [3]Max-Planck-Institut für Quantenoptik, Hans-Kopfermann-Straße 1, 85748 Garching, Germany. [4]Department für Physik, Ludwig-Maximilians-Universität, 80797 München, Germany. [5]Faculty of Engineering and the Institute of Nanotechnology and Advanced Materials, Bar Ilan University, Ramat Gan 5290002, Israel. [6]Raymond and Beverly Sackler School of Physics and Astronomy, Tel-Aviv University, Tel-Aviv 6997801, Israel

Author contributions
I.P.D., M.Gram, M.Gen (responsible of the laboratories) and L.V. (responsible for the theoretical framework) planned the experiment, with the support of F.P., A.A. and E.C. The experimental realisation was achieved (supervised by IPD, M.Gram and M.Gen) by ER (leading role), F.P., A.A. and M.A.de.S. The theoretical aspects were addressed by J.D., E.C. and L.V.. The manuscript was prepared with inputs by all the authors. They also had a fruitful systematic discussion on the progress of the work.

Conflict of interest
The authors declare no competing interests.

Supplementary information The online version contains supplementary material available at https://doi.org/10.1038/s41377-021-00539-0.

Received: 9 October 2020 Revised: 7 April 2021 Accepted: 19 April 2021
Published online: 25 May 2021

References

1. Aharonov, Y., Albert, D. Z. & Vaidman, L. How the result of a measurement of a component of the spin of a spin-1/2 particle can turn out to be 100. *Phys. Rev. Lett.* **60**, 1351–1354 (1988).
2. Ritchie, N. W. M., Story, J. G. & Hulet, R. G. Realization of a measurement of a "weak value". *Phys. Rev. Lett.* **66**, 1107–1110 (1991).
3. Hosten, O. & Kwiat, P. Observation of the spin hall effect of light via weak measurements. *Science* **319**, 787–790 (2008).
4. Dixon, P. B. et al. Ultrasensitive beam deflection measurement via interferometric weak value amplification. *Phys. Rev. Lett.* **102**, 173601 (2009).
5. Xu, X. Y. et al. Phase estimation with weak measurement using a white light source. *Phys. Rev. Lett.* **111**, 033604 (2013).
6. Piacentini, F. et al. Experiment investigating the connection between weak values and contextuality. *Phys. Rev. Lett.* **116**, 180401 (2016).
7. Lundeen, J. S. et al. Direct measurement of the quantum wavefunction. *Nature* **474**, 188–191 (2011).
8. Goggin, M. E. et al. Violation of the Leggett-Garg inequality with weak measurements of photons. *Proc. Natl. Acad. Sci. USA* **108**, 1256–1261 (2011).
9. Magaña Loaiza, O. et al. Amplification of angular rotations using weak measurements. *Phys. Rev. Lett.* **112**, 200401 (2014).
10. Leggett, A. J. Comment on "How the result of a measurement of a component of the spin of a spin-1/2 particle can turn out to be 100". *Phys. Rev. Lett.* **62**, 2325 (1989).
11. Peres, A. Quantum measurements with postselection. *Phys. Rev. Lett.* **62**, 2326 (1989).
12. Aharonov, Y. & Vaidman, L. Aharonov and Vaidman reply. *Phys. Rev. Lett.* **62**, 2327 (1989).
13. Dressel, J. et al. Colloquium: understanding quantum weak values: basics and applications. *Rev. Modern Phys.* **86**, 307 (2014).
14. Ferrie, C. & Combes, J. Weak value amplification is suboptimal for estimation and detection. *Phys. Rev. Lett.* **112**, 040406 (2014).
15. Jordan, A. N., Martínez-Rincón, J. & Howell, J. Technical advantages for weak-value amplification: when less is more. *Phys. Rev. X* **4**, 011031 (2014).
16. Pang, S. S., Dressel, J. & Brun, T. A. Entanglement-assisted weak value amplification. *Phys. Rev. Lett.* **113**, 030401 (2014).
17. Pusey, M. F. Anomalous weak values are proofs of contextuality. *Phys. Rev. Lett.* **113**, 200401 (2014).
18. Vaidman, L. Weak value controversy. *Philos. Trans. R Soc. A, Math. Phys. Eng. Sci.* **375**, 21060395 (2017).
19. Piacentini, F. et al. Investigating the effects of the interaction intensity in a weak measurement. *Sci. Rep.* **8**, 6959 (2018).
20. Ferrie, C. & Combes, J. How the result of a single coin toss can turn out to be 100 heads. *Phys. Rev. Lett.* **113**, 120404 (2014).
21. Mundarain, D. F. & Orszag, M. Quantumness of the anomalous weak measurement value. *Phys. Rev. A* **93**, 032106 (2016).
22. Vaidman, L. et al. Weak value beyond conditional expectation value of the pointer readings. *Phys. Rev. A* **96**, 032114 (2017).
23. Hallaji, M. et al. Weak-value amplification of the nonlinear effect of a single photon. *Nat. Phys.* **13**, 540–544 (2017).
24. Lyons, K. et al. Power-recycled weak-value-based metrology. *Phys. Rev. Lett.* **114**, 170801 (2015).
25. Aharonov, Y. et al. Surprising quantum effects. *Phys. Lett. A* **124**, 199–203 (1987).
26. Aharonov, Y. & Vaidman, L. Properties of a quantum system during the time interval between two measurements. *Phys. Rev. A* **41**, 11 (1990).
27. Dziewior, J. et al. Universality of local weak interactions and its application for interferometric alignment. *Proc. Natl. Acad. Sci. USA* **116**, 2881–2890 (2019).
28. Aharonov, Y. & Botero, A. Quantum averages of weak values. *Phys. Rev. A* **72**, 052111 (2005).
29. Howell, J. C. et al. Interferometric weak value deflections: quantum and classical treatments. *Phys. Rev. A* **81**, 033813 (2010).
30. Berry, M. V. & Popescu, S. Evolution of quantum superoscillations and optical superresolution without evanescent waves. *J. Phys. A: Math. Gen.* **39**, 6965–6977 (2006).
31. Aharonov, Y. et al. Some mathematical properties of superoscillations. *J. Phys. A: Math. Theor.* **44**, 365304 (2011).
32. Piacentini, F. et al. Determining the quantum expectation value by measuring a single photon. *Nat. Phys.* **13**, 1191–1194 (2017).
33. Avella, A. et al. Absolute calibration of an EMCCD camera by quantum correlation, linking photon counting to the analog regime. *Opt. Lett.* **41**, 1841–1844 (2016).

6.2 Weak Traces and Presence of Quantum Particles

6.2.1 Particle Presence in Quantum Mechanics

While classical mechanics is formulated in terms of definite particle trajectories or world-lines, this is not possible in quantum mechanics due to the complementarity of position and momentum. However, also for quantum systems there are length scales on which a classical ballistic motion is observed, as for example particle tracks in cloud chambers [539]. In such scenarios well-localized wave-packets propagate in a well-defined direction, where crucially the product of position and momentum uncertainties is above the limit imposed by the Heisenberg uncertainty relation. In contrast, if the wave-packet would be too well localized, it would experience significant dispersion due to the momentum uncertainty. Note that, as discussed in Sec. 1.2.2, in SQM the "particle" is synonymous with a particular quantum system defined via a certain Hilbert space structure and described by a state vector or density operator. Typically it possesses a spatial degree of freedom as well as other degrees of freedom such as, e.g., spin, called *internal degrees of freedom*. The support of the particle's spatial wave-packet at any point in time defines a spatial region in which the particle could be found if a position measurement would be performed. In this sense the particle can be said to be "present" in this region at a particular point in time [879].

The gedankenexperiments of Wheeler [1021, 1020], as introduced in Sec. 3.4.1, aim to show that a finer attribution of presence beyond just the coarse assertion of presence in the support of the forward-evolving spatial wavefunction is problematic. Ingeniously, instead of considering more fine-grained locations inside the support of a single spatial wave-packet, they establish a paradigm of the illustrative interferometric scenario of paraxial beams, where the delocalization of the particle is coarse-grained, i.e., consists in several well-localized wave-packets following comparatively definite but disjoint paths. Wheeler's delayed choice experiment then excludes the naive interpretation R according to which finding the particle in the support of one wave-packet allows to attribute to it the trajectory of that wave-packet also in the past. The argument crucially rests on the assumption that the future choice of measurement setting cannot have any effect on the past history of the particle in conjecture with the fact that, dependent on that choice, past presence in either only one or in several paths would need to be inferred. Certain interpretations of QM add different consistent definitions of the past presence of quantum particles, such as for example Bohmian mechanics, as discussed in Chapter 7, which attributes a definite trajectory to any particle in addition to its spatial wavefunction. A different strictly operational approach is sketched below.

6.2.2 Weak Trace Approach

In the *weak trace approach* (WTA), as proposed by Vaidman [792] and further developed in [793, 804, 763] as well as **[P9]**, a concept of particle presence is added to quantum mechanics. It is based on the assumption that the propagation of any particle along a certain path always involves interactions with local environments along that path and

defines the presence of this particle by its effect on these environments. For postselected particles, these effects can change when conditioned on successful postselection. This does not mean that the WTA includes retrocausality as necessary to uphold the interpretation R refuted by Wheeler, but rather indicates the fundamentally operational nature of the WTA. The "effect" of the environment is not regarded as the change of a local beable at a certain moment in time t, but operationally as a change in the dispositive expression for the state of this environment, which is simply updated when conditioning on other results. Stating that a postselected particle "affected the environment differently" can be understood in exactly the same manner as the assertions that, upon conditioning on coincidence detection, SPDC "produces photon pairs" or that a delayed choice measurement can decide whether a system "behaved like a wave or particle".

The effect of a pre- and postselected propagating particle on the environment will depend on the interaction strength. According to the WTA, if the interaction is not sufficiently weak, such that entanglement between system and environment cannot be neglected, the particle can no longer be regarded as a separate system and in general a joint description together with the respective environment becomes necessary [758]. The focus of the WTA, however, lies on the other type of scenarios in which the particle interacts only weakly with the various local environments such that an initial pure particle state remains pure and the weak interaction has the two-fold effect derived in Sec. 1.5.2, i.e., the particle experiences at most a unitary evolution (1.23) and a weak trace (1.22) is left on the local environment. The core of the WTA is then that the past presence of the particle at a certain location is defined based on the amplitude of the local weak traces it leaves. As these weak traces fundamentally cannot be detected by a single measurement, i.e., by an "irreversible act of amplification", they do not represent "phenomena" in Wheeler's sense. However, they can be determined with arbitrary precision by measurements on ensembles of identically pre- and postselected systems.

In the WTA to infer conclusions about the presence of the particle from the amplitudes of the local weak traces, the latter are compared to reference cases in which the particle is localized at the respective location. In experimental practice, where the various possible locations correspond for example to different interferometric paths, the particle is localized by preparing it in a definite forward-evolving path state and recording the weak trace left on the respective environment for an ensemble of identically prepared particles. A comparison of the amplitudes of the weak traces α_{loc} and α left by a localized particle and the delocalized particle in question, respectively, then quantifies the *presence* $\mathcal{P}$ of the particle as

$$\mathcal{P} := \frac{\alpha}{\alpha_{\mathrm{loc}}}. \tag{6.27}$$

In the WTA presence is thus not a binary property but fundamentally a gradual concept, i.e., it can have more values than just "present" and "absent". A presence of 1 means that the amplitude of the weak trace is equal to the amplitude of the weak trace for a localized particle. A larger or smaller positive ratio of amplitudes indicates an *increased* and *reduced* presence accordingly. As the presence $\mathcal{P}$ can also become negative or even

complex, the WTA also incorporates such *negative* and *anomalous* presence. It lies in the nature of weak measurements that any assertion of the WTA will be correct only approximately in a suitably weak regime and all theoretical statements will be technically only valid in respective limits of vanishing interaction strength. However, the description of quantum systems in terms of weak traces and corresponding presence $\mathcal{P}$ has proven to be an excellent approximation in several experimental scenarios [706, 817, 799, 746], including **[P3]**, as reproduced in the next section.

6.2.3 Presence and the Weak Value of Local Projection

The local interactions $\mathbf{U}_A$ with the local environments in a certain location A can be always written in the form

$$\mathbf{U}_A = \mathbf{\Pi}_A \otimes \mathbf{U}_I + \mathbf{\Pi}_{\bar{A}} \otimes \mathbb{1}, \tag{6.28}$$

where $\mathbf{\Pi}_A$ is the projector on location A, $\mathbf{\Pi}_{\bar{A}}$ the projector on the remaining locations, and $\mathbf{U}_I$ encompasses the weak interaction between the environment and all internal degrees of freedom of the particle. In the most general case the particle is pre- and postselected both with respect to its internal degrees of freedom as well as to its path state. To infer the presence, the local weak trace of a reference particle is considered, which is pre- and postselected in the same manner on its internal degrees of freedom. Assuming an initially pure state of the local environment $|\chi\rangle$ and a general interaction $\mathbf{U}_I$ with a Hamiltonian of the form (1.21), the weak trace left on the conditioned state of the local environment $|\widetilde{\chi}\rangle$, for a particle localized in A, can be written as

$$|\widetilde{\chi}\rangle \approx e^{-i\varphi} \left(|\chi\rangle + \alpha_{\mathrm{loc}} |\chi_\perp\rangle \right), \tag{6.29}$$

where $\alpha_{\mathrm{loc}} = \Delta_g \mathbf{D}_w$, $\varphi = \mathrm{Re}\big[\langle \mathbf{D}_w \rangle\big]$, the operator $\mathbf{D}_w$ ist given by $\mathbf{D}_w = \sum_j \varepsilon_j (\mathbf{A}_j)_w \mathbf{B}_j / \hbar$, and the generalized standard deviation Δ_g for non-hermitian operators $\mathbf{C}$ is defined as [345, 248]

$$\Delta_g \mathbf{C} := \sqrt{\langle \mathbf{C}^\dagger \mathbf{C} \rangle - |\langle \mathbf{C} \rangle|^2}. \tag{6.30}$$

Accordingly, in the absence of postselection on the internal degrees of freedom, Eq. (6.29) reduces to the simple weak trace (1.22). A similar expression is of course also obtained for the composite weak trace in the case of a mixed state of the local environment.

If now a particle with general delocalized forward and backward-evolving path states is considered, it is straight forward to show that the effect of the interaction is modified to

$$|\widetilde{\chi}\rangle \approx |\chi\rangle + (\mathbf{\Pi}_A)_w \, \alpha_{\mathrm{loc}} |\chi_\perp\rangle, \tag{6.31}$$

as long as both spatial pre- and postselection factorize with the pre- and postselection of the internal degrees of freedom of the particle. By application of definition (6.27) it becomes clear that in such cases the presence $\mathcal{P}$ exactly corresponds to weak value of local

projection on A. Again in case of an initially mixed state of the local environment, the amplitudes of each of the component weak traces are multiplied by $(\mathbf{\Pi}_A)_w$.

The particular presence $\mathcal{P}$ is crucially completely independent of the interaction $\mathbf{U}_I$, at least as long as the latter is sufficiently weak, and implies significant consequences on any weak measurements performed on the particle at location A. If for example the interaction has the form $\mathbf{U}_I = \bigotimes_j \mathbf{U}_j$, where each $\mathbf{U}_j$ corresponds to the measurement of a particular internal degree of freedom of the system by a pointer which is part of the local environment, the effect of each of these measurement interactions will be modified by the presence $\mathcal{P}$ in a similar manner. In particular, for example with $\mathcal{P} > 1$ the shifts of the corresponding pointer observables will all be amplified by the same factor. In this sense an increased presence of the particle increases the values of all its observable quantities. If on the other hand the presence is strictly imaginary, complementary pointer observables will be shifted in all measurements. Finally, for $\mathcal{P} < 0$, all shifts will be reversed, changing, e.g., the effects of certain interactions from repulsive to attractive, as proposed in [703]. Note that, due to the linearity of weak values, the presence of the particle at all locations always sums up to 1 at any point in time.

A special type of local interaction is given if $\mathbf{U}_I$ represents a weak measurement interaction for the measurement of an observable $\mathbf{A}$, acting on some subset of internal degrees of freedom of the particle, by some pointer which is part of the local environment. Assuming again an initially pure pointer state, the modified effect of this measurement interaction can be expressed on the conditional pointer state $|\widetilde{\chi}\rangle$ as

$$|\widetilde{\chi}\rangle \approx e^{-\varepsilon(\mathbf{\Pi}_A)_w(\mathbf{A})_w\mathbf{B}/\hbar}\,|\chi\rangle\,. \tag{6.32}$$

In general if the spatial parts of the pre- and postselection states no longer factorize from the remaining parts, the above expression is no longer correct and, instead of the product of weak values, the weak value $(\mathbf{\Pi}_A \otimes \mathbf{A})_w$ of the product of observables has to be considered. This represents an instance of a failure of product rule, as introduced in Sec. 2.6.2, for weak values [795]. In such cases the presence of the particle is no longer simply described by the weak value of local projection and the spatial degree of freedom has to be considered jointly with the internal degrees of freedom to provide expressions for the presence. In particular, it is possible that the weak value of local projection $(\mathbf{\Pi}_A)_w$ vanishes while the weak value $(\mathbf{\Pi}_A \otimes \mathbf{A})_w$ has a finite value, which represents the weak trace equivalent of a Cheshire cat scenario. In such cases the degree of presence $\mathcal{P}$ at a location A could be defined based on weak values, e.g., as

$$\mathcal{P} = \max_{\mathbf{A}} \frac{|(\mathbf{\Pi}_A \otimes \mathbf{A})_w|}{||\mathbf{A}||}, \tag{6.33}$$

where $\mathbf{A}$ is an arbitrary observable acting on the internal degrees of freedom of the particle, and $||\cdot||$ is an operator norm.

In **[P3]**, as reproduced below in Sec. 6.2.6, a universal modification of the effect of interactions by the weak value of projection is observed using a MZI and the degrees of freedom of the paraxial beam. Instead of coupling different local pointers to various

internal degrees of freedom of a particle, the degrees of freedom of the beam themselves are employed as pointers as is common in many experimental weak measurements. Thus, the interaction Hamiltonian for the j-th degree of freedom has the form $\mathbf{H}_I = ga\mathbf{\Pi}_A \otimes \mathbf{B}_j$, which is equivalent to the measurement of an operator $\mathbf{A}_j$ on the internal degree of freedom, with $\mathbf{H}_I = g\mathbf{\Pi}_A \otimes \mathbf{A}_j \otimes \mathbf{B}_j$, when the state of the degree of freedom is an eigenstate with eigenvalue a. A simultaneous local coupling in one of the interferometric paths to three distinct degrees of freedom is effectively induced by displacing and deflecting the transverse mode in x and y-directions, as well as by introducing a slight change of the polarization of the beam.

6.2.4 Weak Three Box Scenario

A seminal application of WTA is the three box scenario as introduced in Sec. 2.6.2. While in the original version the particle is found with certainty in any of the boxes when a projective measurement is performed, a similar result is obtained when evaluating the weak trace [681, 672]. For the two-state

$$\langle\phi| = \frac{1}{\sqrt{3}}\big(\langle A| - \langle B| + \langle C|\big) \quad |\psi\rangle = \frac{1}{\sqrt{3}}\big(|A\rangle + |B\rangle + |C\rangle\big), \tag{6.34}$$

the weak values of projection

$$(\mathbf{\Pi}_A)_w = 1, \qquad (\mathbf{\Pi}_B)_w = -1, \qquad (\mathbf{\Pi}_C)_w = 1, \tag{6.35}$$

are obtained. According to the WTA the particle thus has a regular presence of 1 in boxes A and C and an anomalous presence of -1 in box B. All those weak values are measurable simultaneously by induced appropriate local weak interactions. Results such as these are the reason why sometimes weak values are claimed to "resolve" quantum paradoxes, see, e.g., [728, 749, 808]. In the context of the three-box paradox the resolution by the WTA consists in providing a concept of presence, which consistently allows to attribute full presence, i.e., presence of order 1, in all three boxes. However, this notion of "resolution" has also been criticized [789, 719, 788]. Note that in some examples the amplitudes of paths A, B, and C are chosen differently, such that the weak values correspond to different numbers, which, however are still of comparable order. Furthermore, in physical scenarios, due to always present interactions with local environments, crucially both pre- and postselection correspond to entangled states and are therefore only approximately given by the pure states (6.34).

The WTA was introduced based on an optical interferometric Gedankenexperiment which corresponds to an extended three-box scenario [792]. Therein light propagates through a nested interferometer, as depicted in Fig. 6.1, and is prepared and postselected such, that the forward and backward evolving states with respect to paths A, B and C correspond approximately to the states (6.34). Accordingly the weak values of projection onto the corresponding paths have the values (6.35) and the photons can be said to be fully present in the corresponding paths, i.e., in the outer path C as well as in the inner

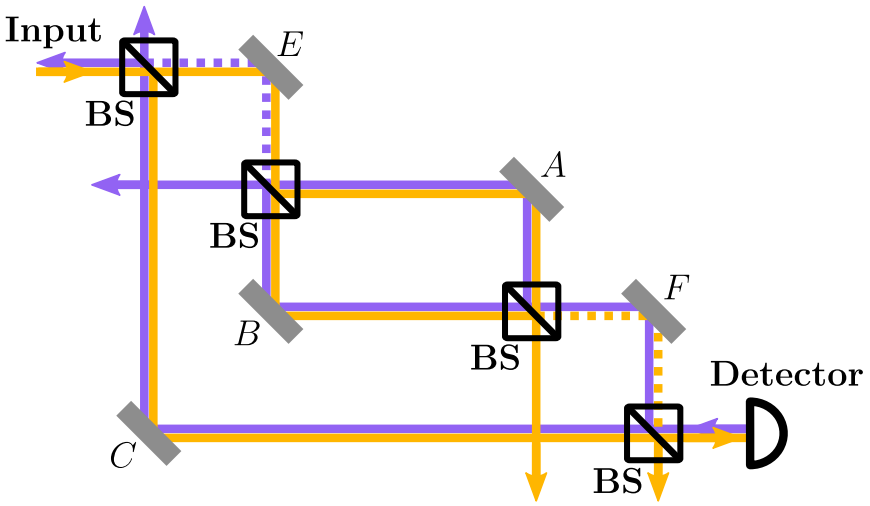

Figure 6.1: **Nested Mach-Zehnder Interferometer** The forward evolving state is represented by the orange lines. When conditioning on successful detection, also a backward evolving state can be assigned to the system, which is represented by the purple lines. The dashed paths denote regions of only very small amplitude of the respective states due to leakage through the dark ports of the inner interferometer. The WTA attributes significant presence only where there is strong overlap between forward and backward evolving states, i.e., in arms A, B and C but not E and F, leading to "disconnected paths". The corresponding weak values of local projection can be measured by inducing vibrations of the mirrors with different frequencies at the five locations.

interferometer. Additionally, however, also paths E and F, leading to and away from the inner interferometer are considered. It turns out that the corresponding weak values of projection $(\mathbf{\Pi}_E)_w$ and $(\mathbf{\Pi}_F)_w$ are vanishing, and thus, according to the WTA, the particle is not present significantly in the corresponding paths. In this sense the WTA concludes that in this particular scenario the particle propagates along "disconnected particle paths". These predictions have been first verified in a seminal experiment by Danan *et al.* [706], in which weak measurements of the corresponding weak values were implemented by imprinting small deflections, varying with different frequencies, at the various locations through the tilting of the respective mirrors.

6.2.5 Criticism of the WTA

Although perfectly consistent with the predictions of SQM, both the WTA and the experiment described above have encountered heavy criticism and are the subject of a still-ongoing heated controversy. The criticism can be coarsely grouped into five points. The first issue is related to the general question whether weak values can be regarded as properties of single PPS, as already discussed in Sec. 6.1.6, which of course has implications for the question whether weak traces can be attributed to single particles or are merely a collective phenomenon [717, 780, 724, 730]. Only in the former case can the weak trace approach provide a consistent concept of particle presence.

The next point concerns the nested interferometer scenario described above and in particular the question of continuity between the case of perfect destructive interference at the dark output port of the inner interferometer and the case of necessary "leakage" of light, whenever weak measurements of presence are performed [748, 787, 726, 724]. These arguments essentially state that the calculation with the pure states (6.34) pertains only to the ideal case and cannot be regarded as valid for cases where the interferometer is disturbed. As clarified in [797, 763] and also discussed above, this criticism clearly rests on a misunderstanding of the WTA, which crucially is an approximate concept based fundamentally on the presence of non-vanishing local weak interactions in any scenario. For example, even if the mirrors in the experiment [706] are not moved, weak traces are left on the spatial state of the mirrors, such that an undisturbed perfectly tuned interferometer has to be regarded as a theoretical fiction. The much stronger controlled weak interactions which are induced in addition to these unavoidable natural interactions simply represent an experimental tool allowing to properly quantify the weak traces.

Third, as argued by some authors, the WTA is inadequate as a concept of presence precisely because it contradicts classical intuition with results such as disconnected paths [717, 724]. However, as discussed above, this clash with classical intuitions is not specific to the WTA but in fact the hallmark of many quantum mechanical phenomena, for which already the uncertainty relation prohibits the notion of particle trajectories, at least in the standard approach, and wavefunctions routinely correspond to superpositions of various locations. Thus in the standard view as championed by Wheeler, no claims about presence of particle can be made at all, as long as no position measurements are performed. In contrast, some authors, see, e.g., [764, 773, 726, 717, 780, 782, 724] appear to implicitly ascribe to concepts of presence which go beyond this minimal view, either by identifying the particle's presence with only a part of the forward evolving wavefunction or by employing some concept of continuity of energy or probability flow, reminiscent of Bohmian mechanics, as introduced in the next chapter. While such alternative definitions of presence might be viable, their incompatibily with the WTA does not in itself represent an a priori reason to dismiss the WTA.

The fourth problem concerns the particular experimental realizations of measurements of weak traces. With exception of the experiment by the group of Steinberg [723], all other measurements employ internal degrees of freedom of the particle as pointers, see, e.g., [706, 817, 746] as well as the three experimental studies reprinted here. In effect, the possible interaction is not restricted to a single point of contact with the pointer, but the latter can interact with the system at various locations. This is exactly the effect present in a proposal by Jordan and Alonso [690], in which the trace imprinted at location E appears in the signal since an additional subsequent interaction with the internal degree of freedom is induced at a different location [804, 770]. Crucially, experiments with internal degrees of freedom as pointers allow to measure weak traces reliably only under the condition that apart from an interaction at a single location no further disturbance or interaction is introduced in this degrees of freedom. Note that in the experiment [706] this condition is fulfilled by the fact that each mirror effectively couples to distinct frequency modes of the beam, which are not affected by the mirrors at the other locations.

Finally, several authors have also criticized the general usefulness of the WTA as a physical concept [734, 724]. This line of criticism is most difficult both to pursue as well as to refute since notions such as "usefulness" or "simplicity" are notoriously hard to define. Of course the WTA does not make any new predictions and any effects are fully explainable by SQM. Furthermore, its suitability as a resolution of so-called quantum paradoxes involving projective measurements, such as the three-box paradox, is plausibly contested, due to the question of different ensembles of PPS, as discussed in Sec. 2.6.2. On the other hand, several hitherto unknown and unexpected effects, such as the results presented in [**P6**] and [**P3**], as reprinted in 6.1.8 and in the next section, respectively, have been highlighted by this new formal approach and in general it is difficult to exclude that this consistent concept of the presence of quantum particles, providing potentially a more complete understanding of the physical world, does not have merit in itself and will not turn out fruitful in the future, such as has been the case with many other strictly foundational concepts. As stated by Aharanov and Vaidman already in one of the earliest works on the TSVF:

> To avoid possible misinterpretations we want to stress from the outset that our work neither contradicts ordinary quantum theory nor extends it in the sense of new physical laws. It is possible, in principle, to obtain all the results presented in this work using the standard formalism. However, using only quantum states evolving towards the future, it is more difficult to prove these results, and in some cases it is almost impossible to foresee them. [673]

Universality of local weak interactions and its application for interferometric alignment

Jan Dziewior[a,b], Lukas Knips[a,b], Demitry Farfurnik[c,1], Katharina Senkalla[a,b], Nimrod Benshalom[c], Jonathan Efroni[c], Jasmin Meinecke[a,b], Shimshon Bar-Ad[c], Harald Weinfurter[a,b], and Lev Vaidman[c,2]

[a]Max-Planck-Institut für Quantenoptik, 85748 Garching, Germany; [b]Department für Physik, Ludwig-Maximilians-Universität, 80797 München, Germany; and [c]Raymond and Beverly Sackler School of Physics and Astronomy, Tel-Aviv University, Tel-Aviv 69978, Israel

Edited by Michael Berry, University of Bristol, Bristol, UK, and approved December 31, 2018 (received for review July 28, 2018)

The modification of the effect of interactions of a particle as a function of its preselected and postselected states is analyzed theoretically and experimentally. The universality property of this modification in the case of local interactions of a spatially preselected and postselected particle has been found. It allowed us to define an operational approach for the characterization of the presence of a quantum particle in a particular place: the way it modifies the effect of local interactions. The experiment demonstrating this universality property provides an efficient interferometric alignment method, in which the position of the beam on a single detector throughout one phase scan yields all misalignment parameters.

quantum physics | quantum experiments | quantum measurement | weak measurements | optics alignment

Preselected and postselected systems are ubiquitous in quantum mechanics. In many quantum information schemes, the intended process is only realized by the interplay of preselection and postselection. The addition of postselection, often together with conditioned transformations, is the basis of protocols such as universal quantum computation within the Knill–Laflamme–Milburn scheme (1), entanglement swapping (2), and heralding in general (3).

The two-state vector formalism (TSVF) (4) provides a general framework for the description of preselected and postselected systems. It introduces a state evolving backward in time and thereby treats the postselection on equal footing as the preselection. The key element of the TSVF is the weak value of an observable. As long as the interaction is sufficiently weak or short, the observable effect on the external system is completely characterized by the weak value (5). For such interactions, the state of the external systems after the postselection can deviate significantly from the states expected by just considering the coupling to preselected systems (6). The concept of weak values became the basis of several successful applications in precision-measurement techniques (7, 8). While there are theoretical controversies about the optimality of the weak value-based tomography and precision-measurement methods (9–20), a plethora of fruitful applications continues to emerge (21–34).

We take a step back and investigate the fundamental properties of preselected and postselected systems. We find that there exists a general universality principle characterizing how the effects of the interactions in one location of a spatially preselected and postselected quantum system are modified as a function of preselection and postselection. All these modifications are specified by a single complex number, the weak value of the spatial projection operator. One of the innovations of our approach is that it does not rely on the specific form of the interaction Hamiltonian. Instead, it expresses the change of the state via the complex amplitude of an orthogonal component, which emerges due to the interaction. If the weak value is a positive number, the size of the changes in every variable is multiplied by this number, and when it is negative, all modifications happen in the opposite direction. If the effect originally changed a particular variable, in the case of an imaginary weak value, the effect will occur in a variable conjugate to the initial one, and when the weak value is a complex number, both effects are combined together. This approach allows a formal definition of a quantum particle's presence.

Until now, most accounts considered the weak value to be limited to the case of weak interactions—e.g., refs. 35–39. It is another crucial innovation of our approach, however, that we explicitly apply the formalism to the case of much stronger interactions. We use an expression for the weak value which takes into account changes due to interactions of finite strength in the time interval between preselection and postselection. Besides incorporating the stronger interactions, we also account for decoherence or imperfections in the measurement system. We show experimentally that this weak value can in fact be measured by using weakly coupled pointers.

An interferometer, especially a Mach–Zehnder-type interferometer (MZI), can be seen as the iconic example for preselected and postselected systems. The reflectivity/transmittivity of the first beam splitter together with the phase shifter defines the preselected state of the system. The final beam splitter together

Significance

In this combined theoretical and experimental work, we describe and demonstrate a universal feature of local couplings of spatially preselected and postselected systems. All weak couplings, independently of their physical nature, are modified in the same universal manner, characterized by the weak value of local projection. We present a general analysis which neither relies on a specific form of the coupling nor is restricted to weak interactions. This allows us to define a consistent paradigm of the presence of a quantum particle, much more intricate than the concept of the presence of a classical particle. Furthermore, we discovered that Gaussian pointers remain reliable beyond the weak regime, which enabled a simple and efficient alignment method for interferometric setups.

Author contributions: J.D., L.K., H.W., and L.V. designed research; J.D., L.K., K.S., and L.V. performed research; J.D., L.K., D.F., and L.V. contributed new analytic tools; J.D., L.K., D.F., K.S., N.B., J.E., S.B.-A., and L.V. analyzed data; J.D., L.K., K.S., N.B., J.M., H.W., and L.V. wrote the paper; D.F., N.B., J.E., and S.B.-A. performed preliminary experimental work on the alignment method; D.F., N.B., J.E., and S.B.-A. participated in the analyses; and D.F. suggested the alignment method.

The authors declare no conflict of interest.

This article is a PNAS Direct Submission.

This open access article is distributed under Creative Commons Attribution License 4.0 (CC BY).

Data deposition: Please contact the authors if you wish to access the raw data.

[1]Present addresses: Racah Institute of Physics, The Hebrew University of Jerusalem, Jerusalem 9190401, Israel; and The Center for Nanoscience and Nanotechnology, The Hebrew University of Jerusalem, Jerusalem 9190401, Israel.

[2]To whom correspondence should be addressed. Email: vaidman@post.tau.ac.il.

Published online February 5, 2019.

Downloaded from https://www.pnas.org by MPDL Quantenoptik on March 30, 2022 from IP address 130.183.91.43.

with detection of the particle in one output of the interferometer sets the postselected state. The effect of weak interactions of the particle with external systems, which can be seen as a trace the particle leaves inside the interferometer, is characterized by the weak value of the projection operator on the corresponding arm. Surprisingly, we also found that for Gaussian states of the external system, the weak value characterizes the modification of the trace for arbitrary strength of the interaction.

The interferometer enables straightforward experimental implementation, where we consider a preselected and postselected photon passing through. We experimentally characterize the various effects of multiple interactions in one of the interferometer's arms using the mode and the polarization of the propagating photon as the external systems coupled to the photon's path. We find that the modifications of the weak effects on the photon can be described by the weak value of the projection operator on the corresponding arm for various types and strengths of couplings.

We can now turn the picture upside-down and view any coupling to the external degrees of freedom as being due to misalignment of the interferometer. For example, a tilted mirror in one of the beams now becomes an interaction deflecting the Gaussian mode of the beam from its ideal direction. This analogy directly leads us to an efficient alignment technique for interferometers, where our analysis provides a simple model for the image observable at the output of an interferometer. More precisely, by measuring the phase-dependent trajectory of the centroid of the output mode on only a single spatially resolving detector, we can extract the misalignment parameters in one go. This technique harnesses the benefits of the weak amplification method (6) to improve precision.

Weak Value of Local Projection and its Connection to the Trace

Let us first consider the effect of a quantum particle on external systems due to all kinds of local interactions in the channel through which it passes. The interactions might be caused by various properties of the particle—e.g., charge, mass, magnetic moment, etc.—but we assume that the particle passing through the channel does not change its quantum state.*

If the quantum particle is not present in the channel, the state of the external systems at a particular time is $|\chi\rangle$. When the quantum particle is localized in the channel, as shown in Fig. 1*A*, the interactions change the total state of the external systems as

$$|\chi\rangle \to |\chi'\rangle \equiv \eta\left(|\chi\rangle + \epsilon|\chi^{\perp}\rangle\right), \qquad [1]$$

where $|\chi^{\perp}\rangle$ denotes the component of $|\chi'\rangle$, which is orthogonal to $|\chi\rangle$. By definition, we choose the phase of $|\chi^{\perp}\rangle$ such that $\epsilon > 0$. For simplicity, but without loss of generality, we also disregard the global phase and consider the coefficient η to be positive, such that $\eta = \langle\chi\,|\,\chi'\rangle = \frac{1}{\sqrt{1+\epsilon^2}}$. The trace left by the particle is manifested by the presence of the orthogonal component $|\chi^{\perp}\rangle$ and is quantified by the parameter ϵ.

Next, let this channel be an arm of an MZI (Fig. 1*B*). We assume that the arm B of the MZI is ideal—i.e., the particle leaves no trace there.† For the creation of the preselected state

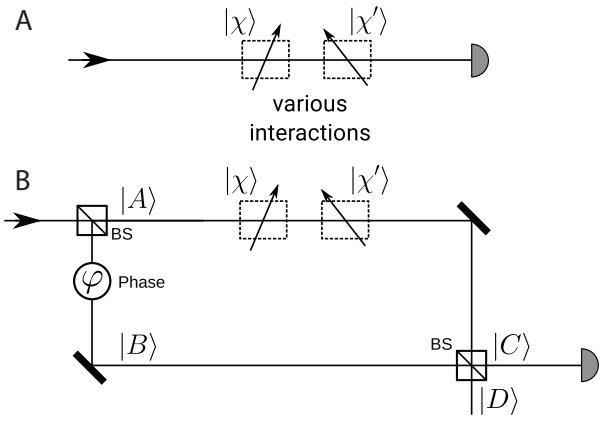

Fig. 1. Comparison between effect of the local coupling of the particle when it passes through a single channel and when it passes through an interferometer. (*A*) The particle interacts with external systems in a single channel originally in the state $|\chi\rangle$. (*B*) The particle passes through an MZI with arm A identical to the channel described in *A* with all its local interactions, while it is assumed that there are no local couplings in arm B.

inside the interferometer $|\psi\rangle$, the unbalanced input beam splitter is followed by a phase shifter, resulting in

$$|\psi\rangle = \cos\alpha|A\rangle + \sin\alpha e^{i\varphi}|B\rangle, \qquad [2]$$

where $|A\rangle$ and $|B\rangle$ represent the eigenstates of the path degree of freedom, and α and φ are the two real parameters of the state.

The second beam splitter is balanced, so its operation can be modeled as

$$|A\rangle \to \frac{1}{\sqrt{2}}(|C\rangle + |D\rangle), \qquad [3a]$$

$$|B\rangle \to \frac{1}{\sqrt{2}}(|C\rangle - |D\rangle). \qquad [3b]$$

We collect photons in output port C, which corresponds to a postselection of the state

$$|\phi\rangle = \frac{1}{\sqrt{2}}(|A\rangle + |B\rangle). \qquad [4]$$

Accounting for the interactions in arm A (Fig. 1*B*), the composite state $|\Psi\rangle$ of the particle and the external systems before the second beam splitter is

$$|\Psi\rangle = \cos\alpha|A\rangle|\chi'\rangle + \sin\alpha e^{i\varphi}|B\rangle|\chi\rangle, \qquad [5]$$

where here and in the rest of the paper, we use a shorthand notation for tensor products with $|A\rangle|\chi'\rangle \equiv |A\rangle \otimes |\chi'\rangle$. After detection of the particle in arm C—i.e., postselection of the particle in state **[4]**—the state of the external systems becomes

$$|\tilde{\chi}\rangle = \mathcal{N}\left(|\chi\rangle + \frac{\eta\epsilon}{\eta + \tan\alpha e^{i\varphi}}|\chi^{\perp}\rangle\right), \qquad [6]$$

where $\mathcal{N}$ is the normalization factor. Here and in the rest of the paper, we use the accent symbol "$\sim$" to denote situations with preselection and postselection.

We start by considering interactions which are sufficiently small, with $\epsilon \ll 1$. In the case of a single channel, the particle passing through it leads to the change of the state of the external systems,

$$|\chi\rangle \to |\chi'\rangle = |\chi\rangle + \epsilon|\chi^{\perp}\rangle + \mathcal{O}(\epsilon^2), \qquad [7]$$

which is just an expansion of **[1]** in orders of ϵ.

*To deal with cases where the states of some degrees of freedom of the particle change, we treat them equivalently to the external degrees of freedom. In fact, this is the case in our experiment (Observing the Universality Property).

†This assumption is made for simplicity of presentation. The main results of the paper about the universality of modification of interactions are easily transformed to the case when some weak traces are left in all parts of the interferometer.

Downloaded from https://www.pnas.org by MPDL Quantenoptik on March 30, 2022 from IP address 130.183.91.43.

Downloaded from https://www.pnas.org by MPDL Quantenoptik on March 30, 2022 from IP address 130.183.91.43.

For the particle that has passed through the corresponding MZI and has been detected in C, we observe a different change of the state of the external systems. Expanding Eq. **6** in orders of ϵ, we can see that the weak effect of the interaction is modified relative to [**7**] by a single parameter, the weak value of projection on arm A,

$$|\chi\rangle \to |\tilde{\chi}\rangle = |\chi\rangle + \epsilon\,(\mathbf{P}_A)_w|\chi^{\perp}\rangle + \mathcal{O}(\epsilon^2), \qquad [8]$$

where, for defining the weak value, we neglect the coupling to external systems

$$(\mathbf{P}_A)_w \equiv \frac{\langle\phi|\mathbf{P}_A|\psi\rangle}{\langle\phi|\psi\rangle} = \frac{1}{1+\tan\alpha\; e^{i\varphi}}. \qquad [9]$$

The design of the interferometer allows the full range of weak values of projection onto arm A, by varying the parameters $\tan\alpha$ and φ. Note that we did not restrict the number of interactions as long as their combined effect is sufficiently weak.

When the trace left in the interferometer is small, $\epsilon \ll 1$, the weak value can be considered neglecting the effect of the interactions, as in [**9**]. In the next section, we will turn toward scenarios with stronger couplings for which the interactions cannot be neglected.

Weak Value Considering Finite Coupling Strength and Imperfections

Calculating the weak value as in Eq. **9**, we have implicitly assumed that it only depends on the preselection and postselection states at the boundaries of the considered time interval. This is correct in the limit of weak coupling, which is considered in most works about weak measurements. However, sometimes even in scenarios with coupling of finite strength, the weak value has been treated as if there was no coupling—i.e., using formula [**9**] (20, 35–40).

To correctly account for couplings of finite strength, we turn to the proper definition of the weak value in the framework of the TSVF, which refers to a single point in time t, at which the particular forward- and backward-evolving quantum states have to be evaluated (41). All interactions of finite strength and imperfections of optical devices between preselection and t, as well as between t and postselection, must be considered. Thus, Eq. **2** correctly describes the forward-evolving state only immediately after the first beam splitter, and Eq. **4** describes the backward-evolving state only immediately before the second beam splitter. Since all evolutions due to imperfections or interactions with the different external systems are local—i.e., they have the common eigenstates $|A\rangle$ and $|B\rangle$—the time ordering of the evolutions is of no consequence. Therefore, the weak value $(\mathbf{P}_A)_w$ stays constant in time, and we are free to choose any moment in time to calculate it. For convenience, we calculate the weak value immediately before postselection on state [**4**] and modify only the forward-evolving state to account for the evolution due to interactions inside the interferometer.

Due to the interactions, the system becomes entangled with the external systems as described by Eq. **5**. Thus, the particle is in the mixed state described by the density matrix in the basis $\{|A\rangle, |B\rangle\}$

$$\rho = \begin{pmatrix} \cos^2\alpha & \cos\alpha\sin\alpha e^{-i\varphi}\eta \\ \cos\alpha\sin\alpha e^{i\varphi}\eta & \sin^2\alpha \end{pmatrix}. \qquad [10]$$

The weak value in the case of mixed states has been derived in ref. 5 (equation 32 therein),

$$A_w = \frac{\mathrm{Tr}\,(\rho_{\mathrm{post}} A \rho_{\mathrm{pre}})}{\mathrm{Tr}\,(\rho_{\mathrm{post}}\rho_{\mathrm{pre}})}. \qquad [11]$$

In our case, this formula is not applicable for arbitrary time between the preselection and postselection due to entanglement in both forward- and backward-evolving states with the same external systems (section VI of ref. 5), but it can be used to calculate the weak value immediately before the last beam splitter since the backward-evolving state is not entangled (see also refs. 35, 42, and 43). As we explained above, the weak value of the projector $\mathbf{P}_A$ is constant between preselection and postselection, so it can be calculated as

$$(\mathbf{P}_A)_w = \frac{\mathrm{Tr}\,(|\phi\rangle\langle\phi|\mathbf{P}_A\rho)}{\mathrm{Tr}\,(|\phi\rangle\langle\phi|\rho)} = \frac{1+\tan\alpha\,\eta e^{-i\varphi}}{1+\tan^2\alpha+2\tan\alpha\,\eta\cos\varphi}. \qquad [12]$$

From Eq. **10**, we see that the overlap η quantifies the loss of coherence between the two arms of the interferometer due to interactions and imperfections, which consequently leads to a reduction of the maximally achievable weak value. The dependence of the weak value [**12**] on η as well as on α and φ is presented in Fig. 2. Fig. 2 *A* and *B* show the case with ideal overlap $\eta = 1$, while Fig. 2 *C*–*F* illustrate the dependence for the nonideal case with reduced overlap and thus smaller $(\mathbf{P}_A)_w$.

The weak value [**12**] which accounts for multiple and even strong interactions is not useful to describe the whole of the external systems when inserted into expansion [**8**] because ϵ is large. However, Eq. **12** can be used to describe the modification for those interactions which are weak, even if some of the other interactions or all of them together are arbitrarily strong. We will show this now.

In our scenario, we neglect the interactions of external systems in arm A among themselves. If between some particular systems, the interaction cannot be neglected, they are considered as a single composite system. Thus, the interactions [**1**] in a single channel (Fig. 1*A*) can be decomposed as

$$|\chi\rangle = \bigotimes_j |\chi_j\rangle \to |\chi'\rangle = \bigotimes_j \eta_j \left(|\chi_j\rangle + \epsilon_j|\chi_j^{\perp}\rangle\right). \qquad [13]$$

Here, as for [**1**], we absorbed the phases in the definitions of states, such that ϵ_j and η_j are positive numbers.

In the case where the coupling to the, say, k-th system, is weak, the change of the state of the system can be also expressed by using density-matrix language in the $\{|\chi_k\rangle, |\chi_k^{\perp}\rangle\}$ basis as

$$\rho_k = \begin{pmatrix} 1 & 0 \\ 0 & 0 \end{pmatrix} \to \rho_k' = \begin{pmatrix} 1 & \epsilon_k \\ \epsilon_k & 0 \end{pmatrix} + \mathcal{O}(\epsilon_k^2). \qquad [14]$$

For a particle passing through the MZI, when both the preselection as well as the postselection state are superpositions of $|A\rangle$ and $|B\rangle$, several interactions in A (Fig. 1*B*) will lead to entanglement between the various external systems. Thus, each of the systems will be described by a mixed state. The modified evolution of the weakly coupled k-th system is

$$\rho_k \to \tilde{\rho}_k = \begin{pmatrix} 1 & (\mathbf{P}_A)_w^*\epsilon_k \\ (\mathbf{P}_A)_w\epsilon_k & 0 \end{pmatrix} + \mathcal{O}(\epsilon_k^2). \qquad [15]$$

Again, the modification of the effect of the weak interaction is characterized by the weak value $(\mathbf{P}_A)_w$.

Manifestation of the Trace as Shifts in Pointer States

In the previous sections, we described the trace a particle leaves as the appearance of an orthogonal component in the quantum state of external systems. Another language, frequently closer to

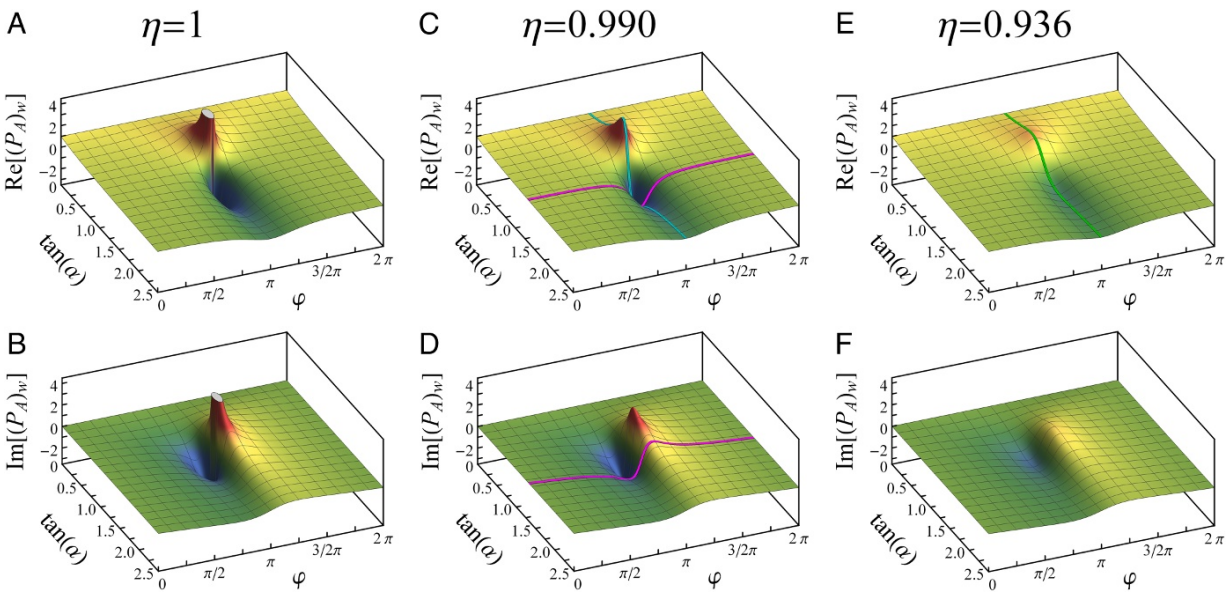

Fig. 2. Exact parameter dependence of weak value. Real (*A*, *C*, and *E*) and imaginary (*B*, *D*, and *F*) parts of weak value of the projection operator on arm *A* for $\eta = 1$, $\eta = 0.990$, and $\eta = 0.936$. Each plot shows the dependence on the phase φ and the amplitude ratio $\tan\alpha$. The highlighted colored lines represent the parameter values that are set in the various measurements (see Figs. 4 and 5).

experimental evidence, is the change in the expectation values of the external systems. Given the small change due to interactions in Fig. 1*A*, expressed in [**7**], every observable O of the external system changes its expectation value as

$$\delta\langle O\rangle \equiv \langle\chi'|O|\chi'\rangle - \langle\chi|O|\chi\rangle = 2\epsilon\,\mathrm{Re}\left[\langle\chi|O|\chi^{\perp}\rangle\right] + \mathcal{O}(\epsilon^2). \quad [16]$$

Then, using [**8**] (or [**15**], respectively), we see that for the preselected and postselected particle (Fig. 1*B*), the change in the expectation value of O is modified according to

$$\tilde{\delta}\langle O\rangle = 2\epsilon\,\mathrm{Re}\left[\langle\chi|O|\chi^{\perp}\rangle\,(\mathbf{P}_A)_w\right] + \mathcal{O}(\epsilon^2). \quad [17]$$

This formula is universal—it is valid for every system which was coupled weakly in arm A to the particle passing through the interferometer.

Eq. **17** represents a result in a very general scenario. Let us now focus on the less general but very common measurement situation, which is usually considered when treating weak values (41). There, a single observable O is the pointer variable Q, the pointer wavefunction $\chi(Q)$ is real, and the interaction with the particle in the channel shifts the wave function in the pointer variable representation as

$$\chi(Q) \to \chi'(Q) = \chi(Q - \delta Q). \quad [18]$$

Obviously, this also shifts the expectation value

$$\delta\langle Q\rangle = \delta Q. \quad [19]$$

In this scenario, $\chi^{\perp}(Q)$ is also real, as well as $\langle\chi|Q|\chi^{\perp}\rangle$. Then, a positive weak value $(\mathbf{P}_A)_w$ just tells us how the effect of the interaction is amplified or reduced according to

$$\tilde{\delta}\langle Q\rangle \approx \delta Q\,\mathrm{Re}[(\mathbf{P}_A)_w]. \quad [20]$$

If $(\mathbf{P}_A)_w$ is negative, it tells us that the pointer will be shifted in the opposite direction.

If the weak value is imaginary, the expectation value of the pointer position will not be changed. However, an orthogonal component in the quantum state of the pointer will still appear. It will manifest itself in the shift of the expectation value of the momentum P_Q conjugate to Q

$$\tilde{\delta}\langle P_Q\rangle \approx 2\delta Q\,(\Delta P_Q)^2\,\mathrm{Im}[(\mathbf{P}_A)_w], \quad [21]$$

where $(\Delta P_Q)^2 = \langle\chi|P_Q^2|\chi\rangle - \langle\chi|P_Q|\chi\rangle^2$ and $\hbar = 1$.

Eqs. **20** and **21** were obtained from [**16**] and [**17**] on the assumption of weak coupling when higher orders of ϵ can be neglected. In the measurement situation [**18**] with a Gaussian pointer, $\chi = e^{-Q^2/4(\Delta Q)^2}$ (we omit normalization), the usual range of validity of the weak value formalism is extended. Even when the coupling is strong and the pointer distribution is significantly distorted during the measurement, the expressions for the shifts of the expectation values of Q, [**16**] and [**17**], remain exact, with

$$\delta\langle Q\rangle = 2\epsilon\mathrm{Re}\left[\langle\chi|Q|\chi^{\perp}\rangle\right], \quad [22a]$$

$$\tilde{\delta}\langle Q\rangle = 2\epsilon\mathrm{Re}\left[\langle\chi|Q|\chi^{\perp}\rangle\,(\mathbf{P}_A)_w\right]. \quad [22b]$$

Indeed, for the Gaussian pointer $\langle\chi|Q|\chi\rangle = 0$, $\langle\chi'|Q|\chi'\rangle = \delta Q$, and also the following expressions are easily calculated as

$$\eta = \langle\chi|\chi'\rangle = e^{-(\delta Q)^2/8(\Delta Q)^2}, \quad \langle\chi|Q|\chi'\rangle = \langle\chi|\chi'\rangle\frac{\delta Q}{2}. \quad [23]$$

Then, [**22a**] is proven by substituting [**19**] and [**1**], while including [**6**] and [**12**] proves [**22b**].

If the pointer is a Gaussian in the position variable Q, it is of course also a Gaussian in the conjugate momentum P_Q representation. Therefore, [**20**] and [**21**], in analogy to the above, become exact formulas with $\Delta P_Q = \frac{1}{2\Delta Q}$. There are corresponding exact formulas for the effect of a shift in momentum δP_Q with

Downloaded from https://www.pnas.org by MPDL Quantenoptik on March 30, 2022 from IP address 130.183.91.43.

$$\tilde{\delta}\langle P_Q\rangle = \delta P_Q \mathrm{Re}[(\mathbf{P}_A)_w], \quad [24a]$$

$$\tilde{\delta}\langle Q\rangle = -2\delta P_Q (\Delta Q)^2 \,\mathrm{Im}[(\mathbf{P}_A)_w], \quad [24b]$$

see also ref. 44.

Direct substitution shows that the expressions remain correct for Gaussians in the regime of strong interactions also in the case of combinations of shifts in Q and P_Q, such that

$$\tilde{\delta}\langle Q\rangle = \delta Q \mathrm{Re}[(\mathbf{P}_A)_w] - 2\delta P_Q (\Delta Q)^2 \,\mathrm{Im}[(\mathbf{P}_A)_w], \quad [25a]$$

$$\tilde{\delta}\langle P_Q\rangle = \delta P_Q \mathrm{Re}[(\mathbf{P}_A)_w] + \frac{\delta Q}{2(\Delta Q)^2}\,\mathrm{Im}[(\mathbf{P}_A)_w]. \quad [25b]$$

These equations are the basis of the alignment method presented in Alignment Method.

Observing the Universality Property

We use an optical MZI to experimentally visualize our central claim—namely, that all kinds of small effects of spatially preselected and postselected systems taking place at a specific location are modified in a universal manner characterized by the weak value of spatial projection. In the experiment, we demonstrate the universal change for three different couplings. In every case, the effect is modified in the same manner.

There are proposals and actual experiments where the photon couples to other particles in one arm of the interferometer (45–49). In ref. 49, one arm of the interferometer is a Kerr medium, and the photon passing through this arm changes the quantum state of the pointer by introducing a shift in the relative phase between the wave packets of the pointer photons. As it is done in most weak-measurement experiments, instead of coupling to external particles, we, rather, study interactions of the photons in an arm of the interferometer by observing the effect on other degrees of freedom of the photons itself. We also used a (weak) laser beam, so all of the results can be explained by using Maxwell equations (although in a much more difficult way), but the observations would not change by using single photons, since intensity measurements are in one-to-one correspondence to single-photon probability distributions.

The interactions in arm A are realized by introducing controlled changes of spatial and polarization degrees of freedom. The initial state of the position degree of freedom can be well approximated by a Gaussian along the x as well as the y coordinates. The interaction is implemented by shifting the center of the Gaussian intensity distribution of the light beam going through arm A by δx, compared with the beam going through arm B,

$$\chi_x(x) = e^{-x^2/w_0^2} \to \chi'_x(x) = e^{-(x-\delta x)^2/w_0^2}, \quad [26]$$

where w_0 denotes the waist of the beam and normalization factors are omitted.

Another degree of freedom is the spatial state in the y direction of the light beam, which we modified by changing the angle of the beam around the x axis, which for small angles corresponds to the momentum shift $\delta p_y = \frac{2\pi}{\lambda}\delta\theta_x$. The resulting modification in arm A can be expressed by

$$\chi_y(p_y) = e^{-w_0^2 p_y^2/4} \to \chi'_y(p_y) = e^{-w_0^2 (p_y-\delta p_y)^2/4}. \quad [27]$$

As a third external system, we use the photon polarization. The interaction parameter here is the rotation of polarization by the angle $\delta\Theta$,

$$|\chi_\sigma\rangle = |H\rangle \to |\chi'_\sigma\rangle = \cos\frac{\delta\Theta}{2}|H\rangle + \sin\frac{\delta\Theta}{2}|V\rangle, \quad [28]$$

where the states $|H\rangle$ and $|V\rangle$ are defined via $\sigma_z|H\rangle = |H\rangle$ and $\sigma_z|V\rangle = -|V\rangle$ for the Pauli matrix σ_z.

All other properties of the photon are expressed in the state $|\chi_O\rangle$. Any imperfections of the interferometer can be understood to lead to a change of the initial state of these properties in arm A, $|\chi_O\rangle \to |\chi'_O\rangle$.

It is a good approximation to assume that there are no interactions between the external degrees of freedom we consider, and thus we can express the quantum state of the photon in arm B just before reaching the final beam splitter of the interferometer as

$$|B\rangle|\chi\rangle = |B\rangle|\chi_x\rangle|\chi_y\rangle|\chi_\sigma\rangle|\chi_O\rangle, \quad [29]$$

while in arm A it is

$$|A\rangle|\chi'\rangle = |A\rangle|\chi'_x\rangle|\chi'_y\rangle|\chi'_\sigma\rangle|\chi'_O\rangle. \quad [30]$$

To test the universality of modifications of effects for various degrees of freedom, one could either perform complete tomographies of the final pointer states [**14**] and [**15**] or, more clearly, show the modification of the effects of the three couplings according to [**20**] and [**21**]. We follow the second approach. More explicitly, we test the differences between effects of the interactions on the expectation values in three degrees of freedom when the particle passes through the single arm (expressed by δ) and when the particle passes through both arms (expressed by $\tilde{\delta}$).[‡] Because of the linear relation between θ_y and p_x, as well as θ_x and p_y, one obtains

$$\tilde{\delta}\langle x\rangle = \delta\langle x\rangle \mathrm{Re}[(\mathbf{P}_A)_w], \quad [31]$$

$$\tilde{\delta}\langle \theta_y\rangle = \frac{\delta\langle x\rangle}{z_R}\mathrm{Im}[(\mathbf{P}_A)_w], \quad [32]$$

$$\tilde{\delta}\langle \theta_x\rangle = \delta\langle \theta_x\rangle \mathrm{Re}[(\mathbf{P}_A)_w], \quad [33]$$

$$\tilde{\delta}\langle y\rangle = -z_R\delta\langle \theta_x\rangle \mathrm{Im}[(\mathbf{P}_A)_w]. \quad [34]$$

Here, we have used the Rayleigh range $z_R \equiv \frac{\pi w_0^2}{\lambda}$ as the characteristic parameter of the Gaussian beam.

The conjugate variable to the angle Θ defining polarization changes in the $\sigma_x - \sigma_z$ plane is an angle Υ describing polarization rotations in the $\sigma_y - \sigma_z$ plane relative to the initial state $|H\rangle$. For small deviations, these angles relate linearly to $\langle\sigma_x\rangle$ and $\langle\sigma_y\rangle$, respectively, and are given by

$$\tilde{\delta}\langle\Theta\rangle = \delta\langle\Theta\rangle \mathrm{Re}[(\mathbf{P}_A)_w], \quad [35]$$

$$\tilde{\delta}\langle\Upsilon\rangle = -\delta\langle\Theta\rangle \mathrm{Im}[(\mathbf{P}_A)_w]. \quad [36]$$

The test was performed for the full range of φ and thus for a large range of values $(\mathbf{P}_A)_w$; see violet lines on the graphs of Fig. 2. The parameters for the calculation of $(\mathbf{P}_A)_w$ necessary for testing relations [**31**–**36**] were also obtained from measurements. The signals from separate arms (when the other arm was blocked) provided $\tan\alpha$. The phase φ and the overlap η were obtained from the intensity of the interference signal and visibility measurements, respectively. The relation between the visibility $\mathcal{V}$ and the overlap η for the phase-dependent output intensity $\mathcal{I} \propto \langle\phi|\rho|\phi\rangle \propto 1 + \tan^2\alpha + 2\tan\alpha\,\eta\cos\varphi$ is given by

$$\mathcal{V} \equiv \frac{\mathcal{I}_{\max} - \mathcal{I}_{\min}}{\mathcal{I}_{\max} + \mathcal{I}_{\min}} = \eta\frac{2\tan\alpha}{1+\tan^2\alpha}. \quad [37]$$

The experiment is shown schematically in Fig. 3. After propagation through a single-mode fiber for spatial filtering, the horizontally polarized light from a laser diode ($\lambda = 780\,\mathrm{nm}$) is split by

[‡]We chose this method since our measurements of the shifts $\delta\langle x\rangle$, $\delta\langle\theta_x\rangle$, and $\delta\langle\Theta\rangle$ in a single channel are more precise than our control of the shifts δx, $\delta\theta_x$, and $\delta\Theta$ via manual stages.

Downloaded from https://www.pnas.org by MPDL Quantenoptik on March 30, 2022 from IP address 130.183.91.43.

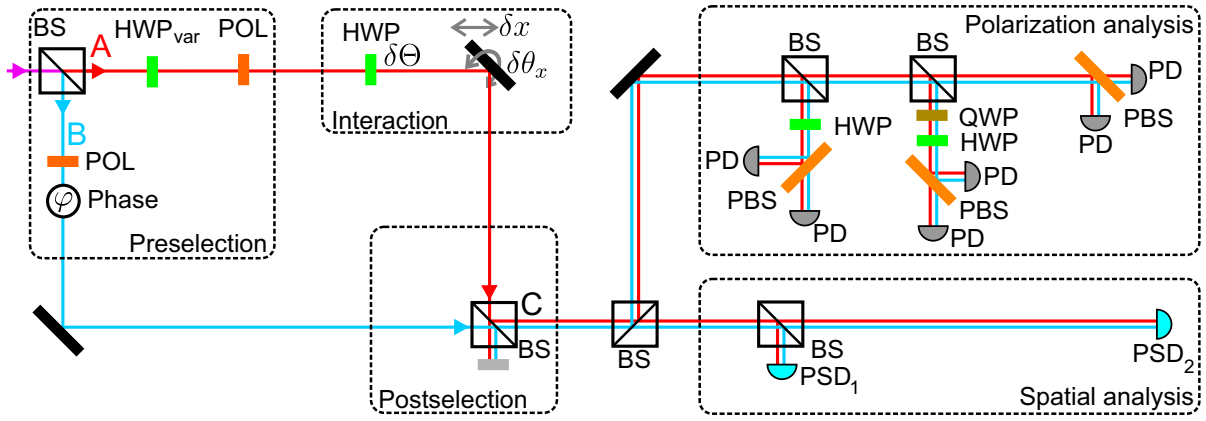

Fig. 3. Schematic experimental setup. The preselection state $|\psi\rangle$ is set by using a nonpolarizing beam splitter (BS), creating a spatial superposition between arms *A* and *B*. Two equally oriented polarizers (POL) and a half-wave plate (HWP$_{var}$) are used to define the relative amplitudes. Angle and position shifts—e.g., $\delta\theta_x$ and δx—are introduced by moving and tilting of optical components, whereas polarization rotations are imposed using a half-wave plate (HWP). The postselection is done by considering only one of the output ports (*C*) of the interferometer. Analysis of the polarization degree of freedom is achieved by means of half- and quarter-wave plates (QWP), polarizing beam splitters (PBS), and photodiodes (PD), allowing the projection onto the polarization states $1/\sqrt{2}(|H\rangle \pm |V\rangle)$, $1/\sqrt{2}(|H\rangle \pm i|V\rangle)$, $|H\rangle$, and $|V\rangle$. Position-sensing detectors (PSD) at different *z*-positions allow us to determine position and angle, respectively, in *x* and in *y* direction.

a nonpolarizing beam splitter. The moduli of the amplitudes of the preselection state [**2**] are controlled by means of rotating the polarization using a half-wave plate in arm A, followed by a horizontal polarization filter. The relative phase between the arms φ is set by an optical trombone system with retroreflecting prisms moved by a piezoelectric crystal (not shown).

This setup enables us to directly implement the three desired interactions along beam A and simultaneously measure their effect. Fig. 3 depicts the setup. The spatial displacement δx, which is schematically depicted as a shift of the mirror, was achieved by lateral movement of the prism from the trombone system. Instead of a vertical tilt of this mirror, we incorporate the vertical rotation $\delta\theta_x$ by tilting the second beam splitter. The polarization rotation $\delta\Theta$ is controlled by rotating a half-wave plate in arm A. Detecting light only from the output port C provides the post-selection onto state $|\phi\rangle$, Eq. **4**.

The photons at port C are distributed onto several detectors using beam splitters for position and polarization analysis. A position-sensing detector PSD_1 placed near the interferometer and a detector PSD_2 placed farther away allows the estimation of position and angle in x and y directions. We perform tomography of the polarization state using half- and quarter-wave plates in combination with polarizing beam splitters, as shown in Fig. 3.

A measurement run consists of three steps—namely, first a measurement of light propagating in arm A alone, second of arm B alone, and last a measurement of the interference signal. The six expectation values obtained from measurements of arm B are used as a reference for the subsequent analysis.

The measurement with only beam A shows the effect of the interactions when the photons pass through a single channel, as in Fig. 1*A*. The results are indicated in the graphs of Fig. 4 as red dashed horizontal lines since they exhibit no dependence on the phase.[§]

The universality is clearly shown by the similarity of the results for the three couplings (Fig. 4). Of course, in all graphs, the observed values are different and have different units. For demonstration purposes, we arranged the scales of the graphs in Fig. 4, *Upper* such that the signals of all interactions, $\langle x\rangle_A$, $\langle\theta_y\rangle_A$, and $\langle\Theta\rangle_A$, have the same size. We were trying to avoid shifts in conjugate variables as much as possible. Our measurement results, red dashed lines in the plots from the Fig. 4, *Lower*, show that the tuning was good, although not perfect.

Continuous violet lines on these graphs provide theoretical predictions based on the weak value $(\mathbf{P}_A)_w$ given by [**12**], and the interactions in the single arms are presented as red and blue dashed lines in the graphs. The intensities obtained by measuring arm A and arm B alone yield $\tan\alpha = 1.3323 \pm 0.0002$. From the visibility measurement, $\mathcal{V} = 95.09 \pm 0.02\%$, we obtained $\eta = 0.9904 \pm 0.0003$. For these parameters, we observed amplifications with factors up to 4 and -3. The very good agreement between experimental data and theoretical predictions, shown in Fig. 4, demonstrates the universality of the modification of several fundamentally distinct forms of interactions for couplings with a preselected and postselected system.

To evaluate the dependence of the weak value on the coherence between the two arms parametrized by η, we measured the effect of the displacement in x on the output beam. For this run, we kept the phase fixed at $\varphi = \pi$ and varied the amplitude ratio $\tan\alpha$ covering another region of the parameter space from Fig. 2. We changed the coherence by varying the polarization misalignment, leading to a smaller overlap between the photon states passing through the two arms. The modification of the shift in the x direction presented in Fig. 5 follows nicely the weak value [**12**].

Alignment Method

In the previous sections, we considered a scenario in which the path state of a photon in an arm of an interferometer is coupled to its other degrees of freedom, in particular, its spatial degrees of freedom in the x and y direction. This scenario exactly represents a situation encountered in real experimental interferometric setups—namely, when the arms of the interferometer are misaligned. The differences in position $\delta\vec{r} \equiv (\delta x, \delta y)$ and angle $\delta\vec{\theta} \equiv (\delta\theta_x, \delta\theta_y)$ between the photons passing through distinct arms of the interferometer can be considered as results of interactions in one arm, which change the initially identical spatial states of the particle.

[§]Please contact J.D. if you desire access to the raw experimental data for this plot as well as for all other plots.

Downloaded from https://www.pnas.org by MPDL Quantenoptik on March 30, 2022 from IP address 130.183.91.43.

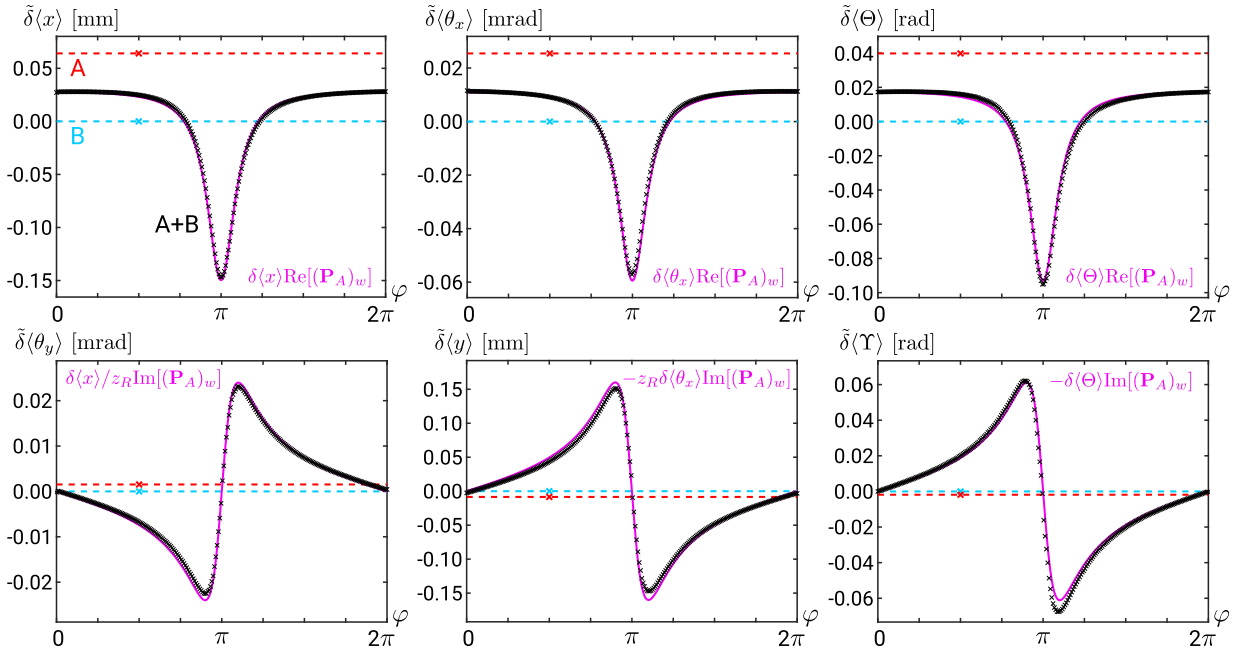

Fig. 4. Observed universality. (*Upper*) The introduced displacements of arm *A* in *x* direction, angle around the *x* axis, and angle of polarization Θ (δx, $\delta\theta_x$, and $\delta\Theta$) can be seen from the single red datapoints plotted at an arbitrary phase position. The blue datapoints corresponding to arm *B* are taken as a reference and thus show zero shift. The axes are scaled such that the readings of *A* agree for the three external systems. For each of these three, the same behavior of the interference signal (black datapoints) is observed for the shifts of the variables $\tilde{\delta}\langle x\rangle$, $\tilde{\delta}\langle\theta_x\rangle$, and $\tilde{\delta}\langle\Theta\rangle$: The effect seen from the measurement of the single arm is multiplied with the phase-dependent real part of the weak value. (*Lower*) The analogous plots for the shift of the respective conjugate variables represented by $\tilde{\delta}\langle\theta_y\rangle$, $\tilde{\delta}\langle y\rangle$, and $\tilde{\delta}\langle\Upsilon\rangle$ show nicely the dependence on the imaginary part of the weak value. The violet theoretical curves represent the rescaled real and imaginary parts of the weak value (no fit).

It is well known that the picture generated by the interference of the beams from a misaligned interferometer displays a strong phase dependence. Fig. 6*A* shows the centroid trajectory during the phase scan of a misaligned interferometer. We demonstrate that it is possible to quantitatively determine the exact misalignment parameters of the interferometer by analyzing this

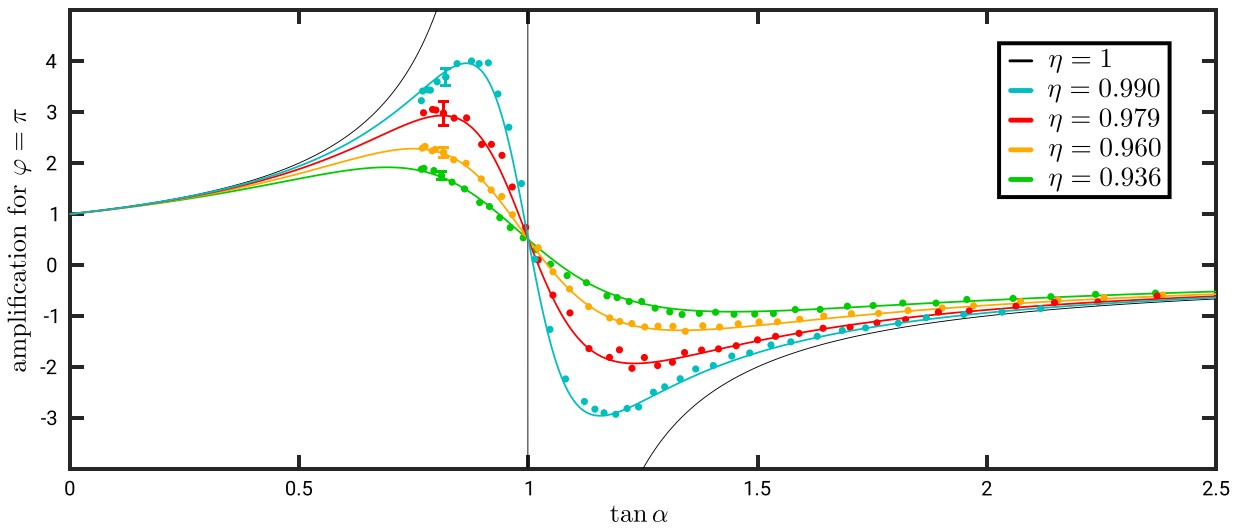

Fig. 5. Modification of weak value due to decoherence. The colored dots represent the measured values for the modification of the shift δx in the interference signal when varying the weak value via the relative amplitudes of the paths *A* and *B* ($\tan\alpha$ in Eq. **12**) and fixed $\varphi = \pi$. The four datasets correspond to four different values of the overlap η, which quantifies the coherence between the states of the external systems from the two arms. The lines are theoretical curves as highlighted by the colored lines in Fig. 2 *C* and *E*. Respective average error bars are shown for each η on one of the first data points. For comparison, also the theoretical line with $\eta = 1$ (Fig. 2*A*) is shown.

Downloaded from https://www.pnas.org by MPDL Quantenoptik on March 30, 2022 from IP address 130.183.91.43.

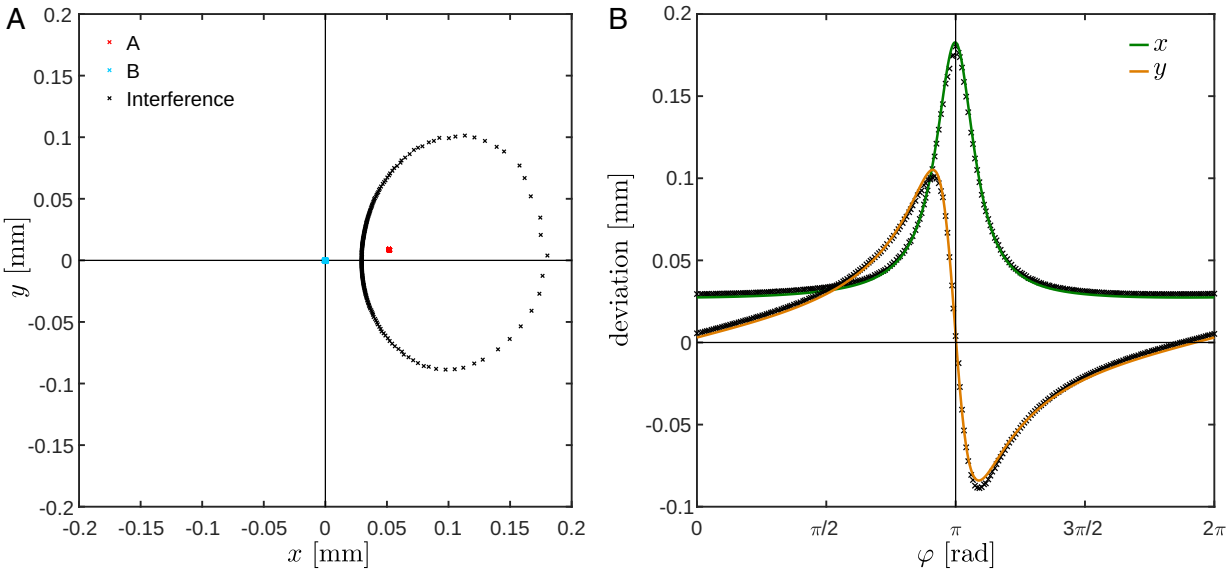

Fig. 6. (*A*) Trajectories of beam centroids in output *C* for misaligned MZI. The blue and red spots correspond to the measurements of the beams from the single arms when the other arm is blocked. While the blue spot at the origin corresponds to beam *B* without interaction, the red spot corresponds to the misaligned beam *A*. The elliptic trajectory of the interference pattern is represented by the black points. (*B*) Fits onto *x* and *y* projections of trajectory. By fitting the vector function [**38**] to the *x* and *y* projections of the interference ellipse, we determine the parameters of the misalignment.

phase-dependent movement. In fact, the misalignment parameters $\delta\vec{r}$ and $\delta\vec{\theta}$ could be calculated from measurements described in the previous section. Disregarding the polarization analysis, it was a measurement of the misalignment parameters based on position measurements of centroids of the beams on two detectors at different locations. But the method is more powerful and can be implemented with only a single position-sensitive detector as well.

The basis for our alignment method are Eqs. **25A** and **25B** which, somewhat surprisingly, remain precise, even for large misalignment. The shift observed on the single detector $\tilde{\delta}\vec{R}$ is the sum of the position shift $\tilde{\delta}\vec{r}$ and the position shift due to the shift in direction $\delta\vec{\theta}\times\vec{L}$, where $\vec{L}=(0,0,z)$ is the vector parallel to the beam with the length equal to the distance z along the beam between the waist and the detector. Thus, the position shift of the centroid on the detector $\tilde{\delta}\vec{R}$ is given by

$$\tilde{\delta}\vec{R}=(\delta x+z\delta\theta_y,\ \delta y-z\delta\theta_x)\mathrm{Re}[(\mathbf{P}_A)_w]+\left(\frac{z}{z_R}\delta x-z_R\delta\theta_y,\ \frac{z}{z_R}\delta y+z_R\delta\theta_x\right)\mathrm{Im}[(\mathbf{P}_A)_w]. \qquad [38]$$

The weak value is given by [**12**]. The parameters $\tan\alpha$, η, z, and z_R are found experimentally as in the previous section. The function [**38**] corresponds to the trajectory of the beam centroid on the detector, as shown in Fig. 6*A*. Even small misalignments, which otherwise might be difficult to resolve, become detectable due to the effect of weak amplification.

Fig. 6*B* shows the x and y components of $\tilde{\delta}\vec{R}$ as functions of φ. A least-squares fit of this function provides the four unknown misalignment parameters $\delta\vec{r}$ and $\delta\vec{\theta}$. It is remarkable that a fit function with so few parameters accurately models the experimental results. For the data shown, the fit provided $\delta\vec{r}=(49\pm 2,7\pm 2)\ \mu\mathrm{m}$ and $\delta\vec{\theta}=(12.7\pm 0.4,0.2\pm 0.4)\ \mu\mathrm{rad}$.

We have performed corrections according to these parameters and repeated our procedure (Fig. 7). The stability of the centroid shows excellent alignment, and a subsequent fit procedure provides the parameters $\delta\vec{r}=(-1\pm 2,2\pm 2)\ \mu\mathrm{m}$ and $\delta\vec{\theta}=(0.2\pm 0.4,-0.6\pm 0.4)\ \mu\mathrm{rad}$.

In our method to obtain the misalignment parameters, we rely on the knowledge of the beam parameters—i.e., Rayleigh range z_R and longitudinal position of the detector relative to the waist z. In some situations, the reversed task might be of interest. If

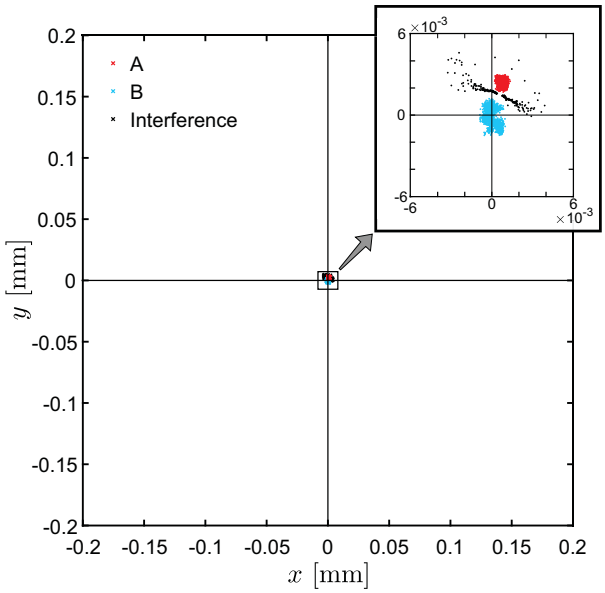

Fig. 7. Trajectories of beam centroids after one alignment step. It can be clearly seen how the size of the ellipse and the distance between the centroids of the single beams *A* (red) and *B* (blue) are significantly reduced in comparison with Fig. 6*A*.

Downloaded from https://www.pnas.org by MPDL Quantenoptik on March 30, 2022 from IP address 130.183.91.43.

we control the misalignment parameters, we can also use our algorithm with the fit to obtain the beam parameters.

In fact, the general idea of alignment using weak values was already used in alignment of the interferometer demonstrating the past of a particle in nested interferometers (50), and, since then, it was significantly developed and improved (51, 52) until it reached the efficiency presented in the present work when a single scan led to a very good alignment.

Trace and Presence

A generic property of weak measurements is the possibility to perform several weak measurements on the same system. Thus, we can interpret our experiment as multiple weak measurements of the projection operator which all yield the same result, the weak value of the projection on the arm of the interferometer. However, it also implies a broader meaning with respect to the discussion of the local presence of quantum particles.

A classical particle can either be in a particular location or not. The presence of a quantum particle in a certain location, however, is a subtle issue, and its analysis strongly depends on the adopted interpretation of quantum mechanics. To avoid controversial interpretational issues, we do not discuss ontological aspects of the concept of the presence of a particle and instead argue within the operational approach.

When the wavefunction of a quantum particle is well localized in a particular location, the trace is specified in a unique way by the local interaction in that location in analogy to the trace of a classical particle when it is present (Eq. **1**). Given that there are only local interactions in nature, there is no trace when the wavefunction vanishes. Similarly, there is no trace in a classical channel when the particle is absent.

Scenarios when the wavefunction does not vanish, but is also not fully localized at this location, are no longer understandable from a classical perspective. The universal relation between the trace in these scenarios and the trace of a fully localized particle which we found in our work can be considered as a basis of an operational concept of presence of a particle. It goes beyond defining the particle as present when it leaves a trace and not present when it does not (53).

According to our operational approach, the "presence" of a preselected and postselected particle in the arm A of an interferometer is defined according to the way it affected the external systems to which it was coupled and is quantified by the complex number $(\mathbf{P}_A)_w$. This definition yields presence 1 when the forward-evolving wavefunction of the particle is solely inside the arm A independently of postselection, but presence 1 can happen also when neither the preselected nor the postselected states are eigenstates of the local projection on arm A. The presence 0 or "absence" of the particle is ensured when the forward-evolving wavefunction of the particle vanishes in arm A, but it is not a necessary condition. The postselected particle might have been absent in arm A (no effect on local external systems can be observed), even when the forward-evolving wavefunction did not vanish there.

Our concept provides a quantification and characterization of presence by describing the modification of effects of the particle's interactions with external systems. It can be increased, decreased, or changed in a particular, well-defined way, and this change is the same for all local interactions—it is universal.

Conclusions

We have analyzed theoretically and experimentally the modifications of the effect of weak interactions on preselected and postselected particles. We have shown that there is a universal description of the modification of these couplings for all weak interactions given by a single complex number, the weak value of the projection on the corresponding location.

Our approach is based on expressing the effect on external systems in terms of the orthogonal components which appear due to the interactions. This allows us to formalize the meaning of the weak value without reference to a specific form of coupling. The weak value not only modifies a shift of expectation values as usual, but also the relative amplitudes of the orthogonal components of all external quantum systems interacting with the particle.

The experiment shows for three different couplings that each of the effects is modified in exactly the same way. This is shown for not just a few cases of preselected and postselected particles, but for a continuum of parameters with a large range of weak values of projection.

The approach derives the general expression [**12**] which allows us to apply the concept of weak values for several couplings which are not necessarily weak. These findings enable one to understand seemingly complicated dependencies seen in experiments—for example, ref. 37—and can facilitate multiparameter precision measurements in the future.

We define an operational paradigm for the presence of a preselected and postselected particle according to the trace it leaves. It is more intricate than the dichotomic concept of the presence of a classical particle, which can only be present or not. This complexity is surprising in light of the fact that in all scenarios, the external systems are in a superposition or a mixture of the undisturbed state with a single particular orthogonal component.

Our demonstration of the universality of the modification of the interactions led us to an alignment method. Its effectiveness relies on the unexpected robustness of the modification of Gaussian pointers, where the weak value expressions remain precise, even for strong couplings. In our method, a single phase scan suffices to recover all misalignment parameters from the analysis of the position of the centroid of a single output beam, clearly reducing the effort in an often-tedious task, while at the same time potentially harnessing the benefits of weak value amplification.

ACKNOWLEDGMENTS. This work has been supported in part by Israel Science Foundation Grant 1311/14; German–Israeli Foundation for Scientific Research and Development Grant I-1275-303.14; DFG Beethoven 2 Project WE2541/7-1; and the German Excellence Initiative Nanosystems Initiative Munich. J.D. was supported by the international Max-Planck-Research School for Quantum Science and Technology. L.K. was supported by the international Ph.D. program ExQM from the Elite Network of Bavaria. J.M. was supported by a Ludwig-Maximilians-Universität research fellowship.

1. Knill E, Laflamme R, Milburn GJ (2001) A scheme for efficient quantum computation with linear optics. *Nature* 409:46–52.
2. Żukowski M, Zeilinger A, Horne MA, Ekert AK (1993) "Event-ready-detectors" Bell experiment via entanglement swapping. *Phys Rev Lett* 71:4287–4290.
3. Zeilinger A, Horne MA, Weinfurter H, Żukowski M (1997) Three-particle entanglements from two entangled pairs. *Phys Rev Lett* 78:3031–3034.
4. Aharonov Y, Vaidman L (2008) The two-state vector formalism: An updated review. *Time in Quantum Mechanics,* Lecture Notes in Physics Vol 734, eds Muga JG, Sala Mayato R, Egusquiza ÍL (Springer, Berlin), 2nd Ed, Vol 1, pp 399–447.
5. Vaidman L, et al. (2017) Weak value beyond conditional expectation value of the pointer readings. *Phys Rev A* 96:032114.
6. Aharonov Y, Albert DZ, Vaidman L (1988) How the result of a measurement of a component of the spin of a spin-1/2 particle can turn out to be 100. *Phys Rev Lett* 60:1351–1354.
7. Hosten O, Kwiat P (2008) Observation of the spin hall effect of light via weak measurements. *Science* 319:787–790.
8. Dixon PB, Starling DJ, Jordan AN, Howell JC (2009) Ultrasensitive beam deflection measurement via interferometric weak value amplification. *Phys Rev Lett* 102:173601.
9. Zilberberg O, Romito A, Gefen Y (2011) Charge sensing amplification via weak values measurement. *Phys Rev Lett* 106:080405.
10. Wu S, Żukowski M (2012) Feasible optical weak measurements of complementary observables via a single Hamiltonian. *Phys Rev Lett* 108:080403.
11. Hofmann HF (2012) How weak values emerge in joint measurements on cloned quantum systems. *Phys Rev Lett* 109:020408.

Downloaded from https://www.pnas.org by MPDL Quantenoptik on March 30, 2022 from IP address 130.183.91.43.

12. Xu X-Y, et al. (2013) Phase estimation with weak measurement using a white light source. *Phys Rev Lett* 111:033604.
13. Dressel J, Malik M, Miatto FM, Jordan AN, Boyd RW (2014) *Colloquium*: Understanding quantum weak values: Basics and applications. *Rev Mod Phys* 86:307–316.
14. Jordan AN, Martínez-Rincón J, Howell JC (2014) Technical advantages for weak-value amplification: When less is more. *Phys Rev X* 4:011031.
15. Ferrie C, Combes J (2014) Weak value amplification is suboptimal for estimation and detection. *Phys Rev Lett* 112:040406.
16. Knee GC, Gauger EM (2014) When amplification with weak values fails to suppress technical noise. *Phys Rev X* 4:011032.
17. Magaña Loaiza OS, Mirhosseini M, Rodenburg B, Boyd RW (2014) Amplification of angular rotations using weak measurements. *Phys Rev Lett* 112:200401.
18. Pusey MF (2014) Anomalous weak values are proofs of contextuality. *Phys Rev Lett* 113:200401.
19. Zhang L, Datta A, Walmsley IA (2015) Precision metrology using weak measurements. *Phys Rev Lett* 114:210801.
20. Piacentini F, et al. (2018) Investigating the effects of the interaction intensity in a weak measurement. *Sci Rep* 8:6959.
21. Martínez-Rincón J, Chen Z, Howell JC (2017) Practical advantages of almost-balanced-weak-value metrological techniques. *Phys Rev A* 95:063804.
22. Li F, Huang J, Zeng G (2017) Adaptive weak-value amplification with adjustable postselection. *Phys Rev A* 96:032112.
23. Araújo MP, De Leo S, Maia GG (2017) Optimizing weak measurements to detect angular deviations. *Annalen der Physik* 529:1600357.
24. Qiu X, et al. (2017) Precision phase estimation based on weak-value amplification. *Appl Phys Lett* 110:071105.
25. Liu X, et al. (2017) Optimal pre- and post-selections of weak measurements for precision parameter estimation. *J Appl Phys* 121:203106.
26. Chen G, et al. (2018) Heisenberg-scaling measurement of the single-photon Kerr nonlinearity using mixed states. *Nat Commun* 9:93.
27. Kim Y, et al. (2018) Direct quantum process tomography via measuring sequential weak values of incompatible observables. *Nat Commun* 9:192.
28. Zhou X, Sheng L, Ling X (2018) Photonic spin hall effect enabled refractive index sensor using weak measurements. *Sci Rep* 8:1221.
29. Li L, et al. (2018) Phase amplification in optical interferometry with weak measurement. *Phys Rev A* 97:033851.
30. Qin L, Wang Z, Zhang C, Li X-Q (2018) Direct measurement of the quantum state of photons in a cavity. *Opt Express* 26:7034–7042.
31. Ren C, Qiu J, Chen J, Shi H (2018) Ultra-precise time tuning and central frequency shift of optical pulses via small weak values. *Opt Commun* 425:19–23.
32. Huang J-Z, Fang C, Zeng G (2018) Weak-value-amplification metrology without spectral analysis. *Phys Rev A* 97:063853.
33. Fang C, Huang J-Z, Zeng G (2018) Robust interferometry against imperfections based on weak value amplification. *Phys Rev A* 97:063818.
34. Li H, et al. (2018) High-precision temperature measurement based on weak measurement using nematic liquid crystals. *Appl Phys Lett* 112:231901.
35. Wu S, Li Y (2011) Weak measurements beyond the Aharonov-Albert-Vaidman formalism. *Phys Rev A* 83:052106.
36. Di Lorenzo A (2012) Full counting statistics of weak-value measurement. *Phys Rev A* 85:032106.
37. Kofman AG, Ashhab S, Nori F (2012) Nonperturbative theory of weak pre- and post-selected measurements. *Phys Rep* 520:43–133.
38. Zhang Y-X, Wu S, Chen Z-B (2016) Coupling-deformed pointer observables and weak values. *Phys Rev A* 93:032128.
39. Denkmayr T, et al. (2017) Experimental demonstration of direct path state characterization by strongly measuring weak values in a matter-wave interferometer. *Phys Rev Lett* 118:010402.
40. Vaidman L (2017) Comment on "Experimental demonstration of direct path state characterization by strongly measuring weak values in a matter-wave interferometer". arXiv:1703.01616.
41. Aharonov Y, Vaidman L (1990) Properties of a quantum system during the time interval between two measurements. *Phys Rev A* 41:11–20.
42. Wiseman HM (2002) Weak values, quantum trajectories, and the cavity-QED experiment on wave-particle correlation. *Phys Rev A* 65:032111.
43. Silva R, et al. (2014) Pre- and postselected quantum states: Density matrices, tomography, and Kraus operators. *Phys Rev A* 89:012121.
44. Dressel J, Jordan AN (2012) Weak values are universal in Von Neumann measurements. *Phys Rev Lett* 109:230402.
45. Simon C, Polzik ES (2011) Fock-state view of weak-value measurements and implementation with photons and atomic ensembles. *Phys Rev A* 83:040101.
46. Feizpour A, Xing X, Steinberg AM (2011) Amplifying single-photon nonlinearity using weak measurements. *Phys Rev Lett* 107:133603.
47. Fu L, Hashmi FA, Jun-Xiang Z, Shi-Yao Z (2015) An ideal experiment to determine the "past of a particle" in the nested Mach-Zehnder interferometer. *Chin Phys Lett* 32:050303.
48. Ben-Israel A, et al. (2017) An improved experiment to determine the 'past of a particle' in the nested Mach-Zehnder interferometer. *Chin Phys Lett* 34: 020301.
49. Hallaji M, Feizpour A, Dmochowski G, Sinclair J, Steinberg AM (2017) Weak-value amplification of the nonlinear effect of a single photon. *Nat Phys* 13:540–544.
50. Danan A, Farfurnik D, Bar-Ad S, Vaidman L (2013) Asking photons where they have been. *Phys Rev Lett* 111:240402.
51. Farfurnik D (2013) Weak value analysis of an optical Mach-Zehnder interferometer. Master's thesis (School of Physics and Astronomy, Tel Aviv University, Tel Aviv).
52. Benshalom N (2017) Quantum weak values in classical interferometry. Master's thesis (School of Physics and Astronomy, Tel Aviv University, Tel Aviv).
53. Vaidman L (2013) Past of a quantum particle. *Phys Rev A* 87:052104.

Downloaded from https://www.pnas.org by MPDL Quantenoptik on March 30, 2022 from IP address 130.183.91.43.

Chapter 7

Nonlocal Effects in Bohmian Mechanics

This final chapter treats the second special topic of this work, namely Bohmian mechanics. In particular the focus lies on the manner in which action-at-a-distance allows this theory to provide a realist description of the physical world, which reproduces all empirical predictions of quantum mechanics. The first three sections mirror the first three chapters of this work and, after introducing the basic formalism of the Bohmian theory, describe the measurement process as well as the behavior of space-like separated systems from the Bohmian perspective. Subsequently, based on the concept of the PWF as introduced in Chapter 4 it is analyzed how the formalism of Bohmian mechanics can be extended to photons, which enables a Bohmian description of a double-slit experiment, where one photon represents the pointer for the which-path measurement of the other. Finally the corresponding photonic experiment, which was begun in the course of this work, is presented, along with a discussion of its possible interpretation.

7.1 Bohmian Mechanics

7.1.1 Basic Principles

Bohmian Mechanics (BM) or *de Broglie-Bohm theory*, as first formulated by de Broglie [8] and later rediscovered and developed further by Bohm [837, 838], represents the most famous hidden-variable extension of quantum mechanics. In its standard non-relativistic formulation [847, 819, 823, 824] it considers physical systems consisting of a number of n point-like particles, with the hidden-variables corresponding to the n definite particle positions $\widetilde{x} := \{\vec{x}_1, \vec{x}_2, \ldots, \vec{x}_n\}$, where $\vec{x}_j$ is the position of the j-th particle. All physical properties of the system depend on the trajectories of these particles relative to their joint spatial wavefunction $\Psi(\vec{x}_1, \vec{x}_2, \ldots, \vec{x}_n, t)$ defined on the so-called *configuration space* $\mathbb{K} := \mathbb{R}^{3n}$ of particle positions. As in SQM the deterministic unitary time-evolution of the wavefunction is given by the Schrödinger equation. Bohmian particles are also fun-

damentally identical and thus the multi-particle wavefunctions are always symmetric or anti-symmetric. Note, however, that this implies a non-trivial topology for the configuration space which actually consists of unordered tuples of n-positions [855, 819, 823, 824]. This structure and the symmetriziation can be neglected for notational convenience for particles which do not interfere, just as in the case of SQM. Other degrees of freedom than position are incorporated by considering vectorial wavefunctions, i.e., spinors, see, e.g., [369, 819, 823, 883, 824]. However, in this work for the most part a more convenient but fully equivalent mixed notation closer to the Dirac formalism will be employed, leading to expressions of the form $|\psi(\widetilde{x},t)\rangle := \sum_j \psi_j(\widetilde{x},t)\,|a_j\rangle$, where $\{|a_j\rangle\}$ is some basis for the Hilbert space of all non-position degrees of freedom. Note that $|\psi(\widetilde{x},t)\rangle$ is a density of states which is normalized via the condition $\int_{\mathbb{K}}\langle\psi(\widetilde{x})|\psi(\widetilde{x})\rangle \mathrm{d}\widetilde{x}/\sqrt{2\pi}^{3n} = 1$. Some authors, e.g., [847, 819, 883] use two different sets of symbols to distinguish the actual configuration of particle positions $\widetilde{x}$ from running variables such as the position arguments in the integral shown above. In this work, however, the degree of mathematical precision is reduced for the benefit of notational convenience, as is typical in treatments of BM from the perspective of physics, see, e.g., [910, 841, 308, 904, 885, 892], and the two usages of spatial coordinates are not formally distinguished. Thus, for example the equivalence

$$\frac{\partial}{\partial x}\psi(x) \equiv \frac{\partial}{\partial x'}\psi(x')\Big|_{x'=x} \tag{7.1}$$

holds, where on the RHS "x" represents the actual position of the particle and "x'" just a variable in contrast to the LHS, where both formal functions are fulfilled by the symbol "x".

Although the laws of BM are strictly deterministic, the probabilistic predictions of SQM are recovered via a strictly epistemological but irreducible uncertainty about the position of each particle, similar to the inaccessibility of the particular micro-state in classical statistical physics [838, 847, 861, 819, 823, 824]. As a consequence of the dynamical laws of the theory, as described below, the only a priori knowledge obtainable about the positions of the particles is a joint probability density $p(\widetilde{x},t)$ given by the Born rule with $p(\widetilde{x},t) = |\Psi(\widetilde{x},t)|^2$. Accordingly, the marginal probability density of the position $p_j(\vec{x}_j,t)$ of a single particle j is given by the diagonal elements of its reduced density operator $\rho_j(t) = \mathrm{tr}_{k\neq j}\big(|\Psi(t)\rangle\langle\Psi(t)|\big)$ in position representation, i.e., $p_j(\vec{x},t) = \langle\vec{x}|\rho_j(t)|\vec{x}\rangle$, where here the ket $|\Psi(t)\rangle$ denotes the full quantum state of the n-particle system *not* projected onto a particular configuration $\tilde{x}$. This particular distribution of particles is called *quantum equilibrium* and the postulate that it is factually realized is known as the *quantum equilibrium hypothesis* (QEH) [849, 847, 819, 823]. In consequence, according to BM, the preparation of a set of copies of a quantum state effectively means preparing an ensemble of particles randomly distributed according to Born rule. Due to the form of Bohmian dynamics, if a multi-particle system is in equilibrium at a certain time, this is also true for all other times [839, 847, 879, 824]. Note that Valentini [907, 906] has proposed a physical motivation of the QEH, where the equilibrium distribution emerges as a consequence of the generalization of the thermodynamical H-theorem to quantum systems, as the state corresponding to maximal entropy, even from an initial configuration which does not cor-

respond to quantum equilibrium. However, the necessity of such a motivation has been criticized with the argument that the QEH is motivated sufficiently by the fact that such a distribution is *typical* in the statistical sense, i.e., the by far most probable configuration given all possible states of the universe [849, 847, 823].

7.1.2 Guiding Wave

The conservation of the equilibrium distribution as given by the quantum mechanical continuity equation imposes restrictions on the possible trajectories of the Bohmian particles, i.e., the particles have to move along the flow lines of the probability current with a certain velocity [819]. This velocity can be obtained by writing the quantum continuity equation in form of classical continuity equation as

$$\frac{\partial}{\partial t}p(\vec{x},t) + \vec{\nabla}\big(\vec{v}(\vec{x},t)\,p(\vec{x},t)\big) = 0, \tag{7.2}$$

where the velocity is given as $\vec{v} = \vec{j}/p$, i.e., the probability current weighted by the local density. For example in the case of non-relativistic massive particles the velocity of the j-th particle is given by [819, 824]

$$\vec{v}_j(\widetilde{x},t) = \frac{\hbar}{m_j}\frac{\mathrm{Im}\big[\,\langle\Psi(\widetilde{x},t)|\,\vec{\nabla}_j\,|\Psi(\widetilde{x},t)\rangle\,\big]}{\langle\Psi(\widetilde{x},t)|\Psi(\widetilde{x},t)\rangle} \tag{7.3}$$

where m_j is its mass and $\vec{\nabla}_j$ the spatial derivative for particle j. For scalar particles the expression simplifies further to the well-known form of the Bohmian velocity

$$\vec{v}_j(\widetilde{x},t) = \frac{\hbar}{m_j}\mathrm{Im}\big[\frac{\vec{\nabla}_j\Psi(\widetilde{x},t)}{\Psi(\widetilde{x},t)}\big]. \tag{7.4}$$

The above *guiding equations* illustrate in what sense the wavefunction Ψ represents a *guiding wave* or *guiding field* for the Bohmian particles [819], also explaining the term "pilot-wave interpretation". Note that in general the velocity of each particle depends on the whole configuration of the n-particle system, i.e., also on the position of all other particles. Since those can be located at arbitrary points in space, this dependence forms the basis for the mechanism of action-at-a-distance in BM [87, 818, 879, 819]. Furthermore, the evolution under the guiding wave is manifestly non-Newtonian and neither momentum nor energy conservation is given for each of the particles separately. Finally, contrary to Newtonian mechanics, Bohmian guiding equations of the form (7.3) represent first-order differential equations, and in effect the resulting trajectories of particles guided by the same field never cross [832, 887, 890]. Note also that the configuration of particles $\widetilde{x}$ can never reach the *nodes* of the wavefunction, i.e., points with $\Psi(\widetilde{x},t) = 0$, and thus the trajectories are always well-defined.

7.1.3 Variants of Bohmian Mechanics

BM reproduces the dispositional results of SQM through the QEH. Additionally, however, it also provides a description of physical reality by establishing a connection between the formalism and the real particle positions it is taken to represent, where in the most prominent formulation, as sketched above, the positions of the point-like Bohmian particles represent the beables. However, the Bohmian approach as described so far, albeit very prominent, is only one among several formulations of Bohmian mechanics.

While the formalism based on a first-order differential equation of the form (7.3) is closest to de Broglies original suggestion [906], the most important alternative formulation is the original formulation by Bohm [837], as championed also by Nelson [882], Hiley [886, 818], and Holland [820]. It has the same ontological structure but expresses the evolution of the Bohmian particles in Newtonian terms [824]. In the simple example of a single scalar particle, by expressing the wavefunction in polar decomposition $\psi = \varrho e^{-i\varphi}$, the Schrödinger equation in coordinate representation can be rewritten in terms of two differential equations corresponding to its real and imaginary parts. In particular, for a non-relativistic Hamiltonian with a kinetic energy term $\vec{\nabla}^2/2m$ and potential V, these equations are given as [837, 818, 820, 825, 821]

$$\frac{\partial}{\partial t}\varrho^2(\vec{x},t) + \frac{\hbar}{m}\vec{\nabla}\left(\varrho^2(\vec{x},t)\vec{\nabla}\varphi(\vec{x},t)\right) = 0 \tag{7.5}$$

$$\hbar\frac{\partial}{\partial t}\varphi(\vec{x},t) + \frac{\hbar^2}{2m}\Big(\vec{\nabla}\varphi(\vec{x},t)\Big)^2 + \Big(V(\vec{x},t) - \frac{\hbar^2}{2m}\frac{\vec{\nabla}^2\varrho(\vec{x},t)}{\varrho(\vec{x},t)}\Big) = 0. \tag{7.6}$$

While, using the equivalence $\vec{v} = \vec{\nabla}\varphi$, the first equation corresponds simply to the continuity equation (7.2), the second is similar to the Hamilton-Jacobi equation of classical mechanics with an addition potential term Q defined as [837, 886, 818, 820]

$$Q(\vec{x},t) = -\frac{\hbar^2}{2m}\frac{\vec{\nabla}^2\varrho(\vec{x},t)}{\varrho(\vec{x},t)}, \tag{7.7}$$

which is called *quantum potential*. Note that the phase φ of the wavefunction plays the role of the classical *action* S, with $S = \hbar\varphi$, from which the trajectories are derived by the variation principle, i.e., by finding a path which minimizes the integrated action [820, 821]. In general this leads to trajectories perpendicular to the surfaces of constant φ, i.e., the phasefronts of ψ. The evolution of the particle can then be expressed in terms of a force [837, 818]

$$F = -\vec{\nabla}\big(V(\vec{x},t) + Q(\vec{x},t)\big) \tag{7.8}$$

derived from a modified effective potential. While this formulation allows to relate the Bohmian approach to classical mechanics, it is arguably artificial in the sense that it does not add any new content to the theory while complicating it significantly [847, 906, 824]. Furthermore, in contrast to the first-order guiding equation (7.3), it cannot be easily generalized to non-scalar particles with internal degrees of freedom such as spin. As criticized by Dürr, Goldstein, and Zanghì:

> ... the connection between classical mechanics and Bohmian mechanics that is suggested by the quantum potential is rather misleading. Bohmian mechanics is not simply classical mechanics with an additional force term. [...] the quantum potential should not be regarded as fundamental, and we should not allow it to obscure, as it all too easily tends to do, the most basic structure defining Bohmian mechanics. [...] We believe that the most serious flaw in the quantum potential formulation of Bohmian mechanics is that it gives a completely wrong impression of the lengths to which we must go in order to convert orthodox quantum theory into something more rational. [...] the artificiality suggested by the quantum potential is the price one pays if one insists on casting a highly nonclassical theory into a classical mold. [847]

Apart from the consideration of a quantum potential, also more fundamental departures from the standard form of BM have been considered. In general the Bohmian velocity is not uniquely defined by the requirement of consistency with the continuity equation (7.2) and it is always possible to add a divergence free term to Bohmian guiding equations of the form (7.3), without changing the empirical predictions [847, 845, 910, 848]. As discussed below, this ambivalence is also relevant for the question in which sense photon trajectories can be identified with the flow lines of the electromagnetic Poynting current. Furthermore, the ontological status of the wavefunction in BM is an intricate question and psi-ontic, psi-epistemic as well as nomological views are possible, where in the latter option the wavefunction is just regarded as the mathematical representation of a physical law [842, 879, 944, 990, 860, 824]. Finally, also variants of Bohmian mechanics can be formulated in which the beables are not given by the positions of the particles but by their momenta or other properties [858, 859, 910, 885]. The discussion of the Bohmian theory in this work is based on the arguably most prominent approach as developed chiefly by Dürr, Goldstein and Zanghi [847, 819, 823], and presented above in Secs. 7.1.1 and 7.1.2.

7.2 Measurement in Bohmian Mechanics

7.2.1 Measurement Process

BM solves the measurement problem straight forwardly by incorporating the measurement apparatus in the quantum description via a set of pointer particles which constitute the measuring device [838, 818, 861, 819]. For example, for a dichotomic measurement, the measurement interaction leads to a final entangled state in which two eigenfunctions of the measurement operator $|\psi_1\rangle$ and $|\psi_2\rangle$ are correlated with two orthogonal pointer states χ_1 and χ_2 as

$$|\Psi(\widetilde{x}_S, \widetilde{x}_P)\rangle = \frac{1}{\sqrt{2}}\Big(|\psi_1(\widetilde{x}_S)\rangle\, \chi_1(\widetilde{x}_P) + |\psi_2(\widetilde{x}_S)\rangle\, \chi_2(\widetilde{x}_P)\Big), \tag{7.9}$$

where $\widetilde{x}_S$ and $\widetilde{x}_P$ denote all positions of system and pointer particles, respectively. The Bohmian explanation of a definite measurement outcome is now based on the fact, that a proper measurement evolution does lead to pointer states which are not merely orthogonal

but necessarily also have disjoint supports in configuration space. In effect, the final configuration of pointer particles can only lie either fully in χ_1 or χ_2 which corresponds to a definite observable macroscopic outcome. The particular states into which the pointer systems evolve are determined by the phenomenon of decoherence [888, 942], as introduced in Sec. 2.5.1. As pointed out by Vaidman [905] this Bohmian explanation involves the tacit postulate that experience "corresponds to Bohmian positions".

In effect, according to BM, every measurement is ultimately a position measurement [818, 918, 847, 861, 905]. In particular, for measurements of any other degree of freedom it is necessary to describe the transition to disjoint spatial states of a pointer due to the measurement interaction. However, this is usually trivial as the vast majority of practical measurements clearly involve spatial pointers. This is true not only for paradigmatic examples such a the Stern-Gerlach experiment but also for typical energy measurements with calorimeters and time-of-flight detectors [611, 660, 818, 536], common electrical measurements of current or voltage [52], and all filtering measurements, where systems propagating in space do or do not pass a filtering mechanism, such as, e.g., polarization measurements via polarizers.

In the rare cases when a clear connection to a position measurement cannot be easily established, a more careful analysis of the measurement process becomes necessary. In fact the scenario of surrealistic trajectories, as sketched in 7.3.2, is exactly based on such a case, where orthogonal states of a non-position degree of freedom are correlated with the system states about to be measured and the readout of this degree of freedom via a position measurement is delayed for a certain amount of time. Accordingly, the experiment, which is subject to this work, is exactly based on a such transition of orthogonal pointer states from joined spatial support to a disjoint one. Note that, since, as discussed in Sec. 2.2.2, the measurement of any generalized observable can be expressed in terms of unitary evolution and pure states, it can also be expressed in terms of Bohmian formalism.

The Bohmian measurement model also accounts for the collapse of the wavefunction, although, just as in the MWI presented in Sec. 2.5.5, this collapse is always only effective and in principle reversible, however, it is irreversible FAPP [838, 818, 918, 819, 1004, 942]. In essence when the measurement interaction has lead to the state (7.9), typically the supports of the two pointer states χ_1 and χ_2 will remain disjoint forever due to particular mechanisms of physical decoherence, and thus one of the parts of the sum will be persistently vanishing. Thus, the future of system and pointer can be described by the product state

$$|\Psi(\widetilde{x}_S, \widetilde{x}_P)\rangle = |\psi_j(\widetilde{x}_S)\rangle \, \chi_j(\widetilde{x}_P)\,, \tag{7.10}$$

which exactly corresponds to the selective post-measurement state of SQM corresponding to the outcome j. In this sense BM shares the global wavefunction of the MWI, with the difference that the "empty waves", i.e., components with supports in regions of configuration space which are not populated, are suppressed and thus can be disregarded [905]. In the words of Dürr and Teufel:

> This collapse is not a physical process, but an act of convenience. It is introduced

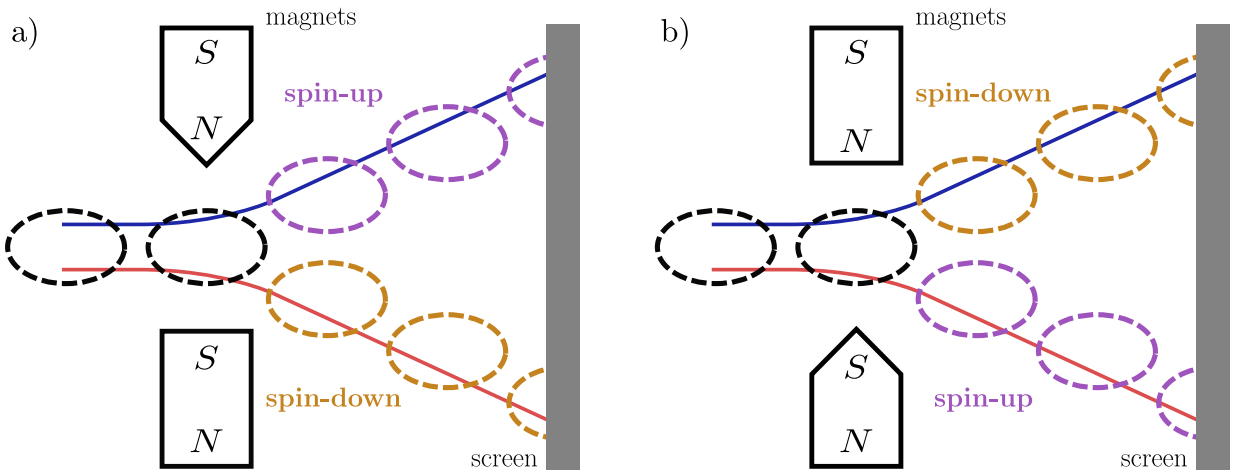

Figure 7.1: **Contextuality in BM - Spin** The two panels show two runs of a Stern-Gerlach measurement with identical initial conditions but different orientations of the apparatus. For illustration the trajectories of two Bohmian particles with different initial positions are depicted. The sequence of dashed ellipses indicates different timesteps in the propagation of the wavepackets which guide the particles. While only the evolution of a single wavefunction is shown, each of the particles is guided by its own copy of such a function. The flip of the magnetic gradient between scenarios a) and b) does only affect the propagation of the wavepackets, i.e., the deflection of spin-up and spin-down components, and not the trajectories of the particles. In effect, the particles are found in different spin states dependent on the orientation of the measurement apparatus.

> because it would simply be uneconomical to keep the ineffective wave functions, and the price we pay for forgetting them amounts to nothing. [819]

Note that, even in the case where no effective collapse occurs, i.e., the wavefunctions χ_j have overlapping supports, it is always possible to express the effective wavefunction or density operator of the system conditioned on the current position of the other particles, known as the *conditional wavefunction* of BM [819, 831, 884]. Conditional wavefunctions are particularly relevant for the explanation of nonlocal effects in BM, as discussed in subsequent sections.

7.2.2 Contextuality in Bohmian Measurement

In accordance with the no-go theorems discussed in Sec. 3.2.2, the structure of the Bohmian theory and the resulting description of quantum measurement necessarily leads to a contextual theory. In BM the only hidden-variables are the eigenvalues of the position operator and, as discussed in above, measurement outcomes for all other observables are explained by the evolutions of this restricted set of parameters, as given by the guiding equation [369, 846, 847, 861, 872, 883]. Accordingly, all non-position properties are linked *not* to the particle itself but rather to the particular wavefunction currently guiding it. In this sense, although BM reintroduces the concept of a classical phase space through the configuration space, it does so only for a limited set of degrees of freedom. A particle *is* at a certain

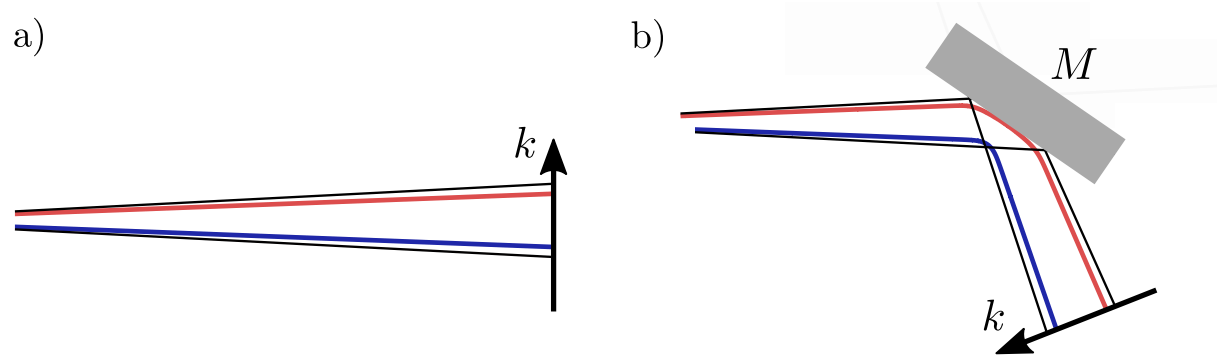

Figure 7.2: **Contextuality in BM - Momentum** Panel a) shows a simple far-field momentum measurement where the position has become fully correlated with momentum and the Bohmian particles follow straight lines accordingly. Since the reflection at a mirror M in panel b) induces a parity transformation, the screen axis has to be adjusted accordingly for a subsequent momentum measurement. However, in the reflection region the Bohmian particles transfer between different momentum states. This can be seen by the fact that they experience different effective reflection angles. Also in this case the particular implementation of the measurement influences in which momentum state a particle will be found.

position but a measurement only *finds* it for example in a certain spin state [819]. In effect, just as in Bohr's view, also in the Bohmian theory the experimental apparatus plays an essential role, however, one that that is part of the physical description [369, 836, 861].

The manner in which a measurement reveals a particle's position but the outcome of the measurement of another degree of freedom is fundamentally contextual is nicely illustrated through a gedankenexperiment proposed by Albert [912]. This scenario effectively represents a delayed-choice Stern-Gerlach measurement, which shows that prior to an irreversible measurement interaction, the particle cannot be said to be definitely in either one of the two spin states. As shown in Fig. 7.1, for a given initial position of a spin-1/2 particle inside the wave-packet propagating through a Stern-Gerlach apparatus the outcome of the measurement is independent of the orientation of the gradient of the magnetic field. However, while in one case the particle is found in the support of the wavefunction component corresponding to spin up, in the other it is found to be spin down. In both cases the outcome of the measurement is explained deterministically by the initial position of the particle. But what spin outcome is observed depends on the measurement context, i.e., in this case the orientation of the magnetic gradient. As put pointedly by Dürr and Teufel:

> What does this tell us? In fact it tells us that the particle changes its spin as a person changes his or her shirt. In other words, spin is not a property of a particle. It is dangerously misleading to speak of a particle with spin such and such. Spin is a property of the guiding wave function, which is a spinor. The particle itself has only one property: position. [819]

Note that for an ensemble of identically prepared particles the quantum mechanical pre-

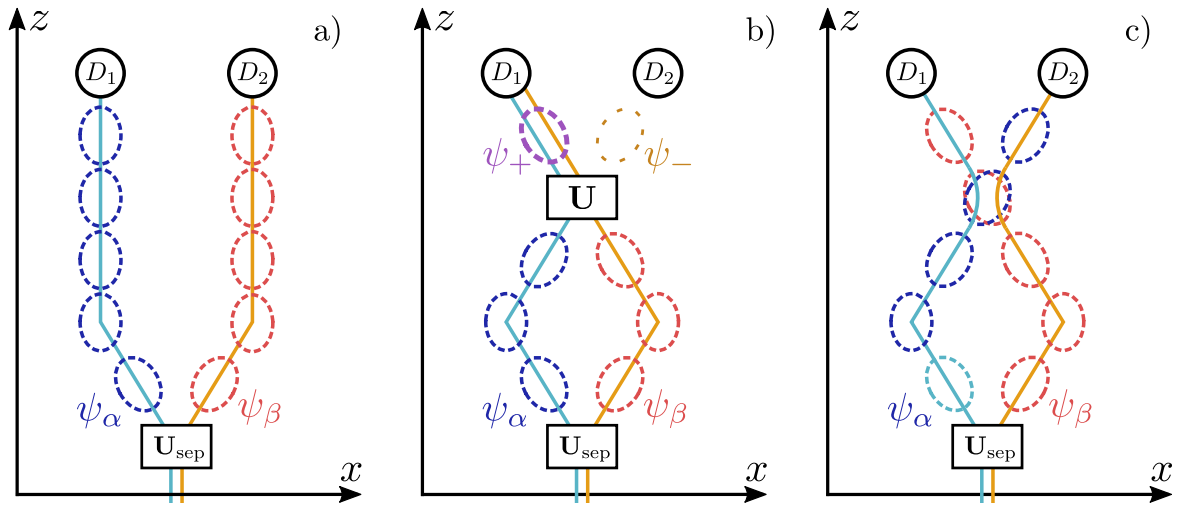

Figure 7.3: **Bohmian Explanation of Wheeler's Delayed Choice Scenario** The three panels depict the Bohmian explanation of the scenario from Fig. 3.4. As introduced in Fig. 7.1, the trajectories of two example particles are shown, with dashed ellipses indicating the timesteps in the propagation of the respective wavepackets. While panels a) and b) correspond to "particle" and "wave" behavior, respectively, panel c) shows a modification of a), where the paths of the wavepackets cross, as in Wheeler's original example. The combination of wave and particle aspects in the Bohmian approach allows to formulate a description of the scenario which is both local and realist.

dictions are perfectly recovered due to the QEH.

While the scenario described above is related to the contextuality of a non-spatial observable, an even more striking example is provided by the contextuality of standard quantum mechanical momentum as represented by the momentum operator $\vec{\mathbf{p}}$ [861]. In Fig. 7.2a the arguably simplest measurement of momentum is depicted, which simply corresponds to a position measurement in the far field of a paraxial beam, where the free evolution has led to a perfect correlation of position and momentum, as derived in Sec. 5.1.3. In this scenario the equivalent of the flip of the magnetic gradient, is, e.g., a reflection of the beam by a mirror, as shown in Fig. 7.2b. Due to the form of the Bohmian trajectories in the reflection region, the particles can transfer between two different regions of support of the wavefunction, which correspond to different momentum states. The initial position of the particle within the wavepacket thus does not determine the outcome of a momentum measurement independently of the employed apparatus, i.e., also momentum measurements depend on the context. Also in this case of course the QEH guarantees empirical equivalence to the predictions of SQM.

7.2.3 Delayed Choice Experiments

It is also instructive to evaluate the Bohmian description of Wheeler's delayed choice scenario, as introduced in Sec. 3.4.1. The realistic interpretation R, as discussed and

subsequently refuted by Wheeler, aimed to explain the detection events by ascribing past presence to the particle in either one or two of the possible paths. Since the choice of setting could be made after the first beam-splitting, this interpretation was proven untenable. In contrast, BM is not exclusive with respect to particle and wave behavior and embraces both [830, 818, 861]. The wavefunction, following the deterministic Schrödinger evolution, propagates along both paths and is thus sensitive to their relative phase. The particle follows a deterministic evolution guided by the wavefunction and has a definite position at all times. This combination of wave and particle behavior allows to circumvent Wheeler's argument and provides a realistic description of the process in which the system is locally influenced by the setting S only when it reaches the interaction region [830, 836, 818, 875, 890]. The vital insight that in the Bohmian explanation the wavefunction is involved in a three-fold manner has been pointed out by Fine, who writes:

> Beyond the wave-particle duality, in Bohmian mechanics the wave function itself acquires a multiple personality. In one guise it behaves as what Einstein dubbed a Führungsfeld (guiding field), directing the particles along trajectories determined by solutions to the velocity equations. [...] In satisfying Schrödinger's equation, however, the wave function also assumes the role of a true Gespensterfeld (spook field), acting as a "spook" or secret agent that reflects and transmits salient information about the environment, including measurement interactions. [...] Finally [...] Ψ has a third role to play; namely, that of a probability measure limiting the localization of particles. [861]

Fig. 7.3 illustrates the Bohmian explanation of different measurement outcomes dependent on the choice of setting S. In each of the panels two possible runs of the experiment with single particles are depicted, where two colors of trajectories distinguish the cases where a particle has traveled either along path α or β before reaching the region where the setting dependent interaction is applied. In scenario a) no beam-splitter is inserted and each particle follows the path it was already on up to detector. Upon insertion of the beam-splitter in scenario b) both particles instead remain in the support of the guiding field ψ_+ and reach the same detector, i.e., the detector D_1 registers a detection event with certainty, corresponding to perfectly constructive interference. Scenario c) represents an alternative scenario in which the beam-splitter is absent but the trajectories of the wave-packets cross, as in Wheeler's original proposal [1020]. In this case the particles transfer from one wave-packet to the other in the region of overlapping supports, i.e., figuratively speaking they "change their shirts" since, as discussed in Sec. 7.2.2, trajectories of particles guided by the same field cannot cross. The outcome statistics at the two detectors, however, are exactly the same as in scenario a). This represents an illustrative instance of a pair of physical scenarios, which, although dispositively equivalent, correspond to very different situations according to the descriptive model of BM.

7.3 The Nonlocality of Bohmian Mechanics

7.3.1 Bohmian Explanation in the Bell-Scenario

Any interpretation of quantum mechanics has to be evaluated in its relation to Bell's theorem, in particular with respect to the question which of the four fundamental assumptions, as derived in Sec. 3.2.4, is violated. As discussed in Sec. 7.2.1, the measurement model of BM functions by explaining the definite outcomes in terms of configurations of ensembles of pointer particles. As such, in contrast to, e.g., the MWI, only one of several possible final pointer states is realized and EBC is given. Although BM is fully deterministic, it does not enforce any superdeterministic correlations between the choices of settings and the hidden-variables and is thus also compatible with FC. Finally through the dependence of the trajectory of each particle on the positions of a number of other particles, as mediated by the guiding field, BM provides an explanatory model for the appearance of quantum correlations [838]. However, just as the dispositive prediction of SQM (3.4), this model does not factorize, i.e., it implies a causal relationship between the events at the two space-like separated sites. Thus, since BM satisfies CCP, EBC, and FC, it necessarily violates RC, i.e., it fundamentally includes action-at-a-distance. Note, however, that this does not imply a violation of signal-locality. The reason for this is the QEH, which leads to a randomization of the nonlocal influence in a way that suppresses any possibility of superluminal communication [838, 908, 818, 820, 906, 819, 826].

Any theory violating RC is faced with the problem of defining causal influences between the space-like separated events in the absence of a definite time-ordering. The most common approach in the context of BM is the postulation of a preferred spacetime foliation, which allows to formulate the wavefunction of all particle positions with a common absolute time [385, 410, 851, 831, 852, 884]. As all events in spacetime are reducible to configurations of particles, the preferred foliation thus establishes a definite absolute global time-ordering of all events, which in itself violates the principle of relativity [851, 819]. Crucially, due to the QEH and no-signaling, again no empirical procedure is able to distinguish between different foliations FAPP, i.e., the preferred foliation is "hidden" as well [474, 851, 884].

The Bohmian explanation of the Bell-scenario can be illustrated by the following simplified model for which the joint state of the systems at the sites A and B, before any of the parties performs their local measurement, can be written as [818, 820, 883]

$$|\Psi(\vec{x}_A, \vec{x}_B)\rangle = \frac{1}{\sqrt{2}}\psi(\vec{x}_A)\chi(\vec{x}_B)\left(|C_A\rangle\,|C_B\rangle + |D_A\rangle\,|D_B\rangle\right), \tag{7.11}$$

where ψ and χ are the respective spatial wavefunctions of the two particles and the states $|C_j\rangle$ and $|D_j\rangle$ denote the bases of other degrees of freedom in which the particles are entangled, such as, e.g., spin. Here the explicit time-dependence of the wavefunctions is neglected for notational convenience. Assuming that with respect to the preferred foliation the measurement on particle A in a basis $\{|E\rangle, |F\rangle\}$ is performed first, as shown in Fig. 7.4,

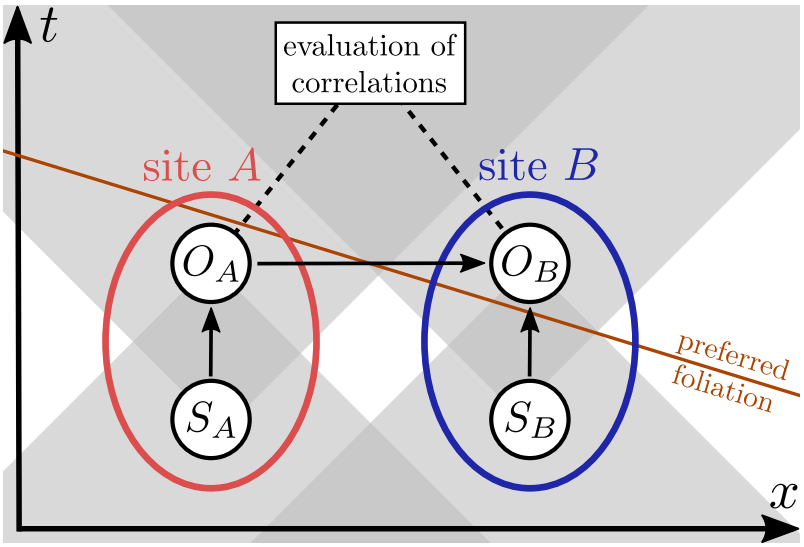

Figure 7.4: **Bohmian Explanation of Bell-Scenario** The Minkowski diagram illustrates the causal structure of the nonlocal model of BM for the generation of correlations in the Bell-scenario shown in Fig. 3.2. Causal relations are indicated as black arrows. Assuming the depicted preferred foliation, the entanglement in the wavefunction of the two systems at the two sites mediates a RC-violating causal influence of the observation at site A on the observation at site B.

the joint state evolves into $|\Psi'\rangle$ with

$$\begin{aligned}|\Psi'(\vec{x}_A,\vec{x}_B)\rangle = \frac{1}{\sqrt{2}}\Big(&\psi_E(\vec{x}_A)\,|E_A\rangle\,\left(\mu_{EC}\,|C_B\rangle + \mu_{ED}\,|D_B\rangle\,\right)\\ &+ \psi_F(\vec{x}_A)\,|F_A\rangle\,\left(\mu_{FC}\,|C_B\rangle + \mu_{FD}\,|D_B\rangle\,\right)\Big)\chi(\vec{x}_B),\end{aligned} \tag{7.12}$$

where ψ_E and ψ_F are spatial wavefunctions with disjoint supports corresponding to the two measurement outcomes E and F, and the amplitudes μ_{jk} are defined as $\mu_{jk} = \langle j|k\rangle$. Such a scenario is for example given by a Stern-Gerlach setup for which the orientation of the magnets determines the basis $\{|E\rangle, |F\rangle\}$ and the separation of the corresponding wave-packets leads to the emergence of two disjoint spatial wavefunctions [820]. Since particle A is localized in only one of the supports, say corresponding to E, an effective collapse occurs into the state

$$|\Psi'(\vec{x}_A,\vec{x}_B)\rangle = \psi_E(\vec{x}_A)\,|E\rangle\,\left(\mu_{EC}\,|C_B\rangle + \mu_{ED}\,|D_B\rangle\,\right)\chi(\vec{x}_B), \tag{7.13}$$

where the particles can now be treated separately since they are no longer correlated. Upon measurement, particle B will show the outcome statistics corresponding to the state $\mu_{EC}\,|C_B\rangle + \mu_{ED}\,|D_B\rangle$, which will exactly reproduce the Bell-correlations. For example if particle A is measured in the basis $\{|C_A\rangle, |D_A\rangle\}$ the state of particle B will collapse to one of the states $\{|C_B\rangle, |D_B\rangle\}$ and, if B is measured in that basis, perfect correlations will be detected since B will be guided by only a single non-vanishing wave-packet.

The outcome of the first measurement of particle A depends solely on the position of particle A since there is no correlation between the two components of its wavefunction ψ_E and ψ_F with the spatial wavefunction of particle B. The measurement on A is thus causally dependent only on the preparation which led to the entanglement in the internal degrees of freedom. In contrast, the subsequent behavior of particle B strongly depends on the position of particle A and also on the choice of measurement basis at site A. In this sense there is thus two-fold causal influence from site A to site B, as also indicated in Fig. 7.4. The causal relation is less clear when there is no such definite time-ordering of the two measurements with respect to the preferred foliation and in such cases the action-at-a-distance mediates causal influences in both directions, which depend on the details of the measurements. Note that of course a similar description can be given if the particles are entangled directly with respect to their spatial wavefunctions, as in the original EPR scenario discussed in Sec. 3.2.1.

7.3.2 The Scenario of "Surrealistic" Trajectories

The nonlocal character of Bohmian explanations in scenarios involving entangled particles has been pointed out by a seminal gedankenexperiment proposed by Englert, Scully, Süssmann, and Walther (ESSW) [857], see also [895], which leads to Bohmian trajectories denoted as "surrealistic" by the authors. The gedankenexperiment represents a modified version of a Bell-type scenario in which one particle is employed as a which-path detector for another, see Fig. 7.5. The propagation of particle A is arranged similarly as in the Wheeler-type delayed choice scenario from Fig. 7.3c, where the trajectories of the wave-packets cross. The second particle B is placed into one of the two possible paths of particle A such that the interaction between the two particles leads to the state

$$|\Psi'(\vec{x}_A, \vec{x}_B)\rangle = \frac{1}{\sqrt{2}}\big(\psi_\alpha(\vec{x}_A)\,|C_B\rangle + \psi_\beta(\vec{x}_A)\,|D_B\rangle\,\big)\psi_B(\vec{x}_B) \tag{7.14}$$

in which the path of particle A is entangled with the internal state of particle B. Note that this state is similar to the state (7.12) after a measurement at one of the sites in the Bell-scenario, where here the internal degrees of freedom of particle A can be neglected.

In a typical projective which-path measurement particle B would be made to interact with a macroscopic measurement device such that its internal states would become entangled with disjoint components of pointer wavefunctions and an effective collapse into one of the spatial components for particle A would occur. In contrast, in the ESSW scenario crucially the entanglement of particle A persists only with the internal degree of freedom of particle B from which the spatial state of the latter factorizes, such that no effective collapse occurs and both ψ_α as well as ψ_β are available to guide particle A. Of course at the time of the which-path interaction, particle A has a definite position in only one of these two disjoint wave-packets. The essential element of the ESSW scenario is the transfer of particle A between the supports of the two wave-packets in the crossing region. Assuming for example that initially particle A is in path α, the $|D\rangle$ component is suppressed for particle B due to the vanishing value of $\psi_\beta(\vec{x}_A)$ in the state (7.14). At that time, any definitive

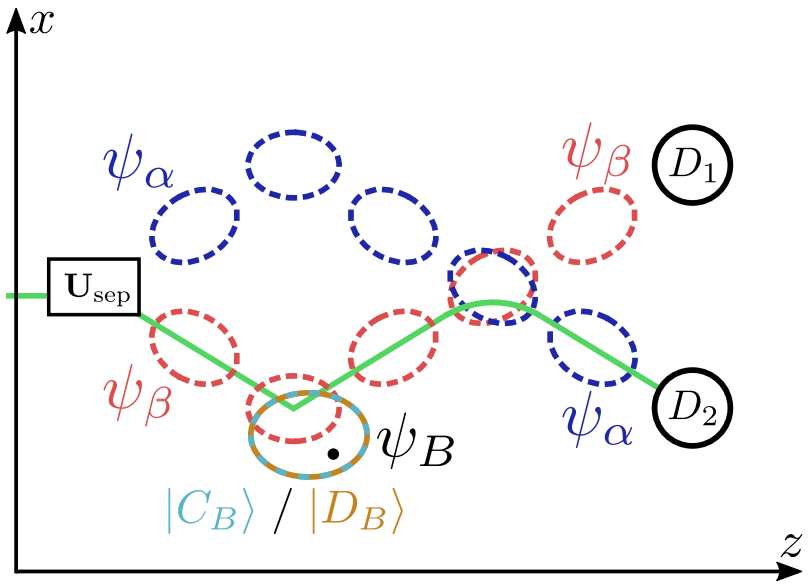

Figure 7.5: **Scenario of "Surrealistic" Trajectories** The scenario represents a modification of Wheeler's scenario with crossing paths, as shown in Fig. 7.3c, with an additional which-path measurement. An example of a possible trajectory for particle A is shown as a green line. The which-path marking is based on the flip of an internal degree of freedom of particle B, i.e., $|C\rangle_B \rightarrow |D_B\rangle$, correlated with the wavepacket component ψ_β. ψ_B is the unchanged spatial wavefunction of particle B, which is assumed to be in rest and represented by a black dot. Crucially, after the crossing region, a particle A propagating towards detector D_2 will have transferred from the support of ψ_β to the support of ψ_α and thus be correlated with finding the path-marker particle B in the state $|C_B\rangle$. In effect, while, for any particle detected in D_2, BM retrodicts a passage through the lower path, this is in contradiction with a straight-forward interpretation of the reading on particle B as a reliable indication of *past* behavior of particle A. This constitutes the alleged "surreal" character of such trajectories.

measurement of the state of particle B would thus yield the result C, where simultaneity is again defined based on some preferred spacetime foliation. At the later time when particle A is in the crossing region, i.e., in the support of both wave-packets, a measurement of particle B in the $\{|C\rangle, |D\rangle\}$-basis can yield both results with probabilities dependent on the particular amplitudes of the two wave-packets at the exact point $\vec{x}_A$. Finally after the transition of particle A between the two packets, the component $|C\rangle$ becomes suppressed for particle B and any measurement of the latter will yield the outcome D with certainty.

According to ESSW, the fact that the which-path detector is found, e.g., in state $|D\rangle$ while the Bohmian reconstruction of the past trajectory indicates that the particle propagated along path α prior to the crossing represents a conceptual problem. The authors take the results indicated by the local detectors placed in the paths as the defining characteristic of particle presence and correctly conclude that, given this assumption, Bohmian trajectories are "macroscopically at variance with recorded track" [857]. For illustration ESSW also mention the example of a bubble-chamber, which is further developed by Aharonov

and Vaidman [827, 905]. In this extension of the gedankenexperiment a set of detectors, such as those described above, is distributed over the whole space, forming an effective "bubble-chamber" of "slow detectors", i.e., detectors which on the timescale of propagation of particle A react exclusively with a change in an internal degree of freedom and only later evolve to show a macroscopic outcome. In such a slow bubble-chamber the track, which forms only after passage of particle A, indeed does not indicate the Bohmian trajectory. In [881] further types of which-path detectors are analyzed in terms of their capability to generate such effects.

7.3.3 Interpretation of the ESSW Scenario

ESSW summarize their conclusion, where in the original example the propagating particle A is an atom, in the following way:

> A supporter of Bohmian mechanics would insist that the atom went along its Bohm trajectory through one of the detectors, but left its mark in the other one. Thus, he concludes, the which-way detectors do not deserve their name. The usual which-way detection, he declares, is an illusion. [857]

This represents an absolutely correct assessment of the standard Bohmian response, see, e.g., [853, 846, 874, 902, 828]. However, the authors proceed to argue:

> But, in arguing this way, is he not putting away with the basics of Bohmian mechanics? For, on the one hand, the retrodicted Bohm trajectories are supposed to be "truly realistic", on the other hand, checking them out is forbidden or, at least, impossible. We conclude: The reality attributed to Bohm trajectories is not physical, it is metaphysical. [857]

While the latter fragment is not easy to understand, a charitable reading seems to indicate that the authors identify two basic tenets of BM which seem to be in contradiction, namely the aim to facilitate a realistic description of the physical world as well as a fundamental impossibility to measure Bohmian trajectories on a single particle level. The first statement is of course true and the second holds only insofar as a measurement of trajectories without disturbance is assumed. In principle a series of spatially-resolving QND measurements would allow to measure the full spatial evolution of a Bohmian particle, where, however, each measurement would change the future evolution due to the effective collapse of the wavefunction as prescribed by the standard IDT relations of quantum mechanics. In any case, ESSW seem to imply that the which-path detector in their scenario represents a valid "check" of particle trajectories and, as mentioned above, should be regarded as the *only* candidate for a realistic criterion of particle presence. Since it contradicts the Bohmian description, Bohmian trajectories are deemed "surrealistic".

The fundamental assumption in the argument of ESSW that the outcome indicated by the which-path detector is to be regarded as an indicator of physical reality is not justified further by the authors and thus only speculation over possible motivations is possible. From the perspective of the standard operational interpretation of quantum mechanics, taking

Wheeler's view as an example, the fact that particle B is found in some state after particle A has already passed does not imply anything about the past of particle A [853, 879]. In Wheeler's view statements about physical systems can be only made based on macroscopic observations and the only observations in the ESSW scenario are the final states of particles A and B at two distinct locations. Just as in the Bell-scenario, these results do not admit any further inference about the common past of the particles. Quantum mechanics is just regarded as a calculational tool that allows to predict the probability to find particle B in either of its internal states after particle A has passed the crossing region and these empirical predictions are exactly reproduced by Bohmian mechanics. In this sense BM takes complementarity more seriously than ESSW. Through its contextuality it provides a physical mechanism of complementarity and the outcome of the which-path measurement is factually undefined until a proper readout of the which-path detector is performed.

Since there is no contradiction with operational quantum mechanics beyond the trivial fact that BM provides a realist model, it appears that ESSW have a particular type of realist interpretation in mind with which BM is in conflict. Again in a charitable reconstruction of their argument the prime candidate for such a view seems to be an insistence on the locality of interactions [874], as sketched in Sec. 3.1.3, which implies the general possibility to reliably isolate the which-path measurement apparatus from the system after the measurement interaction. The argument could then state for example that in any realist interpretation the state of any particle B can only be affected via interaction with another particle A if the particles have been present at the same location at some point in time, which is clearly not the case in the explanation of BM. In this case, however, the whole scenario of ESSW is nothing but a particular example of the inherent nonlocality in Bohmian mechanics, and the titulation of trajectories as "surrealistic" merely a criticism of action-at-a-distance [828]. While thus the gedankenexperiment has no bearing on the validity of BM, it nevertheless ingeniously illustrates the consequences of nonlocality in an explicit manner. In connection with a delayed-choice of the readout of the which-path measurement device it represents the basis for the experiment described in Sec. 7.7. In the following, trajectories of this type are denoted as "ESSW-trajectories". Note that there is a minority of proponents of the Bohmian approach who take a different position than the one described above, and negate that the trajectories postulated by ESSW factually occur, see, e.g., [875].

7.4 Weak Values and Photon Trajectories

7.4.1 Relativistic Bohmian Mechanics

While the non-relativistic version of Bohmian mechanics is well-developed, a straight forward relativistic generalization is not trivial mainly due to the nonlocality of the theory. However, it represents an active area of research and several relativistic approaches have been formulated without a clear consensus with respect to a preferred version, see, e.g., [899, 898, 831, 824, 865] for overviews. For example, models have been proposed which incorpo-

rate probabilistic creation and annihilation events of QFT in between which the particles follow deterministic trajectories [851, 850, 904]. As mentioned above, a preferred spacetime foliation is a prominent solution to the problem of simultaneity [410, 854, 851] and there are proposals to derive the particular nature of the foliation from properties of the wavefunctions [852] or cosmological considerations [904]. Alternatively, also modified versions of relativistic Bohmian dynamics have been suggested which do not require a preferred foliation, but instead rest on a multi-time description [833] or incorporate retrocausality [871, 901, 900].

Also in the case of photons there is no consensus whether a trajectory description is possible due to the problem of photon localization [862, 863, 876], which has already been argued by Bohm [840]. Nevertheless, Bohmian photon trajectories have been proposed by Ghose *et al.* [869, 868, 870], based on a particular formulation of the PWF, different from the one presented here. In contrast, the approach used in this work seems to be more in line with the standard conception of BM, as introduced above, in which the continuity equation is central and the dynamical laws can be generalized to different Hamiltonians. Thus, given the continuity equation obeyed by the PWF, a natural definition of photon velocity $\vec{v}$ is obtained by dividing the probability current through the local density as $\vec{v} = \vec{j}/p$. As the current corresponds to the normalized Poynting current, these trajectories follow the energy flow lines of the electromagnetic field, as it is also the case for the trajectories introduced by Ghose *et al.* with an alternative PWF. A similar understanding of the Poynting current as the correct generalization of non-relativistic Bohmian velocity is also advocated in a range of works by Sanz and collaborators [844, 891, 821, 890], who, however, explicitly denounce a description in terms of point-like particles both in the relativistic and the non-relativistic case. Also in the work by Kocsis *et al.* [878], which represents the first experimental recording of photon trajectories, as well as in its prominent interpretation [834], the recorded trajectories are presented as mere flow lines, without attribution to point-like Bohmian particles.

7.4.2 Operational Definition Based on Weak Values

A crucial step in the debate about Bohmian trajectories in general was provided by an operational definition of velocity of quantum particles based on weak measurements, provided by Wiseman [910]. In fact it had already been known that, at least for scalar wavefunctions, the Bohmian velocity corresponds to the local k-vector, which is in principle measurable for an ensemble of systems prepared in the same state [866, 889]. However, Wiseman's proposal adds two crucial elements, namely first an operational definition of Bohmian velocity connecting it to the classical concept of velocity, which second, illuminates its experimental accessibility via weak measurements leading to simple procedures to record Bohmian particle trajectories.

The velocity of a classical particle can be measured by two successive measurements of its position, $\vec{x}_1$ and $\vec{x}_2$ at times t_1 and t_2 separated by some time-interval τ, where the mean velocity $\bar{v}$ in that time interval is given by $\vec{v}_m = (\vec{x}_2 - \vec{x}_1)/\tau$. If the time interval is chosen smaller, the local velocity at either of the points is approximated better

with $v(\vec{x}_1, t_1) = \lim_{\tau\to 0} \vec{v}_m$. In practice it is sufficient to reduce the time-interval to a timescale which is sufficiently small compared to changes in $\vec{v}$. In quantum mechanics such a procedure is in general not possible since the precise first measurement irreducibly disturbs the momentum state of the particle and leads essentially to a random outcome of the second position measurement due to the increased momentum uncertainty. The same behavior is of course reproduced in BM where the guiding field is changed due to the first measurement interaction, affecting the further evolution of the particle, such that the Bohmian velocity of a single particle is fundamentally unmeasurable [819].

Wiseman's suggestion is instead to measure the first position only weakly, thus avoiding the disturbance of the subsequent evolution [910]. Of course for a single particle this procedure also does not allow to obtain a definite value for the velocity due the large uncertainty of the weak measurement. However, assuming an ensemble of particles following deterministic non-crossing trajectories, the second strong measurement effectively picks out a single trajectory, or a set of close trajectories, such that all particles detected at the second location must have been localized in at least the same region at the time of their respective weak measurements. When a weak value is regarded as a definite property of a single quantum system as presented in Sec. 6.1.6, the outcome of the weak measurement on the ensemble of particles can be seen as an uncertain measurement of that definite position. Formally, this definition of velocity can be expressed as [910]

$$v(\vec{x}, t) := \lim_{\tau\to 0} \frac{1}{\tau} \mathbb{E}\big[\vec{x}_2 - \vec{x}_1^w | \vec{x}_2 = \vec{x}\big], \tag{7.15}$$

in terms of random variables, where $\vec{x}_2$ is the definite outcome of the strong measurement at time $t+\tau$, $\vec{x}_1^w$ is the uncertain outcome of the preceding weak measurement at time t, and the expectation value is conditioned on finding the system at position $\vec{x}$ upon the strong measurement. As argued by Wiseman, this corresponds to a *naive* conception of velocity which does not rest on any knowledge of QM but just on the minimal assumptions that systems cannot be reliably prepared in a specific state as well as that strong measurements disturb the future evolution while weak measurements do not.

Following the straight forward interpretation of weak measurements, as discussed in Sec. 6.1.6, the conditioned mean outcome of weak measurement $\vec{x}_1^w$ is identified with the real part of the weak value of the position operator given as

$$\mathbb{E}\big[\vec{x}_1^w | \vec{x}_2 = \vec{x}\big] = \mathrm{Re}\Big[\frac{\langle\psi|\, \mathbf{\Pi}_{\vec{x}} \mathbf{U}_t^{t+\tau}\, \vec{\mathbf{x}}\, |\psi\rangle}{\langle\psi|\, \mathbf{\Pi}_{\vec{x}} \mathbf{U}_t^{t+\tau}\, |\psi\rangle}\Big] = \mathrm{Re}\big[(\vec{\mathbf{x}})_w\big], \tag{7.16}$$

where the preselection state $|\psi\rangle$ is defined at the time of the weak measurement t and $\mathbf{U}_t^{t+\tau}$ indicates the unitary evolution up until the time of postselection $\mathbf{\Pi}_{\vec{x}}$ at time $t+\tau$. Note that in general the above expression cannot be further reduced since the postselection might only be partial if other degrees of freedom of the system are involved. By assuming a conservative Hamiltonian $\mathbf{H}$ and taking the limit $\tau \to 0$, the unitary operator can be expanded to first order as $\mathbf{U}_t^{t+\tau} \approx 1 - i\mathbf{H}\tau/\hbar$, which leads to final expression for the

operational velocity [910]

$$\vec{v}(\vec{x},t) = \lim_{\tau\to 0}\frac{1}{\tau}\left(\vec{x} - (\vec{\mathbf{x}})_w\right) = \frac{1}{\hbar}\frac{\mathrm{Re}\big[\,\langle\psi|\,\mathbf{\Pi}_{\vec{x}}\; i[\mathbf{H},\vec{\mathbf{x}}]\,|\psi\rangle\,\big]}{\langle\psi|\mathbf{\Pi}_{\vec{x}}|\psi\rangle}, \tag{7.17}$$

where $\langle\psi|\,\mathbf{\Pi}_{\vec{x}}\,|\psi\rangle = p(\vec{x})$ and $\vec{\mathbf{v}} := i[\mathbf{H},\vec{\mathbf{x}}]/\hbar$ can be interpreted as a generalized *velocity operator* [562, 877]. Note that, due to the time-symmetry of QM, the same expression is obtained if the differential quotient (7.15) is formulated in a time-reversed manner, such that $\vec{v} = \lim_{\tau\to 0}\left((\vec{\mathbf{x}})'_w - \vec{x}\right)/\tau$. In this case the operation involves starting with a partial preparation of the system at time t in a well defined position $\vec{x}$ after which a weak measurement of position is performed at time $t+\tau$, followed by an immediate postselection onto the final state $|\phi\rangle$ into which the system would have evolved had it stated in $|\psi\rangle$ at time t without any measurements in between.

The operational definition of particle velocity (7.17) represents a crucial and very general result. In the case of the non-relativistic Hamiltonian for a set of massive particles it immediately reduces to the usual Bohmian velocity (7.3) [848]. It also encompasses arbitrary Hamiltonians $\mathbf{H}$, for which it always leads to particle velocities which conserve quantum mechanical continuity, as defined in (7.2). This establishes a remarkable connection between two seemingly unconnected realistic approaches to quantum mechanics, i.e., the interpretation of weak values as genuine properties of pre- and postselected systems and BM. Note, however, that such measurements by no means imply an empirical proof of Bohmian trajectories [884, 892]. They allow to reconstruct the trajectories for an ensemble of particles, under the two assumptions that the particles follow deterministic trajectories and that weak values are properties of single pre- and postselected quantum systems.

7.4.3 Photon Trajectories

Using the formalism of the PWF, as presented in Sec. 4.7, the operational definition of velocity can be applied to photons. As given by Eq. (7.17), the crucial quantity is the velocity operator $\vec{\mathbf{v}}$, which, employing the single-photon Hamiltonian $c\boldsymbol{\sigma}_z \otimes \vec{\mathbf{s}}\cdot\vec{\mathbf{p}}$ from Eq. (4.60), becomes [562]

$$\vec{\mathbf{v}} = \frac{ic}{\hbar}[\boldsymbol{\sigma}_z \otimes (\vec{\mathbf{s}}\cdot\vec{\mathbf{p}}), \mathbb{1}\otimes\vec{\mathbf{x}}] = c\boldsymbol{\sigma}_z\otimes\vec{\mathbf{s}}. \tag{7.18}$$

This means that

$$\langle\psi|\mathbf{\Pi}_{\vec{x}}\vec{\mathbf{v}}|\psi\rangle = \frac{\vec{S}_{\mathrm{avg}}(\vec{x})}{\langle\mathbf{H}\rangle}, \tag{7.19}$$

which exactly corresponds to the probability current $\vec{j}$ of the PWF, as defined in Eq. 4.61, i.e., the trajectories follow the flow lines of the Poynting current. The operational reasoning in terms of weak values thus not only fits to standard non-relativistic BM, but is also in perfect agreement with the formulation of the PWF in terms of the RS vector, where of course the time-limit should not be extended to subcycle timescales [910] and thus also the

averaged Poynting current, as defined in Eq. (4.19), should be considered. Furthermore, this definition also inherits the ambiguity of the definition of the Poynting current, with respect to an additional curl, although arguments have been made for the uniqueness of this identification [897].

The compatibility of photon trajectories based on the PWF with the operational definition is an indicator for the viability of electromagnetical energy flow lines as the correct description of photons when treated in the framework of BM. The crucial element is a particle velocity which leads to a conservation of energy. Both the approach described here as well as the alternative approach to the PWF as advocated by Ghose *et al.* share this feature. Just as with non-relativistic Bohmian trajectories it is possible to treat these flow-lines as mere calculational or pictorial tools, without any ontological commitments. However, from the perspective of BM they appear as the prime candidates for a trajectory theory of point-like photons similar to the standard Bohmian theory for massive non-relativistic particles. Only equipped with this interpretation can photon experiments be regarded as relevant for the investigation of the Bohmian theory. Accordingly, in the following photons will be treated from the Bohmian perspective as point-like particles following the guiding equation derived above.

7.5 Nonlocal Effects in the Photonic Double-Slit

7.5.1 Transverse Velocity Field of Gaussian Beam

The definition of photon trajectories based on the PWF in the preceding section allows to discuss the functioning of the Bohmian theory in the double-slit scenario realized with single photons. In the experiment described in this work the double-slit is very well approximated by the superposition of two parallel and quasi-monochromatic Gaussian beams, which are displaced in horizontal x-direction, as introduced in Sec. 5.3.2. Furthermore, the two beams are *astigmatic*, which means that they have different widths and longitudinal waist positions with respect to transverse x and y directions. Nevertheless their wavefunction and thus also the total wavefunction still factorizes with respect to the two transverse directions such that the definition of a double-slit is fulfilled.

To calculate the photon trajectories, the Poynting current has to be evaluated, as done, e.g., in [870, 844, 891, 834, 890, 893]. Since the transverse wavefunction factorizes, also the components of these two k-vectors depend only on the corresponding coordinates such that the problem reduces to two one-dimensional problems, where, however, according to Eq. (4.27), each transverse direction of the spin-current depends on the component of the osmotic k-vector in the other transverse direction. For a single astigmatic Gaussian beam the respective k-vector components $k_{\mathrm{loc},j}$ and $k_{\mathrm{osm},j}$ for each of the two transverse dimensions $j = x, y$ are simply given as

$$k_{\mathrm{loc},x}(x,z) = \frac{kx}{R_x(z_x)}, \qquad k_{\mathrm{osm},x}(x,z) = -\frac{2x}{w_x^2(z_x)}, \tag{7.20}$$

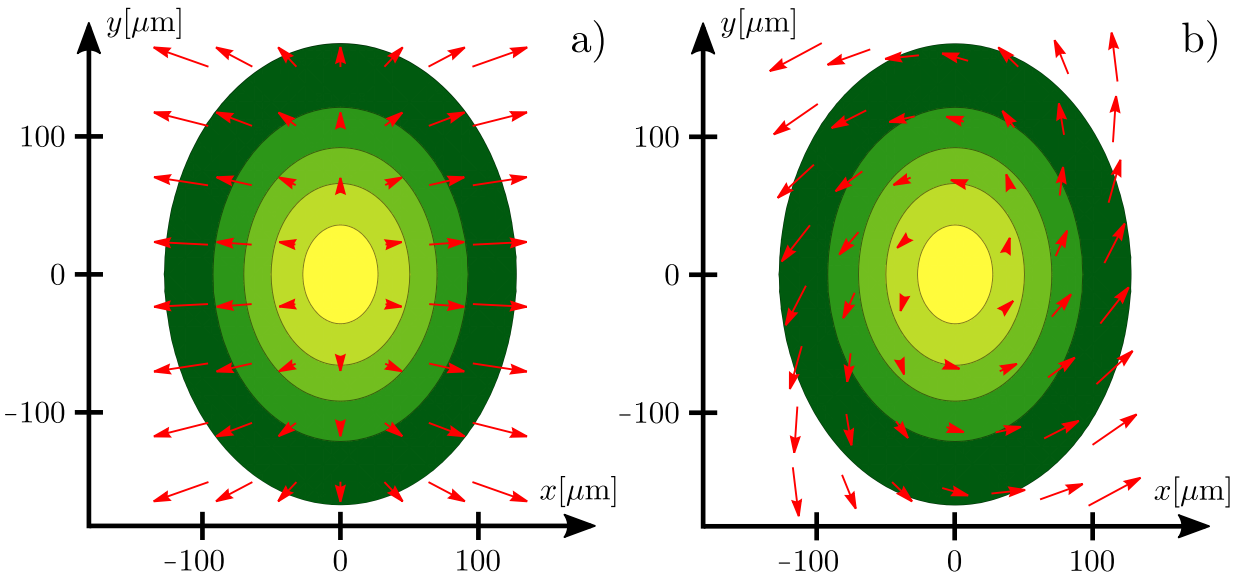

Figure 7.6: **Transverse Velocity Fields for Gaussian Beam** The velocity fields are shown for an astigmatic beam with waists of $w_{x0} = 100\mu$m and $w_{y0} = 150\mu$m and a wavelength of 810nm. The transverse profile is evaluated at a distance of 25mm from the common focus. Panel a) shows the linearly polarized case with orbital-current only. Since the waist in x-direction is smaller, the beam is diverging more in this direction. For circular polarization, as shown in panel b), a divergence-free spin-current is added to the orbital current. From a Bohmian perspective, the spin current does not affect the particle density, but leads to additional collective shifts of the particles, which are absent in the linearly polarized case.

and vice versa for the y-direction, where w_j and R_j are the respective widths and curvatures, and $z_j = z - z_{0j}$ the corresponding longitudinal distances to the focus positions z_{0j}. In the paraxial approximation the z-component of the local k-vector simply corresponds to k and the z-component of the osmotic k-vector depends on various factors such as the beam divergence and the longitudinal part of the wavefunction but is irrelevant for the calculation of Bohmian velocity since the spin-current is purely transverse. Note that, while technically outside of the central axis of the beam it holds that $|\vec{k}_{\mathrm{loc}}| > k$, this does not necessarily imply a superluminal velocity because, due to the paraxial approximation, the longitudinal velocity is approximated as c by default and its potential reduction due to transverse motion is not taken into account. Nevertheless superluminal velocity of Bohmian particles is a possibility and does not constitute a conceptual problem [880]. Its analysis would, however, require to go beyond the paraxial approximation and is thus outside the scope of this work.

Using the above results for the two types of k-vectors, the total current for a single Gaussian beam can be calculated via expressions (4.26) and (4.27), which for linearly and circularly polarized Gaussian beams leads to transverse velocity fields such as those presented in Fig. 7.6. The circularity of polarization results in the appearance of an additional spiraling motion of the photons, which, however, does not contribute to the net

energy flow, i.e., changes in Bohmian particle density, and should also not be confused with orbital angular momentum of light, which is just an effect of orbital current.

7.5.2 Double-Slit Trajectories

The transverse intensity distribution of a Gaussian double-slit is derived in Sec. 5.3.2 in dependence on the two coherence parameters η_{pol} and η_L, which are also shown to be equivalent to a coherence loss due to a which-path measurement in Sec. 5.3.3. To discuss the corresponding photon trajectories in the double-slit field, in the following for simplicity of presentation a homogeneously and linearly polarized field is assumed, i.e., both slits have the same polarization. In effect, the entire velocity field can be expressed in terms of the local k-vector, which depends solely on the relation between the two scalar wavefunctions corresponding to the slits. Certain effects of polarization inhomogeneity are sketched in the context of measurement back-action due to the weak velocity measurement, as introduced below in Sec. 7.6.3. Furthermore, since in the homogeneous case the behavior in x and y-directions can be treated completely independently, most of the discussion is restricted to the horizontal xz-plane in which the slits are separated and in which thus all non-trivial effects of double-slit interference occur. Finally, also beams with resting focus, as introduced in Sec. 4.2.2, are considered for which the slit-functions are stationary.

Neglecting the homogeneous polarization and assuming full longitudinal coherence between the two slits, the general conditional state of the photon in the double-slit $|\Psi\rangle$ can be expressed as

$$|\Psi(\vec{x}_A,t)\rangle = c_\alpha(t)\,\psi_\alpha(\vec{x}_A)\,|\chi_\alpha(t)\rangle + e^{i\varphi(t)}\,c_\beta(t)\,\psi_\beta(\vec{x}_A)\,|\chi_\beta(t)\rangle\,, \tag{7.21}$$

where $c_\alpha, c_\beta \geq 0$ parametrize the relative amplitudes of the two slit-functions, φ their relative phase, and the states $|\chi_\alpha\rangle$ and $|\chi_\beta\rangle$ represent the possible internal states of other particles, with which the photon is potentially entangled. While the slit-functions ψ_α and ψ_β themselves are stationary, the other parameters in general have a time-dependence, which, as described below, is determined by the collective trajectory $\widetilde{x}_B(t)$ of the other particles in configuration space. In any case, at any point in time the state of the slit-particle A can be expressed by the above state. Note that, for simplicity, without loss of generality, it is assumed that $\eta = \langle\chi_\alpha|\chi_\beta\rangle \in [0,1]$ and the corresponding phase is absorbed into φ.

Expression (7.21) allows to express the effective velocity field of the slit particle in terms of the slit-functions ψ_j by including possible incoherence via a general coherence parameter $\eta(t)$, just as done for the transverse intensity distribution (5.32). Employing definition (7.17) along with the simplification due to linear polarization shown in Eq. (4.23), the time-dependent velocity field $\vec{v}_A$ for the slit-particle becomes [892]

$$\begin{aligned}\vec{v}_A(\vec{x}_A,t) &= \frac{c}{k}\,\frac{\mathrm{Im}\big[\,\langle\Psi(\vec{x}_A,t)|\,\vec{\nabla}\,|\Psi(\vec{x}_A,t)\rangle\,\big]}{\langle\Psi(\vec{x}_A,t)|\Psi(\vec{x}_A,t)\rangle} \\ &= \frac{c}{k}\,\frac{c_\alpha^2|\psi_\alpha|^2\vec{k}_{\text{loc}}^{(\alpha)} + c_\beta^2|\psi_\beta|^2\vec{k}_{\text{loc}}^{(\beta)} + \eta c_\alpha c_\beta|\psi_\alpha\psi_\beta|\big(\vec{\sigma}_{\text{loc}}\cos\varphi' + \vec{\delta}_{\text{osm}}\sin\varphi'\big)}{c_\alpha^2|\psi_\alpha|^2 + c_\beta^2|\psi_\beta|^2 + 2\eta c_\alpha c_\beta|\psi_\alpha\psi_\beta|\cos\varphi'}\,,\end{aligned} \tag{7.22}$$

where $\vec{k}^{(j)}_{\mathrm{loc}}(\vec{x}_A)$ and $\vec{k}^{(j)}_{\mathrm{osm}}(\vec{x}_A)$ are local and osmotic k-vectors of slit j, $\vec{\sigma}_{\mathrm{loc}} := \vec{k}^{(\alpha)}_{\mathrm{loc}} + \vec{k}^{(\beta)}_{\mathrm{loc}}$ is the sum of local k-vectors, and $\vec{\delta}_{\mathrm{osm}} := \vec{k}^{(\alpha)}_{\mathrm{osm}} - \vec{k}^{(\beta)}_{\mathrm{osm}}$ is the difference of osmotic k-vectors, defined in analogy to the opposite quantities from Sec. 4.2.4. The phase φ' is defined as the difference of phase φ and the relative phase $\delta\varphi$ of the slit-functions at position $\vec{x}_A$ with $\varphi'(\vec{x}_A, t) = \delta\varphi(\vec{x}_A) - \varphi(t)$. Note that in the second expression for clarity of notation the explicit dependence on time and position $\vec{x}_A$ of the slit-particle has been suppressed.

The velocity field can also be expressed without interference terms depending on η. For example, considering a generalization of the state of photon A (7.21) with

$$|\Psi(\vec{x}_A)\rangle = \sum_j e^{i\varphi_j(t)} c_j(t)\psi_j(\vec{x}_A)\,|\chi_j(t)\rangle\,, \tag{7.23}$$

where again perfect coherence of the internal states is assumed, at any given time t it is always possible to perform a basis transformation with new functions ψ'_j and suitably modified coefficients, such that the new states $|\chi'_j(t)\rangle$ are orthogonal. After tracing out the other particles, the state of photon A can then be conveniently expressed in terms of the density operator

$$\rho(t) = \sum_j p_j(t)|\psi'_j(t)\rangle\langle\psi'_j(t)|, \tag{7.24}$$

where here again $|\psi'_j(t)\rangle$ denotes the full spatial state of the photon without projection on a particular position $\vec{x_A}$. This means that the particle is guided by a set of non-interfering wave-functions ψ'_j and the resulting velocity field has a form similar to (7.22) with $\eta = 0$, where of course in this case the incoherent sum contains more than two elements. Note that crucially *every* single particle propagating through the slit is guided by the full set of incoherent guiding fields, i.e., even for $\eta = 0$, the velocity field (7.22) in general depends both on ψ_α and on ψ_β.

Combining Eq. (7.22) with expressions (7.20) allows to calculate the double-slit trajectories of the photons in the xz-plane, which are shown in Fig. 7.7 for $\varphi = 0$, equal amplitudes $c_\alpha = c_\beta$, as well as full coherence $\eta = 1$. Following the QEH, the transverse density of trajectories is chosen proportionally to the probability density at one longitudinal position. Since the trajectories are defined based on the probability flow, the density of trajectories stays proportional to the transverse probability density at all other times both past and future. The parameters of the beams are chosen such, that the double-slit field transitions from near field to close to far field configuration. Such trajectories have been first derived by Philippidis *et al.* [886] for massive particles and show the same characteristic features, illustrating clearly the guiding mechanism of BM. As put plainly by Bell:

> De Broglie showed in detail how the motion of a particle, passing through just one of two holes in screen [sic], could be influenced by waves propagating through both holes. And so influenced that the particle does not go where the waves cancel out, but is attracted to where they cooperate. This idea seems to me so natural and simple, to resolve the wave-particle dilemma in such a clear and ordinary way, that it is a great mystery to me that it was so generally ignored. [968]

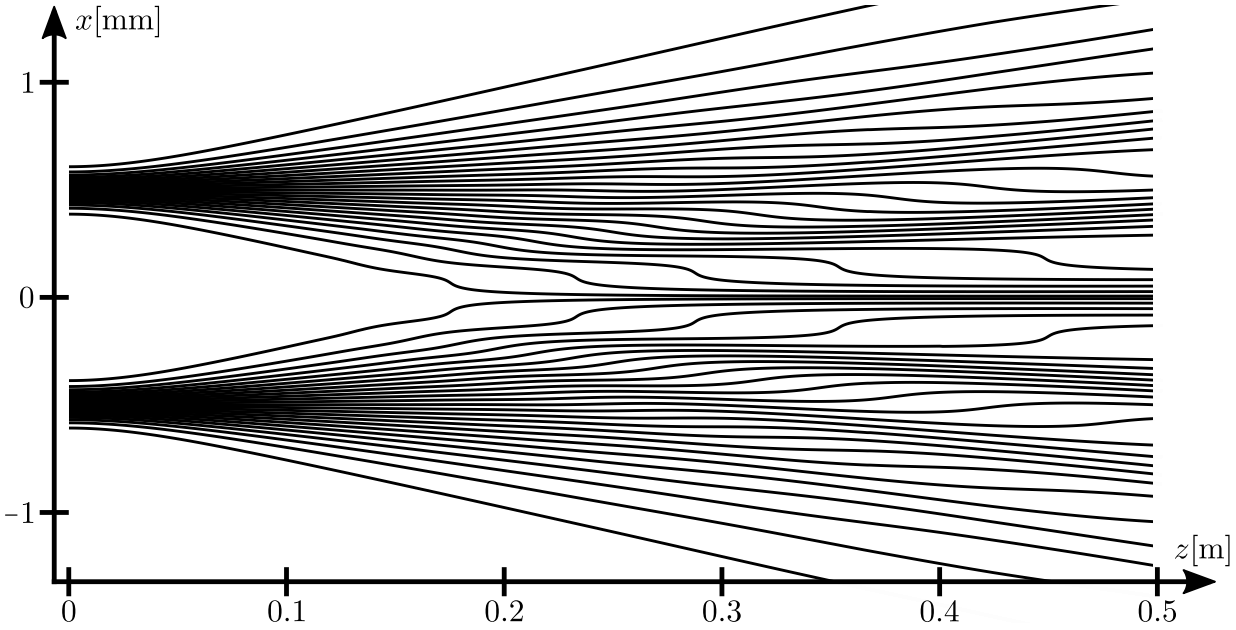

Figure 7.7: **Calculated Double-Slit Trajectories of Single Photons** The starting points of the 40 example trajectories at position $z = 0$ are chosen such that their density is proportional to the transverse probability density given by the guiding PWF, i.e., a superposition of two displaced Gaussian distributions. The two Gaussian beams are separated by 1mm and have equal waists of $w_0 = 110\mu$m and a wavelength of 810nm. The same parameters are used in all subsequent quantitative plots. The bunching of trajectories induced by the guiding equation results in a transverse distribution of particles which complies with the observable probability distribution also at each subsequent transverse plane. Note that in the paraxial approximation the z-axis is equivalent to the time-axis for the transverse propagation.

A similar calculation with different parameters is also the basis of all other figures of trajectories shown below.

For illustration also the horizontal components of the velocity are depicted in Fig. 7.8 for the transverse plane at $z = 0.4$m. The peaks, both in positive as well as negative direction, correspond to fast transitions of the particles through the valleys of the probability density. For valleys close to the center $x = 0$ the particles move towards the center against the general direction of beam diffraction, i.e., for example for $x < 0$ there are locations where the x-component of the velocity is positive. Note that at the inner peaks close to the center of the slit the transverse momenta reach values which are larger than any k-vector components present in the single beams, which is an instance of superoscillations [560], as introduced in Sec. 6.1.4.

7.5.3 ESSW-Trajectories

The realization of the double-slit scenario with single photons is also especially suited to implement a version of the gedankenexperiment of "surrealistic" trajectories, as discussed

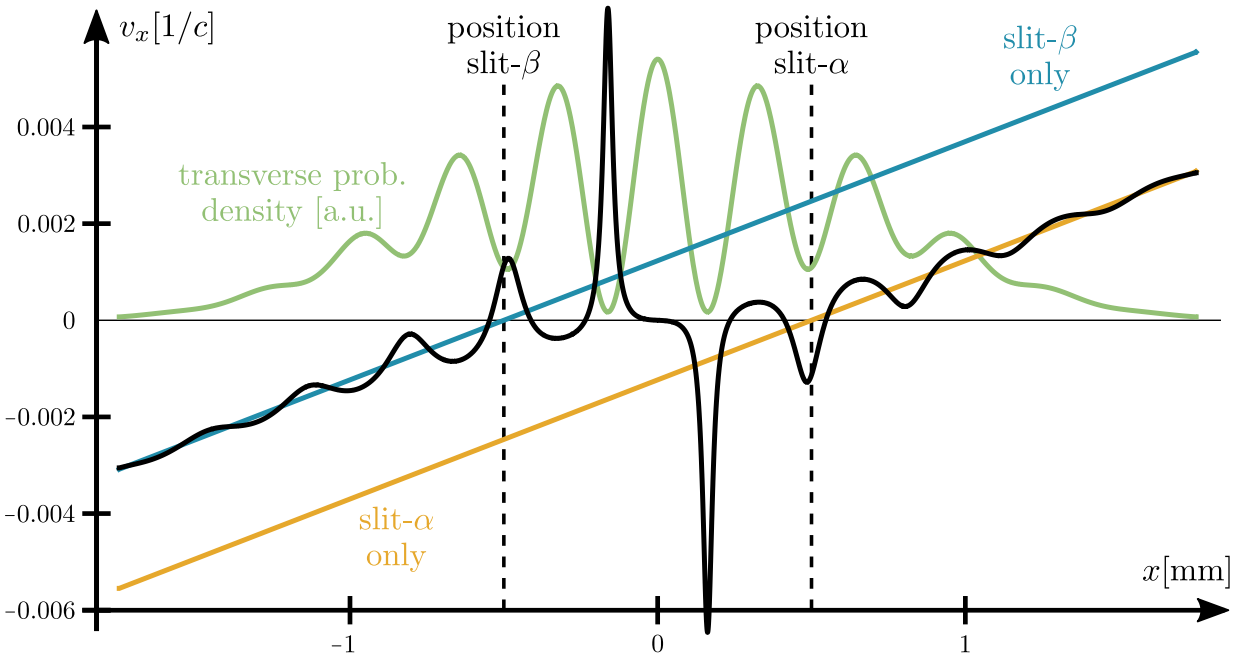

Figure 7.8: **Horizontal Components of Velocity** The black line shows the transverse velocity of the double-slit field with the same parameters as used in Fig. 7.7, evaluated at the longitudinal position $z = 0.4$m. The dashed vertical lines indicate the centers of the two slits At the edges, the velocity approaches asymptotically the velocities of the single slits α and β, shown as the tilted straight yellow and blue lines, respectively. Additionally, the transverse probability density is overlayed for reference. It can be seen that the peaks of the velocity coincide with the minima of the probability density. Furthermore, crucially due to the peaks there are regions on either side of the origin $x = 0$, where the sign of the velocity indicates a propagation towards the origin, against the general beam divergence.

in Sec. 7.3.2. Following the experimental approach of Mahler *et al.* [308] based on a proposal by Braverman and Simon [841], the original scenario of disjoint paths, as devised by ESSW, is replaced by a which-path measurement in a double-slit, as introduced in Sec. 5.3.3. While in this case the correlation between the position of the measured particle in the slit and the observed outcome on the measuring particle are not perfect, the nonlocal influences between the particles can be shown in a graphically illustrative manner.

The crucial physical element of the ESSW scenario is the state (7.14) in which the spatial degree of freedom of particle A is entangled with an internal degree of freedom of a second particle but not with its spatial state. In the photonic setting, instead of aiming to achieve this state via a which-path measurement interaction between two photons, a SPDC source of entangled photons, as described in Sec. 5.2.3, is used. Starting with a polarization-entangled two-photon state of the form (5.28), the double-slit is created through a polarization-dependent splitting of the spatial wavefunction of photon A, followed by a path-dependent rotation of its polarization, see Sec. 7.7.2 for the experimental

details. The resulting two-photon wavefunction $|\Psi\rangle$ has the form

$$|\Psi(\vec{x}_A, \vec{x}_B)\rangle = \frac{1}{\sqrt{2}}\Big(\psi_\alpha(\vec{x}_A)\,|C_B\rangle + \psi_\beta(\vec{x}_A)\,|D_B\rangle\Big)\,|P_A\rangle\,\chi(\vec{x}_B), \tag{7.25}$$

where the spatial wavefunctions ψ_α and ψ_β of photon A are correlated with the orthogonal polarization states $|C_B\rangle$ and $|D_B\rangle$ of photon B. Both the polarization $|P_A\rangle$ of photon A, which is equal for both slits, and the spatial PWF χ of photon B factorize from the entangled degrees of freedom. The above state is a special case of the state (7.21) with equal amplitudes $c_\alpha = c_\beta$ and vanishing coherence $\eta = 0$, such that the relative phase φ is irrelevant for the velocity. Note that all state parameters are time-independent since the spatial wavefunction of particle B factorizes.

For the state (7.25) the velocity field (7.22) simplifies to a simple weighted average of the single-slit velocity fields, with

$$\vec{v}_A(\vec{x}_A) = \frac{c}{k}\left(p_\alpha(\vec{x}_A)\,\vec{k}^{(\alpha)}_{\mathrm{loc}}(\vec{x}_A) + p_\beta(\vec{x}_A)\,\vec{k}^{(\beta)}_{\mathrm{loc}}(\vec{x}_A)\right), \tag{7.26}$$

where the local relative weights of the two slits p_j are given by

$$p_j(\vec{x}_A) = \frac{|\psi_j(\vec{x}_A)|^2}{|\psi_\alpha(\vec{x}_A)|^2 + |\psi_\beta(\vec{x}_A)|^2}. \tag{7.27}$$

Since any dependence on the position of photon B cancels out, the behavior of photon A in this case is strictly local, i.e., it depends solely on the two components of its wavefunction at its location $\vec{x}_A$. In contrast, the evolution of the position of photon A will have a nonlocal effect on photon B and lead to a continuous rotation of its polarization through the nonlocal dependence expressed in Eq. (7.25), where the relative amplitudes of the two polarization states are modified by the complex factors $\psi_j(\vec{x}_A)$. Note, however, that also here, at least from Bohmian perspective, the polarization is strictly not a property of photon B but only of its wavefunction.

Assuming again Gaussian slit functions as in the preceding section, the resulting horizontal trajectories are shown in Fig. 7.9. These trajectories are "surrealistic" in the sense of ESSW since there is non-vanishing support of the two slit function ψ_α and ψ_β on both sides of the symmetry axis $x = 0$ while the trajectories never cross that line. In effect, there will be a subset of outcomes for which the which-path measurement will "indicate" passage through one slit in the sense of ESSW while the Bohmian theory will retrodict passage through the other. From the Bohmian perspective this behavior is not problematic and the possible outcomes of polarization measurements on photon B are fully explained by a nonlocal influence of the current position of photon A, mediated by the entangled two-photon wavefunction.

7.5.4 Bohmian Steering

Apart from nonlocal influences due to the free evolution of the two systems, BM also allows for instantaneous changes of the evolution of a remote system due to experimental

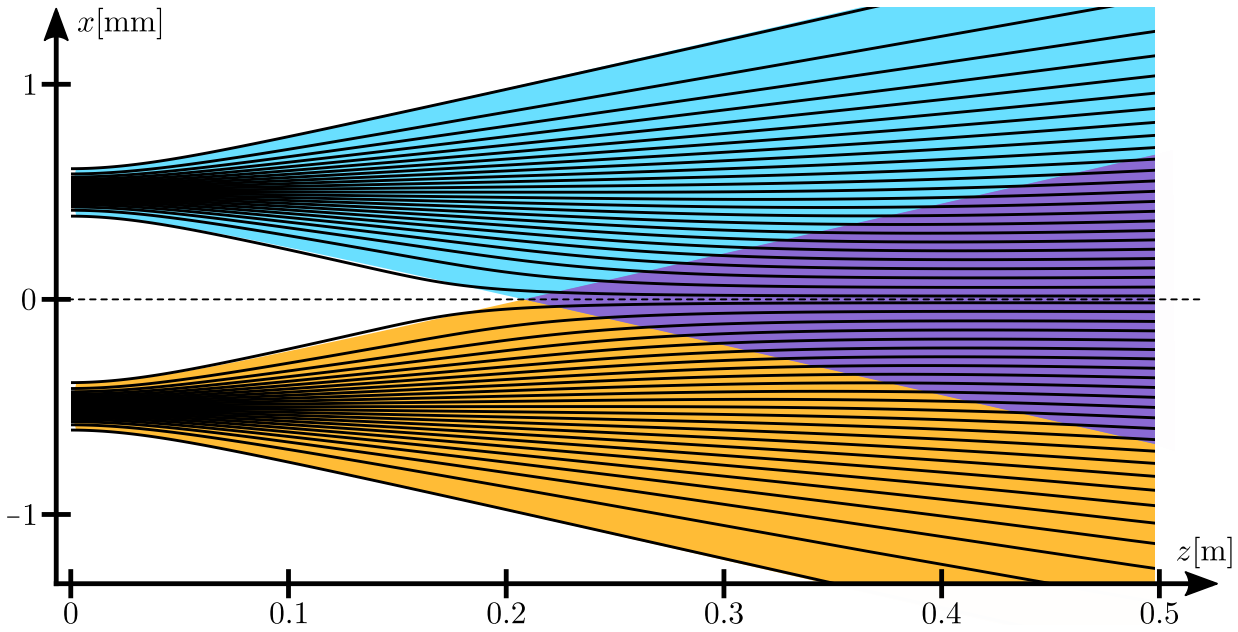

Figure 7.9: **Equivalent of ESSW-Trajectories in Double-Slit** The trajectories are calculated using the same beam parameters as in Fig. 7.7, where additionally, the colored backgrounds (light blue and yellow) indicate the regions of significant support of the two components of the wavefunction corresponding to the two slits. The purple background marks the region where both components have non-vanishing support. Due to the perfect path marking there is no coherence between the two components, i.e., $\eta = 0$, and the resulting guiding field thus corresponds to an incoherent sum of the two single guiding fields, resulting in an absence of interference fringes. As in the ESSW scenario there are some particles which transfer from being in the support of only one of the two components to being in the support of both. For those particles there exists a non-vanishing probability that the result of the which-path measurement will indicate passage through a different slit than the one attributed to them by BM.

interventions at a space-like separated site. These effects go beyond the strictly operational notion of steering, as introduced in 3.4.2, which merely corresponds to the strictly dispositive ascription of effective states to remote or past systems, due to conditioning on certain local measurement outcomes. In contrast, according to BM, in dependence on the time-ordering given by a preferred foliation, changes in the evolution of the system at one site in general have instantaneous effects on the behavior of other systems and thus "steering" in a more literal sense is present [820, 841, 884, 911]. These effects can of course also be realized in the scenario of two entangled photons.

The evolution of photon A in the double-slit interference field can be steered remotely by inducing a measurement of photon B in some particular polarization basis $\{|E\rangle, |F\rangle\}$, as described in the context of the Bell-scenario in Sec. 7.3.1. Assuming the initial path-

marked state $|\Psi\rangle$ from Eq. (7.25) this measurement leads to the state

$$|\Psi'(\vec{x}_A,\vec{x}_B)\rangle = \frac{1}{\sqrt{2}}\Big(\psi_E(\vec{x}_A)\chi_E(\vec{x}_B)\,|E_B\rangle + \psi_F(\vec{x}_A)\chi_F(\vec{x}_B)\,|F_B\rangle\Big)\,|P_A\rangle\,, \tag{7.28}$$

with the effective conditional wavefunctions for the slit photon A

$$\begin{aligned}\psi_E(\vec{x}_A) &= \mu_{EC}\psi_\alpha(\vec{x}_A) + \mu_{ED}\psi_\beta(\vec{x}_A)\\ \psi_F(\vec{x}_A) &= \mu_{FC}\psi_\alpha(\vec{x}_A) + \mu_{FD}\psi_\beta(\vec{x}_A),\end{aligned} \tag{7.29}$$

where the complex amplitudes μ are defined just as in Eq. (7.12). Note that, as shown in Sec. 7.3.1, "measurement" is this context does not need to involve a FAPP irreversible process or macroscopic amplification and instead the only requirement is that the wave-packets χ_E and χ_F have disjoint supports, see also [881]. Such a state is thus realized for example if the state of photon B is separated at a suitably oriented polarizing beam-splitter. Again similarly to the Bell-scenario, since photon B has a definite position in one of the two supports of the two components χ_E and χ_F, an effective collapse occurs and photon A is guided by one of the two superpositions of slit-functions ψ_E or ψ_F, where the relative amplitudes depend on the choice of measurement basis $\{|E_B\rangle\,,|F_B\rangle\}$. The conditional state of the slit-photon then again corresponds to a state of the form (7.21) with $\eta = 1$ and the gradual splitting of the wave-packets of photon B represents an example of a possible time-evolution of the state parameters c_j and φ defined in Eq. 7.21. As discussed in Sec. 5.3.3, erasure of the which-path measurement is achieved whenever $\mu_{jC} = \mu_{jD}$.

In contrast to SQM in BM the exact time-ordering of the measurement of photon B with respect to the propagation of photon A is of crucial importance and leads to different physical situations, which empirically are fully equivalent. In Fig. 7.10 the effective trajectories for three different temporal relations are presented, where photon B is projected onto $|E_B\rangle = (|C_B\rangle + i\,|D_B\rangle)/\sqrt{2}$ and $|F_B\rangle = (|C_B\rangle - i\,|D_B\rangle)/\sqrt{2}$, resulting in interference patterns which are phase-shifted by $\pm\pi/2$ relative to Fig. 7.7. In panel a) the effective collapse happens before photon A propagates through the slit, such that for several repetitions with an ensemble of photon pairs, the ensemble is effectively separated into two groups, dependent on the corresponding position of the respective partner photons B either in the support of χ_E or χ_F. Those two groups, as shown by the different colors, are then guided by two distinct velocity fields corresponding to complementary superpositions of the two slit-functions ψ_α and ψ_β, for the whole duration of the propagation. While these trajectories cross in the phase-space of photon A, they still do not cross in configuration space, since the two species of trajectories are correlated with positions $\vec{x}_B$ in disjoint spatial regions.

In Figs. 7.10b and c the resulting trajectories are shown for cases in which the separation of the wave-packets for photon B is performed at a later point of the evolution of the slit-photon, in particular when the latter has already reached a region of overlapping support of the two slit functions. Up until the time the splitting is induced photon A follows the ESSW-trajectories shown in Fig. 7.9 and after the splitting again two species of trajectories emerge. As discussed above, during the initial propagation the polarization of photon B is

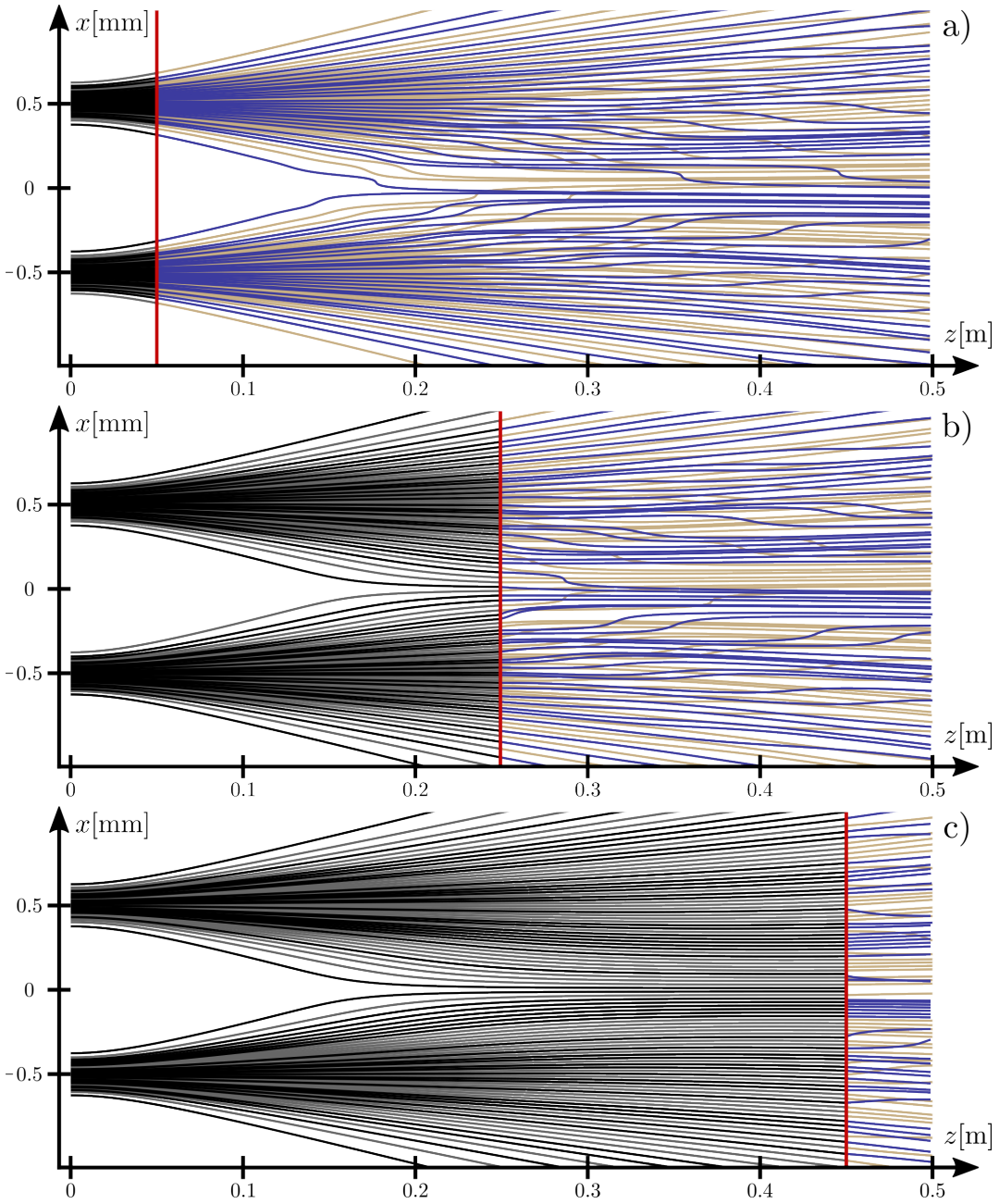

Figure 7.10: **Time-Ordering of Steering** The three figures show the variation of the effect on photon A, when the wavefunction components of photon B are split at different times of the evolution, by projections onto $|E_B\rangle$ (blue) and $|F_B\rangle$ (yellow), where for better illustration trajectories corresponding to $|F_B\rangle$ have reduced opacity. If the splitting is done early (a), the ensemble of slit-photons is split randomly into two groups which are then guided by different fields. The randomness stems from the unknown initial position of particle B and is here simulated via a weighted Monte-Carlo algorithm. In contrast, if the splitting happens at a later stage or after the evolution, as shown in panels b) and c), the location of photon A becomes more and more correlated with the polarization of photon B, such that the splitting of the latter groups the slit-photons according to their location. In all cases exactly the same correlations are observed.

continuously rotated in dependence on the position of photon A according to Eq. (7.25). This rotated polarization determines then the relative probability that photon B will follow any of the two possible paths, corresponding to outcomes E and F upon the separation of its spatial wave-packet, i.e., it is possible that for certain positions $\vec{x}_A$ of photon A the measurement outcome of photon B will be fully or at least approximately determined solely by the position of photon A. This is the case exactly when photon A is currently located in a valley of the corresponding transverse interference pattern and crucial for the correct reproduction of outcome statistics by BM. For example if the photon A happens to be at a position $\vec{x}_A$ where $\psi_\alpha = -\psi_\beta$, i.e., a perfect intensity minimum of the field shown in Fig. 7.7, and photon B is measured in the basis $\{|\pm\rangle = (|C\rangle_B \pm |D\rangle_B)/\sqrt{2}\}$, then the latter will experience only one non-vanishing wave-packet, i.e., the one corresponding to the state $|-\rangle$. In general, however, the attribution of a given photon A to one of the two velocity fields, will have some randomness due to the random position of photon B inside its initial wave-packet χ.

Note that in the three cases presented in Fig. 7.10 at each longitudinal position the transverse probability densities sum up to the incoherent sum of single-slit probability densities, exactly as in the case of ESSW-trajectories shown in Fig. 7.9, and also the average velocity field is the same. Furthermore, it is possible to consider the correlations between a measurement of the transverse probability density for an ensemble of photons A after the full propagation and the outcomes of the respective measurements of the corresponding photons B. These correlations will be exactly the same in all three scenarios. Thus, while according to Bohmian mechanics the separation of the wave-packets of photon B leads to an instantaneous change of the propagation of photon A, there is fundamentally no possibility to verify this change empirically [841, 884, 892]. Only after the classical information about the observed position of photon B in one of the supports of wave-packets χ_E or χ_F has been transmitted to site A, along with the particular time of separation, does it become possible to retrodict the corresponding Bohmian trajectory for each recorded photon at site A. Exactly because of this empirical equivalence of the various scenarios, it is impossible to determine the correct preferred foliation. Any time-ordering of the events at the two sites leads to the same observed correlations, albeit with different ontological explanations. To provide a concrete realist account of the nonlocal influences, as presented here, a particular preferred foliation has to be assumed for which, however, other physical motivations can be found, as mentioned in Sec. 7.4.1.

Further twists can be added to the scenario if the separation between the wave-packets of photon B is reversed while photon A is still propagating through the double-slit field, e.g., via a recombination of the separated wave-packets at a second polarizing beam-splitter, such that the effective collapse is reversed. In this case, illustrated in Fig. 7.11, the ensemble of photons A initially follows ESSW-trajectories, is subsequently split into two groups guided by distinct velocity fields, and finally, after the wave-packets of the corresponding photons B are merged, again follows the initial trajectories, albeit in a reshuffled manner. Such procedures could of course also be repeated and also partial splittings, i.e., weakened measurements of particle B could be implemented, which would lead to intermediate behavior.

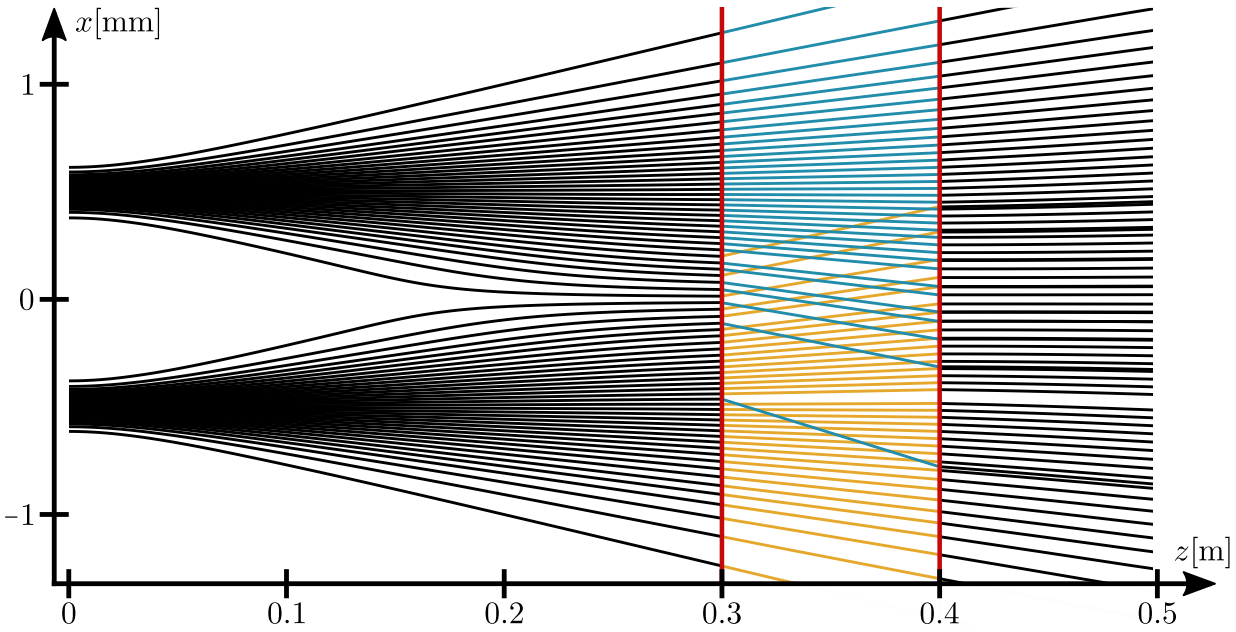

Figure 7.11: **Trajctories for Reversal of Effective Collapse** The splitting of the wavepacket of particle B into $|C_B\rangle$ and $|D_B\rangle$ is indicated, as in Fig. 7.10, by the vertical line at $z = 0.3$m, where the two colors yellow and blue indicate two groups of particles guided by different fields. The randomness in the attribution of each particle A to one of the groups is again simulated via a weighted Monte-Carlo algorithm. At propagation length $z = 0.4$m (indicated by the second vertical line) the wavepackets of particle B are recombined, leading to the recovery of a common guiding field for all particles in the slit field. During transition through the region $z = [0.3, 0.4]$, the trajectories of the particles A will cross, however, crucially in exactly such a manner that the overall transverse probability distribution remains unaffected.

7.6 Experimental Velocity Measurement

7.6.1 Weak Measurement of Bohmian Velocity

As mentioned in Sec. 7.4.2, the connection between Bohmian velocity and weak values has motivated experimental techniques for the reconstruction of Bohmian trajectories. According to Wiseman's basic ansatz a measurement of Bohmian velocity should be comprised of two measurements of particle position, first a weak measurement followed closely by a second ideal measurement, corresponding to a postselection [903]. However, alternatively, according to Eq. (7.17), the velocity can be also obtained by directly measuring the weak value of the velocity operator, along with a postselection performed at the exact time of the measurement. This last requirement can be ignored, whenever the velocity operator commutes with the future evolution of the system, as is the case for free photons.

In general for photons a measurement of velocity operators would require a coupling to the spin-operator $\vec{\mathbf{s}}$, i.e., a quantum measurement of the photonic Poynting current. However, as proposed in [878], for paraxial beams similar information about transverse

components of the velocity operator can be obtained by simply measuring the transverse momentum operator $\vec{\mathbf{p}}_T$, as defined in Sec. 5.1.2. Based on Eq. (7.22) the horizontal component of the velocity can be expressed as

$$v_x(\vec{x}_A) = \frac{c}{\hbar k} \frac{\mathrm{Re}\big[\mathrm{tr}\left(\mathbf{\Pi}_{\vec{x}_A} \mathbf{p}_x \rho\right)\big]}{\mathrm{tr}\left(\mathbf{\Pi}_{\vec{x}_A} \rho\right)} = \frac{c}{\hbar k} \mathrm{Re}\big[(\mathbf{p}_x)_w\big], \tag{7.30}$$

where the density operator ρ from Eq. (7.24), has been used to define the weak value. The real part of the weak value of transverse momentum thus exactly corresponds to the weighted average of local k-vectors

$$\mathrm{Re}\big[(\mathbf{p}_x)_w\big] = \hbar \sum_j p_j \, k^{(j)}_{\mathrm{loc},x}, \tag{7.31}$$

with weights p_j defined according to (7.27), which is exactly equivalent to the Bohmian velocity in case of linearly polarized light.

Additionally the imaginary part of $(\mathbf{p}_x)_w$ contains information about the osmotic k-vector and corresponds to [710, 873]

$$\mathrm{Im}\big[(\mathbf{p}_x)_w\big] = -\hbar \sum_j p_j \, k^{(j)}_{\mathrm{osm},x}, \tag{7.32}$$

which in turn represents a weighted averaging over the horizontal components of osmotic momentum. For a homogeneously circularly polarized field, a measurement of the weak values $(\mathbf{p}_x)_w$ and $(\mathbf{p}_y)_w$ thus allows a reconstruction both of the orbital part and of the spin part of the velocity, where for the latter expression (4.27) can be used.

7.6.2 Coupling via Birefringent Crystal

As introduced in Sec. 5.1, the toolbox of linear optics allows to implement a plethora of interactions between the various degrees of freedom of paraxial beams. Since in the photonic double-slit scenario the polarization degree of freedom of the slit-photon is not part of the entangled state, it is available to be employed as a pointer system in the measurement of the weak value of the transverse momentum $(\mathbf{p}_x)_w$ [878]. The corresponding effective interaction between transverse mode and the polarization degrees of freedom then can be induced via a uniaxial birefringent crystal, as introduced in Sec. 5.1.8. Assuming that the crystal is sufficiently thin, such that the effective relative and absolute retardation of the two polarization components can be ignored, the interaction unitary operator (5.18) acting on $\mathcal{H}_{\mathrm{pol}} \otimes \mathcal{H}_x$ simplifies to

$$\mathbf{U}_{\mathrm{BR}} = e^{-i\frac{\varepsilon}{\hbar}\boldsymbol{\sigma}_z \otimes \mathbf{p}_x}, \tag{7.33}$$

where the crystal is oriented such that the separation by 2ε happens in the horizontal direction with respect to horizontal and vertical polarization states, and furthermore no relative phase between the two components is introduced. The above evolution exactly

corresponds to an indirect measurement of the momentum operator $\mathbf{p}_x$ by coupling it to a pointer via the operator $\boldsymbol{\sigma}_z$, as described in Sec. 2.2.1. A momentum eigenstate, i.e., a plane wave arriving at the crystal with a momentum p_x, would thus experience a definite rotation of polarization of $\exp(-i\varepsilon p_x \boldsymbol{\sigma}_z/\hbar)$. As discussed in Sec. 6.1.3, for a weak measurement with a qubit pointer an initial pointer state from an unbiased basis with respect to the coupling operator has to be chosen. Since additionally linear polarization for the field is required, only one of the states $|\pm\rangle$ can be chosen as the initial polarization of the slits. In the following the pointer is assumed to be initially in the state $|+\rangle$. For a large ensemble of photons, a measurement of the complementary polarization expectation values $\langle\boldsymbol{\sigma}_y\rangle$ and $\langle\boldsymbol{\sigma}_z\rangle$ at some transverse location x, i.e., with postselection on $|x\rangle$, then allows to determine the weak value of transverse momentum with

$$(\mathbf{p}_x)_w \approx \frac{\hbar}{2\varepsilon}\left(\delta\langle\boldsymbol{\sigma}_y\rangle + i\delta\langle\boldsymbol{\sigma}_z\rangle\right), \tag{7.34}$$

where here the equivalent of expressions (6.17) for a qubit pointer has been employed. This allows to calculate the Bohmian velocity v_x via Eq. (7.30).

The same measurement process can also be analyzed without recourse to the formalism of weak values. For each of the slit-functions ψ_j in the state ρ, the birefringent crystal leads to the separation of horizontal and vertical polarization components with

$$\psi_j(x,z)\,|+\rangle \to \frac{1}{\sqrt{2}}\Big(\psi_j^{\varepsilon}(x,z)\,|H\rangle + \psi_j^{-\varepsilon}(x,z)\,|V\rangle\Big), \tag{7.35}$$

where $\psi_j^{\varepsilon}(x,z) = \psi_j(x-\varepsilon,z)$. Thus effectively at each position (x,z) the wavefunction of photon A has the effective polarization state $|P_j\rangle$ with

$$|P_j(x,z)\rangle = N_j(x,z)\Big(\psi_j^{\varepsilon}(x,z)\,|H\rangle + \psi_j^{-\varepsilon}(x,z)\,|V\rangle\Big) \tag{7.36}$$

with normalization

$$N_j(x,z) = \frac{1}{\sqrt{|\psi_j^{\varepsilon}(x,z)|^2 + |\psi_j^{-\varepsilon}(x,z)|^2}}. \tag{7.37}$$

While for the initial polarization state $|+\rangle$ it holds that $\langle+|\boldsymbol{\sigma}_z|+\rangle = \langle+|\boldsymbol{\sigma}_y|+\rangle = 0$, after the interaction small changes of local polarization encode information about the local properties of the scalar functions ψ_j. Since the calculation of $\langle\boldsymbol{\sigma}_z\rangle$ corresponds to a straight subtraction of $\psi_j^{-\varepsilon}$ from ψ_j^{ε}, it is particularly sensitive to the local change of modulus of ψ_j. Thus, it can be shown that for sufficiently small ε

$$\langle P_j(x,z)|\,\boldsymbol{\sigma}_z\,|P_j(x,z)\rangle \approx -2\varepsilon k_{\mathrm{osm},x}^{(j)}. \tag{7.38}$$

Similarly, as the calculation of $\langle\boldsymbol{\sigma}_y\rangle$ involves a subtraction of the projection of $|P_j\rangle$ on right and left-circular polarization, respectively, it is sensitive to changes in the relative phase

between H and V polarization, which is primarily related to the local phase gradient of ψ_j. Thus the local k-vector can be determined as

$$\langle P_j(x,z)|\,\boldsymbol{\sigma}_y\,|P_j(x,z)\rangle \approx 2\varepsilon k^{(j)}_{\mathrm{loc},x}. \tag{7.39}$$

Using Eqs. (7.31) and (7.32), the expressions for the shifts in the qubit expectation values $\langle\boldsymbol{\sigma}_z\rangle$ and $\langle\boldsymbol{\sigma}_y\rangle$ can be shown to exactly correspond to the relation (7.34) derived using the formalism of weak values.

While the approximations for Eqs. (7.34), (7.38) and (7.39) all rest on the assumption of a sufficiently small separation ε, this parameter has to be sufficiently small with respect to two different types of conditions. First, it needs to be sufficiently small compared to the horizontal variation of the modulus ϱ and phase ν of $\psi_j = \varrho e^{i\nu}$ since, among other reasons, in the derivation of the above equations the local derivatives of ϱ and ν are approximated via the differential quotients

$$\frac{\partial}{\partial x}\varrho(x,z) \approx \frac{\varrho(x-\varepsilon,z)-\varrho(x+\varepsilon,z)}{2\varepsilon}, \qquad \frac{\partial}{\partial x}\nu(x,z) \approx \frac{\nu(x-\varepsilon,z)-\nu(x+\varepsilon,z)}{2\varepsilon}. \tag{7.40}$$

The second approximation is strictly related to the particular behavior of qubit pointers and independent from the properties of ψ_j. In contrast to canonical measurements, in general expectation values of qubits are not shifted proportionally to an effective interaction strength ε outside of a weak regime close to their zero value. For example given an evolution of the form $\mathbf{U} = \exp(i\varepsilon\boldsymbol{\sigma}_z)$ acting on the state $|+\rangle$, the $\boldsymbol{\sigma}_y$ expectation value behaves as $\langle\boldsymbol{\sigma}_y\rangle = \sin\varepsilon$. As shown in Fig. 7.12, given the employed range of experimental parameters, the approximation $\sin\big(\varepsilon\mathrm{Re}\big[(\mathbf{p})_x\big]\big) \approx \varepsilon\mathrm{Re}\big[(\mathbf{p})_x\big]$, while valid over significant regions of the horizontal profile, fails noticeably for the extremes of transverse velocity. In contrast, the approximation of slowly varying modulus and phase of ψ_j is satisfied very well. In effect, to reduce the systematic error of the velocity estimation, the non-approximated form of the response of the qubit pointer is taken into account by using the modified expression

$$(\mathbf{p}_x)_w \approx \frac{\hbar}{2\varepsilon}\Big(\arcsin\big(\delta\langle\boldsymbol{\sigma}_y\rangle\big) + i\arcsin\big(\delta\langle\boldsymbol{\sigma}_z\rangle\big)\Big) \tag{7.41}$$

to reconstruct the velocity field from the data.

Since the effective interaction results in a transverse displacement of the two polarization components, its effect is independent from the longitudinal position z at which it is induced. The horizontal polarization profile $|P_A(x,z)\rangle$, which varies for all subsequent transverse planes, correctly encodes the local weak values of transverse momentum. This is equivalent to the fact that the interaction operator $\mathbf{U}_{\mathrm{BR}}$, defined in Eq. (7.33), commutes with the free evolution [878]. Alternatively, as mentioned above, the interaction can also be seen as an imprint of a k_x-dependent definite rotation of polarization for each component of the k-space wavefunction $\widetilde{\psi}(k_x,k_z)$. The resulting polarization at a particular location (x,z) of postselection then depends on the respective superposition of k_x components.

From the Bohmian perspective this weak measurement approach represents a measurement of properties of the wavefunction which is equivalent to a partial tomography of the

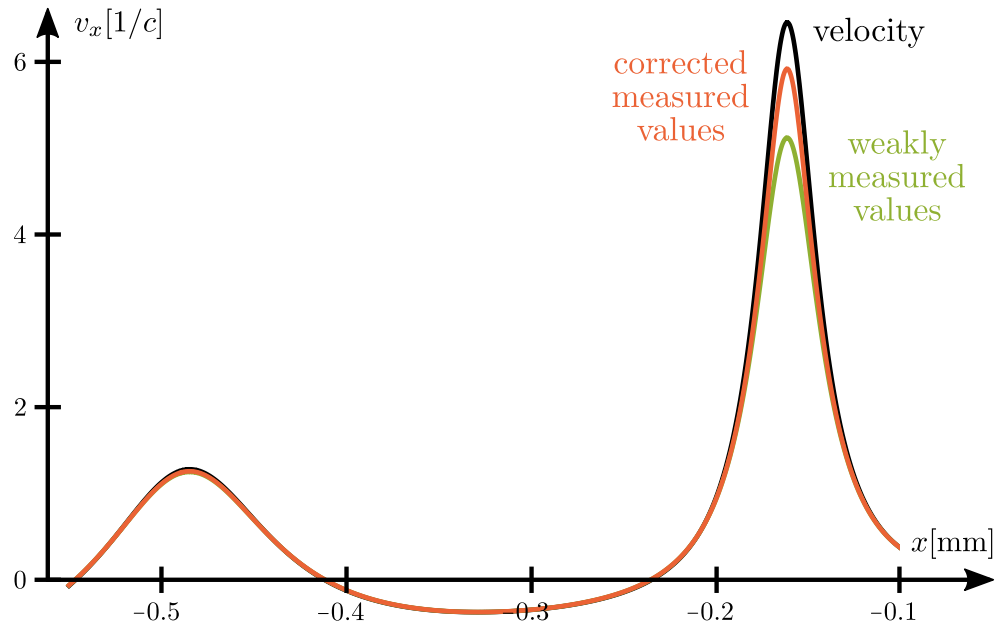

Figure 7.12: **Errors in Weak Approximation** While the black curve represents the correct signal, the green curve shows the value obtained with the weak measurement technique for a coupling strength of $\varepsilon = 10\mu$m (the remaining parameters are the same as for Fig. 7.8). The discrepancy is especially pronounced at peak values of transverse velocity. The error can be reduced significantly by employing the correction with the arcsin, as indicated by the red curve.

spatial state via interference of displaced components of the same wavefunction [625, 648, 894]. However, for a sufficiently fine-grained spatial postselection for which the transverse velocity is effectively constant over the whole postselected region, such weak measurements can be regarded to "map the intrinsic velocity fields" of Bohmian particles [879]. An alternative approach to measure the local k-vector directly via a conventional phase-front measurement has also been analyzed in [909]. Finally it has been proposed to generalize this approach to measure the whole three-dimensional velocity field using three independent pointer degrees of freedom [894].

7.6.3 Measurement Back-Action

Dependent on the amount of separation ε, the weak measurement described in the preceding section will have a varying amount of back-action on the future evolution of each particle in the slit [903]. In general the earlier the interaction is introduced with respect to the propagation through the interference region after the double-slit, the more significant the change of the corresponding trajectories. The back-action can be divided into changes of orbital and spin-current, respectively.

In the case of orbital current the situation is comparatively simple and each guiding field ψ_j is separated into an average of two incoherent slightly displaced guiding fields

according to Eq. (7.35). The orbital velocity field at a given location (x, z) then becomes

$$v_x(x,z) = \frac{c}{k}\big(p_H(x,z)\, k_{\mathrm{loc},x}(x-\varepsilon,z) + p_V(x,z)\, k_{\mathrm{loc},x}(x+\varepsilon,z)\big). \tag{7.42}$$

This effect is dominated not by differences between the local k-vectors but by changes in the relative local densities p_j. In effect, as shown in Fig. 7.13a it is strongest at the minima of the probability density, i.e., at the peaks of the velocity field. For the separation of $\varepsilon = 15\mu$m chosen for the experimental realization in this work, this effect of back-action is clearly negligible.

With respect to spin-current the measurement back-action is more complicated. Since the information about the local weak value of transverse momentum is encoded in local changes of polarization, the latter is no longer homogeneous over the whole profile and components of spin-current appear, which can be calculated according to Eq. (4.24). As shown in Figs. 7.13a and b, the x-component of the emerging spin-current is not homogeneous in y-direction, i.e., particles follow slightly different trajectories in vertically displaced xz-planes of the double-slit. Thus, since the experimental realization as described in the next section, involves an averaging over the whole y-direction of the field, the particles detected at a particular x-position in fact have followed slightly different trajectories as an effect of the back-action of the weak measurement. This effect is strongest at the peaks of velocity, where the maximal amount of circularity is present in the horizontal polarization profile. However, just as with the orbital current, also this disturbance is negligible for the chosen weak measurement strength.

7.7 Experimental Delayed Choice Investigation

7.7.1 Experimental Setup

Bohmian double-slit trajectories of photons have been reconstructed based on weak measurements in three experiments. The first implementation by Kocsis *et al.* [878] employed a single-photon source to reconstruct coherent trajectories of the form showed in Fig. 7.7 on a single-photon basis, where the detection was realized using a cooled CCD camera. Two subsequent experiments addressed the nonlocal influences between entangled photons, one of which is propagating through the double-slit field. While the work by Mahler *et al.* [308] recorded ESSW-trajectories and demonstrated the continuous rotation of the polarization of photon B, the experiment by Xiao *et al.* [911] considered a steering scenario in which the effect of the separation of the wave-packets of photon B in dependence on the chosen measurement basis was investigated. Both latter experiments employ cameras with single-photon resolution, which need to be triggered on the detection of photon B to distinguish the actual detection of photon A from background noise. Since this process of electronic triggering is slow compared to the time particle A spends in the double-slit field, crucially the macroscopic measurement of photon B has to be concluded before particle A even enters the slit. In effect, as shown in Fig. 7.14a for any possible foliation, the measurement of photon B is strictly in the past with respect to the propagation of photon

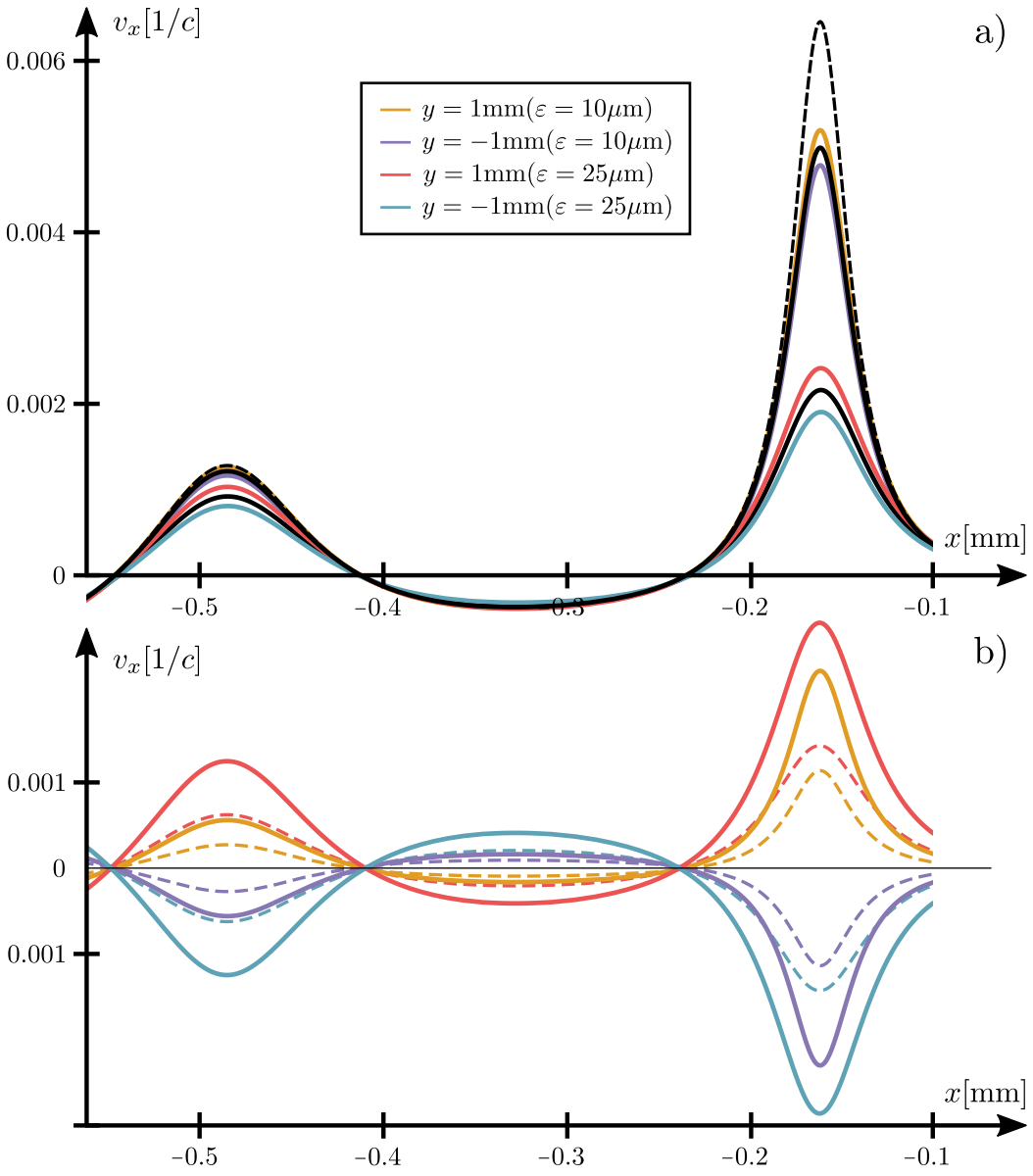

Figure 7.13: **Back-Action due to Weak Measurement** In panel a), the undisturbed velocity is represented by the black dashed line. The two solid black lines show strictly orbital reductions of peak velocity due to guiding via the incoherent sum of the displaced velocity fields (ϵ =10μm, 20μm), corresponding to horizontal and vertical polarizations. The additional effects of spin-current, which appears due to the slight circularity of the polarization, are indicated with colored lines. As indicated, the effect of the spin-current might vary over the vertical position y of the field, which has a width in the order of 1mm. In panel b) the spin-current is re-plotted for clarity without the orbital contribution, where the dashed lines correspond to medium vertical positions with $y = \pm 0.5$mm, respectively.

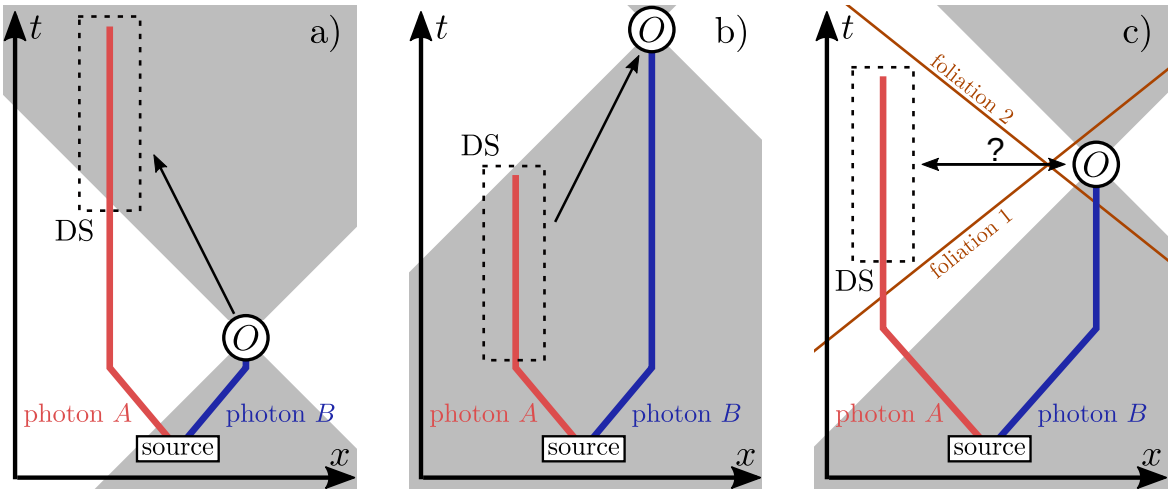

Figure 7.14: **Time-Ordering in Double-Slit Experiments** In the scenario shown in panel a), the observations on photon B lie fully in the causal past of the propagation of photon A through the double-slit field (indicated by a dashed box). The scenario of ESSW-trajectories thus cannot be realized. In contrast, panels b) and c) show experiments with potential ESSW-trajectories. Since in panel b) the observations on photon B are strictly in the future of the double-slit propagation, the structure of BM indicates a causal influence of particle A on particle B. In case c) of space-like separation, the structure of causal influences depends on the foliation and in general mutual causal influences between the two particles are possible.

A through the slit. Since the empirical correlations in the outcomes of the measurements on the two photons are independent of the time-ordering, as discussed in Sec. 7.5.4, in both experiments the nonlocal effects are reproduced via postprocessing and appropriate selection of data. From a Bohmian perspective, however, neither ESSW-trajectories nor actual steering is *factually* realized.

The experiment, which was begun in the course of this work, aims to overcome the shortcoming of the previous experiments described above. The core idea is the usage of a different type of spatially-resolving detection for photon A passing through the double-slit, which does not require a prior triggering but allows to detect both photons simultaneously. The corresponding setup is shown in Fig. 7.15. The polarization-entangled two-photon state is generated by the source briefly sketched in Sec. 5.2.3 and described in detail in [909]. While the weak measurement of the velocity-field of photon A is described above in Sec. 7.6, the generation of the slit and the spatially-resolving polarization measurement are presented in the subsequent subsections. As mentioned in Sec. 7.5.4, the separation of the wave-packets of photon B is achieved via a polarizing beam-splitter. The detection of the photons is implemented by capturing them in multi-mode fibers, which guide them to APDs. An electronic coincidence detection device then filters the sequences of detection signals from detectors for the two photons for events of simultaneous detection. A controlled delay applied to photon B allows to tune the time-ordering between the propagation of photon A and the separation of wave-packets of photon B in the rest frame

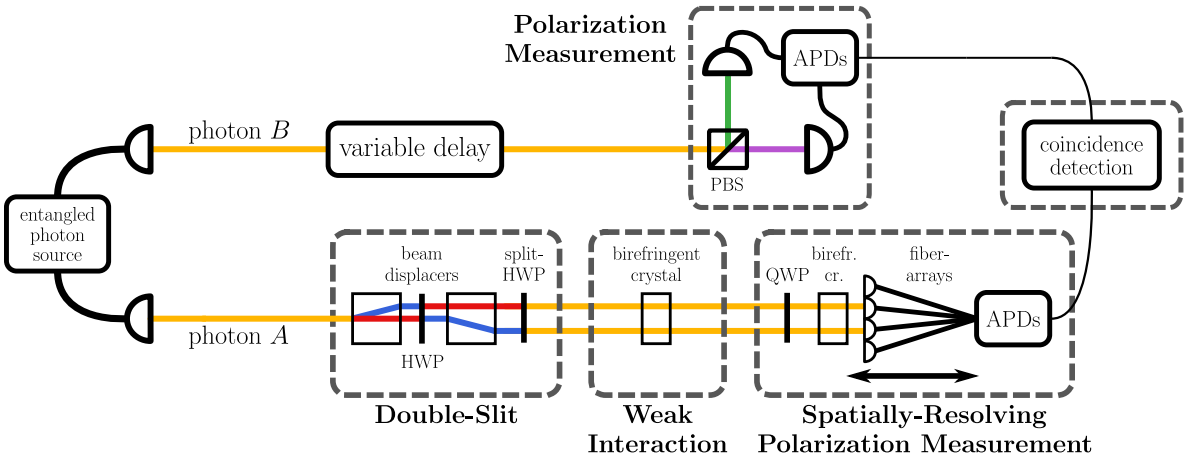

Figure 7.15: **Experimental Setup** After the entangled two-photon states are generated in a SPDC-source, see Sec. 5.2.3, the two photons are coupled into optical fibers and distributed to two distinct experimental sites, where they are out-coupled and continue free propagation. Photon A undergoes the generation of the double-slit, a weak interaction, and finally a spatially-resolving polarization measurement, which are described in Secs. 7.7.2, 7.6.2, and 7.7.3, respectively. For photon B a conventional polarization measurement is performed, after a tunable propagation distance, which effectively constitutes a variable delay. This polarization measurement is realized via a PBS and a pair of fiber-couplers, guiding the light to two APDs. Finally, a multi-channel coincidence unit allows to condition the detection events on two-photon correlations.

of the experimental laboratory. In the evaluation of the data, steering effects are retrodicted, assuming that this reference frame provides the preferred foliation. Nevertheless, as shown in Fig. 7.14b, the spatial separation between the two sites can be chosen sufficiently small, such that interventions performed on particle B are strictly in the causal future of particle's A entry into the slit and in the causal past of the conclusion of the propagation through the double-slit field. In effect, in these experiments at least some factual steering occurs for *any* preferred foliation. Alternatively, also measurement runs with large space-like separation can be performed, which are equivalent to a delayed-choice experiment, as discussed in Sec. 3.4.2, where Bell-correlations between the systems can be observed. In the latter case, however, there can exist foliations for which all interventions on particle B are strictly in the past or in the future of photon's A propagation through the interference field of the double-slit, as shown in Fig. 7.14c.

7.7.2 Generation of the Double-Slit

The basis of the experimental study is the two-photon state (7.14), which involves a perfect which-path marking of the path of photon A by the polarization of photon B. Starting from the polarization-entangled state of the form (5.28) produced by the source, the target state is achieved by using a birefringent polarization dependent beam-displacer to separate the horizontally and vertically polarized components of the slit-photon A in horizontal

direction. This leads to the two-photon state

$$|\Psi(\vec{x}_A, \vec{x}_B)\rangle = \frac{1}{\sqrt{2}}\Big(\psi_\alpha(\vec{x}_A)\,|H_A\rangle\,|H_B\rangle + \psi_\beta(\vec{x}_A)\,|V_A\rangle\,|V_B\rangle\Big)\chi(\vec{x}_B) \tag{7.43}$$

in which path and polarization of photon A together with the polarization of photon B form a three-partite entangled state. The corresponding geometry is sketched in Fig. 7.15. Since directly after the separation the two components of the slit are transversally fully disjoint, it is possible to manipulate them separately via two differently oriented half-waveplates, which allow to rotate them to the same polarization $|+\rangle$. This polarization then represents the initial pointer state for the weak velocity measurement. The unitary polarization rotation disentangles the polarization degree of freedom of photon A from the other two and achieves the state (7.14). Furthermore, in order to minimize loss of longitudinal coherence between the two slit-functions due to different optical path-lengths, *two* crystals in a zero-order configuration, as introduced in Sec. 5.1.8, are employed, with an additional half-waveplate flipping the horizontal and vertical polarizations of the two beam components between the crystals. In effect, both slit-functions experience exactly the same longitudinal evolution and all retardation effects cancel out.

To achieve a Fraunhofer scenario as introduced in Sec. 5.3.1, the beam of photon A is focused in horizontal direction using a cylindrical lens acting only in x-direction, such that the longitudinal position of the focus coincides with the region where the two crystals separate the beam components, as shown in Fig. 7.16. The double-slit function then effectively corresponds to a pair of one-dimensional Gaussian apertures, which spatially filter a plane-wave propagating in z-direction. As described below, the measurement of the horizontal velocity field requires an astigmatic beam profile in which the beam is effectively collimated in y-direction over the whole double-slit field. In effect, the vertical width of the beam at the waist has to be chosen sufficiently large corresponding to a sufficiently long Raleigh range. This collimation can be implemented for example directly using the out-coupler of the beam for photon A. In this case, however, the transverse beam profile at the longitudinal positions of the crystals will have significant extension in y-direction. Due to manufacturing imperfections in the crystals, they exhibit variations of thickness over the transverse surfaces of the facets. In combination with the significant vertical extension of the transverse profile over these facets, in effect the two slit-functions have different relative phases at different heights, which leads to the curved double-slit profile shown in Fig. 7.17a. To avoid this effect a pair of cylindrical lenses acting in y-direction is employed. As also shown in Fig. 7.16, the first of these lenses focuses the beam on the crystals also in vertical direction and the second one re-collimates the beam after it has sufficiently diverged. Since in effect the two slit beams propagate only through a small portion of the cross-section of the separation crystals, imperfections do not play a significant role and an equal phase-relation over the whole vertical extensions of the double-slit profile is achieved, as shown in Fig. 7.17b.

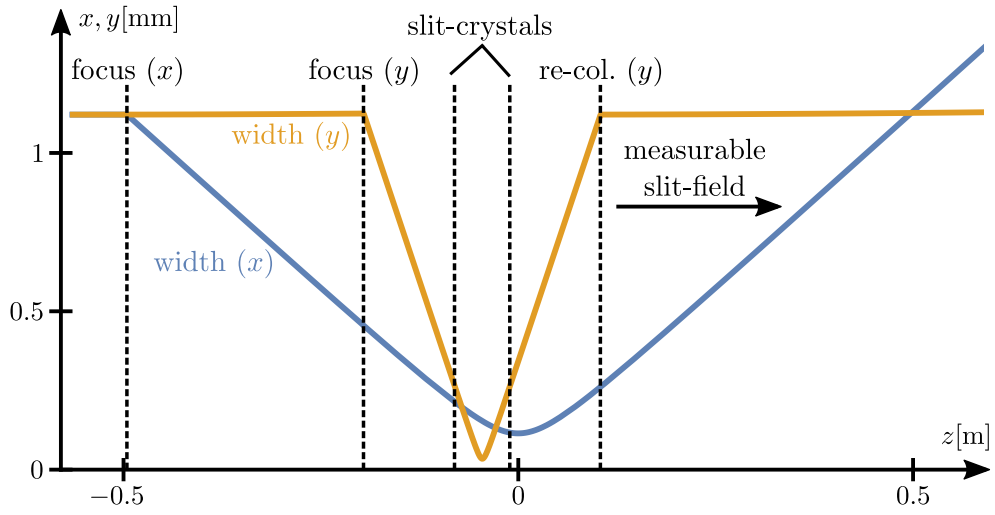

Figure 7.16: **Evolution of Beams over Double-Slit Field** The colored lines show the evolution of the beam width in x-direction (blue) and y-direction (yellow), respectively. After exit from a single mode fiber, the beam is collimated by a fiber-coupler, resulting in a waist in the order of 1.1mm. In x-direction the profile is shaped by only a single cylindrical lens with a focal length of 50cm, such that the longitudinal position of the focus ($w_0 \approx 110\mu$m) roughly coincides with the location of the slit-crystals. This exactly generates the desired interference field in the horizontal plane. For the y-direction a pair of equal cylindrical lenses ($f = 10$cm) allows to focus the beam at the location of the slit-crystals, while still recovering a collimation for the remaining propagation through the interference field, as required by the detection strategy.

7.7.3 Polarization Measurement

To measure the transverse velocity-field of photon A at a given longitudinal position according to Eq. (7.41), it is necessary to conduct a spatially-resolving polarization measurement. Furthermore, as mentioned above, no electronically triggered camera can be used since this would require a too early detection of photon B. The strategy chosen in this work is to employ an array of multi-mode fibers, each connected to a dedicated APD. These fiber-arrays then form the effective pixels of a low-noise single-photon camera with a much better temporal resolution than in the other experiments. Since, as discussed in Sec. 7.5.1, only the horizontal transverse velocity is of interest, it is sufficient to arrange the fiber-array in a horizontal direction. To achieve sufficient experimental efficiency, a cylindrical lens is then employed to focus the vertical transverse mode of the double-slit field into corresponding rows of fibers. As discussed in Sec. 7.6.3, this procedure is based on the assumption that the velocity field is approximately homogeneous in y-direction.

As shown in Fig. 7.18, the polarization is analyzed by combining an additional birefringent beam displacer with a quarter-waveplate, which together effectively implement a measurement of the $\boldsymbol{\sigma}_y$ operator of polarization. By comparing the counts $m_R^{(j)}$ and $m_L^{(j)}$ registered by the two APDs connected to the pair of fibers centered at the same transverse

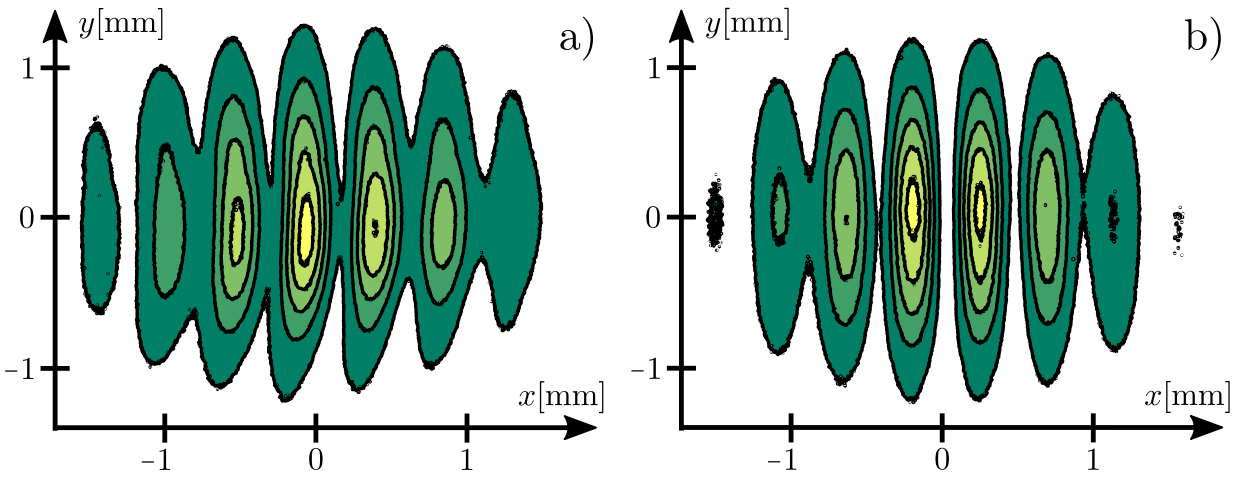

Figure 7.17: **Transverse Double-Slit Profiles** Panel a) shows the transverse double-slit profile without the focusing in y-direction, which was measured with a conventional CMOS camera and laser light. The variance of interferometric phase with vertical position y is larger than $\pi/2$. The additional focusing in y-direction leads the measurement of a decidedly improved profile shown in panel b).

location x_j, the local change of observable polarization $\delta\langle\boldsymbol{\sigma}_y\rangle$ can be determined via

$$\delta\langle\boldsymbol{\sigma}_y\rangle(x_j, z) \approx \frac{m_R^{(j)}(z) - m_L^{(j)}(z)}{m_R^{(j)}(z) + m_L^{(j)}(z)}, \tag{7.44}$$

assuming the initial polarization state $|+\rangle$. This allows to determine the Bohmian velocity via Eqs. (7.41) and (7.30). Note that the effective longitudinal position z of the velocity measurement is determined by the position of the fiber-arrays since they realize the post-selection on a particular position $\vec{x}_j$ and terminate the free evolution of the photon in the double-slit field. Just as the weak measurement interaction, also the final vertical separation of polarization components commutes with the free evolution Hamiltonian of photon A and thus in principle could be implemented at any point of the double-slit propagation, without affecting the observed results. However, the full separation of the two polarization components prior to capturing by the fibers also induces a back-action on the guiding fields, leading to different trajectories for the particles in the upper and lower part. Therefore, it is crucial that the distance from the final separation to the postselection of the photons is sufficiently small, if the photons captured at each horizontal location x in the lower and upper array are to be regarded as having followed similar trajectories, according to the Bohmian picture.

In conclusion, the experimental measurement stage for photon A consist of a cylindrical lens implementing a vertical focusing of the slit-field, followed by a quarter-waveplate and a birefringent crystal, after which two horizontal fiber-arrays capture the photon projected onto different polarization states. The corresponding evolution of the horizontal and vertical beam modes is shown in Fig. 7.19. Since for technical reasons it is impossible to use

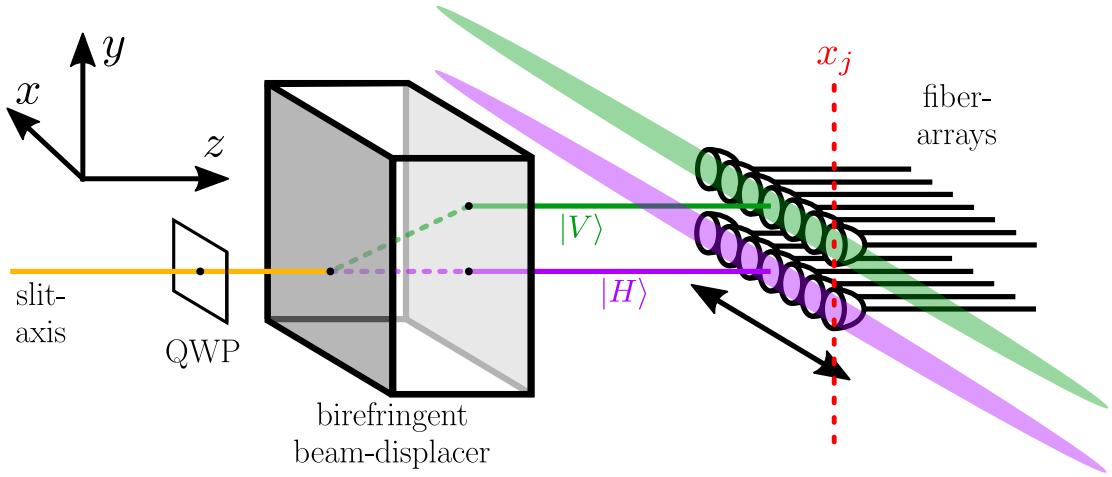

Figure 7.18: **Single-Photon Polarization Measurement** An effective projection onto the polarization states $|\circlearrowleft\rangle$ and $|\circlearrowright\rangle$ is achieved by combining a QWP with a birefringent beam-displacer oriented along the vertical axis. The QWP is set such that $|H\rangle \leftrightarrow |\circlearrowleft\rangle$ and $|V\rangle \leftrightarrow |\circlearrowright\rangle$ and in effect the slight transverse variation of the circularity of polarization, which encodes the transverse velocity, is transferred into a slight difference in the transverse probability distribution between the upper and the lower components of the wavefunction. This difference is detected as a difference in photon counts registered by a range of APDs connected to two vertically displaced horizontal fiber-arrays. By moving these arrays horizontally through the whole interference field, it is possible to determine the x-component of the transverse velocity for each transverse location x_j.

arrays which cover the whole horizontal extent of the slit-field, the arrays are instead moved in x-direction to scan all possible positions. This also allows to allocate more time to the collection of photons in the minima of the transverse intensity profile, which is necessary to achieve sufficient statistics and overcome shot-noise. In order to detect the velocity field at various longitudinal positions, the whole detection stage can be moved longitudinally. For reasons of experimental simplicity it is highly beneficial if the vertical focusing into the fiber arrays does not have to be adjusted at different z-positions. This can be achieved by using astigmatic beams, as described in the preceding subsection, which are collimated along the vertical direction over the length of the double-slit field.

7.7.4 Interpretation of Experimental Results

The implementation of the experiment described in the preceding sections is still ongoing. A preliminary partial test-experiment with a similar slit-geometry and the same weak measurement approach has been realized with coherent laser light and a conventional camera in [867]. This allowed the reconstruction of a velocity-field based on interfering slit-functions, leading to trajectories of the form 7.7. The current experimental effort is focused mainly on implementing the spatially-resolving polarization measurement system with single-photon sensitivity and in particular the faithful reconstruction of the transverse

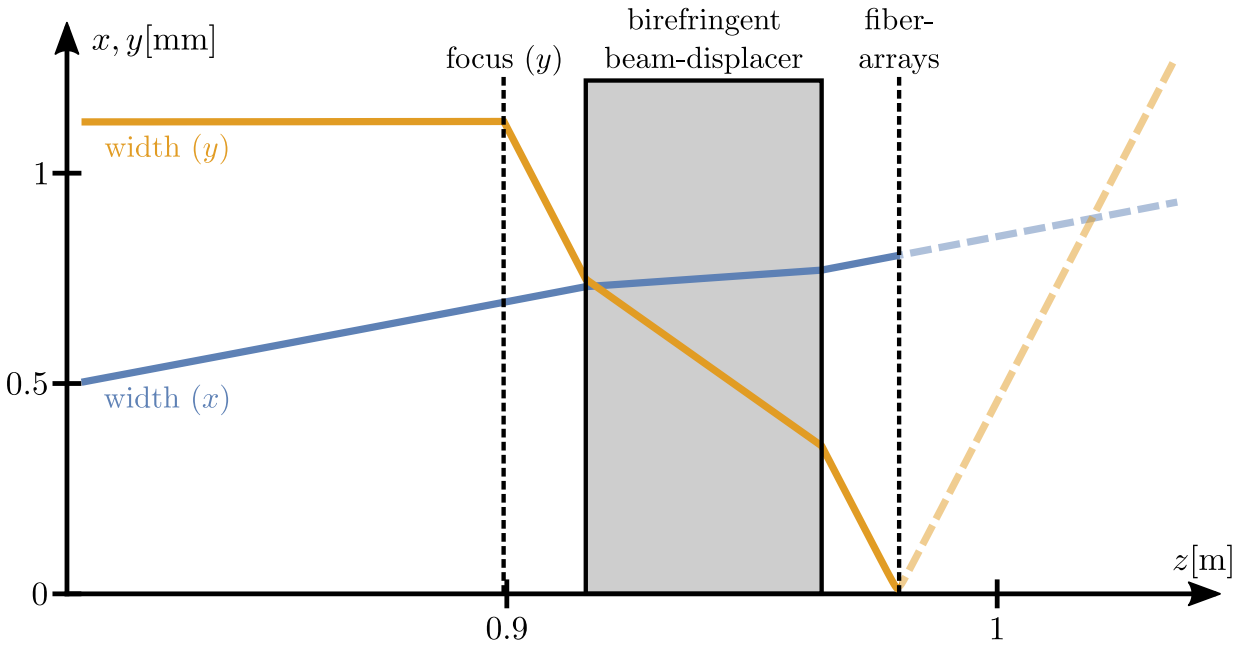

Figure 7.19: **Evolution of Beams at Detection Optics** The figure shows the evolution of the beam width (x-direction in blue, y-direction in yellow) at the detection system, where vertical lines indicate the longitudinal position of an additional cylindrical lens and the fiber arrays, respectively. While the beam propagation in x-direction should remain unaffected, apart from a retardation due to passage through the birefringent beam-displacer, the cylindrical lens ($f = 5$cm), focuses the light in y-direction onto the horizontal fiber-arrays. Since the beam is collimated with respect to the y-direction, the longitudinal position of the focus relative to the lens is not changed when the whole detection system is moved in longitudinal direction through the double-slit interference field to measure the velocity at different transverse planes.

intensity distribution via the multi-mode fibers of the detection array. Further results will be reported in future works.

The final photon-pair experiment will correspond to an implementation of nonlocal Bohmian steering of trajectories due to interventions at a remote site. It will allow to reconstruct the different conditional velocity fields experienced by photon A dependent on choices of measurement basis for photon B. Furthermore, it will demonstrate the empirical equivalence of the various possible time-orderings of measurements on the two photons, up to a full delayed-choice scenario in which the measurement of photon B is performed only after photon A has traversed the slit-field.

The goal of the experiment is not to prove or disprove Bohmian mechanics, which is fundamentally impossible via observations which follow the dispositive predictions of quantum mechanics. As put by Norsen and Struyve:

> First, as Einstein [...] famously remarked: "Whether you can observe a thing or not depends on the theory which you use. It is the theory which decides what can be observed". [...] The result of the empirical procedure coincides with certain things

> that are posited to actually exist by one candidate theory, Bohmian mechanics. But another candidate theory, which does not posit those things, also has no trouble accounting for the results. Indeed, insofar as the two theories are empirically equivalent, the results cannot really count as evidence for or against either theory. [884]

Instead this experiment illustrates, in an especially pronounced manner, the ontological implications of Bohmian mechanics and the particular physical mechanisms which lead to its equivalence with the standard quantum mechanical predictions. In the spirit of Wheeler:

> We search here, not for new experiments or new predictions, but for new insight. Experiments dramatize and predictions spell out the quantum's consequences... [1021]

Conclusion

It remains to assess what the presented work has contributed to answering the two principal questions posed in the introduction. With respect to the first question, three approaches to quantum reality have been discussed. The first of these is the strictly operational approach, sometimes called Copenhagen interpretation. It negates all access to an observer-independent reality based on the fact of complementarity, as codified through the impossibility of NCHV, together with impossibility to provide a locally causal description of the phenomena without recourse to arguably extreme positions such as superdeterminism or a multitude of worlds. Quantum physics is seen as providing a template of an abstract formal apparatus which allows to bring a coherent structure into a strictly dispositive account of empirical phenomena. The study [**P11**] analyzing the probabilistic certification of entanglement is an example of how this formalism can be practically applied without ontological commitments. However, it also highlights that even in the absence of questions about physical reality, other foundational problems remain, in this case the dependence on the justification of statistical conclusions on the foundational attitude towards statistical inference, i.e., either frequentism or Bayesianism.

Also the experiments [**P4**] and [**P8**] are described in the language of operational quantum mechanics. In [**P4**] an experimental procedure is demonstrated to realize a nonlocal QND measurement of a two-qubit system. By employing an entangled initial pointer state, it becomes possible to preserve the entanglement between the two qubits even if local measurements of their joint states are performed. The work [**P8**] is closer connected to applications and represents a first step in the direction of using integrated waveguide array structures as a platform for the simulation of open quantum systems. It nevertheless also has conceptional relevance as it investigates an alternative definition of information, which, while connected to the standard notion as introduced by Shannon and generalized to quantum information, is fundamentally based on the distinguishability of states of physical systems. Furthermore, it analyzes the way this information is distributed in the interaction of the system with its environment, in particular distinguishing two principal cases, where information fully flows to the environment or is stored in the system-environment correlations.

The second approach to quantum reality is based on weak values defined through the TSVF and allows to identify interphenomena, i.e., measurement-independent properties of quantum systems. In the context of the WTA, such weak values emerge as quantifiers of particle presence, which allow to give an account of the past evolution of quantum

particles. While weak values thus go beyond the standard set of statements of quantum mechanics, they do not correspond to beables, at least in the standard interpretation as proposed by Vaidman. Their reality is of epistemic nature, i.e., they represent a particular phenomenon. Crucially, the interpretation of weak values hinges on the question whether the quantum mechanical description can be applied to single systems or whether weak values merely constitute statistical properties of ensembles. The two experiments [**P1**] and [**P6**] both address this question. In the former work the effective coupling with a pre- and postselected system is shown to disturb the other system significantly less than a coupling with an only partially postselected system. In fact in the limit of vanishing coupling strength, there is a sense in which a weak value has the same empirical signature as an eigenvalue, thus inheriting its special status as expressed in the definition of elements of reality by EPR. The latter identification, however, hinges on the replacement of the original criterion of dispositive certainty with the criterion of pure resulting pointer states. In the second experiment a special type of weak value is reliably measured based on a single measurement outcome, i.e., without statistical averaging over an ensemble of particles. While the experimental implementation corresponds to a sequential coupling of several PPS to the same pointer, it is formally equivalent to the measurement of a robust weak value on a correspondingly large system. The concept of particle presence is addressed by [**P3**], where the universal modification of coupling of a PPS to three different pointer systems due to a modified presence is demonstrated. Also this experiment can be seen as a simplified version of a formally equivalent scenario in which a delocalized PPS couples to three distinct parts of local environments via three different degrees of freedom.

Finally Bohmian mechanics was presented as a paradigmatic example of a thoroughly realist interpretation of quantum mechanics. It was shown to solve the contradiction of Bell's theorem by explicitly incorporating action-at-a-distance. The nonlocal effects present in the theory were discussed in the context of a double-slit steering scenario, the experimental realization of which is still ongoing. Possible future avenues of research could involve considering nonlocal effects on two-photon interference or going beyond the paraxial approximation as proposed in [865, 864]. In particular it would be highly illustrative to achieve a scenario in which the reconstructed Bohmian trajectories are superluminal. Furthermore, measurement back-action effects which induce spin-currents could be avoided if the weak coupling to a polarization pointer would be replaced by a direct phasefront measurement.

All three discussed approaches give decidedly different answers to the first principal question of this thesis and all three are in equal agreement with the empirical phenomena. In consequence, while it appears difficult to argue for the unconditional need of a conception of quantum reality, it is in fact impossible to justify its categorical rejection. Nevertheless, the no-go theorems, chiefly Bell's theorem, delineate essential boundaries for any such concept.

The answer to the second question is also not clear cut. Neither of the three experiments involving weak values [**P1**],[**P3**],[**P6**] provides unconditional arguments to rule out a statistical interpretation of the observed results. However, each of them shows a particular phenomenon with a direct correspondence to a formal expression in terms of weak

values. This demonstrates that, at least in some scenarios, the time-symmetric formalism is especially suited to capture an effective epistemic reality. In any case all six experimental studies reported in this work, including the experimental reconstruction of Bohmian trajectories, can be explained in terms of all three interpretations, where in the case of the works [**P4**] and [**P8**] a description via weak values does not fill well due to the absence of weak measurements. However, [**P8**] of course directly addresses a time-symmetric scenario with postselection. Thus, none of these experimental studies demonstrates new physics in the sense of phenomena which go beyond the dispositive capabilities of SQM. They rather follow the tradition of Wheeler's illustrative experiments, which provide "insight" through the observation of particular physical phenomena, tailored specifically with the goal to bring out the prior unnoticed and often surprising consequences of various interpretations and to evaluate their suitability to describe the respective phenomena. As such, they primarily achieve a clarification of how various interpretations are to be applied and furthermore provide arguments of conceptual clarity in favor of one or the other approach.

The evolution of quantum mechanics has fostered a rich field of foundational investigations addressing core questions about the nature of physical science. This development represents a striking historical illustration of how realist and anti-realist positions can apply diametrically opposing interpretations to exactly the same corpus of experimentally observed phenomena. Among all these considerations, Bell's theorem stands out as a paradigmatic example of how basic foundational assumptions can be formally codified, which in turn, remarkably, allows to prove that quantum phenomena are in logical contradiction with a classical worldview. This result and the multitude of other scientific works on which this thesis is built are unified in the sublime scientific endeavor of humanity, which represents a priceless treasure in our times highly deserving of protection given the cynical disinformation rampant in the growing data-sphere of our world. The author has the humble hope that this treatise contributes to motivate the need for a continuing search of a proper understanding of quantum mechanics, as difficult as it might be, going beyond the mere facilitation of technological progress, as important as it is.

Science, after all, is the pursuit of truth.

List of Publications

[**P1**]
L. Vaidman, A. Ben-Israel, **J. Dziewior**, L. Knips, M. Weißl, J. Meinecke, C. Schwemmer, R. Ber, and H. Weinfurter,
Weak value beyond conditional expectation value of the pointer readings,
Physical Review A **96**, 032114 (2017).
Contribution: Conducted experiment and evaluated data together with LK and MW, performed theoretical analysis with LV and ABI, prepared manuscript together with LV, ABI, LK, MW, JM, and HW.

[**P2**]
L. Knips, **J. Dziewior**, A. Hashagen, J. D. A. Meinecke, M. M. Wolf, and H. Weinfurter,
Preprint: Procedures for the Optimal Measurement-Disturbance Tradeoff,
arXiv:1808.07882 (2018).
Contribution: Designed experiment together with LK, conducted experiment and evaluated data together with LK, performed theoretical analysis with AH and MW, prepared manuscript together with LK, AH, JDAM, MMW, and HW.

[**P3**]
J. Dziewior, L. Knips, D. Farfurnik, K. Senkalla, N. Benshalom, J. Efroni, J. Meinecke, S. Bar-Ad, H. Weinfurter, and L. Vaidman,
Universality of weak interaction of a particle in an arm of an interferometer and its application for alignment,
Proceedings of the National Academy of Sciences **116**, 2881 (2019).
Contribution: Designed experiment together with LK, HW, and LV, conducted experiment and evaluated data together with LK and KS, performed theoretical analysis with LV, prepared manuscript together with LK, DF, KS, NB, JE, JM, SBA, HW, and LV.

[**P4**]
X.-Y. Xu, W.-W. Pan, Q.-Q. Wang, **J. Dziewior**, L. Knips, Y. Kedem, K. Sun, J.-S. Xu, Y.-J. Han, C.-F. Li, G.-C. Guo, and L. Vaidman,
Measurements of nonlocal variables and demonstration of the failure of the product rule for a pre and postselected pair of photons,
Physical Review Letters **122**, 100405 (2019).
Contribution: Performed theoretical analysis together with LK and LV, edited the manuscript together with XYX, LK, YK, KS, CFL, and LV.

[**P5**]
L. Knips, **J. Dziewior**, W. Klobus, W. Laskowski, T. Paterek, P. J. Shadbolt, H. Weinfurter, and J. D. A. Meinecke,
Multipartite entanglement analysis from random correlations,
npj Quantum Information **6** (2020).
Contribution: Conducted experiment and evaluated data together with LK and JDAM, wrote manuscript together with LK, WK, WL, TP, HW, and JDAM.

[**P6**]
E. Rebufello, F. Piacentini, A. Avella, M. A. de Souza, M. Gramegna, **J. Dziewior**, E. Cohen, L. Vaidman, I. P. Degiovanni, and M. Genovese,
Anomalous weak values via a single photon detection,
Light: Science & Applications **10**, 106 (2021).
Contribution: Performed theoretical analysis together with EC and LV, wrote the manuscript together with ER, FP, AA, MAdS, MGr, EC, LV, IPD, and MGe.

[**P7**]
W. Kłobus, M. Miller, M. Pandit, R. Ganardi, L. Knips, **J. Dziewior**, J. Meinecke, H. Weinfurter, W. Laskowski, and T. Paterek,
Cooperation and dependencies in multipartite systems,
New Journal of Physics **23** (2021).
Contribution: Edited the manuscript together with WK, MM, MP, RG, LK, JM, HW, WL, and TP.

[**P8**]
J. Dziewior, L. Ruscio, L. Knips, E. Meyer, A. Szameit, and J. D. A. Meinecke,
Tracing Information Flow from Open Quantum Systems,
Laser & Photonics Reviews **19** (2025).
Contribution: Conducted experiment and evaluated data together with LR and JDAM, performed theoretical analysis with LR and JDAM, prepared manuscript together with LR, LK, AS, and JDAM.

[**P9**]
G. Reznik, C. Versmold, **J. Dziewior**, F. Huber, S. Bagchi, H. Weinfurter, J. Dressel, and L. Vaidman,
Photons are lying about where they have been, again,
Physics Letters A **470** (2023).
Contribution: Performed theoretical analysis with GR, CV, FH, JDr, and LV, conducted simulations with CV, prepared manuscript together with GR, CV, FH, SB, HW, JDr, and LV.

[**P10**]
P. Cieśliński, S. Imai, **J. Dziewior**, O. Gühne, L. Knips, W. Laskowski, J. Meinecke, T. Paterek, T. Vértesi,
Analysing quantum systems with randomised measurements,
Physics Reports **1095** (2024).
Contribution: Composed the content with PC and SI, prepared the manuscript with PC, SI, OG, LK, WL, JM, TP, and TV.

[**P11**]
P. Cieśliński, **J. Dziewior**, L. Knips, W. Kłobus, J. Meinecke, T. Paterek, H. Weinfurter, and W. Laskowski,
Valid and efficient entanglement verification with finite copies of a quantum state,
npj Quantum Information **10** (2024).
Contribution: Worked on conceptual analysis together with PC and LK, performed simulations together with PC and LK, prepared the manuscript together with PC, LK, WK, JM, TP, HW, and WL.

[**P12**]
A. Ben-Israel, L. Knips, **J. Dziewior**, J. Meinecke, A. Danan, H. Weinfurter, and L. Vaidman,
An Improved Experiment to Determine the 'Past of a Particle' in the Nested Mach-Zehnder Interferometer,
Chin. Phys. Lett. **34** (2017).
Contribution: Performed theoretical analysis together with ABI, LK, and LV, prepared the manuscript together with ABI, LK, JM, AD, HW, and LV.

Bibliography

Historical

Monographies

[1] N. Bohr. *Atomic Theory and the Description of Nature*. Reprint of the 1934 ed. with new preface. Cambridge University Press, 1961.

[2] P. W. Bridgman. *The Logic of Modern Physics*. New York: Macmillan, 1927.

[3] W. Heisenberg. *The Physical Principles of the Quantum Theory*. University of Chicago Press, 1930.

[4] J. v. Neumann. *Mathematische Grundlagen der Quantenmechanik*. Springer, 1932.

Articles

[5] C. D. Anderson. "The Positive Electron." In: *Phys. Rev.* 43.6 (1933), pp. 491–494.

[6] N. Bohr. "Can Quantum-Mechanical Description of Physical Reality be Considered Complete?" In: *Phys. Rev.* 48.8 (1935), pp. 696–702.

[7] M. Born. "Quantenmechanik der Stoßvorgänge." In: *Zeitschrift für Physik* 38.11 (1926), pp. 803–827.

[8] L. de Broglie. "La nouvelle dynamique des quanta." In: *Solvay* (1928), pp. 105–132.

[9] L. de Broglie. "Recherches sur la théorie des Quanta." Theses. Migration - université en cours d'affectation, 1924.

[10] L. de Broglie. *Research on the theory of quanta*. Minkowski Institute Press, 2021.

[11] H. B. G. Casimir. "On the attraction between two perfectly conducting plates." In: *Proc. K. Ned. Akad. Wet.* 51 (1948), p. 793.

[12] A. H. Compton and A. W. Simon. "Directed Quanta of Scattered X-Rays." In: *Phys. Rev.* 26.3 (1925), pp. 289–299.

[13] P. A. M. Dirac. "The quantum theory of the emission and absorption of radiation." In: *Proceedings of the Royal Society of London. Series A* 114.767 (1927), pp. 243–265.

[14] P. A. M. Dirac. "The quantum theory of the electron." In: *Proceedings of the Royal Society of London. Series A, Containing Papers of a Mathematical and Physical Character* 117.778 (1928), pp. 610–624.

[15] F. J. Dyson. "The Radiation Theories of Tomonaga, Schwinger, and Feynman." In: *Phys. Rev.* 75.3 (1949), pp. 486–502.

[16] A. Einstein. "über einen die Erzeugung und Verwandlung des Lichtes betreffenden heuristischen Gesichtspunkt." In: *Annalen der Physik* 322.6 (1905), pp. 132–148.

[17] A. Einstein. "Zur Elektrodynamik bewegter Körper." In: *Annalen der Physik* 322.10 (1905), pp. 891–921.

[18] A. Einstein, B. Podolsky, and N. Rosen. "Can Quantum-Mechanical Description of Physical Reality Be Considered Complete?" In: *Phys. Rev.* 47.10 (1935), pp. 777–780.

[19] A. Einstein and N. Rosen. "The Particle Problem in the General Theory of Relativity." In: *Phys. Rev.* 48.1 (1935), pp. 73–77.

[20] W. Gerlach and O. Stern. "Der experimentelle Nachweis der Richtungsquantelung im Magnetfeld." In: *Zeitschrift für Physik* 9.1 (1922), pp. 349–352.

[21] W. Heisenberg. "Über den anschaulichen Inhalt der quantentheoretischen Kinematik und Mechanik." In: *Zeitschrift für Physik* 43.3 (1927), pp. 172–198.

[22] W. Heisenberg. "Über quantentheoretische Umdeutung kinematischer und mechanischer Beziehungen." In: *Zeitschrift für Physik* 33 (1925), pp. 879–893.

[23] G. Hermann. “Die naturphilosophischen Grundlagen der Quantenmechanik.” In: *Abhandlugen der Fries'schen Schule* 6.2 (1935), pp. 69–152.

[24] E. H. Kennard. “Zur Quantenmechanik einfacher Bewegungstypen.” In: *Zeitschrift für Physik* 44.4 (1927), pp. 326–352.

[25] W. E. Lamb and R. C. Retherford. “Fine Structure of the Hydrogen Atom by a Microwave Method.” In: *Phys. Rev.* 72.3 (1947), pp. 241–243.

[26] L. Landau and R. Peierls. “Quantum electrodynamics in configuration space.” In: *Zeit. f. Phys.* 62 (1930), pp. 188–200.

[27] J. Larmor. “LXIII. On the theory of the magnetic influence on spectra; and on the radiation from moving ions.” In: *The London, Edinburgh, and Dublin Philosophical Magazine and Journal of Science* 44.271 (1897), pp. 503–512.

[28] G. N. Lewis. “The Conservation of Photons.” In: *Nature* 118.2981 (1926), pp. 874–875.

[29] G. Lüders. “über die Zustandsänderung durch den Meßprozeß.” In: *Annalen der Physik* 443.5-8 (1950), pp. 322–328.

[30] L. Mach. “Über einen Interferenzrefraktor.” In: *Zeitschrift für Instrumentenkunde* 12 (1892), pp. 89–93.

[31] E. Madelung. “Quantentheorie in hydrodynamischer Form.” In: *Zeitschrift für Physik* 40.3 (1927), pp. 322–326.

[32] T. D. Newton and E. P. Wigner. “Localized States for Elementary Systems.” In: *Rev. Mod. Phys.* 21.3 (1949), pp. 400–406.

[33] W. Pauli. “Die allgemeinen Prinzipien der Wellenmechanik.” In: *Quantentheorie*. Ed. by H. Bethe et al. Berlin, Heidelberg: Springer Berlin Heidelberg, 1933, pp. 83–272.

[34] W. Pauli. “über den Zusammenhang des Abschlusses der Elektronengruppen im Atom mit der Komplexstruktur der Spektren.” In: *Zeitschrift für Physik* 31.1 (1925), pp. 765–783.

[35] M. Planck. “Über das Gesetz der Energieverteilung im Normalspectrum.” In: *Annalen der Physik* 309.3 (1901), pp. 553–563.

[36] M. Planck. “Über eine Verbesserung der Wienschen Spektralgleichung.” In: *Verhandl. Dt. Phys. Ges.* 2 (1900), p. 202.

[37] M. Planck. “Zur Theorie des Gesetzes der Energieverteilung im Normalspectrum.” In: *Verhandl. Dt. Phys. Ges.* 2 (1900), p. 237.

[38] H. P. Robertson. “An Indeterminacy Relation for Several Observables and Its Classical Interpretation.” In: *Phys. Rev.* 46.9 (1934), pp. 794–801.

[39] H. P. Robertson. “The Uncertainty Principle.” In: *Phys. Rev.* 34.1 (1929), pp. 163–164.

[40] E. Schrödinger. “Quantisierung als Eigenwertproblem.” In: *Annalen der Physik* 384.4 (1926), pp. 361–376.

[41] E. Schrödinger. “Die gegenwärtige Situation in der Quantenmechanik.” In: *Naturwissenschaften* 23 (1935), pp. 807–812, 823–828, 844–849.

[42] E. Schrödinger. “Zum Heisenbergschen Unschärfeprinzip.” In: *Preuss. Akad. Wiss. Phys.-Math.* (1930), p. 296.

[43] G. I. Taylor. “Interference Fringes with Feeble Light.” In: *Proceedings of the Cambridge Philosophical Society* 15 (1909), pp. 114–115.

[44] H. Weyl. “Quantenmechanik und Gruppentheorie.” In: *Zeitschrift für Physik* 46.1 (1927), pp. 1–46.

[45] E. Wigner. “On the Quantum Correction For Thermodynamic Equilibrium.” In: *Phys. Rev.* 40.5 (1932), pp. 749–759.

[46] T. Young. “II. The Bakerian Lecture. On the theory of light and colours.” In: *Philosophical Transactions of the Royal Society of London* 92 (1802), pp. 12–48.

[47] L. Zehnder. “Ein neuer Interferenzrefraktor.” In: *Zeitschrift für Instrumentenkunde* 11 (1891), pp. 275–285.

Basic Quantum Mechanics

Monographies

[48] D. Bohm. *Quantum Theory*. Prentice-Hall, Inc., 1951.

[49] H. P. Breuer and F. Petruccione. *The theory of open quantum systems*. Oxford University Press, 2002.

[50] C. Cohen-Tannoudji, B. Diu, and F. Laloë. *Quantum Mechanics*. Vol. 1. Wiley-VCH, 2005.

[51] R. P. Feynman. *The Feynman Lectures on Physics. Volume III (Online Edition)*. 2013.

[52] H. S. Kalsi. *Electronic Instrumentation*. McGraw Hill, 2010.

[53] L. D. Landau and E. . Lifshitz. *Quantum Mechanics. Non-Relativistic Theory*. Pergamon Press, 1977.

[54] A. Messiah. *Quantum Mechanics*. Vol. 1. North-Holland, 1965.

[55] A. Messiah. *Quantum Mechanics*. Vol. 2. North-Holland, 1965.

[56] Á. Rivas and S. F. Huelga. *Open Quantum Systems*. Springer Heidelberg Dordrecht London New York, 2012.

[57] J. J. Sakurai. *Modern Quantum Mechanics*. Addison-Wesley, 1994.

[58] B. Thaller. *The Dirac Equation*. Springer, 1992.

[59] R. T. Weidner and R. L. Sells. *Elementary Modern Physics*. Allyn and Bacon, Inc., 1976.

Encyclopedic

[60] L. Ballentine. "States in Quantum Mechanics." In: *Compendium of Quantum Physics*. Ed. by D. Greenberger, K. Hentschel, and F. Weinert. Berlin, Heidelberg: Springer Berlin Heidelberg, 2009, pp. 742–744.

[61] L. E. Ballentine. "States, Pure and Mixed, and Their Representations." In: *Compendium of Quantum Physics*. Ed. by D. Greenberger, K. Hentschel, and F. Weinert. Berlin, Heidelberg: Springer Berlin Heidelberg, 2009, pp. 744–746.

[62] A. Borrelli. "Bose–Einstein Statistics." In: *Compendium of Quantum Physics*. Ed. by D. Greenberger, K. Hentschel, and F. Weinert. Berlin, Heidelberg: Springer Berlin Heidelberg, 2009, pp. 74–78.

[63] M. Breinig. "Schrodinger Equation." In: *Compendium of Quantum Physics*. Ed. by D. Greenberger, K. Hentschel, and F. Weinert. Berlin, Heidelberg: Springer Berlin Heidelberg, 2009, pp. 681–685.

[64] M. Breinig. "Wave Mechanics." In: *Compendium of Quantum Physics*. Ed. by D. Greenberger, K. Hentschel, and F. Weinert. Berlin, Heidelberg: Springer Berlin Heidelberg, 2009, pp. 822–827.

[65] B. Falkenburg. "Correspondence Principle." In: *Compendium of Quantum Physics*. Ed. by D. Greenberger, K. Hentschel, and F. Weinert. Berlin, Heidelberg: Springer Berlin Heidelberg, 2009, pp. 125–131.

[66] C. Held. "Gleason's Theorem." In: *Compendium of Quantum Physics*. Ed. by D. Greenberger, K. Hentschel, and F. Weinert. Berlin, Heidelberg: Springer Berlin Heidelberg, 2009, pp. 263–266.

[67] C. Held. "Kochen–Specker Theorem." In: *Compendium of Quantum Physics*. Ed. by D. Greenberger, K. Hentschel, and F. Weinert. Berlin, Heidelberg: Springer Berlin Heidelberg, 2009, pp. 331–335.

[68] B. J. Hiley. "Hidden Variables." In: *Compendium of Quantum Physics*. Ed. by D. Greenberger, K. Hentschel, and F. Weinert. Berlin, Heidelberg: Springer Berlin Heidelberg, 2009, pp. 284–287.

[69] N. Huggett and T. Imbo. "Indistinguishability." In: *Compendium of Quantum Physics*. Ed. by D. Greenberger, K. Hentschel, and F. Weinert. Berlin, Heidelberg: Springer Berlin Heidelberg, 2009, pp. 311–317.

[70] E. Joos. "Decoherence." In: *Compendium of Quantum Physics*. Ed. by D. Greenberger, K. Hentschel, and F. Weinert. Berlin, Heidelberg: Springer Berlin Heidelberg, 2009, pp. 155–159.

[71] H. Kragh. "Dirac Equation." In: *Compendium of Quantum Physics*. Ed. by D. Greenberger, K. Hentschel, and F. Weinert. Berlin, Heidelberg: Springer Berlin Heidelberg, 2009, pp. 171–172.

[72] H. Kragh. "Relativistic Quantum Mechanics." In: *Compendium of Quantum Physics*. Ed. by D. Greenberger, K. Hentschel, and F. Weinert. Berlin, Heidelberg: Springer Berlin Heidelberg, 2009, pp. 632–637.

[73] H. Kragh. "Wave Function." In: *Compendium of Quantum Physics*. Ed. by D. Greenberger, K. Hentschel, and F. Weinert. Berlin, Heidelberg: Springer Berlin Heidelberg, 2009, pp. 812–813.

[74] H. Kragh. "Wave Packet." In: *Compendium of Quantum Physics*. Ed. by D. Greenberger, K. Hentschel, and F. Weinert. Berlin, Heidelberg: Springer Berlin Heidelberg, 2009, pp. 828–830.

[75] N. P. Landsman. "Born Rule and its Interpretation." In: *Compendium of Quantum Physics*. Ed. by D. Greenberger, K. Hentschel, and F. Weinert. Berlin, Heidelberg: Springer Berlin Heidelberg, 2009, pp. 64–70.

[76] N. P. Landsman. "Quantization (Systematic)." In: *Compendium of Quantum Physics*. Ed. by D. Greenberger, K. Hentschel, and F. Weinert. Berlin, Heidelberg: Springer Berlin Heidelberg, 2009, pp. 510–514.

[77] M. Massimi. "Exclusion Principle (or Pauli Exclusion Principle)." In: *Compendium of Quantum Physics*. Ed. by D. Greenberger, K. Hentschel, and F. Weinert. Berlin, Heidelberg: Springer Berlin Heidelberg, 2009, pp. 220–222.

[78] S. Saunders. "Fermi-Dirac Statistics." In: *Compendium of Quantum Physics*. Ed. by D. Greenberger, K. Hentschel, and F. Weinert. Berlin, Heidelberg: Springer Berlin Heidelberg, 2009, pp. 230–235.

[79] S. Saunders. "Identity of Quanta." In: *Compendium of Quantum Physics*. Ed. by D. Greenberger, K. Hentschel, and F. Weinert. Berlin, Heidelberg: Springer Berlin Heidelberg, 2009, pp. 299–304.

[80] A. Shimony. "Hidden-Variables Models of Quantum Mechanics (Noncontextual and Contextual)." In: *Compendium of Quantum Physics*. Ed. by D. Greenberger, K. Hentschel, and F. Weinert. Berlin, Heidelberg: Springer Berlin Heidelberg, 2009, pp. 287–291.

[81] W. Stulpe. "Density Operator." In: *Compendium of Quantum Physics*. Ed. by D. Greenberger, K. Hentschel, and F. Weinert. Berlin, Heidelberg: Springer Berlin Heidelberg, 2009, pp. 166–169.

[82] W. Stulpe. "Unitary Operator." In: *Compendium of Quantum Physics*. Ed. by D. Greenberger, K. Hentschel, and F. Weinert. Berlin, Heidelberg: Springer Berlin Heidelberg, 2009, pp. 807–807.

[83] R. Tumulka. "Orthonormal Basis." In: *Compendium of Quantum Physics*. Ed. by D. Greenberger, K. Hentschel, and F. Weinert. Berlin, Heidelberg: Springer Berlin Heidelberg, 2009, pp. 447–449.

[84] S. Weigert. "No-Cloning Theorem." In: *Compendium of Quantum Physics*. Ed. by D. Greenberger, K. Hentschel, and F. Weinert. Berlin, Heidelberg: Springer Berlin Heidelberg, 2009, pp. 404–405.

[85] F. Weinert. "Stern–Gerlach Experiment." In: *Compendium of Quantum Physics*. Ed. by D. Greenberger, K. Hentschel, and F. Weinert. Berlin, Heidelberg: Springer Berlin Heidelberg, 2009, pp. 746–750.

[86] C. Witte. "Hamiltonian Operator." In: *Compendium of Quantum Physics*. Ed. by D. Greenberger, K. Hentschel, and F. Weinert. Berlin, Heidelberg: Springer Berlin Heidelberg, 2009, pp. 271–275.

Articles

[87] J. S. Bell. "On the Problem of Hidden Variables in Quantum Mechanics." In: *Rev. Mod. Phys.* 38.3 (1966), pp. 447–452.

[88] H.-P. Breuer. "Genuine quantum trajectories for non-Markovian processes." In: *Phys. Rev. A* 70.1 (2004), p. 012106.

[89] H.-P. Breuer, E.-M. Laine, and J. Piilo. "Measure for the Degree of Non-Markovian Behavior of Quantum Processes in Open Systems." In: *Phys. Rev. Lett.* 103.21 (2009), p. 210401.

[90] H.-P. Breuer et al. "Colloquium: Non-Markovian dynamics in open quantum systems." In: *Rev. Mod. Phys.* 88.2 (2016), p. 021002.

[91] A. Cabello. "How many questions do you need to probe that unasked questions have no answers?" In: *International Journal of Quantum Information* 04.01 (2006), pp. 55–61.

[92] A. Caldeira and A. Leggett. "Quantum tunnelling in a dissipative system." In: *Annals of Physics* 149.2 (1983), pp. 374–456.

[93] D. Chruściński, A. Kossakowski, and Á. Rivas. "Measures of non-Markovianity: Divisibility versus backflow of information." In: *Phys. Rev. A* 83.5 (2011), p. 052128.

[94] A. M. Gleason. "Measures on the Closed Subspaces of a Hilbert Space." In: *The Logico-Algebraic Approach to Quantum Mechanics: Volume I: Historical Evolution*. Ed. by C. A. Hooker. Dordrecht: Springer Netherlands, 1975, pp. 123–133.

[95] T. Heinosaari and M. Ziman. "Guide to Mathematical Concepts of Quantum Theory." In: *Acta Physica Slovaca* 58 (2008), pp. 487–674.

[96] S. Kochen and E. P. Specker. "The Problem of Hidden Variables in Quantum Mechanics." In: *Journal of Mathematics and Mechanics* 17.1 (1967), pp. 59–87.

[97] E.-M. Laine, J. Piilo, and H.-P. Breuer. "Measure for the non-Markovianity of quantum processes." In: *Phys. Rev. A* 81.6 (2010), p. 062115.

[98] L. Li, M. J. Hall, and H. M. Wiseman. "Concepts of quantum non-Markovianity: A hierarchy." In: *Physics Reports* 759 (2018). Concepts of quantum non-Markovianity: A hierarchy, pp. 1–51.

[99] J. Liu, X.-M. Lu, and X. Wang. "Nonunital non-Markovianity of quantum dynamics." In: *Phys. Rev. A* 87.4 (2013), p. 042103.

[100] D. Manzano. "A short introduction to the Lindblad master equation." In: *AIP Advances* 10.2 (2020), p. 025106.

[101] K.-P. Marzlin and T. Landry. "On the connection between the theorems of Gleason and of Kochen and Specker." In: *Canadian Journal of Physics* 93.12 (2015), pp. 1446–1452.

[102] N. D. Mermin. "Simple unified form for the major no-hidden-variables theorems." In: *Phys. Rev. Lett.* 65.27 (1990), pp. 3373–3376.

[103] V. Namias. "The Fractional Order Fourier Transform and its Application to Quantum Mechanics." In: *IMA Journal of Applied Mathematics* 25.3 (1980), pp. 241–265.

[104] Á. Rivas, S. F. Huelga, and M. B. Plenio. "Quantum non-Markovianity: characterization, quantification and detection." In: *Reports on Progress in Physics* 77.9 (2014), p. 094001.

[105] M. Seevinck. "Challenging the Gospel: Grete Hermann on von Neumann's No-Hidden-Variables Proof." In: *Grete Hermann - Between Physics and Philosophy*. Ed. by E. Crull and G. Bacciagaluppi. Dordrecht: Springer Netherlands, 2016, pp. 107–117.

[106] F. Shimizu, K. Shimizu, and H. Takuma. "Double-slit interference with ultracold metastable neon atoms." In: *Phys. Rev. A* 46.1 (1992), R17–R20.

[107] C. Simon et al. "Feasible "Kochen-Specker" Experiment with Single Particles." In: *Phys. Rev. Lett.* 85.9 (2000), pp. 1783–1786.

[108] S. J. Summers. "On the Stone – von Neumann Uniqueness Theorem and Its Ramifications." In: *John von Neumann and the Foundations of Quantum Physics*. Ed. by M. Rédei and M. Stöltzner. Dordrecht: Springer Netherlands, 2001, pp. 135–152.

[109] I. de Vega and D. Alonso. "Dynamics of non-Markovian open quantum systems." In: *Rev. Mod. Phys.* 89.1 (2017), p. 015001.

[110] M. Żukowski. "Definite values for observables versus quantum predictions: a "GHZ-like" test." In: *Physics Letters A* 157.4 (1991), pp. 198–202.

Information, Classical and Quantum

Monographies

[111] S. M. Barnett. *Quantum Information*. Oxford University Press, 2009.

[112] G. Chen et al. *Quantum Computing Devices: Principles, Designs, and Analysis*. Chapman & Hall/CRC, Boca Raton, 2007.

[113] C. W. Helstrom. *Quantum Detection and Estimation Theory*. Academic Press, 1976.

[114] A. Holevo. *Probabilistic and Statistical Aspects of Quantum Theory*. North Holland, 1982.

[115] K. Kraus. *States, Effects, and Operations. Fundamental Notions of Quantum Theory*. Ed. by W. H. W. A. Böhm J. D. Dollard. Vol. 190. Lectures in Mathematical Physics at the University of Texas at Austin. 1983.

[116] N. D. Mermin. *Quantum Computer Science: An Introduction*. Cambridge University Press, 2007.

[117] M. A. Nielsen and I. L. Chuang. *Quantum Computation and Quantum Information: 10th Anniversary Edition*. Cambridge University Press, 2010.

[118] C. E. Shannon and W. Weaver. *The Mathematical Theory of Communication*. University of Illinois Press, Urbana, 1949.

[119] B. L. van der Waerden. *Mathematische Statistik*. Springer, 1971.

Encyclopedic

[120] P. Adriaans. "Information." In: *The Stanford Encyclopedia of Philosophy*. Ed. by E. N. Zalta and U. Nodelman. Winter 2023. Metaphysics Research Lab, Stanford University, 2023.

[121] M. L. Bellac. "Quantum Computation." In: *Compendium of Quantum Physics*. Ed. by D. Greenberger, K. Hentschel, and F. Weinert. Berlin, Heidelberg: Springer Berlin Heidelberg, 2009, pp. 533–538.

Articles

[122] F. Arute et al. "Quantum supremacy using a programmable superconducting processor." In: *Nature* 574.7779 (2019), pp. 505–510.

[123] A. Asadian et al. "Heisenberg-Weyl Observables: Bloch vectors in phase space." In: *Phys. Rev. A* 94.1 (2016), p. 010301.

[124] A. Barenco et al. "Conditional Quantum Dynamics and Logic Gates." In: *Phys. Rev. Lett.* 74.20 (1995), pp. 4083–4086.

[125] H. Barnum et al. "Noncommuting Mixed States Cannot Be Broadcast." In: *Phys. Rev. Lett.* 76.15 (1996), pp. 2818–2821.

[126] S. D. Bartlett, T. Rudolph, and R. W. Spekkens. "Reference frames, superselection rules, and quantum information." In: *Rev. Mod. Phys.* 79.2 (2007), pp. 555–609.

[127] F. B. Basset et al. "Daylight entanglement-based quantum key distribution with a quantum dot source." In: *Quantum Science and Technology* 8.2 (2023), p. 025002.

[128] T. Baumgratz, M. Cramer, and M. B. Plenio. "Quantifying Coherence." In: *Phys. Rev. Lett.* 113.14 (2014), p. 140401.

[129] C. H. Bennett and G. Brassard. "Quantum cryptography: Public key distribution and coin tossing." In: *Proceedings of IEEE International Conference on Computers, Systems, and Signal Processing*. 1984, p. 175.

[130] C. H. Bennett et al. "Postulates for measures of genuine multipartite correlations." In: *Phys. Rev. A* 83.1 (2011), p. 012312.

[131] C. H. Bennett et al. "Teleporting an unknown quantum state via dual classical and Einstein-Podolsky-Rosen channels." In: *Phys. Rev. Lett.* 70.13 (1993), pp. 1895–1899.

[132] R. A. Bertlmann and P. Krammer. "Bloch vectors for qudits." In: *Journal of Physics A: Mathematical and Theoretical* 41.23 (2008), p. 235303.

[133] D. Bouwmeester et al. "Quantum Dense Coding and Quantum Teleportation." In: *The Physics of Quantum Information: Quantum Cryptography, Quantum Teleportation, Quantum Computation*. Ed. by D. Bouwmeester, A. Ekert, and A. Zeilinger. Berlin, Heidelberg: Springer Berlin Heidelberg, 2000, pp. 49–92.

[134] S. L. Braunstein. "Quantum limits on precision measurements of phase." In: *Phys. Rev. Lett.* 69.25 (1992), pp. 3598–3601.

[135] S. L. Braunstein and C. M. Caves. "Statistical distance and the geometry of quantum states." In: *Phys. Rev. Lett.* 72.22 (1994), pp. 3439–3443.

[136] S. L. Braunstein and P. van Loock. "Quantum information with continuous variables." In: *Rev. Mod. Phys.* 77.2 (2005), pp. 513–577.

[137] H. J. Briegel and R. Raussendorf. "Persistent Entanglement in Arrays of Interacting Particles." In: *Phys. Rev. Lett.* 86.5 (2001), pp. 910–913.

[138] D. E. Browne and T. Rudolph. "Resource-Efficient Linear Optical Quantum Computation." In: *Phys. Rev. Lett.* 95.1 (2005), p. 010501.

[139] J. Bub. "Quantum Information and Computation." In: *Philosophy of Physics*. Ed. by J. Butterfield and J. Earman. Handbook of the Philosophy of Science. Amsterdam: North-Holland, 2007, pp. 555–660.

[140] V. Bužek and M. Hillery. "Quantum copying: Beyond the no-cloning theorem." In: *Phys. Rev. A* 54.3 (1996), pp. 1844–1852.

[141] N. J. Cerf and C. Adami. "Negative Entropy and Information in Quantum Mechanics." In: *Phys. Rev. Lett.* 79.26 (1997), pp. 5194–5197.

[142] N. J. Cerf and C. Adami. "Quantum extension of conditional probability." In: *Phys. Rev. A* 60.2 (1999), pp. 893–897.

[143] Y.-A. Chen et al. "An integrated space-to-ground quantum communication network over 4,600 kilometres." In: *Nature* 589.7841 (2021), pp. 214–219.

[144] J. P. Covey, H. Weinfurter, and H. Bernien. "Quantum networks with neutral atom processing nodes." In: *npj Quantum Information* 9.1 (2023), p. 90.

[145] M. Cramer et al. "Efficient quantum state tomography." In: *Nature Communications* 1.1 (2010), p. 149.

[146] G. M. D'Ariano, M. G. Paris, and M. F. Sacchi. "Quantum Tomographic Methods." In: *Quantum State Estimation*. Ed. by M. Paris and J. Řeháček. Berlin, Heidelberg: Springer Berlin Heidelberg, 2004, pp. 7–58.

[147] D. Deutsch et al. "Concepts of Quantum Computation." In: *The Physics of Quantum Information: Quantum Cryptography, Quantum Teleportation, Quantum Computation*. Ed. by D. Bouwmeester, A. Ekert, and A. Zeilinger. Berlin, Heidelberg: Springer Berlin Heidelberg, 2000, pp. 93–132.

[148] D. Deutsch. "Quantum theory, the Church-Turing principle and the universal quantum computer." In: *Proceedings of the Royal Society of London. A. Mathematical and Physical Sciences* 400.1818 (1985), pp. 97–117.

[149] D. Deutsch and R. Jozsa. "Rapid solution of problems by quantum computation." In: *Proceedings of the Royal Society of London. Series A: Mathematical and Physical Sciences* 439.1907 (1992), pp. 553–558.

[150] S. J. Devitt, W. J. Munro, and K. Nemoto. "Quantum error correction for beginners." In: *Reports on Progress in Physics* 76.7 (2013), p. 076001.

[151] D. Dieks. "Communication by EPR devices." In: *Physics Letters A* 92.6 (1982), pp. 271–272.

[152] A. Ekert et al. "Quantum Cryptography." In: *The Physics of Quantum Information: Quantum Cryptography, Quantum Teleportation, Quantum Computation*. Ed. by D. Bouwmeester, A. Ekert, and A. Zeilinger. Berlin, Heidelberg: Springer Berlin Heidelberg, 2000, pp. 15–48.

[153] A. K. Ekert et al. "Decoherence and Quantum Error Correction." In: *The Physics of Quantum Information: Quantum Cryptography, Quantum Teleportation, Quantum Computation*. Ed. by D. Bouwmeester, A. Ekert, and A. Zeilinger. Berlin, Heidelberg: Springer Berlin Heidelberg, 2000, pp. 221–259.

[154] R. P. Feynman. "Simulating physics with computers." In: *International Journal of Theoretical Physics* 21.6 (1982), pp. 467–488.

[155] F. Furrer et al. "Continuous Variable Quantum Key Distribution: Finite-Key Analysis of Composable Security against Coherent Attacks." In: *Phys. Rev. Lett.* 109.10 (2012), p. 100502.

[156] I. M. Georgescu, S. Ashhab, and F. Nori. "Quantum simulation." In: *Rev. Mod. Phys.* 86.1 (2014), pp. 153–185.

[157] A. Gilchrist, N. K. Langford, and M. A. Nielsen. "Distance measures to compare real and ideal quantum processes." In: *Phys. Rev. A* 71.6 (2005), p. 062310.

[158] M. Gimeno-Segovia et al. "From Three-Photon Greenberger-Horne-Zeilinger States to Ballistic Universal Quantum Computation." In: *Phys. Rev. Lett.* 115.2 (2015), p. 020502.

[159] V. Giovannetti, S. Lloyd, and L. Maccone. "Advances in quantum metrology." In: *Nature Photonics* 5.4 (2011), pp. 222–229.

[160] V. Giovannetti, S. Lloyd, and L. Maccone. "Quantum Metrology." In: *Phys. Rev. Lett.* 96.1 (2006), p. 010401.

[161] V. Giovannetti, S. Lloyd, and L. Maccone. "Quantum-Enhanced Measurements: Beating the Standard Quantum Limit." In: *Science* 306.5700 (2004), pp. 1330–1336.

[162] N. Gisin and R. Thew. "Quantum communication." In: *Nature Photonics* 1.3 (2007), pp. 165–171.

[163] N. Gisin et al. "Quantum cryptography." In: *Rev. Mod. Phys.* 74.1 (2002), pp. 145–195.

[164] D. Gottesman. *An Introduction to Quantum Error Correction and Fault-Tolerant Quantum Computation*. preprint: arXiv:0904.2557 (quant-ph). 2009.

[165] C. Gross and I. Bloch. "Quantum simulations with ultracold atoms in optical lattices." In: *Science* 357.6355 (2017), pp. 995–1001.

[166] L. K. Grover. "A Fast quantum mechanical algorithm for database search." In: *Proceedings of 28th Annual ACM Symposium on Theory of Computing* (1996), pp. 212–219.

[167] H. Häffner, C. Roos, and R. Blatt. "Quantum computing with trapped ions." In: *Physics Reports* 469.4 (2008), pp. 155–203.

[168] A.-L. Hashagen. "Universal Asymmetric Quantum Cloning Revisited." In: *Quantum Info. Comput.* 17.9-10 (2017), pp. 747–778.

[169] A. S. Holevo. "Statistical problems in quantum physics." In: *Proceedings of the Second Japan-USSR Symposium on Probability Theory.* Ed. by G. Maruyama and Y. V. Prokhorov. Berlin, Heidelberg: Springer Berlin Heidelberg, 1973, pp. 104–119.

[170] M. Horodecki, J. Oppenheim, and A. Winter. "Partial quantum information." In: *Nature* 436.7051 (2005), pp. 673–676.

[171] P. Horodecki, Ł. Rudnicki, and K. Życzkowski. "Five Open Problems in Quantum Information Theory." In: *PRX Quantum* 3.1 (2022), p. 010101.

[172] Y.-F. Huang et al. "Experimental Test of the Kochen-Specker Theorem with Single Photons." In: *Phys. Rev. Lett.* 90.25 (2003), p. 250401.

[173] R. Jozsa and B. Schumacher. "A New Proof of the Quantum Noiseless Coding Theorem." In: *Journal of Modern Optics* 41.12 (1994), pp. 2343–2349.

[174] M. Keyl. "Fundamentals of quantum information theory." In: *Physics Reports* 369.5 (2002), pp. 431–548.

[175] H. J. Kimble. "The quantum internet." In: *Nature* 453.7198 (2008), pp. 1023–1030.

[176] G. Kimura. "The Bloch vector for N-level systems." In: *Physics Letters A* 314.5 (2003), pp. 339–349.

[177] E. Knill, R. Laflamme, and G. J. Milburn. "A scheme for efficient quantum computation with linear optics." In: *Nature* 409.6816 (2001), pp. 46–52.

[178] E. Knill et al. "Introduction to quantum error correction." In: *Los Alamos Science* 27 (2002), p. 188.

[179] L. Knips et al. *How long does it take to obtain a physical density matrix?* preprint: arXiv:1512.06866 (quant-ph). 2015.

[180] M. Koashi. "Unconditional security of quantum key distribution and the uncertainty principle." In: *Journal of Physics: Conference Series* 36.1 (2006), p. 98.

[181] P. Kok et al. "Linear optical quantum computing with photonic qubits." In: *Rev. Mod. Phys.* 79.1 (2007), pp. 135–174.

[182] K. Kraus. "General state changes in quantum theory." In: *Annals of Physics* 64.2 (1971), pp. 311–335.

[183] T. D. Ladd et al. "Quantum computers." In: *Nature* 464.7285 (2010), pp. 45–53.

[184] H. Lee, P. Kok, and J. P. Dowling. "A quantum Rosetta stone for interferometry." In: *Journal of Modern Optics* 49.14-15 (2002), pp. 2325–2338.

[185] G. Lindblad. "Completely positive maps and entropy inequalities." In: *Communications in Mathematical Physics* 40.2 (1975), pp. 147–151.

[186] A. G. J. MacFarlane, J. P. Dowling, and G. J. Milburn. "Quantum technology: the second quantum revolution." In: *Philosophical Transactions of the Royal Society of London. Series A: Mathematical, Physical and Engineering Sciences* 361.1809 (2003), pp. 1655–1674.

[187] L. S. Madsen et al. "Quantum computational advantage with a programmable photonic processor." In: *Nature* 606.7912 (2022), pp. 75–81.

[188] M. G. A. Paris. "Quantum Estimation for Quantum Technology." In: *International Journal of Quantum Information* 07.supp01 (2009), pp. 125–137.

[189] J. M. Pino et al. "Demonstration of the trapped-ion quantum CCD computer architecture." In: *Nature* 592.7853 (2021), pp. 209–213.

[190] S. Pirandola et al. "Advances in photonic quantum sensing." In: *Nature Photonics* 12.12 (2018), pp. 724–733.

[191] S. Pirandola et al. "Advances in quantum cryptography." In: *Adv. Opt. Photon.* 12.4 (2020), pp. 1012–1236.

[192] E. Polino et al. "Photonic quantum metrology." In: *AVS Quantum Science* 2.2 (2020), p. 024703.

[193] R. Raussendorf and H. J. Briegel. "A One-Way Quantum Computer." In: *Phys. Rev. Lett.* 86.22 (2001), pp. 5188–5191.

[194] M. B. Ruskai. "Inequalities for quantum entropy: A review with conditions for equality." In: *Journal of Mathematical Physics* 43.9 (2002), pp. 4358–4375.

[195] M. B. Ruskai, S. Szarek, and E. Werner. "An analysis of completely-positive trace-preserving maps on M2." In: *Linear Algebra and its Applications* 347.1 (2002), pp. 159–187.

[196] V. Scarani et al. "Quantum cloning." In: *Rev. Mod. Phys.* 77.4 (2005), pp. 1225–1256.

[197] F. Schäfer et al. "Tools for quantum simulation with ultracold atoms in optical lattices." In: *Nature Reviews Physics* 2.8 (2020), pp. 411–425.

[198] B. Schumacher. "Quantum coding." In: *Phys. Rev. A* 51.4 (1995), pp. 2738–2747.

[199] C. Schwemmer et al. "Systematic Errors in Current Quantum State Tomography Tools." In: *Phys. Rev. Lett.* 114.8 (2015), p. 080403.

[200] C. E. Shannon. "A mathematical theory of communication." In: *The Bell System Technical Journal* 27.3 (1948), pp. 379–423.

[201] P. Shor. "Algorithms for quantum computation: discrete logarithms and factoring." In: *Proceedings 35th Annual Symposium on Foundations of Computer Science*. 1994, pp. 124–134.

[202] C. Simon et al. "Quantum memories." In: *The European Physical Journal D* 58.1 (2010), pp. 1–22.

[203] W. F. Stinespring. "Positive Functions on C*-Algebras." In: *Proceedings of the American Mathematical Society* 6.2 (1955), pp. 211–216.

[204] A. Streltsov, G. Adesso, and M. B. Plenio. "Colloquium: Quantum coherence as a resource." In: *Rev. Mod. Phys.* 89.4 (2017), p. 041003.

[205] G. Tóth and I. Apellaniz. "Quantum metrology from a quantum information science perspective." In: *Journal of Physics A: Mathematical and Theoretical* 47.42 (2014), p. 424006.

[206] M. C. Tran et al. "Correlations between outcomes of random measurements." In: *Phys. Rev. A* 94.4 (2016), p. 042302.

[207] R. Ursin et al. "Entanglement-based quantum communication over 144km." In: *Nature Physics* 3.7 (2007), pp. 481–486.

[208] G. Vest et al. "Quantum key Distribution with a Hand-Held Sender Unit." In: *Phys. Rev. Appl.* 18.2 (2022), p. 024067.

[209] P. Walther et al. "Experimental one-way quantum computing." In: *Nature* 434.7030 (2005), pp. 169–176.

[210] S. Wang et al. "Twin-field quantum key distribution over 830-km fibre." In: *Nature Photonics* 16.2 (2022), pp. 154–161.

[211] Y. Watanabe, T. Sagawa, and M. Ueda. "Uncertainty relation revisited from quantum estimation theory." In: *Phys. Rev. A* 84.4 (2011), p. 042121.

[212] J. Watrous. "Semidefinite Programming for Completely Bounded Norms." In: *Theory of Computing* 5 (2009), pp. 217–238.

[213] S. Wehner, D. Elkouss, and R. Hanson. "Quantum internet: A vision for the road ahead." In: *Science* 362.6412 (2018), eaam9288.

[214] S. Wiesner. "Conjugate Coding." In: *SIGACT News* 15.1 (1983), pp. 78–88.

[215] K. Wintersperger et al. "Neutral atom quantum computing hardware: performance and end-user perspective." In: *EPJ Quantum Technology* 10.1 (2023), p. 32.

[216] W. K. Wootters and W. H. Zurek. "A single quantum cannot be cloned." In: *Nature* 299.5886 (1982), pp. 802–803.

[217] J. Yin et al. "Entanglement-based secure quantum cryptography over 1,120 kilometres." In: *Nature* 582.7813 (2020), pp. 501–505.

[218] V. Zapatero et al. "Advances in device-independent quantum key distribution." In: *npj Quantum Information* 9.1 (2023), p. 10.

[219] H.-S. Zhong et al. "Quantum computational advantage using photons." In: *Science* 370.6523 (2020), pp. 1460–1463.

Quantum Measurement and Complementarity

Monographies

[220] V. B. Braginsky and F. Y. Khalili. *Quantum Measurement*. Cambridge University Press, 1992.

[221] P. Busch, M. Grabowski, and P. J. Lahti. *Operational Quantum Physics*. Springer, 1995.

[222] P. Busch, P. J. Lahti, and P. Mittelstaedt. *The Quantum Theory of Measurement*. Springer, 1991.

[223] M. G. A. Paris and J. Řeháček, eds. *Quantum State Estimation*. Springer, 2004.

[224] M. Schlosshauer. *Decoherence and the Quantum to Classical Transition*. Springer, 2007.

[225] H. M. Wiseman and G. J. Milburn. *Quantum Measurement and Control*. Cambridge University Press, 2010.

Encyclopedic

[226] M. Breinig. "Heisenberg Microscope." In: *Compendium of Quantum Physics*. Ed. by D. Greenberger, K. Hentschel, and F. Weinert. Berlin, Heidelberg: Springer Berlin Heidelberg, 2009, pp. 279–280.

[227] P. Busch. "Effect." In: *Compendium of Quantum Physics*. Ed. by D. Greenberger, K. Hentschel, and F. Weinert. Berlin, Heidelberg: Springer Berlin Heidelberg, 2009, pp. 179–180.

[228] P. Busch and B. Falkenburg. "Heisenberg Uncertainty Relation (Indeterminacy Relations)." In: *Compendium of Quantum Physics*. Ed. by D. Greenberger, K. Hentschel, and F. Weinert. Berlin, Heidelberg: Springer Berlin Heidelberg, 2009, pp. 281–283.

[229] P. Busch and G. Jaeger. "Which-Way or Welcher-Weg-Experiments." In: *Compendium of Quantum Physics*. Ed. by D. Greenberger, K. Hentschel, and F. Weinert. Berlin, Heidelberg: Springer Berlin Heidelberg, 2009, pp. 845–851.

[230] P. Busch and P. Lahti. "Measurement Theory." In: *Compendium of Quantum Physics*. Ed. by D. Greenberger, K. Hentschel, and F. Weinert. Berlin, Heidelberg: Springer Berlin Heidelberg, 2009, pp. 374–379.

[231] P. Busch and P. Lahti. "Observable." In: *Compendium of Quantum Physics*. Ed. by D. Greenberger, K. Hentschel, and F. Weinert. Berlin, Heidelberg: Springer Berlin Heidelberg, 2009, pp. 425–428.

[232] S. Goldstein. "Projection Postulate." In: *Compendium of Quantum Physics*. Ed. by D. Greenberger, K. Hentschel, and F. Weinert. Berlin, Heidelberg: Springer Berlin Heidelberg, 2009, pp. 499–501.

[233] B. J. Hiley. "Quantum Eraser." In: *Compendium of Quantum Physics*. Ed. by D. Greenberger, K. Hentschel, and F. Weinert. Berlin, Heidelberg: Springer Berlin Heidelberg, 2009, pp. 546–549.

[234] E. Joos. "Quantum Zeno Effect." In: *Compendium of Quantum Physics*. Ed. by D. Greenberger, K. Hentschel, and F. Weinert. Berlin, Heidelberg: Springer Berlin Heidelberg, 2009, pp. 622–625.

[235] P. Mittelstaedt. "Objectification." In: *Compendium of Quantum Physics*. Ed. by D. Greenberger, K. Hentschel, and F. Weinert. Berlin, Heidelberg: Springer Berlin Heidelberg, 2009, pp. 417–420.

[236] H. Stapp. "Complementarity Principle." In: *Compendium of Quantum Physics*. Ed. by D. Greenberger, K. Hentschel, and F. Weinert. Berlin, Heidelberg: Springer Berlin Heidelberg, 2009, pp. 111–113.

[237] L. Vaidman. "Protective Measurements." In: *Compendium of Quantum Physics*. Ed. by D. Greenberger, K. Hentschel, and F. Weinert. Berlin, Heidelberg: Springer Berlin Heidelberg, 2009, pp. 505–508.

[238] S. Weigert. "Quantum State Reconstruction." In: *Compendium of Quantum Physics*. Ed. by D. Greenberger, K. Hentschel, and F. Weinert. Berlin, Heidelberg: Springer Berlin Heidelberg, 2009, pp. 609–611.

[239] B. R. Wheaton. "Wave-Particle Duality: A Modern View." In: *Compendium of Quantum Physics*. Ed. by D. Greenberger, K. Hentschel, and F. Weinert. Berlin, Heidelberg: Springer Berlin Heidelberg, 2009, pp. 835–840.

[240] B. R. Wheaton. "Wave-Particle Duality: Some History." In: *Compendium of Quantum Physics*. Ed. by D. Greenberger, K. Hentschel, and F. Weinert. Berlin, Heidelberg: Springer Berlin Heidelberg, 2009, pp. 830–835.

Articles

[241] Y. Aharonov, J. Anandan, and L. Vaidman. "The meaning of protective measurements." In: *Foundations of Physics* 26.1 (1996), pp. 117–126.

[242] Y. Aharonov and L. Vaidman. "Measurement of the Schrödinger wave of a single particle." In: *Physics Letters A* 178.1 (1993), pp. 38–42.

[243] D. M. Appleby. "Symmetric informationally complete measurements of arbitrary rank." In: *Optics and Spectroscopy* 103.3 (2007), pp. 416–428.

[244] D. M. Appleby. "Quantum Errors and Disturbances: Response to Busch, Lahti and Werner." In: *Entropy* 18.5 (2016).

[245] M. Arndt et al. "Wave-particle duality of C60 molecules." In: *Nature* 401.6754 (1999), pp. 680–682.

[246] E. Arthurs and J. L. Kelly. "B.S.T.J. briefs: On the simultaneous measurement of a pair of conjugate observables." In: *The Bell System Technical Journal* 44.4 (1965), pp. 725–729.

[247] S.-Y. Baek et al. "Experimental violation and reformulation of the Heisenberg's error-disturbance uncertainty relation." In: *Scientific Reports* 3 (2013), pp. 2221–.

[248] F. Bagarello. "Uncertainty relation for non-Hermitian operators." In: *Journal of Physics A: Mathematical and Theoretical* 56.42 (2023), p. 425201.

[249] K. Banaszek. "Fidelity Balance in Quantum Operations." In: *Phys. Rev. Lett.* 86.7 (2001), pp. 1366–1369.

[250] I. Bengtsson. "Three Ways to Look at Mutually Unbiased Bases." In: *AIP Conference Proceedings* 889.1 (2007), pp. 40–51.

[251] R. Blume-Kohout. "Optimal, reliable estimation of quantum states." In: *New Journal of Physics* 12.4 (2010), p. 043034.

[252] V. B. Braginsky and F. Y. Khalili. "Quantum nondemolition measurements: the route from toys to tools." In: *Rev. Mod. Phys.* 68.1 (1996), pp. 1–11.

[253] V. B. Braginsky, Y. I. Vorontsov, and K. S. Thorne. "Quantum Nondemolition Measurements." In: *Science* 209.4456 (1980), pp. 547–557.

[254] C. Branciard. "Error-tradeoff and error-disturbance relations for incompatible quantum measurements." In: *Proceedings of the National Academy of Sciences* 110.17 (2013), pp. 6742–6747.

[255] S. L. Braunstein, C. M. Caves, and G. Milburn. "Generalized Uncertainty Relations: Theory, Examples, and Lorentz Invariance." In: *Annals of Physics* 247.1 (1996), pp. 135–173.

[256] T. Brougham, E. Andersson, and S. M. Barnett. "Cloning and joint measurements of incompatible components of spin." In: *Phys. Rev. A* 73.6 (2006), p. 062319.

[257] D. Bruß, J. Calsamiglia, and N. Lütkenhaus. "Quantum cloning and distributed measurements." In: *Phys. Rev. A* 63.4 (2001), p. 042308.

[258] F. Buscemi et al. "Unifying different notions of quantum incompatibility into a strict hierarchy of resource theories of communication." In: *Quantum* 7 (2023), p. 1035.

[259] P. Busch. ""No Information Without Disturbance": Quantum Limitations of Measurement." In: *Quantum Reality, Relativistic Causality, and Closing the Epistemic Circle: Essays in Honour of Abner Shimony*. Dordrecht: Springer Netherlands, 2009, pp. 229–256.

[260] P. Busch. "Indeterminacy relations and simultaneous measurements in quantum theory." In: *International Journal of Theoretical Physics* 24.1 (1985), pp. 63–92.

[261] P. Busch, T. Heinonen, and P. Lahti. "Heisenberg's uncertainty principle." In: *Physics Reports* 452.6 (2007), pp. 155–176.

[262] P. Busch, T. Heinonen, and P. Lahti. "Noise and disturbance in quantum measurement." In: *Physics Letters A* 320.4 (2004), pp. 261–270.

[263] P. Busch, P. Lahti, and R. F. Werner. "Colloquium: Quantum root-mean-square error and measurement uncertainty relations." In: *Rev. Mod. Phys.* 86.4 (2014), pp. 1261–1281.

[264] P. Busch, P. Lahti, and R. F. Werner. "Proof of Heisenberg's Error-Disturbance Relation." In: *Phys. Rev. Lett.* 111.16 (2013), p. 160405.

[265] X. Cao et al. "The transition from quantum Zeno to anti-Zeno effects for a qubit in a cavity by varying the cavity frequency." In: *Physics Letters A* 376.4 (2012), pp. 349–357.

[266] A. Z. Chaudhry. "A general framework for the Quantum Zeno and anti-Zeno effects." In: *Scientific Reports* 6.1 (2016), p. 29497.

[267] B. Chen and P. Lian. "Uncertainty relations for multiple operators without covariances." In: *Journal of Physics A: Mathematical and Theoretical* 55.9 (2022), p. 095303.

[268] I. L. Chuang and M. A. Nielsen. "Prescription for experimental determination of the dynamics of a quantum black box." In: *Journal of Modern Optics* 44.11-12 (1997), pp. 2455–2467.

[269] P. J. Coles et al. "Entropic uncertainty relations and their applications." In: *Rev. Mod. Phys.* 89.1 (2017), p. 015002.

[270] G. M. D'Ariano. "On the Heisenberg principle, namely on the information-disturbance trade-off in a quantum measurement." In: *Fortschritte der Physik* 51.4-5 (2003), pp. 318–330.

[271] G. M. D'Ariano, C. Macchiavello, and M. F. Sacchi. "Joint measurements via quantum cloning." In: *Journal of Optics B: Quantum and Semiclassical Optics* 3.2 (2001), pp. 44–50.

[272] N. D. H. Dass and T. Qureshi. "Critique of protective measurements." In: *Phys. Rev. A* 59.4 (1999), pp. 2590–2601.

[273] E. B. Davies and J. T. Lewis. "An operational approach to quantum probability." In: *Communications in Mathematical Physics* 17.3 (1970), pp. 239–260.

[274] B. Demirel, S. Sponar, and Y. Hasegawa. "Measurements of Entropic Uncertainty Relations in Neutron Optics." In: *Applied Sciences* 10.3 (2020).

[275] V. V. Dodonov. "Variance uncertainty relations without covariances for three and four observables." In: *Phys. Rev. A* 97.2 (2018), p. 022105.

[276] J. Dressel, S. Agarwal, and A. N. Jordan. "Contextual Values of Observables in Quantum Measurements." In: *Phys. Rev. Lett.* 104.24 (2010), p. 240401.

[277] J. Dressel and A. N. Jordan. "Contextual-value approach to the generalized measurement of observables." In: *Phys. Rev. A* 85.2 (2012), p. 022123.

[278] J. Dressel and A. N. Jordan. "Quantum instruments as a foundation for both states and observables." In: *Phys. Rev. A* 88.2 (2013), p. 022107.

[279] J. Dressel and F. Nori. "Certainty in Heisenberg's uncertainty principle: Revisiting definitions for estimation errors and disturbance." In: *Phys. Rev. A* 89.2 (2014), p. 022106.

[280] S. Dürr, T. Nonn, and G. Rempe. "Origin of quantum-mechanical complementarity probed by a 'which-way' experiment in an atom interferometer." In: *Nature* 395 (1998), p. 33.

[281] T. Durt et al. "On Mutually Unbiased Bases." In: *International Journal of Quantum Information* 08.04 (2010), pp. 535–640.

[282] A. Elben et al. "The randomized measurement toolbox." In: *Nature Reviews Physics* 5.1 (2023), pp. 9–24.

[283] B.-G. Englert, M. O. Scully, and H. Walther. "Complementarity and uncertainty." In: *Nature* 375.6530 (1995), pp. 367–368.

[284] J. Erhart et al. "Experimental demonstration of a universally valid error-disturbance uncertainty relation in spin measurements." In: *Nat Phys* 8.3 (2012), pp. 185–189.

[285] G. B. Folland and A. Sitaram. "The uncertainty principle: A mathematical survey." In: *Journal of Fourier Analysis and Applications* 3.3 (1997), pp. 207–238.

[286] C. A. Fuchs and K. Jacobs. "Information-tradeoff relations for finite-strength quantum measurements." In: *Phys. Rev. A* 63.6 (2001), p. 062305.

[287] C. A. Fuchs and A. Peres. "Quantum-state disturbance versus information gain: Uncertainty relations for quantum information." In: *Phys. Rev. A* 53.4 (1996), pp. 2038–2045.

[288] G. Gour and A. Kalev. "Construction of all general symmetric informationally complete measurements." In: *Journal of Physics A: Mathematical and Theoretical* 47.33 (2014), p. 335302.

[289] O. Gühne et al. "Colloquium: Incompatible measurements in quantum information science." In: *Rev. Mod. Phys.* 95.1 (2023), p. 011003.

[290] M. J. W. Hall. "Prior information: How to circumvent the standard joint-measurement uncertainty relation." In: *Phys. Rev. A* 69.5 (2004), p. 052113.

[291] A.-L. K. Hashagen and M. M. Wolf. "Universality and Optimality in the Information-Disturbance Tradeoff." In: *Annales Henri Poincaré* 20.1 (2019), pp. 219–258.

[292] T. Heinosaari and M. M. Wolf. "Nondisturbing quantum measurements." In: *Journal of Mathematical Physics* 51.9 (2010), p. 092201.

[293] T. J. Herzog et al. "Complementarity and the Quantum Eraser." In: *Phys. Rev. Lett.* 75.17 (1995), pp. 3034–3037.

[294] Z. Hradil. "Quantum-state estimation." In: *Phys. Rev. A* 55.3 (1997), R1561–R1564.

[295] W. M. Itano et al. "Quantum Zeno effect." In: *Phys. Rev. A* 41.5 (1990), pp. 2295–2300.

[296] D. F. V. James et al. "Measurement of qubits." In: *Phys. Rev. A* 64.5 (2001), p. 052312.

[297] E. Joos and H. D. Zeh. "The emergence of classical properties through interaction with the environment." In: *Zeitschrift für Physik B Condensed Matter* 59.2 (1985), pp. 223–243.

[298] E. Joos. "Dynamical Consequences of Strong Entanglement." In: *Quantum Decoherence*. Ed. by B. Duplantier, J.-M. Raimond, and V. Rivasseau. Basel: Birkhäuser Basel, 2007, pp. 177–192.

[299] F. Kaneda et al. "Experimental Test of Error-Disturbance Uncertainty Relations by Weak Measurement." In: *Phys. Rev. Lett.* 112.2 (2014), p. 020402.

[300] S. Kechrimparis and S. Weigert. "Geometry of uncertainty relations for linear combinations of position and momentum." In: *Journal of Physics A: Mathematical and Theoretical* 51.2 (2017), p. 025303.

[301] S. Kechrimparis and S. Weigert. "Heisenberg uncertainty relation for three canonical observables." In: *Phys. Rev. A* 90.6 (2014), p. 062118.

[302] A. G. Kofman and G. Kurizki. "Acceleration of quantum decay processes by frequent observations." In: *Nature* 405.6786 (2000), pp. 546–550.

[303] K. Korzekwa, D. Jennings, and T. Rudolph. "Operational constraints on state-dependent formulations of quantum error-disturbance trade-off relations." In: *Phys. Rev. A* 89.5 (2014), p. 052108.

[304] P. G. Kwiat, A. M. Steinberg, and R. Y. Chiao. "Observation of a "quantum eraser": A revival of coherence in a two-photon interference experiment." In: *Phys. Rev. A* 45.11 (1992), pp. 7729–7739.

[305] Y. Liu et al. "Experimental test of error-tradeoff uncertainty relation using a continuous-variable entangled state." In: *npj Quantum Information* 5.1 (2019), p. 68.

[306] G. Ludwig. "Versuch einer axiomatischen Grundlegung der Quantenmechanik und allgemeinerer physikalischer Theorien." In: *Zeitschrift für Physik* 181.3 (1964), pp. 233–260.

[307] H. Maassen and J. B. M. Uffink. "Generalized entropic uncertainty relations." In: *Phys. Rev. Lett.* 60.12 (1988), pp. 1103–1106.

[308] D. H. Mahler et al. "Adaptive Quantum State Tomography Improves Accuracy Quadratically." In: *Phys. Rev. Lett.* 111.18 (2013), p. 183601.

[309] R. Mir et al. "A double-slit 'which-way' experiment on the complementarity-uncertainty debate." In: *New Journal of Physics* 9.8 (2007), pp. 287–.

[310] B. Misra and E. C. G. Sudarshan. "The Zeno's paradox in quantum theory." In: *Journal of Mathematical Physics* 18.4 (1977), pp. 756–763.

[311] M. Mohseni, A. T. Rezakhani, and D. A. Lidar. "Quantum-process tomography: Resource analysis of different strategies." In: *Phys. Rev. A* 77.3 (2008), p. 032322.

[312] M. A. Nielsen. "Characterizing mixing and measurement in quantum mechanics." In: *Phys. Rev. A* 63.2 (2001), p. 022114.

[313] M. Ohliger, V. Nesme, and J. Eisert. "Efficient and feasible state tomography of quantum many-body systems." In: *New Journal of Physics* 15.1 (2013), p. 015024.

[314] K. Okamura and M. Ozawa. "Measurement theory in local quantum physics." In: *Journal of Mathematical Physics* 57.1 (2015), p. 015209.

[315] M. Ozawa. "Heisenberg's original derivation of the uncertainty principle and its universally valid reformulations." In: *Current Science* 109.11 (2015), pp. 2006–2016.

[316] M. Ozawa. "Quantum measuring processes of continuous observables." In: *Journal of Mathematical Physics* 25.1 (1984), pp. 79–87.

[317] M. Ozawa. "Uncertainty relations for joint measurements of noncommuting observables." In: *Physics Letters A* 320.5 (2004), pp. 367–374.

[318] M. Ozawa. "Uncertainty relations for noise and disturbance in generalized quantum measurements." In: *Annals of Physics* 311.2 (2004), pp. 350–416.

[319] M. Ozawa. "Universally valid reformulation of the Heisenberg uncertainty principle on noise and disturbance in measurement." In: *Phys. Rev. A* 67.4 (2003), p. 042105.

[320] J. P. Paz and W. H. Zurek. "Environment-Induced Decoherence and the Transition from Quantum to Classical." In: *Coherent atomic matter waves*. Ed. by R. Kaiser, C. Westbrook, and F. David. Berlin, Heidelberg: Springer Berlin Heidelberg, 2001, pp. 533–614.

[321] A. Peres. "Zeno paradox in quantum theory." In: *American Journal of Physics* 48.11 (1980), pp. 931–932.

[322] E. Prugovečki. "Information-theoretical aspects of quantum measurement." In: *International Journal of Theoretical Physics* 16.5 (1977), pp. 321–331.

[323] H. Rauch and S. A. Werner. *Neutron Interferometry: Lessons in Experimental Quantum Mechanics, Wave-Particle Duality, and Entanglement*. Oxford University Press, 2015.

[324] J. M. Renes, V. B. Scholz, and S. Huber. "Uncertainty relations: An operational approach to the error-disturbance tradeoff." In: *Quantum* 1 (2017), p. 20.

[325] J. M. Renes et al. "Symmetric informationally complete quantum measurements." In: *Journal of Mathematical Physics* 45.6 (2004), pp. 2171–2180.

[326] L. A. Rozema et al. "Violation of Heisenberg's Measurement-Disturbance Relationship by Weak Measurements." In: *Phys. Rev. Lett.* 109.10 (2012), p. 100404.

[327] M. Schlosshauer. "Quantum decoherence." In: *Physics Reports* 831 (2019). Quantum decoherence, pp. 1–57.

[328] C. Schwemmer et al. "Experimental Comparison of Efficient Tomography Schemes for a Six-Qubit State." In: *Phys. Rev. Lett.* 113.4 (2014), p. 040503.

[329] M. O. Scully, B.-G. Englert, and H. Walther. "Quantum optical tests of complementarity." In: *Nature* 351.6322 (1991), pp. 111–116.

[330] M. O. Scully and K. Drühl. "Quantum eraser: A proposed photon correlation experiment concerning observation and "delayed choice" in quantum mechanics." In: *Phys. Rev. A* 25.4 (1982), pp. 2208–2213.

[331] K. Siudzińska. "All classes of informationally complete symmetric measurements in finite dimensions." In: *Phys. Rev. A* 105.4 (2022), p. 042209.

[332] R. W. Spekkens. "Contextuality for preparations, transformations, and unsharp measurements." In: *Phys. Rev. A* 71.5 (2005), p. 052108.

[333] S. Sponar et al. "Experimental test of entropic noise-disturbance uncertainty relations for three-outcome qubit measurements." In: *Phys. Rev. Res.* 3.2 (2021), p. 023175.

[334] P. Storey et al. "Path detection and the uncertainty principle." In: *Nature* 367.6464 (1994), pp. 626–628.

[335] G. Sulyok et al. "Experimental Test of Entropic Noise-Disturbance Uncertainty Relations for Spin-1/2 Measurements." In: *Phys. Rev. Lett.* 115.3 (2015), p. 030401.

[336] Y. Sun, N. Li, and S. Luo. "Fidelity-disturbance-entropy tradeoff in quantum channels." In: *Phys. Rev. A* 105.6 (2022), p. 062458.

[337] J. Uffink. "How to protect the interpretation of the wave function against protective measurements." In: *Phys. Rev. A* 60.5 (1999), pp. 3474–3481.

[338] H.-Q.-C. Wang et al. "Uncertainty relations for triples of observables and the experimental demonstrations." In: *Science China Physics, Mechanics & Astronomy* 66.5 (2023), p. 250314.

[339] S. Weigert and M. Wilkinson. "Mutually unbiased bases for continuous variables." In: *Phys. Rev. A* 78.2 (2008), p. 020303.

[340] R. F. Werner. "The uncertainty relation for joint measurement of position and momentum." In: *Quant. Inf. Comput.* 4 (2004), pp. 546–562.

[341] R. F. Werner and T. Farrelly. "Uncertainty from Heisenberg to Today." In: *Foundations of Physics* 49.6 (2019), pp. 460–491.

[342] M. M. Weston et al. "Experimental Test of Universal Complementarity Relations." In: *Phys. Rev. Lett.* 110.22 (2013), p. 220402.

[343] H. M. Wiseman et al. "Nonlocal momentum transfer in welcher Weg measurements." In: *Phys. Rev. A* 56.1 (1997), pp. 55–75.

[344] H. Wiseman and F. Harrison. "Uncertainty over complementarity?" In: *Nature* 377.6550 (1995), pp. 584–584.

[345] X. Zhao and C. Zhang. "Uncertainty Relations of Non-Hermitian Operators: Theory and Experimental Scheme." In: *Frontiers in Physics* 10 (2022).

[346] W. H. Zurek. "Pointer basis of quantum apparatus: Into what mixture does the wave packet collapse?" In: *Phys. Rev. D* 24.6 (1981), pp. 1516–1525.

[347] W. H. Zurek. "Decoherence, einselection, and the quantum origins of the classical." In: *Rev. Mod. Phys.* 75.3 (2003), pp. 715–775.

Bell's Theorem and Relativity

Monographies

[348] M. Bell and S. Gao, eds. *Quantum Nonlocality and Reality: 50 Years of Bell's Theorem*. Cambridge University Press, 2016.

[349] G. L. Naber. *The Geometry of Minkowski Spacetime*. Springer, 1992.

[350] V. Scarani. *Bell Nonlocality*. Oxford University Press, 2019.

Encyclopedic

[351] A. Fine. "The Einstein-Podolsky-Rosen Argument in Quantum Theory." In: *The Stanford Encyclopedia of Philosophy*. Ed. by E. N. Zalta. Summer 2020. Metaphysics Research Lab, Stanford University, 2020.

[352] D. J. Gauthier. "Superluminal Communication in Quantum Mechanics." In: *Compendium of Quantum Physics*. Ed. by D. Greenberger, K. Hentschel, and F. Weinert. Springer Berlin Heidelberg, 2009, pp. 766–769.

[353] D. M. Greenberger. "GHZ (Greenberger–Horne–Zeilinger) Theorem and GHZ States." In: *Compendium of Quantum Physics*. Ed. by D. Greenberger, K. Hentschel, and F. Weinert. Springer Berlin Heidelberg, 2009, pp. 258–263.

[354] A. J. Leggett. "Aspect Experiment." In: *Compendium of Quantum Physics*. Ed. by D. Greenberger, K. Hentschel, and F. Weinert. Springer Berlin Heidelberg, 2009, pp. 14–18.

[355] W. Myrvold, M. Genovese, and A. Shimony. "Bell's Theorem." In: *The Stanford Encyclopedia of Philosophy*. Ed. by E. N. Zalta. Fall 2021. Metaphysics Research Lab, Stanford University, 2021.

[356] H. P. Stapp. "Locality." In: *Compendium of Quantum Physics*. Ed. by D. Greenberger, K. Hentschel, and F. Weinert. Springer Berlin Heidelberg, 2009, pp. 347–348.

[357] G. Weihs. "Loopholes in Experiments." In: *Compendium of Quantum Physics*. Ed. by D. Greenberger, K. Hentschel, and F. Weinert. Springer Berlin Heidelberg, 2009, pp. 348–355.

Articles

[358] Y. Aharonov and D. Z. Albert. "States and observables in relativistic quantum field theories." In: *Phys. Rev. D* 21.12 (1980), pp. 3316–3324.

[359] Y. Aharonov, D. Z. Albert, and L. Vaidman. "Measurement process in relativistic quantum theory." In: *Phys. Rev. D* 34.6 (1986), pp. 1805–1813.

[360] J.-M. A. Allen et al. "Quantum Common Causes and Quantum Causal Models." In: *Phys. Rev. X* 7.3 (2017), p. 031021.

[361] M. L. Almeida et al. "Multipartite fully nonlocal quantum states." In: *Phys. Rev. A* 81.5 (2010), p. 052111.

[362] A. Aspect, J. Dalibard, and G. Roger. "Experimental Test of Bell's Inequalities Using Time-Varying Analyzers." In: *Phys. Rev. Lett.* 49.25 (1982), pp. 1804–1807.

[363] A. Aspect, P. Grangier, and G. Roger. "Experimental Realization of Einstein-Podolsky-Rosen-Bohm Gedankenexperiment: A New Violation of Bell's Inequalities." In: *Phys. Rev. Lett.* 49.2 (1982), pp. 91–94.

[364] A. Aspect, P. Grangier, and G. Roger. "Experimental Tests of Realistic Local Theories via Bell's Theorem." In: *Phys. Rev. Lett.* 47.7 (1981), pp. 460–463.

[365] J.-D. Bancal, N. Gisin, and S. Pironio. "Looking for symmetric Bell inequalities." In: *Journal of Physics A: Mathematical and Theoretical* 43.38 (2010), p. 385303.

[366] J.-D. Bancal et al. "Definitions of multipartite nonlocality." In: *Phys. Rev. A* 88.1 (2013), p. 014102.

[367] D. Beckman et al. "Causal and localizable quantum operations." In: *Phys. Rev. A* 64.5 (2001), p. 052309.

[368] J. S. Bell. "On the Einstein Podolsky Rosen paradox." In: *Physics Physique Fizika* 1.3 (1964), pp. 195–200.

[369] J. S. Bell. "Introduction to the hidden-variable question." In: *Speakable and Unspeakable in Quantum Mechanics: Collected Papers on Quantum Philosophy*. Cambridge University Press, 2004, pp. 29–39.

[370] J. S. Bell. "La nouvelle cuisine." In: *Speakable and Unspeakable in Quantum Mechanics: Collected Papers on Quantum Philosophy*. Cambridge University Press, 2004, pp. 232–248.

[371] J. S. Bell. "The theory of local beables." In: *Speakable and Unspeakable in Quantum Mechanics: Collected Papers on Quantum Philosophy*. Cambridge University Press, 2004, pp. 52–62.

[372] J. S. Bell. "The Theory of Local Beables." In: *Dialectica* 39 (1985). Ed. by M. Bell, K. Gottfried, and M. J. G. Veltman, pp. 86–96.

[373] D. Bohm and Y. Aharonov. "Discussion of Experimental Proof for the Paradox of Einstein, Rosen, and Podolsky." In: *Phys. Rev.* 108.4 (1957), pp. 1070–1076.

[374] C. Branciard. "Detection loophole in Bell experiments: How postselection modifies the requirements to observe nonlocality." In: *Phys. Rev. A* 83.3 (2011), p. 032123.

[375] N. Brunner et al. "Bell nonlocality." In: *Rev. Mod. Phys.* 86.2 (2014), pp. 419–478.

[376] H. Buhrman et al. "Nonlocality and communication complexity." In: *Rev. Mod. Phys.* 82.1 (2010), pp. 665–698.

[377] E. G. Cavalcanti and R. Lal. "On modifications of Reichenbach's principle of common cause in light of Bell's theorem." In: *Journal of Physics A: Mathematical and Theoretical* 47.42 (2014), p. 424018.

[378] R. Chaves, G. B. Lemos, and J. Pienaar. "Causal Modeling the Delayed-Choice Experiment." In: *Phys. Rev. Lett.* 120.19 (2018), p. 190401.

[379] B. S. Cirel'son. "Quantum generalizations of Bell's inequality." In: *Letters in Mathematical Physics* 4.2 (1980), pp. 93–100.

[380] J. F. Clauser and A. Shimony. "Bell's theorem. Experimental tests and implications." In: *Reports on Progress in Physics* 41.12 (1978), p. 1881.

[381] J. F. Clauser et al. "Proposed Experiment to Test Local Hidden-Variable Theories." In: *Phys. Rev. Lett.* 23.15 (1969), pp. 880–884.

[382] D. Collins et al. "Bell Inequalities for Arbitrarily High-Dimensional Systems." In: *Phys. Rev. Lett.* 88.4 (2002), p. 040404.

[383] R. Corry. "Retrocausal models for {EPR}." In: *Studies in History and Philosophy of Science Part B: Studies in History and Philosophy of Modern Physics* 49 (2015), pp. 1–9.

[384] B. d'Espagnat. "The Quantum Theory and Reality." In: *Scientific American* 241 (1989), pp. 158–181.

[385] P. H. Eberhard. "Bell's theorem and the different concepts of locality." In: *Il Nuovo Cimento B (1971-1996)* 46.2 (1978), pp. 392–419.

[386] A. K. Ekert. "Quantum cryptography based on Bell's theorem." In: *Phys. Rev. Lett.* 67.6 (1991), pp. 661–663.

[387] A. Fine. "Correlations and efficiency: Testing the Bell inequalities." In: *Foundations of Physics* 19.5 (1989), pp. 453–478.

[388] A. Fine. "Hidden Variables, Joint Probability, and the Bell Inequalities." In: *Phys. Rev. Lett.* 48.5 (1982), pp. 291–295.

[389] S. J. Freedman and J. F. Clauser. "Experimental Test of Local Hidden-Variable Theories." In: *Phys. Rev. Lett.* 28.14 (1972), pp. 938–941.

[390] M. Giustina et al. "Significant-Loophole-Free Test of Bell's Theorem with Entangled Photons." In: *Phys. Rev. Lett.* 115.25 (2015), p. 250401.

[391] D. M. Greenberger et al. "Bell's theorem without inequalities." In: *American Journal of Physics* 58.12 (1990), pp. 1131–1143.

[392] M. J. W. Hall. *Comment on 'Non-realism: deep thought or soft option?', by N. Gisin.* preprint: arXiv:0909.0015 (quant-ph). 2009.

[393] T. Hellmuth et al. "Delayed-choice experiments in quantum interference." In: *Phys. Rev. A* 35.6 (1987), pp. 2532–2541.

[394] B. Hensen et al. "Loophole-free Bell inequality violation using electron spins separated by 1.3 kilometres." In: *Nature* 526.7575 (2015), pp. 682–686.

[395] R. Horodecki, P. Horodecki, and M. Horodecki. "Violating Bell inequality by mixed spin-12 states: necessary and sufficient condition." In: *Physics Letters A* 200.5 (1995), pp. 340–344.

[396] H.-L. Huang et al. "Compatibility of causal hidden-variable theories with a delayed-choice experiment." In: *Phys. Rev. A* 100.1 (2019), p. 012114.

[397] R. Ionicioiu and D. R. Terno. "Proposal for a Quantum Delayed-Choice Experiment." In: *Phys. Rev. Lett.* 107.23 (2011), p. 230406.

[398] V. Jacques et al. "Experimental Realization of Wheeler's Delayed-Choice Gedanken Experiment." In: *Science* 315.5814 (2007), pp. 966–968.

[399] T. Jennewein et al. "Experimental Nonlocality Proof of Quantum Teleportation and Entanglement Swapping." In: *Phys. Rev. Lett.* 88.1 (2001), p. 017903.

[400] S. J. Jones, H. M. Wiseman, and A. C. Doherty. "Entanglement, Einstein-Podolsky-Rosen correlations, Bell nonlocality, and steering." In: *Phys. Rev. A* 76.5 (2007), p. 052116.

[401] F. Kaiser et al. "Entanglement-Enabled Delayed-Choice Experiment." In: *Science* 338.6107 (2012), pp. 637–640.

[402] D. Kaszlikowski et al. "Violations of Local Realism by Two Entangled N-Dimensional Systems Are Stronger than for Two Qubits." In: *Phys. Rev. Lett.* 85.21 (2000), pp. 4418–4421.

[403] G. C. Krizek. "Einstein's 1935 papers: EPR=ER?" In: *arxiv* (2017).

[404] L. J. Landau. "On the violation of Bell's inequality in quantum theory." In: *Physics Letters A* 120.2 (1987), pp. 54–56.

[405] N. Linden et al. "Quantum Nonlocality and Beyond: Limits from Nonlocal Computation." In: *Phys. Rev. Lett.* 99.18 (2007), p. 180502.

[406] Y. Liu et al. "Multipartite nonlocality in an Ising model with a tilted magnetic field at zero and finite temperatures." In: *Physics Letters A* 450 (2022), p. 128396.

[407] X.-S. Ma et al. "Quantum erasure with causally disconnected choice." In: *Proceedings of the National Academy of Sciences* 110.4 (2013), pp. 1221–1226.

[408] X.-s. Ma et al. "Experimental delayed-choice entanglement swapping." In: *Nature Physics* 8.6 (2012), pp. 479–484.

[409] J. Maldacena and L. Susskind. "Cool horizons for entangled black holes." In: *Fortschritte der Physik* 61.9 (2013), pp. 781–811.

[410] T. Maudlin. "Space-Time in the Quantum World." In: *Bohmian Mechanics and Quantum Theory: An Appraisal*. Ed. by J. T. Cushing, A. Fine, and S. Goldstein. Springer Netherlands, 1996, pp. 285–307.

[411] T. Maudlin. "What Bell did." In: *Journal of Physics A: Mathematical and Theoretical* 47.42 (2014), p. 424010.

[412] N. D. Mermin. "Quantum mechanics vs local realism near the classical limit: A Bell inequality for spin s." In: *Phys. Rev. D* 22.2 (1980), pp. 356–361.

[413] N. D. Mermin. "Hidden variables and the two theorems of John Bell." In: *Rev. Mod. Phys.* 65.3 (1993), pp. 803–815.

[414] N. D. Mermin. "Quantum mysteries revisited." In: *American Journal of Physics* 58.8 (1990), pp. 731–734.

[415] M. Michler, H. Weinfurter, and M. Żukowski. "Experiments towards Falsification of Noncontextual Hidden Variable Theories." In: *Phys. Rev. Lett.* 84.24 (2000), pp. 5457–5461.

[416] T. Norsen. "Against 'Realism'." In: *Foundations of Physics* 37.3 (2007), pp. 311–340.

[417] T. Norsen. "John S. Bell's concept of local causality." In: *American Journal of Physics* 79.12 (2011), pp. 1261–1275.

[418] P. M. Pearle. "Hidden-Variable Example Based upon Data Rejection." In: *Phys. Rev. D* 2.8 (1970), pp. 1418–1425.

[419] D. Pegg. "Objective reality, causality and the aspect experiment." In: *Physics Letters A* 78.3 (1980), pp. 233–234.

[420] A. Peres. "Delayed choice for entanglement swapping." In: *Journal of Modern Optics* 47.2-3 (2000), pp. 139–143.

[421] A. Peres. "Finite violation of a Bell inequality for arbitrarily large spin." In: *Phys. Rev. A* 46.7 (1992), pp. 4413–4414.

[422] A. Peres and D. R. Terno. "Quantum information and relativity theory." In: *Rev. Mod. Phys.* 76.1 (2004), pp. 93–123.

[423] M. Piani and J. Watrous. "Necessary and Sufficient Quantum Information Characterization of Einstein-Podolsky-Rosen Steering." In: *Phys. Rev. Lett.* 114.6 (2015), p. 060404.

[424] S. Pironio. "All Clauser-Horne-Shimony-Holt polytopes." In: *Journal of Physics A: Mathematical and Theoretical* 47.42 (2014), p. 424020.

[425] E. Polino et al. "Device-independent test of a delayed choice experiment." In: *Phys. Rev. A* 100.2 (2019), p. 022111.

[426] S. Popescu. "Bell's Inequalities and Density Matrices: Revealing "Hidden" Nonlocality." In: *Phys. Rev. Lett.* 74.14 (1995), pp. 2619–2622.

[427] S. Popescu and D. Rohrlich. "Quantum nonlocality as an axiom." In: *Foundations of Physics* 24.3 (1994), pp. 379–385.

[428] S. Popescu and L. Vaidman. "Causality constraints on nonlocal quantum measurements." In: *Phys. Rev. A* 49.6 (1994), pp. 4331–4338.

[429] H. Price. "Toy models for retrocausality." In: *Studies in History and Philosophy of Science Part B: Studies in History and Philosophy of Modern Physics* 39.4 (2008), pp. 752–761.

[430] D. Rauch et al. "Cosmic Bell Test Using Random Measurement Settings from High-Redshift Quasars." In: *Phys. Rev. Lett.* 121.8 (2018), p. 080403.

[431] W. Rosenfeld et al. "Event-Ready Bell Test Using Entangled Atoms Simultaneously Closing Detection and Locality Loopholes." In: *Phys. Rev. Lett.* 119.1 (2017), p. 010402.

[432] M. A. Rowe et al. "Experimental violation of a Bell's inequality with efficient detection." In: *Nature* 409.6822 (2001), pp. 791–794.

[433] L. K. Shalm et al. "Strong Loophole-Free Test of Local Realism." In: *Phys. Rev. Lett.* 115.25 (2015), p. 250402.

[434] L. Susskind. "Copenhagen vs Everett, Teleportation, and ER=EPR." In: *Fortschritte der Physik* 64.6-7 (2016), pp. 551–564.

[435] G. Svetlichny. "Distinguishing three-body from two-body nonseparability by a Bell-type inequality." In: *Phys. Rev. D* 35.10 (1987), pp. 3066–3069.

[436] J.-S. Tang et al. "Realization of quantum Wheeler's delayed-choice experiment." In: *Nature Photonics* 6.9 (2012), pp. 600–604.

[437] The BIG Bell Test Collaboration. "Challenging local realism with human choices." In: *Nature* 557.7704 (2018), pp. 212–216.

[438] F. J. Tipler. "Quantum nonlocality does not exist." In: *Proceedings of the National Academy of Sciences* 111.31 (2014), pp. 11281–11286.

[439] J. Tura et al. "Detecting nonlocality in many-body quantum states." In: *Science* 344.6189 (2014), pp. 1256–1258.

[440] R. Uola et al. "Quantum steering." In: *Rev. Mod. Phys.* 92.1 (2020), p. 015001.

[441] L. Vaidman. "Instantaneous Measurement of Nonlocal Variables." In: *Phys. Rev. Lett.* 90.1 (2003), p. 010402.

[442] L. Vaidman. "Lorentz-invariant "elements of reality" and the joint measurability of commuting observables." In: *Phys. Rev. Lett.* 70.22 (1993), pp. 3369–3372.

[443] L. Vaidman. "Teleportation of quantum states." In: *Phys. Rev. A* 49.2 (1994), pp. 1473–1476.

[444] L. Vaidman. "The Bell Inequality and the Many-Worlds Interpretation." In: *Quantum Nonlocality and Reality: 50 Years of Bell's Theorem*. Ed. by M. Bell and S. Gao. Cambridge University Press, 2016, pp. 195–203.

[445] M. Waegell and K. J. McQueen. "Reformulating Bell's theorem: The search for a truly local quantum theory." In: *Studies in History and Philosophy of Science Part B: Studies in History and Philosophy of Modern Physics* 70 (2020), pp. 39–50.

[446] G. Weihs et al. "Violation of Bell's Inequality under Strict Einstein Locality Conditions." In: *Phys. Rev. Lett.* 81.23 (1998), pp. 5039–5043.

[447] R. F. Werner. "Comment on 'What Bell did'." In: *Journal of Physics A: Mathematical and Theoretical* 47.42 (2014), p. 424011.

[448] R. F. Werner. "Quantum states with Einstein-Podolsky-Rosen correlations admitting a hidden-variable model." In: *Phys. Rev. A* 40.8 (1989), pp. 4277–4281.

[449] R. F. Werner and M. M. Wolf. "Bell Inequalities and Entanglement." In: *Quantum Information and Computation* 1.3 (2001), pp. 1–25.

[450] H. M. Wiseman. "The two Bell's theorems of John Bell." In: *Journal of Physics A: Mathematical and Theoretical* 47.42 (2014), p. 424001.

[451] H. M. Wiseman, S. J. Jones, and A. C. Doherty. "Steering, Entanglement, Nonlocality, and the Einstein-Podolsky-Rosen Paradox." In: *Phys. Rev. Lett.* 98.14 (2007), p. 140402.

[452] H. Wiseman. "Physics: Bell's theorem still reverberates." In: *Nature* 510.7506 (2014), pp. 467–469.

[453] H. M. Wiseman and E. G. Cavalcanti. "Causarum Investigatio and the Two Bell's Theorems of John Bell." In: *Quantum [Un]Speakables II: Half a Century of Bell's Theorem*. Ed. by R. Bertlmann and A. Zeilinger. Springer International Publishing, 2017, pp. 119–142.

[454] C. J. Wood and R. W. Spekkens. "The lesson of causal discovery algorithms for quantum correlations: causal explanations of Bell-inequality violations require fine-tuning." In: *New Journal of Physics* 17.3 (2015), p. 033002.

[455] M. Żukowski et al. ""Event-ready-detectors" Bell experiment via entanglement swapping." In: *Physical Review Letters* 71.26 (1993), pp. 4287–4290.

[456] M. Żukowski and Č. Brukner. "Bell's Theorem for General N-Qubit States." In: *Phys. Rev. Lett.* 88.21 (2002), p. 210401.

[457] M. Żukowski and Č. Brukner. "Quantum non-locality-it ain't necessarily so..." In: *Journal of Physics A: Mathematical and Theoretical* 47.42 (2014), p. 424009.

Entanglement and its Application

Encyclopedic

[458] D. Bruß. "Creation and Detection of Entanglement." In: *Compendium of Quantum Physics*. Ed. by D. Greenberger, K. Hentschel, and F. Weinert. Berlin, Heidelberg: Springer Berlin Heidelberg, 2009, pp. 145–149.

[459] D. Bruß. "Entanglement Purification and Distillation." In: *Compendium of Quantum Physics*. Ed. by D. Greenberger, K. Hentschel, and F. Weinert. Berlin, Heidelberg: Springer Berlin Heidelberg, 2009, pp. 202–205.

[460] D. Janzing. "Entropy of Entanglement." In: *Compendium of Quantum Physics*. Ed. by D. Greenberger, K. Hentschel, and F. Weinert. Berlin, Heidelberg: Springer Berlin Heidelberg, 2009, pp. 205–209.

Articles

[461] A. Acín, N. Gisin, and L. Masanes. "From Bell's Theorem to Secure Quantum Key Distribution." In: *Phys. Rev. Lett.* 97.12 (2006), p. 120405.

[462] J.-D. Bancal et al. "Device-Independent Witnesses of Genuine Multipartite Entanglement." In: *Phys. Rev. Lett.* 106.25 (2011), p. 250404.

[463] C. H. Bennett et al. "Purification of Noisy Entanglement and Faithful Teleportation via Noisy Channels." In: *Phys. Rev. Lett.* 76.5 (1996), pp. 722–725.

[464] S. Bose, V. Vedral, and P. L. Knight. "Multiparticle generalization of entanglement swapping." In: *Phys. Rev. A* 57.2 (1998), pp. 822–829.

[465] J. Bowles et al. "Device-Independent Entanglement Certification of All Entangled States." In: *Phys. Rev. Lett.* 121.18 (2018), p. 180503.

[466] H.-J. Briegel et al. "Entanglement Purification." In: *The Physics of Quantum Information: Quantum Cryptography, Quantum Teleportation, Quantum Computation*. Ed. by D. Bouwmeester, A. Ekert, and A. Zeilinger. Berlin, Heidelberg: Springer Berlin Heidelberg, 2000, pp. 261–293.

[467] H.-J. Briegel et al. "Quantum Repeaters: The Role of Imperfect Local Operations in Quantum Communication." In: *Phys. Rev. Lett.* 81.26 (1998), pp. 5932–5935.

[468] D. Bruß et al. "Reflections upon separability and distillability." In: *Journal of Modern Optics* 49.8 (2002), pp. 1399–1418.

[469] V. Coffman, J. Kundu, and W. K. Wootters. "Distributed entanglement." In: *Phys. Rev. A* 61.5 (2000), p. 052306.

[470] D. Deutsch et al. "Quantum Privacy Amplification and the Security of Quantum Cryptography over Noisy Channels." In: *Phys. Rev. Lett.* 77.13 (1996), pp. 2818–2821.

[471] A. Dimić and B. Dakić. "Single-copy entanglement detection." In: *npj Quantum Information* 4.1 (2018), p. 11.

[472] D. P. DiVincenzo et al. "Evidence for bound entangled states with negative partial transpose." In: *Phys. Rev. A* 61.6 (2000), p. 062312.

[473] W. Dür and J. I. Cirac. "Classification of multiqubit mixed states: Separability and distillability properties." In: *Phys. Rev. A* 61.4 (2000), p. 042314.

[474] W. Dür, J. I. Cirac, and R. Tarrach. "Separability and Distillability of Multiparticle Quantum Systems." In: *Phys. Rev. Lett.* 83.17 (1999), pp. 3562–3565.

[475] W. Dür, G. Vidal, and J. I. Cirac. "Three qubits can be entangled in two inequivalent ways." In: *Phys. Rev. A* 62.6 (2000), p. 062314.

[476] C. Eltschka and J. Siewert. "Quantifying entanglement resources." In: *Journal of Physics A: Mathematical and Theoretical* 47.42 (2014), p. 424005.

[477] N. Friis et al. "Entanglement certification from theory to experiment." In: *Nature Reviews Physics* 1.1 (2019), pp. 72–87.

[478] S. Gharibian. "Strong NP-Hardness of the Quantum Separability Problem." In: *Quantung Information and Computation* 10.3 & 4 (2012), pp. 0343–0360.

[479] O. Gühne and G. Tóth. "Energy and multipartite entanglement in multidimensional and frustrated spin models." In: *Phys. Rev. A* 73.5 (2006), p. 052319.

[480] O. Gühne and G. Tóth. "Entanglement detection." In: *Physics Reports* 474.1 (2009), pp. 1–75.

[481] O. Gühne, G. Tóth, and H. J. Briegel. "Multipartite entanglement in spin chains." In: *New Journal of Physics* 7.1 (2005), p. 229.

[482] M. Horodecki, P. Horodecki, and R. Horodecki. "Mixed-State Entanglement and Distillation: Is there a "Bound" Entanglement in Nature?" In: *Phys. Rev. Lett.* 80.24 (1998), pp. 5239–5242.

[483] M. Horodecki, P. Horodecki, and R. Horodecki. "Separability of mixed states: necessary and sufficient conditions." In: *Physics Letters A* 223.1 (1996), pp. 1–8.

[484] R. Horodecki et al. "Quantum entanglement." In: *Rev. Mod. Phys.* 81.2 (2009), pp. 865–942.

[485] P. Hyllus et al. "Fisher information and multiparticle entanglement." In: *Phys. Rev. A* 85.2 (2012), p. 022321.

[486] T. Jennewein et al. "Quantum Cryptography with Entangled Photons." In: *Phys. Rev. Lett.* 84.20 (2000), pp. 4729–4732.

[487] D. Kaszlikowski et al. "Quantum Correlation without Classical Correlations." In: *Phys. Rev. Lett.* 101.7 (2008), p. 070502.

[488] W. Kłobus et al. "Higher dimensional entanglement without correlations." In: *The European Physical Journal D* 73.2 (2019), p. 29.

[489] L. Knips et al. "Multipartite Entanglement Detection with Minimal Effort." In: *Phys. Rev. Lett.* 117.21 (2016), p. 210504.

[490] L. M. Knips. "Efficient Quantum State Analysis and Entanglement Detection." PhD thesis. Ludwig-Maximilians-Universität München, 2019.

[491] W. Laskowski et al. "Entanglement witnesses with variable number of local measurements." In: *Phys. Rev. A* 88.2 (2013), p. 022304.

[492] W. Laskowski et al. "Experimental Schmidt Decomposition and State Independent Entanglement Detection." In: *Phys. Rev. Lett.* 108.24 (2012), p. 240501.

[493] W. Laskowski et al. "Optimized state-independent entanglement detection based on a geometrical threshold criterion." In: *Phys. Rev. A* 88.2 (2013), p. 022327.

[494] M. Lewenstein et al. "Optimization of entanglement witnesses." In: *Phys. Rev. A* 62.5 (2000), p. 052310.

[495] H. Lu et al. "Entanglement Structure: Entanglement Partitioning in Multipartite Systems and Its Experimental Detection Using Optimizable Witnesses." In: *Phys. Rev. X* 8.2 (2018), p. 021072.

[496] H. Ollivier and W. H. Zurek. "Quantum Discord: A Measure of the Quantumness of Correlations." In: *Phys. Rev. Lett.* 88.1 (2001), p. 017901.

[497] T. J. Osborne and F. Verstraete. "General Monogamy Inequality for Bipartite Qubit Entanglement." In: *Phys. Rev. Lett.* 96.22 (2006), p. 220503.

[498] K. F. Pál, T. Vértesi, and M. Navascués. "Device-independent tomography of multipartite quantum states." In: *Phys. Rev. A* 90.4 (2014), p. 042340.

[499] S. Pallister, N. Linden, and A. Montanaro. "Optimal Verification of Entangled States with Local Measurements." In: *Phys. Rev. Lett.* 120.17 (2018), p. 170502.

[500] A. Peres. "Separability Criterion for Density Matrices." In: *Phys. Rev. Lett.* 77.8 (1996), pp. 1413–1415.

[501] M. B. Plenio and S. Virmani. "An Introduction to Entanglement Measures." In: *Quantum Information and Computation* 7.1 (2007), pp. 1–51.

[502] Á. Rivas, S. F. Huelga, and M. B. Plenio. "Entanglement and Non-Markovianity of Quantum Evolutions." In: *Phys. Rev. Lett.* 105.5 (2010), p. 050403.

[503] V. Saggio et al. "Experimental few-copy multipartite entanglement detection." In: *Nature Physics* 15.9 (2019), pp. 935–940.

[504] C. Schwemmer et al. "Genuine Multipartite Entanglement without Multipartite Correlations." In: *Phys. Rev. Lett.* 114.18 (2015), p. 180501.

[505] R. Taghiabadi, S. J. Akhtarshenas, and M. Sarbishaei. "Reexamination of strong subadditivity: A quantum-correlation approach." In: *Phys. Rev. A* 95.3 (2017), p. 032315.

[506] G. Tóth. "Multipartite entanglement and high-precision metrology." In: *Phys. Rev. A* 85.2 (2012), p. 022322.

[507] M. C. Tran et al. "Genuine N-partite entanglement without N-partite correlation functions." In: *Phys. Rev. A* 95.6 (2017), p. 062331.

[508] G. Vidal and R. F. Werner. "Computable measure of entanglement." In: *Phys. Rev. A* 65.3 (2002), p. 032314.

[509] F. Xu et al. "Secure quantum key distribution with realistic devices." In: *Rev. Mod. Phys.* 92.2 (2020), p. 025002.

[510] X.-D. Yu, J. Shang, and O. Gühne. "Statistical Methods for Quantum State Verification and Fidelity Estimation." In: *Advanced Quantum Technologies* 5.5 (2022), p. 2100126.

Optics, Quantum Optics and Quantum Field Theory

Monographies

[511] H.-A. Bachor and T. C. Ralph. *A Guide to Experiments on Quantum Optics*. Wiley-VCH, 2004.

[512] I. Bałynicki-Birula and Z. Bałynicka-Birula. *Elektrodynamika Kwantowa*. Pergamon Press, 1974.

[513] M. Bass et al., eds. *OSA Handbook of Optics. Volume I, Fundamentals, Techniques, and Design*. McGraw-Hill, 1995.

[514] M. Born and E. Wolf. *Principles of Optics*. 6th. Pergamon Press Ltd., 1986.

[515] R. W. Boyd. *Nonlinear Optics*. Academic Press, 2020.

[516] V. G. Dmitriev, G. G. Gurzadyan, and D. N. Nikogosyan. *Handbook of Nonlinear Optical Crystals*. Springer, 1999.

[517] G. R. Fowles. *Introduction to Modern Optics*. 2nd. Dover Publications, INC., New York, 1989.

[518] A. Gerrard and J. M. Burch. *Introduction to Matrix Methods in Optics*. Dover Publications. Inc., 1975.

[519] J. W. Goodman. *Introduction to Fourier Optics*. McGraw-Hill, 1996.

[520] D. J. Griffiths. *Introduction to elementary particles*. John Wiley & Sons, Inc., 1987.

[521] R. Haag. *Local Quantum Physics: Fields, Particles, Algebras*. Springer Berlin Heidelberg New York, 1996.

[522] R. Hanbury-Brown. *The Intensity Interferometer*. Taylor & Francis, 1974.

[523] J. D. Jackson. *Classical Electrodynamics*. John Wiley & Sons, Inc., 1999.

[524] R. Loudon. *The Quantum Theory of Light*. 3rd. Oxford University Press, 2000.

[525] L. Mandel and E. Wolf. *Optical Coherence and Quantum Optics*. Cambridge University Press, 1995.

[526] F. Mandl and G. Shaw. *Quantum Field Theory*. John Wiley & Sons, 1984.

[527] R. Menzel. *Photonics*. Springer Berlin, Heidelberg, 2001.

[528] P. Meystre and M. Sargent. *Elements of Quantum Optics*. Springer, 2007.

[529] G. J. Milburn and D. Walls. *Quantum Optics*. Springer, 1994.

[530] B. E. A. Saleh and M. C. Teich. *Fundamentals of Photonics*. John Wiley & Sons, 2007.

[531] M. O. Scully and M. S. Zubairy. *Quantum Optics*. Cambridge University Press, 1997.

[532] W. A. Shurcliff. *Polarized Light*. Harvard University Press, 1966.

[533] A. W. Snyder and J. D. Love. *Optical Waveguide Theory*. Springer, 1983.

[534] S. Weinberg. *The Quantum Theory of Fields*. Vol. 1. Cambridge University Press, 1995.

[535] S. Weinberg. *The Quantum Theory of Fields*. Vol. 2. Cambridge University Press, 1996.

[536] R. Wigmans. *Calorimetry: Energy Measurement in Particle Physics*. Oxford University Press, 2017.

[537] W. Zinth and U. Zinth. *Optik*. Oldenburg, 2009.

Encyclopedic

[538] A. Borrelli. "Renormalization." In: *Compendium of Quantum Physics*. Ed. by D. Greenberger, K. Hentschel, and F. Weinert. Berlin, Heidelberg: Springer Berlin Heidelberg, 2009, pp. 637–640.

[539] B. Falkenburg. "Particle Tracks." In: *Compendium of Quantum Physics*. Ed. by D. Greenberger, K. Hentschel, and F. Weinert. Berlin, Heidelberg: Springer Berlin Heidelberg, 2009, pp. 460–465.

[540] C. Gearhart. "Black-Body Radiation." In: *Compendium of Quantum Physics*. Ed. by D. Greenberger, K. Hentschel, and F. Weinert. Berlin, Heidelberg: Springer Berlin Heidelberg, 2009, pp. 39–42.

[541] G. Jaeger. "Double-Slit Experiment (or Two-Slit Experiment)." In: *Compendium of Quantum Physics*. Ed. by D. Greenberger, K. Hentschel, and F. Weinert. Berlin, Heidelberg: Springer Berlin Heidelberg, 2009, pp. 174–178.

[542] B. R. Judd. "Second Quantization." In: *Springer Handbook of Atomic, Molecular, and Optical Physics*. Ed. by G. W. F. Drake. Springer International Publishing, 2023, pp. 111–117.

[543] D. Kaiser. "Feynman Diagrams." In: *Compendium of Quantum Physics*. Ed. by D. Greenberger, K. Hentschel, and F. Weinert. Berlin, Heidelberg: Springer Berlin Heidelberg, 2009, pp. 235–239.

[544] P. G. Kwiat. "One- and Two-Photon Interference." In: *Compendium of Quantum Physics*. Ed. by D. Greenberger, K. Hentschel, and F. Weinert. Berlin, Heidelberg: Springer Berlin Heidelberg, 2009, pp. 428–434.

[545] P. Milonni and U. Mohideen. "Casimir Effect." In: *Compendium of Quantum Physics*. Ed. by D. Greenberger, K. Hentschel, and F. Weinert. Berlin, Heidelberg: Springer Berlin Heidelberg, 2009, pp. 87–88.

[546] P. Milonni and M. M. Nieto. "Coherent States." In: *Compendium of Quantum Physics*. Ed. by D. Greenberger, K. Hentschel, and F. Weinert. Berlin, Heidelberg: Springer Berlin Heidelberg, 2009, pp. 106–108.

[547] P. W. Milonni. "Zero-Point Energy." In: *Compendium of Quantum Physics*. Ed. by D. Greenberger, K. Hentschel, and F. Weinert. Berlin, Heidelberg: Springer Berlin Heidelberg, 2009, pp. 864–866.

[548] K. A. Milton. "Particle Physics." In: *Compendium of Quantum Physics*. Ed. by D. Greenberger, K. Hentschel, and F. Weinert. Berlin, Heidelberg: Springer Berlin Heidelberg, 2009, pp. 455–459.

[549] M. B. Plenio. "Squeezed States." In: *Compendium of Quantum Physics*. Ed. by D. Greenberger, K. Hentschel, and F. Weinert. Berlin, Heidelberg: Springer Berlin Heidelberg, 2009, pp. 736–738.

[550] J. R. Sapirstein. "Quantum Electrodynamics." In: *Springer Handbook of Atomic, Molecular, and Optical Physics*. Ed. by G. W. F. Drake. Cham: Springer International Publishing, 2023, pp. 415–431.

[551] B. R. Wheaton. "Photoelectric Effect." In: *Compendium of Quantum Physics*. Ed. by D. Greenberger, K. Hentschel, and F. Weinert. Berlin, Heidelberg: Springer Berlin Heidelberg, 2009, pp. 472–475.

[552] F. Wilczek. "Quantum Field Theory." In: *Compendium of Quantum Physics*. Ed. by D. Greenberger, K. Hentschel, and F. Weinert. Berlin, Heidelberg: Springer Berlin Heidelberg, 2009, pp. 549–564.

Articles

[553] J. Aasi et al. "Enhanced sensitivity of the LIGO gravitational wave detector by using squeezed states of light." In: *Nature Photonics* 7.8 (2013), pp. 613–619.

[554] L. Allen et al. "Orbital angular momentum of light and the transformation of Laguerre-Gaussian laser modes." In: *Phys. Rev. A* 45.11 (1992), pp. 8185–8189.

[555] P. K. Amiri et al. "Tight-Binding Analysis of Coupled Dielectric Waveguide Structures." In: *Fiber and Integrated Optics* 25.1 (2006), pp. 11–27.

[556] F. T. Arecchi. "Measurement of the Statistical Distribution of Gaussian and Laser Sources." In: *Phys. Rev. Lett.* 15.24 (1965), pp. 912–916.

[557] R. S. Aspden, M. J. Padgett, and G. C. Spalding. "Video recording true single-photon double-slit interference." In: *American Journal of Physics* 84.9 (2016), pp. 671–677.

[558] A. Bekshaev and M. Soskin. "Transverse energy flows in vectorial fields of paraxial beams with singularities." In: *Optics Communications* 271.2 (2007), pp. 332–348.

[559] A. Bekshaev, K. Y. Bliokh, and M. Soskin. "Internal flows and energy circulation in light beams." In: *Journal of Optics* 13.5 (2011), p. 053001.

[560] M. V. Berry. "Optical currents." In: *Journal of Optics A: Pure and Applied Optics* 11.9 (2009), p. 094001.

[561] I. Białynicki-Birula. "On the Wave Function of the Photon." In: *Acta Physica Polonica A* 86.1-2 (1994), pp. 97–116.

[562] I. Białynicki-Birula. "The Photon Wave Function." In: *Coherence and Quantum Optics VII: Proceedings of the Seventh Rochester Conference on Coherence and Quantum Optics, held at the University of Rochester, June 7-10, 1995*. Ed. by J. H. Eberly, L. Mandel, and E. Wolf. Boston, MA: Springer US, 1996, pp. 313–322.

[563] I. Bialynicki-Birula and Z. Bialynicka-Birula. "Quantum-mechanical description of optical beams." In: *Journal of Optics* 19.12 (2017), p. 125201.

[564] K. Y. Bliokh and F. Nori. "Transverse and longitudinal angular momenta of light." In: *Physics Reports* 592 (2015). Transverse and longitudinal angular momenta of light, pp. 1–38.

[565] D. Bouwmeester et al. "Experimental quantum teleportation." In: *Nature* 390.6660 (1997), pp. 575–579.

[566] R. W. Boyd, A. L. Gaeta, and E. Giese. "Nonlinear Optics." In: *Springer Handbook of Atomic, Molecular, and Optical Physics*. Ed. by G. W. F. Drake. Springer International Publishing, 2023, pp. 1097–1110.

[567] J. B. Brask. *Gaussian states and operations - a quick reference*. preprint: arXiv:2102.05748 (quant-ph). 2022.

[568] B. Brecht et al. "Photon Temporal Modes: A Complete Framework for Quantum Information Science." In: *Phys. Rev. X* 5.4 (2015), p. 041017.

[569] G. Breitenbach, S. Schiller, and J. Mlynek. "Measurement of the quantum states of squeezed light." In: *Nature* 387.6632 (1997), pp. 471–475.

[570] R. H. Brown and R. Q. Twiss. "Correlation between Photons in two Coherent Beams of Light." In: *Nature* 177.4497 (1956), pp. 27–29.

[571] R. H. Brown, R. Q. Twiss, and A. C. B. Lovell. "Interferometry of the intensity fluctuations in light - III. Applications to astronomy." In: *Proceedings of the Royal Society of London. Series A. Mathematical and Physical Sciences* 248.1253 (1958), pp. 199–221.

[572] R. H. Brown et al. "Interferometry of the intensity fluctuations in light - I. Basic theory: the correlation between photons in coherent beams of radiation." In: *Proceedings of the Royal Society of London. Series A. Mathematical and Physical Sciences* 242.1230 (1957), pp. 300–324.

[573] F. Capasso. "Chapter 1 Physics of Avalanche Photodiodes." In: *Lightwave Communications Technology*. Ed. by W. Tsang. Vol. 22. Semiconductors and Semimetals. Elsevier, 1985, pp. 1–172.

[574] C. M. Caves. "Quantum-mechanical noise in an interferometer." In: *Phys. Rev. D* 23.8 (1981), pp. 1693–1708.

[575] N. J. Cerf and J. Fiuràšek. "Optical quantum cloning." In: *Progress in Optics*. Ed. by E. Wolf. Vol. 49. Elsevier, 2006, pp. 455–545.

[576] Y. Chen et al. "Tight-binding model in optical waveguides: Design principle and transferability for simulation of complex photonics networks." In: *Phys. Rev. A* 104.2 (2021), p. 023501.

[577] R. Y. Chiao, E. Garmire, and C. H. Townes. "Self-Trapping of Optical Beams." In: *Phys. Rev. Lett.* 13.15 (1964), pp. 479–482.

[578] W. Chmara. "A Quantum Open-systems Theory Approach to Photodetection." In: *Journal of Modern Optics* 34.3 (1987), pp. 455–467.

[579] C. Couteau et al. "Applications of single photons to quantum communication and computing." In: *Nature Reviews Physics* 5.6 (2023), pp. 326–338.

[580] V. Debierre. "The Photon Wave Function in Principle and in Practice." Theses. Ecole Centrale Marseille ; École centrale de Marseille, 2015.

[581] I. H. Deutsch and J. C. Garrison. "Paraxial quantum propagation." In: *Phys. Rev. A* 43.5 (1991), pp. 2498–2513.

[582] B.-G. Englert. "Fringe Visibility and Which-Way Information: An Inequality." In: *Phys. Rev. Lett.* 77.11 (1996), pp. 2154–2157.

[583] M. Erhard et al. "Twisted photons: new quantum perspectives in high dimensions." In: *Light: Science & Applications* 7.3 (2018), pp. 17146–17146.

[584] P. G. Evans et al. "Bright Source of Spectrally Uncorrelated Polarization-Entangled Photons with Nearly Single-Mode Emission." In: *Phys. Rev. Lett.* 105.25 (2010), p. 253601.

[585] M. Fleming and A. Mooradian. "Spectral characteristics of external-cavity controlled semiconductor lasers." In: *IEEE Journal of Quantum Electronics* 17.1 (1981), pp. 44–59.

[586] T. Fortier and E. Baumann. "20 years of developments in optical frequency comb technology and applications." In: *Communications Physics* 2.1 (2019), p. 153.

[587] T. Giordani et al. "Integrated photonics in quantum technologies." In: *La Rivista del Nuovo Cimento* 46.2 (2023), pp. 71–103.

[588] R. J. Glauber. "Coherent and Incoherent States of the Radiation Field." In: *Phys. Rev.* 131.6 (1963), pp. 2766–2788.

[589] R. J. Glauber. "Optical Coherence and Photon Statistics." In: *Quantum Optics and Electronics: Lectures delivered at Les Houche sduring the 1964 session of the Summer School of Theoretical Physics*. Gordon and Breach, 1965, pp. 63–185.

[590] R. J. Glauber. "The Quantum Theory of Optical Coherence." In: *Phys. Rev.* 130.6 (1963), pp. 2529–2539.

[591] M. Gräfe and A. Szameit. "Integrated photonic quantum walks." In: *Journal of Physics B: Atomic, Molecular and Optical Physics* 53.7 (2020), p. 073001.

[592] P. D. Group et al. "Review of Particle Physics." In: *Progress of Theoretical and Experimental Physics* 2022.8 (2022), p. 083C01.

[593] C. Guerlin et al. "Progressive field-state collapse and quantum non-demolition photon counting." In: *Nature* 448.7156 (2007), pp. 889–893.

[594] J. L. Hall. "Nobel Lecture: Defining and measuring optical frequencies." In: *Rev. Mod. Phys.* 78.4 (2006), pp. 1279–1295.

[595] T. W. Hänsch. "Nobel Lecture: Passion for precision." In: *Rev. Mod. Phys.* 78.4 (2006), pp. 1297–1309.

[596] C. J. Hawthorn, K. P. Weber, and R. E. Scholten. "Littrow configuration tunable external cavity diode laser with fixed direction output beam." In: *Review of Scientific Instruments* 72.12 (2001), pp. 4477–4479.

[597] C. K. Hong, Z. Y. Ou, and L. Mandel. "Measurement of subpicosecond time intervals between two photons by interference." In: *Phys. Rev. Lett.* 59.18 (1987), pp. 2044–2046.

[598] G. Jaeger, A. Shimony, and L. Vaidman. "Two interferometric complementarities." In: *Phys. Rev. A* 51.1 (1995), pp. 54–67.

[599] S. Keiber et al. "Electro-optic sampling of near-infrared waveforms." In: *Nature Photonics* 10.3 (2016), pp. 159–162.

[600] O. Keller. "On the theory of spatial localization of photons." In: *Physics Reports* 411.1 (2005), pp. 1–232.

[601] P. L. Kelley and W. H. Kleiner. "Theory of Electromagnetic Field Measurement and Photoelectron Counting." In: *Phys. Rev.* 136.2A (1964), A316–A334.

[602] M. K.-H. Kiessling and A. S. Tahvildar-Zadeh. "On the quantum-mechanics of a single photon." In: *Journal of Mathematical Physics* 59.11 (2018), p. 112302.

[603] H. J. Kimble, M. Dagenais, and L. Mandel. "Photon Antibunching in Resonance Fluorescence." In: *Phys. Rev. Lett.* 39.11 (1977), pp. 691–695.

[604] H. J. Kimble and L. Mandel. "Photoelectric detection of polychromatic light." In: *Phys. Rev. A* 30.2 (1984), pp. 844–850.

[605] H. Kogelnik and T. Li. "Laser Beams and Resonators." In: *Appl. Opt.* 5.10 (1966), pp. 1550–1567.

[606] F. Krausz and M. Ivanov. "Attosecond physics." In: *Rev. Mod. Phys.* 81.1 (2009), pp. 163–234.

[607] P. G. Kwiat et al. "New High-Intensity Source of Polarization-Entangled Photon Pairs." In: *Phys. Rev. Lett.* 75.24 (1995), pp. 4337–4341.

[608] W. E. Lamb. "Anti-photon." In: *Applied Physics B* 60.2 (1995), pp. 77–84.

[609] S. K. Lamoreaux. "The Casimir force: background, experiments, and applications." In: *Reports on Progress in Physics* 68.1 (2004), p. 201.

[610] U. Leonhardt. "Quantum physics of simple optical instruments." In: *Reports on Progress in Physics* 66.7 (2003), p. 1207.

[611] P. D. Lett et al. "Observation of Atoms Laser Cooled below the Doppler Limit." In: *Phys. Rev. Lett.* 61.2 (1988), pp. 169–172.

[612] R. Loudon and P. Knight. "Squeezed Light." In: *Journal of Modern Optics* 34.6-7 (1987), pp. 709–759.

[613] A. Luis. "Gaussian beams and minimum diffraction." In: *Opt. Lett.* 31.24 (2006), pp. 3644–3646.

[614] K. B. MacAdam, A. Steinbach, and C. Wieman. "A narrow-band tunable diode laser system with grating feedback, and a saturated absorption spectrometer for Cs and Rb." In: *American Journal of Physics* 60.12 (1992), pp. 1098–1111.

[615] T. H. Maiman. "Stimulated Optical Radiation in Ruby." In: *Nature* 187.4736 (1960), pp. 493–494.

[616] L. Mandel. "Squeezed States and Sub-Poissonian Photon Statistics." In: *Phys. Rev. Lett.* 49.2 (1982), pp. 136–138.

[617] L. Mandel. "Sub-Poissonian photon statistics in resonance fluorescence." In: *Opt. Lett.* 4.7 (1979), pp. 205–207.

[618] L. Mandel and E. Wolf. "Coherence Properties of Optical Fields." In: *Rev. Mod. Phys.* 37.2 (1965), pp. 231–287.

[619] G. D. Marshall et al. "Laser written waveguide photonic quantum circuits." In: *Opt. Express* 17.15 (2009), pp. 12546–12554.

[620] M. A. M. Marte and S. Stenholm. "Paraxial light and atom optics: The optical Schrödinger equation and beyond." In: *Phys. Rev. A* 56.4 (1997), pp. 2940–2953.

[621] J. C. F. Matthews et al. "Observing fermionic statistics with photons in arbitrary processes." In: *Scientific Reports* 3.1 (2013), p. 1539.

[622] T. Meany et al. "Laser written circuits for quantum photonics." In: *Laser & Photonics Reviews* 9.4 (2015), pp. 363–384.

[623] R. Menzel and P. W. Milonni. "Laser Principles." In: *Springer Handbook of Atomic, Molecular, and Optical Physics*. Ed. by G. W. F. Drake. Cham: Springer International Publishing, 2023, pp. 1069–1080.

[624] P. J. Mosley et al. "Heralded Generation of Ultrafast Single Photons in Pure Quantum States." In: *Phys. Rev. Lett.* 100.13 (2008), p. 133601.

[625] E. Mukamel et al. "Direct measurement of the spatial Wigner function with area-integrated detection." In: *Opt. Lett.* 28.15 (2003), pp. 1317–1319.

[626] A. Muthukrishnan, M. O. Scully, and M. S. Zubairy. "The Photon Wave Function." In: *The Nature of Light. What is a Photon?* Ed. by C. Roychoudhuri, A. F. Kracklauer, and K. Creath. CRC Press, 2008. Chap. 10, pp. 155–162.

[627] A. Muthukrishnan, M. Scully, and M. Zubairy. "The concept of the photon - Revisited." In: *Optics and Photonics News* 14 (2003), pp. 18–27.

[628] D. Niemietz et al. "Nondestructive detection of photonic qubits." In: *Nature* 591.7851 (2021), pp. 570–574.

[629] J.-W. Pan et al. "Multiphoton entanglement and interferometry." In: *Rev. Mod. Phys.* 84.2 (2012), pp. 777–838.

[630] S. Parker. "A Single-Photon Double-Slit Interference Experiment." In: *American Journal of Physics* 39.4 (1971), pp. 420–424.

[631] M. Pavšič. "Localized States in Quantum Field Theory." In: *Advances in Applied Clifford Algebras* 28.5 (2018), p. 89.

[632] E. Pelucchi et al. "The potential and global outlook of integrated photonics for quantum technologies." In: *Nature Reviews Physics* 4.3 (2022), pp. 194–208.

[633] X. Qiang et al. "Large-scale silicon quantum photonics implementing arbitrary two-qubit processing." In: *Nature Photonics* 12.9 (2018), pp. 534–539.

[634] R. S. Quimby and R. C. Powell. "Types of Lasers." In: *Springer Handbook of Atomic, Molecular, and Optical Physics*. Ed. by G. W. F. Drake. Cham: Springer International Publishing, 2023, pp. 1081–1095.

[635] M. G. Raymer and B. J. Smith. "The Maxwell wave function of the photon (Invited Paper)." In: *Proc.SPIE* 5866 (2005), pp. 5866 - 5866 –5.

[636] E. Recami, M. Zamboni-Rached, and H. E. Hernàndez-Figueroa. "Localized Waves: A Historical and Scientific Introduction." In: *Localized Waves*. Ed. by E. Recami, M. Zamboni-Rached, and H. E. Hernàndez-Figueroa. John Wiley & Sons, Ltd, 2008. Chap. 1, pp. 1–41.

[637] O. Rosas-Ortiz. "Coherent and Squeezed States: Introductory Review of Basic Notions, Properties, and Generalizations." In: *Integrability, Supersymmetry and Coherent States: A Volume in Honour of Professor Véronique Hussin*. Ed. by Ş. Kuru, J. Negro, and L. M. Nieto. Cham: Springer International Publishing, 2019, pp. 187–230.

[638] R. Rosenfelder. *Path Integrals in Quantum Physics*. 2017.

[639] W. Rueckner and J. Peidle. "Young's double-slit experiment with single photons and quantum eraser." In: *American Journal of Physics* 81.12 (2013), pp. 951–958.

[640] P. Saari. "Photon Localization Revisited." In: *Quantum Optics and Laser Experiments*. Ed. by S. Lyagushyn. Rijeka: IntechOpen, 2012. Chap. 3.

[641] M. O. Scully and M. Sargent. "The concept of the photon." In: *Physics Today* 25.3 (1972), pp. 38–47.

[642] L. K. Shalm et al. "Quantum Optical Tests of the Foundations of Physics." In: *Springer Handbook of Atomic, Molecular, and Optical Physics*. Ed. by G. W. F. Drake. Cham: Springer International Publishing, 2023, pp. 1231–1257.

[643] J. Shapiro, H. Yuen, and A. Mata. "Optical communication with two-photon coherent states-Part II: Photoemissive detection and structured receiver performance." In: *IEEE Transactions on Information Theory* 25.2 (1979), pp. 179–192.

[644] C. Silberhorn. "Detecting quantum light." In: *Contemporary Physics* 48.3 (2007), pp. 143–156.

[645] J. E. Sipe. "Photon wave functions." In: *Phys. Rev. A* 52.3 (1995), pp. 1875–1883.

[646] S. Slussarenko et al. "Unconditional violation of the shot-noise limit in photonic quantum metrology." In: *Nature Photonics* 11.11 (2017), pp. 700–703.

[647] B. J. Smith and M. G. Raymer. "Photon wave functions, wave-packet quantization of light, and coherence theory." In: *New Journal of Physics* 9.11 (2007), p. 414.

[648] B. J. Smith et al. "Measurement of the transverse spatial quantum state of light at the single-photon level." In: *Opt. Lett.* 30.24 (2005), pp. 3365–3367.

[649] D. T. Smithey et al. "Measurement of the Wigner distribution and the density matrix of a light mode using optical homodyne tomography: Application to squeezed states and the vacuum." In: *Phys. Rev. Lett.* 70.9 (1993), pp. 1244–1247.

[650] M. Sparnaay. "Measurements of attractive forces between flat plates." In: *Physica* 24.6 (1958), pp. 751–764.

[651] E. C. G. Sudarshan. "Equivalence of Semiclassical and Quantum Mechanical Descriptions of Statistical Light Beams." In: *Phys. Rev. Lett.* 10.7 (1963), pp. 277–279.

[652] L. Susskind and J. Glogower. "Quantum mechanical phase and time operator." In: *Physics Physique Fizika* 1.1 (1964), pp. 49–61.

[653] F. Tamburini and D. Vicino. "Photon wave function: A covariant formulation and equivalence with QED." In: *Phys. Rev. A* 78.5 (2008), p. 052116.

[654] S. M. Tan and D. F. Walls. "Loss of coherence in interferometry." In: *Phys. Rev. A* 47 (6 1993), pp. 4663–4676.

[655] U. M. Titulaer and R. J. Glauber. "Density Operators for Coherent Fields." In: *Phys. Rev.* 145.4 (1966), pp. 1041–1050.

[656] A. Tonomura et al. "Demonstration of single-electron buildup of an interference pattern." In: *American Journal of Physics* 57.2 (1989), pp. 117–120.

[657] D. F. Walls. "Squeezed states of light." In: *Nature* 306.5939 (1983), pp. 141–146.

[658] J. Wang et al. "Multidimensional quantum entanglement with large-scale integrated optics." In: *Science* 360.6386 (2018), pp. 285–291.

[659] H. Weinfurter. "Experimental Bell-State Analysis." In: *Europhysics Letters* 25.8 (1994), p. 559.

[660] D. S. Weiss et al. "Optical molasses and multilevel atoms: experiment." In: *J. Opt. Soc. Am. B* 6.11 (1989), pp. 2072–2083.

[661] L.-A. Wu, M. Xiao, and H. J. Kimble. "Squeezed states of light from an optical parametric oscillator." In: *J. Opt. Soc. Am. B* 4.10 (1987), pp. 1465–1475.

[662] A. Wünsche. "Quantization of Gauss-Hermite and Gauss-Laguerre beams in free space." In: *Journal of Optics B: Quantum and Semiclassical Optics* 6.3 (2004), S47.

[663] M. Xiao, L.-A. Wu, and H. J. Kimble. "Precision measurement beyond the shot-noise limit." In: *Phys. Rev. Lett.* 59.3 (1987), pp. 278–281.

[664] S. Yefet and A. Pe'er. "A Review of Cavity Design for Kerr Lens Mode-Locked Solid-State Lasers." In: *Applied Sciences* 3.4 (2013), pp. 694–724.

[665] H. P. Yuen. "Two-photon coherent states of the radiation field." In: *Phys. Rev. A* 13.6 (1976), pp. 2226–2243.

[666] H. Zeh. "There is no "first" quantization." In: *Physics Letters A* 309.5 (2003), pp. 329–334.

[667] A. Zeilinger et al. "Three-Particle Entanglements from Two Entangled Pairs." In: *Physical Review Letters* 78.16 (1997), pp. 3031–3034.

[668] H. Zhang et al. "Coherent optical frequency combs: From principles to applications." In: *Journal of Electronic Science and Technology* 20.2 (2022), p. 100157.

[669] X. T. Zou and L. Mandel. “Photon-antibunching and sub-Poissonian photon statistics.” In: *Phys. Rev. A* 41.1 (1990), pp. 475–476.

Time-Symmetric Approach and Weak Values

Monographies

[670] Y. Aharonov and D. Rohrlich. *Quantum Paradoxes: Quantum Theory for the Perplexed*. Wiley-VCH Verlag Berlin GmbH, 2005.

Encyclopedic

[671] L. Vaidman. "Two-State Vector Formalism." In: *Compendium of Quantum Physics*. Ed. by D. Greenberger, K. Hentschel, and F. Weinert. Berlin, Heidelberg: Springer Berlin Heidelberg, 2009, pp. 802–806.

[672] L. Vaidman. "Weak Value and Weak Measurements." In: *Compendium of Quantum Physics*. Ed. by D. Greenberger, K. Hentschel, and F. Weinert. Berlin, Heidelberg: Springer Berlin Heidelberg, 2009, pp. 840–842.

Articles

[673] Y. Aharonov and L. Vaidman. "Complete description of a quantum system at a given time." In: *Journal of Physics A: Mathematical and General* 24.10 (1991), p. 2315.

[674] Y. Aharonov et al. "Novel Properties of Preselected and Postselected Ensembles." In: *Annals of the New York Academy of Sciences* 480.1 (1986), pp. 417–421.

[675] Y. Aharonov, D. Z. Albert, and L. Vaidman. "How the result of a measurement of a component of the spin of a spin-1/2 particle can turn out to be 100." In: *Phys. Rev. Lett.* 60.14 (1988), pp. 1351–1354.

[676] Y. Aharonov, P. G. Bergmann, and J. L. Lebowitz. "Time Symmetry in the Quantum Process of Measurement." In: *Phys. Rev.* 134.6B (1964), B1410–B1416.

[677] Y. Aharonov, E. Cohen, and A. C. Elitzur. "Foundations and applications of weak quantum measurements." In: *Phys. Rev. A* 89.5 (2014), p. 052105.

[678] Y. Aharonov and E. Y. Gruss. *Two-time interpretation of quantum mechanics*. preprint: arXiv:quant-ph/0507269. 2005.

[679] Y. Aharonov, S. Popescu, and J. Tollaksen. "A time-symmetric formulation of quantum mechanics." In: *Physics Today* 63.11 (2010), pp. 27–32.

[680] Y. Aharonov and L. Vaidman. "Properties of a quantum system during the time interval between two measurements." In: *Phys. Rev. A* 41.1 (1990), pp. 11–20.

[681] Y. Aharonov and L. Vaidman. "The Two-State Vector Formalism: An Updated Review." In: *Time in Quantum Mechanics*. Ed. by J. Muga, R. S. Mayato, and Í. Egusquiza. Berlin, Heidelberg: Springer Berlin Heidelberg, 2008, pp. 399–447.

[682] Y. Aharonov et al. "Finally making sense of the double-slit experiment." In: *Proceedings of the National Academy of Sciences* 114.25 (2017), pp. 6480–6485.

[683] Y. Aharonov et al. "Measurement and collapse within the two-state vector formalism." In: *Quantum Studies: Mathematics and Foundations* 1.1 (2014), pp. 133–146.

[684] Y. Aharonov et al. "Peculiar features of entangled states with postselection." In: *Phys. Rev. A* 87.1 (2013), p. 014105.

[685] Y. Aharonov et al. "Quantum Cheshire Cats." In: *New Journal of Physics* 15.11 (2013), p. 113015.

[686] Y. Aharonov et al. "Quantum violation of the pigeonhole principle and the nature of quantum correlations." In: *Proceedings of the National Academy of Sciences* 113.3 (2016), pp. 532–535.

[687] Y. Aharonov et al. "Surprising quantum effects." In: *Physics Letters A* 124.4 (1987), pp. 199–203.

[688] Y. Aharonov et al. "The Weak Reality That Makes Quantum Phenomena More Natural: Novel Insights and Experiments." In: *Entropy* 20.11 (2018).

[689] Y. Aharonov et al. "Time-symmetry and topology of the Aharonov-Bohm effect." In: *Journal of Physics A: Mathematical and Theoretical* 56.47 (2023), p. 475302.

[690] M. A. Alonso and A. N. Jordan. "Can a Dove prism change the past of a single photon?" In: *Quantum Studies: Mathematics and Foundations* 2.3 (2015), pp. 255–261.

[691] G. B. Alves et al. "Achieving metrological precision limits through postselection." In: *Phys. Rev. A* 95.1 (2017), p. 012104.

[692] D. R. M. Arvidsson-Shukur et al. "Quantum advantage in postselected metrology." In: *Nature Communications* 11.1 (2020), p. 3775.

[693] S. M. Barnett, J. Jeffers, and D. T. Pegg. "Quantum Retrodiction: Foundations and Controversies." In: *Symmetry* 13.4 (2021).

[694] S. M. Barnett, D. T. Pegg, and J. Jeffers. "Bayes' theorem and quantum retrodiction." In: *Journal of Modern Optics* 47.11 (2000), pp. 1779–1789.

[695] B. N. Bauml. *On the Validity of the Weak Value Approximation*. preprint: arXiv:2312.10397 (quant-ph). 2023.

[696] M. V. Berry and S. Popescu. "Evolution of quantum superoscillations and optical superresolution without evanescent waves." In: *Journal of Physics A: Mathematical and General* 39.22 (2006), p. 6965.

[697] M. V. Berry. "Evanescent and real waves in quantum billiards and Gaussian beams." In: *Journal of Physics A: Mathematical and General* 27.11 (1994), p. L391.

[698] S. L. Braunstein and H. J. Kimble. "A posteriori teleportation." In: *Nature* 394.6696 (1998), pp. 840–841.

[699] A. Brodutch. "Comment on "How the Result of a Single Coin Toss Can Turn Out to be 100 Heads"." In: *Phys. Rev. Lett.* 114.11 (2015), p. 118901.

[700] N. Brunner et al. "Optical Telecom Networks as Weak Quantum Measurements with Postselection." In: *Phys. Rev. Lett.* 91.18 (2003), p. 180402.

[701] J. Bub and H. Brown. "Curious Properties of Quantum Ensembles Which Have Been Both Preselected and Post-Selected." In: *Phys. Rev. Lett.* 56.22 (1986), pp. 2337–2340.

[702] P. Busch and P. J. Lahti. "The determination of the past and the future of a physical system in quantum mechanics." In: *Foundations of Physics* 19.6 (1989), pp. 633–678.

[703] M. F. B. Cenni, R. Corrêa, and P. L. Saldanha. "Effective electrostatic attraction between electrons due to quantum interference." In: *Phys. Rev. A* 100.2 (2019), p. 022101.

[704] M.-C. Chen et al. "Experimental demonstration of quantum pigeonhole paradox." In: *Proceedings of the National Academy of Sciences* 116.5 (2019), pp. 1549–1552.

[705] J. Combes et al. "Quantum limits on postselected, probabilistic quantum metrology." In: *Phys. Rev. A* 89.5 (2014), p. 052117.

[706] A. Danan et al. "Asking Photons Where They Have Been." In: *Phys. Rev. Lett.* 111.24 (2013), p. 240402.

[707] T. Denkmayr et al. "Experimental Demonstration of Direct Path State Characterization by Strongly Measuring Weak Values in a Matter-Wave Interferometer." In: *Phys. Rev. Lett.* 118.1 (2017), p. 010402.

[708] T. Denkmayr et al. "Observation of a quantum Cheshire Cat in a matter-wave interferometer experiment." In: *Nature Communications* 5.1 (2014), p. 4492.

[709] P. B. Dixon et al. "Ultrasensitive Beam Deflection Measurement via Interferometric Weak Value Amplification." In: *Phys. Rev. Lett.* 102.17 (2009), p. 173601.

[710] J. Dressel and A. N. Jordan. "Significance of the imaginary part of the weak value." In: *Phys. Rev. A* 85.1 (2012), p. 012107.

[711] J. Dressel and A. N. Jordan. "Weak Values are Universal in Von Neumann Measurements." In: *Phys. Rev. Lett.* 109.23 (2012), p. 230402.

[712] J. Dressel et al. "*Colloquium* : Understanding quantum weak values: Basics and applications." In: *Rev. Mod. Phys.* 86.1 (2014), pp. 307–316.

[713] J. Dressel et al. "Strengthening weak-value amplification with recycled photons." In: *Phys. Rev. A* 88.2 (2013), p. 023821.

[714] I. M. Duck, P. M. Stevenson, and E. C. G. Sudarshan. "The sense in which a "weak measurement" of a spin-1/2 particle's spin component yields a value 100." In: *Phys. Rev. D* 40.6 (1989), pp. 2112–2117.

[715] J. A. Dziewior. "The Concept of Weak Values." MA thesis. Ludwig-Maximilian-Universität München, 2016.

[716] P. Egan and J. A. Stone. "Weak-value thermostat with 0.2mK precision." In: *Opt. Lett.* 37.23 (2012), pp. 4991–4993.

[717] B.-G. Englert et al. "Past of a quantum particle revisited." In: *Phys. Rev. A* 96.2 (2017), p. 022126.

[718] A. Feizpour, X. Xing, and A. M. Steinberg. "Amplifying Single-Photon Nonlinearity Using Weak Measurements." In: *Phys. Rev. Lett.* 107.13 (2011), p. 133603.

[719] C. Ferrie and J. Combes. "How the Result of a Single Coin Toss Can Turn Out to be 100 Heads." In: *Phys. Rev. Lett.* 113.12 (2014), p. 120404.

[720] C. Ferrie and J. Combes. "Weak Value Amplification is Suboptimal for Estimation and Detection." In: *Phys. Rev. Lett.* 112.4 (2014), p. 040406.

[721] S. Gammelmark, B. Julsgaard, and K. Mølmer. "Past Quantum States of a Monitored System." In: *Phys. Rev. Lett.* 111.16 (2013), p. 160401.

[722] J. L. Garretson et al. "The uncertainty relation in 'which-way' experiments: how to observe directly the momentum transfer using weak values." In: *Journal of Optics B: Quantum and Semiclassical Optics* 6.6 (2004), S506.

[723] M. Hallaji et al. "Weak-value amplification of the nonlinear effect of a single photon." In: *Nature Physics* 13 (2017), p. 540.

[724] J. R. Hance, J. Rarity, and J. Ladyman. "Weak values and the past of a quantum particle." In: *Phys. Rev. Res.* 5 (2 2023), p. 023048.

[725] J. Harris, R. W. Boyd, and J. S. Lundeen. "Weak Value Amplification Can Outperform Conventional Measurement in the Presence of Detector Saturation." In: *Phys. Rev. Lett.* 118.7 (2017), p. 070802.

[726] F. A. Hashmi et al. "Two-state vector formalism and quantum interference." In: *Journal of Physics A: Mathematical and Theoretical* 49.34 (2016), p. 345302.

[727] H. F. Hofmann. "Complete characterization of post-selected quantum statistics using weak measurement tomography." In: *Phys. Rev. A* 81.1 (2010), p. 012103.

[728] H. F. Hofmann. *On the resolution of quantum paradoxes by weak measurements.* preprint: arXiv:0911.0071 (quant-ph). 2009.

[729] O. Hosten and P. Kwiat. "Observation of the Spin Hall Effect of Light via Weak Measurements." In: *Science* 319.5864 (2008), pp. 787–790.

[730] A. C. Ipsen. "Anomalous Weak Values are Caused by Disturbance." In: *Foundations of Physics* 52.1 (2022), p. 20.

[731] A. C. Ipsen. "Disturbance in weak measurements and the difference between quantum and classical weak values." In: *Phys. Rev. A* 91.6 (2015), p. 062120.

[732] A. N. Jordan, J. Martínez-Rincón, and J. C. Howell. "Technical Advantages for Weak-Value Amplification: When Less Is More." In: *Phys. Rev. X* 4.1 (2014), p. 011031.

[733] R. Jozsa. "Complex weak values in quantum measurement." In: *Phys. Rev. A* 76.4 (2007), p. 044103.

[734] R. E. Kastner. "Demystifying Weak Measurements." In: *Foundations of Physics* 47.5 (2017), pp. 697–707.

[735] R. E. Kastner. "The Three-Box "Paradox" and Other Reasons to Reject the Counterfactual Usage of the ABL Rule." In: *Foundations of Physics* 29.6 (1999), pp. 851–863.

[736] A. Kent. "Consistent Sets Yield Contrary Inferences in Quantum Theory." In: *Phys. Rev. Lett.* 78.15 (1997), pp. 2874–2877.

[737] Y. Kim et al. "Direct quantum process tomography via measuring sequential weak values of incompatible observables." In: *Nature Communications* 9.1 (2018), p. 192.

[738] K. A. Kirkpatrick. "Classical three-box "paradox"." In: *Journal of Physics A: Mathematical and General* 36.17 (2003), p. 4891.

[739] G. C. Knee and G. A. D. Briggs. "Seeing opportunity in every difficulty: protecting information with weak value techniques." In: *Quantum Studies: Mathematics and Foundations* 5.3 (2018), pp. 505–517.

[740] G. C. Knee et al. "Weak-value amplification: state of play." In: *Quantum Measurements and Quantum Metrology* 3.1 (2016).

[741] A. G. Kofman, S. Ashhab, and F. Nori. "Nonperturbative theory of weak pre- and post-selected measurements." In: *Physics Reports* 520.2 (2012), pp. 43–133.

[742] C. Krafczyk et al. "Enhanced Weak-Value Amplification via Photon Recycling." In: *Phys. Rev. Lett.* 126.22 (2021), p. 220801.

[743] A. Kumari, A. K. Pan, and P. K. Panigrahi. "Joint weak value for all order coupling using continuous variable and qubit probe." In: *The European Physical Journal D* 71.11 (2017), p. 275.

[744] A. J. Leggett. "Comment on "How the result of a measurement of a component of the spin of a spin-1/2 particle can turn out to be 100"." In: *Phys. Rev. Lett.* 62.19 (1989), pp. 2325–2325.

[745] M. S. Leifer and R. W. Spekkens. "Pre- and Post-Selection Paradoxes and Contextuality in Quantum Mechanics." In: *Phys. Rev. Lett.* 95.20 (2005), p. 200405.

[746] H. Lemmel et al. "Quantifying the presence of a neutron in the paths of an interferometer." In: *Phys. Rev. Res.* 4.2 (2022), p. 023075.

[747] L. Li et al. "Phase amplification in optical interferometry with weak measurement." In: *Phys. Rev. A* 97.3 (2018), p. 033851.

[748] Z.-H. Li, M. Al-Amri, and M. S. Zubairy. "Comment on "Past of a quantum particle"." In: *Phys. Rev. A* 88.4 (2013), p. 046102.

[749] J. S. Lundeen and A. M. Steinberg. "Experimental Joint Weak Measurement on a Photon Pair as a Probe of Hardy's Paradox." In: *Phys. Rev. Lett.* 102.2 (2009), p. 020404.

[750] J. S. Lundeen and C. Bamber. "Procedure for Direct Measurement of General Quantum States Using Weak Measurement." In: *Phys. Rev. Lett.* 108.7 (2012), p. 070402.

[751] J. S. Lundeen et al. "Direct measurement of the quantum wavefunction." In: *Nature* 474.7350 (2011), pp. 188–191.

[752] K. Lyons et al. "Power-Recycled Weak-Value-Based Metrology." In: *Phys. Rev. Lett.* 114.17 (2015), p. 170801.

[753] L. Maccone and C. C. Rusconi. "State estimation: A comparison between direct state measurement and tomography." In: *Phys. Rev. A* 89.2 (2014), p. 022122.

[754] M. Malik et al. "Direct measurement of a 27-dimensional orbital-angular-momentum state vector." In: *Nat Commun* 5 (2014), pp. -.

[755] J. Martínez-Rincón et al. "Ultrasensitive inverse weak-value tilt meter." In: *Opt. Lett.* 42.13 (2017), pp. 2479–2482.

[756] M. Mirhosseini et al. "Compressive Direct Measurement of the Quantum Wave Function." In: *Phys. Rev. Lett.* 113.9 (2014), p. 090402.

[757] Y. Mori, J. Lee, and I. Tsutsui. "On the validity of weak measurement applied for precision measurement." In: *Journal of Physics B: Atomic, Molecular and Optical Physics* 53.1 (2019), p. 015501.

[758] D. Paneru and E. Cohen. "Past of a particle in an entangled state." In: *International Journal of Quantum Information* 15.08 (2017), p. 1740019.

[759] A. D. Parks. "Weak values and the Aharonov-Vaidman gauge." In: *Journal of Physics A: Mathematical and Theoretical* 43.3 (2009), p. 035305.

[760] A. D. Parks and J. E. Gray. "Variance control in weak-value measurement pointers." In: *Phys. Rev. A* 84.1 (2011), p. 012116.

[761] D. Pegg, S. Barnett, and J. Jeffers. "Quantum Theory of Preparation and Measurement." In: *Journal of Modern Optics* 49.5-6 (2002), pp. 913–924.

[762] D. T. Pegg, S. M. Barnett, and J. Jeffers. "Quantum retrodiction in open systems." In: *Phys. Rev. A* 66.2 (2002), p. 022106.

[763] U. Peleg and L. Vaidman. "Comment on "Past of a quantum particle revisited"." In: *Phys. Rev. A* 99.2 (2019), p. 026103.

[764] V. Potoček and G. Ferenczi. "Which-way information in a nested Mach-Zehnder interferometer." In: *Phys. Rev. A* 92.2 (2015), p. 023829.

[765] K. L. Pregnell and D. T. Pegg. "Retrodictive quantum optical state engineering." In: *Journal of Modern Optics* 51.11 (2004), pp. 1613–1626.

[766] G. J. Pryde et al. "Measurement of Quantum Weak Values of Photon Polarization." In: *Phys. Rev. Lett.* 94.22 (2005), p. 220405.

[767] M. F. Pusey and M. S. Leifer. "Logical Pre- and Post-Selection Paradoxes are Proofs of Contextuality." In: *Proc. 12th International Workshop on Quantum Physicsand Logic (QPL2015)*. 2015.

[768] T. Ravon and L. Vaidman. "The three-box paradox revisited." In: *Journal of Physics A: Mathematical and Theoretical* 40.11 (2007), p. 2873.

[769] K. J. Resch et al. "Time-Reversal and Super-Resolving Phase Measurements." In: *Phys. Rev. Lett.* 98.22 (2007), p. 223601.

[770] G. Reznik et al. "Photons are lying about where they have been, again." In: *Physics Letters A* 470 (2023), p. 128782.

[771] N. W. M. Ritchie, J. G. Story, and R. G. Hulet. "Realization of a measurement of a "weak value"." In: *Phys. Rev. Lett.* 66.9 (1991), pp. 1107–1110.

[772] A. Romito et al. "Weak values are quantum: you can bet on it." In: *Quantum Studies: Mathematics and Foundations* 3.1 (2016), pp. 1–4.

[773] H. Salih. "Commentary: "Asking photons where they have been" - without telling them what to say." In: *Frontiers in Physics* 3 (2015).

[774] J. Z. Salvail et al. "Full characterization of polarization states of light via direct measurement." In: *Nat Photon* 7.4 (2013), pp. 316–321.

[775] W. D. Sharp and N. Shanks. "The Rise and Fall of Time-Symmetrized Quantum Mechanics." In: *Philosophy of Science* 60.3 (1993), pp. 488–499.

[776] Z. Shi et al. "Scan-free direct measurement of an extremely high-dimensional photonic state." In: *Optica* 2.4 (2015), pp. 388–392.

[777] R. Silva et al. "Pre- and postselected quantum states: Density matrices, tomography, and Kraus operators." In: *Phys. Rev. A* 89.1 (2014), p. 012121.

[778] J. Sinclair et al. "Interpreting weak value amplification with a toy realist model." In: *Physics Letters A* 383.24 (2019), pp. 2839–2845.

[779] J. Sinclair et al. "Weak-value amplification and optimal parameter estimation in the presence of correlated noise." In: *Phys. Rev. A* 96.5 (2017), p. 052128.

[780] D. Sokolovski. "Asking photons where they have been in plain language." In: *Physics Letters A* 381.4 (2017), pp. 227–232.

[781] D. R. Solli et al. "Fast Light, Slow Light, and Phase Singularities: A Connection to Generalized Weak Values." In: *Phys. Rev. Lett.* 92.4 (2004), p. 043601.

[782] S. Sponar et al. "Asking Neutrons where they have been." In: *Journal of Physics: Conference Series* 1316.1 (2019), p. 012002.

[783] S. Sponar et al. "Weak values obtained in matter-wave interferometry." In: *Phys. Rev. A* 92.6 (2015), p. 062121.

[784] A. M. Steinberg. "Conditional probabilities in quantum theory and the tunneling-time controversy." In: *Phys. Rev. A* 52.1 (1995), pp. 32–42.

[785] A. M. Steinberg. "How Much Time Does a Tunneling Particle Spend in the Barrier Region?" In: *Phys. Rev. Lett.* 74.13 (1995), pp. 2405–2409.

[786] A. M. Steinberg. "Quantum measurement: A light touch." In: *Nature* 463.7283 (2010), pp. 890–891.

[787] B. E. Y. Svensson. "Non-representative Quantum Mechanical Weak Values." In: *Foundations of Physics* 45.12 (2015), pp. 1645–1656.

[788] B. E. Y. Svensson. "Quantum Weak Values and Logic: An Uneasy Couple." In: *Foundations of Physics* 47.3 (2017), pp. 430–452.

[789] B. E. Y. Svensson. "What Is a Quantum-Mechanical "Weak Value" the Value of?" In: *Foundations of Physics* 43.10 (2013), pp. 1193–1205.

[790] G. S. Thekkadath et al. "Direct Measurement of the Density Matrix of a Quantum System." In: *Phys. Rev. Lett.* 117.12 (2016), p. 120401.

[791] J. P. Torres and L. J. Salazar-Serrano. "Weak value amplification: a view from quantum estimation theory that highlights what it is and what isn't." In: *Scientific Reports* 6.1 (2016), p. 19702.

[792] L. Vaidman. "Past of a quantum particle." In: *Phys. Rev. A* 87.5 (2013), p. 052104.

[793] L. Vaidman. "Tracing the past of a quantum particle." In: *Phys. Rev. A* 89.2 (2014), p. 024102.

[794] L. Vaidman. "Weak value controversy." In: *Philosophical Transactions of the Royal Society of London A: Mathematical, Physical and Engineering Sciences* 375.2106 (2017).

[795] L. Vaidman. *"Elements of Reality" and the Failure of the Product Rule*. preprint: arXiv:hep-th/9310176. 1993.

[796] L. Vaidman. "Backward evolving quantum states." In: *Journal of Physics A: Mathematical and Theoretical* 40.12 (2007), p. 3275.

[797] L. Vaidman. "Comment on 'Two-state vector formalism and quantum interference'." In: *Journal of Physics A: Mathematical and Theoretical* 51.6 (2018), p. 068002.

[798] L. Vaidman. *Lying particles*. preprint: arXiv:2401.06735 (quant-ph). 2024.

[799] L. Vaidman. "Neutrons and photons inside a nested Mach-Zehnder interferometer." In: *Phys. Rev. A* 101.5 (2020), p. 052119.

[800] L. Vaidman. "The Meaning of Elements of Reality and Quantum Counterfactuals: Reply to Kastner." In: *Foundations of Physics* 29.6 (1999), pp. 865–876.

[801] L. Vaidman. "Time Symmetry and the Many-Worlds Interpretation." In: *Many Worlds?: Everett, Quantum Theory & Reality*. Ed. by S. Saunders et al. Oxford University Press, 2010.

[802] L. Vaidman. "Time-Symmetrized Counterfactuals in Quantum Theory." In: *Foundations of Physics* 29.5 (1999), pp. 755–765.

[803] L. Vaidman. "Weak-measurement elements of reality." In: *Foundations of Physics* 26.7 (1996), pp. 895–906.

[804] L. Vaidman and I. Tsutsui. "When Photons Are Lying about Where They Have Been." In: *Entropy* 20.7 (2018).

[805] A. Vella et al. "Simultaneous Measurement of Multiple Parameters of a Subwavelength Structure Based on the Weak Value Formalism." In: *Phys. Rev. Lett.* 122.12 (2019), p. 123603.

[806] G. I. Viza et al. "Experimentally quantifying the advantages of weak-value-based metrology." In: *Phys. Rev. A* 92.3 (2015), p. 032127.

[807] M. Waegell and J. Tollaksen. "Contextuality, Pigeonholes, Cheshire Cats, Mean Kings, and Weak Values." In: *Quantum Studies: Mathematics and Foundations* 5.2 (2018), pp. 325–349.

[808] M. Waegell et al. "Quantum reality with negative-mass particles." In: *Proceedings of the National Academy of Sciences* 120.32 (2023), e2018437120.

[809] S. Watanabe. "Symmetry of Physical Laws. Part III. Prediction and Retrodiction." In: *Rev. Mod. Phys.* 27.2 (1955), pp. 179–186.

[810] H. M. Wiseman. "Weak values, quantum trajectories, and the cavity-QED experiment on wave-particle correlation." In: *Phys. Rev. A* 65.3 (2002), p. 032111.

[811] H. Wiseman. "Directly observing momentum transfer in twin-slit "which-way" experiments." In: *Physics Letters A* 311.4 (2003), pp. 285–291.

[812] S. Wu. "State tomography via weak measurements." In: *Scientific Reports* 3.1 (2013), p. 1193.

[813] S. Wu and Y. Li. "Weak measurements beyond the Aharonov-Albert-Vaidman formalism." In: *Phys. Rev. A* 83.5 (2011), p. 052106.

[814] S. Wu and K. Mølmer. "Weak measurements with a qubit meter." In: *Physics Letters A* 374.1 (2009), pp. 34–39.

[815] L. Xu et al. "Approaching Quantum-Limited Metrology with Imperfect Detectors by Using Weak-Value Amplification." In: *Phys. Rev. Lett.* 125.8 (2020), p. 080501.

[816] X.-Y. Xu et al. "Phase Estimation with Weak Measurement Using a White Light Source." In: *Phys. Rev. Lett.* 111.3 (2013), p. 033604.

[817] Z.-Q. Zhou et al. "Experimental observation of anomalous trajectories of single photons." In: *Phys. Rev. A* 95.4 (2017), p. 042121.

Bohmian Mechanics

Monographies

[818] D. Bohm and B. Hiley. *The Undivided Universe: An Ontological Interpretation of Quantum Theory*. Routledge, 1993.

[819] D. Dürr and S. Teufel. *Bohmian Mechanics. The Physics and Mathematics of Quantum Theory*. Springer, 2009.

[820] P. R. Holland. *The Quantum Theory of Motion: An Account of the de Broglie-Bohm Causal Interpretation of Quantum Mechanics*. Cambridge University Press, 1993.

[821] Á. S. Sanz and S. Miret-Artés. *A Trajectory Description of Quantum Processes. I. Fundamentals*. Springer, 2012.

[822] Á. S. Sanz and S. Miret-Artés. *A Trajectory Description of Quantum Processes. II. Applications*. Springer, 2014.

Encyclopedic

[823] D. Dürr et al. "Bohmian Mechanics." In: *Compendium of Quantum Physics*. Ed. by D. Greenberger, K. Hentschel, and F. Weinert. Berlin, Heidelberg: Springer Berlin Heidelberg, 2009, pp. 47–55.

[824] S. Goldstein. "Bohmian Mechanics." In: *The Stanford Encyclopedia of Philosophy*. Ed. by E. N. Zalta. Fall 2021. Metaphysics Research Lab, Stanford University, 2021.

[825] B. J. Hiley. "Bohm Interpretation of Quantum Mechanics." In: *Compendium of Quantum Physics*. Ed. by D. Greenberger, K. Hentschel, and F. Weinert. Berlin, Heidelberg: Springer Berlin Heidelberg, 2009, pp. 43–47.

[826] B. J. Hiley. "Bohm's Approach to the EPR Paradox." In: *Compendium of Quantum Physics*. Ed. by D. Greenberger, K. Hentschel, and F. Weinert. Berlin, Heidelberg: Springer Berlin Heidelberg, 2009, pp. 55–58.

Articles

[827] Y. Aharonov and L. Vaidman. "About Position Measurements Which do Not Show the Bohmian Particle Position." In: *Bohmian Mechanics and Quantum Theory: An Appraisal*. Ed. by J. T. Cushing, A. Fine, and S. Goldstein. Dordrecht: Springer Netherlands, 1996, pp. 141–154.

[828] J. A. Barrett. "The Persistence of Memory: Surreal Trajectories in Bohm's Theory." In: *Philosophy of Science* 67.4 (2000), pp. 680–703.

[829] J. S. Bell. "On the impossible pilot wave." In: *Foundations of Physics* 12.10 (1982), pp. 989–999.

[830] J. S. Bell. "de Broglie-Bohm, delayed-choice double-slit experiment, and density matrix." In: *Speakable and Unspeakable in Quantum Mechanics: Collected Papers on Quantum Philosophy*. Cambridge University Press, 2004, pp. 111–116.

[831] A. Benseny et al. "Applied Bohmian mechanics." In: *The European Physical Journal D* 68.10 (2014), p. 286.

[832] K. Berndl. "Global Existence and Uniqueness of Bohmian Trajectories." In: *Bohmian Mechanics and Quantum Theory: An Appraisal*. Ed. by J. T. Cushing, A. Fine, and S. Goldstein. Dordrecht: Springer Netherlands, 1996, pp. 77–86.

[833] K. Berndl et al. "Nonlocality, Lorentz invariance, and Bohmian quantum theory." In: *Phys. Rev. A* 53.4 (1996), pp. 2062–2073.

[834] K. Y. Bliokh et al. "Photon trajectories, anomalous velocities and weak measurements: a classical interpretation." In: *New Journal of Physics* 15.7 (2013), p. 073022.

[835] D. Bohm and B. Hiley. "Non-locality and locality in the stochastic interpretation of quantum mechanics." In: *Physics Reports* 172.3 (1989), pp. 93–122.

[836] D. J. Bohm, C. Dewdney, and B. H. Hiley. "A quantum potential approach to the Wheeler delayed-choice experiment." In: *Nature* 315 (1985), pp. 294–297.

[837] D. Bohm. "A Suggested Interpretation of the Quantum Theory in Terms of "Hidden" Variables. I." In: *Phys. Rev.* 85.2 (1952), pp. 166–179.

[838] D. Bohm. "A Suggested Interpretation of the Quantum Theory in Terms of "Hidden" Variables. II." In: *Phys. Rev.* 85.2 (1952), pp. 180–193.

[839] D. Bohm. "Proof That Probability Density Approaches $|\psi|^2$ in Causal Interpretation of the Quantum Theory." In: *Phys. Rev.* 89.2 (1953), pp. 458–466.

[840] D. Bohm, B. J. Hiley, and P. N. Kaloyerou. "An ontological basis for the quantum theory." In: *Physics Reports* 144 (1987), pp. 321–375.

[841] B. Braverman and C. Simon. "Proposal to Observe the Nonlocality of Bohmian Trajectories with Entangled Photons." In: *Phys. Rev. Lett.* 110.6 (2013), p. 060406.

[842] C. Callender and R. Weingard. "Trouble in Paradise? Problems for Bohm's Theory." In: *The Monist* 80.1 (1997), pp. 24–43.

[843] C.-C. Chou et al. "Quantum interference within the complex quantum Hamilton-Jacobi formalism." In: *Annals of Physics* 325.10 (2010), pp. 2193–2211.

[844] M. Davidović et al. "Electromagnetic energy flow lines as possible paths of photons." In: *Physica Scripta* 2009.T135 (2009), p. 014009.

[845] E. Deotto and G. C. Ghirardi. "Bohmian Mechanics Revisited." In: *Foundations of Physics* 28.1 (1998), pp. 1–30.

[846] C. Dewdney, L. Hardy, and E. Squires. "How late measurements of quantum trajectories can fool a detector." In: *Physics Letters A* 184.1 (1993), pp. 6–11.

[847] D. Dürr, S. Goldstein, and N. Zanghì. "Bohmian Mechanics as the Foundation of Quantum Mechanics." In: *Bohmian Mechanics and Quantum Theory: An Appraisal*. Ed. by J. T. Cushing, A. Fine, and S. Goldstein. Dordrecht: Springer Netherlands, 1996, pp. 21–44.

[848] D. Dürr, S. Goldstein, and N. Zanghì. "On the Weak Measurement of Velocity in Bohmian Mechanics." In: *Journal of Statistical Physics* 134.5 (2009), pp. 1023–1032.

[849] D. Dürr, S. Goldstein, and N. Zanghì. "Quantum equilibrium and the origin of absolute uncertainty." In: *Journal of Statistical Physics* 67.5 (1992), pp. 843–907.

[850] D. Dürr et al. "Bell-type quantum field theories." In: *Journal of Physics A: Mathematical and General* 38.4 (2005), R1.

[851] D. Dürr et al. "Bohmian Mechanics and Quantum Field Theory." In: *Phys. Rev. Lett.* 93.9 (2004), p. 090402.

[852] D. Dürr et al. "Can Bohmian mechanics be made relativistic?" In: *Proceedings of the Royal Society A: Mathematical, Physical and Engineering Sciences* 470.2162 (2014), p. 20130699.

[853] D. Dürr et al. "Comment on "Surrealistic Bohm Trajectories"." In: *Zeitschrift für Naturforschung A* 48.12 (1993), pp. 1261–1262.

[854] D. Dürr et al. "Hypersurface Bohm-Dirac models." In: *Phys. Rev. A* 60.4 (1999), pp. 2729–2736.

[855] D. Dürr et al. "Topological Factors Derived from Bohmian Mechanics." In: *Annales Henri Poincaré* 7.4 (2006), pp. 791–807.

[856] B.-G. Englert, M. O. Scully, and H. W. Georg Süssmann. "Reply to Comment on "Surrealistic Bohm Trajectories"." In: *Zeitschrift für Naturforschung A* 48.12 (1993), pp. 1263–1264.

[857] B.-G. Englert et al. "Surrealistic Bohm Trajectories." In: *Zeitschrift für Naturforschung A* 47.12 (1992), pp. 1175–1186.

[858] S. T. Epstein. "The Causal Interpretation of Quantum Mechanics." In: *Phys. Rev.* 89.1 (1953), pp. 319–319.

[859] S. T. Epstein. "The Causal Interpretation of Quantum Mechanics." In: *Phys. Rev.* 91.4 (1953), pp. 985–985.

[860] M. Esfeld et al. "The Ontology of Bohmian Mechanics." In: *British Journal for the Philosophy of Science* 65.4 (2014), pp. 773–796.

[861] A. Fine. "On the Interpretation of Bohmian Mechanics." In: *Bohmian Mechanics and Quantum Theory: An Appraisal*. Ed. by J. T. Cushing, A. Fine, and S. Goldstein. Dordrecht: Springer Netherlands, 1996, pp. 231–250.

[862] R. Flack and B. J. Hiley. "Weak measurement and its experimental realisation." In: *Journal of Physics: Conference Series* 504.1 (2014), p. 012016.

[863] R. Flack and B. J. Hiley. *Weak Values of Momentum of the Electromagnetic Field: Average Momentum Flow Lines, Not Photon Trajectories*. preprint: arXiv:1611.06510 (quant-ph). 2016.

[864] J. Foo, A. P. Lund, and T. C. Ralph. *Measurement-based Lorentz-covariant Bohmian trajectories of interacting photons*. preprint: arXiv:2309.16011 (quant-ph). 2023.

[865] J. Foo et al. "Relativistic Bohmian trajectories of photons via weak measurements." In: *Nature Communications* 13.1 (2022), p. 4002.

[866] W. Gale, E. Guth, and G. T. Trammell. "Determination of the Quantum State by Measurements." In: *Phys. Rev.* 165.5 (1968), pp. 1434–1436.

[867] M. Galli. "Measurement of average Bohmian trajectories of photons in a double slit interferometer." MA thesis. Università degli Studi di Milano, 2021.

[868] P. Ghose. "Relativistic quantum mechanics of spin-0 and spin-1 bosons." In: *Foundations of Physics* 26.11 (1996), pp. 1441–1455.

[869] P. Ghose, D. Home, and M. Roy. "Relativistic quantum mechanics of bosons." In: *Physics Letters A* 183.4 (1993), pp. 267–271.

[870] P. Ghose et al. "Bohmian trajectories for photons." In: *Physics Letters A* 290.5-6 (2001), pp. 205–213.

[871] S. Goldstein and R. Tumulka. "Opposite arrows of time can reconcile relativity and nonlocality." In: *Classical and Quantum Gravity* 20.3 (2003), p. 557.

[872] L. Hardy. "Contextuality in Bohmian Mechanics." In: *Bohmian Mechanics and Quantum Theory: An Appraisal*. Ed. by J. T. Cushing, A. Fine, and S. Goldstein. Dordrecht: Springer Netherlands, 1996, pp. 67–76.

[873] B. J. Hiley. "Weak Values: Approach through the Clifford and Moyal Algebras." In: *Journal of Physics: Conference Series* 361.1 (2012), p. 012014.

[874] B. J. Hiley, R. E. Callaghan, and O. Maroney. *Quantum trajectories, real, surreal or an approximation to a deeper process?* preprint: arXiv:quant-ph/0010020. 2000.

[875] B. J. Hiley and R. E. Callaghan. "Delayed-choice experiments and the Bohm approach." In: *Physica Scripta* 74.3 (2006), p. 336.

[876] B. J. Hiley and P. Van Reeth. "Quantum Trajectories: Real or Surreal?" In: *Entropy* 20.5 (2018).

[877] D. H. Kobe. "A Relativistic Schrödinger-like Equation for a Photon and Its Second Quantization." In: *Foundations of Physics* 29.8 (1999), pp. 1203–1231.

[878] S. Kocsis et al. "Observing the Average Trajectories of Single Photons in a Two-Slit Interferometer." In: *Science* 332.6034 (2011), pp. 1170–1173.

[879] C. R. Leavens. "Weak Measurements from the Point of View of Bohmian Mechanics." In: *Foundations of Physics* 35.3 (2005), pp. 469–491.

[880] C. Leavens and R. Sala Mayato. "Superluminal systematic particle velocity in relativistic stochastic Bohmian mechanics." In: *Physics Letters A* 263.1 (1999), pp. 1–8.

[881] G. Naaman-Marom, N. Erez, and L. Vaidman. "Position measurements in the de Broglie-Bohm interpretation of quantum mechanics." In: *Annals of Physics* 327.10 (2012), pp. 2522–2542.

[882] E. Nelson. "Derivation of the Schrödinger Equation from Newtonian Mechanics." In: *Phys. Rev.* 150.4 (1966), pp. 1079–1085.

[883] T. Norsen. "The pilot-wave perspective on spin." In: *American Journal of Physics* 82.4 (2014), pp. 337–348.

[884] T. Norsen and W. Struyve. "Weak measurement and Bohmian conditional wave functions." In: *Annals of Physics* 350 (2014), pp. 166–178.

[885] A. O. T. Pang et al. "Experimental Comparison of Bohm-like Theories with Different Primary Ontologies." In: *Quantum* 4 (2020), p. 365.

[886] C. Philippidis, C. Dewdney, and B. J. Hiley. "Quantum interference and the quantum potential." In: *Il Nuovo Cimento B (1971-1996)* 52.1 (1979), pp. 15–28.

[887] D. A. Rice. "A geometric approach to nonlocality in the Bohm model of quantum mechanics." In: *American Journal of Physics* 65.2 (1997), pp. 144–147.

[888] J. Rosaler. "Is de Broglie-Bohm Theory Specially Equipped to Recover Classical Behavior?" In: *Philosophy of Science* 82.5 (2015), pp. 1175–1187.

[889] A. Royer. "Measurement of quantum states and the Wigner function." In: *Foundations of Physics* 19.1 (1989), pp. 3–32.

[890] A. S. Sanz. "Investigating Puzzling Aspects of the Quantum Theory by Means of Its Hydrodynamic Formulation." In: *Foundations of Physics* 45.10 (2015), pp. 1153–1165.

[891] A. Sanz et al. "Understanding interference experiments with polarized light through photon trajectories." In: *Annals of Physics* 325.4 (2010), pp. 763–784.

[892] À. S. Sanz. "Young's Experiment with Entangled Bipartite Systems: The Role of Underlying Quantum Velocity Fields." In: *Entropy* 25.7 (2023).

[893] À. S. Sanz, M. D. Davidović, and M. Božić. "Bohmian-Based Approach to Gauss-Maxwell Beams." In: *Applied Sciences* 10.5 (2020).

[894] W. P. Schleich, M. Freyberger, and M. S. Zubairy. "Reconstruction of Bohm trajectories and wave functions from interferometric measurements." In: *Phys. Rev. A* 87.1 (2013), p. 014102.

[895] M. O. Scully. "Do Bohm trajectories always provide a trustworthy physical picture of particle motion?" In: *Physica Scripta* 1998.T76 (1998), p. 41.

[896] E. J. Squires. "Why is position special?" In: *Foundations of Physics Letters* 3.1 (1990), pp. 87–93.

[897] W. Struyve et al. "On the uniqueness of paths for spin-0 and spin-1 quantum mechanics." In: *Physics Letters A* 322.1 (2004), pp. 84–95.

[898] W. Struyve. "Pilot-wave approaches to quantum field theory." In: *Journal of Physics: Conference Series* 306.1 (2011), p. 012047.

[899] W. Struyve. "Pilot-wave theory and quantum fields." In: *Reports on Progress in Physics* 73.10 (2010), p. 106001.

[900] R. I. Sutherland. "Lagrangian Description for Particle Interpretations of Quantum Mechanics: Entangled Many-Particle Case." In: *Foundations of Physics* 47.2 (2017), pp. 174–207.

[901] R. I. Sutherland. "Causally symmetric Bohm model." In: *Studies in History and Philosophy of Science Part B: Studies in History and Philosophy of Modern Physics* 39.4 (2008), pp. 782–805.

[902] G. Tastevin and F. Laloë. "Surrealistic Bohmian trajectories do not occur with macroscopic pointers." In: *The European Physical Journal D* 72.10 (2018), p. 183.

[903] F. L. Traversa et al. "Robust weak-measurement protocol for Bohmian velocities." In: *Phys. Rev. A* 87.5 (2013), p. 052124.

[904] R. Tumulka. "On Bohmian Mechanics, Particle Creation, and Relativistic Space-Time: Happy 100th Birthday, David Bohm!" In: *Entropy* 20.6 (2018).

[905] L. Vaidman. "The Reality in Bohmian Quantum Mechanics or Can You Kill with an Empty Wave Bullet?" In: *Foundations of Physics* 35.2 (2005), pp. 299–312.

[906] A. Valentini. "Pilot-Wave Theory of Fields, Gravitation and Cosmology." In: *Bohmian Mechanics and Quantum Theory: An Appraisal*. Ed. by J. T. Cushing, A. Fine, and S. Goldstein. Dordrecht: Springer Netherlands, 1996, pp. 45–66.

[907] A. Valentini. "Signal-locality, uncertainty, and the subquantum H-theorem. I." In: *Physics Letters A* 156.1 (1991), pp. 5–11.

[908] A. Valentini. "Signal-locality, uncertainty, and the subquantum H-theorem. II." In: *Physics Letters A* 158.1 (1991), pp. 1–8.

[909] C. Versmold. "Bohmian Trajectories in a Double Slit Experiment." MA thesis. Ludwig-Maximilian-Universität München, 2021.

[910] H. M. Wiseman. "Grounding Bohmian mechanics in weak values and bayesianism." In: *New Journal of Physics* 9.6 (2007), p. 165.

[911] Y. Xiao et al. "Experimental nonlocal steering of Bohmian trajectories." In: *Opt. Express* 25.13 (2017), pp. 14463–14472.

Interpretation and Philosophy

Monographies

[912] D. Z. Albert. *Quantum Mechanics and Experience*. Harvard University Press, 1992.

[913] T. Aquinas. *Quaestiones Disputatae de Veritate*. Trans. by R. W. Mulligan, J. V. McGlynn, and R. W. Schmidt. Henry Regnery Company, 1952.

[914] Aristotle. *Metaphysics*. Trans. by H. G. Apostle. Indiana University Press, 1966.

[915] Augustine. *Against the Academicians (Contra academicos)*. Trans. by M. P. Garvey. Marquette University Press, 1942.

[916] J. O. Berger. *Statistical Decision Theory and Bayesian Analysis*. Springer New York, NY, 2010.

[917] M. Born and A. Einstein. *The Born-Einstein Letters. Correspondence between Albert Einstein and Max and Hedwig Born from 1916-1955*. Macmillan, 1971.

[918] J. T. Cushing. *Quantum Mechanics. Historical Contingency and the Copenhagen Hegemony*. The University of Chicago Press, 1994.

[919] B. d'Espagnat. *Conceptual Foundations of Quantum Mechanics*. Perseus Books Publishing, 1976.

[920] B. d'Espagnat. *Veiled Reality*. Westview Press, 2003.

[921] R. Descartes. *Meditationes de prima philosophia*. Ed. by A. Buchenau. Project Gutenberg, 2007.

[922] H. G. Frankfurt. *On Bullshit*. Princeton University Press, 2005.

[923] I. Hacking. *Representing and Intervening*. Cambridge University Press, 1983.

[924] W. Heisenberg. *Physics and Philosophy. The Revolution in Modern Science*. Harper & Brothers, 1958.

[925] R. I. G. Hughes. *The Structure and Interpretation of Quantum Mechanics*. Harvard University Press, 1992.

[926] D. Hume. *An Enquiry Concerning Human Understanding*. Ed. by S. L. A. Selby-Bigge. Project Gutenberg, 2006.

[927] M. Jammer. *The Philosophy of Quantum Mechanics*. John Wiley and Sons, 1974.

[928] I. Kant. *Kritik der reinen Vernunft. Nach der ersten und zweiten Originalausgabe*. Ed. by J. Timmermann. Felix Meiner Verlag, 1998.

[929] E. L. Lehmann and J. P. Romano. *Testing Statistical Hypotheses*. Springer Cham, 2005.

[930] J. Locke. *An Essay Concerning Humane Understanding*. Ed. by A. C. Fraser. Clarendon Press, 1894.

[931] P. Mittelstaedt. *The Interpretation of Quantum Mechanics and the Measurement Process*. Cambridge University Press, 1998.

[932] P. Mittelstaedt and P. A. Weingartner. *Laws of Nature*. Springer, 2005.

[933] Plato. "Parmenides." In: *The Collected Dialogues of Plato*. Ed. by E. Hamilton and H. Cairns. Princeton University Press, 1961.

[934] Plato. "Timaeus." In: *The Collected Dialogues of Plato*. Ed. by E. Hamilton and H. Cairns. Princeton University Press, 1961.

[935] M. Redhead. *Incompleteness Nonlocality and Realism*. Clarendon Press, 1987.

[936] H. Reichenbach. *The Direction of Time*. Univ. of Calif. Press, 1971.

[937] C. P. Robert. *The Bayesian Choice*. Springer New York, 2013.

[938] W. C. Salmon. *Causality and Explanation*. Oxford University Press, 1997.

[939] W. C. Salmon. *Scientific Explanation and the Causal Structure of the World*. Princeton University Press, 1984.

[940] S. Saunders et al., eds. *Many Worlds?: Everett, Quantum Theory & Reality*. Oxford University Press, 2010.

[941] D. Wallace. *The Emergent Multiverse*. Oxford University Press, 2012.

Encyclopedic

[942] G. Bacciagaluppi. "The Role of Decoherence in Quantum Mechanics." In: *The Stanford Encyclopedia of Philosophy*. Ed. by E. N. Zalta. Fall 2020. Metaphysics Research Lab, Stanford University, 2020.

[943] J. A. Barrett. "Many Worlds Interpretation of Quantum Mechanics." In: *Compendium of Quantum Physics*. Ed. by D. Greenberger, K. Hentschel, and F. Weinert. Berlin, Heidelberg: Springer Berlin Heidelberg, 2009, pp. 363–367.

[944] C. Callender. "Metaphysics of Quantum Mechanics." In: *Compendium of Quantum Physics*. Ed. by D. Greenberger, K. Hentschel, and F. Weinert. Berlin, Heidelberg: Springer Berlin Heidelberg, 2009, pp. 384–389.

[945] A. Chakravartty. "Scientific Realism." In: *The Stanford Encyclopedia of Philosophy*. Ed. by E. N. Zalta. Summer 2017. Metaphysics Research Lab, Stanford University, 2017.

[946] H. Chang. "Operationalism." In: *The Stanford Encyclopedia of Philosophy*. Ed. by E. N. Zalta. Fall 2021. Metaphysics Research Lab, Stanford University, 2021.

[947] J. Faye. "Copenhagen Interpretation of Quantum Mechanics." In: *The Stanford Encyclopedia of Philosophy*. Ed. by E. N. Zalta. Winter 2019. Metaphysics Research Lab, Stanford University, 2019.

[948] S. French. "Identity and Individuality in Quantum Theory." In: *The Stanford Encyclopedia of Philosophy*. Ed. by E. N. Zalta. Winter 2019. Metaphysics Research Lab, Stanford University, 2019.

[949] R. Frigg. "GRW Theory (Ghirardi, Rimini, Weber Model of Quantum Mechanics)." In: *Compendium of Quantum Physics*. Ed. by D. Greenberger, K. Hentschel, and F. Weinert. Berlin, Heidelberg: Springer Berlin Heidelberg, 2009, pp. 266–270.

[950] G. Ghirardi and A. Bassi. "Collapse Theories." In: *The Stanford Encyclopedia of Philosophy*. Ed. by E. N. Zalta. Summer 2020. Metaphysics Research Lab, Stanford University, 2020.

[951] C. Hitchcock. "Probabilistic Causation." In: *The Stanford Encyclopedia of Philosophy*. Ed. by E. N. Zalta. Spring 2021. Metaphysics Research Lab, Stanford University, 2021.

[952] M. Kuhlmann. "Quantum Field Theory." In: *The Stanford Encyclopedia of Philosophy*. Ed. by E. N. Zalta and U. Nodelman. Summer 2023. Metaphysics Research Lab, Stanford University, 2023.

[953] P. Mittelstaedt. "Ignorance Interpretation of Quantum Mechanics." In: *Compendium of Quantum Physics*. Ed. by D. Greenberger, K. Hentschel, and F. Weinert. Berlin, Heidelberg: Springer Berlin Heidelberg, 2009, pp. 305–306.

[954] L. Vaidman. "Many-Worlds Interpretation of Quantum Mechanics." In: *The Stanford Encyclopedia of Philosophy*. Ed. by E. N. Zalta. Fall 2021. Metaphysics Research Lab, Stanford University, 2021.

[955] S. Weinstein and D. Rickles. "Quantum Gravity." In: *The Stanford Encyclopedia of Philosophy*. Ed. by E. N. Zalta and U. Nodelman. Summer 2023. Metaphysics Research Lab, Stanford University, 2023.

Articles

[956] S. L. Adler. "Why decoherence has not solved the measurement problem: a response to P.W. Anderson." In: *Studies in History and Philosophy of Science Part B: Studies in History and Philosophy of Modern Physics* 34.1 (2003), pp. 135–142.

[957] Y. Aharonov and J. Anandan. *Meaning of the Density Matrix*. preprint: arXiv:quant-ph/9803018. 1998.

[958] D. Albert. "Probability in the Everett Picture." In: *Many Worlds?: Everett, Quantum Theory & Reality*. Ed. by S. Saunders et al. Oxford University Press, 2010.

[959] D. Albert and B. Loewer. "Interpreting the many worlds interpretation." In: *Synthese* 77.2 (1988), pp. 195–213.

[960] V. Allori et al. "On the Common Structure of Bohmian Mechanics and the Ghirardi-Rimini-Weber Theory: Dedicated to GianCarlo Ghirardi on the occasion of his 70th birthday." In: *The British Journal for the Philosophy of Science* 59.3 (2008), pp. 353–389.

[961] G. Andreoletti and L. Vervoort. "Superdeterminism: a reappraisal." In: *Synthese* 200.5 (2022), p. 361.

[962] A. Baas and B. Le Bihan. "What Does the World Look Like according to Superdeterminism?" In: *The British Journal for the Philosophy of Science* 74.3 (2023), pp. 555–572.

[963] L. E. Ballentine. "The Statistical Interpretation of Quantum Mechanics." In: *Rev. Mod. Phys.* 42.4 (1970), pp. 358–381.

[964] L. Ballentine. "Classicality without Decoherence: A Reply to Schlosshauer." In: *Foundations of Physics* 38.10 (2008), pp. 916–922.

[965] A. Bassi and G. Ghirardi. "Dynamical reduction models." In: *Physics Reports* 379.5-6 (2003), pp. 257–426.

[966] J. S. Bell. "Against 'measurement'." In: *Physics World* 3.8 (1990), p. 33.

[967] J. S. Bell. "Are there quantum jumps?" In: *Speakable and Unspeakable in Quantum Mechanics: Collected Papers on Quantum Philosophy*. Cambridge University Press, 2004, pp. 201–212.

[968] J. S. Bell. "Six possible worlds of quantum mechanics." In: *Speakable and Unspeakable in Quantum Mechanics: Collected Papers on Quantum Philosophy*. Cambridge University Press, 2004, pp. 181–195.

[969] Č. Brukner. "On the Quantum Measurement Problem." In: *Quantum [Un]Speakables II*. Ed. by R. Bertlmann and A. Zeilinger. Springer, 2017, pp. 95–118.

[970] Č. Brukner and A. Zeilinger. "Information and Fundamental Elements of the Structure of Quantum Theory." In: *Time, Quantum and Information*. Ed. by L. Castell and O. Ischebeck. Berlin, Heidelberg: Springer Berlin Heidelberg, 2003, pp. 323–354.

[971] J. Bub. "Quantum Mechanics is About Quantum Information." In: *Foundations of Physics* 35.4 (2005), pp. 541–560.

[972] A. Cabello. "Interpretations of Quantum Theory: A Map of Madness." In: *What is Quantum Information?* Ed. by O. Lombardi et al. Cambridge University Press, 2017, pp. 138–144.

[973] M. Carlesso et al. "Present status and future challenges of non-interferometric tests of collapse models." In: *Nature Physics* 18.3 (2022), pp. 243–250.

[974] N. Cartwright. "Causal Laws and Effective Strategies." In: *Noûs* 13.4 (1979), pp. 419–437.

[975] L. Castellani. *All quantum mixtures are proper*. preprint: arXiv:2201.04143 (quant-ph). 2022.

[976] E. K. Chen. "Realism about the wave function." In: *Philosophy Compass* 14.7 (2019), e12611.

[977] M. E. Cuffaro and S. Hartmann. "The Open Systems View." In: *Philosophy of Physics* (2024).

[978] B. d'Espagnat. *Reply to Aharonov and Anandan's "Meaning of the Density Matrix"*. preprint: arXiv:quant-ph/9804063. 1998.

[979] B. d'Espagnat. *Reply to K. A. Kirkpatrick*. preprint: arXiv:quant-ph/0111081. 2001.

[980] D. Deutsch. "Quantum theory as a universal physical theory." In: *International Journal of Theoretical Physics* 24.1 (1985), pp. 1–41.

[981] D. Deutsch. "The structure of the multiverse." In: *Proceedings of the Royal Society of London. Series A: Mathematical, Physical and Engineering Sciences* 458.2028 (2002), pp. 2911–2923.

[982] B. S. DeWitt. "The Many-Universes Interpretation of Quantum Mechanics." In: *The Many-Worlds Interpretation of Quantum Mechanics*. Ed. by B. S. DeWitt and N. Graham. Princeton University Press, 1973.

[983] H. Everett. ""Relative State" Formulation of Quantum Mechanics." In: *Rev. Mod. Phys.* 29.3 (1957), pp. 454–462.

[984] C. A. Fuchs. *QBism, the Perimeter of Quantum Bayesianism*. preprint: arXiv:1003.5209 (quant-ph). 2010.

[985] C. A. Fuchs, N. D. Mermin, and R. Schack. "An introduction to QBism with an application to the locality of quantum mechanics." In: *American Journal of Physics* 82.8 (2014), pp. 749–754.

[986] C. A. Fuchs and A. Peres. "Quantum Theory Needs No 'Interpretation'." In: *Phys. Today* 70 (2000), p. 012343.

[987] G. C. Ghirardi, R. Grassi, and F. Benatti. "Describing the macroscopic world: Closing the circle within the dynamical reduction program." In: *Foundations of Physics* 25.1 (1995), pp. 5–38.

[988] G. C. Ghirardi, A. Rimini, and T. Weber. "Unified dynamics for microscopic and macroscopic systems." In: *Phys. Rev. D* 34.2 (1986), pp. 470–491.

[989] J. R. Hance and S. Hossenfelder. "What does it take to solve the measurement problem?" In: *Journal of Physics Communications* 6.10 (2022), p. 102001.

[990] N. Harrigan and R. W. Spekkens. "Einstein, Incompleteness, and the Epistemic View of Quantum States." In: *Foundations of Physics* 40.2 (2010), pp. 125–157.

[991] S. Hossenfelder and T. Palmer. "Rethinking Superdeterminism." In: *Frontiers in Physics* 8 (2020).

[992] D. Howard. "Who Invented the "Copenhagen Interpretation"? A Study in Mythology." In: *Philosophy of Science* 71.5 (2004), pp. 669–682.

[993] K. A. Kirkpatrick. *Indistinguishability and improper mixtures*. preprint: arXiv:quant-ph/0109146. 2001.

[994] G. C. Krizek. *A classification scheme for interpretations of Quantum Mechanics*. preprint: arXiv:1707.00097 (quant-ph). 2017.

[995] A. J. Leggett. "The Quantum Measurement Problem." In: *Science* 307.5711 (2005), pp. 871–872.

[996] A. C. Lobo, I. L. Paiva, and P. R. Dieguez. *Proper and improper density matrices and the consistency of the Deutsch model for Local Closed Timelike Curves*. preprint: arXiv:1110.6361 (quant-ph). 2012.

[997] X.-s. Ma, J. Kofler, and A. Zeilinger. "Delayed-choice gedanken experiments and their realizations." In: *Rev. Mod. Phys.* 88.1 (2016), p. 015005.

[998] P. Markie and M. Folescu. "Rationalism vs. Empiricism." In: *The Stanford Encyclopedia of Philosophy*. Ed. by E. N. Zalta and U. Nodelman. Spring 2023. Metaphysics Research Lab, Stanford University, 2023.

[999] T. Maudlin. "Three measurement problems." In: *Topoi* 14.1 (1995), pp. 7–15.

[1000] D. N. Mermin. "What's Wrong with this Pillow?" In: *Physics Today* 42.4 (1989), pp. 9–11.

[1001] N. D. Mermin. "Making better sense of quantum mechanics." In: *Reports on Progress in Physics* 82.1 (2018), p. 012002.

[1002] N. D. Mermin. "Could Feynman Have Said This?" In: *Physics Today* 57.5 (2004), pp. 10–11.

[1003] N. D. Mermin. "There is no quantum measurement problem." In: *Physics Today* 75.6 (2022), pp. 62–63.

[1004] T. Norsen and S. Nelson. *Yet Another Snapshot of Foundational Attitudes Toward Quantum Mechanics*. preprint: arXiv:1306.4646 (quant-ph). 2013.

[1005] A. Pais. "Einstein and the quantum theory." In: *Rev. Mod. Phys.* 51.4 (1979), pp. 863–914.

[1006] P. Pearle. "Combining stochastic dynamical state-vector reduction with spontaneous localization." In: *Phys. Rev. A* 39.5 (1989), pp. 2277–2289.

[1007] P. Pearle. "Reduction of the state vector by a nonlinear Schrödinger equation." In: *Phys. Rev. D* 13.4 (1976), pp. 857–868.

[1008] A. Peres. "Unperformed experiments have no results." In: *American Journal of Physics* 46.7 (1978), pp. 745–747.

[1009] M. Ringbauer et al. "Measurements on the reality of the wavefunction." In: *Nat Phys* 11.3 (2015), pp. 249–254.

[1010] S. Saunders. "Many Worlds? An Introduction." In: *Many Worlds?: Everett, Quantum Theory & Reality*. Ed. by S. Saunders et al. Oxford University Press, 2010.

[1011] M. Schlosshauer. "Decoherence, the measurement problem, and interpretations of quantum mechanics." In: *Rev. Mod. Phys.* 76.4 (2005), pp. 1267–1305.

[1012] M. Schlosshauer. "Decoherence: From Interpretation to Experiment." In: *From Quantum to Classical: Essays in Honour of H.-Dieter Zeh*. Ed. by C. Kiefer. Cham: Springer International Publishing, 2022, pp. 45–64.

[1013] M. Schlosshauer, J. Kofler, and A. Zeilinger. "A snapshot of foundational attitudes toward quantum mechanics." In: *Studies in History and Philosophy of Science Part B: Studies in History and Philosophy of Modern Physics* 44.3 (2013), pp. 222–230.

[1014] S. Sivasundaram and K. H. Nielsen. *Surveying the Attitudes of Physicists Concerning Foundational numbers of Quantum Mechanics*. preprint: arXiv:1612.00676 (quant-ph). 2016.

[1015] C. Sommer. *Another Survey of Foundational Attitudes Towards Quantum Mechanics*. preprint: arXiv:1303.2719 (quant-ph). 2013.

[1016] M. Tegmark. "The Interpretation of Quantum Mechanics: Many Worlds or Many Words?" In: *Fortschritte der Physik* 46.6-8 (1998), pp. 855–862.

[1017] R. Tumulka. "A Relativistic Version of the Ghirardi-Rimini-Weber Model." In: *Journal of Statistical Physics* 125.4 (2006), pp. 821–840.

[1018] L. Vaidman. "All is ψ." In: *Journal of Physics: Conference Series* 701.1 (2016), p. 012020.

[1019] L. Vaidman. "Quantum theory and determinism." In: *Quantum Studies: Mathematics and Foundations* 1.1 (2014), pp. 5–38.

[1020] J. A. Wheeler. "Law without Law." In: *Quantum Theory and Measurement*. Ed. by J. A. Wheeler and W. H. Zurek. Princeton University Press, 1983.

[1021] J. A. Wheeler. "The "Past" and the "Delayed-Choice" Double-Slit Experiment." In: *Mathematical Foundations of Quantum Theory*. Academic Press, 1978, pp. 9–48.

[1022] E. P. Wigner. "Remarks on the mind-body question." In: *Quantum Theory and Measurement*. Ed. by J. A. Wheeler and W. H. Zurek. Princeton University Press, 1983.

[1023] H. D. Zeh. "On the interpretation of measurement in quantum theory." In: *Foundations of Physics* 1.1 (1970), pp. 69–76.

[1024] H. Zeh. "The Wave Function: It or Bit?" In: *Science and Ultimate Reality. Quantum Theory, Cosmology, and Complexity*. Ed. by J. D. Barrow, P. C. W. Davies, and C. L. H. Jr. Cambridge University Press, 2004.

[1025] A. Zeilinger. "Experiment and the foundations of quantum physics." In: *Rev. Mod. Phys.* 71.2 (1999), S288–S297.

Acknowledgements

Here, I want to convey my gratitude to the people that I have encountered in the course of this work. Foremost, I want to thank my supervisor Harald. When many many years ago I came to your office asking for the possibility to do a master thesis I know I wasn't the most attractive candidate. But, as you generously do for so many people, you took a chance with me and unconditionally supported me during the next years to pursue so many different projects, not always in the lab. This incredible adventure has been the time of my life and I cannot thank you enough for this opportunity. In our joint work you exemplified deep integrity, a joyous desire to get to the bottom of things, and an encouraging trust in your apprentices to develop the responsibility and drive to become autonomous researchers. I very much hope I could absorb at least a bit of these qualities and live up to the opportunities I was given.

Secondly, I want to thank Lev, who, over the course of many joint projects, developed into a sort of unofficial co-supervisor for me. It is a rare thing in our contemporary scientific culture to have someone stand so firmly by their convictions and be so openly dedicated to their proliferation. And while finding it strange at first, I came to deeply appreciate this attitude of a self-described Don Quichote who goes beyond the status quo and challenges the prevailing and convenient consensus. Is not the presence of such voices an indispensable part in our joint endeavor towards scientific progress? It was a pleasure to be Sancho on some of your adventures. I thank you for all your advice, support, and the profound encouragement you gave.

Next, I want to thank my direct master-thesis supervisor and later co-PhD-student Lukas. I always looked up to you not only as a paragon of scientific excellence but also as a shining example of how people can treat each other. In my life I have not met a kinder and more thoughtful person, to whom I always could turn in the darkest moments of this journey. Your continued friendship means the world to me.

I also met many other amazing people during my time at MPQ: Jasmin, my longest standing office partner with whom I shared many laughs and one or the other spontaneous discovery, and from whom I at least tried to learn the value of "just trying things out" over too much futile overthinking. Carlotta, whom I had the pleasure to accompany during her master-thesis and who later became my co-PhD-student displaying amazing leadership qualities encouraging productive communication and positive change against my often too defeatist attitude. Florian, who I initially supervised as a Bachelor student and who eventually also caught up to become my co-PhD-student in Garching exhibiting

an ingenious attitude towards technology and an admirable and unbroken drive to always obtain a full consistent picture of things. Thanks to all of you for the many essential therapy sessions on Garching couches, unblocking the Bloch coffee machine due to your otherworldly social skills, and just the many fun times.

I also greatly appreciate all the others with whom I had the pleasure to share parts of the journey in Garching, including Christian, Mira, Katharina, Maria, Leonardo, Sholeh, Jasper, Elina, Benedikt, Vinay, and Ozan, as well as all other members of XQP, such as Gwen, Martin, Kai, Peter, Lars, Robert, Tim, Florian F., Pooja, Michi A., Adomas, Yiru, Manpreet, Moritz, Michi S., and also Karabee and Akhil who happened to share with me the surreal minutes waiting in the corridor for my exam grade. I cannot find the words to do you all justice, so just thanks again for the awesome hat!

It was a great pleasure and benefit to cross paths with the Hänsch and Hunger groups. I want to give huge thanks to Prof. Hänsch, Thomas, David, Vitaly, Matthias, Johannes, Savely, Akira, as well as so many others, and importantly also to our amazing administrative staff Ms. Hermann, Ms. Gschwendtner, and Marianne.

I also want to thank our collaboration partners, including, among many others, Wiesiu, Tomek, Paweł, Marco, Fabrizio, Alon, Shimshon, Gregory, Michael, Anna, and Alex. I cherish our time together and am grateful for your enrichment of my scientific and human horizons. Warm thanks go out to Stephan for taking the time to read and evaluate this long thesis and Jörg for being part of my exam preparation and committee.

Finally, there comes the place to address my family. Of course none of this would have come to fruition without my parents who not only gave a great portion of their life energy to sustain the sprawling weed of me, but without whose readiness to take over a good portion of childcare, while still working themselves, my elongated office habitations and thus also this thesis would not have been possible. Thank you forever. I am also eternally thankful for my sisters and brothers-in-law, together with their partners and families. It is so good to have all of you guys. In particular I want to thank my sister Martha for being an example of stoic strength in the face of crippling despair and my sister Mary for being the first to read this thesis and fixing my most embarrassing English mistakes. Susi my dear wife, I am genuinely baffled by your resilience and ability to cope with everything I put you through while pursuing this dream. I have no idea how you are able to sustain the constant stream of joy and support that gives me strength to live every day, but I am so grateful for it. And also to my own three little weeds Sophia, Lea, and Simon to which I wholeheartedly want to give all my life energy, you are the ultimate goal of all of this, since, to say it in the words of Cooper, what are we but *the ghosts of our children's future*.